



N.M. Belyaev

The image features a technical drawing of a cube with various stress distribution diagrams overlaid. The cube is shown in a 3D perspective. Several dashed lines represent the cube's edges and internal planes. Overlaid on the cube are several diagrams: a top face with vertical hatching, a side face with horizontal hatching, and a bottom face with vertical hatching. A diagonal line runs from the top-left corner of the front face to the bottom-right corner of the back face. The diagrams illustrate the distribution of stress or strain across different planes and directions of the cube.

# Strength of Materials

MIR PUBLISHERS MOSCOW



**Н. М. БЕЛЯЕВ**

**СОПРОТИВЛЕНИЕ МАТЕРИАЛОВ**

**ИЗДАТЕЛЬСТВО «НАУКА» МОСКВА**

N. M. BELYAEV

# Strength of Materials

*translated from the Russian  
by N. K. Mehta*

MIR PUBLISHERS MOSCOW

**First published 1979**

**Revised from the 1976 Russian edition**

*На английском языке*

© Издательство «Наука», 1976

© English translation, Mir Publishers, 1979

*Printed in the Union of Soviet Socialist Republics*

# **Nikolai Mikhailovich Belyaev**

## **(1890—1944)**

Nikolai Mikhailovich Belyaev occupied a leading position among eminent Soviet scientists who worked on the technical application of theory of elasticity and strength of materials and structures.

After graduating from the St. Petersburg Institute of Railway Engineering in 1916, Nikolai Mikhailovich Belyaev was invited to stay at the Strength of Materials Department, where he worked under S. P. Timoshenko.

Nikolai Mikhailovich Belyaev was associated with this Institute (now the Leningrad Institute of Railway Engineering) throughout his life. At the institute he taught subjects like engineering structures, bridges, theoretical mechanics, strength of materials and theory of elasticity, and from 1924 to the end of his life was Head of the Strength of Materials Department.

All his life Nikolai Mikhailovich Belyaev was a leading engineer and research worker. He was the first to formulate and solve the problem of stability of prismatic bars under variable axial loading—a problem interesting from the theoretical aspect and important from the point of view of applications. Simultaneously, Nikolai Mikhailovich Belyaev worked on the problem of local stresses in bodies in contact under compression. Here he considerably developed the works of Hertz. The work first published by Nikolai Mikhailovich Belyaev in 1924 has completely retained its value to this day.

In the Soviet Union Belyaev was one of the first to undertake the study of the theory of plastic deformation, and he contributed a lot towards the development of this field.

Nikolai Mikhailovich Belyaev spent the last years of his life in fruitful research on problems of creep and relaxation of metals under high temperatures.

Nikolai Mikhailovich Belyaev was a rare talent who successfully combined theory with experimental research. In 1924 he took over as Head of the mechanical engineering laboratory of the Leningrad Institute of Railway Engineering, and in the course of 16 years of administration changed the laboratory into a leading scientific research centre.

New technical specifications ensuring long and reliable performance of rails were compiled as a result of the research conducted at the laboratory under the guidance and with direct participation of Nikolai Mikhailovich Belyaev. These specifications with minor additions are in force to this day.

Research done by Nikolai Mikhailovich Belyaev in the field of technology of concrete won wide acclaim all over the Soviet Union.

The pedagogical activity of Nikolai Mikhailovich Belyaev was not restricted to the Leningrad Institute of Railway Engineering. He worked at the Leningrad Technological Institute (1919-1926), Leningrad Institute of Civil Aviation (1931-1934), and from 1934 onwards was Head of the Strength of Materials Department at the Leningrad Polytechnical Institute—the biggest institute in the country.

In 1939 Nikolai Mikhailovich Belyaev was elected Corresponding Member of the USSR Academy of Sciences, and from 1942 occupied the post of Deputy Director of the Institute of Mechanics of the Academy of Sciences of the USSR.

His book *Strength of Materials* has won wide recognition in the USSR.

# Preface to the Fifteenth Russian Edition

The new edition of *Strength of Materials* by N. M. Belyaev has been published after 11 years. In 33 years that lapsed between the publication by N. M. Belyaev of the first edition in 1932 and the last fourteenth edition in 1965 a total of 675 000 copies of the book were sold, testifying to its wide popularity. During this period the book was periodically enlarged and revised by N. M. Belyaev and, after his death in 1944, by a group of four of his co-workers. This group, which prepared from the fifth to the fourteenth editions for publication, did not consider it proper to make substantial changes in the original work of N. M. Belyaev. Additions were done at one time or another only when they became absolutely necessary due to changes in standards and technical specifications and in the light of recent research.

In the present edition, prepared by the same group, a number of topics have been dropped either owing to their irrelevance to strength of materials or because they are rarely taught in the main course. The topics that have been dropped include Contact Stresses, Riveted Beams, Reinforced Concrete Beams, Approximate Methods for Calculating Deflection of Beams, Beams on Elastic Foundation, Design of Thin-walled Bars, all graphical methods, and a part of Complicated Problems of Stability Analysis, the other part of the last topic being presented in an abbreviated version. The reader may refer to the earlier editions of this book or special monographs in case information is required on these topics.

Considering the availability of a large number of problem books (see, for instance, *Problems on Strength of Materials* edited by V. K. Kachurin) on the market, most of the examples have been dropped from the present edition. Only examples that are essential for the explanation of theoretical part have been retained.

For greater compactness the problem of design for safe loads has now been included in Chapter 26. For the first time the chapter includes the principles of design for limiting states, which though beyond the limits of the basic course of strength of materials are important enough to require an exposition of the basic concepts even at this stage of teaching.

The problems of strength, which in the previous editions occupied two chapters, have been grouped into one. The part dealing with actual stresses has been transferred to Chapter 2, where it has been presented in a sufficiently detailed manner.

The tables containing data on materials have been dropped from the appendices. A part of the data on materials has been transferred to



corresponding sections. The obsolete steel profiles grading has been replaced by new ones.

As in the previous editions it was our endeavour to preserve Belyaev's style and method of presentation of material. Therefore the author's text has in general been preserved. If Nikolai Mikhailovich Belyaev were alive today he would possibly write many things in a different way. However, since the book won wide popularity as written by N. M. Belyaev, we tried to preserve the original text as far as possible.

The work involved in preparing the fifteenth edition for publication was distributed among the group as follows: Chapter 13, § 80 of Chapter 14, Chapters 15-19, 24-25—L. A. Belyavskii; Chapters 6, 8-12, 27-28—Ya. I. Kipnis; Chapters 1-5, 26 and appendices—N. Yu. Kushelev; Chapter 7, § 79 of Chapter 14, Chapters 20-23, 29-32—A. K. Sinitskii.

*A. K. Sinitskii*

March 1976

# Contents

Nikolai Mikhailovich Belyaev 5  
Preface to the Fifteenth Russian Edition 7

## PART I. Introduction. Tension and Compression

### Chapter 1. Introduction 17

- § 1. The science of strength of materials 17
- § 2. Classification of forces acting on elements of structures 18
- § 3. Deformations and stresses 21
- § 4. Scheme of a solution of the fundamental problem of strength of materials 23
- § 5. Types of deformations 27

### Chapter 2. Stress and Strain in Tension and Compression Within the Elastic Limit. Selection of Cross-sectional Area 27

- § 6. Determining the stresses in planes perpendicular to the axis of the bar 27
- § 7. Permissible stresses. Selecting the cross-sectional area 30
- § 8. Deformations under tension and compression. Hooke's law 32
- § 9. Lateral deformation coefficient. Poisson's ratio 36

### Chapter 3. Experimental Study of Tension and Compression in Various Materials and the Basis of Selecting the Permissible Stresses 40

- § 10. Tension test diagram. Mechanical properties of materials 40
- § 11. Stress-strain diagram 47
- § 12. True stress-strain diagram 48
- § 13. Stress-strain diagram for ductile and brittle materials 52
- § 14. Rupture in compression of brittle and ductile materials. Compression test diagram 54
- § 15. Comparative study of the mechanical properties of ductile and brittle materials 57
- § 16. Considerations in selection of safety factor 59
- § 17. Permissible stresses under tension and compression for various materials 64

## PART II. Complicated Cases of Tension and Compression

### Chapter 4. Design of Statically Indeterminate Systems for Permissible Stresses 66

- § 18. Statically indeterminate systems 66
- § 19. The effect of manufacturing inaccuracies on the forces acting in the elements of statically indeterminate structures 73
- § 20. Tension and compression in bars made of heterogeneous materials 77
- § 21. Stresses due to temperature change 79
- § 22. Simultaneous account for various factors 82
- § 23. More complicated cases of statically indeterminate structures 85

**Chapter 5. Account for Dead Weight in Tension and Compression. Design of Flexible Strings 88**

- § 24. Selecting the cross-sectional area with the account for the dead weight (in tension and compression) 86
- § 25. Deformations due to dead weight 91
- § 26. Flexible cables 92

**Chapter 6. Compound Stressed State. Stress and Strain 99**

- § 27. Stresses along inclined sections under axial tension or compression (unifacial stress) 99
- § 28. Concept of principal stresses. Types of stresses of materials 101
- § 29. Examples of biaxial and triaxial stresses. Design of a cylindrical reservoir 103
- § 30. Stresses in a biaxial stressed state 107
- § 31. Graphic determination of stresses (Mohr's circle) 110
- § 32. Determination of the principal stresses with the help of the stress circle 114
- § 33. Stresses in triaxial stressed state 117
- § 34. Deformations in the compound stress 121
- § 35. Potential energy of elastic deformation in compound stress 124
- § 36. Pure shear. Stresses and strains, Hooke's law. Potential energy 127

**Chapter 7. Strength of Materials in Compound Stress 132**

- § 37. Resistance to failure. Rupture and shear 132
- § 38. Strength theories 136
- § 39. Theories of brittle failure (theories of rupture) 138
- § 40. Theories of ductile failure (theories of shear) 140
- § 41. Reduced stresses according to different strength theories 147
- § 42. Permissible stresses in pure shear 149

**PART III. Shear and Torsion****Chapter 8. Practical Methods of Design on Shear 151**

- § 43. Design of riveted and bolted joints 151
- § 44. Design of welded joints 158

**Chapter 9. Torsion. Strength and Rigidity of Twisted Bars 164**

- § 45. Torque 164
- § 46. Calculation of torques transmitted to the shaft 167
- § 47. Determining stresses in a round shaft under torsion 168
- § 48. Determination of polar moments of inertia and section moduli of a shaft section 174
- § 49. Strength condition in torsion 176
- § 50. Deformations in torsion. Rigidity condition 176
- § 51. Stresses under torsion in a section inclined to the shaft axis 178
- § 52. Potential energy of torsion 180
- § 53. Stress and strain in close-coiled helical springs 181
- § 54. Torsion in rods of non-circular section 187

## PART IV. Bending. Strength of Beams

- Chapter 10. Internal Forces in Bending. Shearing-force and Bending-moment Diagrams 195**
- § 55. Fundamental concepts of deformation in bending. Construction of beam supports 195
  - § 56. Nature of stresses in a beam. Bending moment and shearing force 200
  - § 57. Differential relation between the intensity of a continuous load, shearing force and bending moment 205
  - § 58. Plotting bending-moment and shearing-force diagrams 207
  - § 59. Plotting bending-moment and shearing-force diagrams for more complicated loads 214
  - § 60. The check of proper plotting of  $Q$ - and  $M$ -diagrams 221
  - § 61. Application of the principle of superposition of forces in plotting shearing-force and bending-moment diagrams 223
- Chapter 11. Determination of Normal Stresses in Bending and Strength of Beams 225**
- § 62. Experimental investigation of the working of materials in pure bending 225
  - § 63. Determination of normal stresses in bending. Hooke's law and potential energy of bending 228
  - § 64. Application of the results derived above in checking the strength of beams 235
- Chapter 12. Determination of Moments of Inertia of Plane Figures 239**
- § 65. Determination of moments of inertia and section moduli for simple sections 239
  - § 66. General method of calculating the moments of inertia of complex sections 244
  - § 67. Relation between moments of inertia about two parallel axes one of which is the central axis 246
  - § 68. Relation between the moments of inertia under rotation of axes 247
  - § 69. Principal axes of inertia and principal moments of inertia 250
  - § 70. The maximum and minimum values of the central moments of inertia 254
  - § 71. Application of the formula for determining normal stresses to beams of non-symmetrical sections 254
  - § 72. Radii of inertia. Concept of the momental ellipse 256
  - § 73. Strength check, choice of section and determination of permissible load in bending 258
- Chapter 13. Shearing and Principal Stresses In Beams 263**
- § 74. Shearing stresses in a beam of rectangular section 263
  - § 75. Shearing stresses in I-beams 270
  - § 76. Shearing stresses in beams of circular and ring sections 272
  - § 77. Strength check for principal stresses 275
  - § 78. Directions of the principal stresses 280
- Chapter 14. Shear Centre. Composite Beams 283**
- § 79. Shearing stresses parallel to the neutral axis. Concept of shear centre 283
  - § 80. Riveted and welded beams 289

## PART V. Deformation of Beams due to Bending

### Chapter 15. Analytical Method of Determining Deformations 292

- § 81. Deflection and rotation of beam sections 292
- § 82. Differential equation of the deflected axis 294
- § 83. Integration of the differential equation of the deflected axis of a beam fixed at one end 296
- § 84. Integrating the differential equation of the deflected axis of a simply supported beam 299
- § 85. Method of equating the constants of integration of differential equations when the beam has a number of differently loaded portions 301
- § 86. Method of initial parameters for determining displacements in beams 304
- § 87. Simply supported beam unsymmetrically loaded by a force 305
- § 88. Integrating the differential equation for a hinged beam 307
- § 89. Superposition of forces 310
- § 90. Differential relations in bending 312

### Chapter 16. Graph-analytic Method of Calculating Displacement in Bending 313

- § 91. Graph-analytic method 313
- § 92. Examples of determining deformations by the graph-analytic method 317
- § 93. The graph-analytic method applied to curvilinear bending-moment diagrams 320

### Chapter 17. Non-uniform Beams 324

- § 94. Selecting the section in beams of uniform strength 324
- § 95. Practical examples of beams of uniform strength 325
- § 96. Displacements in non-uniform beams 326

## PART VI. Potential Energy. Statically Indeterminate Beams

### Chapter 18. Application of the Concept of Potential Energy in Determining Displacements 331

- § 97. Statement of the problem 331
- § 98. Potential energy in the simplest cases of loading 333
- § 99. Potential energy for the case of several forces 334
- § 100. Calculating bending energy using internal forces 336
- § 101. Castigliano's theorem 337
- § 102. Examples of application of Castigliano's theorem 341
- § 103. Method of introducing an external force 344
- § 104. Theorem of reciprocity of works 346
- § 105. The theorem of Maxwell and Mohr 347
- § 106. Vereshchagin's method 349
- § 107. Displacements in frames 351
- § 108. Deflection of beams due to shearing force 353

### Chapter 19. Statically Indeterminate Beams 356

- § 109. Fundamental concepts 356
- § 110. Removing static indeterminacy via the differential equation of the deflected beam axis 357

- § 111. Concepts of redundant unknown and base beam 359
- § 112. Method of comparison of displacements 360
- § 113. Application of the theorems of Castigliano and Mohr and Vereshchagin's method 362
- § 114. Solution of a simple statically indeterminate frame 364
- § 115. Analysis of continuous beams 366
- § 116. The theorem of three moments 368
- § 117. An example on application of the theorem of three moments 372
- § 118. Continuous beams with cantilevers. Beams with rigidly fixed ends 375

## PART VII. Resistance Under Compound Loading

### Chapter 20. Unsymmetric Bending 378

- § 119. Fundamental concepts 378
- § 120. Unsymmetric bending. Determination of stresses 379
- § 121. Determining displacements in unsymmetric bending 385

### Chapter 21. Combined Bending and Tension or Compression 389

- § 122. Deflection of a beam subjected to axial and lateral forces 389
- § 123. Eccentric tension or compression 392
- § 124. Core of section 396

### Chapter 22. Combined bending and torsion 401

- § 125. Determination of twisting and bending moments 401
- § 126. Determination of stresses and strength check in combined bending and torsion 404

### Chapter 23. General Compound Loading 408

- § 127. Stresses in a bar section subjected to general compound loading 408
- § 128. Determination of normal stresses 410
- § 129. Determination of shearing stresses 413
- § 130. Determination of displacements 414
- § 131. Design of a simple crank rod 417

### Chapter 24. Curved Bars 428

- § 132. General concepts 423
- § 133. Determination of bending moments and normal and shearing forces 424
- § 134. Determination of stresses due to normal and shearing forces 426
- § 135. Determination of stresses due to bending moment 427
- § 136. Computation of the radius of curvature of the neutral layer in a rectangular section 433
- § 137. Determination of the radius of curvature of the neutral layer for circle and trapezoid 434
- § 138. Determining the location of neutral layer from tables 436
- § 139. Analysis of the formula for normal stresses in a curved bar 436
- § 140. Additional remarks on the formula for normal stresses 439
- § 141. An example on determining stresses in a curved bar 441
- § 142. Determination of displacements in curved bars 442
- § 143. Analysis of a circular ring 445

- Chapter 25. Thick-walled and Thin-walled Vessels 446**
- § 144. Analysis of thick-walled cylinders 446
  - § 145. Stresses in thick spherical vessels 453
  - § 146. Analysis of thin-walled vessels 454
- Chapter 26. Design for Permissible Loads. Design for Limiting States 467**
- § 147. Design for permissible loads. Application to statically determinate systems 457
  - § 148. Design of statically indeterminate systems under tension or compression by the method of permissible loads 458
  - § 149. Determination of limiting lifting capacity of a twisted rod 462
  - § 150. Selecting beam section for permissible loads 465
  - § 151. Design of statically indeterminate beams for permissible loads. The fundamentals. Analysis of a two-span beam 468
  - § 152. Analysis of a three-span beam 472
  - § 153. Fundamentals of design by the method of limiting states 474

## PART VIII. Stability of Elements of Structures

- Chapter 27. Stability of Bars Under Compression 477**
- § 154. Introduction. Fundamentals of stability of shape of compressed bars 477
  - § 155. Euler's formula for critical force 480
  - § 156. Effect of constraining the bar ends 484
  - § 157. Limits of applicability of Euler's formula. Plotting of the diagram of total critical stresses 488
  - § 158. The stability check of compressed bars 494
  - § 159. Selection of the type of section and material 498
  - § 160. Practical importance of stability check 502
- Chapter 28. More Complicated Questions of Stability in Elements of Structures 504**
- § 161. Stability of plane surface in bending of beams 504
  - § 162. Design of compressed-bent bars 512
  - § 163. Effect of eccentric compressive force and initial curvature of bar 517

## PART IX. Dynamic Action of Forces

- Chapter 29. Effect of Forces of Inertia. Stresses due to Vibrations 521**
- § 164. Introduction 521
  - § 165. Determining stresses in uniformly accelerated motion of bodies 523
  - § 166. Stresses in a rotating ring (flywheel rim) 524
  - § 167. Stresses in connecting rods 525
  - § 168. Rotating disc of uniform thickness 529
  - § 169. Disc of uniform strength 533
  - § 170. Effect of resonance on the magnitude of stresses 535
  - § 171. Determination of stresses in elements subjected to vibration 536
  - § 172. The effect of mass of the elastic system on vibrations 541
- Chapter 30. Stresses Under Impact Loading 548**
- § 173. Fundamental concepts 548
  - § 174. General method of determining stresses under impact loading 549

- § 175. Concrete cases of determining stresses and conducting strength checks under impact 554
- § 176. Impact stresses in a non-uniform bar 559
- § 177. Practical conclusions from the derived results 560
- § 178. The effect of mass of the elastic system on impact 562
- § 179. Impact testing for failure 565
- § 180. Effect of various factors on the results of impact testing 568

**Chapter 31. Strength Check of Materials Under Variable Loading 571**

- § 181. Basic ideas concerning the effect of variable stresses on the strength of materials 571
- § 182. Cyclic stresses 573
- § 183. Strength condition under variable stresses 575
- § 184. Determination of endurance limit in a symmetrical cycle 576
- § 185. Endurance limit in an unsymmetrical cycle 579
- § 186. Local stresses 582
- § 187. Effect of size of part and other factors on endurance limit 589
- § 188. Practical examples of failure under variable loading. Causes of emergence and development of fatigue cracks 593
- § 189. Selection of permissible stresses 597
- § 190. Strength check under variable stresses and compound stressed state 600
- § 191. Practical measures for preventing fatigue failure 602

**Chapter 32. Fundamentals of Creep Analysis 605**

- § 192. Effect of high temperatures on mechanical properties of metals 605
- § 193. Creep and after-effect 607
- § 194. Creep and after-effect curves 609
- § 195. Fundamentals of creep design 615
- § 196. Examples on creep design 620

- Appendix 630
- Name index 639
- Subject index 641





# PART I

## Introduction.

### Tension and Compression

#### CHAPTER 1

#### Introduction

#### § 1. The Science of Strength of Materials

In designing structures and machines, an engineer has to select the material and the cross-sectional area of each element of the structure or machine so that it enables the element to have strength to resist external forces transmitted to it by adjacent elements of the structure without failure of strength or distortion of shape, i. e. the element should function properly. Strength of materials provides the engineer with fundamentals for a proper solution of this problem.

*Strength of materials* deals with the behaviour of various materials under the action of external forces and points out how to select the appropriate material and the cross-sectional area of each element of the structure so as to provide fully reliable functioning and the most economic design.

Sometimes, strength of materials has to deal with the problem in a modified form—to check the dimensions of a designed or existing structure.

The conditions for maximum economy in design and reliability of functioning are contradictory. The former demand minimum consumption of materials whereas the latter lead to increase in consumption. This contradiction forms the basis of the technique, which has facilitated the development of strength of materials.

Often the existing methods of checking the strength and the available materials are unable to meet the practical requirements for providing answers to new problems (for example, attaining high speeds in engineering in general and in aerostatics in particular, long-span structures, dynamic stability, etc.). This initiates a search for new materials and study of their properties, and inspires research for improving the existing methods of designing and devising the new ones. Strength of materials must keep pace with the general development of engineering and technology.

Sometimes, besides the chief requirements of maximum reliability and economy, an engineer has to ensure fulfilment of other conditions too, such as quick building (when restoring broken structures), minimum weight (in aircraft design), etc. These conditions influence the dimensions, the shape and the material of the various elements comprising the structure.

The emergence of strength of materials as a separate science dates back to 1638 and is intimately connected with the works of Galileo Galilei, the great Italian scientist. Galileo was a professor of mathematics at Padua. He lived in a period which saw the disintegration of the feudal system, the development of trade capital and international maritime transport, and the birth of mining and metallurgical industries.

The rapid economic developments of those times called for speedy solutions of new technological problems. Increase in international maritime trade perpetuated the need for bigger ships which in turn entailed changes in their design; at the same time it became necessary to reconstruct the existing and to build new internal waterways, including canals and sluices. These new technical problems could not be solved by simply copying the existing designs of ships; it became necessary to judge the strength of elements keeping in mind their size and the forces acting upon them.

Galileo devoted a considerable part of his work to the study of the dependence between the dimensions of beams and bars and the loads they could withstand. He pointed out that the results of his experiments may prove very useful in building big ships, especially in strengthening the deck and covering because low weight is very important in structures of this type. Galileo's works have been published in his book *Discorsi e Dimostrazioni Matematiche . . .* ("Dialogue on Two New Sciences . . .") (1638, Leiden, Holland).

Further development of strength of materials went on in step with the progress of mechanical and civil engineering, and materialized owing to the research work done by a large number of eminent scientists, mathematicians, physicists and engineers. Russian and Soviet scientists occupy an important place amongst them. Brief informative sketches about the role played by individual scientists in the development of some problems of strength of materials are given in corresponding chapters of the book.

## § 2. Classification of Forces Acting on Elements of Structures

When in operation, the elements of structures and machines are subjected to external loads, which they transmit to one another. A dam bears its own weight and the pressure of water that it holds and transmits these forces to the foundation. The steel trusses of bridges take

the weight of the train through the wheels and rails and transmit it to the stone supports, and the latter, in turn, communicate this load to the foundation. The steam pressure in the cylinder of a steam engine is transmitted to a piston rod. The pulling force of the locomotive is transmitted to the train through a coupler which connects the tender with the wagons. Hence, the elements of structures are subject to either *volume forces* acting on each element of the structure (dead weight) or *forces of interaction\** between the element under consideration and adjoining elements or between the element and the surrounding medium (water, steam or air). In future, when we say that an external force is being applied to an element of the structure, this will imply the transmission of force of pressure (motion) to the element under consideration from adjoining elements of the structure or the surrounding medium.

The forces may be classified according to a number of criteria.

We distinguish between the concentrated and distributed forces.

A *concentrated force* is defined as the force of pressure transmitted to the element of structure through an area which is very small as compared to the size of the element, for example, the pressure of the wheels of a moving train on the rails.

In practice the concentrated force is considered to be acting at a point owing to the small area through which the pressure is transmitted. We must keep in mind that this is an approximation which has been introduced to simplify the calculations; actually, no pressure can be transmitted through a point. However, the error due to this approximation is so small that it may be generally ignored.

A *distributed force* is defined as the force applied continually over a certain length or area of the structure. A layer of sand of uniform thickness spread over the sidewalk of a bridge represents a force which is uniformly distributed over a certain area; if the thickness of the sand layer is not uniform we shall obtain a non-uniformly distributed load. The dead weight of a beam in the ceiling represents a load distributed over its length.

The concentrated loads are measured in units of force (tons, kilograms, newtons \*\*); the loads distributed over an area are measured in terms of force per unit area ( $\text{tf}/\text{m}^2$ ,  $\text{kgf}/\text{cm}^2$ ,  $\text{N}/\text{m}^2$ , etc.); the loads distributed along the length of an element are expressed as force per unit length ( $\text{kgf}/\text{m}$ ,  $\text{N}/\text{m}$ , etc.).

The loads may further be classified as permanent and temporary. The *permanent loads* act throughout the whole life of the structure, e.g. dead weight. The *temporary loads* act on the structure only for a

---

\* To be precise, the weight of a body is the force of interaction between the body and the earth.

\*\* In the SI system, which is now preferred and recommended, the force is measured in newtons ( $1 \text{ N} \approx 0.102 \text{ kgf}$ ).

certain period of time—the weight of the train moving along the bridge may be cited as an example.

According to the nature of action, the loads may be classified as static and dynamic.

*Static loads* act on the structure gradually, after being applied to the structure they either do not change at all or change insignificantly; the majority of loads acting in civil and hydraulic structures are of this nature. Under the influence of static loading all elements of the construction remain in equilibrium; accelerations in the elements of the structure are either totally absent or so small that they may be neglected.

If, however, the acceleration is considerable and the change in velocity of the machine or structure takes place in a short time, the load is known as *dynamic*.

The examples of dynamic loads are suddenly applied load, impact load and repeated variable load.

*Suddenly applied loads* are transmitted instantaneously in their total magnitude. An example of this type of loading is the force of pressure of the wheels of a locomotive when it enters a bridge.

*Impact loads* appear when there is a sharp change in the velocity of adjoining elements of a structure, for example the impact of drop hammer during pile driving.

The *repeated variable loads* act on the elements of structures for a considerable number of times. For example, repeated steam pressure, alternately stretching and compressing the piston rod and the connecting rod of the steam engine. In a number of cases the load represents a combination of dynamic loads of different nature.

We shall first of all study the resistance of materials to static loads; the selection of material and cross-sectional area for each element of the structure does not present many difficulties in this case.

In Chapters 29-31 we shall discuss the action of dynamic loads in a number of instances which occur as often as static loads; they require careful study because their effect on the elements of structures differs from that of static loads, and the material also resists them in a different manner.

Concluding the classification of forces acting on the elements of structures, let us consider the action of parts which support these elements; the forces acting on these supports are known as the *reaction forces*—they are unknown quantities and are determined from the condition that each element of the structure must remain in equilibrium under the action of all the external forces applied to it and the reaction forces.

### § 3. Deformations and Stresses

In theoretical mechanics (statics) we study the equilibrium of a perfectly rigid body; this concept of material in statics is sufficient to determine the conditions in which the body will remain in equilibrium under the action of external forces applied to it. However, this rough and approximate concept of the properties of materials does not hold good in strength of materials; here we must take into account the fact that there does not exist a perfectly rigid body.

The elements of a structure, as well as the structure as a whole, change their dimensions and shape to some extent under the action of external forces and are liable to complete failure in the end. This change in shape and size is called *deformation*.

The magnitude and nature of the deformation depend upon the structure of the material used. All materials may be divided into two groups: crystalline and amorphous.

*Crystalline materials* consist of a very large number of extremely small crystals. Each of these is a system of atoms arranged very close to each other in regular rows. These rows form the so-called *crystalline lattice*. In *amorphous materials* the atoms are not arranged in a particular order. They are held in equilibrium by the forces of interaction. The deformation of bodies takes place due to change in the location of atoms, i.e. due to their getting closer or farther.

Deformations are divided into elastic and plastic. *Elastic deformation* disappears when the force causing the deformation is removed; in this case, the body completely regains its initial shape and dimensions. This deformation occurs due to elastic distortion in the crystalline lattice. It has been experimentally observed that the elastic deformation continues till the forces being applied do not exceed a certain limit.

If, however, the external force exceeds this particular limit, the body fails to regain completely its initial shape and size after the force is removed; the difference in size which thus remains is called the *plastic (residual) deformation*. In crystalline materials, this deformation is caused by the irreversible displacement of one layer of crystalline lattice with respect to the other. After the removal of external forces the displaced layers of atoms retain their position.

In deformation, the displacement of atoms under the action of external forces is accompanied by a change in the forces of interaction between the atoms, i.e. the forces of attraction and repulsion.

Additional internal forces accompanying the deformation appear in the elements of structures under the action of external forces. These internal forces resist the external forces and try to prevent them from breaking the element, changing its shape or separating one part from the other. They try to regain the initial shape and size of a deformed part of the structure. In order to assess the effect of the external forces on the deformed element, we must know how to measure and calculate

the interatomic forces that appear as a result of the deformation caused by the action of external forces.

In strength of materials this is achieved by the *method of sections*, which we shall try to explain by the following example. Let us imagine a bar (Fig. 1), which is subjected to the action of two equal and opposite forces,  $P$ , and let us imagine that the bar is cut in two parts  $I$

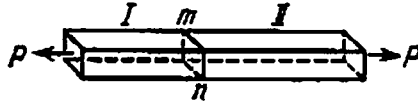


Fig. 1

and  $II$  by a plane  $mn$ . Under the action of forces  $P$  both halves of the bar tend to go apart, but are held together owing to the forces of interaction between the atoms located on both sides of plane  $mn$ . The resultant of the forces of interaction is the *internal force* transmitted through  $mn$  from one half of the bar to the other, and vice versa. The internal force of interaction per unit area around any point of section  $mn$  is called the *stress* at the point of the given section. The stresses acting from part  $II$  on part  $I$  and from part  $I$  on part  $II$  are equal in magnitude according to the law of action and reaction.

A number of planes dividing the bar in two parts in different ways can be drawn through a single point of the bar. The magnitude and direction of the stresses transmitted through the given point from one part of the bar to the other will depend upon how the plane cuts the bar.

Thus, it is wrong to speak of stresses without indicating the plane through which they are being transmitted. Therefore we speak about "the stress on a particular area in a particular plane". Since stress is a force per unit area, it is measured in  $\text{kgf}/\text{cm}^2$ ,  $\text{kgf}/\text{mm}^2$ ,  $\text{tf}/\text{cm}^2$ ,  $\text{tf}/\text{m}^2$ ,  $\text{N}/\text{m}^2$ , etc.

In future, we shall denote stress by letters  $p$ ,  $\sigma$ , and  $\tau$ ; letter  $p$  is used for stresses applied to certain area in any plane inclined at an arbitrary angle,  $\sigma$  denotes stress at right angles to the plane, i.e. *normal stress*, and  $\tau$  denotes stress in the plane, i.e. *shearing stress*.

The stress at any point is the measure of internal forces which appear in the material owing to its deformation under the action of external forces. The force transmitted from part  $I$  of the bar to part  $II$  (see Fig. 1) holds part  $II$  in equilibrium, i.e. counterbalances the system of external forces acting on part  $II$ . This force may be expressed in terms of the stress to be determined: if we consider an elementary area  $dA$  in the plane of cutting, then the elementary force acting on this elementary area will be  $p dA$ , where  $p$  is the stress at the point around which the elementary area is located. The sum of these elementary forces gives us the total force transmitted through the particular plane.

Thus, to determine the stresses, it is necessary to imagine the element to be cut in two parts and write down the conditions of equilibrium for the system of forces acting on one of the cutoff parts; this system includes the external forces applied to the part of the bar under consideration and also the force transmitted through the given plane and expressed in terms of stresses sought. This is the method of sections, which we shall constantly apply in future.

Let us point out, that, in strength of materials, the term "stress" is very often used instead of the expression "internal forces of interaction between parts of the bar"; therefore in future when we mention "uniform and non-uniform distribution of stresses over the section" and "force as the sum of stresses", we must bear in mind that these expressions are to a certain degree conventional. For example, to determine the force one cannot sum up the stresses at various points; as mentioned above, it is necessary to find at each point of section the *elementary force* which is transmitted through an elementary area  $dA$  and then sum up all these values. Recapitulating what has been written above, we come to the conclusion that when an external force is applied to an element of structure, the latter gets deformed and the deformation is accompanied by stresses in the element.

Strength of materials studies, on the one hand, the relation between the external forces and, on the other hand, the deformations and stresses due to them. This enables the engineer to solve the important problem of selecting a bar of proper dimensions and appropriate material to resist the external forces. In the next section we shall give an outline of the solution to this problem.

#### § 4. Scheme of a Solution of the Fundamental Problem of Strength of Materials

While selecting the size and material for an element of the structure we must provide for a certain safety factor against its failure and plastic deformation. The element should be designed so that the maximum stresses that occur during its operation should always be less than the stresses at which the material fails or undergoes plastic deformation.

The stress at which the material fails is called the *ultimate (tensile) strength*; we shall denote it with the same letter as stress but with subscript  $u$ . The stress beyond which the material deforms insignificantly and only up to a predetermined value is known as the *elastic limit*.<sup>\*</sup> These quantities are known as the mechanical characteristics of resistance of materials to failure and plastic deformations. To ensure the smooth functioning of the structure without a risk of failure, we must see to it that the element is only subjected to stresses which are less than its ultimate strength.

---

\* Ultimate strength and elastic limit will be more precisely explained in § 10.



The *permissible stress* is denoted by the same letter but is put in square brackets; it is related to the ultimate strength  $p_u$  by the following expression:

$$[\rho] = \frac{p_u}{k}$$

where  $k$  is the *safety factor* which shows how many times the permissible stress is less than the ultimate (tensile) strength. The value of this factor varies from 1.7-1.8 to 8-10 and depends upon the operating conditions of the structure. It will be discussed in greater detail in §§ 16 and 17.

Denoting by  $p_{\max}$  the maximum stress that appears in the designed element under the action of external forces, we may write the basic condition, which the size and material of the element must satisfy, as follows:

$$p_{\max} \leq [\rho] \quad (1.1)$$

This is the *strength condition*, which states that the actual stress must be not greater than the permissible.

Now we may compile the plan for solving the problems of strength of materials as follows.

(1) Ascertain the magnitude and nature of all the external forces, including the reactions, acting on the element under consideration.

(2) Select an appropriate material that is most suitable in the working conditions of the element (structure) and the nature of loading; determine the permissible stress.

(3) Set the cross-sectional area of the element in numerical or algebraic form, and calculate the maximum actual stress  $p_{\max}$  which develops in it.

(4) Write down the strength condition  $p_{\max} \leq [\rho]$  and with the help of it calculate the cross-sectional area of the element or check whether the set value is sufficient.

The plan of solution of problems in strength of materials is sometimes altered; in some structures the safety factor for the whole structure is found to be greater than that for the material in the point of greatest stress. If the limiting lifting capacity of the material is exhausted at this point, this does not necessarily mean that the limiting lifting capacity of the whole structure has also been reached. In such cases, the strength condition  $p_{\max} \leq [\rho]$  is replaced by the strength condition for the structure as a whole:

$$P \leq P_{\text{per}} = \frac{P_u}{k}$$

here  $P$  is the load on the structure,  $P_{\text{per}}$  is its permissible value, and  $P_u$  is the limiting force which the structure can withstand without brea-

king down. Thus, the design based on permissible stresses is replaced by the design based on permissible loads.

In this case, it is necessary to:

- (1) ascertain the magnitude and nature of all the external forces, acting on the given element;
- (2) select the appropriate material that is most suitable in the working conditions of the structure and also takes into consideration the nature of loading; determine the safety factor;
- (3) set the cross-sectional area of the elements of structure in numerical or algebraic form, and calculate the maximum permissible load  $P_{\text{per}}$ ;
- (4) write down the strength condition  $P \leq P_{\text{per}}$  and with its help calculate the cross-sectional area of the elements of structure or check whether the set dimensions are sufficient.

In a number of cases, as we shall see later (§ 150), both methods give similar results.

In general, we shall be using the conventional method of design based on permissible stresses; however, along with this, the method of design based on permissible loads will be explained, especially in cases where the two methods give dissimilar results.

In the majority of cases the strength condition must be supplemented by stability and rigidity tests. The first test ensures that the elements of structure must not change their predetermined type of equilibrium, and the second test sets limits to the deformations of elements.

While solving problems on strength of materials, we have to take the help of theoretical mechanics and experimental techniques. The determination of external forces is based on equations of statics; in statically indeterminate structures, it is essential to determine the deformation of the material. This, as shown in § 18, is possible only if we have reliable experimental data on the relation between deformations and forces or stresses.

To estimate the permissible stresses we must know the ultimate strength of the material and its other mechanical properties. This information can also be obtained by a study of the properties of material in special material testing laboratories. Finally, to determine actual stresses we seek the help of not only mathematical analysis and mechanics but also the available experimental data. Thus strength of materials consists of two methods of solving a problem: analytical, based on mathematics and mechanics, and experimental. Both these methods are closely interrelated.

Strength of materials should not be considered a branch of science which deals only with theoretical determination of stresses in some homogeneous elastic body. The problems studied in strength of materials can be solved only if we have sufficient experimental data on the mechanical properties of real materials, keeping in mind their structure, methods of fabrication and machining. Therefore, we have paid

considerable attention to this aspect in our book. Experiments play an important role in the understanding of a subject and must be carried out by the students along with their theoretical studies. These experiments, worked out on the basis of facilities and equipment available in the strength testing laboratories, have been presented in a separate manual.\*

Although at the very outset strength of materials was identified with the necessity for solving a number of purely practical problems, its further development was more on the theoretical side, resulting at times in discrepancies between the outcome of experimental investi-

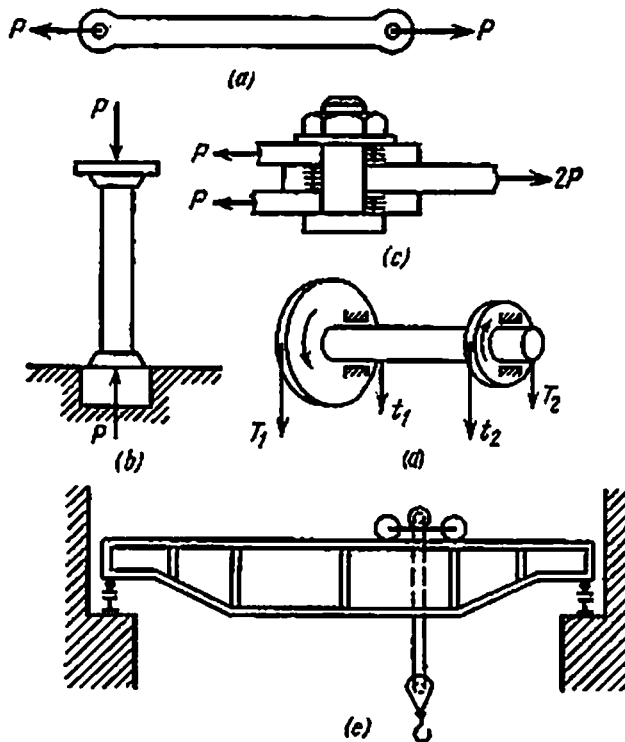


Fig. 2

gations and their practical application. Laboratory research went along a special path, chiefly to set the acceptable standards for various types of materials. Now strength of materials studies real materials in accordance with their operation in structures accentuated by intensive experimental and theoretical investigations for solving developing day-to-day practical problems. These problems, for example, are those connected with the study of the strength of new materials, conditions pertaining to their failure, determination of stresses not only within the limits of elasticity but also beyond them, etc.

\* N. M. Belyaev, *Laboratory Experiments in Strength of Materials*, Gostekhizdat, 1951 (in Russian).

## § 5. Types of Deformations

Having accepted a general method of solving problems of strength of materials, we may now go over to studying individual problems. These may be divided into a number of groups depending upon the type of deformations.

The common types of deformations (Fig. 2) are: (1) tension or compression, (*a*) and (*b*), as in chains, ropes, cables, bars of trusses working under tension or compression, columns; (2) shearing (*c*), as in bolts and rivets; (3) torsion (*d*), as in shafts; (4) bending (*e*), as in beams of all types. These four types of deformations are called *simple deformations*.

The operation of elements in structures is generally more complex; they are subjected to two or more types of deformations simultaneously, for example, tension or compression and bending, bending and torsion, etc. These are cases of the so-called *composite deformation*. For each of the abovementioned types of deformations, we shall find out methods for determining the stresses, selecting the material and cross-sectional area of the elements and determining the magnitude of deformation.

To make it easy for the reader to understand, initially we shall consider only those elements of structures and machines which are in the form of *prismatic bars with a straight axis*. A body which has a uniform cross-sectional area all along its length may be considered a prismatic bar. The centres of gravity of all the sections of the body lie on one straight line, which is called the *axis of the bar*. Later on we shall also consider bars with a non-uniform cross-sectional area and curved axis.

## CHAPTER 2

### Stress and Strain in Tension and Compression Within the Elastic Limit. Selection of Cross-sectional Area

## § 6. Determining the Stresses in Planes Perpendicular to the Axis of the Bar

We shall start the study of strength of materials with the simplest case of tension or compression of a prismatic bar.

*Axial tension or compression* of such a bar is its deformation under the action of two equal and opposite forces applied at the end faces of the bar along its axis. If these forces are directed outwards, the bar is

said to be under tension (Fig. 3a); in the opposite case, under compression (Fig. 3b).

According to the general method of solving problems of strength of materials, we must first determine the magnitude of the external forces  $P$  stretching (compressing) the bar. The value of force  $P$  can usually be determined by considering the interaction of the bar with the other elements of the structure.

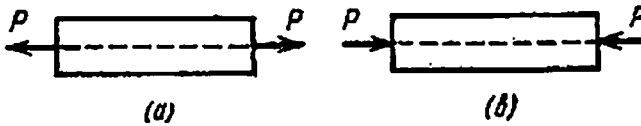


Fig. 3

As a simple example, consider a round steel coupler threaded at the ends and loaded by axial tensile forces  $P=25$  tf (Fig. 4). Our task is to select the cross-sectional area of the shaft which provides sufficient strength. It is required to find out the stresses due to forces  $P$ , deter-

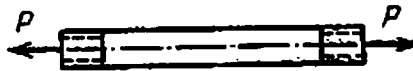


Fig. 4

mine the permissible stress and select the cross-sectional area in such a way that the actual stress does not exceed its maximum permissible value.

To determine the stresses, it is essential to select the planes by which the bar is to be cut into two parts. Strength should be checked in the critical section, i.e. in the section through which the maximum stress is transmitted. We shall first derive formulas for determining stresses in a plane perpendicular to the axis of the bar, and later on in inclined planes too; we will thus be in a position to find the critical section.

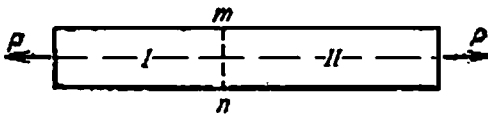


Fig. 5

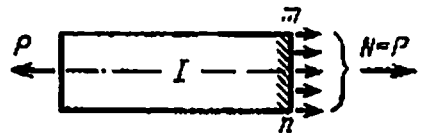


Fig. 6

Let us take a stretched bar and cut it in two parts by a plane  $mn$  (Fig. 5), perpendicular to the axis of the bar. Let us discard the second part; to retain the equilibrium of the first part, we must replace the discarded part by the forces transmitted through section  $mn$  (Fig. 6).

The equivalent forces must balance force  $P$ . Therefore they must compose a resultant force  $N$  equal in magnitude to force  $P$  and directed along the axis in the opposite direction (Fig. 6). This resultant  $N$  is the force acting in the bar.

In future the resultant of internal elastic forces, transferred from one part to the other across the imaginary section, will be called *normal* or *axial force*. However, since the cutoff portion of the bar must remain in equilibrium under the action of the normal force and the external forces acting on it, the normal force may also be calculated through the external forces. It is numerically equal to the resultant of external forces applied to the part of the bar under consideration and acts in the opposite direction. If the normal force acts inwards into the part under consideration, the bar is said to be compressed; if it acts in the opposite direction, the bar is said to be in tension.

Thus, the conditions of equilibrium of the remaining portion of the bar only give us the magnitude of the resultant of the internal forces transmitted through section  $mn$ , its direction and point of application. They, however, do not give us any idea of how the stresses are distributed over the section, i.e. what forces are being transmitted through various unit areas of the section. Let us point out that to ascertain the maximum danger of failure of a material, it is essential to determine the maximum stress and also the unit area of the critical section through which it is transmitted.

Experiments on tensile loading of bars of various materials reveal that if the forces are directed along the axis sufficiently accurately, then the elongations of lines drawn on the surface of the bar parallel to the axis are equal. This gives rise to the hypothesis of uniform distribution of stresses over the section. Only at the faces of the bar, where force  $P$  is directly transmitted to it, the distribution of stresses over different parts of the section is not uniform. The portions to which force  $P$  is applied directly get overloaded; but just a small distance away from the point of application of the force the material starts behaving more uniformly and stress distribution over the section perpendicular to the axis becomes uniform. These stresses are directed parallel to force  $P$ , i.e. perpendicular to the section; therefore they are called *normal stresses* and denoted by the letter  $\sigma$ . Since they are distributed uniformly over the section,  $N = \sigma A$ ; on the other hand,  $N = P$ . Hence

$$\sigma = \frac{P}{A} \quad (2.1)$$

This formula enables us to determine stress  $\sigma$  if the tensile force and the cross-sectional area are known. On the other hand, if we know the maximum permissible normal stress, this formula helps us to find the required cross-sectional area  $A$ .

## § 7. Permissible Stresses.

### Selecting the Cross-sectional Area

To ascertain the permissible stress limit for proper functioning of a bar of the given material, we must experimentally establish the relation between the strength of the bar and the stresses that appear in it. For this, it is essential to prepare a specimen (usually of a round or rectangular cross section) of the given material, clamp its ends in a machine for tensile loading and gradually increase the tensile force  $P$ . The specimen will stretch and ultimately break down.

Let  $P_u$  be the maximum load which the specimen can sustain before rupture. The normal stress due to this load is

$$\sigma_u = \frac{P_u}{A}$$

and is called the *ultimate (tensile) strength* of the material under tension. It is usually expressed in the units  $\text{kgf}/\text{mm}^2$  or  $\text{kgf}/\text{cm}^2$ .

As pointed out earlier in § 4, the maximum permissible normal stress  $[\sigma]$  is several times less than the ultimate strength  $\sigma_u$ ; the permissible stress is obtained by dividing the ultimate strength by the safety factor  $k$ . The value of  $k$  depends upon a number of factors, which shall be discussed in detail later on (§ 16). At any rate, the value of the safety factor must ensure not only the normal working of the element, i.e. working without failure, but also prevent the formation of plastic deformations which may affect the working of the machine or structure. The safety factor depends upon the material of the element, nature of the forces acting on the element, economic conditions and a number of other factors.

In view of the importance of properly selecting the safety factor and the permissible stress, these quantities have been standardized for a large number of structures and machines, and must be strictly followed by the designers. Hence, the permissible stress  $[\sigma]$  may be considered in each case a known quantity. Therefore, to determine the cross-sectional area of a stretched bar one may, using formula (2.1), write down the *strength condition*; this condition states that under the action of a force  $P$ , the actual stress in a stretched bar must not exceed the permissible stress  $[\sigma]$ :

$$\sigma = \frac{P}{A} \leq [\sigma] \quad (2.2)$$

From this condition the minimum cross-sectional area of the bar may be determined as

$$A \geq \frac{P}{[\sigma]} \quad (2.3)$$

With the help of formula (2.3), one can select the cross-sectional area of the bar.

Sometimes the cross-sectional area is preset. Then, from formula (2.3) we can find the permissible load

$$P \leq A[\sigma] \quad (2.4)$$

Returning to the design of the wagon coupler (§ 6, Fig. 4), it is required to select the material and the permissible stress. The coupler is made of steel with an ultimate strength of about 50 kgf/mm<sup>2</sup>. The material is selected such that the coupler is not too heavy, this condition being fulfilled only by using a high-strength material. At the same time, the material should have good resistance to shocks and impacts. A steel of a very high ultimate strength cannot be used because it is brittle.

The coupler should not only withstand fracture but also resist any noticeable plastic deformation to prevent jamming of the coupler thread. The elastic limit for the selected steel is approximately 0.6 times its ultimate strength  $\sigma_u$ . We shall see later that the stress under sudden loading is nearly twice its value under static loading, i.e. its value as determined under laboratory conditions. The permissible stress should therefore not exceed

$$0.5 \times 0.6\sigma_u = 0.3\sigma_u$$

Hence, the safety factor

$$k = \frac{1}{0.3} \approx 3.3$$

Therefore, in this case we may take the permissible stress

$$[\sigma] = \frac{\sigma_u}{k} = 0.3\sigma_u = 50 \times 0.3 = 15 \text{ kgf/mm}^2 = 1500 \text{ kgf/cm}^2$$

The required cross-sectional area at  $P=25$  tf is

$$A \geq \frac{P}{[\sigma]} = \frac{25\,000}{1500} = 16.7 \text{ cm}^2$$

The diameter of the coupler  $d$  is computed from the condition

$$\frac{\pi d^2}{4} = A \geq 16.7$$

wherefrom

$$d \geq \sqrt{\frac{16.7 \times 4}{\pi}} = 4.55 \text{ cm} \approx 4.5 \text{ cm}$$

The calculated diameter corresponds to the base of the thread with the minimum cross-sectional area. When the cross-sectional area of the bar is decreased in a particular place, for example due to a bolt or a rivet hole, a circular cut or a groove (threading), it is essential to determine the minimum cross-sectional area, called *net area* and denoted



by  $A_{\text{net}}$  or  $A_n$ . The cross-sectional area without weakening is called the *gross area* and denoted by  $A_{\text{gross}}$  or  $A_{\text{gr}}$ . Having computed the net area  $A_n$ , we can obtain the gross area  $A_{\text{gr}}$  from design considerations.

The formulas derived above are valid for tension. They can be used for compression as well without any changes. The difference will be in the direction of normal stresses and the magnitude of the permissible stress  $[\sigma]$ . The compression of bars is more complex in that the bar may become unstable, i.e. it may suddenly bend. Designing for stability will be discussed in Part VIII.

Figure 7 shows normal distribution in a section perpendicular to the axis of the bar for tension and compression. For a number of materials (e.g. steel) the permissible stress value is the same in tension and com-

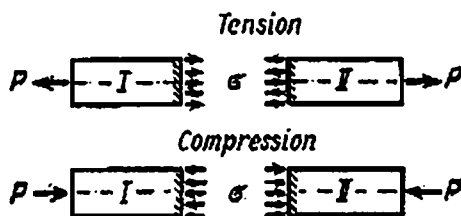


Fig. 7

pression (for short bars, i.e. bars in which the length does not exceed five times the diameter of cross section). In other materials (e.g. cast iron) the permissible stress is different in tension and compression, depending upon the ultimate strength for the recorded deformations.

In a number of cases, compressive stresses are transmitted from one element of construction to another through a comparatively small area of contact between them. This type of stress is generally called the *bearing*, or *contact stress*. Stress distribution around the area of contact is very complex and can be analyzed only by methods of the theory of elasticity. Usually, in simple designing, these stresses are considered as compressive stresses and a special permissible stress limit is fixed. Later on the question of selecting permissible stresses in special cases will be dealt with in greater details.

## § 8. Deformations Under Tension and Compression.

### Hooke's Law

To have complete idea about the working of a stretched or compressed element, it is essential to know ways of calculating the change in its dimensions. The corresponding laws can be obtained only on the basis of experiments with a stretched or compressed specimen of the given material; these experiments also help to study the strength of the material and determine its ultimate strength and other characteristics (§ 10).

These experiments are conducted in the laboratory on special machines which deform the specimen till it breaks down and measure the force required for this purpose.

Simultaneously, the deformation of the specimen is measured with the help of sufficiently accurate measuring instruments — strain gauges (tensometers). The testing machines are capable of applying a sufficiently large load on the specimen and accurately measure the same. Whole parts of structures (columns, portions of walls) can be tested for compression on presses having a capacity of up to 5000 tf. Tension test can be conducted in the laboratory on machines which are capable of exerting a tensile load of up to 1500 tf. However, in a majority of the laboratories machines of considerably less capacity (from 5 to 100 tf for tension test and 200 to 500 tf for compression test) are employed.

A detailed description of these machines and measuring instruments, particularly of the well-known Gagarin Press, is available in the book *Laboratory Experiment in Strength of Materials*, and also in special manuals on mechanical testing of materials. With the help of these machines and measuring instruments one can establish how the material specimen will change its dimensions under tension or compression.

Experiments enable us to conclude that up to a certain limit of loading, the elongation is directly proportional to the tensile force  $P$  and length of the specimen  $l$  but inversely proportional to the cross-sectional area  $A$ . Denoting by  $\Delta l$  the elongation of the specimen due to force  $P$ , we may write down the following relation between these quantities:

$$\Delta l = \frac{Pl}{EA} \quad (2.5)$$

where  $E$  is the proportionality factor which depends upon the material. Quantity  $\Delta l$  is called the *absolute elongation* of the bar due to force  $P$ . Formula (2.5) is called *Hooke's law* after the scientist who founded the law of proportionality in 1660.

Relation (2.5) may be presented in a different form. Let us divide both sides of the relation by  $l$ , the initial length of the bar:

$$\frac{\Delta l}{l} = \frac{P}{EA}$$

The ratio  $\frac{\Delta l}{l}$  of the absolute elongation to the initial length  $l$  is called the *relative elongation (strain)*; it is denoted by the letter  $\epsilon$ .

Relative elongation is a dimensionless quantity, as it is the ratio between two lengths  $\Delta l$  and  $l$  and is numerically equal to the elongation of a unit length of the bar. Replacing  $\frac{\Delta l}{l}$  by  $\epsilon$  and  $\frac{P}{A}$  by the normal

stress  $\sigma$ , we get another expression for Hooke's law:

$$\epsilon = \frac{\sigma}{E} \quad (2.6)$$

or

$$\sigma = \epsilon E \quad (2.7)$$

Thus, the normal stress under tension or compression is directly proportional to the relative elongation or shortening of the bar.

Proportionality factor  $E$ , which links the normal stress with the relative elongation, is called the *modulus of elasticity* of the material under tension (compression). The greater the modulus of elasticity of a material, the less the bar is stretched (compressed) provided all other conditions (length, cross-sectional area, force  $P$ ) remain unchanged. Thus, in physical interpretation, the modulus of elasticity characterizes the resistance of a material to elastic deformation under tension (compression).

Since relative elongation  $\epsilon$  is dimensionless quantity, it follows from formula (2.7) that the modulus of elasticity has the same units as stress  $\sigma$ , i.e. it is expressed in units of force divided by area.

It should be noted that the modulus of elasticity  $E$  does not remain constant even for one material, but varies slightly. In some materials the modulus of elasticity has the same value under tension and compression (steel, copper), in other materials it has different values for each of these deformations. In general this difference is ignored in designing, and for a vast majority of materials a single value of  $E$  is accepted both for tension and compression.

It should be borne in mind that Hooke's law has been represented by a formula which sums up the experimental data only approximately; it cannot therefore be considered an accurate relation.

In all materials the deformation under tension or compression more or less deviates from Hooke's law. In some materials (most of the metals) this deviation is negligible and it may be assumed that there is exact proportionality between deformation and load; in other materials (cast iron, stone, concrete) the deviation is considerably greater.

However, for practical purposes we may ignore the small deviation from formulas (2.5) and (2.6) and use them as such in determining deformation of the bar.

The mean values of the modulus of elasticity  $E$  for a number of materials are given in Table 1.

From formula (2.5) it is evident that the greater its denominator the less is the elongation (pliability) or, in other words, the greater is the rigidity of a bar. Therefore, the denominator of formula (2.5), the quantity  $EA$ , is called the *rigidity of the bar under tension or compression*. We see that the rigidity of a bar under tension or compression depends, on the one hand, upon the material (modulus of elasticity  $E$ ) and, on

Table I

## Modulus of Elasticity and Lateral Deformation Coefficient (Poisson's Ratio)

Material	Modulus of elasticity $E$ ( $10^4$ kgf/cm <sup>2</sup> )	Coefficient of lateral deformation $\mu$
Iron grey, white	1.15-1.60	0.23-0.27
Carbon steel	2.0-2.1	0.24-0.28
Alloy steel	2.1	0.25-0.30
Rolled copper	1.1	0.31-0.34
Rolled phosphor bronze	1.15	0.32-0.35
Cold-drawn brass	0.91-0.99	0.32-0.42
Rolled naval brass	1.0	0.36
Rolled manganese bronze	1.1	0.35
Rolled aluminium	0.69	0.32-0.36
Rolled zinc	0.84	0.27
Lead	0.17	0.42
Glass	0.56	0.25
Granite, limestone, marble	0.42-0.56	
Sandstone	0.18	
Masonry: { from granite from limestone from brick	0.09-0.1 0.06 0.027-0.030	0.16-0.34
Concrete having ultimate strength { 100 kgf/cm 150 kgf/cm 200 kgf/cm	0.146-0.196 0.164-0.214 0.182-0.232	0.16-0.18
Timber along the fibres	0.1-0.12	
Timber across the fibres	0.005-0.01	
Ice * at temperatures { -1°C -3°C -5°C and below	0.04 0.07 0.10	≈0.36
Rubber	0.00008	0.47
Bakelite	0.02-0.03	
Celluloid	0.0174-0.0193	0.39
Textolite	0.06-0.1	
Laminated Bakelite insulation	0.1-0.17	
Rigid polyvinyl chloride (PVC)	0.040	0.22-0.3
Caprolan	0.02-0.023	0.28-0.34
High-pressure polyethylene	0.002-0.0025	0.40-0.46
Phenoplast	0.15-0.20	0.22-0.27
Polycarbonate	0.022-0.024	0.24-0.28
Plexiglas	0.028	

\* SNIP 11-57-75 (SNIP stands for Construction Specifications and Regulations [in the USSR]).

the other hand, upon its cross-sectional area  $A$ . Sometimes it is more convenient to use the term *relative rigidity*  $\frac{EA}{l}$ , i.e. the ratio of rigidity to the length of the bar.

Formulas (2.5) and (2.6) enable us to determine the elongation or shortening in the bar of a structure under tension or compression. Conversely, knowing the elongation, dimensions and the material of the bar one may calculate the normal stresses acting in it. Thus, normal stress can be determined by two methods. If the tensile or compressive force  $P$  is known,  $\sigma$  is calculated from the formula (2.1):

$$\sigma = \frac{P}{A}$$

If the external force is not known but the elongation of the bar can be measured,  $\sigma$  is determined from formula (2.7):

$$\sigma = \varepsilon E$$

The relative elongation may be calculated according to the following formula if the total elongation  $\Delta l$  for a length  $l$  of the bar can be measured:

$$\varepsilon = \frac{\Delta l}{l}$$

We shall show later that the second method has to be employed very often to determine stresses in a number of cases.

## § 9. Lateral Deformation Coefficient. Poisson's Ratio

Apart from longitudinal deformation, the bars working under tension or compression are also subjected to lateral deformation.

Experiments show that under tension (Fig. 8) the length of a bar increases by  $\Delta l$ , whereas its width decreases by  $\Delta b = (b - b_1)$ . The relative elongation

$$\varepsilon = \frac{\Delta l}{l}$$

and the relative lateral deformation

$$\varepsilon_l = \frac{\Delta b}{b}$$

In compression, the shortening of the bar is its longitudinal deformation and the increase in its cross-sectional area is the lateral deformation. It has been experimentally proved that for a majority of the materials  $\varepsilon_l$  is from 3 to 4 times less than  $\varepsilon$ .

The modulus of the ratio of the relative lateral deformation  $\epsilon_1$  to the relative longitudinal deformation  $\epsilon$  is called the *coefficient of lateral deformation*, or *Poisson's ratio*  $\mu$ :

$$\mu = \frac{\epsilon_1}{\epsilon} \quad (2.8)$$

Like the modulus of elasticity  $E$ , Poisson's ratio  $\mu$  is also characteristic of elastic properties of materials. For materials which have identical elastic properties in all directions, these properties can be completely characterized by constants  $E$  and  $\mu$ . Such materials are called *isotropic*. With sufficient accuracy as far as practical application is concerned, we may consider steel and other metals, most of the stones, concrete, rubber and non-laminate plastics as belonging to the group of isotropic materials.

In addition to the isotropic materials, we also have *anisotropic* materials, i.e. materials having dissimilar properties in different directions. To this group of materials belong wood, laminate plastics, some of the stones, cloth, etc. A single value of  $E$  and  $\mu$  cannot characterize their elastic properties; it is essential to have a number of values of these constants in various directions.

For numerical determination of  $\mu$ , it is essential to measure simultaneously the longitudinal and lateral deformation of a bar under tension or compression. Generally, these deformations are measured in stretching a specimen in the form of a long and wide plate (metals), or for a prismatic specimen (stone) under compression.

The values of the coefficient of lateral deformation of various materials are given in Table 1 for deformations within the elastic limits.

Knowing the value of  $\mu$ , we can calculate the change in the volume of the specimen under tension or compression. The length of the deformed specimen is  $l(1+\epsilon)$ . The cross-sectional area of the deformed specimen is  $A(1-\mu\epsilon)^2$ . The volume of the deformed specimen is

$$V_1 = Al(1+\epsilon)(1-\mu\epsilon)^2 = V(1+\epsilon)(1-\mu\epsilon)^2$$

where  $V$  is the initial volume.

Since  $\epsilon$  is a negligibly small quantity up to the limit of proportionality, we may ignore its square. Then volume  $V_1$  becomes

$$V_1 = V[1 + \epsilon(1 - 2\mu)]$$

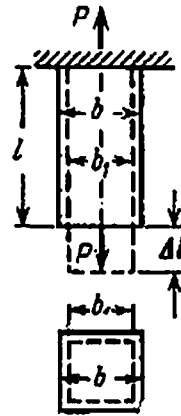


Fig. 8

The relative increase in volume (volume strain) is

$$\frac{V_1 - V}{V} = \epsilon (1 - 2\mu)$$

If Poisson's ratio  $\mu = 0.5$ , there is no change in the volume due to deformation. However, since  $\mu < 0.5$  for a majority of the materials, tension is accompanied by an increase and compression by a decrease in the volume. For rubber  $\mu \approx 0.5$ , therefore there is almost no change in its volume when it is stretched.

The lateral deformation that accompanies the longitudinal deformation has great practical significance. More light will be thrown on this aspect in the succeeding discussion.

Let us consider the following example of applying the methods and formulas derived above.

**Example.** A load of  $Q = 4$  tf is suspended from bracket  $ABC$ , consisting of a wooden rod  $AC$  and an iron pull rod  $AB$  (Fig. 9). Pull rod  $AB$

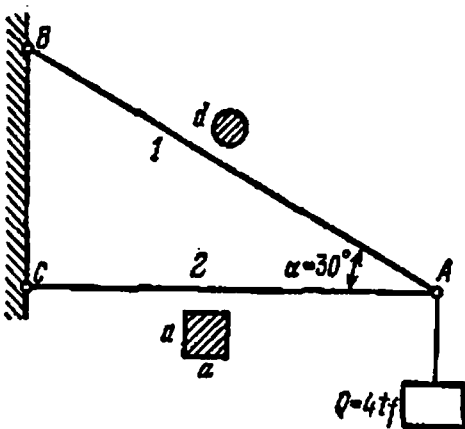


Fig. 9

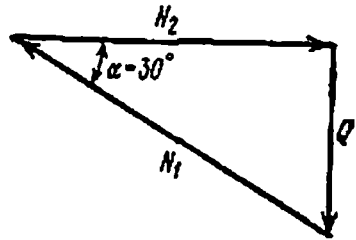


Fig. 10

has a round section and rod  $AC$  a square section. Find diameter  $d$  of rod  $AB$  and sides  $a$  of the square section of rod  $AC$  if the permissible stress for wood is  $|\sigma_-| = 25$  kgf/cm<sup>2</sup>, for steel  $|\sigma_+| = 900$  kgf/cm<sup>2</sup> ( $|\sigma_-|$  is the permissible stress under compression,  $|\sigma_+|$  is the permissible stress under tension); determine the vertical and horizontal displacements of point  $A$ . The length of rod  $AC$  is  $l_2 = 1$  m.

Forces  $N_1$  and  $N_2$  in rods  $AB$  and  $AC$  can be determined from the equilibrium condition of hinge  $A$ , at which the given force  $Q$  and the unknown forces  $N_1$  and  $N_2$  are applied.

By plotting the equilibrium triangle for these forces (Fig. 10), we get

$$N_1 = \frac{Q}{\sin 30^\circ} = 2Q = 8 \text{ tf}$$

$$N_2 = Q \cot 30^\circ = Q\sqrt{3} = 6.93 \text{ tf}$$

The required cross-sectional areas of rods  $AB$  and  $AC$  are

$$A_1 = \frac{N_1}{[\sigma_+]} = \frac{8000}{900} = 8.89 \text{ cm}^2$$

$$A_2 = \frac{N_2}{[\sigma_-]} = \frac{6930}{25} = 277 \text{ cm}^2$$

Diameter of rod  $AB$  is

$$d = \sqrt{\frac{4A_1}{\pi}} = \sqrt{\frac{4 \times 8.89}{\pi}} = 3.34 \text{ cm} \approx 3.4 \text{ cm}$$

Side of the square section of rod  $AC$  is

$$a = \sqrt{A_2} = \sqrt{277} = 16.6 \text{ cm} \approx 17 \text{ cm}$$

Both the values have been rounded—for the steel rod to the nearest mm, and for the wooden rod to the nearest cm.

To determine the displacement  $f$  of point  $A$ , we disconnect the rods and represent them by their new lengths  $BA_1$  and  $CA_2$ , increasing and

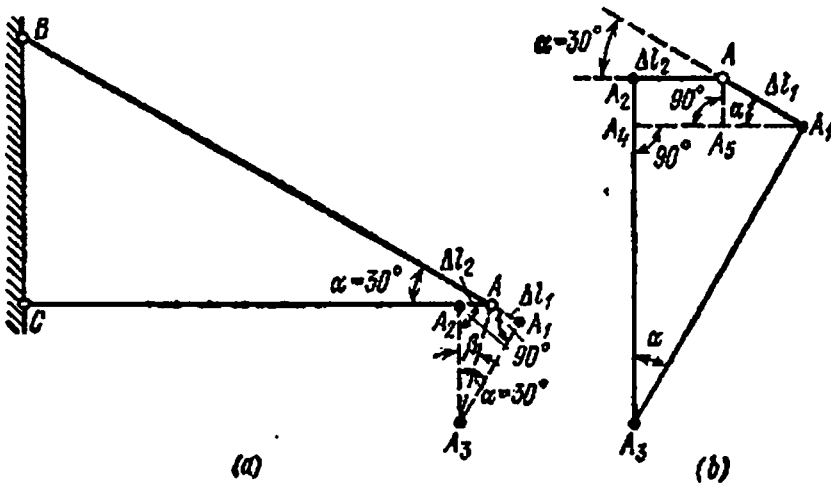


Fig. 11

decreasing their initial lengths by  $\Delta l_1 = AA_1$  and  $\Delta l_2 = AA_2$ , respectively, without changing their direction (Fig. 11(a)). The new position of point  $A$  can be located by bringing together the deformed rods by rotating them about points  $B$  and  $C$ . Points  $A_1$  and  $A_2$  will move along arcs  $A_1A_3$  and  $A_2A_3$ , which due to their small length may be considered as straight lines, perpendicular to  $BA_1$  and  $CA_2$ . The horizontal displacement of point  $A$  will be

$$f_2 = AA_2 = \Delta l_2$$



and the vertical displacement (Fig. 11 (b))

$$f_1 = A_2 A_3 = A_2 A_4 + A_1 A_3$$

The segment

$$A_2 A_4 = A A_3 = \Delta l_1 \sin \alpha$$

and

$$A_1 A_3 = A_1 A_4 \frac{1}{\tan \alpha}$$

But

$$A_1 A_4 = A_1 A_2 + A_3 A_4 = \Delta l_1 \cos \alpha + \Delta l_2$$

Therefore

$$A_1 A_3 = (\Delta l_1 \cos \alpha + \Delta l_2) \frac{1}{\tan \alpha} = \frac{\Delta l_1 \cos^2 \alpha + \Delta l_2 \cos \alpha}{\sin \alpha}$$

Consequently,

$$f_1 = A_2 A_4 + A_1 A_3 = \Delta l_1 \sin \alpha + \frac{\Delta l_1 \cos^2 \alpha + \Delta l_2 \cos \alpha}{\sin \alpha} = \frac{\Delta l_1 + \Delta l_2 \cos \alpha}{\sin \alpha}$$

Deformation of the rods is determined by the formulas

$$\Delta l_2 = \frac{N_2 l_2}{E_2 A_2} = \frac{6930 \times 100}{10^8 \times 17^2} = 2.4 \times 10^{-2} \text{ cm}$$

$$\Delta l_1 = \frac{N_1 l_1}{E_1 A_1} = \frac{8000 \times 100 \times 2}{2 \times 10^8 \times \frac{\pi \times 3.4^2}{4} \times \sqrt{3}} = 5.07 \times 10^{-2} \text{ cm}$$

Hence the horizontal displacement of point  $A$  is  $f_2 = 0.24$  mm, and the vertical displacement is

$$f_1 = \frac{\Delta l_1 + \Delta l_2 \cos \alpha}{\sin \alpha} = \frac{0.507 + 0.24 \times \frac{\sqrt{3}}{2}}{0.5} = 1.43 \text{ mm}$$

Total displacement  $AA_3$  is

$$f = \sqrt{f_1^2 + f_2^2} = \sqrt{1.43^2 + 0.24^2} = 1.45 \text{ mm}$$

## CHAPTER 3

### Experimental Study of Tension and Compression in Various Materials and the Basis of Selecting the Permissible Stresses

#### § 10. Tension Test Diagram.

##### Mechanical Properties of Materials

In the previous chapter, while determining the cross-sectional area and deformation, we came across a number of quantities which characterize a material not only within the limit of proportionality (modulus

of elasticity, limit of proportionality) but also beyond it up to its complete breakdown (ultimate strength). To have a good idea about the mechanical properties of materials under tension or compression, it is essential to study experimentally the phenomena that accompany these processes.

By the difference in their mechanical properties under simple tension or compression at room temperature, the materials may be classified as *brittle* and *ductile*. The brittle materials break down under a very small residual deformation. The failure in case of ductile materials occurs after a considerable residual deformation. Cast iron, stone and concrete, are examples of brittle materials. The low-carbon steels and copper belong to the group of ductile materials.

Let us examine the behaviour of both types of material when subjected to tension till failure. A prismatic specimen of round or rectangular section is prepared. The working portion of the specimen is calibrated in centimetres or fractions of centimetre, to be able to ascertain the change in its length after the experiment. The specimen is placed on the testing machine and its ends are clamped. By straining the specimen axially it is stretched with a load, which increases gradually without shocks or impacts. A number of successive load values are applied, and the corresponding increases in the length  $l$  marked on the specimen are measured.

The experimental results can best be represented in the form of a tension test diagram; a majority of the testing machines have an attachment which automatically plots this diagram when the specimen is stretched. In this diagram, load  $P$  is plotted along the vertical axis and elongation  $\Delta l$  along the horizontal axis.

The tension test diagram for a specimen from ductile material, e.g. low-carbon steel, is of the pattern shown in Fig. 12. The first part of the diagram up to the point  $A$  corresponding to the limit of proportionality is a straight line. Ordinate  $OA_1$  is the value of the tensile force that corresponds to the *limit of proportionality*  $\sigma_p$ , i.e. the maximum stress which, if exceeded, results in deviation from Hooke's law; for low-carbon steel  $\sigma_p$  is approximately equal to 2000 kgf/cm<sup>2</sup>. This stress is determined from formula (2.1) in which the original value of the cross-sectional area  $A$  is used. This stress is known as *conditional stress*. In future, no special mention will be made when the original cross-sectional area is used. The word conditional will also be dropped.

When the tensile force is increased beyond ordinate  $OA_1$ , the deformation starts increasing more rapidly than the force—the diagram takes a curved shape bulging outwards. Then we notice a sharp change in the behaviour of the material; at a certain value of the tensile force  $OC_1$ , the material begins to “flow”. Almost no force is required to further deform the body. A horizontal (or almost horizontal) plateau is obtained on the diagram. The stress at which the material starts to flow, i.e. at which the deformation increases at an almost constant load, is

called the *yield stress*  $\sigma_y$ . For the material under consideration  $\sigma_y$  is approximately equal to 2400 kgf/cm<sup>2</sup>.

During the flow of metal the *Lüder's flow lines* appear on the surface of the material more or less distinctly (Fig. 13). These lines are caused by relative displacement of the material particles when considerable plastic deformation of the specimen takes place.

After the *yielding zone* the material again starts resisting further tensile strain and to elongate it by a length  $\Delta l$  the force should be increased. Point *D* of the diagram corresponds to the maximum load.

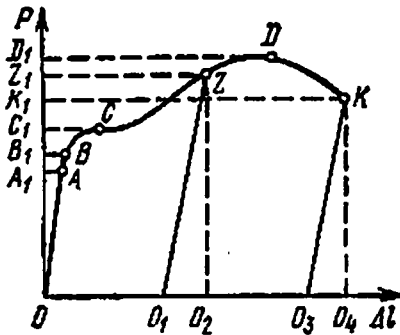


Fig. 12

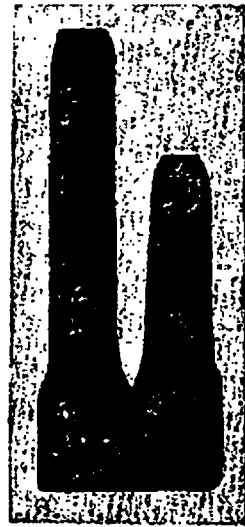


Fig. 13

At this instant there is again a sharp change in the behaviour of the material. Up to this point, the whole bar was being deformed; each unit length of the specimen elongated almost equally. Similarly there was a uniform decrease in the cross-sectional area of the specimen.

From the instant the load achieves the value  $OD_1$ , the deformation gets concentrated in a certain part of the specimen. A small portion of the specimen around this spot is from now on subjected to the maximum stress. This results in a localized reduction of the cross section, and a "neck" is formed (Fig. 14).

As a result of the decrease in the cross-sectional area of the deformed portion, a continuously decreasing load is required to further elongate the specimen. Finally at a load  $OK_1$  the specimen breaks down.

If we stop the experiment at a load less than  $OA_1$  and unload the specimen, then the relation between the force and deformation will be represented by the same straight line as during loading up to  $OA$ . The deformation disappears when the force is removed, implying thereby that the deformation was elastic.

If we start unloading the specimen from a point *Z* on the diagram,

lying between points  $C$  and  $D$ , then unloading will take place along line  $ZO_1$ , which is almost parallel to the line  $OA$ . The specimen in this case will not regain its initial dimensions, segment  $O_1O_2$  will represent the elastic deformation, which, as in the previous case, changes in direct proportion with the load at constant modulus of elasticity. Segment  $OO_1$  will represent the *residual deformation* and segment  $OO_2$  the *total deformation* at a load  $OZ_1$ . We may find a load  $OB_1$  below which only elastic deformations occur. The corresponding point  $B$  on the diagram usually lies a little above but very close to point  $A$ , which represents the limit of proportionality. The stress which if exceeded results in very small (of the order of 0.001-0.03%) residual deformations is called the elastic limit  $\sigma_e$ . On the tension test diagram (Fig. 12) the load causing this stress is represented by the ordinate  $OB_1$ .

Points  $A$  and  $B$  are so close to each other that generally the limit of proportionality and the elastic limit are considered to be the same. Therefore although it is commonly said that a material follows Hooke's law till it reaches the elastic limit, it would be more precise to say till it reaches the limit of proportionality.

The maximum tensile force stretching the specimen is represented by the ordinate  $OD_1$ ; it is commonly referred to as the *crushing load*, because it is essential to apply this load for rupture to begin; the ultimate breakdown occurs at a load represented on the diagram by the ordinate of point  $K$ . The stress caused by the maximum load is called the ultimate strength or ultimate resistance  $\sigma_u$ . The ultimate strength, obtained as a ratio of the maximum load to the initial cross-sectional area of the specimen, characterizes the force required to crush the specimen of the given material under tension; for low-carbon steel it reaches 4000 kgf/cm<sup>2</sup>.

While studying the tension test diagram, we marked on it a number of ordinates representing loads connected with various mechanical properties of the material. Table 2 contains a summary of these loads and their corresponding characteristics (stresses) with their notations. Any of the required stress can be obtained by dividing the corresponding load by the initial cross-sectional area of the specimen.

All the mechanical properties (limit of proportionality and elastic limit, yield stress, and ultimate strength) characterize the ability of a material to resist the tensile forces tending to deform and crush a specimen made from it.



Fig. 14

Table 2

## Mechanical Properties of Materials

Load	Corresponding stress and its notation
Load corresponding to the end of straight line $OA_1$	Limit of proportionality $\sigma_p$
Load corresponding to the beginning of residual deformations $OB_1$	Elastic limit $\sigma_e$
Load corresponding to the flow of the material (increase in deformation at constant load $OC_1$ )	Yield stress $\sigma_y$
Maximum load $OD_1$	Ultimate strength or ultimate resistance $\sigma_u$

The  $x$ -coordinates of the diagram characterize another property of the material, namely, the ability to deform to a certain degree before breaking down.

Segment  $O_3O_1$  (Fig. 12) gives the value of elastic deformation at the time of breakdown, which disappears as soon as the breakdown occurs. Its length  $OO_3 = \Delta l_0$  is the residual deformation of the specimen of length  $l$  after its breakdown. The greater the measured length of the specimen and the greater the pliability of the material, the greater will be this residual deformation.

The ratio of elongation  $\Delta l_0$  to the initial length  $l$  is a *measure of the plasticity* of the material, i.e. its ability to undergo considerable deformations before breaking down.

This ratio expressed in per cents is denoted by  $\delta$  and is called the *residual relative elongation* of the specimen after breakdown and for the commonly used grades of steel varies from 8 to 28%. Thus,

$$\delta = \frac{\Delta l_0}{l} \times 100$$

It must be noted that the residual relative elongation of the specimen depends to a large extent upon its shape and chiefly upon the ratio of its length to its cross-sectional area. Therefore, in laboratory experiments the residual elongation after breakdown is not measured over the full length of the specimen, but only over its certain part called the *reduced length*. In round specimens the reduced length is generally taken equal to  $10d$ ; sometimes it is taken as  $5d$ . In rectangular specimens the reduced length is selected in such a way that the ratio of length and cross-sectional area of a round specimen having the same cross-sectional area  $A$  as the rectangular specimen remains the same. For example, the reduced length of a rectangular specimen corresponding to the length  $10d$  of a round specimen should be  $11.3\sqrt{A}$ . The specimens are prepared

such that the length between the heads somewhat exceeds the estimated length.

The pliability of a material under tension or compression can also be ascertained by another quantity called the *permanent relative reduction* (of area). After the maximum load is reached, a "neck" starts forming in a particular section of the bar, and at the place of failure the cross-sectional area of the specimen is generally less than its initial value (Fig. 14). Let us denote the initial cross-sectional area by  $A_0$ , and the area of the section at which the specimen breaks down by  $A_1$ ; the quantity

$$\psi = \frac{A_0 - A_1}{A_0} \times 100$$

(in per cents) is called the relative reduction after breakdown. The greater is this quantity, the more pliable is the material.

Finally, the tension test diagram shown in Fig. 12 enables us to study one more mechanical property of materials related to their resistance to impact loading.\* The greater is the amount of work required to break the specimen, the higher is its resistance to impact loading. Therefore, the amount of work done in stretching the specimen up to the elastic limit or crushing point may be taken as a characteristic of the resistance of material to suddenly applied loads. This work is represented by the area of the tension test diagram (Fig. 12).

Let us consider the part of the diagram which is within the limits of applicability of Hooke's law (Fig. 15). When the specimen fixed at one end is stretched by applying a gradually increasing force  $P$  at the other end, the displacement of this end is equal to the gradually increasing elongation  $\Delta l = \frac{Pl}{EA}$ ; this relation is expressed by the straight line  $OB$ .

An elongation  $\Delta l$  (segment  $OB_2$  in Fig. 15) corresponds to a particular value of the force  $P$  (segment  $B_1B_2$ ). If we increase the force by  $dP$ , the elongation increases by  $d\Delta l$  and the tensile force having an average value of  $P + \frac{1}{2}dP$  will perform the work

$$dW = \left( P + \frac{1}{2}dP \right) d\Delta l = P d\Delta l + \frac{1}{2} dP d\Delta l$$

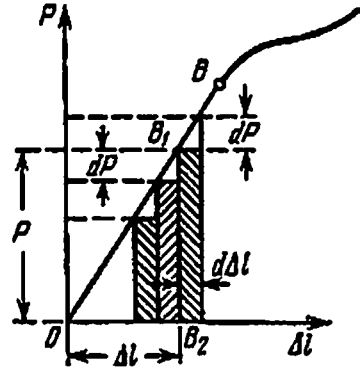


Fig. 15

\* For greater details see § 179.

Neglecting the second-order term  $\frac{1}{2} dP d\Delta l$ , we get

$$dW = P d\Delta l$$

Graphically work  $dW$  is expressed by the area of the shaded rectangle of height  $P$  and base  $d\Delta l$ .

Considering the gradual increase of force  $P$  as a number of successive elementary additions of loads  $dP$ , we find that the work done by the external forces in gradually stretching the specimen is the sum of the areas of the elementary rectangles (Fig. 15). When the load  $P$  is increased continuously, i.e.  $dP$  and  $d\Delta l$  are infinitesimal quantities, for particular values of  $P$  and  $\Delta l$ , this sum may be obtained as the area of triangle  $OB_1B_2$  equal to

$$\frac{1}{2} B_1 B_2 O B_2 = \frac{1}{2} P \Delta l$$

Thus, the work performed in elastic deformation of a bar by  $\Delta l$  may be expressed by the formula

$$W = \frac{1}{2} P \Delta l \quad (3.1)$$

and graphically represented by the corresponding part of the tension test diagram.

The same argument holds good for the whole of the tension test diagram (Fig. 12). The area of the diagram represents the total work  $W$ , expended in breaking a specimen of length  $l$  and cross-sectional area  $A$ .

To obtain the quantity which is a characteristic of a material and not the specimen, we divide work  $W$  by the volume of the specimen. The ratio  $a = \frac{W}{A_0 l}$  is called the *specific work of elastic deformation* under tension.

Similarly, we may determine the *total specific work*  $w_t = \frac{W_t}{A_0 l}$ ; this is the work, required to break the specimen. The greater this quantity, the more reliably the material withstands shock and suddenly applied loads.

We have seen above that the specimen material continues to experience elastic deformation in accordance with Hooke's law even after the yield stress has been passed; in this case are added residual deformations. This is observed while unloading the specimen after loading it beyond the yield stress (point  $Z$  on the tension test diagram in Fig. 12).

If we now start stretching the specimen after unloading it, the loading diagram will be represented by almost the same unloading line  $O_1 Z$  parallel to  $OA$ , and beyond point  $Z$ , by the same curve  $ZDK$  as prior to unloading. Hence, if we compare tension test diagram  $OCZDK$  of a specimen not experiencing unloading with diagram  $O_1 ZDK$  of a

specimen of the same material, which has been preliminarily loaded up to point  $Z$  and then loaded back to point  $O_1$ , we see that the limit of proportionality increases to reach the stress up to which the specimen has been preliminarily loaded, whereas the plastic deformation decreases by  $OO_1$ , i.e. by the residual deformation incurred during preliminary loading.

This increase in the limit of proportionality and decrease in plastic deformation due to preliminary loading beyond yield stress and subsequent unloading is called *cold hardening*. Under cold hardening, corresponding portion of the tension test diagram is, so to say, cut off, resulting in a decrease in the total specific work  $w_t$ . In fact, cold hardening is much more complex than the simple process by which it has been explained here. In particular, if the specimen is allowed to "rest" and reloaded only one-two hours after unloading, the corresponding part  $ZDK$  of the tension test diagram passes a little higher than with the absence of "rest".

## § 11. Stress-strain Diagram

The tension test diagram shown in Fig. 12 illustrates the behaviour of a material for a specimen of the given dimensions; therefore, to get a curve characteristic of the behaviour of the material irrespective of the dimensions of the specimen, the tension test diagram is slightly modified.

The ordinates of the curve in Fig. 12 depicting loads are divided by the initial (before the start of experiment) cross-sectional area of the specimen  $A_0$ , and the abscissas  $\Delta l$  are divided by the estimated length  $l$ . Then in the new diagram we plot along the vertical axis

$$\sigma = \frac{P}{A_0}$$

and along the horizontal axis

$$\epsilon = \frac{\Delta l}{l}$$

Such a diagram, shown in Fig. 16, is called the *stress-strain diagram* for the given material *under tension*. It is similar to the tension test diagram in Fig. 12. In this diagram all the stresses that characterize the mechanical properties of the material are marked: limit of proportionality  $\sigma_p$ , yield stress  $\sigma_y$ , and ultimate strength  $\sigma_u$ .

If we consider a portion of the diagram  $OA$ , up to the limit of proportionality, then for a certain stress  $\sigma$  and its corresponding relative elongation  $\epsilon$ , the area of triangle  $OAB$  (Fig. 17) equal to  $\frac{\sigma\epsilon}{2}$  will represent the specific work in stretching the material to stress  $\sigma$ . We know



that

$$\frac{\sigma e}{2} = \frac{P \Delta l}{2 A l} = w$$

Knowing that  $e = \frac{\sigma}{E}$ , one may write down the expression for specific work of deformation within the elastic limits as follows:

$$w = \frac{\sigma e}{2} = \frac{\sigma^2}{2E} \tag{3.2}$$

By analogy, the total area of the diagram shown in Fig. 16 represents the total specific work  $w_t$  at the moment of breakdown of a specimen of the given material. This quantity may be expressed as the product of

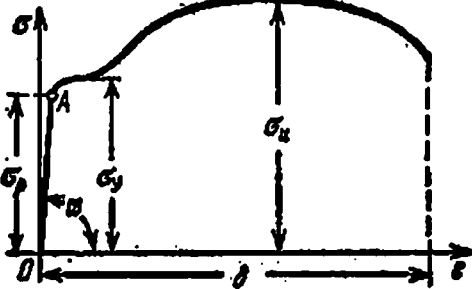


Fig. 16

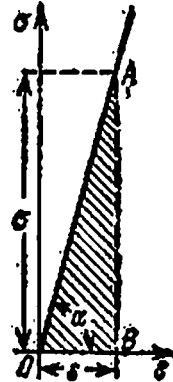


Fig. 17

the length  $\delta$  by the maximum ordinate  $\sigma_u$  and a coefficient  $\eta$  which represents the ratio of the area of the diagram to that of a rectangle having sides  $\delta$  and  $\sigma_u$ :

$$w_t = \eta \sigma_u \delta \tag{3.3}$$

Thus, the total specific work at rupture depends to a certain degree upon the product of the ultimate strength and the strain after the rupture. Therefore, very often, the ability of a material to withstand shocks is judged by the product  $\sigma_u \delta$ .

From the diagram in Fig. 17, it is evident that

$$\tan \alpha = \frac{\sigma}{e} = E$$

Hence, graphically the modulus of elasticity  $E$  is represented by the slope of the straight portion of the diagram.

### § 12. True Stress-strain Diagram

The stress-strain diagram for tension shown in Fig. 16 may be considered as characterizing the properties of the given material under tension.

However, this diagram is only a conditional characteristic of the mechanical properties of the material. In the initial stages of the test, the cross-sectional area of the specimen almost remains constant, but beginning from the yield stress a noticeable reduction takes place, which is initially uniform over the entire length of the specimen, and after crossing the ultimate strength it becomes localized. Therefore, beyond the ultimate strength the ordinates of the curve shown in Fig. 16 represent conditional stresses calculated for the initial cross-sectional area and not the real one.

Similarly, until the ultimate strength is reached the abscissas in Fig. 16 depend only upon the ability of material to elongate. However, once the neck is formed, the relative elongation also becomes dependent upon the dimensions of the specimen (its length and diameter) and thus is no more a characteristic of the material only. Therefore, to obtain a more precise diagram characterizing the properties of the material, the true stress-strain diagram is plotted. It illustrates the relation between stress and strain in the section of rupture.

To plot the true stress-strain diagram it is essential to register the tensile force at various moments and at the same time measure the cross-sectional area of the specimen in the narrowest place.

Let the true stress be denoted by  $\bar{\sigma}$  and the true cross-sectional area in the narrowest section by  $\bar{A}$ , then

$$\bar{\sigma} = \frac{P}{\bar{A}} \quad (3.4)$$

When deformation is large, the original length of the specimen also changes considerably. Consequently, the true elongation  $\bar{e}$  must be related to the actual length of the bar at the given instant of test and may be calculated by the formula

$$\bar{e} = \int_{l_0}^{l_1} \frac{dl}{l} \quad (3.5)$$

where  $l_0$  is the original length of the specimen, and  $l_1$  its length at the time of measurement. When true elongation is large in magnitude, it is denoted by  $\bar{e}$  instead of  $\bar{\epsilon}$ .

Let us establish the relationship between true and conditional strains and true and conditional stresses.

When the specimen deforms uniformly along its length

$$\bar{e} = \int_{l_0}^{l_1} \frac{dl}{l} = \ln l \Big|_{l_0}^{l_1} = \ln l_1 - \ln l_0 = \ln \frac{l_1}{l_0} = \ln \frac{l_0 + \Delta l}{l_0}$$

Finally

$$\bar{e} = \ln(1 + e) \quad (3.6)$$

where

$$e = \frac{\Delta l}{l_0}$$

is the conditional strain.

Formula (3.6) cannot be used in case of non-uniform deformation because it is difficult to measure  $\Delta l$  for computing  $e$ .

It is known that the specimen volume does not change under non-uniform deformation beginning from the moment of neck formation. This is known as the *law of constancy of volume* and may be expressed as

$$A_0 l_0 = \bar{A} l$$

where  $A_0$  is the original cross-sectional area. It ensues that

$$A_0 l_0 = (A_0 - \Delta A) (l_0 + \Delta l)$$

after dividing by  $A_0 l_0$

$$1 = \frac{A_0 - \Delta A}{A_0} \frac{l_0 + \Delta l}{l_0}$$

or

$$(1 - \psi)(1 + e) = 1, \quad \text{where } \psi = \frac{\Delta A}{A_0}$$

wherefrom

$$1 + e = \frac{1}{1 - \psi}$$

Upon substituting the last expression in formula (3.6), we finally obtain

$$\bar{e} = \ln \frac{1}{1 - \psi} \quad (3.7)$$

It should be noted that  $\psi$  is determined in the narrowest part of the neck.

In order to obtain the relationship between true and conditional stresses it should be recalled that

$$P = \sigma A_0 = \bar{\sigma} \bar{A}$$

where  $\sigma$  is conditional stress, i.e. stress related to the original cross-sectional area. Further,

$$\sigma = \bar{\sigma} \frac{\bar{A}}{A_0} = \bar{\sigma} \frac{A_0 - \Delta A}{A_0} = \bar{\sigma} (1 - \psi)$$

and

$$\bar{\sigma} = \sigma \frac{1}{1 - \psi}$$

Considering the relationship between  $\epsilon$  and  $\psi$ , earlier obtained for conditions of uniform deformation, we obtain

$$\bar{\sigma} = \sigma(1 + \epsilon) \tag{3.8}$$

Under conditions of non-uniform deformation, beginning from the moment of neck formation, true stress  $\bar{\sigma}$  is found directly from formula (3.4) as it is meaningless to determine conditional stresses in this state of the specimen because of the large difference between  $\bar{A}$  and  $A_0$ .

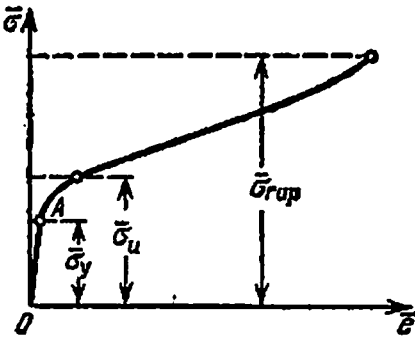


Fig. 18

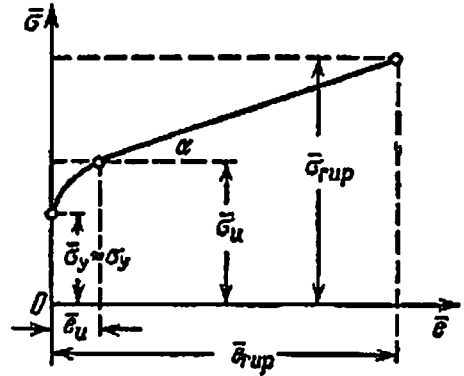


Fig. 19

The true stress-strain diagram is shown in Fig. 18. However, for practical use this diagram is somewhat simplified. It is considered that  $\bar{\sigma}_y \approx \sigma_y$  and a small portion of the curve just preceding rupture is ignored. The diagram is then plotted as shown in Fig. 19.

Yield stress  $\sigma_y = \frac{P_y}{A_0}$ . The true ultimate strength  $\bar{\sigma}_u$  is calculated from the formula (3.8).

The true rupture stress is found from formula (3.4), i.e.

$$\bar{\sigma}_{rup} = \frac{P_{rup}}{\bar{A}}$$

The true uniform elongation is determined from formula (3.6) i.e.  $\bar{\epsilon}_u = \ln(1 + \epsilon)$ , where  $\epsilon$  is the conditional strain at the moment when the neck begins to form.

Finally, the total true rupture strain is found from formula (3.7), where  $\psi$  is computed for the cross section of rupture:

$$\bar{\epsilon}_{rup} = \ln \frac{1}{1 - \psi}$$

It is evident from the diagram of Figs. 18 and 19 that the stress  $\bar{\sigma}$  increases right up to the moment of rupture, rapidly at first but comparatively slowly after the maximum (stress  $\bar{\sigma}_u$ ) is reached. At the

moment of rupture the stress corresponding to the actual cross-sectional area is more than the ultimate strength obtained by the conventional method.

However, it would be erroneous to use the latter value for calculating the maximum load which the bar can withstand before breaking down, which is very important from the practical point of view. This is clear from the tension test diagram in Fig. 12. The maximum load that the specimen withstands corresponds not to the moment of breakdown but to an earlier moment—the magnitude of this load is characterized by the ultimate strength for the specimen of a given cross-sectional area. The actual stress increase in this case is due to the sharp reduction in the working cross-sectional area of the specimen, i.e. due to its rupture.

We may set a number of mechanical properties using the true stress-strain diagram. They were enumerated (marked by italics) when the plotting of true stress-strain tension test diagram was explained.

The ordinates of the true stress-strain diagram show the ability of material to resist plastic deformation.

To increase the plastic (residual) deformation, we must subject the material to a continuously increasing stress; the greater the plastic deformation of the material, the greater is its resistance to such a deformation. This is known as *strengthening*. The ability of a material to strengthening is judged by the steepness of the true stress-strain diagram, i.e. by  $\tan \alpha$ .

The difference of true total and uniform elongation is characteristic of the ability of material to deform locally (at the neck) and is known as *local elongation*.

### § 13. Stress-strain Diagram for Ductile and Brittle Materials

In the preceding sections, we have discussed the physical aspect of the process in which a specimen of ductile material, such as low-carbon steel, is subjected to tension. Stress-strain diagrams similar to the one shown in Fig. 16 are obtained for other ductile materials capable of plastic deformation.

Some (special) grades of steel, copper and bronze do not have the yielding zone. There is a smooth transition of the straight-line portion of the diagram into the curved portion. As an example, the stress-strain diagrams for cast steel (*a*), bronze (*b*), nickel steel (*c*), and manganese steel (*d*) are shown in Fig. 20.

For the materials which do not have a yielding zone, the yield stress is conditionally taken as the stress for which the residual deformation is the same as with a yielding zone. The residual relative elongation in this case is usually taken as 0.2%.

Brittle materials are characterized by the breakdown even at small deformations. When a specimen from a typical brittle material, such

as cast iron, is stretched, inconsiderable deformation is observed right up to the moment of rupture. The specimen breaks down suddenly. The relative elongation and relative reduction in area are found to be

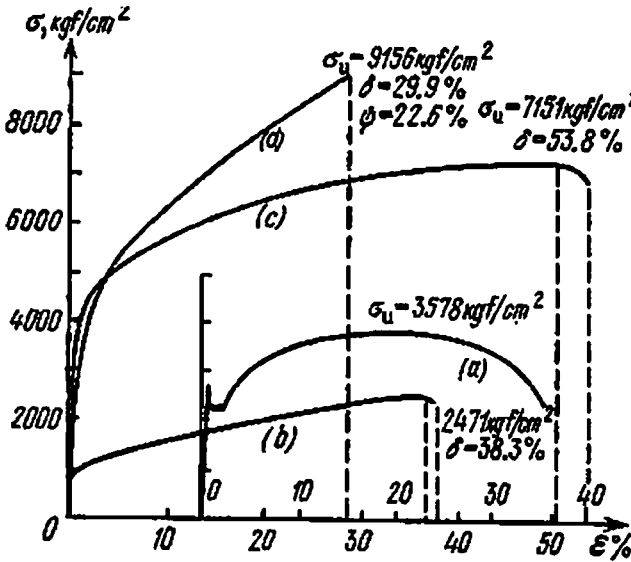


Fig. 20

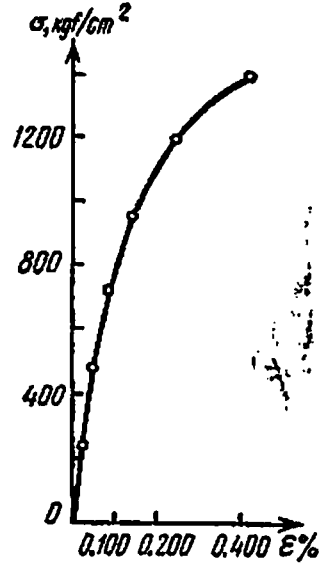


Fig. 21

very small. The stress-strain diagram of cast iron under tension is given in Fig. 21. It should be noted that in Fig. 21 the horizontal scale of the diagram is approximately 40 times more, and the vertical scale is approximately 6 times more than the corresponding scales in Fig. 20.

As a rule, brittle materials have poor resistance to tension; their ultimate strength is less than that of the ductile materials.

The relation between stress and strain when stretching brittle materials does not concur well with Hooke's law; even at low stresses we get a slightly curved line instead of the straight line on the diagram, i.e. a strictly linear proportionality between the force or stress and the corresponding deformation is absent.

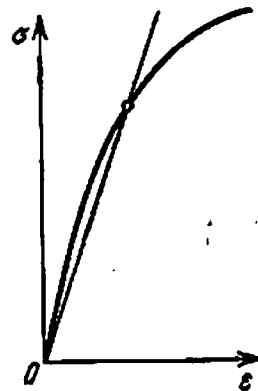


Fig. 22

Therefore, the modulus of elasticity  $E$ , which is equal to the slope of the diagram (see § 11) cannot be considered a constant quantity for brittle materials; it changes depending upon the stress for

which the deformation is to be calculated. As the stress increases, the modulus of elasticity increases or decreases depending upon the direction in which the curve is bulging—upwards or downwards.

However, the deviation from Hooke's law is insignificant for the stress range in which the materials generally function in structures. Therefore, in practice, the curved portion of the diagram (Fig. 22) is replaced by the corresponding chord, and the modulus of elasticity  $E$  is considered constant. This is permissible, the more so because for different specimens the mechanical properties of brittle materials change in a greater range than those of ductile materials; hence, there is no sense in using a very accurate expression for the relation between stress and strain.

#### § 14. Rupture in Compression of Ductile and Brittle Materials. Compression Test Diagram

Specimens in the shape of a cube or a cylinder whose height is just a little more than its diameter are used in studying the strength of materials under compression. In longer specimens it is difficult to avoid bending.

The size of the specimens varies for different materials and fluctuates (for the cube edge) from 2 cm (wood) to 20-30 cm (concrete).

Under compression at stresses below the limit of proportionality or yield stress, a specimen from ductile material behaves as under tension. The limit of proportionality (as also the yield stress for steel) and the modulus of elasticity are almost equal under tension and compression for ductile materials.

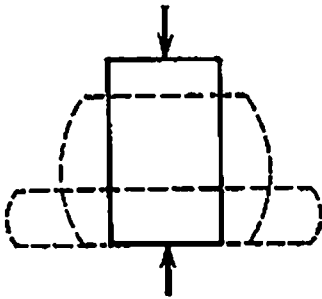


Fig. 23

After passing the limit of proportionality, noticeable residual deformations appear resulting in a shortening of the specimen and an increase in its diameter. The lateral deformations of the specimen at the ends are hindered due to friction between the faces of the specimen and the bearing plates of the press; the specimen acquires the shape of a barrel (Fig. 23).

As the cross-sectional area of the specimen increases, it requires a greater force for further deformation; the specimen continues to compress and ultimately becomes oblate. The stress which may be said to be analogous to ultimate strength in tension is not observed.

A typical stress-strain compression diagram for a ductile material (low-carbon steel) is shown in Fig. 24. As under tension, cold hardening takes place under compression too.

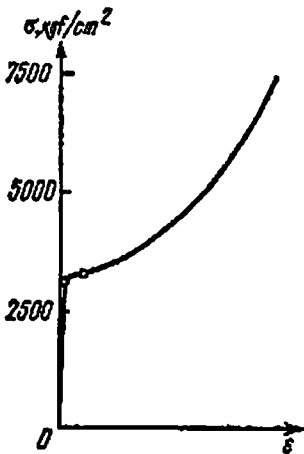


Fig. 24

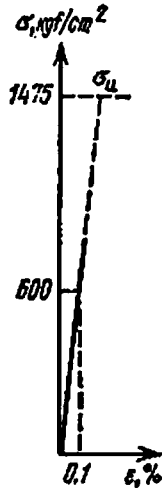


Fig. 25

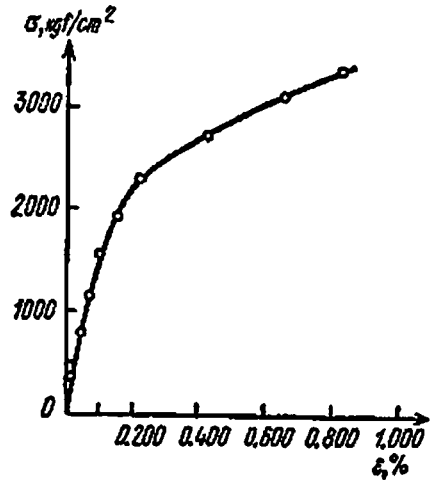


Fig. 26

As under tension, the brittle materials, such as stone, cast iron, and concrete, fail after a small deformation under compression. Figure 25 shows the stress-strain diagram of a stone specimen under compression (a granite cube  $10 \times 10 \times 10$  cm). Figure 26 shows the stress-strain diagram for a cast iron specimen under compression. Here also it

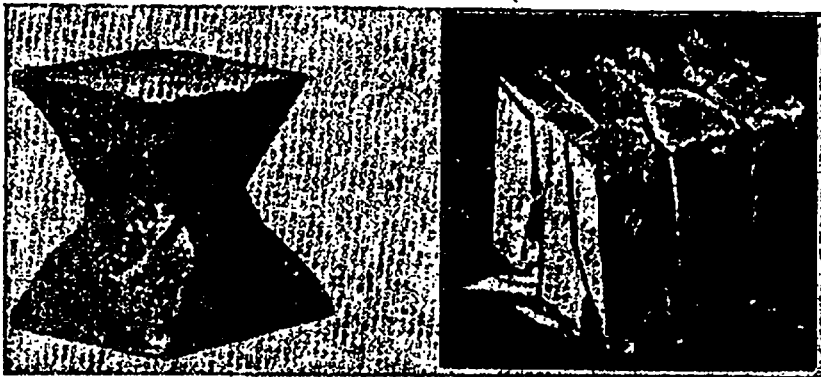


Fig. 27

Fig. 28

should be noted that the scales of diagrams in Figs. 25 and 26, especially the horizontal ones, are much larger than the scale of the diagram in Fig. 24.



The nature of rupture in a stone specimen is shown in Fig. 27; the crushed specimen represents truncated pyramids joined by their smaller bases. This form of rupture is due to the friction force between the specimen and the bearing plates of the press. If we remove this friction, for example, by greasing the specimen faces with paraffin, the nature of rupture will be different: the stone will break into parts with cracks running parallel to the direction of the compressive force (Fig. 28). The crushing load for such a cube will be less than for a cube tested by the common method, without greasing. Therefore, the ultimate strength in compression is to a considerable extent a *conditional*

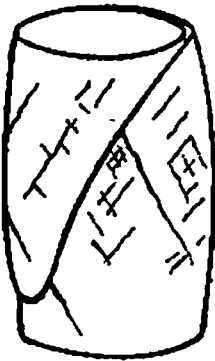


Fig. 29

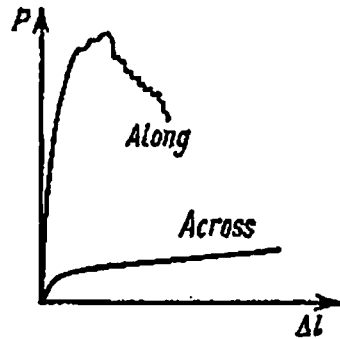


Fig. 30

characteristic of the strength of material. This must be taken into consideration when fixing the safety factor.

It has been observed that when a prismatic specimen made of stone or concrete is compressed slowly, the rupture starts with the appearance of lengthwise cracks parallel to the direction of the force. Therefore, we may say that the material of the specimen under compression ruptures apparently due to the failure of certain portions.

The nature of rupture for cast iron is close to that observed in case of stone. Figure 29 shows a cylindrical cast-iron specimen crushed by axial compression. It must be noted that the resistance of brittle materials to compression is much greater than their resistance to tension.

Compression of a timber specimen gives sharply differing results depending upon the direction of compression with respect to the fibres; timber is an *anisotropic* material, i.e. it has different properties in different directions. The ultimate strength of timber compressed along the fibres is about 10 times more than when it is compressed across the fibres, whereas the deformation is much less. Figure 30 shows the compression test diagram for a timber cube tested along and across the fibres. Table 3 contains data on ultimate strength under tension and compression for most important materials.

normal stress reached. In central axis; through the



section by sum of the

equal portion brought pressed and therefore, the the section.

we see that

lower halves a condition

$$(26.5)$$

presence of

equation of a by determi-

In statically indeterminate beams the formation of one ductile hinge is not enough for full utilization of their bending capacity; it is essential that at least one more ductile hinge be formed. We shall explain this with the help of an example.

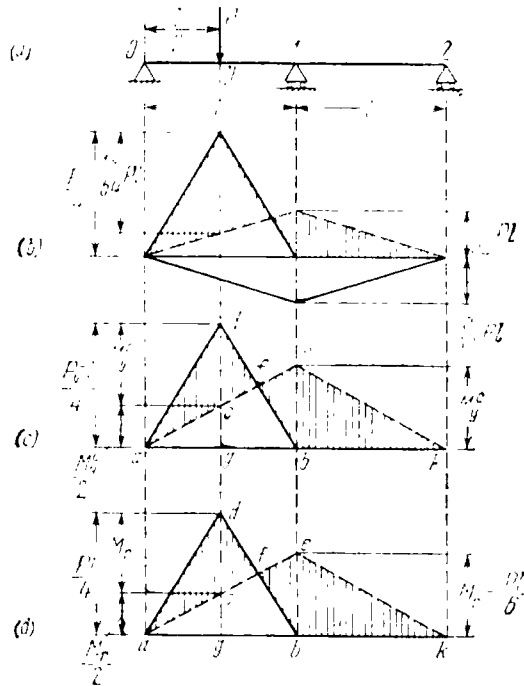


Fig. 377

Let us consider a two-span continuous beam of uniform section (Fig. 377(a)). Its bending moment diagram for work within the elastic limits (Fig. 377(b)) is the difference of the bending moment diagrams for force  $P$  and support moment  $M_1 = \frac{3}{32} Pl$ . Graphic subtraction of the diagrams is shown by dotted lines. The resultant bending moment diagram is hatched. The maximum stressed sections are the section of application of the load with a moment  $M_p = \frac{Pl}{4} - \frac{3}{64} Pl = \frac{13}{64} Pl$  and the middle support with moment  $M_1 = \left| \frac{3}{32} Pl \right| < \frac{13}{64} Pl$ . When the load is increased, stresses in the beam become equal to the yield stress  $\sigma_y$  first of all in the top and bottom layers of the section under load  $P_y$  and may be expressed by the relation

$$\frac{13 P_y l}{64 W} = \sigma_y, \quad \text{wherefrom} \quad P_y = \frac{64 W \sigma_y}{13 l}$$

The amount of work required to crush ductile materials is greater than that required for brittle materials. Therefore, ductile materials are more suitable for structures designed to absorb the maximum possible kinetic energy of impact without failure.

The brittle materials fail easily under impacts just because their specific work of deformation is very small. Due to their small deformation up to stresses close to the ultimate strength, the same brittle materials are sometimes capable of bearing far greater stresses than the ductile materials provided deformation is under the action of a placid, gradually increasing compressive force.

The second distinguishing feature between these materials is that in the initial stages of deformation, the ductile materials may be considered to behave identically under tension and compression. The resistance of an overwhelming majority of the brittle materials to tension is considerably lower than their resistance to compression. This restricts the field of application of brittle materials or requires that special measures be taken to ensure their safe working under tension as, for example, in reinforcement of concrete elements, working under tension, with steel.

A sharp difference is observed in the behaviour of ductile and brittle materials with respect to the so-called *local stresses*, which are distributed over a comparatively small portion of the cross section of the element but the magnitude of which exceeds the average or *nominal* value, calculated from common formulas. Local stresses will be discussed in detail in § 186.

Since we do not observe any considerable deformation in brittle materials almost up to the moment of failure, the non-uniform stress distribution shown above remains unchanged under tension as well as compression right until the ultimate strength is reached. Due to this, a weakened bar of brittle material with local stresses will fail or crack at a much lower value of the *average* normal stress  $\sigma = \frac{P}{A}$  as compared to a similar bar without local stresses. Thus, we may say that local stresses greatly reduce the strength of brittle materials.

The ductile materials are affected by local stresses to a much lower degree. The role of ductility as regards local stresses is to level them to some extent. The mechanism behind this levelling will be discussed in Chapter 31.

We have given a very simplified picture of the working of a bar with a non-uniform distribution of stresses. Actually, levelling out of stresses is hindered not only by strain hardening, but also by the change in the stressed state at the location of stress concentration, its transition from a linear stressed state to a three-dimensional stressed state. This compound stressed state will be discussed later in Chapter 6.

There is one more factor which stipulates the selection of one or the other type of material for practical purposes. Often, while assembling a

structure, it is necessary to bend or to straighten a bent element. Since the brittle materials are capable of withstanding only very small deformations, such operations on them usually give rise to cracks. The ductile materials, capable of taking considerable deformations without rupture, can be bent and straightened without any difficulty.

Thus, brittle materials have poor resistance to tension and impacts, are very sensitive to local stresses and cannot bear change in the shape of elements made from them.

The ductile materials are free from these drawbacks; therefore ductility is one of the most important and desirable property in materials.

The points in favour of brittle materials are that they are usually cheaper and often have a high ultimate strength under compression; this property may be utilized for work under placid loading.

Thus, we see that ductile and brittle materials have exceedingly different and contrasting properties as far as their strength under tension and compression is concerned. However, this difference in properties is only relative. A brittle material may acquire the properties of a ductile material, and vice versa. Both brittleness and ductility depend upon the treatment of the material, stressed state and temperature. Stone, which is conventionally a brittle material under compression, may be made to deform like a ductile material; in some experiments this was achieved by pressing a cylindrical specimen not only at its faces but also on its side surface. On the other hand, mild steel, conventionally a ductile material, may under certain conditions, e.g. low temperature, behave exactly like a brittle material.

Hence the properties "brittleness" and "ductility", which we assign to a material on the basis of compression and tension tests, are related to the materials behaviour only at ordinary temperatures and for the given kinds of deformation. In general, a brittle material may change into a ductile material, and vice versa. Hence it would be more precise to speak not of "brittle" and "ductile" materials but of brittle and plastic states of materials.

It must be noted that a comparatively small increase in the ductility of a brittle material (even up to 2% relative elongation before breakdown) enables its use in a number of cases which are otherwise precluded for brittle materials (in machine parts). Therefore, research work on improving the ductility of brittle materials such as concrete and cast iron demands the maximum possible attention.

## § 16. Considerations in Selection of Safety Factor

A. In the preceding sections, we discussed the methods of computing stresses, determining the mechanical properties of materials under tension and compression, and gave recommendations for selecting one or the other type of materials (ductile or brittle) depending upon the working conditions.

However, the information given till now is not sufficient to find out the permissible stresses suitable for different types of loading. The values of all the mechanical properties of materials (ultimate strength, relative elongation, limit of proportionality, etc.) are obtained from laboratory experiments under static loading, i.e. when the load increases gradually without impacts, shocks and change of sign. Similarly, the formulas correlating normal stress  $\sigma$  with the tensile or compressive force  $P$  have been derived for static loading. It was assumed that the external forces and stresses acting on the cut-off portion of the bar balance each other. In practice, however, we often come across dynamic and systematically changing loads.

As compared to the static load, the suddenly applied load has a two-fold effect; on the one hand, the brittle and ductile materials react differently to the dynamic action of the load and, on the other hand, the stresses are also different. This problem will be discussed in greater details in the chapters on dynamic loading. Here we shall pay attention only to the fact that stresses are generally higher under a dynamic load than under a static load of the same magnitude. This statement is confirmed by experimental results and may also be proved theoretically, as has been done in Part IX.

The ratio of stress  $\sigma_d$  due to dynamic action of the load to stress  $\sigma$  due to static action of the same load is called the *coefficient of dynamic response* and denoted by  $K_d$ :

$$\frac{\sigma_d}{\sigma} = K_d$$

The coefficient of dynamic response depends upon the type of dynamic loading and has a very large value in a number of cases.

**B.** The strength of materials under loads systematically changing their magnitude or magnitude and sign is much different from their strength under static and impact loads.

If, for example, we alternately subject a steel bar to a large number of tensions and compressions, we shall observe that after a definite number of such changes in stresses, the bar in some cases cracks and then ruptures at a stress considerably lower than its ultimate strength. Even for plastic materials the plastic deformation of the specimen before breakdown under similar loading is very small: a brittle fracture takes place.

The failure of materials under a variable load at stresses lower than the ultimate strength is called *fatigue*. This name does not reflect the physical nature of the phenomenon, but it has become such a customary term that it is used to this day.

Experiments show that under alternative tension or compression a decrease in the acting force results in an increase in the number of alterations of this force required to break the specimen. Each material has a maximum normal stress  $\sigma$  at which the specimen can withstand

practically an unlimited number of alterations of the force without breaking down. This stress is denoted by  $\sigma_e$  and is called the *endurance limit* or the *fatigue limit*. The element will not fail until stresses in it do not exceed this limit, irrespective of the number of alterations of the stresses.

Thus, in systematically varying loads, it is essential to specify another mechanical property of the material, namely, endurance limit; it determines the resistance of the material to alternating stresses. The fatigue of materials for various types of loads will be studied in greater detail in Chapter 31.

All that has been stated above must be taken into account when selecting the permissible stresses in tension or compression or, which is the same, when determining the safety factor  $k$  from the formula (see §§ 4 and 7)

$$[\sigma] = \frac{\sigma_n}{k} \quad (3.9)$$

The safety factor should be so selected that the normal stresses acting on the whole section do not exceed the elastic limit (or yield stress) of the material, otherwise the bar will get plastically deformed; under a varying load the normal stresses should not exceed the endurance limit, which is usually lower than the yield stress.

It should be taken into consideration that the stresses are generally higher under impact loading. Since the stresses in this case are also usually determined by assuming the load to be static, the dynamic action of the load must be accounted for by a corresponding increase in the safety factor.

C. As far as the local stresses are concerned (see § 15), it is possible to reconcile to their exceeding the elastic limit or yield stress in the case of ductile materials provided the alternating load is absent. In this case plastic deformation occurs over an extremely small portion of the section and does not affect the working of the construction. Due to plastic deformations the local stresses stop increasing and partially approach the normal stresses in the remaining portion of the section. The brittle materials do not have this property (see § 15): in their case a higher safety factor has to be taken, the more so because their strength under impact loading is lower than that of ductile materials.

Under an alternating load, when we have to reckon with the possibility of developing cracks due to fatigue, it is very essential to take into consideration the local stresses, which seriously affect the selection of safety factor of ductile materials. For the crack due to fatigue to appear, the actual stresses in a particular section must exceed the endurance limit. Since the local stresses are greater than the stresses elsewhere (acting over a larger portion of the section), the chances of the crack appearing are due to namely the local stresses exceeding the endurance limit. As the dimensions of the section are computed from considera-

tions of the maximum general stresses from the formula

$$\sigma_{\max} = \frac{P}{A} \leq [\sigma] = \frac{\sigma_u}{k}$$

the safety factor selected for the general permissible stresses should ensure that the local stresses do not exceed the endurance limit. This requires considerable increase of the safety factor  $k$  as compared to its value under static loading.

In the case of ductile materials, when the endurance limit exceeds the yield stress, the local stresses may be ignored as yielding reduces the possibility of their spreading, playing the role of a buffer.

For brittle materials, which do not have a yield plateau, the danger of fatigue cracks appearing under variable loading is more pronounced, and this requires that the corresponding safety must be increased in comparison with that under static loading.

Thus, since the choice of the safety factor depends upon the properties of the material and the method of applying the external forces, its value is generally greater for brittle materials than for ductile ones; similarly, a higher value of the safety factor has to be taken for dynamic and varying loads as compared to static loads.

**D.** A number of other factors have to be taken into account when selecting the permissible stresses. The magnitudes of forces required for computations are not known exactly; the mechanical properties of materials frequently deviate considerably from their known values; the methods of computation and our knowledge of the interaction between different parts of structures are usually simplified and approximate. The safety factor must cover all these unavoidable inaccuracies of computation and design.

The less the homogeneity of material, the poorer is our knowledge of the forces acting on it, the more simplified is our presentation of the interaction between various elements of the structure, and the greater has to be the safety factor. In operation, machine parts wear out; therefore, in a number of cases a "wear factor" has to be provided for. Similarly corrosion and rotting have to be taken into account in the design of metal and wooden structures.

On the other hand, in certain machines (aeroplanes), the safety factor has to be reduced to the lower possible value to ensure minimum weight.

Hence, proper selection of the permissible stresses is a highly complicated problem, connected with the method of computation, investigation of properties of the material and a large number of other considerations including economic ones. A particular value of the permissible stress determines the consumption of the given material and ways of its use in the structure; this value determines the life of the structure and the field of application of the various materials.

In a large number of structures the standard values of permissible stresses are defined by the standards, and the engineer should only be

able to properly apply them. However, in exceptional cases, say, for example, during war time, the engineer has to abandon the standard values; he may then follow the general considerations, laid down in this section and in Chapter 31.

E. Summing up all that has been stated above, we may formulate the following main points.

The safety factor should be selected in a way so as to provide a definite reserve against the appearance of the so-called *critical state of the material*, which may endanger the working of the machine.

Under static or impact dynamic loading, this state is characterized in ductile materials by the appearance of large plastic deformations (yielding), and in brittle materials by the appearance of cracks preceding ultimate failure. Under repeatedly varying loads the critical state of material is characterized by the appearance and development of fatigue cracks. We shall denote the stress corresponding to the start of critical state by  $\sigma^0$ . This stress is

$$\sigma^0 = \begin{cases} \sigma_y & \text{(yield stress) when the ductile material} \\ & \text{begins to yield} \\ \sigma_u & \text{(ultimate strength) when the brittle} \\ & \text{material ruptures (cracks)} \\ \sigma_e & \text{(endurance limit) when the fatigue} \\ & \text{crack appears} \end{cases}$$

Hence, formula (3.9) may now be written more precisely and replaced by the three formulas depending upon the nature of critical state:

$$[\sigma] = \frac{\sigma_y}{k_y}; \quad [\sigma] = \frac{\sigma_u}{k_u}; \quad [\sigma] = \frac{\sigma_e}{k_e} \quad (3.10)$$

where  $k_y$ ,  $k_u$  and  $k_e$  are the corresponding safety factors. The three formulas may be generalised in the form

$$[\sigma] = \frac{\sigma^0}{k}$$

Here  $\sigma^0$  implies either  $\sigma_y$ , or  $\sigma_u$ , or  $\sigma_e$ , and  $k$  implies either  $k_y$ , or  $k_u$ , or  $k_e$ .

However, formula (3.9) still retains its practical importance. As the yield stress and endurance limit are to a certain extent related to the ultimate strength, the safety factor for all the critical states may be expressed in terms of the ultimate strength.

These in general are the basis considerations essential for properly evaluating the permissible stresses.

F. Passing over to the considerations in assigning the value of the safety factor, we shall give some very brief instructions. The non-homogeneity of the material, inaccuracy in force determination, error of computation, i.e. the common factors are accounted for by the main



safety factor  $k_0$ . For ductile materials (steel) it is taken as  $k_y = k_0 = 1.4-1.6$ , for brittle materials and wood  $k_u = k_0 = 2.5-3$ . Other factors, such as the dynamic nature of the forces, alteration of their action and the effect of local stresses are taken accounted for by additional coefficients, by which the main safety factor is multiplied.

It should be borne in mind that the permissible stress  $[\sigma]$  obtained according to formula (3.9) should be compared to the actual stresses in the part of the structure without considering the dynamic action of the force and other additional factors.

If only the general points are considered while assigning the safety factor, i.e. the overall safety factor is taken equal to the main safety factor, the dynamic action of forces and the local stresses are taken account of, as far as possible, in the value of the actual stress, multiplying the main stress under static loading by the coefficients of dynamic loading and stress concentrations. It is not difficult to see that the results in both the cases will be identical.

Table 4 contains approximate values of the overall safety factor with respect to the ultimate strength for various types of materials and loads including the factors accounting for the dynamic nature of loading and local stresses.

Table 4

## Safety Factors

Loading	Type of material	$k_u$
Static load	{ Ductile	2.4-2.6
	{ Brittle	3.0-9.0
Impact load	Ductile	2.8-5.0
Varying load (tension and compression of equal magnitude)	Ductile (steel)	5.0-15.0

The table is only of a tentative nature; it gives an idea about the change in the safety factor depending upon circumstances. Numerous aspects affecting the safety factor under impact and alternating loads will be discussed in greater details in Chapters 30 and 31.

### § 17. Permissible Stresses Under Tension and Compression for Various Materials

In the preceding section we tried to elucidate the numerous factors which affect the safety factor and consequently the value of permissible stress. In Table 5 are given the tentative values of permissible stresses under tension and compression for some important materials used in engineering and machine building. The table has been compiled on the basis of present Soviet standards.

Table 5

**Tentative Values of the Permissible Stresses for Some Commonly Used Materials**

Material	Permissible stress (kgf/cm <sup>2</sup> )	
	Under tension	Under compression
Gray cast iron	280-800	1200-1500
Low-carbon steel	1600-2000	—
Structural carbon steel used in machine building	600-2500	
Structural alloy steel used in machine building	1000-4000 and higher	
Copper	300-1200	
Brass	700-1400	
Bronze	600-1200	
Aluminium	300-800	
Aluminium bronze	800-1200	
Duraluminium	800-1500	
Textolite	300-400	
Laminated Bakelite insulation	500-700	
Bakelite impregnated veneer	400-500	
Pine along the fibres	70-100	100-120
Pine across the fibres	—	15-20
Oak along the fibres	90-130	130-150
Oak across the fibres	—	20-35
Stonework	up to 3	4-40
Brickwork	up to 2	6-25
Concrete	1-7	10-90

The materials enumerated in the Table 5 must satisfy the requirements and norms (of strength, ductility, production process, chemical composition, etc.) of the corresponding standards. It does not cover all materials, nor the diverse conditions in which they work. In each design problem the permissible stresses should be specified in accordance with the official technical specifications and design standards for the given structure, and, in their absence, on the basis of factors discussed in the preceding section.

# PART II

## Complicated Cases of Tension and Compression

### CHAPTER 4

## Design of Statically Indeterminate Systems for Permissible Stresses

### § 18. Statically Indeterminate Systems

Our ability to calculate the deformation of bars under tension and compression enables us to determine the changes in the shape and size of parts of structures under the action of external forces. Usually these deformations are so small that they seem devoid of any practical importance.

However, in a number of structures, it is impossible to check the strength and determine the cross-sectional area of the various elements without the knowledge of deformation; these structures are known as *statically indeterminate systems*; finding the forces acting in the elements of these structures in a *statically indeterminate problem*.

In all the examples which we have considered till now, the tensile or compressive forces acting on the bar were determined from static conditions of a solid body.

In case of weight  $Q$  suspended from two bars (Fig. 31),  $AB$  and  $AC$ , we find tensile forces  $N_1$  and  $N_2$  stretching the bars from the equilibrium conditions of point  $A$ . Three forces applied to point  $A$  must satisfy two equations of equilibrium: the sum of the projections of these forces on the two coordinate axes must be zero. Thus, we see that the number of unknown quantities (two) is equal to the number of equations (two), therefore forces  $N_1$  and  $N_2$  may be determined from these equations. This is statically determinate problem.

The conditions will be different if weight  $Q$  is suspended from three bars (Fig. 32). In this case point  $A$  is in equilibrium under the action of four forces:  $Q$ ,  $N_1$ ,  $N_2$ , and  $N_3$ , three of the forces being unknown. The number of equations remains the same, i.e. two. Hence, the number of unknown quantities exceeds by one the number of equations, the structure is one degree indeterminate, and the problem cannot be solved with the help of static equations only.

The additional equation required for the solution of the problem can be compiled using the ideas gained in passing over from the theoretical mechanics to the strength of materials. We must take account for the deformability of material. One more equation can be found in studying the deformations of the structure. It turns out that it is always possible to find as many additional equations as is required to complete the number of static equations so that the number of equations be equal to the number of unknown quantities.

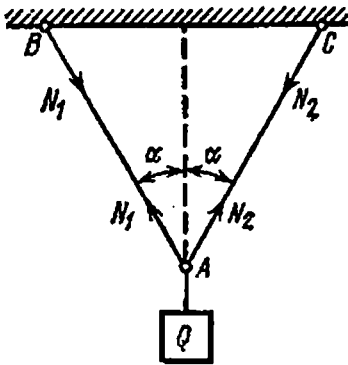


Fig. 31

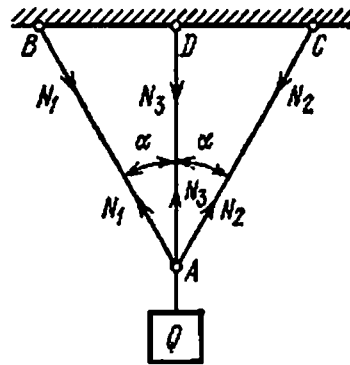


Fig. 32

The extra equations are formed on the basis of the common principle; they should express the *conditions of joint deformations* of the system.

Any structure deforms in such a way that there are no ruptures of the bars, their disconnection or any unforeseen relative displacement of one part of the structure with respect to the other. This in brief is the *principle of joint deformation* of the elements of a system.

The general method of solving statically indeterminate systems is as follows. First of all we must decide what are the forces to be determined, then write down all the static equations of a solid body, and finally derive the required number of extra equations to find the unknown forces.

A course of the solution of the problem is shown for the particular example (Fig. 32). Suppose the side bars of equal cross-sectional areas are made of steel, whereas the middle bar is made of copper. The length of the middle bar is  $l_3$  and that of the side bars,  $l_1$ . Suppose the permissible stress for steel is  $[\sigma_s]$  and for copper  $[\sigma_c]$ . It is required to determine the safe dimensions of the cross sections of these bars under the action of suspended weight  $Q$ .

First of all we shall determine the forces acting on each of the three bars. Since there are hinges at points  $A$ ,  $B$ ,  $C$  and  $D$ , all the three bars can be subjected to only axial forces. Let us consider these forces to be tensile. In order to determine these forces, we must consider the equilibrium of point  $A$  to which the only known force  $Q$  is applied. A scheme of the forces acting on point  $A$  and the location of coordinate

axes are given in Fig. 33. Let us equate to zero the sum of projections of the forces acting on point  $A$  on the coordinate axes:

$$\begin{aligned} N_2 \sin \alpha - N_1 \sin \alpha &= 0 \\ Q - N_3 - N_1 \cos \alpha - N_2 \cos \alpha &= 0 \end{aligned}$$

From the first equation we get  $N_1 = N_2$ ; replacing  $N_2$  by  $N_1$  in the second equation, we obtain

$$N_3 + 2N_1 \cos \alpha = Q \quad (4.1)$$

Now we have one equation with two unknowns.

To obtain the extra equation we must study the deformation of the structure. All the three bars will elongate under the action of force  $Q$ , and point  $A$  will descend. Since  $N_1$  and  $N_2$  are equal and bars 1 and 2

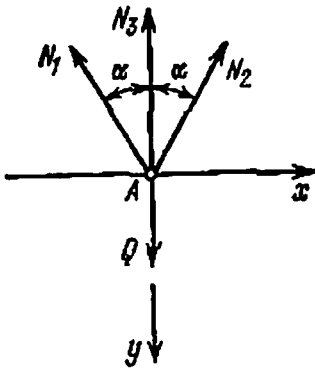


Fig. 33

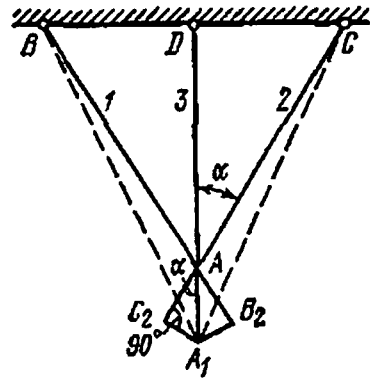


Fig. 34

are of the same material, elongations  $\Delta l_1$  and  $\Delta l_2$  will be equal if the bars are of equal length, point  $A$  will descend vertically downwards. Let us denote the elongation of the third bar by  $\Delta l_3$ .

The elongation of all the three bars is joined, i.e. the bars remain hinged at point  $A$  after deformation. To find the new position of this point, we assume the bars to be disconnected and plot on the diagram (Fig. 34) the new lengths of the side bars  $CC_2$  and  $BB_2$  by increasing their initial lengths by  $\Delta l_1 = AB_2$  and  $\Delta l_2 = AC_2$ . The new position of point  $A$  is obtained by rotating the elongated bars  $CC_2$  and  $BB_2$  about points  $B$  and  $C$ . Points  $B_2$  and  $C_2$  will coincide at point  $A_1$ , moving along the arcs  $C_2A_1$  and  $B_2A_1$  which due to the small deformation may be considered as straight lines perpendicular to  $CC_2$  and  $BB_2$ , respectively.

The new position of the side bars  $BA_1$  and  $CA_1$  is shown by dotted lines. Since the end of the middle bar is also fastened to the hinge, it will also come to point  $A_1$ , and elongation  $\Delta l_3$  will be equal to  $AA_1$ .

According to Hooke's law, the elongations  $\Delta l_1$ ,  $\Delta l_2$ , and  $\Delta l_3$  of all the three bars will be directly proportional to the tensile forces stret-

ching them. After finding the relation between these elongations from the figure, we shall obtain the extra equation correlating the unknown forces in the bars. From triangle  $A_1AB_2$ , we have

$$AB_2 = AA_1 \cos \alpha \quad \text{or} \quad \Delta l_1 = \Delta l_2 \cos \alpha \quad (4.2)$$

Let us express  $\Delta l_1$  and  $\Delta l_2$  in terms of the forces  $N_1$  and  $N_2$ . This is possible only if we know the cross-sectional area of the bars. Here we must state a very important feature of the statically indeterminate systems: to determine the forces acting in bars we must know beforehand either the cross-sectional area of these bars or their ratio.

Let  $A_1$  and  $A_2$  be the cross-sectional areas of the bars; let us denote the modulus of elasticity of steel by  $E_s$  and that of copper by  $E_c$ . Then

$$\Delta l_1 = \frac{N_1 l_1}{E_s A_1}; \quad \Delta l_2 = \frac{N_2 l_2}{E_c A_2} \quad (4.3)$$

Putting these values of  $\Delta l_1$  and  $\Delta l_2$  in equation (4.2), we get

$$\frac{N_1 l_1}{E_s A_1} = \frac{N_2 l_2}{E_c A_2} \cos \alpha$$

It is evident from triangle  $ABD$  (Fig. 34) that

$$l_2 = l_1 \cos \alpha$$

Therefore,

$$N_1 = N_2 \frac{E_s A_1}{E_c A_2} \cos^2 \alpha \quad (4.4)$$

Thus, by examining the joint deformation of the system, we have obtained an extra equation correlating  $N_1$  and  $N_2$ .

Joint deformation takes place in statically determinate structures too, but there it does not impose any constraints on force distribution. Only one system of forces satisfying the equilibrium conditions is possible in this case. Since the number of unknowns is equal to the number of static equations in such structures, the deformation is compatible with the conditions of joint deformation. For example, the forces acting in the bars can be fully determined from the equilibrium conditions of point  $A$ . Both the bars may elongate under the action of these forces without getting disconnected, and the condition of joint deformation is automatically fulfilled.

On the contrary, in statically indeterminate structures, there can be any number of force systems satisfying the equilibrium conditions, because the number of unknowns is greater than the number of equations. From all the possible combinations of forces, the combination which actually occurs is the one that corresponds to the condition of joint deformation.

In the statically indeterminate system (Fig. 32), the location of point *A* after deformation combines the elongations of all the three bars. For the condition of joint deformation to be satisfied it is essential that the elongations should be in a definite ratio. This condition gives us the extra equation (4.4) required for determining the unknown force.

Continuing the solution of the problem we put the value of  $N_1$  from (4.4) into Eq. (4.1) and obtain

$$N_3 + 2N_3 \frac{E_s A_1}{E_c A_3} \cos^3 \alpha = Q$$

whence from

$$N_3 = \frac{Q}{1 + 2 \frac{E_s A_1}{E_c A_3} \cos^3 \alpha} \quad (4.5)$$

and from (4.4)

$$N_1 = \frac{Q \frac{E_s A_1}{E_c A_2} \cos^2 \alpha}{1 + 2 \frac{E_s A_1}{E_c A_3} \cos^3 \alpha} = N_2 \quad (4.6)$$

It is evident from the formulas obtained that the value of  $N$  depends not upon the absolute values of the cross-sectional areas  $A$  and moduli of elasticity  $E$ , but upon their ratio. By setting different values of the ratio  $n = \frac{A_1}{A_2}$  we obtain various combinations of the forces  $N_1$ ,  $N_2$ , and  $N_3$ .

Knowing the forces and the permissible stress we can find  $A_1$  and  $A_3$  from the conditions

$$\frac{N_1}{A_1} \leq [\sigma_s]; \quad \frac{N_3}{A_3} \leq [\sigma_c] \quad (4.7)$$

Calculating  $A_1$  from the first condition and knowing the selected ratio  $n = \frac{A_1}{A_2}$ , we can find  $A_2 = \frac{A_1}{n}$ . This value can be checked up by seeing whether it satisfies the second condition of (4.7); if not, the value of  $A_2$  is found from this condition, and  $A_1$  is determined by the formula

$$A_1 = n A_2 \quad (4.8)$$

Thus, in a statically indeterminate structure with a given load we may obtain a number of different modifications of force distribution between the bars by changing the ratio of their cross-sectional areas. Let us take a numerical example for greater clarification.

Let  $Q=4$  tf;  $\alpha=30^\circ$ ;  $[\sigma_s]=1000$  kgf/cm<sup>2</sup>;  $E_s=2 \times 10^6$  kgf/cm<sup>2</sup>,  $[\sigma_c]=600$  kgf/cm<sup>2</sup>;  $E_c=1 \times 10^6$  kgf/cm<sup>2</sup>.

For preliminary calculation let us assume an arbitrary value of

$$n = \frac{A_1}{A_3} = 1$$

Then

$$N_1 = N_2 = \frac{4 \times \frac{2 \times 10^6}{1 \times 10^6} \cos^2 30^\circ}{1 + 2 \times \frac{2 \times 10^6}{1 \times 10^6} \cos^2 30^\circ} = 1.67 \text{ tf}$$

$$N_3 = \frac{4}{1 + 2 \times \frac{2 \times 10^6}{1 \times 10^6} \cos^2 30^\circ} = 1.11 \text{ tf}$$

From strength condition we obtain

$$A_1 = \frac{N_1}{[\sigma_s]} = \frac{1670}{1000} = 1.67 \text{ cm}^2$$

As we have assumed  $A_1 = A_3$ , then  $A_3 = 1.67 \text{ cm}^2$

Let us check whether these dimensions will satisfy the strength condition for the middle bar:

$$\frac{N_3}{A_3} = \frac{1110}{1.67} = 667 \text{ kgf/cm}^2 > 600 \text{ kgf/cm}^2$$

The assumed value of  $A_3$  is not enough; it should be

$$A_3 = \frac{N_3}{[\sigma_c]} = \frac{1100}{600} = 1.85 \text{ cm}^2$$

To maintain the condition  $A_1 = A_3$  which formed the basis of our calculation, we must take  $A_1 = A_3 = 1.85 \text{ cm}^2$  instead of the required value of  $1.67 \text{ cm}^2$  obtained from the first condition. In this way we shall have an additional reserve in the side bars.

If we wish to avoid this extra reserve and take

$$A_1 = A_2 = 1.67 \text{ cm}^2, \quad A_3 = 1.83 \text{ cm}^2 \quad (4.9)$$

then forces  $N_1$ ,  $N_2$ , and  $N_3$  will change immediately; the ratio  $A_1/A_3$  will no longer equal 1, as assumed earlier, but will be 0.9. In formula (4.5) the denominator becomes less and  $N_3$  increases; in formula (4.6) the decrease in the value of the denominator will be less as compared to the numerator, therefore  $N_1$  and  $N_2$  will decrease.

By decreasing the cross-sectional area of the side bars as compared to that of the middle bar, we reduce the forces acting on the side bars and increase the forces acting on the middle bar.

This reflects the general law which governs the force distribution between the elements of all statically indeterminate systems: the forces are distributed in accordance with the rigidity of the bars; the



greater the cross-sectional area of a given bar, the greater is the share of total force that it takes, and vice versa.

If we approximate the areas  $A_1$  and  $A_2$  to zero, then forces  $N_1$  and  $N_2$  will tend to zero and  $N_3$  to  $Q$ . If, on the other hand, we decrease  $A_3$ , then  $N_3$  will decrease, whereas  $N_1$  and  $N_2$  will increase.

For a value of  $n=0.9$  [formula (4.8)],  $N_1=N_2=1.60$  tf,  $N_3=1.20$  tf. This requires  $A_3=2.0$  cm<sup>2</sup> and  $A_1=1.8$  cm<sup>2</sup> instead of 1.6 cm<sup>2</sup> as found from the strength condition for steel bars.

Had we assumed  $A_1=1.6$  cm<sup>2</sup> for the side bars, the ratio  $n$  would have been reduced again, and the middle bar would have again got overloaded. Thus we should again be reconciled with the reserve in side bars. From formula (4.4) it follows that a particular ratio,  $n = \frac{A_1}{A_3}$ , which ensures that the stresses in all the bars are equal to the permissible stresses, is possible only for a definite value of the angle  $\alpha$ . Indeed, had we determined the areas  $A$  exactly in accordance with the permissible stresses, we would have got the relations

$$N_1 = A_1 [\sigma_s], \quad N_3 = A_3 [\sigma_c] \quad (4.10)$$

Putting these values in (4.4), we get

$$A_1 [\sigma_s] = A_3 [\sigma_c] \frac{E_s A_1}{E_c A_3} \cos^2 \alpha \quad (4.11)$$

wherefrom we have

$$\cos^2 \alpha = \frac{[\sigma_s]}{[\sigma_c]} \frac{E_c}{E_s} \quad (4.12)$$

i.e. in order to select the cross-sectional area without excessive reserve for any value of the ratio  $n$  it is essential that  $\cos \alpha$  should satisfy condition (4.12).

Table 6

Results of Calculations for Various Values of  $n$

$n = \frac{A_1}{A_3}$	$N_1 = N_2$ (tf)	$N_3$ (tf)	$A_1 = A_2$ (cm <sup>2</sup> )		$A_3$ (cm <sup>2</sup> )
			required	assumed	
0.8	1.56	1.30	1.56	1.74	2.17
0.9	1.60	1.20	1.60	1.80	2.00
1.0	1.67	1.11	1.67	1.85	1.85
1.2	1.75	0.97	1.75	1.94	1.62
1.5	1.83	0.82	1.83	2.06	1.37

In our numerical example we obtain

$$\cos^2 \alpha = \frac{1000 \times 1 \times 10^6}{600 \times 2 \times 10^6}, \quad \text{hence} \quad \alpha = 24^\circ$$

Since in the given structure  $\alpha = 30^\circ$ , then for an arbitrary  $n$  we shall either have to give excess reserve in one group of bars, or overload the other group. The value of  $n$  itself should be selected from economic considerations. Table 6 contains the values of different quantities for various values of  $n$ . Knowing the cross-sectional areas, lengths and materials of the bars, we can select a combination which is economically most effective as far as the cost of material is concerned.

### § 19. The Effect of Manufacturing Inaccuracies on the Forces Acting in the Elements of Statically Indeterminate Structures

In the preceding sections we established the main features of the working and design of statically indeterminate systems.

1. The extra equations required to calculate the forces may be obtained only from the condition of joint deformation of the system.

2. The force distribution between the elements of statically indeterminate structures depends upon the ratio of their cross-sectional areas, moduli of elasticity and lengths.

3. The more rigid an element, i.e. the smaller its length and the greater its cross-sectional area and modulus of elasticity, the greater will be the share of force that it will take.

In this section we shall study another property of statically indeterminate structures which is of great practical importance.

It is impossible to manufacture parts of structures with absolute accuracy; small manufacturing errors and inaccuracies must always be taken into account. In a statically determinate structure, these inaccuracies cannot give rise to stresses in the system. Thus, for example, if bar  $AB$  (Fig. 31) is made a little shorter than it should be according to the drawing, all that will happen is a slight distortion of triangle  $CAB$ . In the absence of force  $Q$  the forces in bars  $AB$  and  $AC$  will be equal to zero irrespective of the manufacturing accuracy of the bar length.

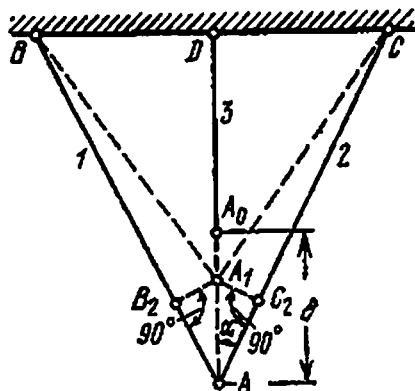


Fig. 35

The statically indeterminate structure shown in Fig. 32 will behave in an entirely different manner. Let the manufactured length of the bar be less than the required by  $AA_0 = \delta$  (Fig. 35). To join the end of the middle bar  $A_0$  with the ends  $A$  of the side bars somewhere at point  $A_1$ , it is necessary to stretch the middle bar by  $\Delta l_1 = A_0A_1$ , and to compress the side bars by  $\Delta l_2 = AB_2 = AC_2$ . Drawing through points  $C_2$  and  $B_2$  perpendiculars to the initial positions of the side bars as explained in § 18, we get the point of junction  $A_1$  of the ends of all the three bars. From the figure we may write down the condition of joint deformation:

$$A_0A = A_0A_1 + A_1A$$

or

$$\delta = \Delta l_1 + \frac{\Delta l_2}{\cos \alpha} \quad (4.13)$$

Since there are no external forces and  $N_1$  is a compressive force whereas  $N_2$  is tensile, the equilibrium condition (4.1) takes the form

$$N_2 - 2N_1 \cos \alpha = 0 \quad (4.14)$$

Replacing in (4.13)  $\Delta l_1$  and  $\Delta l_2$  by their values

$$\Delta l_1 = \frac{N_1 l_1}{E_s A_1} \quad \text{and} \quad \Delta l_2 = \frac{N_2 l_2}{E_c A_2} = \frac{N_2 l_1 \cos \alpha}{E_c A_2}$$

and solving equations (4.13) and (4.14), we have

$$N_2 = \frac{\delta E_c A_2}{l_2 \left[ 1 + \frac{E_c A_2}{2E_s A_1 \cos^2 \alpha} \right]}, \quad N_1 = \frac{N_2}{2 \cos \alpha} \quad (4.15)$$

The plus sign before the values of  $N_1$  and  $N_2$  signifies that our assumptions about the directions of these forces are correct.

It should be pointed out that in formula (4.3) the length of the middle bar can be replaced by  $l_1$  and not by  $l_1 - \delta$ , because  $\delta$  is an infinitesimal as compared to  $l_1$ . This simplification can always be applied when the manufacturing inaccuracies are being considered.

The above computations reveal that the manufacturing inaccuracies will give rise to stresses in the bars even if there are no external forces acting on the structure. Hence, the possibility of the so-called initial stresses is also an important property of the statically indeterminate structures.

If all the three bars are of the same material and have the same cross-sectional area, then under weight  $Q$  (Fig. 32) the tensile force in the middle bar will be greater than in the side bars (4.4). The manufacturing inaccuracy gives rise to an additional tensile force in the middle bar and to compressive forces in the side bars. In this particular example

the initial stresses increase the non-uniformity in the working of the bars and are therefore harmful.

Had the middle bar been longer by  $\delta$ , the initial stresses would have had opposite signs and would have levelled off to some extent the non-uniformity in force distribution between the middle and the side bars

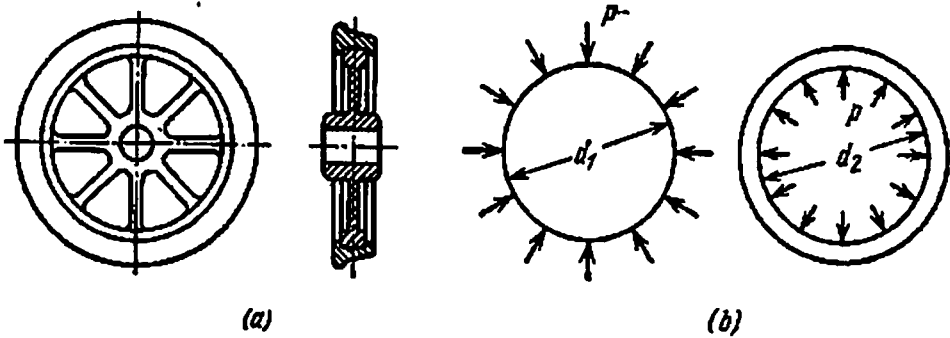


Fig. 36

under the action of weight  $Q$ . In this case, the particular property of the statically indeterminate systems discussed above would have helped in better working of the structure.

Another example of the expedient use of initial stresses is putting on the tyre on the wheels of a rolling stock. The wheel consists of two parts: the central cast portion and the steel tyre which is put on

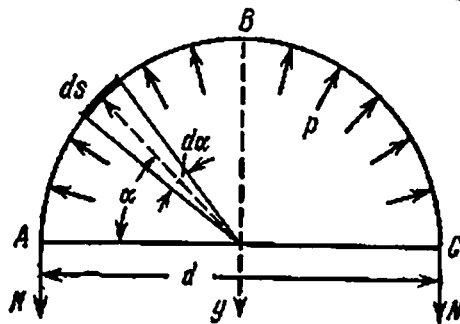


Fig. 37

it (Fig. 36 (a) and (b)). The tyre is fastened to the central portion by means of special fixtures; besides, its internal diameter  $d_2$  is made a little less than  $d_1$ . Usually this difference is of the order of  $\frac{1}{n} d_1$ —approximately  $\frac{1}{2000} d_1$ . Before slipping the tyre on the central portion, it is heated so that its internal diameter becomes greater than the diameter of the central portion; the fitted tyre contracts upon cooling and presses the central portion. A tensile force  $N$  appears in the tyre, and a reaction  $p$ , between the tyre and the central portion (Fig. 36 (b)).

If we cut the tyre across the diameter (Fig. 37), the two forces  $N$  must balance the total pressure on the internal surface of the cutoff portion of the tyre. Let us write down the equilibrium condition by projecting all the forces on the  $y$ -axis (Fig. 37). A pressure  $p ds$  acts upon the element of length  $ds$  of the tyre; its projection on the  $y$ -axis is equal to  $-pds \sin \alpha = -p \frac{d}{2} \sin \alpha d\alpha$ , because  $ds = \frac{d}{2} d\alpha$ . The equilibrium condition takes the form

$$2N - \int_{AKC} p \frac{d}{2} \sin \alpha d\alpha = 0, \quad \text{or} \quad 2N - p \frac{d}{2} \int_0^\pi \sin \alpha d\alpha = 0$$

whencefrom

$$2N - pd = 0 \quad \text{and} \quad N = \frac{pd}{2}, \quad \text{or} \quad p = \frac{2N}{d}$$

Thus we have one static equation for two unknowns  $N$  and  $p$ ; this is a statically indeterminate problem. The unknown forces can be determined only by considering the joint deformation of the structure.

The tension in the tyre and the compression in the central portion should be such that they level the difference between the diameters  $d_1$  and  $d_2$ . Neglecting the deformation of the central portion due to its much greater mass as compared to that of the tyre, we find that the levelling of the difference in diameters takes place chiefly due to elongation of the tyre. If this difference is  $\frac{1}{n}$  of the tyre diameter, then the relative elongation  $\varepsilon_n$  of the diameter and, consequently, of the whole tyre will also be  $\frac{1}{n}$ .

The relative elongation of the tyre under force  $N$  is  $\varepsilon_N = \frac{N}{EA}$ , where  $A$  is the cross-sectional area of the tyre. Equating the values  $\varepsilon_n = \varepsilon_N$ , we obtain an extra equation

$$\frac{N}{EA} = \frac{1}{n}, \quad N = \frac{EA}{n}$$

whence

$$p = \frac{2EA}{nd} \quad (4.16)$$

The stress in the tyre is  $\sigma = \frac{N}{A} = \frac{E}{n}$ .

In formula (4.16)  $d$  may be replaced (instead of the original diameter  $d_2$ ) by  $d_1$ , because the difference in the diameters is infinitely small.

Let us consider a numerical example (the tyre of a freight wagon 13 cm broad and 7.5 cm thick). Let  $d = d_1 = 900$  mm;  $\frac{1}{n} = \frac{1}{1000}$ ;  $E =$

$=2 \times 10^6 \text{ kgf/cm}^2$ ;  $A=7.5 \times 13=97.5 \text{ cm}^2$ . Then we have

$$\sigma = \frac{2 \times 10^6}{1000} = 2000 \text{ kgf/cm}^2$$

$$N = \frac{2 \times 10^6 \times 97.5}{1000} = 195\,000 \text{ kgf} = 195 \text{ tf}$$

$$p = \frac{2 \times 2 \times 10^6 \times 97.5}{90 \times 1000} = 4330 \text{ kgf/cm}$$

### § 20. Tension and Compression in Bars Made of Heterogeneous Materials

This type of bars belongs to the group of statically indeterminate. As an example, we shall discuss how to determine the dimensions of a composite column (Fig. 38) under the action of compressive forces  $P$ . The column consists of a round steel bar of diameter  $d_s$  and is

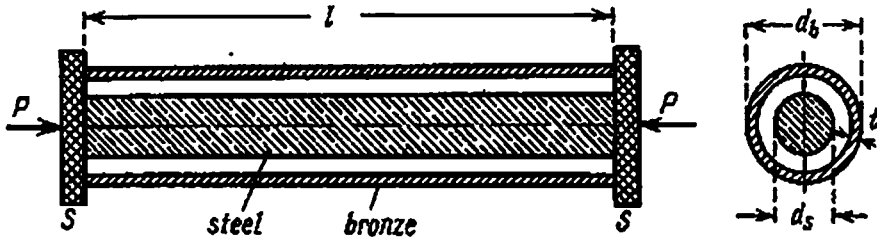


Fig. 38

located inside a bronze jacket of external diameter  $d_b$  and wall thickness  $t$ .

Let us introduce the following notations:

$A_b$ — cross-sectional area of the bronze pipe;

$A_s$ — cross-sectional area of the steel bar;

$[\sigma_b]$ ,  $[\sigma_s]$ ,  $E_b$ ,  $E_s$ — permissible stresses and moduli of elasticity of bronze and steel, respectively.

The required dimensions of the bar should be such that enable it to withstand load  $P$ .

Let us find stresses  $\sigma_b$  and  $\sigma_s$  due to load  $P$  over areas  $A_b$  and  $A_s$ , respectively, and write down the strength condition.

The bar is axially compressed by forces  $P$  applied at the centre of gravity of the section through rigid slabs  $S$  whose deformations are considered negligible (Fig. 38). The part  $P_b$  of the compressive forces is transmitted through the bronze jacket, and part  $P_s$ , through the central steel bar (Fig. 39). We have only one equation of statics to determine these two forces which give rise to stresses in the steel bar and bronze jacket:

$$P_s + P_b = P \quad (4.17)$$

This is a statically indeterminate problem. The second equation is obtained from the condition of joint deformation according to

which both the bronze jacket and steel bar of the column (Fig. 39) must shorten by the same length  $\Delta l$ , since the top and the bottom planes of both coincide. From Hooke's law we have

$$\Delta l = \frac{P_b l}{E_b A_b} = \frac{P_s l}{E_s A_s} \quad (4.18)$$

This is the second equation correlating  $P_b$  and  $P_s$ . From (4.18) we find

$$P_s = P_b \frac{A_s E_s}{A_b E_b}$$

Substituting this value of  $P_s$  in (4.17), we get

$$P_b \left( 1 + \frac{A_s E_s}{A_b E_b} \right) = P$$

and

$$P_b = \frac{P}{1 + \frac{A_s E_s}{A_b E_b}}, \quad P_s = \frac{P \frac{A_s E_s}{A_b E_b}}{1 + \frac{A_s E_s}{A_b E_b}} = \frac{P}{1 + \frac{A_b E_b}{A_s E_s}} \quad (4.19)$$

$$\sigma_b = \frac{P}{A_b + A_s \frac{E_s}{E_b}}, \quad \sigma_s = \frac{P}{A_s + A_b \frac{E_b}{E_s}} \quad (4.20)$$

The distribution of forces between the elements of statically indeterminate structures depends upon the ratios of their cross-sectional

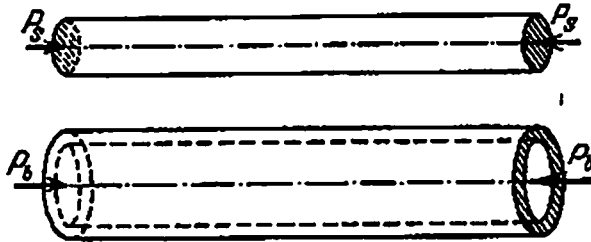


Fig. 39

areas and moduli of elasticity. From equation (4.18), taking into consideration that

$$\frac{P_b}{A_b} = \sigma_b \quad \text{and} \quad \frac{P_s}{A_s} = \sigma_s$$

we find that the ratio of the stresses in bronze and steel depends only upon the ratio of their moduli of elasticity:

$$\frac{\sigma_s}{\sigma_b} = \frac{E_s}{E_b}$$

and the stresses are directly proportional to the moduli of elasticity. Assuming that under compression  $E_s = 2 \times 10^6$  kgf/cm<sup>2</sup> and  $E_b = 1 \times 10^6$  kgf/cm<sup>2</sup> (Table 1), it is obvious that stresses in steel bar will always be two times higher than the stresses in bronze jacket. The permissible stresses for steel are usually three times greater than permissible stresses for bronze. Therefore, if the stresses in the bronze jacket are equal to the permissible stress for bronze, the stresses in the steel bar will be smaller than the permissible stress for steel. Hence the dimensions of the column are obtained from strength condition of bronze jacket under compression:

$$\sigma_b = \frac{P}{A_b + A_s \frac{E_s}{E_b}} = \frac{P}{A_b \left(1 + \frac{A_s}{A_b} \frac{E_s}{E_b}\right)} \leq [\sigma_b] \quad (4.21)$$

Let  $P = 25$  tf. The ratio  $A_s/A_b$  of the cross-sectional areas is usually selected from design considerations. Let  $A_s/A_b = 2$ , and the permissible stress  $[\sigma_b] = 500$  kgf/cm<sup>2</sup>. Equation (4.21) will then be written as

$$\frac{25\,000}{A_b (1 + 2 \times 2)} \leq 500,$$

wherefrom

$$A_b \geq \frac{25\,000}{5 \times 500} = 10 \text{ cm}^2 \quad \text{and} \quad A_s = 2 \times 10 = 20 \text{ cm}^2$$

The diameter of the steel bar is calculated from the condition

$$\frac{\pi d_s^2}{4} \geq A_s, \quad \text{wherefrom} \quad d_s = \sqrt{\frac{4A_s}{\pi}} = \sqrt{\frac{4 \times 20}{3.14}} = 5.05 \text{ cm} \approx 51 \text{ mm}$$

The dimensions of the bronze jacket section can be found if we assume a particular value of wall thickness  $t$  from design considerations. Let  $t = 5 \text{ mm} = 0.5 \text{ cm}$ . Now, applying the approximate formula for a ring, we have

$$A_b \leq \pi d_b t, \quad \text{wherefrom} \quad d_b \geq \frac{A_b}{\pi t} = \frac{10}{3.14 \times 0.5} = 6.48 \text{ cm} \approx 65 \text{ mm}$$

The deformations of such structures are calculated according to the general principles. Since the steel and bronze portions of the column shorten by the same amount, it is immaterial which of the formulas in equation (4.18) is employed for calculating  $\Delta l$ .

## § 21. Stresses Due to Temperature Change

In statically indeterminate systems, stresses without any external loading occur not only due to the inaccuracy of manufacturing and assembling, but also due to a change in temperature.

Considerable stresses of this type may arise in rails welded into a continuous line. The rails are subjected to tensile or compressive stresses.



ses when the temperature changes with respect to that at which they were welded. The problem may be schematically expressed as follows: we have a restrained bar whose both ends have been rigidly fixed at a temperature  $t_1$ ; find the stresses arising when the temperature changes to  $t_2$  (Fig. 40). The length of the bar is  $l$ , cross-sectional area is  $A$  and modulus of elasticity is  $E$ .

Let us ascertain the forces which will act on the bar when the temperature rises from  $t_1$  to  $t_2$ . The bar will tend to elongate and push apart

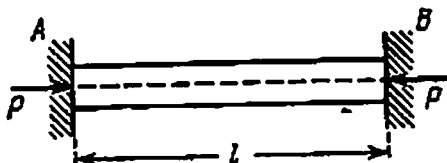


Fig. 40

the supports  $A$  and  $B$ . The supports will resist this with reactions directed as shown in the figure. These forces will cause the bar to be compressed.

These forces cannot be found from static conditions, because all that we come to know from the single equilibrium condition is that the reactions at points  $A$  and  $B$  are equal in magnitude and opposite to each other. The value of the reaction  $P$  remains unknown, and hence the structure may be considered statically indeterminate.

The additional equation can be written from the consideration that length  $l$  of the restrained bar remains unchanged in spite of the change in temperature. This implies that shortening  $\Delta l_p$  due to force  $P$  is equal in its absolute value to the temperature elongation  $\Delta l_t$  which the bar would have experienced had the end  $A$  been fixed and end  $B$  free to move. Hence

$$\Delta l_t - \Delta l_p = 0 \quad (4.22)$$

This is the condition of joint deformation; it shows that the length of the bar remains constant despite the temperature change, since it does not tear away from the fixed supports.

Since

$$\Delta l_p = \frac{Pl}{EA} \quad \text{and} \quad \Delta l_t = \alpha l (t_2 - t_1)$$

where  $\alpha$  is the linear thermal expansion coefficient of the bar material, we have

$$\frac{Pl}{EA} = \alpha l (t_2 - t_1)$$

and

$$\frac{P}{A} = \sigma = \alpha E (t_2 - t_1) \quad (4.23)$$

i.e. the stress due to temperature change in a restrained bar of uniform cross-sectional area depends only upon the modulus of elasticity of the material, its linear expansion coefficient and the temperature difference and not upon its length or the cross-sectional area.

Force  $P$  may be calculated from the expression

$$P = \alpha EA (t_2 - t_1)$$

In this example, if  $t_2 > t_1$ , stress  $\sigma$  will be compressive, because the direction of reaction  $P$  inside the bar has been considered positive. If we follow the generally accepted convention of writing the compressive stresses with a minus sign, and the tensile stresses with a plus sign, then formula (4.23) should be written in the following manner to automatically give the proper sign:

$$\sigma = \alpha E (t_1 - t_2)$$

If the cross-sectional area of the bar is not constant along its length or if it is made from different materials, or if the supports permit a slight change in length, or if all these conditions take place simultaneously, the method of determining thermal stresses somewhat changes although basically it remains the same.

The variability in the cross-sectional area and the use of different materials must be taken into account when calculating  $\Delta l$ ; it is determined as the sum of elongations calculated separately for each portion. The possibility of the bar to slightly change its length is reflected in the equation of joint deformation (4.22); the difference of deformations caused by the temperature change and the forces is in this case not equal to zero, but equal to the length, by which the bar is free to elongate.

A steel bar consisting of two parts of length  $l_1 = 40$  cm and  $l_2 = 60$  cm and cross-sectional area  $A_1 = 10$  cm<sup>2</sup> and  $A_2 = 20$  cm<sup>2</sup>, respectively, has one end rigidly fixed whereas the other end misses the support by  $\Delta_0 = 0.3$  mm (Fig. 41). Find the stresses in both the parts if the temperature increases by 50°C,  $\alpha = 125 \times 10^{-7}$ .

Increase in temperature causes elongation of the bar by  $\Delta l_t$ , and the compression from the support reaction  $P$  results in its shortening by  $\Delta l_p$ . The difference of these two deformations (in absolute value)

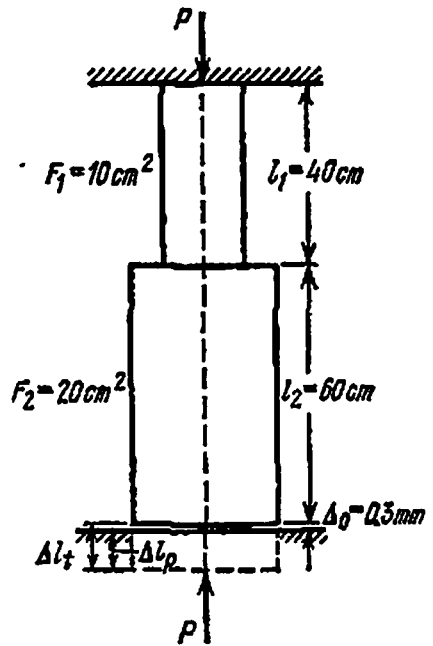


Fig. 41

is  $\Delta_0$  (see Fig. 41):

$$\Delta l_t - \Delta l_p = \Delta_0$$

This is the condition of joint deformation. The respective values of  $\Delta l_t$  and  $\Delta l_p$  are

$$\Delta l_t = \alpha t (l_1 + l_2), \quad \Delta l_p = \frac{Pl_1}{EA_1} + \frac{Pl_2}{EA_2} = \frac{Pl_1}{EA_1} \left[ 1 + \frac{l_2 A_1}{l_1 A_2} \right]$$

Therefore

$$\alpha t (l_1 + l_2) - \frac{Pl_1}{EA_1} \left[ 1 + \frac{l_2 A_1}{l_1 A_2} \right] = \Delta_0$$

whencefrom

$$P = \frac{[\alpha t (l_1 + l_2) - \Delta_0] EA_1}{l_1 \left[ 1 + \frac{l_2 A_1}{l_1 A_2} \right]} = \frac{[125 \times 10^{-7} \times 100 \times 50 - 0.03] \times 2 \times 10^8 \times 10}{40 \left[ 1 + \frac{60 \times 10}{40 \times 20} \right]} = 9300 \text{ kgf}$$

Stress in the upper portion is

$$\sigma' = \frac{P}{A_1} = \frac{9300}{10} = 930 \text{ kgf/cm}^2$$

Stress in the lower portion is

$$\sigma'' = \frac{P}{A_2} = \frac{9300}{20} = 465 \text{ kgf/cm}^2$$

(both the stresses are compressive).

Had there been no gap  $\Delta_0$ , the force as well as the stresses would have increased 1.92 times.

## § 22. Simultaneous Account for Various Factors

Sometimes, in statically indeterminate systems, we have to consider simultaneously the effect of external forces, change of temperature and manufacturing inaccuracies. The problem can be solved in two ways: first method—simultaneous account for all the factors. In this case the equation of joint deformation must contain terms reflecting the effect of all the factors (load, temperature and manufacturing inaccuracies). The forces and stresses obtained as a result of such a computation are final.

In the second method, we compute separately the forces and stresses due to the load, temperature and manufacturing inaccuracies. In other words, a number of separate problems are solved, each problem taking into account only one factor. The final forces and stresses are obtained as the algebraic sum of the values obtained from each of the solutions. The second method is often simpler and more convenient,

although it calls for more calculation. It is known as the *method of cumulative action of forces*. This method is valid because of the applicability of the *principle of superposition of forces*. When deformations are small in magnitude, the deformation caused by a force or a group of forces either does not affect the deformation due to another force or group of forces, or the effect is so small (less by an order) that it may

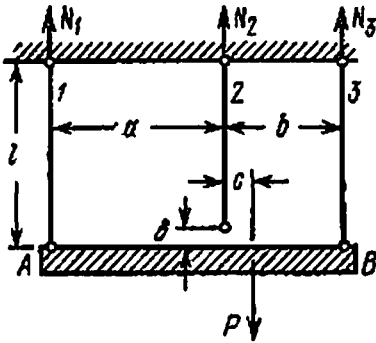


Fig. 42

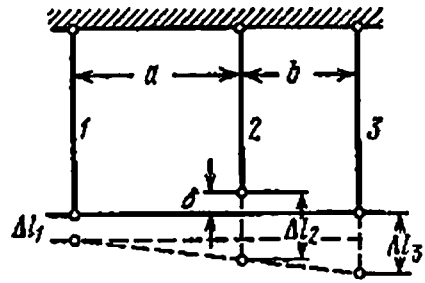


Fig. 43

be neglected. This principle is not applicable for extremely flexible or highly deformable structures like long thin bars, membranes, rubber parts, etc.

We shall solve the following example to illustrate the technique of simultaneous accounting of various factors.

Three parallel vertical rods of equal length  $l=2$  m support a rigid beam  $AB$  to which a force  $P=4$  tf (Fig. 42) is applied. The distance between the rods and from the middle rod to the point of application of force  $P$  are  $a=1.5$  m,  $b=1$  m and  $c=0.25$  m, respectively. The middle bar is shorter than its design length by  $\delta=0.2$  mm. Data about the bars are given in Table 7.

Table 7

No. of rod	Material	$A$ ( $\text{cm}^2$ )	$E$ ( $\text{kg/cm}^2$ )	$\alpha$
1	Copper	2	$1 \times 10^6$	$17 \times 10^{-6}$
2	Steel	1	$2 \times 10^6$	$13 \times 10^{-6}$
3	Steel	3	$2 \times 10^6$	$13 \times 10^{-6}$

During operation the temperature of the structure may rise up by  $20^\circ\text{C}$ .

Find the stresses in each of the three rods.

Let us suppose that forces  $N_1$ ,  $N_2$ , and  $N_3$  in all the rods are tensile. The reactions at the supporting points, equal to them, are shown in

Fig. 42. As the forces are parallel, we can write down only two equilibrium equations. The first is the sum of the projections of forces on the vertical axis and has the following form:

$$N_1 + N_2 + N_3 - P = 0 \quad (4.24)$$

For the second equation let us take the sum of moments of all forces with respect to the point of support of the second rod:

$$N_1 a - N_3 b + P c = 0 \quad (4.25)$$

These two equations are insufficient to determine three unknown forces. We must consider the deformations. Figure 43 shows a sketch diagram of the structure, with the assumption that all the three rods are subjected to tensile forces. From this diagram we may write down the following condition of joint deformation:

$$\frac{\Delta l_3 - \Delta l_1}{\Delta l_2 - \Delta l_1 - \delta} = \frac{a+b}{a} \quad (4.26)$$

The values of the deformations entering into the equation (taking into account the temperature change) will be as follows:

$$\Delta l_1 = \frac{N_1 l}{E_1 A_1} + \alpha_1 l \Delta t, \quad \Delta l_2 = \frac{N_2 l}{E_2 A_2} + \alpha_2 l \Delta t$$

$$\Delta l_3 = \frac{N_3 l}{E_3 A_3} + \alpha_3 l \Delta t$$

Putting these values in equation (4.26) we get

$$\frac{\frac{N_3 l}{E_3 A_3} + \alpha_3 l \Delta t - \frac{N_1 l}{E_1 A_1} - \alpha_1 l \Delta t}{\frac{N_2 l}{E_2 A_2} + \alpha_2 l \Delta t - \frac{N_1 l}{E_1 A_1} - \alpha_1 l \Delta t - \delta} = \frac{a+b}{a} \quad (4.27)$$

Solving equations (4.24), (4.25), and (4.27) simultaneously, we determine  $N_1$ ,  $N_2$ , and  $N_3$ . Their values are

$$N_1 = 792 \text{ kgf}, \quad N_2 = 1020 \text{ kgf}, \quad \text{and} \quad N_3 = 2188 \text{ kgf}$$

Had our assumption about the direction of the forces been wrong for any of the rods, the value of that force would have been obtained with a negative sign.

Let us now determine the corresponding stresses:

$$\text{in the first rod } \sigma_1 = \frac{N_1}{A_1} = \frac{792}{2} = 396 \text{ kgf/cm}^2$$

$$\text{in the second rod } \sigma_2 = \frac{N_2}{A_2} = \frac{1020}{1} = 1020 \text{ kgf/cm}^2$$

$$\text{in the third rod } \sigma_3 = \frac{N_3}{A_3} = \frac{2188}{3} = 729 \text{ kgf/cm}^2$$

The problem could also have been solved by considering separately the effect of load, temperature and manufacturing inaccuracies and subsequently adding the stresses. The result would obviously have been the same.

§ 23. More Complicated Cases of Statically Indeterminate Structures

In all the statically indeterminate systems that we have considered till now, the number of unknown forces exceeded by one the number of static equations. They were all first-order statically indeterminate problems; one of the unknown forces may be considered as a redundant unknown, which cannot be determined from the static equations.

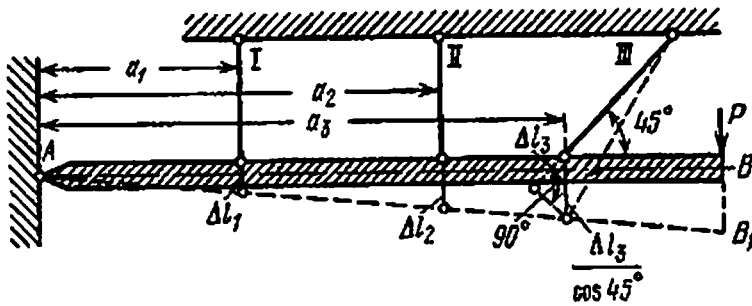


Fig. 44

There may be cases when the number of these redundant unknowns is greater; in such cases it becomes necessary to write down an equal number of extra equations from the conditions of joint deformation of the system. The structure shown in Fig. 44 may be taken as an example: a very rigid bar is hinged to a fixed support suspended from three rods and loaded with force  $P$ .

We may write down three static equations for bar  $AB$ . The number of unknowns is however five: forces in the three rods and the horizontal and vertical components of the reaction at hinge  $A$ .

The extra equations can be written by considering the deformation of the system. Since we are considering bar  $AB$  to be very rigid, its deformation may be ignored. Remaining straight, it will occupy position  $AB_1$ . From the similarity of triangles we may find the relation between  $\Delta l_1$ ,  $\Delta l_2$ , and  $\Delta l_3$ ; this will give us two extra equations, namely:

$$\frac{\Delta l_1}{\Delta l_2} = \frac{a_1}{a_2} \quad \text{and} \quad \frac{\Delta l_1}{\Delta l_3} = \frac{a_1}{a_3 \cos 45^\circ}$$

Further solution is the same as in the example discussed above (§ 18).

## CHAPTER 5

## Account for Dead Weight in Tension and Compression. Design of Flexible Strings

### § 24. Selecting the Cross-sectional Area with the Account for the Dead Weight (in Tension and Compression)

Till now, in determining the external forces stretching or compressing the elements of structures, we ignored the dead weight of these elements. The question arises: Does not this simplification introduce a considerable error in the computations? Let us therefore determine the stresses and deformations of a stretched or compressed bar accounting for its dead weight.

Let a vertical bar (Fig. 45 (a)) be fixed at its upper end and load  $P$  suspended from its lower end. The length of the bar is  $l$ , its cross-

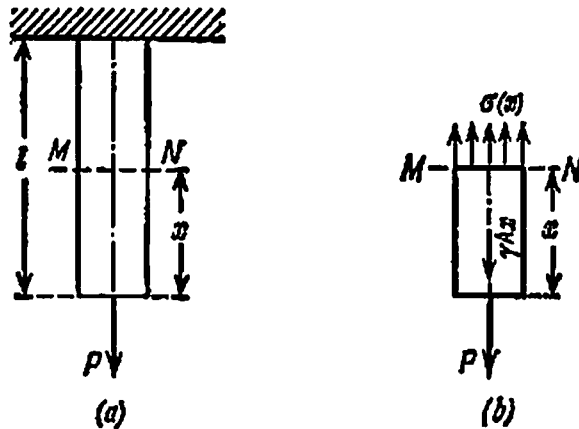


Fig. 45

tional area is  $A$ , modulus of elasticity  $E$  and specific weight  $\gamma$ . Let us calculate the stresses in section  $MN$  located at a distance  $x$  from the free end of the bar.

Cut the bar through section  $MN$  and separate the lower part of length  $x$  loaded by force  $P$  and its own dead weight  $\gamma Ax$  (Fig. 45 (b)). These two forces are balanced by stresses acting on face  $MN$  from cut-off portion. These stresses will be normal, uniformly distributed and directed outwards of the portion of bar under consideration, i.e. they will be tensile. The magnitude of these stresses will be

$$\sigma(x) = \frac{P + \gamma Ax}{A} = \frac{P}{A} + \gamma x \quad (5.1)$$

Thus, when the dead weight is accounted for, the normal stresses are found to be not constant along the length of the bar. The most stressed and hence the critical section will be the uppermost section

for which  $x$  has the maximum value equal to  $l$ ; stress in this section will be

$$\sigma_{\max} = \frac{P}{A} + \gamma l \quad (5.2)$$

It is this section which must satisfy the strength condition

$$\sigma_{\max} = \left( \frac{P}{A} + \gamma l \right) \leq [\sigma] \quad (5.3)$$

Herefrom the required cross-sectional area may be calculated as

$$A \geq \frac{P}{[\sigma] - \gamma l} \quad (5.4)$$

The only difference between this formula and the one for determining the cross-sectional area of a stretched bar without account for the dead weight is that quantity  $\gamma l$  is subtracted from the permissible stress.

Let us calculate the stresses for both the cases to evaluate the importance of this correction. Consider a mild-steel bar 10 m long having  $[\sigma] = 1600 \text{ kgf/cm}^2$  and the quantity  $\gamma l = 7.85 \times 10^{-3} \times 10^3 = 7.85 \text{ kgf/cm}^2$ . Thus, for a mild-steel bar the correction in the cross-sectional area will be  $\frac{7.85}{1600}$ , i.e. approximately 0.5%. Let us now consider a brick column also 10 m long, which has  $[\sigma] = 12 \text{ kgf/cm}^2$  and the quantity  $\gamma l = 1.8 \times 10^{-3} \times 10^3 = 1.8 \text{ kgf/cm}^2$ . Therefore, the correction for the brick column will be  $\frac{1.8}{12}$ , i.e. 15%.

It is obvious that the effect of dead weight in tension and compression may be neglected if the bar (column) is not very long or if it is not made from a low-strength material (brick, stone) with a great weight. The dead weight has to be considered when designing long elevator ropes, various types of long rods and high stone structures (beacon towers, supports of bridge trusses, etc.).

In such cases it becomes necessary to determine the most expedient shape of the element. If we select the cross-sectional area of a rod (Fig. 45) according to formula (5.4) and take it uniform along the whole length, the material of the element will be poorly utilized: the normal stress will reach the permissible limit only in the uppermost section. In all other sections we will have margin of stress and consequently excessive material. Therefore, it is desirable to design the element in such a way that the normal stresses are the same in all its sections (perpendicular to the axis).

Such an element is classified as the *bar of uniform strength under tension and compression*. The element will have minimum weight if the stresses are equal to the permissible stress.



Let us consider a long bar subjected to compression by the force  $P$  and its own weight (Fig. 46). The nearer a section is to the base, the greater is the force causing stresses in the section and therefore the greater must be the dimensions of the section area. The bar will have a shape continuously widening downwards. Cross-sectional area  $A$  will change along the height depending upon the value of  $x$ , i.e.  $A = f(x)$ .

Let us establish a relation between the cross-sectional area of a section and its distance  $x$  from the top end.

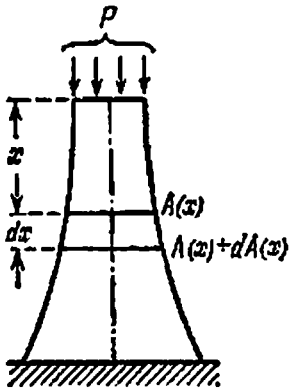


Fig. 46

The cross-sectional area of the top end  $A_0$  is determined from the strength condition:

$$\frac{P}{A_0} = [\sigma] \quad \text{or} \quad A_0 = \frac{P}{[\sigma]}$$

where  $[\sigma]$  is the permissible stress under compression; stresses in all other sections must also be equal to

$$\sigma = [\sigma] = \frac{P}{A_0}$$

Let us take two infinitely close sections at a distance  $x$  from the top end to elucidate the variation of cross-sectional area with the height of the section. Let the distance between the sections be  $dx$ . Let us denote the area of the upper section by  $A(x)$  and the area of the adjoining section by  $A(x) + dA(x)$ . Increment  $dA(x)$  of the area between the two sections must bear the weight  $\gamma A(x) dx$  of the element of the bar enclosed between these two sections. Since it should cause a stress equal to the permissible stress  $[\sigma]$  on the area  $dA(x)$ , we may determine the increment of area  $dA(x)$  from the condition

$$\frac{\gamma A(x) dx}{dA(x)} = [\sigma] \quad (5.5)$$

wherefrom

$$\frac{dA(x)}{A(x)} = \frac{\gamma}{[\sigma]} dx$$

Integrating both sides, we get

$$\ln A(x) + C = \frac{\gamma}{[\sigma]} x \quad (5.6)$$

At  $x=0$  the area  $A(x) = A_0$ ; putting this value in equation (5.6), we have

$$\ln A_0 + C = 0, \quad \text{or} \quad C = -\ln A_0$$

Therefore,

$$\frac{\gamma}{|\sigma|} x = \ln A(x) - \ln A_0 = \ln \frac{A(x)}{A_0}, \quad \frac{A(x)}{A_0} = e^{\frac{\gamma}{|\sigma|} x}$$

and

$$A(x) = A_0 e^{\frac{\gamma}{|\sigma|} x} \quad (5.7)$$

If the cross-sectional area changes exactly according to this law, the lateral faces of the bar have a curved shape (Fig. 46), which complicates the machining operation and increases production cost. For this reason usually a shape approximately corresponding to the shape of a uniform-strength bar is employed, for example a truncated pyramid with plane faces.

The above computation is only approximate. We had assumed that only normal stresses are transmitted through the whole section of the uniform-strength bar; actually, near the edges, the stresses are directed along the tangent to the lateral surface.

In long ropes or stretched rods the shape of a uniform-strength bar is obtained approximately by dividing the bar lengthwise into a number of parts, the cross-sectional area remaining constant over each separate section (Fig. 47)—a so-called step bar is obtained.

For a given length the cross-sectional areas  $A_1, A_2, \dots$  are determined in the following manner. The cross-sectional area of the first portion from the bottom will, according to formula (5.4), be

$$A_1 = \frac{P}{|\sigma| - \gamma l_1}$$

The cross-sectional area of the second portion can be determined by considering it to be loaded by external force  $P$  and the weight of the first portion  $\gamma A_1 l_1$ :

$$A_2 = \frac{P + \gamma A_1 l_1}{|\sigma| - \gamma l_2}$$

The cross-sectional area of the third portion is determined by adding the weight of both the first and second portions to force  $P$ . The cross-sectional area of all other portions can be determined in identical man-

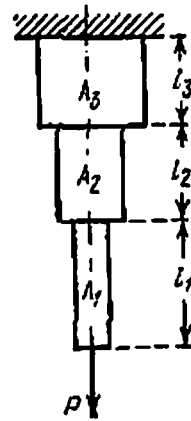


Fig. 47

ner. Let us consider the following example to compare the effectiveness of using uniform-strength bars, step bars and bars of constant section.

A support with height  $h=42$  m is subjected to compression by axial force  $P=400$  tf. Assuming the unit weight of the laying as  $2.2$  tf/m<sup>3</sup>, and the permissible stress under compression as  $12$  kgf/cm<sup>2</sup>, compare the volume of laying for

support of constant section;

support made of three prismatic parts of equal length;

support of uniform strength under compression.

We shall carry out the calculations in tons (force) and metres.

For the first case the cross-sectional area is

$$A = \frac{P}{[\sigma] - h\gamma} = \frac{400}{120 - 42 \times 2.2} = 14.5 \text{ m}^2$$

The volume

$$V = Ah = 14.5 \times 42 \approx 610 \text{ m}^3$$

In the second case, the area of the upper portion is

$$A_1 = \frac{P}{[\sigma] - \frac{h}{3}\gamma} = \frac{400}{120 - 14 \times 2.2} = 4.48 \text{ m}^2$$

The cross-sectional area of the second portion is

$$A_2 = \frac{P + \gamma A_1 \frac{h}{3}}{[\sigma] - \frac{h}{3}\gamma} = \frac{400 + 2.2 \times 4.48 \times 14}{120 - 14 \times 2.2} = 6.04 \text{ m}^2$$

The cross-sectional area of the third portion is

$$A_3 = \frac{P + \gamma A_1 \frac{h}{3} + \gamma A_2 \frac{h}{3}}{[\sigma] - \frac{h}{3}\gamma} = \frac{400 + 2.2 \times 4.48 \times 14 + 2.2 \times 6.04 \times 14}{120 - 14 \times 2.2} = 8.12 \text{ m}^2$$

The total volume of the laying is

$$V = (A_1 + A_2 + A_3) \frac{h}{3} = (4.48 + 6.04 + 8.12) 14 = 261 \text{ m}^3$$

The same result may be obtained from the condition that the force at the bottom of the third portion, equal to  $P+G$  (where  $G$  is the total weight of the support), is simultaneously equal to  $[\sigma]A_3$ ; therefore

$$V = \frac{G}{\gamma} = \frac{[\sigma] A_3 - P}{\gamma} = 261 \text{ m}^3$$

In the case of support of uniform strength under compression, the cross-sectional area of the upper face is

$$A_0 = \frac{P}{[\sigma]} = \frac{400}{120} = 3.33 \text{ m}^2$$

The area of the bottom section is

$$A_h = A_0 e^{\frac{\gamma}{[\sigma]} h} = 3.33 e^{\frac{2.2 \times 12}{120}} = 3.33 e^{0.77} = 7.15 \text{ m}^2$$

The weight of the support of uniform strength  $G$  is determined from the condition

$$P + G = [\sigma] A_h$$

wherefrom

$$G = [\sigma] A_h - P = 120 \times 7.15 - 400 = 460 \text{ tf}$$

The volume of the support is

$$V = \frac{G}{\gamma} = \frac{460}{2.2} = 209 \text{ m}^3$$

which is 20% less than the volume of the step support and approximately three times less than that of the support of constant section.

## § 25. Deformations Due to Dead Weight

In determining the effect of dead weight on deformation under tension and compression we must take into account that the relative elongation of various portions of the bar will vary just as stress  $\sigma(x)$ . To calculate the total elongation of the bar of constant section let us first determine the elongation of an infinitely small portion of length  $dx$ , which is located at distance  $x$  from the end of the rod (Fig. 48). The absolute elongation of this portion (equation (2.5)) is

$$\Delta dx = \frac{P + \gamma x A}{EA} dx = \frac{dx}{E} \left[ \frac{P}{A} + \gamma x \right]$$

The total elongation of the bar

$$\Delta l = \int_0^l \Delta dx = \int_0^l \frac{dx}{E} \left[ \frac{P}{A} + \gamma x \right] = \frac{Pl}{EA} + \frac{\gamma l^2}{2E}$$

As for deformation in uniform-strength bars, the relative elongation is the same over the whole length because the normal stresses are the same in all the sections and equal to the permissible stress  $[\sigma]$ :

$$\epsilon = \frac{[\sigma]}{E}$$

The absolute elongation of a bar of length  $l$  will be

$$\Delta l = \epsilon l = \frac{[\sigma] l}{E} = \frac{Pl}{EA_0}$$

(the notations correspond to Fig. 46).

The deformation of step bars should be determined by parts, calculating the deformation separately for each prismatic portion. The deformation of each portion has to be determined by considering not only its dead weight, but also the weight of portions which affects its deformation in addition to the external force. The total deformation is obtained as the sum of deformations of separate portions.

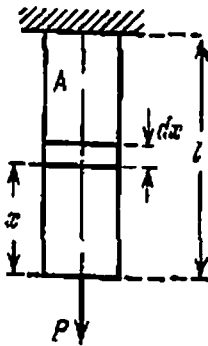


Fig 48

### § 26. Flexible Cables

A. In engineering practice, we come across one more type of a stretched element in which the dead weight plays an important part in determining its strength. These are the so-called *flexible cables*. This term

covers the flexible elements in electric transmission lines, cableways, suspension bridges and other structures.

Let us consider (Fig. 49) a flexible cable of constant section loaded by its own weight and suspended from two supports at different heights. The cable sags along curve  $AOB$  under its own weight. The horizontal projection of the distance between the supports (points of fixation) is called the *span* and is denoted by  $l$ .

As the cable is of a constant section, its weight must be distributed uniformly over its length. Generally, the sag of the cable is small as compared to its span, and there is little difference (not more than 10%) between the length of curve  $AOB$  and its chord  $AB$ . In this case we may consider with a sufficient degree of accuracy that the weight of the cable is distributed uniformly not over its length, but over the horizontal projection of its length, i.e. along the span  $l$ . We shall study only this type of flexible cables. Let us assume that the intensity of the load uniformly distributed along the cable span is  $q$ . This load, having dimensionality [force]/[length], may be not only due to the weight of the cable per unit span but also the weight of ice or any other load also distributed uniformly. This assumption about the law of load distribution considerably simplifies the calculations, but simultaneously renders them approximate. In exact calculations (load

distribution along the curve) the sag curve is a catenary, whereas in approximate calculations it is found to be a quadratic parabola.

Let us take the lowest point of sag  $O$  as the origin of coordinates (Fig. 49); its position, which is as yet unknown, obviously depends upon the magnitude of  $q$ , upon the ratio of the length of cable along the curve to the span and also upon the relative location of the supports. Evidently, tangent to the curve at point  $O$  is horizontal. Let us direct the  $x$ -axis to the right along this tangent.

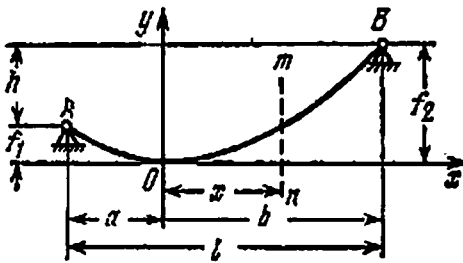


Fig. 49

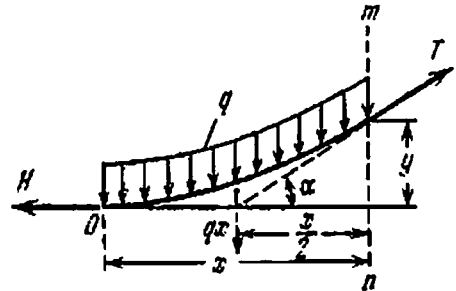


Fig. 50

Let us cut a part of the cable by two sections—one passing through the origin of coordinates and the other at a distance  $x$  from it (section  $mn$ ). Since the cable is flexible, i.e. capable of resisting only tension, the discarded portion can act on the remaining portion only in the form of a force directed along the tangent to the sag curve at the point of section. Any other direction of the force is ruled out.

Figure 50 depicts the cut-out portion of the cable with the forces acting on it. The uniformly distributed load of intensity  $q$  is directed vertically downwards. The action of the left discarded portion (horizontal force  $H$ ) is directed to the left because the cable is working under tension. The action of the right discarded portion, force  $T$ , is directed to the right along the tangent to the sag curve at this point.

Let us write down the equation of equilibrium for the cut-out portion of the cable. Let us take the sum of the moments of all forces about the point of application of force  $T$  and equate it to zero. Proceeding from the approximation introduced earlier, we consider that the resultant of distributed load of intensity  $q$  is  $qx$  and that it acts at the midpoint of segment  $x$  (Fig. 50). We get

$$Hy - qx \frac{x}{2} = 0, \quad \text{whence} \quad y = \frac{qx^2}{2H} \tag{5.8}$$

It follows from this equation that the sag curve is a parabola. When both the supports are at the same level,  $f_1 = f_2 = f$ . In this case  $f$  is called the *sag*. It can be easily determined from equation (5.8) that due to symmetry the lowest point of the cable is at the middle of the span, and  $a = b = \frac{l}{2}$ . Substituting the values of  $x = b = \frac{l}{2}$  and  $y = f$  in

equation (5.8), we get

$$f = \frac{ql^2}{8H} \quad (5.9)$$

From this formula we determine the value of  $H$ :

$$H = \frac{ql^2}{8f} \quad (5.10)$$

The quantity  $H$  is called the *horizontal tension of the cable*.

Thus, if load intensity  $q$  and tensile force  $H$  are known, we can determine sag  $f$  from formula (5.9). If  $q$  and  $f$  are given, then the tensile force  $H$  may be determined by formula (5.10). The relation between these quantities and the length of wire  $s$  along the sag curve may be established with the help of the well-known approximate mathematical formula \*

$$s \approx l \left( 1 + \frac{8f^2}{3l^2} \right) \quad (5.11)$$

Let us return to Fig. 50 and write down one more equilibrium condition for the cut-out portion of the cable, namely, let us equate to zero the sum of projections of all the forces on the  $x$ -axis:

$$-H + T \cos \alpha = 0$$

From this equation we find  $T$ , the tensile force at an arbitrary point:

$$T = \frac{H}{\cos \alpha} \quad (5.12)$$

It is evident from equation (5.12) that force  $T$  increases from the lowest point of the cable towards the supports and is maximum at the suspension points, where the tangent to the sag curve makes the maximum angle with the horizontal axis. This angle is small when the sag is not considerable, therefore we may consider with sufficient accuracy for practical purposes that the cable is subjected to the action of a constant force equal in magnitude to horizontal tension  $H$ . The strength design of a cable is generally carried out for this value. If, however, it is essential to design for the maximum force at the supports,

\* Element of curve length  $ds = dx \sqrt{1 + \left(\frac{dy}{dx}\right)^2}$ ; from formulas (5.8) and (5.10) it follows that  $\frac{dy}{dx} = \frac{qx}{H} = \frac{8fx}{l^2}$ . Therefore

$$ds = dx \left( 1 + \frac{64f^2 x^2}{l^4} \right)^{1/2} \approx dx \left( 1 + \frac{32f^2 x^2}{l^4} \right)$$

After integrating from  $x=0$  to  $x=l/2$  and multiplying by 2, we obtain formula (5.11).

its value for a symmetrical cable is determined in the following manner. The vertical components of support reactions have the same value equal to half of the total load on the cable, i.e.  $\frac{ql}{2}$ . The horizontal components are equal to force  $H$  which is determined by formula (5.10). Total reactions of the supports are obtained as the geometrical sum of these components:

$$T_{\max} = \sqrt{\left(\frac{ql^2}{8f}\right)^2 + \left(\frac{ql}{2}\right)^2} = \frac{ql^2}{8f} \sqrt{1 + \frac{16f^2}{l^2}} = H \sqrt{1 + \frac{16f^2}{l^2}}$$

If the cross-sectional area is denoted by  $A$ , the strength condition for a flexible cable may be written as

$$\sigma = \frac{H}{A} \leq [\sigma]$$

Replacing  $H$  by its value from formula (5.10), we get

$$\frac{ql^2}{8fA} \leq [\sigma]$$

Sag  $f$  can be determined from this formula provided  $l$ ,  $q$ ,  $A$  and  $[\sigma]$  are known. The solution is much simpler if  $q$  is considered to account for the dead weight of the cable only; then  $q = \gamma A$ , where  $\gamma$  is the unit weight of cable material, and

$$f = \frac{\gamma A l^3}{8A [\sigma]} = \frac{\gamma l^3}{8 [\sigma]}$$

i.e. cross-sectional area  $A$  does not affect the value of  $f$ .

B. If the suspension points are at different levels, we find  $f_1$  and  $f_2$  by putting  $x = -a$  and  $x = b$  in equation (5.8):

$$f_1 = \frac{qa^2}{2H}, \quad f_2 = \frac{qb^2}{2H} \quad (5.13)$$

From the second expression we determine tension

$$H = \frac{qb^2}{2f_2} \quad (5.14)$$

Dividing the first expression by the second one, we find

$$\frac{f_1}{f_2} = \frac{a^2}{b^2} \quad \text{or} \quad a = \pm b \sqrt{\frac{f_1}{f_2}}$$

Keeping in view that  $b + a = l$ , we get

$$b \pm b \sqrt{\frac{f_1}{f_2}} = l \quad \text{or} \quad b = \frac{l}{1 \pm \sqrt{\frac{f_1}{f_2}}}$$



Substituting this value for  $b$  in formula (5.14), we finally determine \*

$$H = \frac{ql^2}{2(\sqrt{f_2} \pm \sqrt{f_1})^2} \tag{5.15}$$

Two signs in the denominator indicate that the cable may have two main shapes of sagging. The first mode, corresponding to the smaller value of  $H$  (plus sign before the second root), gives us the peak of the parabola between the cable supports (Fig. 49 and the dashed curve  $AO_1B$  in Fig. 51). At the higher value of tensile force  $H$  (minus sign before the second root) the peak of the parabola will be located to the

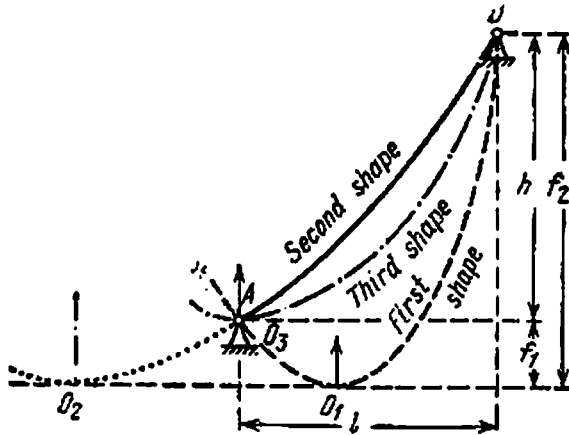


Fig. 51

left of support  $A$  (solid curve  $O_2AB$  in Fig. 51). We get the second mode of the curve.

A third shape (intermediate between the two main) of sag is also possible; it corresponds to the condition  $f_1=0$ . In this case the origin of coordinates  $O_3$  coincides with point  $A$ . One or the other shape will be obtained depending upon the ratio between the length of cable along sag curve  $AOB$  (Fig. 49) and chord  $AB$ .

If sags  $f_1$  and  $f_2$  are not known for a cable hanging from supports at different heights but tension  $H$  is known, then the values of  $a$  and  $b$  as well as sags  $f_1$  and  $f_2$  can be easily determined.

The difference  $h$  in the level of supports (Figs. 49 and 51) is

$$h = f_2 - f_1$$

Let us substitute the values of  $f_1$  and  $f_2$  from equation (5.13) in the above expression and transform it keeping in mind that  $a+b=l$ :

$$h = \frac{qb^2}{2H} - \frac{qa^2}{2H} = \frac{q}{2H} (b^2 - a^2) = \frac{q}{2H} (b+a)(b-a) = \frac{ql}{2H} (b-a)$$

\* The formula for  $H$  in this form was first obtained by Prof. I. Ya. Shtaerman (*Nauka i Tekhnika*, Odessa Polytechnical Institute Journal, 1925).

wherefrom

$$b - a = \frac{2Hh}{ql}$$

and since  $a + b = l$ ,

$$a = \frac{l}{2} - \frac{Hh}{ql} \quad \text{and} \quad b = \frac{l}{2} + \frac{Hh}{ql}$$

It should be noted that for  $a > 0$  the first shape of sag will occur (Fig. 51), at  $a < 0$ , the second shape of sag, and at  $a = 0$ , the third shape. Putting the values of  $a$  and  $b$  in expressions (5.13), we get the values of  $f_1$  and  $f_2$ :

$$f_1 = \frac{ql^2}{8H} + \frac{Hh^2}{2ql^2} - \frac{h}{2}$$

and

$$f_2 = \frac{ql^2}{8H} + \frac{Hh^2}{2ql^2} + \frac{h}{2}$$

C. Let us now see what will happen to a symmetrical cable covering a span  $l$  if its temperature increases to  $t_2$  and the load intensity to  $q_2$  (say, for example, due to ice-covering), the initial temperature and load intensity being  $t_1$  and  $q_1$ , respectively. We assume that in the initial condition either sag  $f_1$  or tension  $H$  is known. [Knowing one of these two quantities we can always determine the other from formula (5.10).]

While calculating the deformation of the cable, which is considerably smaller quantity as compared to the cable length, we make two assumptions: the length of the cable is equal to its span, and tensile force is constant and equal to  $H$ . These assumptions give a small error in gently sloping cables.

In this case the cable elongation due to the increase in temperature will be

$$\Delta s_1 = \alpha (t_2 - t_1) l \quad (5.16)$$

where  $\alpha$  is the linear thermal expansion coefficient of the cable material.

The cable elongates when the temperature increases. This will result in an increase in its sag and, consequently, in accordance with formula (5.10) decrease in its tension. On the other hand, from the same formula (5.10) it is evident that tensile force will increase due to increase in load. Let us assume that the final effect is the lightening of the cable. Then, according to Hooke's law, the elongation of the cable due to increase in tension will be

$$\Delta s_2 = \frac{(H_2 - H_1) l}{EA} \quad (5.17)$$

If  $H_2 < H_1$ ,  $\Delta s_2$  will be negative. When the temperature decreases,  $\Delta s_1$  is negative.

Thus, the length of the cable in its second condition will be the sum of its length in the first condition and the deformations due to the increase in temperature and tensile force:

$$s_2 = s_1 + \Delta s_1 + \Delta s_2 \quad (5.18)$$

The change in the length of the cable will also cause change in its sag. Instead of  $f_1$  it will become  $f_2$ .

Let us now substitute for  $s_1$  and  $s_2$  in equation (5.18) their expressions from formula (5.11), and for the deformations  $\Delta s_1$  and  $\Delta s_2$  their values from formulas (5.16) and (5.17). Then equation (5.18) takes the following form:

$$l \left( 1 + \frac{8f_2^2}{3l^2} \right) = l \left( 1 + \frac{8f_1^2}{3l^2} \right) + \alpha (t_2 - t_1) l + \frac{H_2 - H_1}{EA} l \quad (5.19)$$

Replace  $f_1$  and  $f_2$  by their values from formula (5.19):

$$f_1 = \frac{q_1 l^2}{8H_1} \quad \text{and} \quad f_2 = \frac{q_2 l^2}{8H_2}$$

After certain transformations, equation (5.19) may be written in the form

$$H_2^3 = \left[ \frac{EAq_1^2 l^3}{24H_1^2} + EA\alpha(t_2 - t_1) - H_1 \right] H_2^2 - \frac{EAq_2^2 l^2}{24} = 0 \quad (5.20)$$

Having determined tension  $H_2$  from equation (5.20), we can find  $f_2$  from formula (5.9).

If the transition from the first condition to the second one occurs only due to a change of temperature without any change in the load, then in equation (5.20) load intensity  $q_2$  is replaced by  $q_1$ . If the transition occurs only due to a change in the load intensity without a change of temperature, the middle term in the square bracket is equated to zero.

Obviously, equation (5.20) is also valid for decrease in temperature and reduction in load intensity.

When the sag is not small compared to the length of span, the formulas derived above strictly speaking are not valid, because the actual sag curve—catenary—will differ appreciably from the parabola obtained by assuming uniform load distribution over the span and not over the length of the cable, what in reality takes place.

Accurate calculations reveal that the errors in the value of  $H$  are as follows: for  $\frac{f}{l} < \frac{1}{20}$  the error does not exceed 0.3%, for  $\frac{f}{l} = \frac{1}{10}$ , the error reaches 1.3%, and for  $\frac{f}{l} = \frac{1}{5}$  the error is slightly more than 5%.

## CHAPTER 6

## Compound Stressed State. Stress and Strain

## § 27. Stresses Along Inclined Sections Under Axial Tension or Compression (Uniaxial Stress)

In the preceding sections, while testing the strength of a stretched or compressed bar, we determined stresses only in a section perpendicular to its axis. However, proper evaluation of the critical stresses in the bar is possible only if we know its state completely; this requires the ability to calculate stresses not only in sections perpendicular to the axis.

Let us calculate stresses acting in an arbitrarily inclined section. Let us consider a prismatic bar stretched by forces  $P$  (Fig. 52). Suppose



Fig. 52

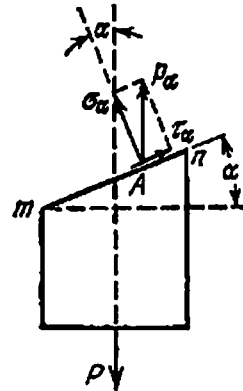
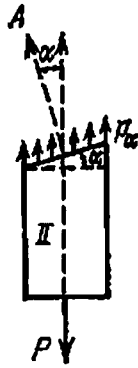


Fig. 53

the bar is cut into two portions  $I$  and  $II$  by plane  $mn$  forming angle  $\alpha$  with cross section  $mk$  perpendicular to the axis. The normals to these sections also form the same angle.

Let us assume that angle  $\alpha$  is positive if  $mk$  coincides with  $mn$  when rotated counterclockwise. We shall call normal  $OA$  directed outwards with respect to the cut-off portion of the bar the outer normal to section  $mn$ . Let us denote the cross-sectional area  $mk$  by  $A_0$ , and the area of section  $mn$  by  $A_\alpha$ .

To determine the stresses transmitted through the given section from the upper portion ( $I$ ) to the lower portion ( $II$ ), we imagine the upper portion to be removed and its action on the lower portion replaced by stresses  $p_\alpha$ . To maintain the equilibrium of the lower portion, stresses  $p_\alpha$  must compensate for force  $P$  and must be directed parallel to the axis of the bar. It is evident that the stresses are not perpendicular to the plane on which they are acting. Their value will also differ from that in section  $mk$ .

Assuming that at a sufficient distance from the point of application of external forces  $P$  stresses  $p_\alpha$  are uniformly distributed over section  $mn$ , we find

$$p_\alpha = \frac{P}{A_\alpha}$$

But since  $A_\alpha = \frac{A}{\cos \alpha}$ ,

$$p_\alpha = \frac{P \cos \alpha}{A_0} = \sigma_0 \cos \alpha$$

where  $\sigma_0 = \frac{P}{A_0}$  is the normal stress in section  $mk$  perpendicular to the direction of the tensile force.

The magnitude of stresses  $p_\alpha$  changes with angle  $\alpha$ . In order that we may have to study only one and the same type of stresses irrespective of angle  $\alpha$ , we resolve stresses  $p_\alpha$  into two components: one in plane  $mn$  and the other in a plane perpendicular to it (Fig. 53). Thus,

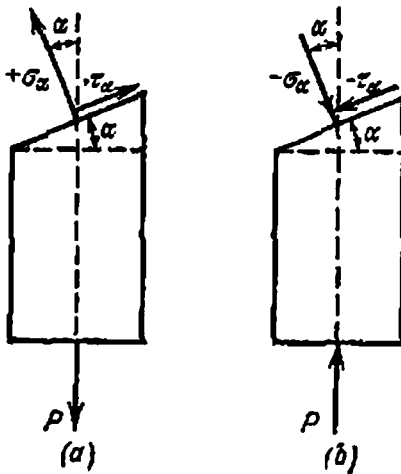


Fig. 54

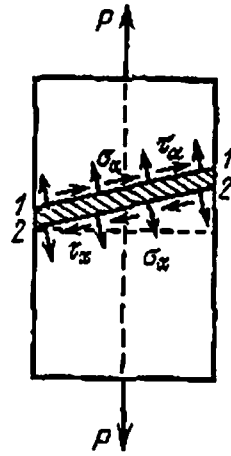


Fig. 55

stress  $p_\alpha$  acting at point  $A$  of plane  $mn$  may be replaced by two mutually perpendicular stresses: normal stress  $\sigma_\alpha$  and shearing stress  $\tau_\alpha$ . The magnitude of these stresses will depend upon angle  $\alpha$  which the normal to the section forms with the direction of the tensile force. From Fig. 53 we have

$$\sigma_\alpha = p_\alpha \cos \alpha = \sigma_0 \cos^2 \alpha \tag{6.1}$$

$$\tau_\alpha = p_\alpha \sin \alpha = \sigma_0 \sin \alpha \cos \alpha = \frac{1}{2} \sigma_0 \sin 2\alpha \tag{6.2}$$

Let us lay down the following conditions as regards the signs of stresses  $\sigma_\alpha$  and  $\tau_\alpha$ . Tensile stresses  $\sigma_\alpha$ , i.e. stresses coinciding with the direction of the outer normal will be considered positive; normal stres-

ses in the opposite direction, i.e. compressive stresses, will be considered negative.

We will consider the shearing stresses positive if their direction is such that the outer normal has to be rotated clockwise to make it coincide with them. The reverse direction of  $\tau_\alpha$  will be considered negative.

Figure 54 shows the accepted convention as regards the signs of  $\alpha$ ,  $\sigma$ , and  $\tau$ .

We always have only two types of stresses acting at every point of the cutting plane irrespective of its angle of inclination  $\alpha$ : normal and shearing.

Figure 55 shows these stresses acting on a thin layer of the material (hatched in the figure) cut out of the stretched bar by two parallel sections 1-1 and 2-2. Each of the planes experiences normal tensile stresses  $\sigma_\alpha$  as well as shearing stresses  $\tau_\alpha$  which make sections 1-1 and 2-2 shear one parallel to the other.

It means that the two types of stresses correspond to two types of deformations: lengthwise deformation (elongation or shortening) and shear. Corresponding to these two types of deformations we have two modes of failure of the material: by *breaking away* and by *shearing*.

To check the strength of the material, it is essential to determine the *maximum* values of  $\sigma_\alpha$  and  $\tau_\alpha$  depending upon the location of plane *mn*.

It follows from formulas (6.1) and (6.2) that  $\sigma_\alpha$  reaches its maximum value when  $\cos^2 \alpha$  is equal to unity, i.e.  $\alpha=0$ . The maximum value of  $\tau_\alpha$  is obtained when  $\sin 2\alpha=1$ , i.e. when  $2\alpha=90^\circ$  or  $\alpha=45^\circ$ . The maximum values of  $\sigma_\alpha$  and  $\tau_\alpha$  will be

$$\max \sigma_\alpha = \sigma_0 = \frac{P}{A_0}, \quad \max \tau_\alpha = \frac{\sigma_0}{2} \quad (6.3)$$

Hence, the maximum normal stresses are acting in sections perpendicular to the axis of the bar; the maximum shearing stresses act in sections forming an angle of  $45^\circ$  with the axis of the bar and are half of the maximum value of the normal stresses.

A logical question that arises is for which of these stresses should the bar be tested, which of these stresses plays the decisive role in the failure of material. These points will be discussed in detail in Chapter 7.

## § 28. Concept of Principal Stresses.

### Types of Stresses of Materials

In the preceding chapters we got acquainted with the behaviour of materials under axial (or, as it is often called, simple) tension or compression. However, there may be cases in practice when the element is subjected to tension or compression in two or three directions under the action of external forces, i.e. it finds itself in a composite stressed state.

In § 27 we showed that even under simple tension two types of stresses are possible: normal  $\sigma$  and shearing  $\tau$ . It follows from formulas (6.1) and (6.2) that in sections perpendicular to the axis of the stretched bar ( $\alpha=0$ ), we have only normal stresses ( $\tau=0$ ), and in sections parallel to its axis ( $\alpha=90^\circ$ ), we have neither normal nor shearing stresses ( $\sigma=0$  and  $\tau=0$ ).

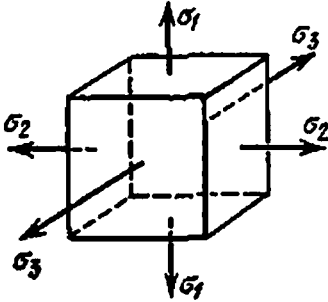


Fig. 56

The planes in which the shearing stresses are totally absent are called *principal planes*; the normal stresses acting in these planes are called *principal stresses*.

It has been proved in the theory of elasticity that three mutually perpendicular principal planes through which three principal (normal) stresses are transferred can be drawn through an arbitrary point of a stressed body. Two of them have extreme values: one is the maximum normal stress, the other is the minimum normal stress; the third prin-

incipal stress is intermediate between the above two. In every point of a stressed body we can isolate an elementary cube whose faces are the principal planes. The cube material is stretched or compressed by three mutually perpendicular principal stresses which are transmitted through the principal planes (Fig. 56).

In the case of simple tension (§ 27) one principal plane at every point is perpendicular to the bar axis ( $\alpha=0^\circ$ ), and the other two are parallel to it ( $\alpha=90^\circ$ ). Since the normal stress is not zero ( $\sigma_\alpha \neq 0$ ) in the first principal plane and in the other two it vanishes, it may be concluded that in simple tension and compression out of the three principal stresses only one is not equal to zero at any point of the bar; this principal stress is parallel to the tensile force and the bar axis. This stress of the material is called *uniaxial*. The element isolated from the bar is deformed in only one direction.

There are cases when the cubic element of the material is subjected to tension or compression in two mutually perpendicular directions or even in all three directions (Fig. 56). When two principal stresses are not equal to zero, the material is said to be in *biaxial (plane) stress*. When all the three principal stresses are not equal to zero in the given point, this pertains to the most general case of stress distribution in the material, the *triaxial (volumetric) stress*; the elementary cube is subjected to tension or compression in all three mutually perpendicular directions.

In future we shall denote the principal stresses by  $\sigma_1$ ,  $\sigma_2$  and  $\sigma_3$ .

The order of numbering the principal stresses will be set in such a way that  $\sigma_1$  represents the maximum stress in algebraic value, and  $\sigma_3$  the minimum one. The compressive stresses will be taken, as before, negative. Therefore, if, for example, the principal stresses have the values of  $+1000 \text{ kgf/cm}^2$ ,  $-600 \text{ kgf/cm}^2$ , and  $+400 \text{ kgf/cm}^2$ , the numeration should be

$$\sigma_1 = +1000 \text{ kgf/cm}^2, \quad \sigma_2 = +400 \text{ kgf/cm}^2, \quad \sigma_3 = -600 \text{ kgf/cm}^2$$

then the condition  $\sigma_1 > \sigma_2 > \sigma_3$  will be satisfied.

Thus, we distinguish three kinds of stressed states:

1. triaxial stress, when all the three principal stresses are not equal to zero (for example, tension or compression in three mutually perpendicular directions);
2. biaxial stress, when one principal stress is equal to zero (tension or compression in two directions);
3. uniaxial stress, when two principal stresses are equal to zero (tension or compression in one direction).

In § 27 we studied the stress distribution in uniaxial stressed state; below we give examples of planar and volumetric stressed states explaining how stresses are distributed in different planes in these cases.

## § 29. Examples of Biaxial and Triaxial Stresses. Design of a Cylindrical Reservoir

A. As an example of a composite stressed state we shall consider the stresses in the material of a thin-walled cylindrical reservoir which is filled with gas, steam or water at pressure of  $q$  atm, i.e.  $q \text{ kgf/cm}^2$ . The

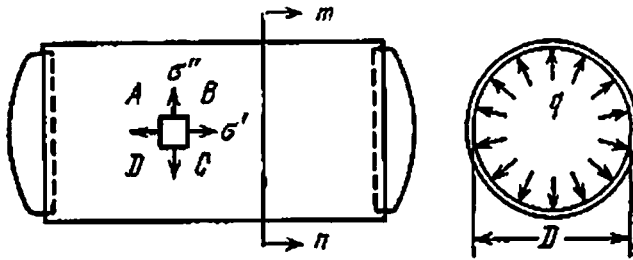


Fig. 57

side walls and the bottom of the reservoir are subjected to a uniformly distributed pressure  $q$ . The dead weight of the fluid in the reservoir is ignored.

The pressure on the bottom will tend to break the cylindrical portion across the cross section; on the other hand, the pressure on the side walls will tend to burst the reservoir along the generatrix of the cylinder. Thus, if we isolate rectangular element ABCD from the cylindrical portion of the reservoir, this element will be subjected to tension



in two directions: by stresses  $\sigma'$  in sections perpendicular to the generatrix and stresses  $\sigma''$  in sections along the generatrix (Fig. 57).

The method of sections will be employed for calculating stresses  $\sigma'$  and  $\sigma''$ . Suppose the internal diameter of the reservoir is  $D$ , and the thickness of its walls is  $l$ . We shall consider  $l$  to be small as compared to  $D$  ( $l < \frac{D}{20}$ ).

Let us imagine the reservoir (Fig. 57) cut along the plane and consider the equilibrium of the cutoff part, for instance, the right one

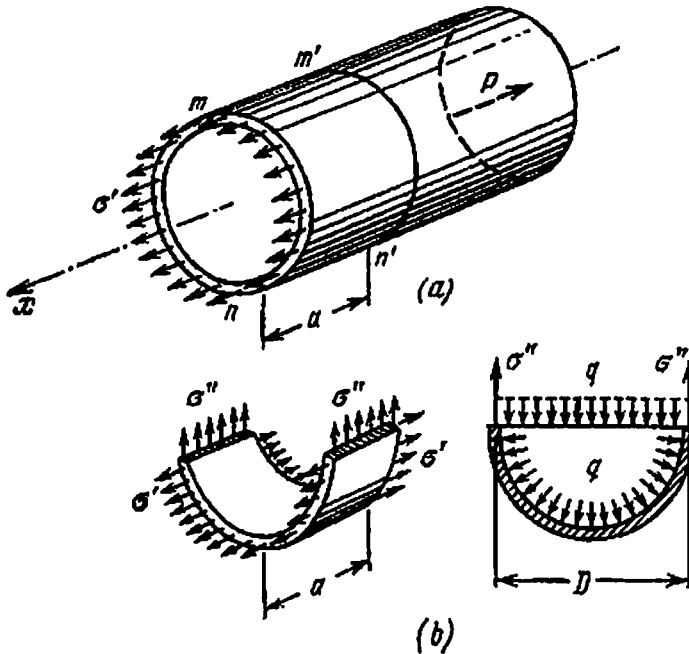


Fig. 58

(Fig. 58 (a)). The resultant of the forces acting on the bottom and stretching the cylindrical portion of the reservoir along the generatrix is

$$P = q \frac{\pi D^2}{4}$$

The area of the ring (a thin strip of thickness  $l$  and approximate length  $\pi D$ ) upon which this force acts is

$$A \approx l\pi D$$

Hence normal stress in this section is:

$$\sigma' = \frac{P}{A} = \frac{q \frac{\pi D^2}{4}}{l\pi D} = \frac{qD}{4l}$$

Stresses  $\sigma''$  in sections parallel to the cylinder generatrix will be found by isolating a ring at some distance from the reservoir bottom cut by sections  $mn$  and  $m'n'$  at a distance  $a$  from each other and by considering a diametrical section of this ring (Fig. 58 (b)). The diametrical surface of the gas (or fluid) experiences a pressure  $q$  which has a resultant  $P_1 = qDa$ . The area of the diametrical section (two walls) which bears this pressure is  $A_1 = 2la$ , and stresses in the walls are

$$\sigma'' = \frac{qDa}{2la} = \frac{qD}{2l}$$

These stresses are two times greater than stresses  $\sigma'$  acting in the ring section.

Since there are no shearing stresses in the ring and diametrical sections, the sections  $A$  and  $A_1$  qualify as principal planes, and stresses  $\sigma'$  and  $\sigma''$  as principal stresses. The third principal stress  $\sigma''' = -q$  acting on the reservoir wall in the radial direction is negligibly small as compared to  $\sigma'$  and  $\sigma''$ ; it may therefore be considered equal to zero.

Consequently, element  $ABCD$  cut out of the reservoir wall (Fig. 57) is subjected to plane stress (biaxial tension). In accordance with the accepted numeration, the principal stresses are

$$\sigma_1 = \frac{qD}{2l}, \quad \sigma_2 = \frac{qD}{4l} \quad \text{and} \quad \sigma_3 = 0 \quad (6.4)$$

Biaxial state of stress also occurs in spherical, conical and other thin-walled vessels, plates, various types of shells, etc.

**B.** The example of a triaxial stress is transfer of pressure from the balls to the race in a ball-bearing or from the wheels of a rolling stock to the rails.

As the contact between the rail head and the tyre may be looked upon as that between two cylinders of different diameters and crosswise generatrices, these surfaces must touch each other at a point. The normal stresses arising at the point of contact when pressure is transmitted from one body to the other are known as contact stresses.

When force is transmitted, the materials of the tyre and the rail get deformed around the point of contact, and pressure is transferred through a contact surface of elliptical shape. The area of contact depends upon the pressure and the radii of the contacting surfaces. If we cut out a small cube (for example, with sides of 1 mm) of the rail material at the centre of the contacting surface, and if the faces of this cube are parallel and perpendicular to the rail axis (Fig. 59), then the stresses acting on the faces will be normal compressive\*. Thus (Fig. 59 (b)) we have three mutually perpendicular planes loaded by principal stresses  $\sigma'$ ,  $\sigma''$ , and  $\sigma'''$ . The emergence of lateral stresses

\* These stresses are calculated in the theory of elasticity.

$\sigma''$  and  $\sigma'''$  can be explained as follows: under the action of stress  $\sigma'$  perpendicular to the plane of transmission of pressure, the cube material tends to expand laterally, and this results in reactions  $\sigma''$  and  $\sigma'''$  from the rail material surrounding the cube, that hinder transverse deformation.

The computed values of these stresses\* show that they actually attain high values. Thus, for example, the values of  $\sigma'$ ,  $\sigma''$ ,  $\sigma'''$  at the contact between the locomotive runner and rail are

$$\sigma' = -110 \text{ kgf/mm}^2, \quad \sigma'' = -90 \text{ kgf/mm}^2, \quad \sigma''' = -80 \text{ kgf/mm}^2$$

By applying the convention of numeration of principal stresses to this example, we get

$$\begin{aligned} \sigma_1 = \sigma''' &= -80 \text{ kgf/mm}^2, & \sigma_2 = \sigma'' &= -90 \text{ kgf/mm}^2, \\ \sigma_3 = \sigma' &= -110 \text{ kgf/mm}^2 \end{aligned}$$

In the given example all the three principal stresses are negative. This is a case of triaxial compression. An example of triaxial tension is the yielding of material at the neck in a specimen subjected to ten-

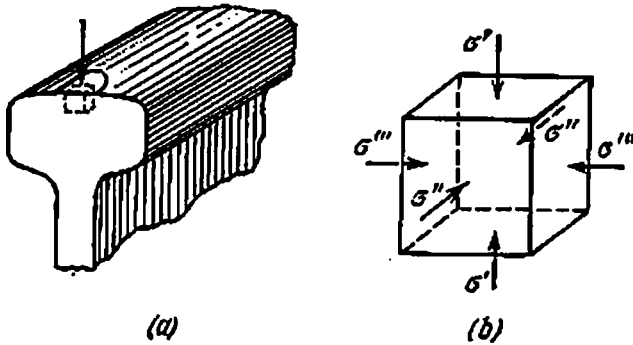


Fig 59

sion. We also often come across cases of composite triaxial stressed state in which the principal stresses have opposite signs:  $\sigma_1 > 0$  and  $\sigma_3 < 0$  (for instance, in the wall of a thick-walled boiler).

The triaxial stressed state is the most general state of stress at a point; the biaxial and uniaxial stressed states are the particular cases when one or two of the three principal stresses become equal to zero.

\* N. M. Belyaev, "Computation of maximum design stresses in compression of contacting bodies", in *Proceedings of the Leningrad Institute of Railroad Engineers*, issues 99 and 102 (1929).

### § 30. Stresses in a Biaxial Stressed State

It is essential to determine the maximum normal and shearing stresses to check the strength of a material in biaxial or triaxial stress.

Let us begin with the biaxial stress. Let us assume that principal stresses  $\sigma_1$  and  $\sigma_2$  are acting on the side faces of a right-angled parallelepiped (Fig. 60). Both these stresses are tensile. There are no stresses on the front faces of the element; therefore the third principal stress is zero. If one of the principal stresses  $\sigma_1$ ,  $\sigma_2$  or both are compressive,

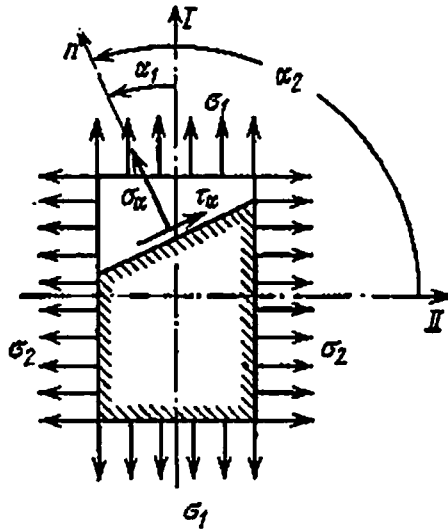


Fig. 60

then their values in the succeeding formulas must be taken with a minus sign, and the numeration should be altered in accordance with the order given in § 28. Thus, if one of the principal stresses is tensile and the other is compressive, then the first will have to be numbered  $\sigma_1$  and the second  $\sigma_2$ ; if both of the stresses are compressive, then the stress having lower absolute value will have to be numbered  $\sigma_2$ , and the greater  $\sigma_1$ .

Our aim is to determine the maximum normal and shearing stresses in sections perpendicular to the front faces.

Let us draw a section the normal to which forms angle  $\alpha_1$  with direction  $I$  (Fig. 60). The same normal forms angle  $\alpha_2$  with direction  $II$ . This section will be subjected to both normal stress  $\sigma_x$  and shearing stress  $\tau_x$ , which depend upon  $\sigma_1$  and  $\sigma_2$ . Their values can be obtained by studying the action of  $\sigma_1$  and  $\sigma_2$  separately and summing up the results. The fraction of the normal stress caused by  $\sigma_1$  may be expressed according to formula (6.1) as  $\sigma_1 \cos^2 \alpha_1$ ; the other fraction of  $\sigma_x$ , caused by stress  $\sigma_2$ , may be written according to the same formula as

$\sigma_2 \cos^2 \alpha_2$ . The total normal stress then becomes

$$\sigma_\alpha = \sigma_1 \cos^2 \alpha_1 + \sigma_2 \cos^2 \alpha_2 = \sigma_1 \cos^2 \alpha_1 + \sigma_2 \cos^2 (\alpha_1 + 90^\circ)$$

or

$$\sigma_\alpha = \sigma_1 \cos^2 \alpha_1 + \sigma_2 \sin^2 \alpha_1 \tag{6.5}$$

By similar reasoning and with the help of formula (6.2) we may find the shearing stresses in the given section:

$$\tau_\alpha = \frac{1}{2} [\sigma_1 \sin 2\alpha_1 + \sigma_2 \sin 2\alpha_2] = \frac{1}{2} [\sigma_1 \sin 2\alpha_1 + \sigma_2 \sin 2(\alpha_1 + 90^\circ)]$$

or

$$\tau_\alpha = \frac{\sigma_1 - \sigma_2}{2} \sin 2\alpha_1 \tag{6.6}$$

In these formulas angle  $\alpha_1$  has been measured from the direction of axis  $l$  (stress  $\sigma_1$ ) up to the normal to the given section by rotating counterclockwise. We shall follow the rules laid down earlier in § 27 in choosing proper signs for  $\sigma_\alpha$  and  $\tau_\alpha$  as well as for angles  $\alpha_1$  and  $\alpha_2$ .

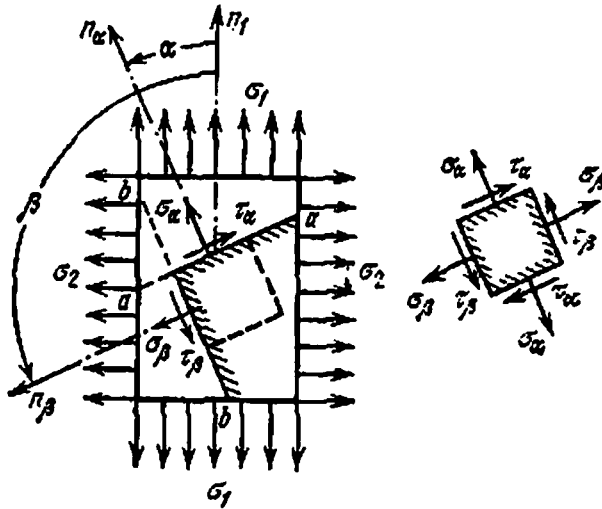


Fig. 61

In future, in formulas giving the values of  $\sigma_\alpha$  and  $\tau_\alpha$  we shall denote  $\alpha_1$  by  $\alpha$ , always measuring it from the maximum (algebraic) principal stress in the anticlockwise direction.

Employing formulas (6.5) and (6.6) which give the stresses in section  $a-a$  (Fig. 61), we can easily determine the stresses in perpendicular section  $b-b$  which has normal  $n_\beta$  forming angle  $\beta = \alpha + 90^\circ$  with the

direction of the maximum principal stress:

$$\left. \begin{aligned} \sigma_{\beta} &= \sigma_1 \cos^2 \beta + \sigma_2 \sin^2 \beta = \sigma_1 \cos^2 (\alpha + 90^\circ) + \sigma_2 \sin^2 (\alpha + 90^\circ) \\ \sigma_{\beta} &= \sigma_1 \sin^2 \alpha + \sigma_2 \cos^2 \alpha \end{aligned} \right\} (6.5')$$

$$\left. \begin{aligned} \tau_{\beta} &= \frac{\sigma_1 - \sigma_2}{2} \sin 2\beta = \frac{\sigma_1 - \sigma_2}{2} \sin (2\alpha + 180^\circ) \\ \tau_{\beta} &= -\frac{\sigma_1 - \sigma_2}{2} \sin 2\alpha \end{aligned} \right\} (6.6')$$

The formulas derived above clarify the properties of stresses acting in mutually perpendicular planes. For normal stresses we have

$$\begin{aligned} \sigma_{\alpha} &= \sigma_1 \cos^2 \alpha + \sigma_2 \sin^2 \alpha \\ \sigma_{\beta} &= \sigma_1 \sin^2 \alpha + \sigma_2 \cos^2 \alpha \end{aligned}$$

Summing up, we get

$$\sigma_{\alpha} + \sigma_{\beta} = \sigma_1 + \sigma_2 = \text{const} \quad (6.7)$$

i.e. the sum of normal stresses in two mutually perpendicular planes is constant and equal to the sum of the principal stresses.

For the shearing stresses, by comparing (6.6) and (6.6'), we get

$$\tau_{\beta} = -\tau_{\alpha} \quad (6.8)$$

Hence, the shearing stresses in two mutually perpendicular planes are equal in magnitude but opposite in sign. This property is generally called the *law of complementary shearing stresses*, this law being valid in all cases in which shearing stresses are acting.

The system of stresses  $\sigma_{\alpha}$ ,  $\sigma_{\beta}$ ,  $\tau_{\alpha}$ ,  $\tau_{\beta}$  depicted in Fig. 61 acts on the faces of an elementary parallelepiped turned through angle  $\alpha$  with respect to the directions of principal stresses  $\sigma_1$  and  $\sigma_2$ . The pair of shearing stresses that tends to rotate the element in the clockwise direction will be considered positive. In Fig. 61 these stresses are denoted by  $\tau_{\alpha}$ . It should be noted that this rule for choosing the sign for  $\tau$  coincides with the convention already decided upon (§ 27).

It is evident from formulas (6.5) and (6.6) that the normal and shearing stresses in a plane depend upon its inclination.

Let us study expression (6.5) for maximum to determine the maximum normal stress. By differentiating with respect to  $\alpha$  and equating the first derivative to zero, we get

$$\frac{d\sigma_{\alpha}}{d\alpha} = -2\sigma_1 \cos \alpha \sin \alpha + 2\sigma_2 \sin \alpha \cos \alpha = 0$$

or

$$\frac{d\sigma_{\alpha}}{d\alpha} = -(\sigma_1 - \sigma_2) \sin 2\alpha = 0 \quad (6.9)$$

A comparison of expressions (6.9) and (6.6) reveals that the condition for maximum of  $\sigma_\alpha$  is the same as obtained by equating to zero the shearing stresses in the corresponding planes. From the same expression it follows that  $\sigma_\alpha = \sigma_1 \cos^2 \alpha + \sigma_2 \sin^2 \alpha$  is maximum either for  $\alpha = 0$  or for  $\alpha = 90^\circ$ . Since  $\sigma_1 > \sigma_2$ , then

$$\begin{aligned} \max \sigma_\alpha &= \sigma_1 && (\text{at } \alpha = 0) \\ \min \sigma_\alpha &= \sigma_2 && (\text{at } \alpha = 90^\circ) \end{aligned}$$

i.e. the maximum and minimum normal stresses at the given point are the principal stresses  $\sigma_1$  and  $\sigma_2$  acting in mutually perpendicular planes free of shearing stresses.

It is evident from formula (6.6) that the maximum shearing stress is

$$\max \tau_\alpha = \frac{\sigma_1 - \sigma_2}{2} \quad (\text{at } \sin 2\alpha = 1, \text{ i.e. at } \alpha = 45^\circ) \quad (6.10)$$

Hence, the maximum shearing stress is half of the difference of the principal stresses and acts in planes inclined at  $45^\circ$  to the principal ones and perpendicular to the plane of the diagram. In planes parallel to  $\sigma_2$ , the maximum shearing stress is

$$\max \tau_2 = \frac{\sigma_1}{2} \quad (6.10')$$

### § 31. Graphic Determination of Stresses (Mohr's Circle)

The calculation of  $\sigma_\alpha$  and  $\tau_\alpha$  from formulas (6.5) and (6.6) may be replaced by graphic determination (Fig. 62).

Let us take a rectangular coordinate system with axes  $\sigma$  and  $\tau$ . The  $\sigma$ -axis directed to the right is taken positive. On the  $\sigma$ -axis we plot

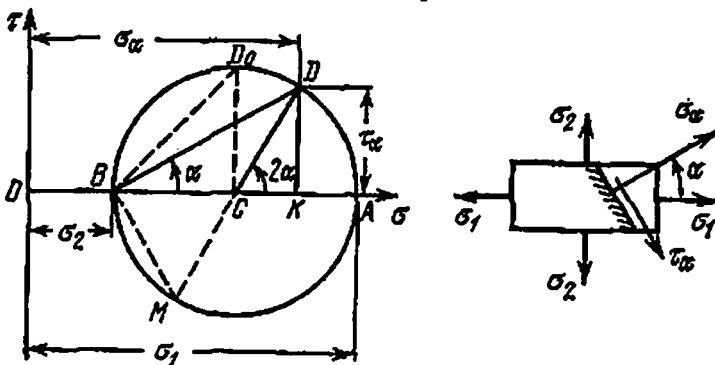


Fig. 62

segments  $OA$  and  $OB$  representing in a certain scale the numerical values of  $\sigma_1$  and  $\sigma_2$  (it is convenient to draw the  $\sigma$ -axis parallel to the maximum principal stress  $\sigma_1$ ).

In Fig. 62 both these stresses are considered tensile and are laid off on the  $\sigma$ -axis in the positive direction. Had one or both of the stresses been compressive, we would have laid them off in the opposite direction. Taking segment  $AB$  as the diameter, we draw a circle with the centre at  $C$ , which is called the stress circle (Mohr's circle). To determine normal stress  $\sigma_\alpha$  and shearing stress  $\tau_\alpha$  in a plane the normal to which makes angle  $\alpha$  with the maximum principal stress  $\sigma_1$ , we must draw a central angle  $2\alpha$  at point  $C$ , plotting its positive value from the  $\sigma$ -axis counterclockwise. Point  $D$  of the stress circle will correspond to the required plane; its coordinates  $OK$  and  $DK$  will be equal to  $\sigma_\alpha$  and  $\tau_\alpha$ , respectively. This can be easily proved. From the diagram, the radius of the stress circle is

$$CD = AC = BC = \frac{AB'}{2} = \frac{OA - OB}{2} = \frac{\sigma_1 - \sigma_2}{2}$$

From the right-angled triangle  $KDC$  we have

$$DK = CD \sin 2\alpha = \frac{\sigma_1 - \sigma_2}{2} \sin 2\alpha = \tau_\alpha$$

Further

$$\begin{aligned} OK &= OB + BC + CK = \sigma_2 + \frac{\sigma_1 - \sigma_2}{2} + \frac{\sigma_1 - \sigma_2}{2} \cos 2\alpha \\ &= \sigma_2 + \frac{\sigma_1 - \sigma_2}{2} (1 + \cos 2\alpha) = \sigma_2 + \frac{\sigma_1 - \sigma_2}{2} 2 \cos^2 \alpha \\ &= \sigma_2 + \sigma_1 \cos^2 \alpha - \sigma_2 \cos^2 \alpha = \sigma_1 \cos^2 \alpha + \sigma_2 \sin^2 \alpha = \sigma_\alpha \end{aligned}$$

Thus, the coordinates of points on the circle determine the stresses. The values of  $\sigma_\alpha$  are measured by the segments along the  $\sigma$ -axis. Positive values of  $\sigma_\alpha$  are plotted in the positive direction of the  $\sigma$ -axis. The values of  $\tau_\alpha$  are measured by the segments parallel to the  $\tau$ -axis. Positive values of  $\tau_\alpha$  are directed upwards, because according to the convention decided upon by us, the values of  $\alpha$  between 0 and 90° correspond to positive values of  $\tau_\alpha$ ; this is also obvious from the formula

$$\tau_\alpha = \frac{\sigma_1 - \sigma_2}{2} \sin 2\alpha$$

in which the maximum principal stress is taken as  $\sigma_1$ .

Having determined stresses  $\sigma_\alpha$  and  $\tau_\alpha$  from the stress circle, let us represent them on the diagram of the cutoff element, taking care of their signs (Fig. 62). Let us recapitulate that we have decided to plot angle  $\alpha$  specifying the location of the outer normal to the cutting plane always from the line of action of the maximum (algebraic) principal stress. Let us therefore bring the direction of the maximum principal stress  $\sigma_1$  in line with the  $\sigma$ -axis on the stress circle. Then line  $BD$  inclined at an angle  $\alpha$  to the  $\sigma$ -axis will be parallel to the normal to the cutting plane, i.e. parallel to  $\sigma_\alpha$ . Line  $BM$  will be parallel to  $\tau_\alpha$ .



As is clear from Fig. 62, the maximum shearing stress is equal to segment  $CD_0$ , i.e. the radius of the stress circle:

$$\max \tau_\alpha = \frac{\sigma_1 - \sigma_2}{2}$$

angle  $2\alpha$  corresponding to this condition is  $90^\circ$  and, consequently,  $\alpha=45^\circ$ . In the stress circle  $\max \tau_\alpha$  is represented by the ordinate  $CD_0$  whose abscissa is  $OC = \frac{\sigma_1 + \sigma_2}{2}$ , i.e. in the plane where  $\tau_\alpha = \tau_{\max}$ , the normal stress has an average value.

It is similarly clear from Fig. 62 that the maximum normal stress is represented by segment  $OA$  which is equal to  $\sigma_1$ , and the minimum, by segment  $OB$  equal to  $\sigma_2$ . It ensues that the normal stress in any plane at an angle  $\alpha$  must be between the principal stresses  $\sigma_1$  and  $\sigma_2$ .

Thus, knowing the principal stresses at a point of a body in biaxial stress we can find the stresses and their directions in any other plane passing through this point with the help of Mohr's circle.

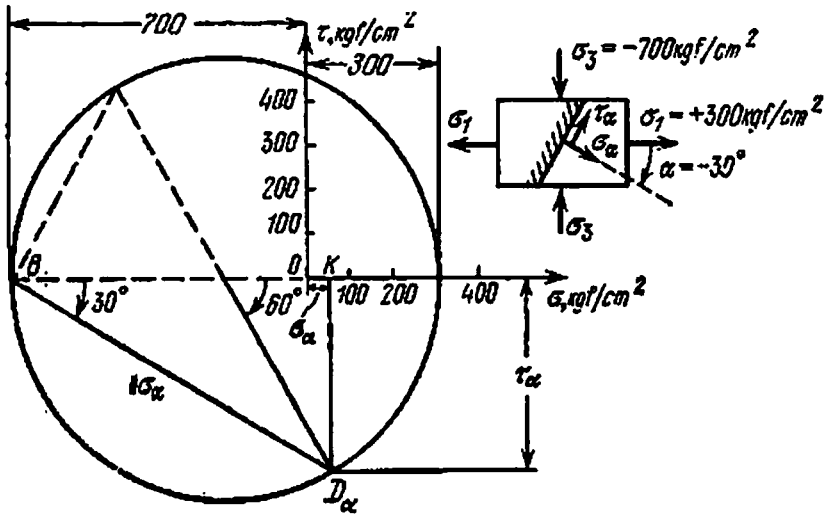


Fig. 63

Let, for example, the principal stresses at some point of the material be  $\sigma_1=300 \text{ kgf/cm}^2$  and  $\sigma_2=-700 \text{ kgf/cm}^2$ . We shall find the normal and shearing stresses in a plane inclined at  $\alpha=-30^\circ$  to the direction of  $\sigma_1$ . The construction is shown in Fig. 63. For the chosen scale the stresses were found to be  $\sigma_\alpha=50 \text{ kgf/cm}^2$  and  $\tau_\alpha=-430 \text{ kgf/cm}^2$ . Their directions are shown in Fig. 63 on the right.

If the principal stresses  $\sigma_1$  and  $\sigma_2$  are known, then with the help of the stress circle we can determine the stresses in two mutually perpendicular sections  $a-a$  and  $b-b$  the normals to which (Fig. 64) make angles  $\alpha$  and  $\beta$ , respectively, with the direction of the maximum principal stress  $\sigma_1$ .

Let us plot angle  $2\alpha$  at point  $C$  of the stress circle (Fig. 64). Point  $D_\alpha$  will correspond to section  $a-a$ , and segments  $D_\alpha K_\alpha$  and  $OK_\alpha$  will represent the respective shearing and normal stresses in the plane.

To determine the stresses in section  $b-b$  we must plot angle  $2\beta$ , i.e. add  $180^\circ$  to angle  $2\alpha$ . All that is required for that is to extend radius  $CD_\alpha$ ; point  $D_\beta$  will correspond to section  $b-b$ .

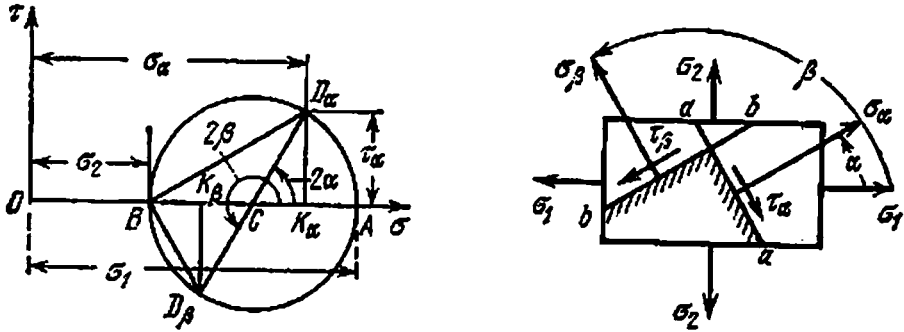


Fig. 64

Stresses  $\tau_\beta$  and  $\sigma_\beta$  are represented by segments  $D_\beta K_\beta$  and  $OK_\beta$ , respectively. It is clear from the diagram that  $\tau_\beta = -\tau_\alpha$  and

$$\sigma_\alpha + \sigma_\beta = \sigma_1 + \sigma_2 = \text{const}$$

The stresses acting on the faces of the element cut by planes  $a$  and  $b$  are shown in Fig. 64 on the right.

By bringing in line the direction of the maximum (algebraically) principal stress  $\sigma_1$  with the  $\sigma$ -axis on the stress circle (Fig. 64), we

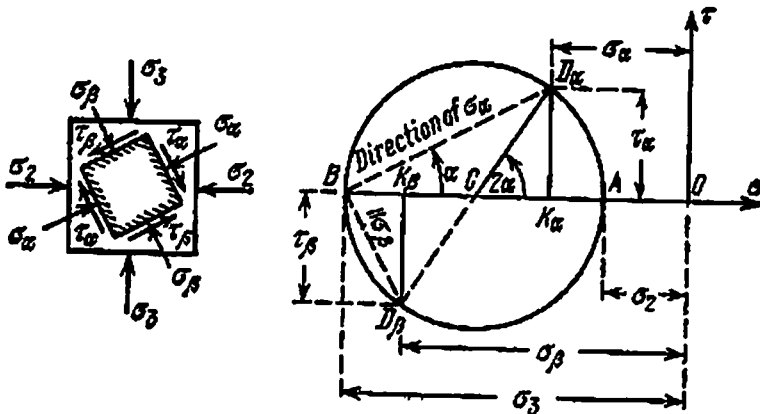


Fig. 65

find that line  $BD_\alpha$  joining the extreme left point of the circle with point  $D_\alpha$  is parallel to stress  $\sigma_\alpha$ , and line  $BD_\beta$  is parallel to stress  $\sigma_\beta$ . The arrows are put in accordance with the signs obtained.

Figure 65 shows how to construct Mohr's circle when both of the principal stresses are compressive.

§ 32. Determination of the Principal Stresses with the Help of the Stress Circle

Sometimes it is required to solve a problem opposite to the one discussed in the preceding section, i.e. determine the principal stresses if the stresses  $\sigma_\alpha, \tau_\alpha, \sigma_\beta,$  and  $\tau_\beta$  are known. The easiest way of doing that is by plotting Mohr's circle.

Assume that the normal and shearing stresses in two mutually perpendicular planes having normals  $n_x$  and  $n_y$  are known (Fig. 66). Let

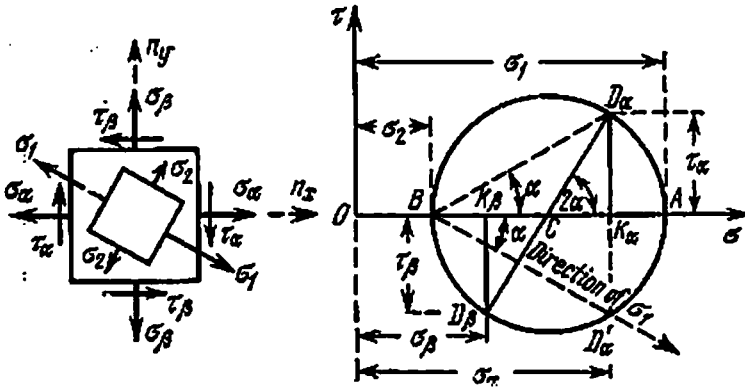


Fig. 66

us denote the normal stresses in the vertical plane ( $n_x$ ) by  $\sigma_\alpha$ , and in the horizontal plane, by  $\sigma_\beta$  since they make certain angles  $\alpha$  and  $\beta$  ( $\beta = \alpha + 90^\circ$ ) with the principal stresses  $\sigma_1$  as yet unknown. The shearing stresses are correspondingly denoted by  $\tau_\alpha$  and  $\tau_\beta$ ; according to the law of complementary shearing stresses,  $\tau_\alpha = -\tau_\beta$ . For the sake of definiteness while constructing Mohr's circle let us assume that  $\sigma_\alpha > \sigma_\beta > 0$ , and  $\tau_\alpha > 0$ .

Let us plot stresses  $\sigma_\alpha, \sigma_\beta, \tau_\alpha,$  and  $\tau_\beta$  using the coordinate system of the required stress circle (Fig. 66):

$$\begin{aligned} \sigma_\alpha &= OK_\alpha, & \sigma_\beta &= OK_\beta, & \tau_\alpha &= K_\alpha D_\alpha \\ \tau_\beta &= K_\beta D_\beta, & \overline{K_\alpha D_\alpha} &= -\overline{K_\beta D_\beta} \end{aligned}$$

Since points  $D_\alpha$  and  $D_\beta$  corresponding to mutually perpendicular sections must lie at the opposite ends of the circle diameter, the point of intersection of line  $D_\alpha D_\beta$  with the  $\sigma$ -axis will give centre  $C$  of the stress circle. Circumscribing a circle of radius  $CD_\alpha$  or  $CD_\beta$  around centre  $C$ , we get segments  $OA$  and  $OB$  on the  $\sigma$ -axis which represent the principal stresses:  $OA = \sigma_1$  and  $OB = \sigma_2$ .

The direction of  $\sigma_\alpha$  is represented on the stress circle by  $BD_\alpha$  which is inclined at a positive angle  $\alpha$  to the  $\sigma$ -axis. Consequently, angle  $\alpha$  should be plotted in the anticlockwise direction moving from point  $A$  towards  $D_\alpha$  in order to pass over from line  $\sigma_1$  to line  $\sigma_\alpha$  in the circle. In our example, we assume the direction of  $\sigma_\alpha$  to be known. This means that in order to represent the direction of  $\sigma_1$  in the diagram of the element under consideration, we must plot angle  $\alpha$  in the opposite direction from  $\sigma_\alpha$ , i.e. in the clockwise direction. The relative disposition of stresses  $\sigma_1$  and  $\sigma_2$  shown on the stress circle by  $OA$  and  $BD_\alpha$  must be retained in the diagram of the element as well.

We may also show on the stress circle the true direction of principal stress  $\sigma_1$  as coinciding with the direction obtained on the diagram of the element by the method explained above. For this from the extreme left point  $B$  of the circle, we must plot an angle  $\alpha$  in the clockwise direction from the  $\sigma$ -axis which is parallel to  $\sigma_\alpha$ , in other words, point  $D_\alpha$  should be brought down to  $D'_\alpha$ . Line  $BD'_\alpha$  coincides in direction with stress  $\sigma_1$ , and  $\sigma_2$  will be directed perpendicular to it. While representing the principal stresses (in our example  $\sigma_1$  and  $\sigma_2$ ) it is essential to take care of their signs obtained by plotting the circle, and also follow the rule of numeration of the principal stresses.

Let us point out that in the problems on biaxial stress discussed here, the third principal stress is zero. Therefore, if both principal stresses obtained from the stress circle are positive (Fig. 66), then the higher one will be  $\sigma_1$  and the lower  $\sigma_2$ ; if one of the stresses is positive and the other negative, then the former will be  $\sigma_1$  and the latter  $\sigma_3$ ; finally, if both stresses are negative, then the one with the greater absolute value will be  $\sigma_3$  and one with the smaller absolute value  $\sigma_2$ .

Angle  $\alpha$  may be determined by the formulas (Fig. 66)

$$\left. \begin{aligned} \tan 2\alpha &= -\frac{D'_\alpha K_\alpha}{CK_\alpha} = -\frac{2\tau_\alpha}{\sigma_\alpha - \sigma_\beta} \\ \tan \alpha &= -\frac{D'_\alpha K_\alpha}{BK_\alpha} = -\frac{\tau_\alpha}{\sigma_\alpha - \sigma_2} = -\frac{\tau_\alpha}{\sigma_1 - \sigma_\beta} \end{aligned} \right\} \quad (6.11)$$

The minus sign is used because for positive values of  $\sigma_\alpha$  and  $\tau_\alpha$  angle  $\alpha$  (the angle of rotation of plane  $\sigma_\alpha$  to the principal direction) is measured in the clockwise direction.

From Fig. 66, we can get the formulas for calculating the principal stresses in biaxial stress; they are represented by segments  $OA$  and  $OB$ . From the diagram we have

$$\overline{OA} = \overline{OC} + \overline{CA} \quad \text{and} \quad \overline{OB} = \overline{OC} - \overline{CB}$$

Further

$$\overline{OC} = \frac{\sigma_\alpha + \sigma_\beta}{2}, \quad \overline{CK}_\alpha = \overline{CK}_\beta = \frac{\sigma_\alpha - \sigma_\beta}{2}$$

The radii of the stress circle  $CA=CB$  are equal to  $CD_\alpha=CD_\beta$  which may be found from the following expression:

$$\begin{aligned} CA = CB = CD_\alpha &= \sqrt{CK_\alpha^2 + K_\alpha D_\alpha^2} = \sqrt{\frac{(\sigma_\alpha - \sigma_\beta)^2}{4} + \tau_\alpha^2} \\ &= \frac{1}{2} \sqrt{(\sigma_\alpha - \sigma_\beta)^2 + 4\tau_\alpha^2} \end{aligned}$$

Therefore,

$$\left. \begin{aligned} \sigma_1 &= \overline{OA} \\ \sigma_2 &= \overline{OB} \end{aligned} \right\} = \frac{1}{2} [(\sigma_\alpha + \sigma_\beta) \pm \sqrt{(\sigma_\alpha - \sigma_\beta)^2 + 4\tau_\alpha^2}] \quad (6.12)$$

In practice we often come across the cases of biaxial stress when  $\sigma_\beta=0$ . For these cases the formulas for principal stresses will take the form

$$\left. \begin{aligned} \sigma_1 \\ \sigma_2 \end{aligned} \right\} = \frac{1}{2} [\sigma_\alpha \pm \sqrt{\sigma_\alpha^2 + 4\tau_\alpha^2}] \quad (6.13)$$

Here the minimum principal stress is denoted by  $\sigma_2$  because it is negative (the quantity under the radical sign is greater than  $\sigma_\alpha$ ).

The angle of inclination of the first principal stress to the  $\sigma$ -axis is determined by formulas which are a corollary of (6.11):

$$\left. \begin{aligned} \tan 2\alpha &= -\frac{2\tau_\alpha}{\sigma_\alpha} \\ \tan \alpha &= -\frac{\tau_\alpha}{\sigma_1} \end{aligned} \right\} \quad (6.14)$$

Given below are examples on determining the principal stresses with the help of stress circle.

Suppose we know the stresses at a given point of the material, acting in two mutually perpendicular planes:

$$\begin{aligned} \sigma_\alpha &= 400 \text{ kgf/cm}^2, & \tau_\alpha &= -300 \text{ kgf/cm}^2 \\ \sigma_\beta &= -200 \text{ kgf/cm}^2, & \tau_\beta &= 300 \text{ kgf/cm}^2 \end{aligned}$$

Figure 67 shows Mohr's circle constructed for these data. The principal stresses are

$$\sigma_1 = 530 \text{ kgf/cm}^2, \quad \sigma_2 = -330 \text{ kgf/cm}^2 \quad (\sigma_3 = 0)$$

and the angle between  $\sigma_\alpha$  and  $\sigma_1$  is  $\alpha=22^\circ$ .

In another example

$$\begin{aligned} \sigma_\alpha &= 1000 \text{ kgf/cm}^2, & \tau_\alpha &= 400 \text{ kgf/cm}^2 \\ \sigma_\beta &= 0, & \tau_\beta &= -400 \text{ kgf/cm}^2 \end{aligned}$$

The plotting of the stress circle is shown in Fig. 68 from which it ensues that  $\sigma_1=1140$  kgf./cm<sup>2</sup> and  $\sigma_3=-140$  kgf./cm<sup>2</sup>. On the front face that lies in the plane of the figure,  $\sigma_2=0$ .

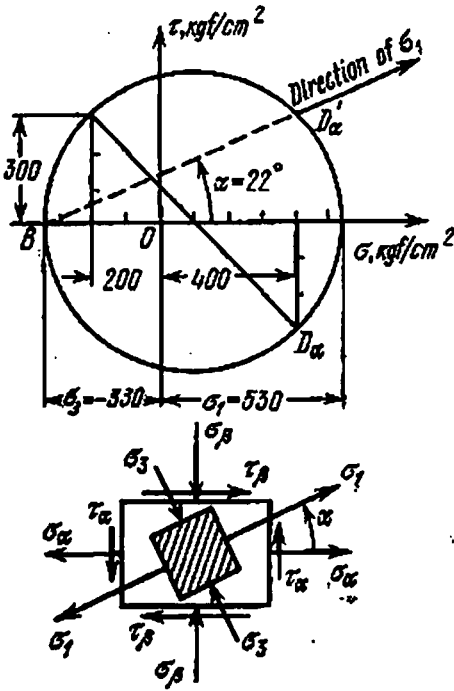


Fig. 67

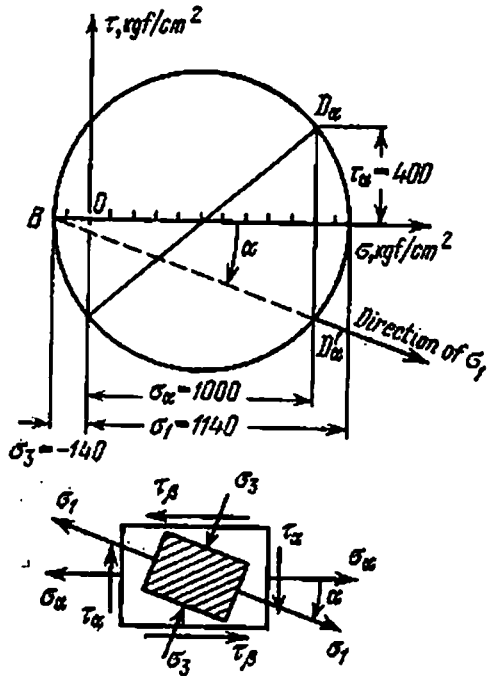


Fig. 68

For both examples the reader is advised to calculate the principal stresses according to formula (6.12) and compare the analytical values with those obtained by graphic construction.

### § 33. Stresses in Triaxial Stressed State

In the general case of a state of triaxial stress, normal as well as shearing, stresses act on the faces of an elementary cube cut out of the material of a body (Fig. 69). In accordance with the law of complementary shearing stresses,  $\tau_{xy}=\tau_{yx}$ ,  $\tau_{xz}=\tau_{zx}$ , and  $\tau_{yz}=\tau_{zy}$ \*. The set of six stresses  $\sigma_x, \sigma_y, \sigma_z$  and  $\tau_{xy}, \tau_{xz}, \tau_{yz}$  completely describes the state of stress at a point and is known as the *stress tensor*.

It is established in the theory of elasticity that around any point of stressed material we can always isolate an elementary cube in which no shearing stresses act on the faces by rotation of planes. In this case the stress tensor is determined by three principal stresses  $\sigma_1, \sigma_2,$  and  $\sigma_3$ .

\* The subscripts on  $\tau$  should be deciphered as follows: the first subscript denotes the plane in which they act (direction of the normal to the plane), the second subscript denotes the direction of shearing stress (along which axis  $\tau$  is acting).

In particular, when  $\sigma_1 = \sigma_2 = \sigma_3 = \sigma$  (uniform triaxial tension or compression), the stress tensor is known as *spherical*.

Suppose we have a cubic element cut from the body. The faces of the cube are subjected to principal stresses  $\sigma_1, \sigma_2$  and  $\sigma_3$  (Fig. 70). Our aim is to determine the normal and shearing stresses in any inclined plane cutting the given cube, provided  $\sigma_1 > \sigma_2 > \sigma_3 > 0$ .

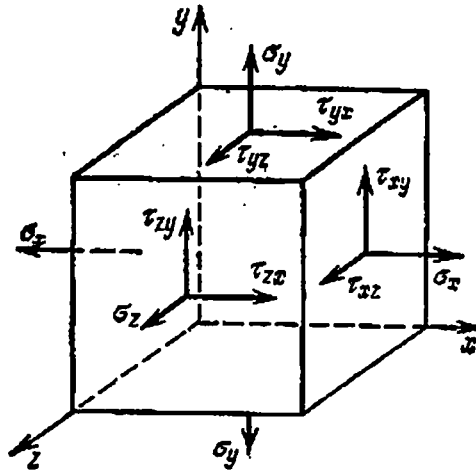


Fig. 69

First we shall determine these stresses in planes parallel to one of the principal stresses, for example  $\sigma_2$ . This plane is hatched in Fig. 70 (a).

We have seen earlier (§ 30) that the principal stress parallel to a given plane gives rise to neither normal nor shearing stresses in it.

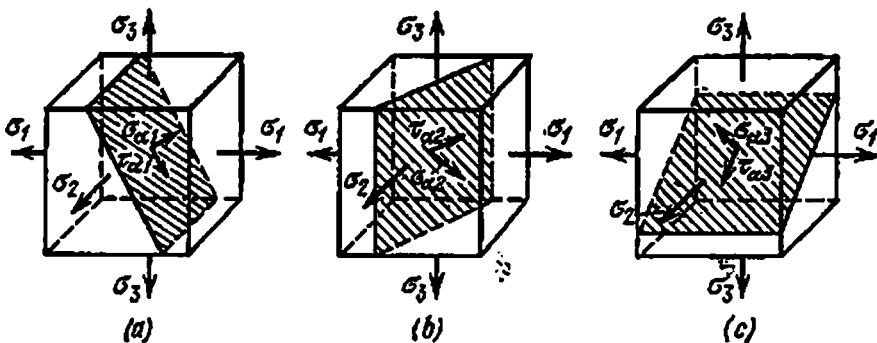


Fig. 70

Therefore, stresses in the planes under consideration will depend only upon  $\sigma_1$  and  $\sigma_3$ —we will again deal with the biaxial stress. Points on the stress circle drawn for the principal stresses  $\sigma_1$  and  $\sigma_3$  (Fig. 71) will correspond to these planes.

Identically, stresses in planes parallel to  $\sigma_3$  (Fig. 70 (b)) will be represented by the coordinates of the points of the stress circle constructed for stresses  $\sigma_1$  and  $\sigma_2$ . In planes parallel to  $\sigma_1$ , the stresses will be represented by points of the stress circle constructed for  $\sigma_2$  and  $\sigma_3$  (Fig. 70 (c)).

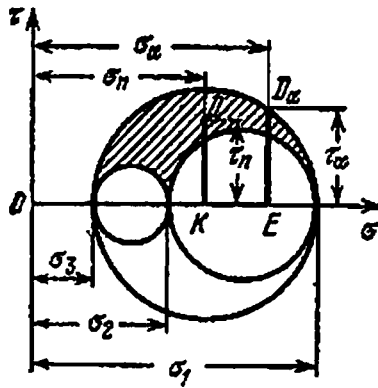


Fig. 71

Thus, coordinates of the points on three stress circles (Fig. 71) represent the normal and shearing stresses in sections of the cube which are parallel to one of the principal stresses.

As for the planes cutting all the three axes of principal stresses, it has been proved in the theory of elasticity that stresses  $\sigma_n$  and  $\tau_n$  are represented by coordinates of points  $D$  in the hatched area of Fig. 71.

The values of these stresses may be calculated by the following formulas:

$$\sigma_n = \sigma_1 \cos^2 \alpha_1 + \sigma_2 \cos^2 \alpha_2 + \sigma_3 \cos^2 \alpha_3 \quad (6.15)$$

$$\tau_n = \sqrt{\sigma_1^2 \cos^2 \alpha_1 + \sigma_2^2 \cos^2 \alpha_2 + \sigma_3^2 \cos^2 \alpha_3 - \sigma_n^2} \quad (6.16)$$

Here  $\alpha_1$ ,  $\alpha_2$  and  $\alpha_3$  are angles which the normal  $n$  to the plane makes with the directions of principal stresses  $\sigma_1$ ,  $\sigma_2$  and  $\sigma_3$ , respectively.

It is clear from Fig. 71 that in triaxial stress the maximum and minimum normal stresses are equal to the maximum and minimum principal stresses, respectively.

The maximum shearing stress is equal to the radius of the largest circle and, consequently, half of the difference of the maximum and minimum principal stresses. It acts in planes inclined at  $45^\circ$  to the direction of these principal stresses, the normal stresses in these planes being equal to half of the sum of the maximum and minimum principal stresses ( $\sigma_1 > \sigma_2 > \sigma_3$ ).

Thus, in the most general case of the stressed state of a material, when all the three principal stresses are nonzero at the given point,



we have

$$\max \sigma_n = \sigma_1, \quad \min \sigma_n = \sigma_3, \quad \max \tau_n = \frac{\sigma_1 - \sigma_3}{2} \quad (6.17)$$

In planes parallel to one of the principal stresses and inclined at  $45^\circ$  to the other two, the shearing stresses will be  $\max \tau = \tau_{1,3}$  according to formula (6.17), and further

$$\tau_{1,2} = \frac{\sigma_1 - \sigma_2}{2}, \quad \tau_{2,3} = \frac{\sigma_2 - \sigma_3}{2} \quad (6.17')$$

The stresses  $\tau_{1,2}$ ,  $\tau_{1,3}$ , and  $\tau_{2,3}$  are sometimes called the *principal shearing stresses*.

For checking the strength of material in compound stressed state (see Chapter 7) it is of interest to know the stresses in the *octahedral*

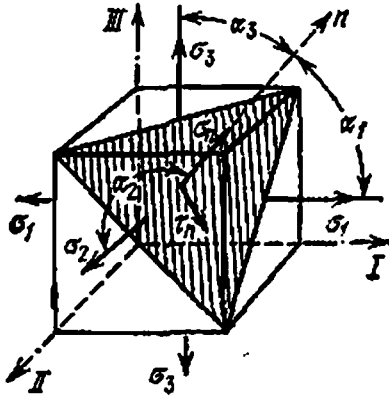


Fig. 72

plane, the normal to which makes equal angles with the directions of all the three principal stresses (Fig. 72). Bearing in mind that

$$\cos^2 \alpha_1 + \cos^2 \alpha_2 + \cos^2 \alpha_3 = 1$$

and when the angles are equal ( $\alpha_1 = \alpha_2 = \alpha_3 = \alpha$ ),  $3 \cos^2 \alpha = 1$ , or  $\cos^2 \alpha = 1/3$ , from formulas (6.15) and (6.16) we obtain

$$\sigma_{\text{oct}} = \frac{1}{3} (\sigma_1 + \sigma_2 + \sigma_3) = \sigma_{\text{mean}} \quad (6.18)$$

$$\tau_{\text{oct}} = \frac{1}{3} \sqrt{(\sigma_1 - \sigma_2)^2 + (\sigma_2 - \sigma_3)^2 + (\sigma_1 - \sigma_3)^2} \quad (6.19)$$

Using expression (6.17) for the principal shearing stresses, we get

$$\tau_{\text{oct}} = \frac{2}{3} \sqrt{\tau_{1,2}^2 + \tau_{2,3}^2 + \tau_{1,3}^2} \quad (6.19')$$

It is evident from expressions (6.18) and (6.19) that the normal octahedral stress is equal to the arithmetic mean of the three principal stresses, whereas the octahedral shearing stress is proportional to the geometric sum of the principal shearing stresses.

An expression of the type (6.19) will be used in Chapter 7 under the name of *stress intensity*, which also characterizes the stresses in a material:

$$\sigma_i = \frac{1}{\sqrt{2}} \sqrt{(\sigma_1 - \sigma_2)^2 + (\sigma_2 - \sigma_3)^2 + (\sigma_1 - \sigma_3)^2} \quad (6.20)$$

It can be easily seen that when  $\sigma_2 = \sigma_3 = 0$ , i.e. in the case of simple uniaxial tension, intensity  $\sigma_i = \sigma_1$ .

### § 34. Deformations in the Compound Stress

When testing the strength of an element (Fig. 56) whose faces are subjected to stresses  $\sigma_1$ ,  $\sigma_2$ , and  $\sigma_3$ , it becomes essential to determine the corresponding deformations. Let us number the edge parallel to principal stress  $\sigma_1$  as first, and those parallel to principal stresses  $\sigma_2$  and  $\sigma_3$  as second and third. Let us now determine the relative longitudinal deformations of the element along these edges by considering the effect of each stress separately and then summing up the results.

Under stress  $\sigma_1$ , the element will get elongated in the direction of the first edge, and the relative elongation is

$$e_1' = \frac{\sigma_1}{E}$$

The first edge, however, is simultaneously the lateral dimension for stresses  $\sigma_2$  and  $\sigma_3$ ; therefore, the element undergoes relative shortening in the direction of the first edge due to stress  $\sigma_2$  and stress  $\sigma_3$ , which is equal to (see § 9)

$$e_1'' = -\mu \frac{\sigma_2}{E}, \quad e_1''' = -\mu \frac{\sigma_3}{E}$$

The total relative deformation in the direction of the first edge may be written as

$$e_1 = e_1' + e_1'' + e_1''' = \frac{\sigma_1}{E} - \mu \frac{\sigma_2}{E} - \mu \frac{\sigma_3}{E}$$

Similar expressions may be written for deformations in the other two directions, and we finally get

$$\left. \begin{aligned} \epsilon_1 &= \frac{\sigma_1}{E} - \mu \left( \frac{\sigma_2}{E} + \frac{\sigma_3}{E} \right) \\ \epsilon_2 &= \frac{\sigma_2}{E} - \mu \left( \frac{\sigma_1}{E} + \frac{\sigma_3}{E} \right) \\ \epsilon_3 &= \frac{\sigma_3}{E} - \mu \left( \frac{\sigma_2}{E} + \frac{\sigma_1}{E} \right) \end{aligned} \right\} \quad (6.21)$$

If some of the stresses  $\sigma_1$ ,  $\sigma_2$ ,  $\sigma_3$  are compressive, their numerical values should be put in formulas (6.21) with a minus sign.

Now from (6.21) we can easily get expressions for tension or compression in two directions by putting one of the principal stresses equal to zero. For example, for the case shown in Fig. 60, we have

$$\left. \begin{aligned} \epsilon_1 &= \frac{\sigma_1}{E} - \mu \frac{\sigma_3}{E} \\ \epsilon_2 &= \frac{\sigma_2}{E} - \mu \frac{\sigma_1}{E} \\ \epsilon_3 &= -\mu \frac{\sigma_1}{E} - \mu \frac{\sigma_2}{E} \end{aligned} \right\} \quad (6.21a)$$

Let us calculate the change in the volume of a rectangular parallelepiped having edges of  $a$ ,  $b$  and  $c$ , if it is under triaxial stress. Its volume before deformation is  $V_0 = abc$ . After deformation, due to elongation of its edges its volume becomes

$$V_1 = (a + \Delta a)(b + \Delta b)(c + \Delta c)$$

or, neglecting the product of small deformations,

$$V_1 = abc + ab\Delta c + ac\Delta b + bc\Delta a = V_0(1 + \epsilon_1 + \epsilon_2 + \epsilon_3)$$

The relative change in volume is

$$\epsilon_V = \frac{V_1 - V_0}{V_0} = \epsilon_1 + \epsilon_2 + \epsilon_3 \quad (6.22)$$

Replacing the sum of relative elongations by some mean

$$\epsilon_{\text{mean}} = \frac{\epsilon_1 + \epsilon_2 + \epsilon_3}{3}$$

we express the relative change in volume as

$$\epsilon_V = 3\epsilon_{\text{mean}} \quad (6.22')$$

Replacing in (6.22) the values of  $\epsilon_1$ ,  $\epsilon_2$ , and  $\epsilon_3$  from (6.21), we get

$$\epsilon_V = \epsilon_1 + \epsilon_2 + \epsilon_3 = \frac{1 - 2\mu}{E} (\sigma_1 + \sigma_2 + \sigma_3) \quad (6.23)$$

It is evident from (6.23) that if Poisson's ratio  $\mu$  is equal to  $\frac{1}{2}$ , the relative change in volume is zero. We have already obtained this result for uniaxial stress in § 9. It is clear from the same formula that if the sum of the three principal stresses is equal to zero, there will be no change of volume within the limits of elastic deformation.

It should be noted that formulas (6.21), (6.22), and (6.23) can also be used for an arbitrarily orientated element of the material the faces of which experience both the normal and shearing stresses (Fig. 69). For this all that is required is to replace  $\sigma_1$ ,  $\sigma_2$ , and  $\sigma_3$  by normal stresses  $\sigma_x$ ,  $\sigma_y$ , and  $\sigma_z$ , and  $\epsilon_1$ ,  $\epsilon_2$ ,  $\epsilon_3$  by  $\epsilon_x$ ,  $\epsilon_y$ , and  $\epsilon_z$ . It will be shown later (§ 36) that shearing stresses change neither the linear dimensions of the element nor its volume.

Let us return to formula (6.23) from which it is obvious that the change in volume depends only on the sum of the principal stresses and not on their ratio. This means that the volume will change by the same value if the cube's faces are subjected to equal mean stresses

$$\sigma_{\text{mean}} = \frac{\sigma_1 + \sigma_2 + \sigma_3}{3}$$

The relative change in volume may in this case be expressed as

$$e_v = \frac{1-2\mu}{E} 3\sigma_{\text{mean}} \quad (6.23')$$

The quantity  $K = \frac{E}{3(1-2\mu)}$  is called the *bulk modulus*. Introducing this notation in formula (6.23), we obtain

$$e_v = \frac{\sigma_{\text{mean}}}{K} = \frac{\sigma_1 + \sigma_2 + \sigma_3}{3K} \quad (6.24)$$

or

$$\sigma_{\text{mean}} = K e_v = 3K e_{\text{mean}} \quad (6.24')$$

Formulas (6.24) and (6.24') describe the general Hooke's law similar to Hooke's law for uniaxial tension. It is evident from these formulas that if equal mean stresses

$$\sigma_{\text{mean}} = \frac{\sigma_1 + \sigma_2 + \sigma_3}{3}$$

forming the spherical stress tensor are applied to the cube's faces, all the edges experience identical strain

$$e_{\text{mean}} = \frac{\sigma_{\text{mean}}}{3K} \quad (6.25)$$

In this case the change in volume of the cube is not accompanied by a change of its shape—the cube remains a cube, but the dimensions of the new cube are different. Therefore, if we are interested in problems related to the change in volume and shape under compound stress, it is convenient to represent each of the principal stresses as a sum of two stresses:

$$\sigma_1 = \sigma_{\text{mean}} + \sigma'_1, \quad \sigma_2 = \sigma_{\text{mean}} + \sigma'_2, \quad \sigma_3 = \sigma_{\text{mean}} + \sigma'_3$$

The given stress tensor formed by the principal stresses  $\sigma_1, \sigma_2,$  and  $\sigma_3$  consists of two terms: the spherical tensor (made up of equal stresses

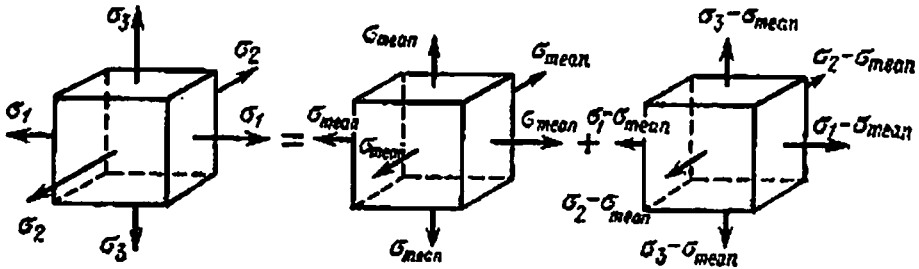


Fig. 73

$\sigma_{\text{mean}}$ ) and a supplementary tensor known as the *stress deviator* (Fig. 73) which represents a system of normal stresses

$$\sigma'_1 = \sigma_1 - \sigma_{\text{mean}}, \quad \sigma'_2 = \sigma_2 - \sigma_{\text{mean}}, \quad \sigma'_3 = \sigma_3 - \sigma_{\text{mean}}$$

It can be easily seen that the sum of these supplementary stresses is equal to zero. Obviously,  $\sigma'_1 + \sigma'_2 + \sigma'_3 = \sigma_1 + \sigma_2 + \sigma_3 - 3\sigma_{\text{mean}} = 0$ , therefore they do not cause any change in volume (§ 34). The stress deviator (Fig. 73 on the right) is only responsible for the change of shape.

We shall return to the problem of the change in volume and shape later while discussing problems of strength of materials in compound stressed state (Chapter 7).

### § 35. Potential Energy of Elastic Deformation in Compound Stress

Potential energy of deformation is the energy accumulated by the material as a result of elastic deformation caused by external forces.

To calculate the potential energy accumulated by an elastic system, we may use the law of conservation of energy.

Let us first consider the case of simple tension (Fig. 74). If we load a bar statically by gradually suspending small loads  $\Delta P$ , then after each addition the suspended load comes down and its potential energy decreases, whereas the potential energy of deformation of the stretched bar increases.

When the load increases slowly and gradually, the velocity of displacement of the free end of the bar is very small. Therefore, we may neglect the inertia of the moving mass and, consequently, assume that the deformation is not accompanied by any change in the kinetic energy of the system.

Under these conditions the potential energy of the lowering load is transformed into the potential energy of elastic deformation of the bar (we neglect the dissipation of energy due to thermal and electromagnetic processes accompanying the elastic deformation). Thus an elastic system under static loading may be considered as a machine transforming one form of potential energy into another.

As the potential energy lost by the load is equal to the work accomplished by it in lowering, the problem of determining the potential energy of deformation comes to calculating the work done by the external forces. In § 10 we obtained expression (3.1) for the work done by the external forces in simple tension:

$$W = \frac{P\Delta l}{2}$$

This implies that the potential energy of tension is also

$$U = W = \frac{P^2 l}{2EA} = \frac{\sigma^2 Al}{2E} \quad (6.26)$$

since  $\Delta l = \frac{Pl}{EA}$ .

The potential energy accumulated by a unit volume of material is

$$u = w = \frac{\sigma^2}{2E} = \frac{\sigma\epsilon}{2} \quad (6.27)$$

Let us now pass over to the determination of potential energy accumulated in a unit volume of a material which is in a compound (planar or volumetric) stress. Making use of the principle of superposition of forces and assuming that the principal stresses increase gradually, we can determine the potential energy as the sum of the energies accumulated by a unit volume of the material under the action of each of the principal stresses  $\sigma_1$ ,  $\sigma_2$ , and  $\sigma_3$  according to (6.27)

$$u = w = \frac{\sigma_1 \epsilon_1}{2} + \frac{\sigma_2 \epsilon_2}{2} + \frac{\sigma_3 \epsilon_3}{2}$$

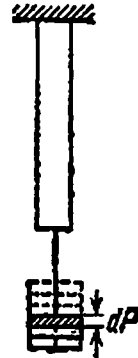


Fig. 74

where  $\epsilon_1$ ,  $\epsilon_2$  and  $\epsilon_3$  are strains calculated from formulas (6.21). The specific energy of deformation will be

$$u = \frac{1}{2} \left[ \sigma_1 \left( \frac{\sigma_1}{E} - \mu \frac{\sigma_2}{E} - \mu \frac{\sigma_3}{E} \right) + \sigma_2 \left( \frac{\sigma_2}{E} - \mu \frac{\sigma_1}{E} - \mu \frac{\sigma_3}{E} \right) + \sigma_3 \left( \frac{\sigma_3}{E} - \mu \frac{\sigma_1}{E} - \mu \frac{\sigma_2}{E} \right) \right]$$

or after multiplication

$$u = \frac{1}{2E} [\sigma_1^2 + \sigma_2^2 + \sigma_3^2 - 2\mu (\sigma_1\sigma_2 + \sigma_1\sigma_3 + \sigma_2\sigma_3)] \quad (6.28)$$

Hence, the *total energy of deformation* accumulated in a unit volume of the material (a cube with edges of unit length) may be calculated from formula (6.28). It may be considered as consisting of two parts: (1)  $u_v$  due to the volumetric change in the cube under consideration (i.e. uniform change of all its dimensions without any change in its shape) and (2)  $u_{sh}$  due to the change in its shape (i.e. energy spent in transforming the cube into a parallelepiped).

This division of the potential energy in two parts facilitates the study of strength of materials in volumetric stress (Chapter 7).

Let us calculate the values of both the components of the specific potential energy. It had been shown earlier (§ 34) that when the edges of the cube deform uniformly, i.e. when there is a change in the volume only, the relative elongation of each edge of the cube may be calculated from formula (6.25):

$$\epsilon_{\text{mean}} = \frac{\sigma_{\text{mean}}}{3K}$$

where  $\sigma_{\text{mean}} = \frac{\sigma_1 + \sigma_2 + \sigma_3}{3}$ , and the bulk modulus  $K = \frac{E}{3(1-2\mu)}$ .

The specific energy due to the change in volume will be

$$u_v = 3 \frac{\sigma_{\text{mean}} \epsilon_{\text{mean}}}{2} = \frac{\sigma_{\text{mean}}^2}{2K} = \frac{(\sigma_1 + \sigma_2 + \sigma_3)^2}{18K}$$

or

$$u_v = \frac{1-2\mu}{6E} (\sigma_1 + \sigma_2 + \sigma_3)^2 \quad (6.29)$$

The potential energy corresponding to the change in shape of the isolated element may now be calculated as the difference

$$u_{sh} = u - u_v = \frac{1}{2E} [\sigma_1^2 + \sigma_2^2 + \sigma_3^2 - 2\mu (\sigma_1\sigma_2 + \sigma_1\sigma_3 + \sigma_2\sigma_3)] - \frac{1-2\mu}{6E} (\sigma_1 + \sigma_2 + \sigma_3)^2$$

After simplifying, we get

$$u_{sh} = \frac{1+\mu}{3E} (\sigma_1^2 + \sigma_2^2 + \sigma_3^2 - \sigma_1\sigma_2 - \sigma_1\sigma_3 - \sigma_2\sigma_3) \quad (6.30)$$

Formula (6.30) may also be expressed through octahedral stresses (6.19) by writing the expression in brackets as the difference of squares:

$$u_{sh} = \frac{1+\mu}{6E} [(\sigma_1 - \sigma_2)^2 + (\sigma_2 - \sigma_3)^2 + (\sigma_1 - \sigma_3)^2] = \frac{3(1+\mu)}{2E} \tau_{oct}^2 \quad (6.30')$$

In simple tension, when  $\sigma_1 = \sigma = \frac{P}{A}$ ,  $\sigma_2 = 0$ , and  $\sigma_3 = 0$ , the specific potential energy corresponding to the volumetric change in the elementary cube is

$$u_v = \frac{(1-2\mu)\sigma^2}{6E} \quad (6.31)$$

and due to change in shape

$$u_{sh} = \frac{(1+\mu)\sigma^2}{3E} \quad (6.32)$$

Obviously, the sum of the two will give the total specific energy of tension:

$$u = u_v + u_{sh} = \frac{\sigma^2}{2E}$$

### § 36. Pure Shear. Stresses and Strains. Hooke's Law. Potential Energy

A. While dealing with compound state of stress (§ 33) it was noticed that like in simple tension or compression (§ 27) planes inclined to the direction of principal stresses experience normal stresses that result in elongation (shortening) as well as shearing stresses which correspond to shear.

In studying shear deformation it is desirable to find planes in which only shearing stresses act, i.e. planes that are free of normal stresses. An analysis of formulas (6.5) and (6.6) reveals that in biaxial stress under certain conditions ( $\alpha = 45^\circ$  and  $\sigma_1 + \sigma_3 = 0$ ) the normal stresses in the inclined plane vanish ( $\sigma_\alpha = \sigma_\beta = 0$ ); only shearing stresses  $\tau_\alpha = \tau_{max}$  act in this plane.

The stressed state in which only shearing stresses act on the faces of an element of a material is known as *pure shear*.

Consider a cubic element with a front face  $abcd$  (Fig. 75). We apply equal shearing stresses  $\tau$  to the faces perpendicular to the front face (recall that  $\tau_\alpha = -\tau_\beta$ ). The front face experiences neither normal nor shearing stresses; it is, therefore, a principal plane in which the principal stress is zero. The two other principal stresses can be found by solving the reverse problem: we determine them through known stresses acting in two mutually perpendicular planes (§ 32). Let us use Mohr's



circle for solving the problem with the following data:

$$\begin{aligned} \text{on the vertical face } \sigma_\alpha &= 0, & \tau_\alpha &= \tau \\ \text{on the horizontal face } \sigma_\beta &= 0, & \tau_\beta &= -\tau \end{aligned}$$

Since the normal stresses laid off on the  $\sigma$ -axis are equal to zero, from point  $O$  (Fig. 76(b)) we plot segment  $OD_\alpha = \tau_\alpha = \tau$  upwards and segment  $OD_\beta = \tau_\beta = -\tau$  downwards. As points  $D_\alpha$  and  $D_\beta$  lie at the end

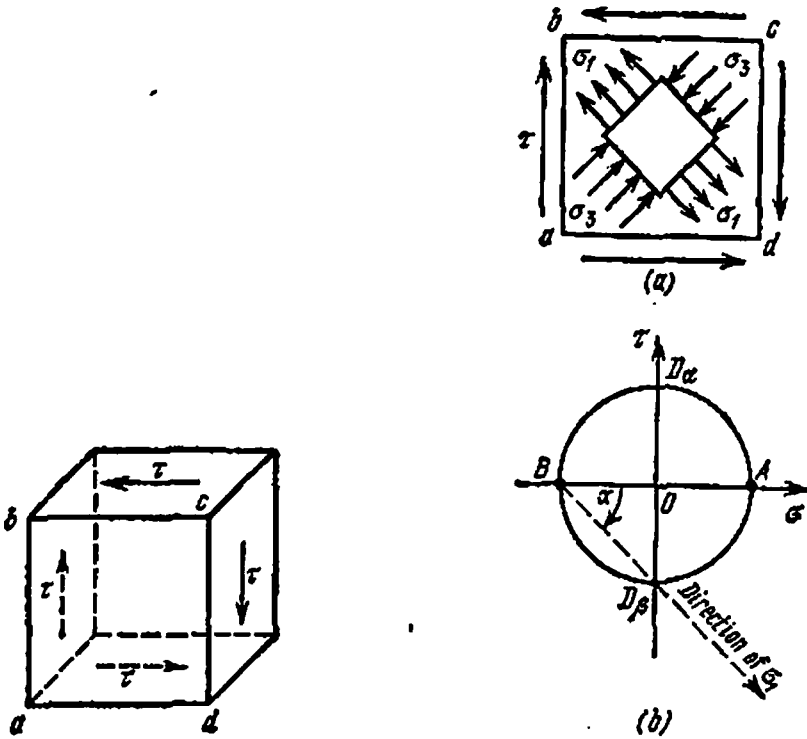


Fig. 75

Fig. 76

points of the diameter of Mohr's circle, its radius is equal to  $OD_\alpha = \tau$ . The segments  $OA$  and  $OB$  cut by the circle on the  $\sigma$ -axis are also equal to the radius and determine the magnitudes of the principal stresses:

$$OA = \sigma_1 = \tau, \quad OB = \sigma_3 = -\tau, \quad \sigma_2 = 0 \quad (6.33)$$

Identical results are obtained if we put  $\sigma_\alpha = \sigma_\beta = 0$  and  $\tau_\alpha = \tau$  in formulas (6.12).

The direction of principal stress  $\sigma_1$  is shown on Mohr's circle by the line  $BD_\beta$  which makes an angle of  $45^\circ$  with the normal to plane  $bc$ . A similar conclusion ensues from formula (6.11). The element cut out of the material around the same point by the principal planes (Fig. 76(a)) is stretched by stresses  $\sigma_1$  along diagonal  $bd$  and compressed by

stresses  $\sigma_s$  along diagonal  $ac$ . This can also be proved by considering the equilibrium conditions of a part of the cube cut out by a diagonal plane (Fig. 77).

Thus, pure shear is equivalent to a combination of two equal principal stresses—one of them tensile and the other compressive (the third equal to zero). In other words this is a particular case of biaxial stress when  $\sigma_1 = -\sigma_2$ . Planes inclined at  $45^\circ$  to the direction of principal stresses experience only shearing stresses which subject the ele-

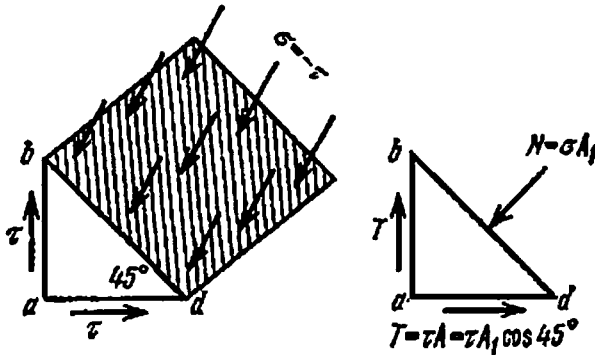


Fig. 77

ment to shear. At the same time, the material of this element is stretched and compressed in the direction of principal stresses. It should be noted that shear is always accompanied by tension (compression), and vice versa.

B. We shall now consider deformations in pure shear. Let a cubic element of the material be in a state of equilibrium in pure shear (Fig. 78). If we fix the face  $AB$  of this element, then the shearing stresses will displace the face  $CD$  parallel to  $AB$  by a distance  $DD_1 = CC_1 = \Delta s$  called the *absolute displacement*. The element  $ABCD$  gets warped and the right angles transform into acute or obtuse angles changing by a value  $\gamma$ . This angle is called the *relative shear* or angle of shear, and serves as a measure of distortion (warping) of the angles of the rectangular element. Since in structures we usually come across only elastic deformations, this angle is extremely small.

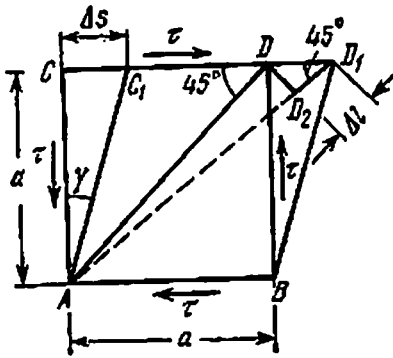
The magnitude of the angle of shear is connected with the absolute displacement and distance  $a$  between the planes  $AB$  and  $CD$ :

$$\gamma = \tan \gamma = \frac{\Delta s}{a} \quad (6.34)$$

i.e. the angle of shear is equal to the absolute displacement divided by the distance between the shearing planes; it is expressed in radians.

It can be shown that the angle of shear is directly proportional to shearing stress  $\tau$ . Thus the angle of shear numerically defines the shear deformation,

Let us study Fig. 78 to establish the relation between  $\tau$  and  $\gamma$ . Due to warping of the given element, diagonal  $AD$  gets elongated. This elongation may on the one hand be related to the acting stresses and on the other, to the angle of shear; combining the two relations we can establish the dependence between  $\tau$  and  $\gamma$ .



From Fig. 78, we can obtain the absolute elongation of the diagonal by cutting the new diagonal  $AD_1$  by an arc with a centre  $A$  and radius  $AD$ . We get a right-angled triangle  $DD_1D_2$  in which arm  $DD_1$  represents the absolute elongation  $\Delta s$  and arm  $D_2D_1$  represents the elongation  $\Delta l$  of the diagonal. The angle at point  $D_1$  may be taken as  $45^\circ$  due to the small value of deformation. Then

Fig. 78

$$\Delta l = \Delta s \cos 45^\circ$$

The relative elongation of the diagonal is

$$\epsilon = \frac{\Delta l}{l}$$

where  $l = \frac{a}{\sin 45^\circ}$ . Therefore

$$\epsilon = \frac{\Delta s}{a} \cos 45^\circ \sin 45^\circ$$

Since  $\frac{\Delta s}{a} = \gamma$ , and  $\cos 45^\circ \sin 45^\circ = 0.5$ , we get

$$\epsilon = \frac{\gamma}{2} \tag{6.35}$$

On the other hand, the relative elongation of the diagonal caused by the principal stresses  $\sigma_1 = \tau$  and  $\sigma_3 = -\tau$  (Fig. 76 (a)) may be expressed by formula (6.21):

$$\epsilon = \epsilon_1 = \frac{\sigma_1}{E} - \mu \frac{\sigma_3}{E} = \frac{\tau}{E} (1 + \mu)$$

Putting this value of  $\epsilon$  in formula (6.34), we get

$$\frac{\tau}{E} (1 + \mu) = \frac{1}{2} \gamma$$

wherefrom

$$\tau = \frac{E}{2(1 + \mu)} \gamma \tag{6.36}$$

Thus, angle of shear  $\gamma$  and shearing stress  $\tau$  are directly proportional to each other, i.e. in shear the stress and corresponding strain are related by Hooke's law.

Denoting the proportionality factor  $\frac{E}{2(1+\mu)}$  correlating  $\tau$  and  $\gamma$  by  $G$ , we get

$$\tau = G\gamma \quad (6.37)$$

where

$$G = \frac{E}{2(1+\mu)} \quad (6.38)$$

Quantity  $G$  is called the *modulus of elasticity in shear*, or *shear modulus*, and expression (6.37) is Hooke's law for shear. We see that it is completely identical to Hooke's law for tension ( $\sigma = E\epsilon$ ). Shear modulus  $G$ , like  $E$ , has the dimensions of stress.

Since in formula (6.38) for the shear modulus only two of the three elastic constants  $E$ ,  $\mu$  and  $G$  are independent, the third may be expressed through the first two. However, it can also be determined directly from experiments on torsion of round bars (Chapter 9).

The absolute displacement depends not only upon shearing stress but also upon the dimensions of the isolated element. Let us denote by  $A$  the area of the faces on which the shearing stresses are acting; the distance between the parallel faces is denoted by  $a$  (Fig. 78), and the force acting along these faces, which is a resultant of stresses  $\tau$  (with the assumption that shearing stresses  $\tau$  are uniformly distributed over area  $A$ ), by  $Q = \tau A$ . Substituting  $\tau$  and  $\gamma$  in equation (6.37), we obtain

$$\frac{Q}{A} = \frac{\Delta s}{a} G, \quad \text{wherefrom} \quad \Delta s = \frac{Qa}{GA} \quad (6.39)$$

Absolute displacement is directly proportional to the shearing force and the distance between the sheared planes and inversely proportional to the cross-sectional areas of the sheared planes and the shear modulus, i.e. we have a formula which expresses Hooke's law for shear that is identical to the formula for absolute elongation under tension:

$$\Delta l = \frac{Pl}{EA}$$

With the help of expression (6.39) we can also calculate the potential energy of shear through the work done by force  $Q$ . Considering that force  $Q$  is applied statically, gradually increasing from zero to a finite value, we can express the work done by this force in affecting a displacement  $\Delta s$  as

$$W = \frac{1}{2} Q \Delta s$$

Substituting  $\Delta s$  from equation (6.39), we get

$$U = \frac{Q^2 a}{2GA} = \frac{\tau^2 A a}{2G} \quad (6.40)$$

Dividing by volume  $V = aA$ , we find the potential energy in pure shear as

$$u = \frac{U}{V} = \frac{\tau^2}{2G} \quad (6.41)$$

The same result could have been obtained from formula (6.28), § 35, by considering pure shear as a compound stressed state with principal stresses  $\sigma_1 = \tau$ ,  $\sigma_2 = 0$ , and  $\sigma_3 = -\tau$ .

It should be noted that in pure shear the potential energy is spent only on changing the shape, as the change in the volume in shear is zero. This becomes clear from formula (6.23) if it is taken into account that in pure shear the sum of principal stresses is equal to zero.

## CHAPTER 7

### Strength of Materials in Compound Stress

#### § 37. Resistance to Failure. Rupture and Shear

Some problems related to the strength of the elements of structures under uniaxial loading were discussed in §§ 16 and 17. It is well known that among other conditions, the design of a structure must also satisfy the strength condition which requires that maximum stress in each part of a machine or structure must not exceed the permissible stress that constitutes a certain fraction of the failing stress. In order to select the permissible stress it is essential to study the behaviour of material during its deformation from the moment the load is applied right up to failure. The latter is also required for other purposes, for instance, for controlling the plastic deformation processes (wire drawing, stamping, rolling, forging, metal cutting, pressing of laminated plastics and other materials).

We do not meet any difficulty in experimentally investigating the behaviour of materials in uniaxial tension or compression with machines commonly installed in material testing laboratories. The tension or compression test diagrams obtained as a result of these experiments give a clear idea about the resistance of a given material to elastic or plastic deformation and enable us to determine mechanical characteristics like yield stress and ultimate strength which are so important for assessing the strength of material and specifying permissible stress.

The behaviour of material under loading depends upon its properties and the state of stress. In some cases strain remains more or less pro-

portional to stress right up to failure; failure occurs without any plastic deformation (Fig. 25). In other cases elastic deformation is succeeded by plastic deformation of considerable magnitude that ends in failure (Figs. 16 and 18). A continuously increasing plastic deformation may not necessarily lead to failure (Fig. 24).

The first diagram (Fig. 25) describes the behaviour of a brittle material in uniaxial tension or compression. In this case failure should be considered as the critical state of the material, and the ultimate strength as the failure stress. Under tension failure occurs in a section perpendicular to the tensile force, and under compression (with regular lubrication of the specimen faces that come in contact with the press plates) in sections parallel to the direction of compressive force (Fig. 28). In both cases failure takes place through separation of material particles from one another, i.e. through rupture. In the case of tension, rupture can be caused both by the maximum normal tensile stress and the maximum elongation in the direction of action of the tensile force. In the case of compression, failure may be considered to occur due to considerable tension in the direction perpendicular to the compressive force. It is noteworthy that under compression brittle materials often fail in sections that are inclined with respect to the direction of the compressive force. It may therefore be assumed that failure is more complicated in nature than described above and the cause of failure are normal as well as shearing stresses acting on these inclined planes (see § 40B for a more detailed discussion).

The second diagram shows the behaviour of ductile materials under uniaxial tension (Fig. 18 depicts the true stress-strain diagram for tension). The critical states in this case may be the beginning of yielding, neck formation, and rupture. The corresponding failure stresses will be yield stress, ultimate strength and true stress at rupture. The appearance of shear lines (Lüder's lines) after permanent plastic deformation (Fig. 13) and failure of specimens in planes inclined at  $\pi/4$  to the direction of tensile force (§ 27) enable us to consider that the starting and growth of plastic deformation and the final failure occur due to slip and shear under the action of maximum shearing stresses. Such a failure is known as *failure due to shear*.

The third diagram describes the behaviour of a ductile material under compression when plastic deformation does not lead to failure (Fig. 24 shows the compression test diagram). The beginning of yielding should be considered as the critical state, and yield stress, which does not differ much from yield stress under tension, as the failure stress. In this case plastic deformation begins and develops due to shear under the action of shearing stresses.

The two different concepts of failure of materials discussed above, namely (1) failure in the form of rupture due to elongation or mainly under the action of normal tensile stresses and (2) failure as a shear under the influence of shearing stresses, have been known for a long

time. These concepts led to two types of resistance of materials to failure: *resistance to rupture* and *resistance to shear*.

Till recent past it was considered that every material possessed only one type of resistance to failure—either resistance to rupture or resistance to shear. Such a one-sided concept of failure prevented a general solution to the problem of strength of materials from being found.

A few years ago a new concept that has a sound experimental support was put forward in the Soviet Union. According to this concept every material depending upon the working conditions may fail both due to rupture and shear and may therefore possess resistance to both types of failure. This new approach to failure helped us to clarify the concept of failure. Therefore, at the present stage of the science of strength of materials only the new approach should be considered correct.

The possibility of failure of materials due to rupture, supported by experimental evidence was not subjected to any doubts till now. On the contrary, many scientists tend to explain all cases of failure by the rupture phenomena.

The nature of failure due to rupture depends both on the type of material and the state of the stress. In principle it is possible that failure may occur in some cases on account of brittle rupture without any plastic deformation and in other cases due to ductile rupture accompanied by the plastic deformation of more or less considerable magnitude. Thus, for instance, it is experimentally established that some grades of bronze and aluminium alloys are capable of failure due to rupture even after undergoing permanent set of about 20%.

The resistance to rupture is best studied by the testing of brittle non-metallic materials (glass, plastics, concrete, and stone).

It is extremely difficult to study the resistance to rupture of ductile materials because during testing it is, as a rule, impossible to avoid the stage of plastic deformation and hence the shearing stresses of a considerable magnitude. On account of the fact that ductile materials have a much lower resistance to shearing stresses (shear) as compared to their resistance to rupture, it is difficult to achieve rupture of these materials by conventional tests because failure due to shear takes place earlier. Therefore in order to determine the resistance to rupture the test conditions (type of stressed state, temperature, rate of deformation) should be altered so that the resistance to shear improves considerably without any change in the resistance to rupture.

Available experimental data enable us to consider that resistance to rupture does not depend much upon the rate of deformation and test temperature. It therefore follows that by conducting dynamic tests at low temperatures we can find, with certain approximation, the resistance to rupture in normal conditions.

Numerous experimental investigations reveal that the resistance to rupture of brittle materials is constant for different types of loading.

However, we do not have sufficient data to be able to come to a similar conclusion for ductile materials. Some experimental studies point out that resistance to rupture depends upon cold hardening—it increases with the degree of cold hardening.

Failure due to shear is more complicated than rupture because it is usually preceded by considerable plastic deformations which result in redistribution of stresses and other complications. The existence of this type of failure, caused mainly by shearing stresses, is confirmed by a number of experimental data.

The failure of materials under tension accompanied by neck formation, shear, torsion and bending usually occurs along planes close to the planes of maximum shearing stresses. Although it is not always possible to conclude about the type of failure (rupture or shear) merely from the angle of rupture, in a number of cases the location of the plane of failure and the appearance of the breakdown surface can be decisive factors in this respect. Thus, for instance, if failure under torsion occurs in planes perpendicular to the bar axis, it is undoubtedly caused by shearing stresses because in this case the surface of breakdown plane is completely free of normal stresses.

It is much more difficult to differentiate between failures due to rupture and shear when the body is under a compound stress. Still in a number of cases of complex loading it was established that shearing stresses played a major role in many instances of failure, which were earlier considered obvious examples of failure due to rupture.

In ductile materials shear occurring without preceding permanent set, usually of a considerable magnitude, is highly improbable, because failure due to shear takes place due to shearing stresses, which also play the major role in plastic deformation of materials. At least it has not been possible till now to practically achieve such failure in metals although some of them (for example, compressed magnesium and its alloys) fail due to shear after small plastic deformation (5-15%). This is known as the so-called "brittle shear".

Experimental data show that resistance to shear practically does not depend upon the type of stressed state for pure metals (copper, aluminium, iron) and some alloys. It is also established that it depends upon the rate of deformation and temperature to a much greater extent than the resistance to rupture. Resistance to shear increases with increase in rate of deformation and reduction in temperature.

The assumption about materials having resistance to both types of failure is confirmed by experiments on failure of cold-short metals and some brittle materials. For one and the same material the magnitudes of resistance to rupture and shear are different: for ductile materials usually  $\bar{\tau}_{sh} < \bar{\sigma}_{rup}$  on the contrary, for brittle materials  $\bar{\tau}_{sh} > \bar{\sigma}_{rup}$ . The laws governing  $\bar{\tau}_{sh}$  and  $\bar{\sigma}_{rup}$  may differ depending upon the changes in composition of material and its machining and heat treatment.



The above discussion about the resistance of materials to failure may serve as a basis for strength test in simple and compound states of stress. The application of the resistance characteristics is discussed in succeeding sections. The considerable growth of research on failure of materials in recent years is fully reflected in the book *Fundamentals of the Mechanics of Failure* by L. M. Kachanov, Nauka, Moscow, 1974.

### § 38. Strength Theories

As has been already stated, in the case of uniaxial loading it is not difficult to find the breakdown stress which is used as a basis for designating permissible stresses.

It is much more difficult to find the breakdown stress in compound stressed state which is in general characterized by the three different principal stresses. Experiments show that the breakdown state of an element of structure (yield, rupture) depends upon the nature of stres-

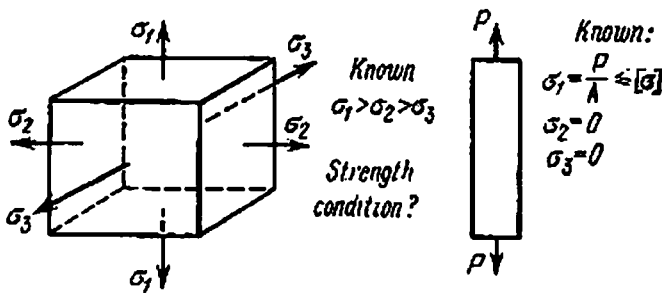


Fig. 79

sed state, i.e. upon the ratio between the three principal stresses. Since the number of various possible ratios between the principal stresses is infinitely large, there exist a corresponding infinite number of potential states of failure of the structure element. Hence, for each new ratio between the principal stresses it is necessary to experimentally find the permissible stresses anew. It should be borne in mind that it is much more difficult to conduct tests in compound stressed state as compared to simple tension or compression; these tests are more time consuming and expensive, and, as a rule, require special accessories to the machines available in laboratories.

Therefore, it is necessary to find ways of expressing the strength condition under compound stress in terms of  $\sigma_y$  and  $\sigma_u$  obtained from experiments for the uniaxial stress.

Thus, in the general case, when all the three principal stresses are nonzero, the strength of the material is tested according to the following plan:

- (1) the three principal stresses  $\sigma_1 > \sigma_2 > \sigma_3$  are calculated;
- (2) the material is selected;

(3) the critical stresses  $\sigma^n = \sigma_y$  or  $\sigma^n = \sigma_u$  and the permissible stresses are determined experimentally for the given material under simple tension or compression.

It is required to write down the strength condition for the compound stress knowing  $\sigma_1$ ,  $\sigma_2$ , and  $\sigma_3$  and retaining the same safety factor  $k$  (Fig. 79).

The above problem can be solved only on the basis of the assumption (hypothesis) about the type of function relating the strength of material to the value and sign of the principal stresses, and the factor that causes the critical state.

These factors may be numerous. As a matter of fact, even in simple tension of a bar of ductile material we may put the question: what is the cause of yielding?

We may assume that yielding starts when the maximum normal stresses in the bar reach the yield point  $\sigma_y$ . However, one may as well look at the problem from a different point of view and assume that yielding starts when the maximum elongation of the material reaches a certain limit. One may also assume that large plastic deformations begin to occur when the maximum shearing stresses achieve a certain value.

Thus, we can put forward a number of hypotheses and on their basis formulate various theories of strength. We shall see later that in simple tension or compression (in uniaxial stress) the results obtained by the strength tests are the same irrespective of the hypothesis used. This is so because the strength test is based directly upon experimental data.

The matters will be very much different in compound stress. In the succeeding sections we shall show how the strength condition changes depending upon the accepted theory. One or the other theory is selected for practical application only after it has been experimentally verified for the compound stressed state.

Whichever strength hypothesis we choose, it can be expressed analytically as some function of principal stresses

$$\Phi(\sigma_1, \sigma_2, \sigma_3) = \text{const} = C \quad (7.1)$$

In this form the strength theory expresses the condition of constancy (irrespective of the nature of stressed state) of the set of principal stresses that has one or the other physical interpretation. At the same time, equation (7.1) also describes some limiting surface in three-dimensional space of the principal stresses. Thus, for example, if  $C = \sigma_y$  or  $C = \sigma_u$ , the corresponding limiting surface is the surface which determines the conditions under which yielding or failure of material takes place.

Before we begin to expound various theories of strength, let us take note that the critical state for ductile materials (appearance of large plastic deformations) as well as brittle materials (appearance of cracks) lies at the boundary of application of Hooke's law (with known approxi-

mation sufficient for practical purposes). This enables us to use the formulas which have been derived in the preceding sections and which are valid only within the limits of application of Hooke's law for calculations relating to the strength test.

Our earlier discussion about the resistance of materials to rupture and shear emphasizes the need to distinguish between the strength theories for materials that fail due to rupture and the theories in which failure due to shear is considered the breakdown state. These theories are dealt with in §§ 39 and 40 separately.

### § 39. Theories of Brittle Failure (Theories of Rupture)

As has been already stated, failure in the form of rupture may be considered to occur either due to maximum normal tensile stress or due to maximum elastic elongation.

A. The assumption that failure is related to the maximum tensile stresses was put forward as early as the seventeenth century and subsequently supported by G. Lamé (1833) and W. J. M. Rankine (1856). At present the theory in which the maximum tensile stress is taken as the strength criterion is known as the *theory of maximum tensile stresses* or the *first strength theory*.

If  $\sigma_1 \geq \sigma_2 \geq \sigma_3$ , then the stress  $\sigma_1$  will be the maximum tensile stress  $\sigma_{\max}$ . According to the first strength theory, failure will occur irrespective of the stressed state when

$$\sigma_{\max} = \sigma_1 = \sigma_{rup}$$

where  $\sigma_{rup}$  is the resistance to rupture which is constant for a given material. For many brittle materials  $\sigma_{rup}$  is equal to the stress  $\sigma_u$  at the moment of failure under tensile loading. The safe state will obviously correspond to the condition

$$\sigma_{\max} = \sigma_1 \leq \frac{\sigma_{rup}}{k} = [\sigma]_t \quad (7.2)$$

where  $[\sigma]_t$  is the permissible stress in tension. Equation (7.2) represents the strength condition according to the first strength theory. It is applicable only when  $\sigma_1 > 0$ .

This theory is confirmed by tensile tests of brittle materials such as stone, brick, concrete, glass, and porcelain. In the case of compound stress the theory often comes into conflict with experimental data because it does not take into account the other two principal stresses upon which the strength of material depends in many cases.

B. The idea that brittle failure is connected not with the maximum tensile stress but with maximum strain was first expressed by French scientists Ed. Mariotte (in 1686) and C. M. L. Navier (in 1826) and later supported by other French scientists, J. V. Poncelet (1839) and

B. Saint-Venant (1837). The strength theory based upon this supposition is known as the *theory of maximum strain*, or the *second strength theory*. According to this theory failure occurs irrespective of the state of stress when maximum elastic strain  $\epsilon_{\max}$  becomes equal to a certain value  $\epsilon_{rup}$  which is constant for the given material. In general

$$\epsilon_{\max} = \epsilon_1 = \frac{1}{E} [\sigma_1 - \mu (\sigma_2 + \sigma_3)]$$

whereas in simple tension  $\epsilon = \sigma/E$ ; it is obvious that  $\epsilon_{rup} = \sigma_{rup}/E$ . In the compound stress, failure will occur when

$$\sigma_1 - \mu (\sigma_2 + \sigma_3) = \sigma_{rup}$$

The stressed state may be considered safe if in this expression  $\sigma_{rup}$  is replaced by  $[\sigma]_t$ . The strength condition in the second strength theory may be written as

$$\sigma_1 - \mu (\sigma_2 + \sigma_3) \leq \frac{\sigma_{rup}}{k} = [\sigma]_t \quad (7.3)$$

Thus in the theory of maximum strain, the permissible stress under tension is compared not to one of the principal stresses but to a combination of all of them, called the *reduced stress* and determined by the formula

$$\sigma_{red} = \sigma_1 - \mu (\sigma_2 + \sigma_3)$$

This hypothesis is also not supported by some experiments on the strength of ductile materials. If it were true for ductile materials, then the specimen stretched in two or three directions should be stronger than the specimen stretched in only one direction; this is not confirmed by experiments. This hypothesis is similarly not confirmed for uniform bulk compression.

For brittle materials, the theory of maximum strain generally gives results which match well with the available experimental data. Expression (7.3) may be applied if  $\sigma_1 - \mu (\sigma_2 + \sigma_3) > 0$ . Application of the second strength theory for the case of compression enables us to satisfactorily explain the reasons behind the failure of brittle materials along planes parallel to the direction of compressive force and also explain more or less correctly why the strength of brittle materials under compression is considerably higher than their strength in tension

(in tension  $\epsilon_{\max} = \frac{\sigma_1^0}{E} = \epsilon_{rup}$  and  $\sigma_1^0 = E\epsilon_{rup}$ , whereas in compression  $\epsilon_{\max} = -\frac{\mu}{E} \sigma_c^0 = \epsilon_{rup}$  and  $|\sigma_c^0| = \frac{E}{\mu} \epsilon_{rup}$ , i.e.  $\frac{1}{\mu}$  times greater). However, the second strength theory is also confirmed mainly by experiments on brittle materials only.

Both theories discussed above are theories of rupture; none of them is universal, i.e. valid in all the cases of failure due to rupture.

Sometimes the first theory conforms better to experimental data, sometimes the second. For a solid uniform body the second theory appears to be more logical and well founded than the first one.

#### § 40. Theories of Ductile Failure (Theories of Shear)

A. The fact that shear lines appear on the specimen surface during plastic deformation and that under tension ductile materials fail along the planes of maximum shearing stresses enables us to accept these stresses as the criterion of strength. This idea was first proposed by the French physicist Ch. A. Coulomb in 1773 and supported by the experiments of H. Tresca (1868), J. J. Guest (1900) and others. The strength theory based upon this assumption came to be known as the *theory of maximum shearing stresses* or the *third strength theory*. According to this theory the critical state of material (in the form of yield or failure) occurs, irrespective of the stressed state, when the maximum shearing stress  $\tau_{\max}$  becomes equal to a certain value  $\tau^0$  which is constant for the given material, i.e.

$$\tau_{\max} = \tau_1^0 = \tau_y$$

or

$$\tau_{\max} = \tau_{II}^0 = \tau_{sh}$$

where  $\tau_y$  is the yield stress in shear and  $\tau_{sh}$  is the maximum shearing stress when the material fails due to shear. The safe functioning of material is obviously governed by the strength condition

$$\tau_{\max} \leq \frac{\tau_y}{k} = [\tau] \quad (7.4)$$

In compound stress  $\tau_{\max} = (\sigma_1 - \sigma_2)/2$ . If we assume, following this theory, that permissible stress  $[\tau]$  does not depend upon the type of stressed state, we shall find its value from experiments on simple tension in which failure occurs as a result of shear. In this case  $\sigma_2 = 0$  and  $\tau_{\max} = \frac{\sigma_1}{2}$ . If stress  $\sigma_1$  in the right-hand side of the last expression is raised to permissible stress  $[\sigma]$ , the left-hand side of the same expression will represent the permissible value of shearing stress  $\tau$ ; thus,  $[\tau] = \frac{[\sigma]}{2}$ . Substituting now the values of  $\tau_{\max}$  and  $[\tau]$  in expression (7.4), we obtain

$$\tau_{\max} = \frac{1}{2} (\sigma_1 - \sigma_2) \leq \frac{1}{2} [\sigma]$$

or

$$\sigma_1 - \sigma_2 \leq [\sigma] \quad (7.5)$$

Thus, for strength check according to this theory the permissible stress in tension or compression is compared not with the maximum normal stress, but with the difference between the maximum and minimum normal (principal) stresses. The reduced stress in this case is

$$\sigma_{red} = \sigma_1 - \sigma_3$$

The advantage of the theory of maximum shearing stresses lies in its simplicity and the linearity of the strength condition, as in the first and second theories. It is well supported by experiments on ductile materials that have equal resistance to tension and compression, and also by experiments on bulk compression. This theory usually ensures sound dimensions of the designed elements of structures; sometimes the dimensions are even slightly on the higher side.

The drawback of the theory of maximum shearing stresses, which is seen immediately, is that it completely ignores the effect of the average principal stress on the working of the material. It implies that for constant maximum normal stress  $\sigma_1$  and minimum normal stress  $\sigma_3$ , we may vary  $\sigma_2$  in any way without changing working conditions of the material as long as it is less than  $\sigma_1$  and greater than  $\sigma_3$ . This statement is quite dubious, and experiments reveal that  $\sigma_2$  does have an effect upon the strength of materials. The theory also underestimates the danger of failure of elements subjected to approximately equal tensile stresses in the three principal axes. To this may be added that, according to this theory, the stressed states in cubic elements isolated near inclined planes (Fig. 54 (a) and (b)) must be identical from the point of view of failure if shearing stresses  $\tau_\alpha$  in these planes are equal to each other. As  $\tau_\alpha$  increases the yielding and failure in the material in these elements begin simultaneously. Experiments show that for materials having higher resistance under compression as compared to tension, case (a) in which the normal stresses in the plane of shearing stresses are tensile is more dangerous than case (b), when the normal stresses in the plane of  $\tau_\alpha$  are compressive. As the shearing stress  $\tau_\alpha$  increases, the material of the element will begin to yield or rupture earlier in case (a) than in case (b). Thus, the strength of material is influenced not only by the shearing stress but also by the normal stress acting on the same plane. This factor is taken into account by Mohr's theory (1900) which is discussed below.

B. The breakdown conditions  $\frac{\sigma_1 - \sigma_3}{2} = \tau_y$  or  $\frac{\sigma_1 - \sigma_3}{2} = \tau_{sh}$  discussed above should be looked upon in a broader aspect than as mere interpretation of the theory of maximum shearing stresses. According to these formulas, it can be considered that critical state is determined only by the maximum and minimum principal stresses. Experiments do not fully confirm this hypothesis; however, the maximum possible error due to ignoring medium principal stress  $\sigma_2$  does not exceed 15% and in a majority of cases is considerably smaller. Therefore while writing

the strength conditions it is permissible to restrict ourselves to studying the effect on strength only of the maximum and minimum principal stresses.

It is common knowledge that various cases of stress can be graphically represented by Mohr's stress circles. Figure 80 depicts a number of such circles: circle 1 represents simple tension:  $\sigma_1 \neq 0, \sigma_2 = \sigma_3 = 0$ ;

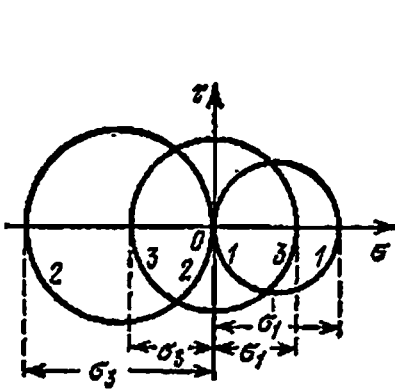


Fig. 80

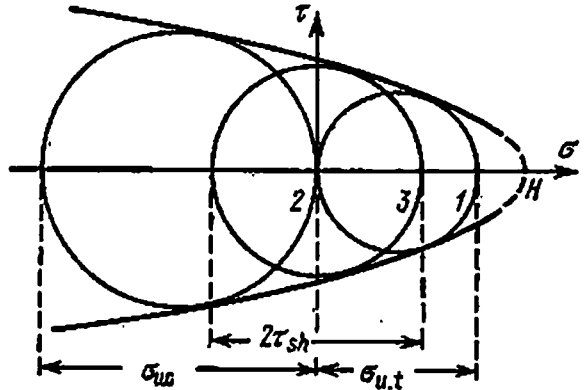


Fig. 81

circle 2, simple compression:  $\sigma_1 = \sigma_2 = 0, \sigma_3 \neq 0$ ; circle 3, pure shear:  $\sigma_3 = -\sigma_1, \sigma_2 = 0$ . The stress circles constructed for principal stress values corresponding to the critical state of materials will be called *limiting stress circles*. The limiting stress circles corresponding to the

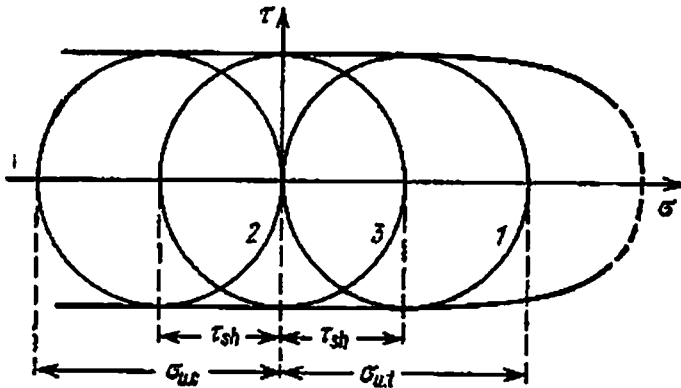


Fig. 82

state of stress depicted in Fig. 80 are shown in Fig. 81. The diameter of the limiting circle which depicts the critical state in simple tension is  $\sigma_{u,t}$ , the ultimate strength in tension; in the case of simple compression the ultimate circle diameter is  $\sigma_{u,c}$ , ultimate strength in compression; and in the case of pure shear the limiting circle diameter is equal to  $2\tau_{sh}$ .

O. Mohr postulated that all the limiting stress circles constructed from arbitrary centres can be inscribed into a smooth curve, the *envelope of the family of limiting stress circles*, which is tangent to all of them (Fig. 81). The envelope intersects the  $\sigma$ -axis at a certain point  $H$ , which corresponds to uniform triaxial tension (if  $\sigma_1 = \sigma_2 = \sigma_3$ , the stress circle becomes a point). The envelope is open on the opposite side because the failure of material under uniform triaxial compression is impossible. Plotting the envelope can be simplified by considering it, in the first approximation, as a straight line tangent to the limiting circles

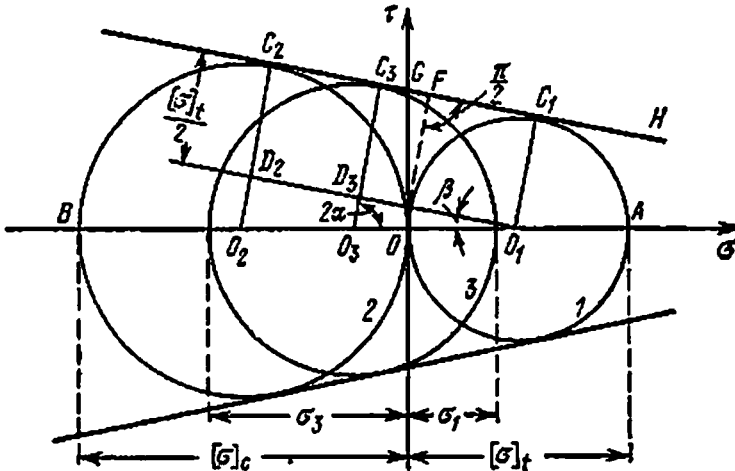


Fig. 83

of tension and compression. If the ultimate strengths under tension and compression are equal, the envelope branches remain parallel to the  $\sigma$ -axis over a large distance (Fig. 82). In this case Mohr's theory coincides with the theory of maximum shearing stresses.

By reducing the diameters of all limiting circles  $k$  times, where  $k$  is the safety factor, we obtain a family of circles which represents the permissible stressed states instead of the limiting stresses (Fig. 83). In Fig. 83 segment  $OA$  (the diameter of circle 1), represents the permissible stress under simple tension  $[\sigma]_t$ , segment  $OB$  (the diameter of circle 2) represents permissible stress under simple compression  $|\sigma|_c$ . The intermediate circle 3 with centre at  $O_3$  touches the envelope  $C_2C_1H$  at point  $C_3$  and represents a stressed state with principal stresses  $\sigma_1$  and  $\sigma_2$ .

From the similarity of triangles  $O_1O_2D_2$  and  $O_1O_3D_3$  it ensues that

$$\frac{O_3D_3}{O_2D_2} = \frac{O_1O_3}{O_1O_2} \quad \text{or} \quad \frac{O_3C_3 - O_1C_1}{O_2C_2 - O_1C_1} = \frac{OO_1 + OO_3}{OO_1 + OO_2}$$

By substituting corresponding stresses in place of segments, we obtain

$$\frac{\sigma_1 - \sigma_2 - [\sigma]_t}{|\sigma|_c - [\sigma]_t} = \frac{[\sigma]_t - (\sigma_1 + \sigma_2)}{[\sigma]_t + |\sigma|_c}$$



After some transformations we get the strength condition according to Mohr's theory:

$$\sigma_1 - \frac{|\sigma|_t}{|\sigma|_c} \cdot \sigma_3 = \sigma_1 - p\sigma_3 \leq [\sigma]_t, \quad p = \frac{|\sigma|_t}{|\sigma|_c} \quad (7.6)$$

The same condition can be derived without using stress circles\* if it is kept in mind that shear (according to Mohr) leading to failure occurs in that (breakdown) plane which has the most unfavourable combination of normal and shearing stresses. The condition restricting the value of a particular reduced shearing stress  $\tau_{red}$  in the breakdown plane may be written as

$$\tau_{red} = |\tau| + f\sigma \leq [\tau]_{red} \quad (7.7)$$

where  $|\tau|$  and  $\sigma$  are stresses in the breakdown plane (the sign of normal stress is taken into account) and  $f$  is the coefficient of friction. The location of the plane of maximum reduced shearing stress (in Fig. 83 this plane corresponds to point  $C_3$ ) is determined by angle  $\alpha$  which this plane makes with the plane of principal stress  $\sigma_1$ :  $\tan 2\alpha = \frac{1}{f} = \frac{1}{\tan \beta}$ . It can be shown (Fig. 83) that

$$f = \frac{|\sigma|_c - |\sigma|_t}{2\sqrt{|\sigma|_t|\sigma|_c}} \quad \text{and} \quad [\tau]_{red} = \frac{1}{2}\sqrt{[\sigma]_t[\sigma]_c} = OG$$

when  $f=0$  strength condition (7.7) changes into the similar condition of the third strength theory; if  $\sigma > 0$  (tension), condition (7.7) is satisfied only when the value of  $|\tau|$  is reduced as compared to the value for  $\sigma=0$ ; if  $\sigma < 0$  (compression), condition (7.7) is satisfied even with a higher value of  $|\tau|$  as compared to the value for  $\sigma=0$ . These conclusions are supported by experiments discussed earlier at the end of § 40A.

It can be easily seen that the strength condition (7.6) according to Mohr's theory coincides with the strength condition according to the theory of maximum shearing stresses if  $p=1$ , i.e.  $|\sigma|_t = |\sigma|_c$ . If the permissible stress under tension is very small (brittle materials), i.e. if it can be considered that  $|\sigma|_t = 0$  and  $p=0$ , Mohr's theory changes into the theory of maximum normal stresses. In biaxial stress, when  $\sigma_3=0$  and  $p \approx \mu$ , Mohr's theory coincides with the theory of maximum strain. Thus, to a certain extent Mohr's theory generalizes the first three strength theories; it correctly describes plastic deformation and failure due to shear of materials having different resistances to tension and compression. All experiments that verify the first and third theories and some experiments verifying the second theory also support Mohr's theory. It undoubtedly represents a forward step as

\* See S. I. Druzhinin and Yu. I. Yagn, *Strength of Materials*, "Kubuch", 1933 (in Russian).

compared to the first three theories. Yet it cannot be considered universal, since in a number of cases it does not correctly reflect the nature of failure due to rupture, and like the third strength theory it does not take into account the intermediate principal stress.

B. A number of authors suggested that the appearance of the critical state in materials depends not upon the magnitude of deformations and stresses separately but upon their combination and other factors like the potential energy or the numerically equal to it specific work of deformation. The amount of this work is expressed in terms of all the three principal stresses.

By the end of last century (1885) Italian scientist F. Beltrami proposed that the total potential energy of deformation per unit volume of the material should be taken as the criterion of pliability and strength of materials. On the basis of this hypothesis the condition expressing the approach of the critical state may be written as

$$u = u^0$$

where  $u^0$  is the potential energy accumulated in a unit volume of the material when yield or rupture sets in.

This hypothesis was not confirmed by experiments and is only of historical importance. It, however, formed the foundation upon which the new *energy theory of strength* was built; the latter generally gives results matching well with the experiments.

Considering the fact that plastic deformation takes place without any change in volume, F. Huber in 1904, R. Mises in 1913 and H. Hencky in 1924 proposed that instead of total potential energy of deformation only that part of the energy which was spent on changing the shape of a body should be accepted as the strength criterion. According to this hypothesis, irrespective of the stress yielding or rupture of the material starts when the potential energy of distortion per unit volume,  $u_{sh}$ , reaches a certain limiting (critical) value  $u_{sh}^0$  for the given material, i.e.

$$u_{sh} = u_{sh}^0 \quad (7.8)$$

where  $u_{sh}^0 = u_{sh.y}$  or  $u_{sh}^0 = u_{sh.rup}$ .

It is known that in compound stressed state (see formula (6.30'), § 35)

$$u_{sh} = \frac{1+\mu}{6E} [(\sigma_1 - \sigma_2)^2 + (\sigma_2 - \sigma_3)^2 + (\sigma_3 - \sigma_1)^2] = \frac{3(1+\mu)}{2E} \tau_{oct}^2$$

and in uniaxial tension

$$u_{sh} = \frac{1+\mu}{6E} 2\tau_1^2$$

If we accept, as already stated, that the critical value of the potential energy of distortion (for example, corresponding to the beginning

of yielding of material) does not depend upon the type of stressed state, we can consider that in uniaxial as well as in any other type of stress

$$u_{sh}^0 = \frac{1+\mu}{6E} 2\tau_y^2$$

Substituting the expressions for  $u_{sh}$  and  $u_{sh}^0$  in equation (7.8), dividing both sides by  $2\frac{1+\mu}{6E}$  and extracting from them square roots, we get the following expression which determines the beginning of critical state:

$$\frac{1}{\sqrt{2}} \sqrt{(\sigma_1 - \sigma_2)^2 + (\sigma_2 - \sigma_3)^2 + (\sigma_3 - \sigma_1)^2} = \frac{3}{\sqrt{2}} \tau_{oct} = \sigma_y$$

It can be easily noticed that this equation represents the condition of constancy of stress (or constancy of the octahedral shearing stress). The strength condition according to this theory, known as the *theory of potential energy of distortion* or the *fourth strength theory*, may be written as

$$\begin{aligned} \frac{1}{\sqrt{2}} \sqrt{(\sigma_1 - \sigma_2)^2 + (\sigma_2 - \sigma_3)^2 + (\sigma_3 - \sigma_1)^2} \\ = \sigma_l = \frac{3}{\sqrt{2}} \tau_{oct} \leq \frac{\sigma_y}{k} = [\sigma] \quad (7.9) \end{aligned}$$

The theory of potential energy of distortion is well supported by experiments on ductile materials, but fails when applied to brittle materials. This is natural because it is the theory of octahedral or medium shearing stresses unlike the third theory, which is the theory of maximum shearing stresses. The fourth strength theory takes into account all the three principal stresses and is therefore more complete than the theory of maximum shearing stresses. Unlike the first three strength theories and Mohr's theory, the fourth strength theory is non-linear, which somewhat complicates its practical application.

Keeping in mind that the resistance of materials to plastic deformation is to some extent affected by the mean normal stress  $\sigma_{mean}$ , the condition expressing the onset of yielding according to the theory of potential energy of distortion may be written more precisely as

$$\sigma_l + A\sigma_{mean} = B\sigma_y \quad (7.10)$$

where  $A$  and  $B$  are constants that depend upon the properties of a material. The strength condition may then be written in the form

$$\begin{aligned} \frac{1}{\sqrt{2}} \sqrt{(\sigma_1 - \sigma_2)^2 + (\sigma_2 - \sigma_3)^2 + (\sigma_3 - \sigma_1)^2} \\ + \frac{A_1}{3} (\sigma_1 + \sigma_2 + \sigma_3) \leq B_1 [\sigma] \quad (7.11) \end{aligned}$$

This expression can apparently be employed for checking the strength of parts of machines and structures made not only of ductile but also of some brittle materials. Unfortunately the possibility of applying this condition to brittle materials has not been studied sufficiently till now.

#### § 41. Reduced Stresses According to Different Strength Theories

In conclusion of our discussion of strength theories, we may write the strength condition in triaxial stress as follows:

$$\sigma_{red} \leq [\sigma] \quad (7.12)$$

where  $\sigma_{red}$  is the reduced stress and  $[\sigma]$  is the permissible stress in simple tension or compression. The reduced stress  $\sigma_{red}$  may be interpreted as the tensile stress in uniaxial loading equivalent to the compound stressed state under consideration as far as the danger of failure is concerned.

The expressions for  $\sigma_{red}$  according to different theories are as follows:

$$\begin{aligned} \sigma_{red}^I &= \sigma_{max} = \sigma_1 \\ \sigma_{red}^{II} &= E \epsilon_{max} = \sigma_1 - \mu (\sigma_2 + \sigma_3) \\ \sigma_{red}^{III} &= 2\tau_{max} = \sigma_1 - \sigma_3, \quad \sigma_{red}^M = \sigma_1 - p\sigma_3 \\ \sigma_{red}^{IV} &= \frac{1}{\sqrt{2}} \sqrt{(\sigma_1 - \sigma_2)^2 + (\sigma_2 - \sigma_3)^2 + (\sigma_3 - \sigma_1)^2} \end{aligned}$$

With a number of theories at his disposal for assessing the strength of parts from brittle and ductile materials, an engineer must choose in each particular case the most suitable theory proceeding from the actual properties of material. It is difficult to make the proper choice because of the fact that in compound stress the division of materials into ductile and brittle is conditional. A material having good ductility under simple tension and compression may behave like a brittle material in compound stress and fail without undergoing large plastic deformation. On the other hand, a material that shows brittle in uniaxial loading may behave as a ductile material when subjected to other types of stress. Hence, ductility and brittleness of materials depend upon the condition in which the given structure functions. Therefore it is more correct not to speak of brittle and ductile materials but of brittle and ductile states of materials.

The main factors that affect brittleness and ductility are temperature (low temperature increases brittleness, high temperature as a rule improves ductility), rate of deformation (in case of fast dynamic loading brittleness increases, whereas ductility is retained when loading is

static and gradual), type of stress (states of stress close to uniform triaxial tension are known as "tough" and they lead to higher brittleness; on the contrary stressed states close to uniform triaxial compression are known as "soft" and improve ductility).

At present many materials can be made to acquire brittle or ductile state by different means. If a material can deform and fail both as brittle and ductile, then, as was earlier stated, it also has two characteristics of resistance to failure that are determined experimentally: resistance to rupture and resistance to shear. The resistance to rupture  $\sigma_{rup}$  is found as the maximum normal tensile stress required for causing rupture  $\sigma_{max} = \sigma_1$  (first strength theory) or the reduced normal stress which is the product of maximum strain  $\epsilon_{max} = e_1$  and modulus of elasticity  $E$ , i.e.  $\sigma_{red} = \sigma_1 - \mu(\sigma_2 + \sigma_3)$  (second strength theory). The resistance to shear is determined by the maximum shearing stress when failure occurs due to shear  $\tau_{sh} = \tau_{max}^0 = \frac{1}{2}(\sigma_1 - \sigma_3)^0$  (third strength theory), by the limiting value of stress  $\sigma_1^0$  at the moment of failure (fourth strength theory) and the limiting value of reduced stress  $(\sigma_1 - \frac{\sigma_{u,t}}{\sigma_{u,c}})^0$  in the case of shear failure (Mohr's theory).

In the light of above, while designing, for instance, the elements of structures from mild steel, a ductile material in certain conditions (static loading, room temperature, uniaxial stress), it is not always possible to apply the third or fourth strength theories without taking into account the actual working conditions of the structures; similarly, while designing parts from concrete—a brittle material under the afore-mentioned conditions, the first theory is not always applicable.

The problem of applying one or the other strength theory can be solved to the first approximation with the help of the so-called mechanical state diagram proposed by Prof. Ya. B. Fridman on the basis of research on the strength of materials carried out by Prof. N. N. Davidenkov and his followers.\*

As an example consider the transmission of pressure from the locomotive wheel to the rail (Fig. 59). The elementary cube with edges of 1 mm cut at the centre of the area through which the pressure from the wheel is being transmitted to the rail is subjected to compressive principal stresses:  $\sigma_1 = -80$  kgf/mm<sup>2</sup>;  $\sigma_2 = -90$  kgf/mm<sup>2</sup>;  $\sigma_3 = -110$  kgf/mm<sup>2</sup>. We shall calculate by the third and fourth strength theories the reduced stress which should be compared with the permissible stress. According to the theory of maximum shearing stresses

$$\sigma_{red}^{III} = \sigma_1 - \sigma_3 = -80 + 110 = 30 \text{ kgf/mm}^2$$

\* For instance, see N. M. Belyaev, *Strength of Materials*, 10-14 editions, § 252 (in Russian).

According to the distortion energy theory

$$\sigma_{red}^{IV} = \frac{1}{\sqrt{2}} \sqrt{(-80 + 90)^2 + (-90 + 110)^2 + (-110 + 80)^2} \\ = 26.4 \text{ kgf/mm}^2$$

Since the yield stress for commercial rail steel is approximately 40 kgf/mm<sup>2</sup> and the elastic limit is nearly 30 kgf/mm<sup>2</sup>, the computed principal stresses are within the permissible limits. This is confirmed by the behaviour of rail steel in exploitation.

Finally, it should be noted that all the preceding discussions of the strength theories pertain to the materials which may be sufficiently accurately considered as isotropic. The formulas derived above are not applicable for anisotropic materials. For example, in the case of timber the direction of force with respect to fibres has to be taken into account.

## § 42. Permissible Stresses in Pure Shear

The permissible shearing stress in pure shear could, it seems, be determined as in uniaxial tension or compression, i.e. by experimentally establishing the critical stress (corresponding to yielding or rupture) and dividing it by the factor of safety. There are, however, some practical difficulties in applying such a method. It is very difficult to simulate pure shear in laboratory conditions; the working of bolts and riveted joints is complicated due to the presence of normal stresses. In the case of torsion\* of solid bars of round and other cross sections the stressed state is not uniform in the whole volume of the bar. Moreover, the plastic deformation preceding failure is accompanied by redistribution of stresses, which complicates the determination of critical stress. When thin-walled bars are subjected to torsion, the bar walls can easily lose stability. In the light of all these considerations the permissible stresses in torsion and pure shear are chosen on the basis of one or the other strength theory depending upon the permissible tensile stress that can be determined more reliably.

Keeping in mind that in pure shear  $\sigma_1 = \tau$ ,  $\sigma_2 = 0$ , and  $\sigma_3 = -\tau$  (see formulas (6.33) in § 36), we can establish relationships between  $[\tau]$  and  $[\sigma]$  according to the different strength theories.

After substituting  $\sigma_1 = \tau$  in the first strength theory condition  $\sigma_1 \leq [\sigma]_t$ , it may be written as  $\tau \leq [\sigma]_t$ , wherefrom

$$[\tau]_t = [\sigma]_t \quad (7.13)$$

After substituting in the second strength theory condition

$$\sigma_1 - \mu(\sigma_2 + \sigma_3) \leq [\sigma]_t$$

\* The material of a bar subjected to torsion experiences pure shear (see Chapter 9).

the values of principal stresses in pure shear, we get

$$\tau - \mu(-\tau) = (1 + \mu)\tau \leq [\sigma]_t$$

or

$$\tau \leq \frac{[\sigma]_t}{1 + \mu}$$

wherefrom

$$[\tau]^{II} = \frac{[\sigma]_t}{1 + \mu} \quad (7.14)$$

After substituting in the third strength theory condition

$$\sigma_1 - \sigma_3 \leq [\sigma]$$

the values of  $\sigma_1$  and  $\sigma_3$ , it takes the form

$$\tau - (-\tau) = 2\tau \leq [\sigma]$$

or

$$\tau \leq \frac{1}{2} [\sigma]$$

i.e.

$$[\tau]^{III} = \frac{1}{2} [\sigma] \quad (7.15)$$

The strength condition according to Mohr's theory is  $\sigma_1 - \rho\sigma_3 \leq [\sigma]_t$ ; in the case of pure shear we get  $\tau - \rho(-\tau) = (1 + \rho)\tau \leq [\sigma]_t$ , wherefrom  $\tau \leq \frac{1}{1 + \rho} [\sigma]_t$ , or

$$[\tau]^M = \frac{1}{1 + \rho} [\sigma]_t = \frac{[\sigma]_t [\sigma]_c}{[\sigma]_t + [\sigma]_c} \quad (7.16)$$

In Fig. 83 permissible stress  $[\tau]^M$  is represented by segment  $OF$ . Applying the fourth strength theory, we find

$$\frac{1}{\sqrt{2}} \sqrt{(\tau - 0)^2 + (0 + \tau)^2 + (\tau + \tau)^2} = \sqrt{3}\tau \leq [\sigma]$$

i.e.

$$\tau \leq \frac{[\sigma]}{\sqrt{3}} \quad \text{and} \quad [\tau]^{IV} = \frac{[\sigma]}{\sqrt{3}} \quad (7.17)$$

Expressions (7.15) and (7.17) should be used in the design of the elements of structures from ductile materials that have equal resistance to tension and compression. The difference between  $[\tau]^{III}$  and  $[\tau]^{IV}$  is about 15%. Expression (7.16) must be used in the case of materials that have unequal resistance to tension and compression. Expression (7.13) is used rarely. It is desirable to use expression (7.14) only for brittle materials; however, it is also used in the design of parts working in shear (bolts, and rivets). Since  $\mu \approx 0.3$  for steel, then

$$[\tau]^{II} = \frac{1}{1.3} [\sigma]_t = (0.75 - 0.8) [\sigma]_t$$

# PART III

## Shear and Torsion

### CHAPTER 8 Practical Methods of Design on Shear

#### § 43. Design of Riveted and Bolted Joints

While studying the stresses acting in inclined planes (§ 27) we saw that even in simple tension or compression two parts of a bar cut by an inclined plane tend not only to separate from each other but to shear along the sectioning plane. This is due to the fact that both normal and shearing stresses act in the plane. We came across these types of deformations—tension or compression and shear—while discussing compound stress and, in particular, in pure shear (§ 36).

In practice a number of parts of structures work mainly under shear due to which strength test for shearing stresses acquires major importance. The simplest examples of such parts are bolted and riveted joints. In many fields rivets have been replaced by welding; however, riveted joints are still widely used for joining all types of metal structures: rafters, bridge trusses, cranes, for joining plates in boilers, ships, reservoirs, etc.

To make a riveted joint, holes are drilled or pressed in both plates. A red-hot rivet with one head is placed in these holes and its other end is riveted by strokes from a special hammer or by pressure from a hydraulic press (riveting machine) to make the second head. Small rivets (having diameter less than 8 mm) are deformed in a cold state (in aviation structures).

A. Let us take the simplest riveted joint to study the working of rivets (Fig. 84). Six rivets placed in two rows join two plates by a *lapped joint*. Under the action of forces  $P$  these plates tend to shift over one another, this being hampered by the rivets to which forces  $P$  are transferred.\*

While checking the strength of rivets we shall stick to the established order of solving problems of strength of materials. Two equal and

---

\* The resistance due to friction is not taken into account.



opposite forces are transferred to each rivet: one acting from the first plate and the other, from the second plate. It has been experimentally shown that some of the rivets in a row carry greater load than the others. However, at the moment of breakdown, the forces acting on various rivets more or less level out due to plastic deformation. Therefore, it is generally accepted that all the rivets work under similar conditions.

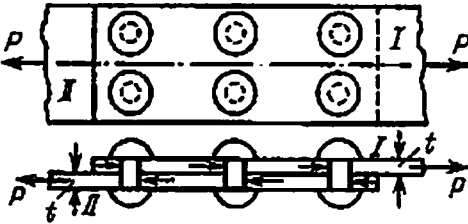


Fig. 84

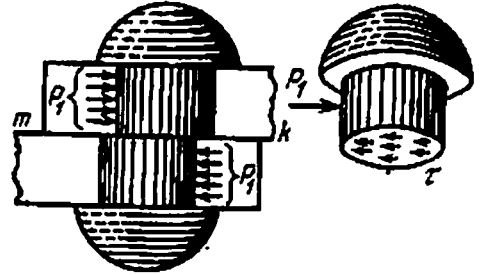


Fig. 85

Thus if there are  $n$  rivets in the joint shown in Fig. 84, then each of the rivets will be subjected to two equal and opposite forces  $P_1 = \frac{P}{n}$  (Fig. 85). These forces are transmitted to the rivet through the pressure of the corresponding plate on the semicylindrical surface of the shank. Forces  $P_1$  tend to shear the rivet along plane  $mk$  which is the parting plane of the plates.

To determine the stresses acting in this plane let us imagine the rivet shank to be cut by section  $mk$  and the lower portion removed (Fig. 85). The internal forces which are transferred through this section from the lower portion to the upper one will balance force  $P_1$ , i.e. they will act parallel to it in the cutting plane and will give a resultant force  $P_1$ . Therefore, the stresses appearing in this section and acting tangentially to it will be called shearing stresses  $\tau$ . Generally it is assumed that they are distributed uniformly over the whole section. If the rivet shank has diameter  $d$ , then the stress per unit area of the section will be

$$\tau = \frac{P_1}{\frac{\pi d^2}{4}} = \frac{P}{n \frac{\pi d^2}{4}}$$

Denoting the permissible stress in shear by  $[\tau]$ , we may write the strength condition of the rivet under shear as follows:

$$\tau = \frac{P_1}{A} = \frac{P}{n \frac{\pi d^2}{4}} \leq [\tau] \quad (8.1)$$

i.e. the actual shearing stress  $\tau$  acting in the rivet material should not exceed the permissible shearing stress (see § 42).

From this condition we can determine the required diameter of the rivets if their number is known, and vice versa. Usually the diameter of the rivet shank  $d$  is given in accordance with the thickness  $t$  of the parts to be joined (generally  $d \approx 2t$ ) and the required number of rivets  $n$  is determined from the relation

$$n \geq \frac{P}{\frac{\pi d^2}{4} [\tau]} \quad (8.1')$$

The denominator of this formula represents the force which each of the rivets can withstand safely.

While deriving formula (8.1) one more inaccuracy had been allowed. Actually forces  $P_1$  acting on the rivet are not directed along a straight line but constitute a force couple. This couple is balanced by another force couple, formed by the reaction of the riveted plates on the rivet head (Fig. 86) and gives rise to normal stresses acting in plane  $mk$ .

Besides these normal stresses, section  $mk$  is subjected to normal stresses from another source: during cooling the rivet shank tends to shorten which is hindered by the stop of the rivet heads by the plates. This, on the one hand, leads to tightening of the plates by the rivets giving rise to forces of friction between them, and on the other hand causes considerable normal stresses in the sections of the rivet shank.

These stresses are not very harmful. The rivets are made of steel possessing sufficient ductility; therefore, even if the normal stresses attain the yield point we can only expect some plastic deformation (elongation) of the rivet shank, which will reduce the friction between the plates. The rivets will however continue to work on shear as designed. These normal stresses are therefore not taken into consideration while designing riveted joints.

Expression (8.1) has been derived for single-shear riveted joints. If the joint is lapped by two cover plates (Fig. 87), each rivet experiences shear in two planes— $mk$  and  $gf$  (Fig. 88). Such rivets are known as *double-shear rivets*. If  $n$  rivets are required to transmit force  $P$  from one plate to the cover plates, then force acting on one rivet is  $P_1 = P/n$ . The area of shear  $A_{sh} = \frac{2\pi d^2}{4}$  and the shearing stresses in sec-

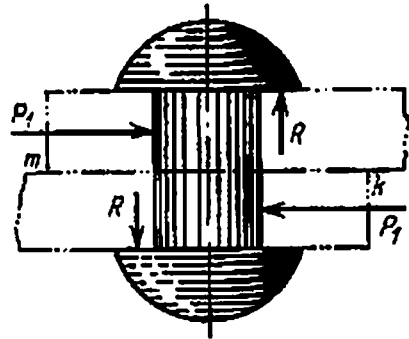


Fig. 86

tions *mk* and *gf* (Fig. 88) are

$$\tau = \frac{P}{n \frac{2\pi d^2}{4}}$$

The strength condition for a double-shear rivet may be written as

$$\tau \leq [\tau], \text{ wherefrom } n \geq \frac{P}{2 \frac{\pi d^2}{4} [\tau]} \tag{8.2}$$

Hence, in a joint having two shear planes, the number of rivets required according to the strength condition against shear is two times less than that required in single shear (formula (8.1)).

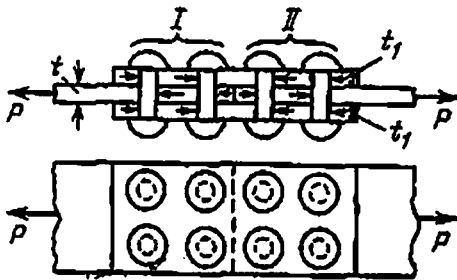


Fig. 87

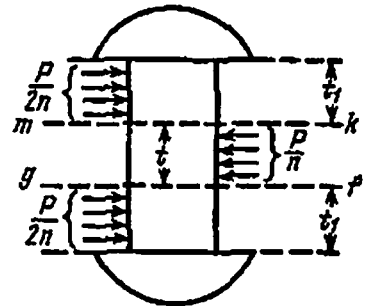


Fig. 88

In the case of multiple-shear rivets that are sometimes used in metal structures, the shear area of each rivet is  $A_{sh} = \frac{k\pi r^2}{4}$  and the strength condition is

$$n \geq \frac{P}{k \frac{\pi d^2}{4}} \tag{8.3}$$

where *k* is the number of shear planes.

However, the observance of strength conditions for shear alone does not always ensure that the riveted joint is sufficiently strong. The joint will be spoiled if the hole walls or the rivet shank get crushed along the semicylindrical contact surface when the force is being transmitted from the plate to the rivet. Therefore, in order to ensure reliable working of the riveted joint it is essential to check the rivets (or plates) against crushing.

Figure 89 presents an approximate picture of transmission of pressure to the rivet shank. The distribution of this pressure over the cylindrical surface is not known; it depends to a large extent upon the conditions of manufacturing the structure. It is assumed that the non-uniform pressure transmitted to the semicylindrical surface of a rivet is distributed uniformly over the diametral plane *BC* of the rivet. The stress

in this diametral plane is found to be equal to the maximum bearing stress  $\sigma_b$  at point *A* of the rivet surface (Fig. 89).

This conditional bearing stress can be calculated by dividing the force acting on each rivet with the area of the diametral section *BCC'B'* (Fig. 89). This area is a rectangle one side of which is the rivet diameter and the other the thickness of the plate through which the pressure is transmitted to the rivet.

The pressure on each rivet is  $\frac{P}{n}$ , therefore

$$\sigma_b = \frac{P}{n t d}$$

The strength condition for bearing will be

$$\sigma_b = \frac{P}{n t d} \leq [\sigma_b] \tag{8.4}$$

where  $[\sigma_b]$  is the permissible bearing stress. From this formula the required number of rivets may be determined as

$$n \geq \frac{P}{t d [\sigma_b]} \tag{8.5}$$

The permissible bearing stress is generally taken from 2 to 2.5 times greater than the permissible stress under tension or compression  $[\sigma]$ , because the test for bearing strength is actually a simplified test of

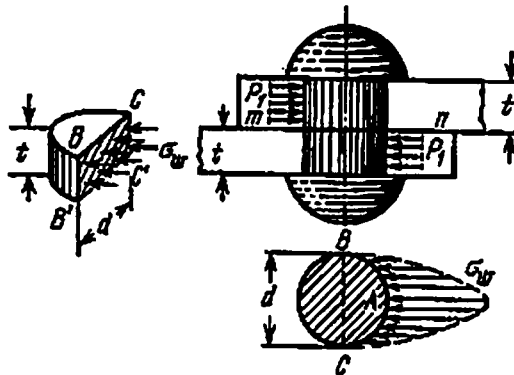


Fig. 89

strength for contact stresses. Expressions (8.4) and (8.5) are equally valid for single-shear and double-shear rivets.

We shall illustrate with an example how to calculate the required number of rivets. Let us compare two types of a riveted joint, one lap-joint with single-shear rivets (Fig. 84) and the other with double-shear rivets (Fig. 87). Let  $P=48\,000$  kgf,  $t=1$  cm,  $[\tau]=1000$  kgf/cm<sup>2</sup> and  $[\sigma_b]=2400$  kgf/cm<sup>2</sup>. The thickness of cover plates  $t_1$  is always more than  $0.5 t$ .

(a) For a lap joint we have according to the strength condition for shear (8.1)

$$n \geq \frac{P}{\frac{\pi d^2}{4} [\tau]} = \frac{48\,000}{\frac{3.14 \times 2^2}{4} 1000} \approx 15$$

according to the bearing strength condition (8.5)

$$n > \frac{P}{td[\sigma_b]} = \frac{48\,000}{1 \times 2 \times 2400} = 10$$

Number of rivets required is 15.

(b) For a butt joint with two cover plates according to strength condition for shear (8.2)

$$n \geq \frac{P}{2 \frac{\pi d^2}{4} [\tau]} \approx 8$$

according to bearing strength condition (8.5)

$$n \geq \frac{P}{td[\sigma_b]} = 10$$

We should use 10 rivets (on each side of the joint).

We see that the number of single-shear rivets was determined by the strength condition for shear, whereas that of double-shear rivets by the bearing strength condition.

**B.** The presence of rivets introduces certain changes in the methods of checking the tensile or compressive strength of the plates themselves. The critical section of each plate (Fig. 90) is the section which passes through the rivet holes. The effective width of the plate is minimum in this section; it is said that the section is weakened by the rivet holes. If  $b$  is the total width of the plate, then we get the following strength condition:

$$\frac{P}{t(b-md)} \leq [\sigma] \quad (8.6)$$

where  $m$  is the number of holes in the section (in our case there are two of them).

Knowing the plate thickness  $t$ , we can find its width  $b$  from the above condition. The area of the weakened section  $(b-md)t$  is called the net area, whereas the area of the full section  $bt$  is called the gross area.

The account of the effect of the rivet holes on the strength of riveted plates is generally accepted but is rather conditional. Actually, considerable local stresses arise over the contour of the plate, at the ends of the diameter perpendicular to the direction of tension. These local stresses in the material may reach the yield point and cause plastic deformations, though in a small volume of the plate material.

These local stresses are potentially capable of causing cracks only in a material having low fatigue limit when it is subjected to a variable load (§ 16). However, in the usual working conditions of riveted joints this danger may be ruled out. To avoid failure of riveted plates due to rivets the latter should be located at a certain distance from each other and from the edge of the plates. The location of rivets in the top view is conditioned not only by the strength and lightness of the joint but also by manufacturing considerations.

C. Like rivets, link bolts of lugs and the common bolted joints experience shearing and bearing stresses, therefore their design does not differ from that of riveted joints.

A somewhat different method is employed for designing high-strength bolted joints which have found wide application in recent years, es-

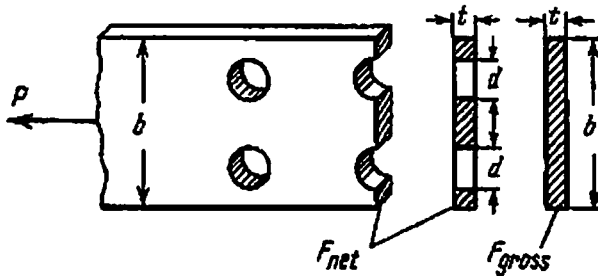


Fig. 90

pecially in bridge building. These bolts are used instead of rivets and are tightened by means of torque wrenches to a very high values of tensile forces, which ensure such tight pressing of the joined elements that the frictional forces at the interface are able to bear all the forces transmitted through the joint. The high-strength bolts experience neither shear nor bearing strain.

The basic idea behind the design of these bolts lies in providing the equilibrium between external forces  $P$  transmitted through the joint and the frictional forces that develop between the joined elements. If we denote the tensile force for one bolt by  $N$  and the coefficient of friction by  $f$ , we get the following strength condition for the joint:

$$P = \alpha N f n \quad (8.7)$$

Here  $n$  is the number of bolts and  $\alpha$  is a coefficient that accounts for possible deviations of  $N$  and  $f$  from their nominal values ( $\alpha < 1$ ). The required number of high-strength bolts is calculated from equation (8.7):

$$n \geq \frac{P}{\alpha N f} \quad (8.8)$$

In accordance with the existing standards for steel bridges, we assume

$$N = 0.6 \sigma_u A$$

where  $A$  is the area of bolt section weakened by thread and  $\sigma_u$  is the ultimate strength of bolt material which is not less than 12 000 kgf/cm<sup>2</sup>. Depending upon the grade of steel, the following values are used:  $\alpha = 0.78$  and  $f = 0.4-0.45$ .

#### § 44. Design of Welded Joints

In manufacturing metal structures electric-arc welding is often employed. It was invented at the end of the XIX century by Russian engineers N. N. Benardos (1882) and N. G. Slavyanov (1888) and ultimately found wide application throughout the world.

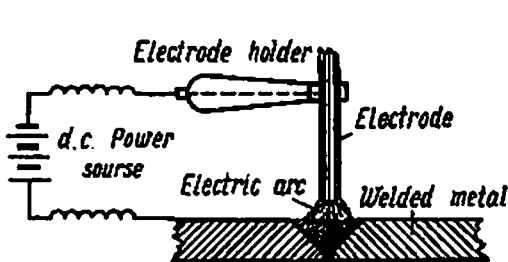


Fig. 91

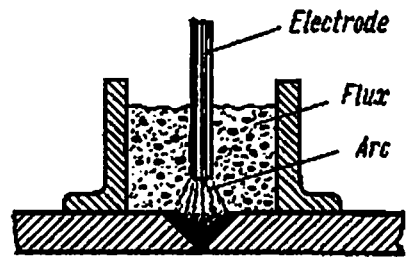


Fig. 92

In electric-arc welding by Slavyanov's method the electrode material (steel) melts under the heat of the electric arc and fills the joint of the elements to be welded, which are also heated to the fusion point by the electric arc. As a result, upon cooling the molten metal forms a weld which rigidly joins the elements (Fig. 91).

A thick protective coating is applied to the electrode to shield the molten metal from the harmful influence of the surrounding atmosphere. When the electrode melts, the protective coating forms a large amount of slag and gases which isolate the molten metal from the surrounding atmosphere. This ensures high quality of the weld metal, which may otherwise have very poor mechanical properties due to atmospheric oxygen and nitrogen (if the electrode is not coated or if the coating is thin).

At present manual arc welding is used mainly in joints requiring relatively short welds, for example, in welding steel trusses, tacking of angles, etc. Structures requiring long welds (such as mass produced welded beams, ship bodies and gas holders) are welded by automatic arc welding under a flux layer (Fig. 92). In automatic arc welding the electrode wire rolled into a coil is fed to the joint at a certain distance from the weld, thus ensuring constant arc length. The carriage with the electrode moves along the joint at a rate which is determined by the welding conditions. The arc and weld are protected from atmospheric oxygen and nitrogen by a layer of flux (granulated slag of special com-

position) which also melts in the arc flame, forming a brittle, easily removable skin.

Structures made of aluminium alloys, that have won wide popularity in recent years, are welded by argon-arc welding using an infusible tungsten electrode and an aluminium welding rod. The distinguishing feature of argon-arc welding is that the arc and molten metal are protected from the atmospheric undesirable impurities by an argon jet.

Besides arc welding, resistance spot welding is employed in some cases when thin metal sheets have to be welded (for example, welding of thin plating and thin profiles). In spot welding the parts to be joined are placed between tightly pressed to them copper electrodes through which electric current is passed. The metal around the points of contact gets heated up to a temperature which is sufficient to ensure welding of the elements.

If the joint design, the electrode material and the welding method are properly selected, the welded joint is found to be in no way inferior to the riveted joint under static as well as dynamic loading (including impact and alternating ones). In addition, electric-arc welding has a number of advantages over riveting, the most important of which are lower labour consumption and the absence of weakening of the section of the elements due to rivet holes. This gives considerable saving of resources and metal besides the economy due to greater compactness of the joint. The economic gains from electric-arc welding and the fact that it simplifies the structures have in the last few years led to gradual replacement of riveted joints by welded.

The welded joints, like the riveted joints, are designed on the assumption that the stresses are uniformly distributed in the weld section. The design is closely connected to the welding method; in particular, this is reflected in the permissible stresses, which are selected for the particular weld material in accordance with the welding method (manual or automatic welding) and also the thickness and composition of the electrode coating.

According to existing standards, the permissible stress for weld material is taken the same as for the base metal in the case of automatic arc welding under a flux layer and manual arc welding with top-quality electrodes. For welding with common electrodes the permissible stresses are reduced by 10%.

The gauge length of the weld is often assumed to be 10 mm less than the actual length to account for poor fusion at the beginning and crater formation at the end of the weld and also to take into consideration the difference in structure of the base and weld metals.

Let us discuss the design methods for some types of welded joints.

The butt joint is the simplest and most reliable of all joints. It is obtained by filling the gap between the end faces of the elements to be welded with fillet metal. The butt joint, depending upon the thickness of the elements is made according to one of the methods shown in



Fig. 93. The strength test is done for tension or compression according to the following formula

$$\sigma_w = \frac{P}{l_f} \leq [\sigma_w] \quad (8.9)$$

Here  $l_f = A_w$  is the nominal effective cross-sectional area of the weld having gauge length of the joint  $l = b$  and weld height  $h$  equal to the thickness of the plates  $t$ .

Taking into account the possibility of poor fusion at the ends the weld length is taken as  $l = b - 10$  mm and the weld has a different strength as compared to the base metal. It should be noted that with

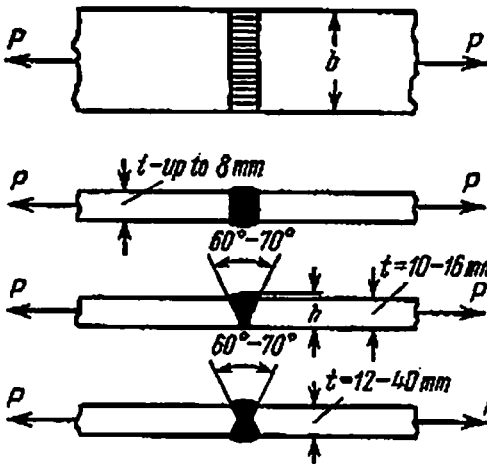


Fig. 93

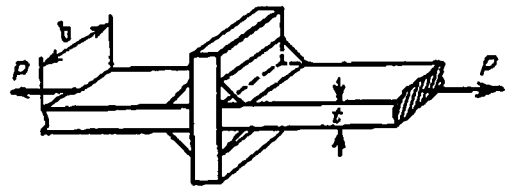


Fig. 94

an appropriate quality of welding the strength of the butt joint is not less than that of the base metal even under impact loading.\*

In order to achieve greater joint strength, it is sometimes made in the form of a cross-shaped joint with the help of a plate which is welded by means of fillet welds (Fig. 94). Similar welds are employed in lap and butt joints which are made with the help of cover plates.

The fillet welds laid perpendicular to the direction of force are called edge transverse fillet welds, whereas those laid parallel to the force acting on the lap joint are known as side or side fillet welds.

The fillet weld does not have a very definite shape of section (Fig. 95(a)). In theoretical calculations of strength the weld section is considered to be an isosceles triangle (shown by dotted lines) of height  $h$ \*\* (Fig. 95(b)).

\* Ya. I. Kipnis, D. I. Navrotskii, *Investigation of Strength of Welded Joints Under Impact*, Transzheldorizdat, 1956 (In Russian).

\*\* Sometimes transverse fillet welds are made concave with height  $h < 0.7t$ . The cathetus of the weld may be even less than the thickness of the plate.

The joints made with the edge (end-lap) welds are shown in Figs. 94 and 96. These welds fail in the weakest section *AB*, as established experimentally.

It is clear from Fig. 95 (b) that the total stress acting in section *AB* may be resolved into normal and shearing components. As the resistance

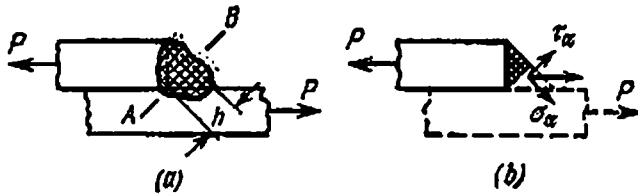


Fig. 95

of steel to shear is lower than that to tension, the transverse fillet welds are designed for shear assuming that the shearing stresses are distributed uniformly over the area of section *AB*. Keeping in mind that

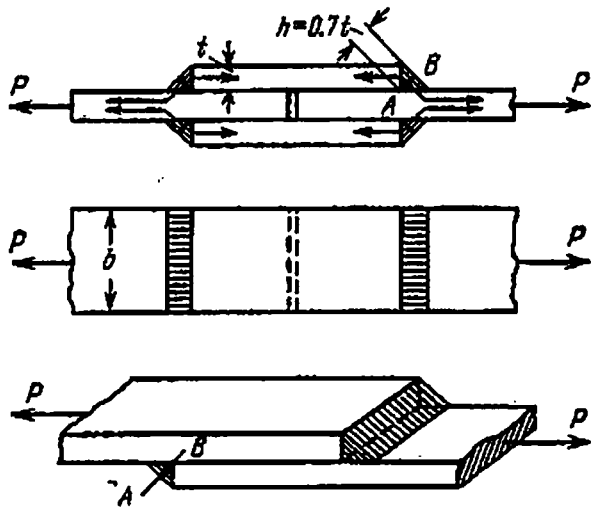


Fig. 96

force *P* acting on the joint is taken by two end-lap welds (Fig. 96), the upper and the lower ones, we get

$$\tau_w = \frac{P}{2A_w}$$

As the area of the weld section is  $A_w = hl = ll \cos 45^\circ \approx 0.7ll$ , and the gauge length is  $l = b$ , the strength condition may be written as

$$\tau_w = \frac{P}{1.4ll} \leq [\tau_w] \tag{8.10}$$

The cross-shaped butt joint depicted in Fig. 94 is designed similarly.

Actually, the weld material is subject to compound loading, the distribution of stresses in section  $AB$  being non-uniform. A study of the welds by the methods of the theory of elasticity, which has a sound experimental support, reveals that there is a high stress concentration at the corners of welds.

Apart from this, due to shrinkage of the joints in the welding zone during cooling, additional stresses occur not only in the weld material but also in the base metal, thus subjecting it to a compound stress.

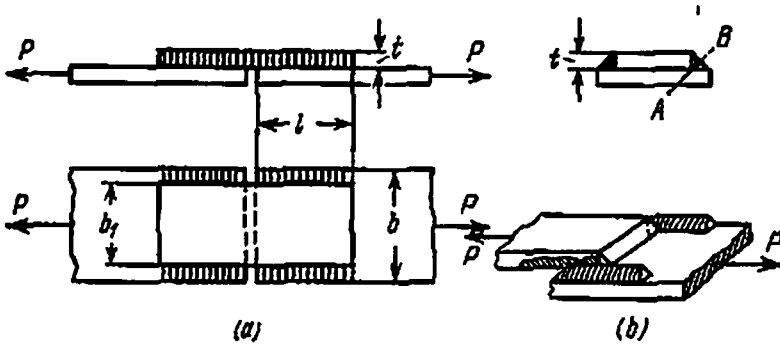


Fig. 97

This factor may result in lower ductility of the weld metal thus making the joint (with transverse fillet welds) less reliable, especially under impact or alternating loads, as compared to butt joints without cover plates.

A joint with side (longitudinal) fillet weld is shown in Fig. 97(a). The weld shown in Fig. 97(b) fails over a considerable length of the joint due to shearing of the weld metal parallel to the weld in the weakest section  $AB$ . The strength condition for two symmetrically placed welds may be written as

$$\tau_w = \frac{P}{2 \times 0.7tl} \leq [\tau_w] \quad (8.11)$$

The number of welds doubles if two overlapping plates cover the joint, and the strength condition takes the form

$$\tau_w = \frac{P}{4 \times 0.7tl} \leq [\tau_w] \quad (8.12)$$

The required gauge length  $l$  of the side fillet welds is generally calculated from formulas (8.11) and (8.12). The actual length of each weld is taken as  $l_0 = l + 10$  mm.

Experiments show that the side fillet welds fail in a way similar to the failure of ductile materials with large permanent deformation. This makes the working of side fillet welds more favourable as compared to that of end-lap (transverse fillet) welds. However, it should be borne

in mind that there is high stress concentration at the ends of side fillet welds too.

In designing welded joints greater reliability of the joint is sought to be achieved by using, instead of a butt joint, or in addition to it, overlapping cover plates, which are welded by side fillet welds or edge welds or both. As was earlier pointed out, under impact and alternating loads such "strengthening" of the butt joint may do greater harm than benefit.

In design of a combined joint using end-lap welds and side fillet welds simultaneously, it is considered that the joint resistance is the sum of the resistances of individual welds, i.e.  $P = P_e + P_s$ , where the resistance of the edge weld for a gauge length  $l_e$  is  $P_e = 0.7 t l_e [\tau_w]$ , and the resistance of the side welds is  $P_s = 2 \times 0.7 t l_s [\tau_w]$ ; here  $l_e = b$ , where  $b$  is the width of the cover plate. By substituting these values we get

$$P = (0.7 t l_e + 1.4 t l_s) [\tau_w] \quad (8.13)$$

The length of the side fillet weld  $l_s$ , can be determined if the length of the edge weld is known. If cover plates are used on both sides, the number of welds doubles, i.e. the right-hand side of formula (8.13) should be doubled.

The wide application of electric-arc welding in metal structures has led to the development of various types of welded joints, the design and analysis of which are discussed in special literature\*.

The methods discussed in this chapter on the design of riveted and welded joints for permissible stresses are accepted in machine building, ship building, aircraft building, etc. A fundamentally new method of design for limiting state (Chapter 25) is applied in the Soviet Union for designing engineering structures (civil and industrial buildings, bridges, tunnels, etc.). This method, however, does not differ much from the design for permissible stresses.

The joints in timber structures (grooves, keys, etc.) working under shear and bearing are also designed by the limiting-state method. The distinguishing feature of timber is its anisotropy due to which it has different shearing and bearing strength depending upon the angle between the direction of force acting on the element and the direction of fibres. Timber has higher shearing and bearing strength along the fibres than across the fibres or in an inclined direction; this is taken into account by means of coefficients. The design and analysis of these joints is available in special literature\*\*.

\* See, for example, G. A. Nikolaev, S. A. Kurkin, and V. A. Vinokurov, *Analysis, Design and Preparation of Welded Structures*, Vysshaya Shkola, 1971 (in Russian).

\*\* See, for example, A. P. Pavlov, *Timber Structures*, Goslesizdat, 1959 (in Russian). See also *Building Structures*, edited by G. Ovechkin, Gosstroizdat, 1975 (in Russian).

## CHAPTER 9

## Torsion.

## Strength and Rigidity of Twisted Bars

## § 45. Torque

The results obtained during the study of shear enable us to pass over to the study of strength under torsion. In practice we come across torsion very often; the examples of rods working under torsion are axes of a rotating wheel, transmission shafts, elements of three-dimensional mechanisms, springs and even an ordinary ward key.

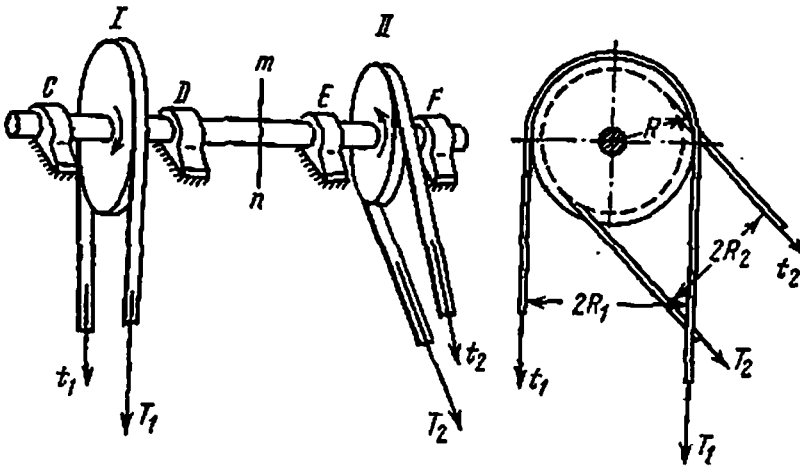


Fig. 98

We shall first study torsion in round shafts. Let us imagine (Fig. 98) shaft  $CF$  on which two pulleys,  $I$  and  $II$ , are fitted tightly. The shaft is supported by bearings  $C$ ,  $D$ ,  $E$ , and  $F$ . Pulley  $I$  rotates the shaft with the help of a belt drive from an electric motor. Pulley  $II$  transmits this rotation to the machine tool through another belt drive.

Pulley  $I$  is acted upon from the tight and slack sides of the belt by pulling forces  $T_1$  and  $t_1$ , respectively, which lie in a plane perpendicular to the shaft axis. Similarly pulling forces  $T_2$  and  $t_2$  act on pulley  $II$  and transmit to it the resistance offered by the machine tool. On the one hand, these forces exert pressure on the bearings (in the same way as the dead weight of the pulley) and, on the other hand, they constitute force couples lying in a plane perpendicular to the shaft axis.

Denoting the radius of any of the two pulleys by  $R$  and keeping in mind that tension ( $T$ ) of the tight side is greater than tension ( $t$ ) of the slack side, we can write the following equation of moments with

\* This arrangement of the bearings has been decided upon so that the bending of the shaft may become negligible.

respect to the centre of circle (Fig. 98):

$$M_1 = TR - tR = (T - t)R \quad (9.1)$$

Thus forces  $T_1$  and  $t_1$  form a torque  $(T_1 - t_1)R_1$  which twists the shaft in one direction (shown by arrow), whereas the resistance of machine tool gives a torque  $(T_2 - t_2)R_2$  which is directed oppositely.

For uniform operation of the machine all the forces acting on the shaft must be in equilibrium; the torque  $(T_1 - t_1)R_1$  should all the time be balanced by the resisting torque  $(T_2 - t_2)R_2$ , i.e.

$$(T_1 - t_1)R_1 = (T_2 - t_2)R_2 = M \quad (9.1')$$

There always exists an equilibrium between the torque transmitted from the motor to the machine tool through the shaft and the reactive torque on the shaft due to the resistance offered by the machine tool, irrespective of the type of transmission employed (V-belt, tooth gearing, friction gearing, etc.).

The portion of the shaft between the centres of the pulleys is subjected to the action of two equal and opposite force couples, acting in

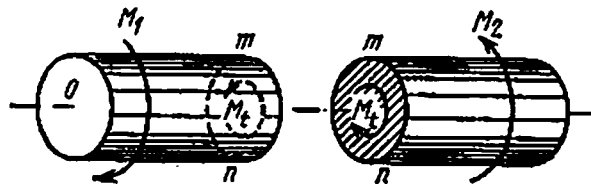


Fig. 99

parallel planes, that rotate one with respect to the other: the shaft gets twisted. Thus torsion is caused by force couples lying in planes perpendicular to the shaft axis.

We shall employ the method of sections in order to investigate the internal forces acting in cross sections of the shaft under the action of these force couples. Let us consider, for example, the part of the shaft which is located to the left of section  $mn$  (Fig. 99). It ensues from the conditions of equilibrium of the part under consideration that the internal forces must result in a moment  $M_1 = M_1$  that balances the external moment, i.e. acts in the opposite direction. Similarly, if we consider the equilibrium of the part to the right of section  $mn$  we find that in the same section the internal forces create a moment  $M_1 = M_2$ .

The moment of internal forces acting in an arbitrary section of the shaft subjected to torsion that tends to rotate this section about the shaft axis is called *torque* or *twisting moment*. The magnitude and direction of torque depend upon the magnitude of the external moments acting on the length of shaft under consideration.

It is easier to determine the signs of torques through the directions of external moments. Torque  $M_t$  will be considered positive if the external moment acts in the anticlockwise direction when seen from the side of the section; in Fig. 99,  $M_t > 0$ .

This sign convention for  $M_t$  corresponds to the direction of internal forces that are transmitted from the part of the shaft under consideration to the other part, for instance, from left to right.

In the above case there were only two pulleys on the shaft, which transmitted to it equal and opposite torques (9.1'); this resulted in torsion of the portion of the shaft between the pulleys by the torque  $M_t = M$ .

There are more complex situations when a number of pulleys are mounted on the shaft, one of them being the driving pulley and the rest driven. Each pulley transmits its torque to the shaft, and if the shaft is running uniformly, the sum of all the moments acting on the shaft must be zero.

Figure 100 shows a shaft which is acted upon by torsional moments  $M_1, M_2, M_3, M_4$ ; torque  $M_1$  acts in one direction (from the driving pulley), and  $M_2, M_3$  and  $M_4$  in the opposite direction (from the driven pulleys). For uniform rotation of the shaft

$$-M_1 + M_2 + M_3 + M_4 = 0 \quad (a)$$

The torque will have different values in different portions of the shaft. The portion of the shaft to the left of section 1-1 will be in equilibrium under the action of torsional moment  $M_4$  and the torque in section 1-1. Thus,  $M_t$  for this section will be equal to  $M_4$  with a minus sign because  $M_4$  acts in the clockwise direction when seen from the side of section. Therefore,

$$M_{t_1} = -M_4$$

Similarly, if we consider the portion of the shaft located to the left of section 2-2 (Fig. 100), we find that the moment of internal forces in this section is  $M_{t_2} = -M_4 + M_1$ . We would have obtained the same value of torque in section 2-2 if we considered the equilibrium of the portion of the shaft to the right of section 2-2. In this case the expression for torque would have been  $M_{t_2} = M_2 + M_3$ ; moreover, according to condition (a)

$$M_2 + M_3 = M_1 - M_4$$

Finally, for section 3-3, considering the right portion of the shaft, we get  $M_{t_3} = M_3$  or  $M_{t_3} = M_1 - M_2 - M_4$ . From the expressions for  $M_t$  which are given here it is evident that the torque in an arbitrary section of the shaft is numerically equal to the algebraic sum of the moments of external forces acting either to the left or right of this section.

The value of the torque in different portions of the shaft may be represented graphically by plotting the so-called torsional moment diagram. For this, the  $x$ -axis is plotted below the shaft drawing and the ordinates representing the value of torsional moments in the particular section are laid off from it with proper signs (positive upwards).

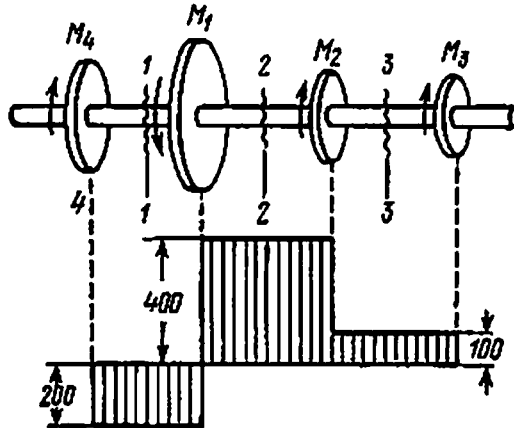


Fig. 100

The torque diagram is plotted in the form of rectangles because within the limits of a particular portion, the value of the torque  $M_1$  does not depend upon the position of the section between the pulleys.

Suppose in Fig. 100  $M_1=600$  kgf·m,  $M_2=300$  kgf·m,  $M_3=100$  kgf·m, and  $M_4=200$  kgf·m. The distribution of torsional moments along the length of the shaft is shown in Fig. 100.

#### § 46. Calculation of Torques Transmitted to the Shaft

To find the torques acting on a shaft we must know the moments, transmitted to it by all the pulleys. These moments may be determined if we know the number of revolutions of the shaft and the power transmitted by the pulley. Let a force couple having moment  $M$  be acting on the pulley (Fig. 101). We can imagine the couple to be consisting of two forces  $P$  applied at the contour of the pulley. Upon rotation the couple performs work; the magnitude of this work per unit time is equal to the power transmitted by the pulley.

Let us calculate the work done by the couple when the pulley is rotating. As the pulley revolves through an angle  $\alpha$ , each force of the couple covers a distance  $R\alpha$ , where  $R$  is the radius of the pulley. The total work done by the couple of forces will be

$$W = 2PR\alpha = M\alpha$$



Thus, the work done by a force couple when it is revolved through an angle  $\alpha$  is equal to the moment of the couple multiplied by the angle of rotation (in radians).

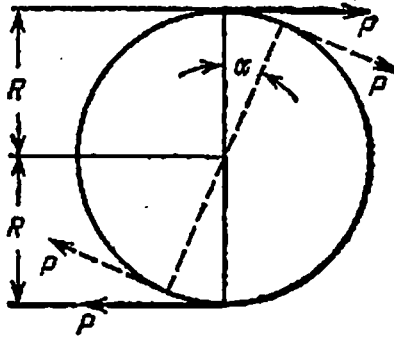


Fig. 10f

If the shaft completes  $m$  revolutions per unit time, then the work done will be  $W=2\pi m M$ . On the other hand, work per unit time is the power  $N$ . Therefore, the torque may be expressed through the given values of power and number of revolutions per unit time of the shaft:

$$M = \frac{N}{2\pi m} \quad (9.2)$$

If the power is given in h.p., then  $N=L$  h. p. or  $N=75 L$  kgf·m/sec and if the speed is  $m=n$  r.p.m., or per second  $n/60$ , then

$$M = \frac{75 \times 60 \times L}{2\pi n} = \frac{2250L}{\pi n} = 716.2 \frac{L}{n} \text{ kgf} \cdot \text{m} \quad (9.3)$$

The power may also be given in kilowatts,  $N=K$  kW. As 1 kW is approximately equal to 102 kgf·m/sec, we get

$$M = \frac{102 \times 60}{2\pi} \frac{K}{n} \text{ kgf} \cdot \text{m} = 973.6 \frac{K}{n} \text{ kgf} \cdot \text{m} \quad (9.4)$$

For given  $L$  or  $K$  we calculate the moment transmitted by each pulley from formulas (9.3) and (9.4), plot the twisting moment diagram and find the critical section in which  $M_t = M_{t, \max}$ .

#### § 47. Determining Stresses in a Round Shaft Under Torsion

Having plotted the  $M_t$ -diagram, we can find in any section of the shaft the twisting moment made up of the moments of internal forces acting in this section. Let us try to determine these internal forces and the corresponding stresses in the section. For solving this problem we shall use the results of experimental research given below.

A. Experiments show that when a round shaft is twisted by a couple of  $M$  (Fig. 102), the following points are observed.

All the generating lines revolve through an angle  $\gamma$ , and squares drawn on the shaft surface warp changing into rhomb, i.e. they are subjected to shear.

Each cross section revolves w.r.t. the other about the shaft axis through an angle called the *angle of twist*. The value of this angle is

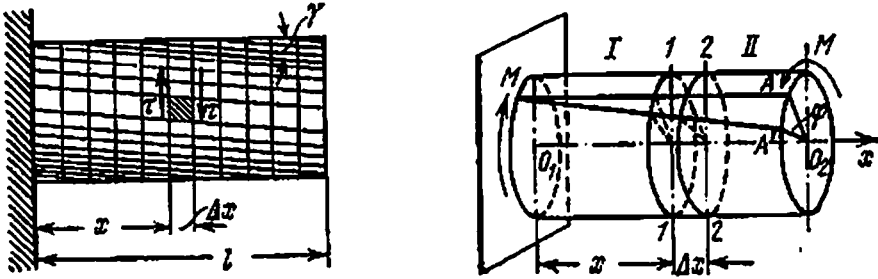


Fig. 102

directly proportional to the torque and the distance between the sections.

The end face remains a plane and the contours of all the sections remain undistorted (circles remain circles). Radii marked on the end face remain straight lines even after deformation.

The distance between adjacent sections practically does not change, i.e. sections 1-1 and 2-2, while turning with respect to one another through angle  $\Delta\phi$  retain their relative distance  $\Delta x$ .

Thus, the experiments show that a bar in torsion represents a system of rigid discs mounted centrally on a common axis  $O_1O_2$ . Upon deformation all these discs turn w.r.t. one another without changing their shape, size and relative distance.

The experimental observations enumerated above give us the basis for formulating the following hypotheses:

1. all cross sections remain planes;
2. radii on the sections remain straight lines;
3. distances between the sections remain unchanged.

The applicability of these hypotheses is further supported by the fact that the formulas obtained on their basis give results which agree well with those obtained experimentally.

B. Let us now pass over to determining stresses in sections perpendicular to the shaft axis. Let us imagine (Fig. 103) the twisted shaft  $O_1O_2$  to be cut in two portions I and II by a section 1-1 perpendicular to the shaft axis and located at a distance  $x$  from section  $O_1$ . Let us remove portion II and consider portion I. This part must remain in equilibrium under the action of external moment  $M$  applied in section  $O_1$  and torque  $M_t$  acting in section 1-1. The equilibrium condition

of the cutoff portion may be expressed as

$$M_t = M$$

According to its definition, torque  $M_t$  is the moment of internal forces that replace the action of the removed portion of the shaft. In order to be able to create moment  $M_t$ , the internal forces in the section and the corresponding stresses must be tangential to the section and perpendicular to the radii\*. For calculating the moments of these

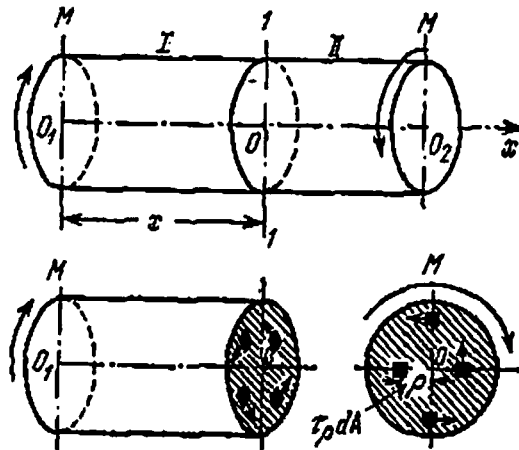


Fig. 103

elementary forces and their sum  $\Sigma M_\tau = M_t$ , let us consider an arbitrary point at a distance  $\rho$  from the centre of the circle and isolate an elementary area  $dA$  around it (Fig. 103). The force acting on the elementary area will be  $dP = \tau_\rho dA$ , where  $\tau_\rho$  is the shearing stress at the given point. The moment of this force about point  $O$  is

$$dM_\tau = \tau_\rho \rho dA$$

Considering area  $dA$  to be infinitely small, we can find the sum of the moments of all the forces as a definite integral over the area of the section:

$$\Sigma M_\tau = \int_A \tau_\rho \rho dA$$

or, since  $\Sigma M_\tau = M_t$ ,

$$\int_A \tau_\rho \rho dA = M_t \quad (9.5)$$

\* If we assume that  $\tau$  is not perpendicular to radius, then it must have a component along the radius, which, according to the law of complementary shearing stresses, must give rise to shearing stresses along the cylinder generatrices, including the ones on the external surface of the shaft which is free of all stresses (see Fig. 122).

However, we cannot yet find  $\tau$  from the above equation as we do not know how the shearing stresses are distributed over the section. C. It is not possible to determine the stresses in section 1-1 with

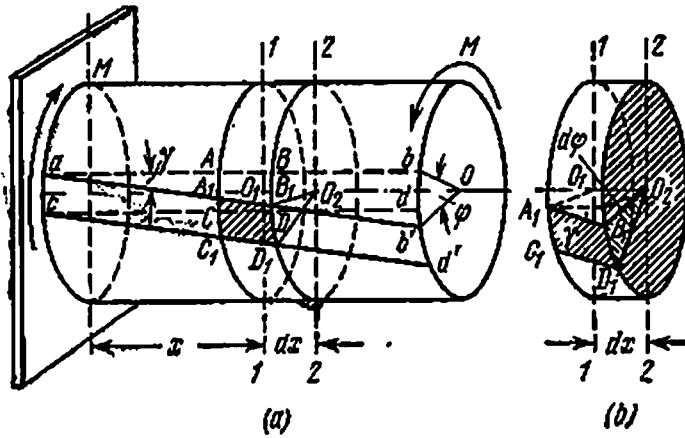


Fig. 104

the help of static equations only. It is a statically indeterminate problem, and to solve it completely we must take into account the deformation of the shaft shown in Figs. 102 and 104.

Let us isolate (Fig. 104) on the surface of the shaft, prior to deformation, a rectangle  $ABDC$  by two adjacent generating lines  $ab$  and  $cd$  and two portions of sections 1-1 and 2-2.

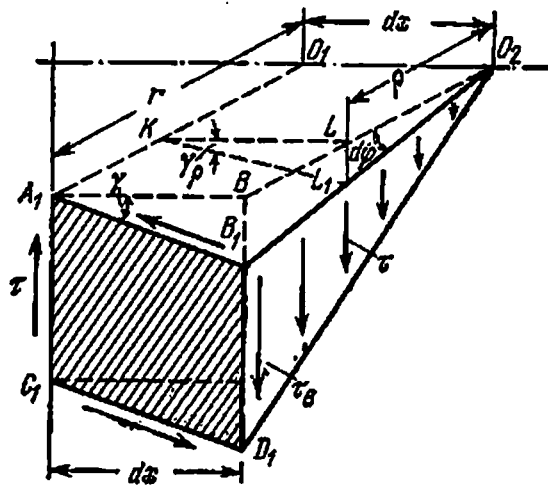


Fig. 105

After deformation both sections 1-1 and 2-2 turn about the fixed end through angles  $\phi_x$  (section 1-1) and  $\phi_x + d\phi$  (section 2-2). On the basis of the accepted hypotheses, we can say that both sections will remain planes, radii  $O_2B$ ,  $O_1A$ ,  $O_1C$  and  $O_2D$  will remain straight

lines and distance  $dx$  between sections 1-1 and 2-2 will remain unchanged. Under these conditions the whole element  $ABDCO_1O_2$  will be displaced and warped because its right face which lies in section 2-2 turns through  $d\varphi$  w.r.t. the left face which lies in section 1-1.

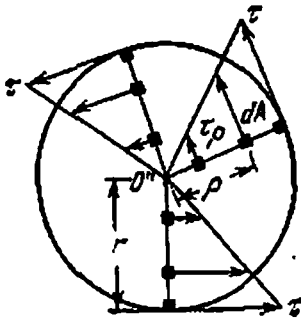


Fig. 106

Rectangle  $ABDC$  occupies the position which is shown in Fig. 104 by hatched lines. The warped element  $A_1B_1D_1C_1O_1O_2$  is shown in Fig. 105; on the same figure is shown the form of the element if it had remained undistorted, i.e. if its left and right faces both had turned through the same angle.

The warping caused by unequal turning of sections 1-1 and 2-2 transforms right angles of rectangle  $ABDC$  into acute and obtuse angles; the material of the element experiences shear (Figs. 102 and 104). The magnitude of this deformation is characterized by the *angle of*

*distortion* or the angle of shear. On the shaft surface in rectangle  $A_1B_1D_1C_1$  this angle is equal to  $\angle BA_1B_1$ ; it is denoted in Fig. 105 by  $\gamma$ .

We already know that shear is accompanied by appearance of shearing stresses in the faces of the warped element (§ 36).

Figure 105 depicts the stresses acting on an elementary area  $B_1D_1O_2$  enclosed between the right face (section 2-2) and the horizontal surface of the element  $A_1B_1O_2O_1$ . Their value may be expressed through the angle of shear  $\gamma$  which characterizes the warping of the rectangle  $A_1B_1D_1C_1$  by formula (6.37):

$$\tau = \gamma G$$

As the absolute displacement of the element on the shaft surface is  $BB' = r d\varphi$ , at the angle of shear  $\gamma = \frac{BB'}{A_1B} = r \frac{d\varphi}{dx}$ , the stress around point  $B_1$  will be

$$\tau_B = G\gamma = rG \frac{d\varphi}{dx}$$

Let us now determine the stress  $\tau_\rho$  at another point of section  $L_1$ , which is at a distance  $\rho$  from the centre (Fig. 105). For this we must find the angle of shear of the material at point  $L_1$ . In Fig. 105 the angle of shear or the angle of warping  $\angle LKL_1$  is denoted by  $\gamma_\rho$ . It will be less than the angle of shear  $\gamma$  at the shaft surface. By the same

reasoning as in determining  $\gamma$ , we find that  $\gamma_\rho = \rho \frac{d\phi}{dx}$  and get

$$\tau_\rho = \rho G \frac{d\phi}{dx} \quad (9.6)$$

The angle of shear and the shearing stress at any point in the cross section of the twisted shaft are directly proportional to the distance  $\rho$  of this point from the centre of the section. Graphically, the variation of the shearing stresses may be depicted by a straight line (Fig. 106). The shearing stresses  $\tau$  are maximum at points lying on the edge of the section and zero at the centre.

Thus, we have established the law of distribution of shearing stresses in cross sections of a twisted shaft.

D. The shearing stress may now be determined from equation (9.5). Replacing  $\tau_\rho$  by its value from equation (9.6) and taking the quantity  $G \frac{d\phi}{dx}$  (which is constant when integrating over area) out of the integral sign, we get

$$G \frac{d\phi}{dx} \int_A \rho^2 dA = M_t$$

( $\int_A \rho^2 dA$ , i.e. the sum of the products of elementary areas into the squares of their distances from point  $O$ , is called the *polar moment of inertia* and denoted by  $J_p$ . Consequently,

$$G \frac{d\phi}{dx} J_p = M_t$$

From the equation we can find the twisting angle per unit length of the rod

$$\frac{d\phi}{dx} = \frac{M_t}{GJ_p} \quad (9.7)$$

Substituting  $\frac{d\phi}{dx}$  into (9.6), we get

$$\tau_\rho = \frac{M_t}{J_p} \rho \quad (9.8)$$

The shearing stress is maximum at points of the section which lie at the rod surface, i.e. when  $\rho = \rho_{\max} = r$ :

$$\tau_{\max} = \frac{M_t \rho_{\max}}{J_p} = \frac{M_t r}{J_p} \quad (9.9)$$

The formulas for  $\tau_{\max}$  may be written in another form:

$$\tau_{\max} = \frac{M_t \rho_{\max}}{J_p} = \frac{M_t}{\left( \frac{J_p}{\rho_{\max}} \right)} = \frac{M_t}{W_p} \quad (9.10)$$

The ratio  $\frac{J_p}{\rho_{\max}^3} = W_p$  is called the *section modulus*; as the moment of inertia  $J_p$  is expressed in units of length to the fourth power, the section modulus  $W_p$  is measured in units of length to the third power.

The quantities  $J_p$  and  $W_p$  are geometrical characteristics of the section under torsion, i.e. they show how shape and size of the section influence the torsional resistance of the rod. As described later (§ 48), their values are determined through the rod's diameter.

#### § 48. Determination of Polar Moments of Inertia and Section Moduli of a Shaft Section

To determine  $J_p = \int_A \rho^2 dA$  we isolate a circular ring between radii  $\rho$  and  $\rho + d\rho$  (Fig. 107). Now in this ring we isolate an elementary area  $dA$ . We sum up the products  $\rho^2 dA$  for the ring and then sum up the

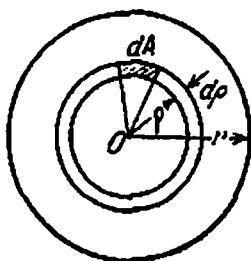


Fig. 107

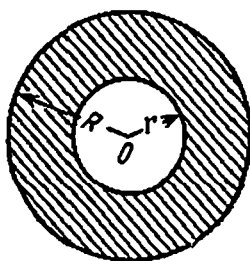


Fig. 108

values obtained from all the rings into which the section may be divided. As all the elementary areas in a particular ring are located at a fixed distance from the centre,  $\rho$ , we have

$$\sum \rho^2 dA = \rho^2 \sum dA$$

In a ring  $\sum dA$  is the area of a thin circular strip;  $\sum dA = 2\pi\rho d\rho$  and therefore  $\rho^2 \sum dA = 2\pi\rho^3 d\rho$ . Summing these quantities for the whole of the section, we get

$$J_p = \int_0^r 2\pi\rho^3 d\rho = 2\pi \int_0^r \rho^3 d\rho = \frac{\pi r^4}{2}$$

or expressing  $r$  through the diameter

$$J_p = \frac{\pi d^4}{32} \approx 0.1 d^4 \quad (9.11)$$

This is the polar moment of inertia of a circular section. The section modulus of a circular section under torsion will be

$$W_p = \frac{J_p}{\rho_{\max}} = \frac{\pi r^4}{2r} = \frac{\pi r^3}{2} = \frac{\pi d^3}{16} \approx 0.2d^3 \quad (9.12)$$

It is clear from formula (9.8) that shearing stress  $\tau$  is not large at points of the section close to the centre (where  $\rho$  is small). The twisting moment is balanced, chiefly, by stresses acting in the section near its surface; the material of the central portion of the shaft experiences low stresses and does not contribute much to the resistance to torsion. Therefore the shafts of large diameters are sometimes made hollow to make them lighter and cheaper (Fig. 108). In this manner we remove the central portion of the shaft, which is incidentally the weakest portion of the forging, affected most by harmful inclusions.

We shall determine the moment of inertia and section modulus of such a tubular section. Let us denote the outer radius by  $R$  and the inner radius by  $r$ . Then substituting  $dA = 2\pi\rho d\rho$ , we get

$$\left. \begin{aligned} J_p &= \int_A \rho^2 dA = 2\pi \int_r^R \rho^3 d\rho = \frac{\pi}{2} (R^4 - r^4) \\ J_p &= \frac{\pi}{32} (D^4 - d^4) \approx 0.1 (D^4 - d^4) \end{aligned} \right\} \quad (9.13)$$

The section modulus is

$$W_p = \frac{J_p}{\rho_{\max}} = \frac{\pi (R^4 - r^4)}{2R} = \frac{\pi (D^4 - d^4)}{16D} \quad (9.14)$$

If we assume the ratio  $d/D = \alpha$ , or  $d = \alpha D$ , we get

$$J_p = \frac{\pi D^4}{32} (1 - \alpha^4) \quad (9.13')$$

$$W_p = \frac{\pi D^3}{16} (1 - \alpha^4) \quad (9.14')$$

If the thickness of the tubular section is small ( $t < 0.1R$ ), then denoting the mean radius of the pipe by  $r_0 = \frac{R+r}{2}$  and keeping in mind that  $R - r = t$ , we obtain

$$J_p = \frac{\pi}{2} (R^4 - r^4) = \frac{\pi}{2} (R^2 + r^2)(R + r)(R - r) = \frac{\pi}{2} (R^2 + r^2) 2r_0 t$$

Replacing  $R$  by  $r_0 + \frac{t}{2}$  and  $r$  by  $r_0 - \frac{t}{2}$  and neglecting the square of the thickness  $t$  we get

$$J_p \approx 2\pi r_0^3 t \quad (9.15)$$



Similarly the section modulus may be found as

$$W_p \approx 2\pi r_0^3 l \quad (9.16)$$

These approximate formulas are very convenient for practical calculations.

It is obvious that for each cross section the polar moment of inertia and the section modulus have a single definite value which depends upon the dimensions of the shaft section.

### § 49. Strength Condition in Torsion

Knowing the section modulus we can determine  $\max \tau$  from formula (9.10).

According to the strength condition the maximum shearing stress must not exceed the permissible stress, i.e.

$$\max \tau = \frac{M_t}{W_p} \leq [\tau] \quad (9.17)$$

From this formula we can determine the section modulus for a known twisting moment and the assumed permissible stress, and then from the determined section modulus we can calculate the required radius or diameter of the shaft.

As explained earlier (§ 42), the permissible stress  $[\tau]$  should be taken 0.5 to 0.6 of the principal permissible tensile stress, as in the case of pure shear. In practice the value of  $[\tau]$  for mild steel varies from 200 to 1000 kgf/cm<sup>2</sup>, and for carbon steel from 300 to 1200 kgf/cm<sup>2</sup>, depending upon the type of load (static, alternating, impact) and the magnitude of local stresses that occur in the keyways, bosses and other places where the shape of the shaft section changes.

### § 50. Deformations in Torsion. Rigidity Condition

We had seen in § 47 that the torsional deformation of a cylindrical bar is distinguished by relative rotation of adjacent sections. The angle of rotation of one section with respect to another was called the angle of torsion  $\varphi$ . For sections located at distance  $dx$  from one another we had obtained expression (9.7)

$$\frac{d\varphi}{dx} = \frac{M_t}{GJ_p}, \quad \text{or} \quad d\varphi = \frac{M_t dx}{GJ_p}$$

If the distance between the sections is  $l$ , the angle of torsion is

$$\varphi = \int_0^l \frac{M_t dx}{GJ_p} \quad (9.18')$$

Usually the torque is constant within the limits of a particular portion; therefore integrating with respect to  $x$ , we obtain

$$\varphi = \frac{M_t l}{GJ_p} \quad (9.18)$$

Formula (9.18) has complete analogy with the corresponding formula for tension and compression and expresses Hooke's law for torsion. It is evident from formula (9.18) that the greater the *torsional rigidity*  $GJ_p$ , the smaller is the angle of twist  $\varphi$  (for a given  $M_t$ ). Thus,  $J_p$  reflects the effect of the dimensions of the cross section on the deformability of the rod under torsion, and  $G$  the effect of elastic properties.

If the shaft is mounted by a number of pulleys which divide it into portions subjected to different twisting moments  $M_i$ , then formula (9.18) enables us to calculate the angle of twist of one end w.r.t. the other for all the portions.

Computation of the angle of torsion has practical importance: firstly it is required for determining the reactions of support of twisted shafts in statically indeterminate systems; however, this is a rare case. Secondly, we must know the angle of torsion to check the rigidity of the shaft.

The maximum permissible limits of angle  $\varphi$ , which should not be exceeded to ensure safe working of the machine, have been established experimentally. These limits are as follows: under normal conditions  $[\varphi] = 0.3^\circ$  per unit length of the shaft; under alternating loads  $[\varphi] = 0.25^\circ$ ; under suddenly changing (impact) loads  $[\varphi] = 0.15^\circ$ . Sometimes under normal working conditions we take  $[\varphi] = 1^\circ$  per 20 times the shaft's diameter\*.

Hence, the shaft dimensions should be calculated not only from the strength condition (9.17) but also the rigidity condition

$$\varphi = \frac{M_t l}{GJ_p} \leq [\varphi] \quad (9.19)$$

This condition is often the most important when designing long shafts. We shall explain the rigidity check with the help of the following example.

Suppose a shaft transmits  $N = 150$  hp at  $n = 60$  r.p.m. It is required to select shaft diameter from the strength condition and check it for rigidity if the permissible stress  $[\tau] = 600$  kgf/cm<sup>2</sup> and the permissible angle of torsion per metre length of the shaft is  $[\varphi] = 0.3^\circ$ . Shear modulus  $G = 8 \times 10^8$  kgf/cm<sup>2</sup>.

---

\* For some time now the permissible angle of torsion  $[\varphi]$  is taken up to  $2^\circ$  and more per metre length of the shaft depending upon its functioning. Thus, for instance, angles of torsion of up to  $2.5^\circ$  per unit length are permitted for automobile cardan shafts.

The moment transmitted by the shaft may be calculated from expression (9.3):

$$M = 716.2 \frac{N}{n} = 716.2 \frac{150}{60} \approx 1800 \text{ kgf} \cdot \text{m} = 18 \times 10^4 \text{ kgf} \cdot \text{cm}$$

From strength condition (9.17) the section modulus may be found as

$$W_p \geq \frac{M_t}{[\tau]} = \frac{M}{[\tau]} = \frac{18 \times 10^4}{600} = 300 \text{ cm}^3$$

As  $W_p \approx 0.2d^3$  [formula (9.12)], the shaft diameter will be

$$d \geq \sqrt[3]{\frac{300}{0.2}} = 11.45 \text{ cm}$$

Let us take  $d = 11.5$  cm and check the section for rigidity. According to formula (9.11) the polar moment of inertia may be calculated as

$$J_p \approx 0.1d^4 = 0.1 \times (11.5)^4 = 1745 \text{ cm}^4$$

The angle of torsion per metre (or 100 cm) length of the shaft is calculated from formula (9.18):

$$\varphi = \frac{M_t l}{G J_p} = \frac{18 \times 10^4 \times 100}{8 \times 10^8 \times 1745} = 0.129 \text{ rad} = 0.78^\circ > [\varphi]$$

We see that although the strength condition is satisfied, the shaft diameter should be increased to improve rigidity and it should be calculated from expression (9.19):

$$J_p \geq \frac{M_t l}{G [\varphi]}$$

wherefrom, by substituting the value of permissible angle of torsion in radians  $[\varphi] = 0.3 \frac{\pi}{180}$ , we obtain

$$d \geq \sqrt[4]{\frac{18 \times 10^4 \times 180}{0.1 \times 8 \times 10^8 \times 0.3}} = 14.56 \text{ cm}$$

Hence, the shaft's diameter should be taken  $d = 14.6$  cm to ensure required rigidity.

### § 51. Stresses Under Torsion in a Section Inclined to the Shaft Axis

While studying the stresses in a round shaft under torsion (§ 47), we saw that shearing stress  $\tau$  acts at every point of a section perpendicular to the shaft axis. According to the law of complementary shearing stresses, a similar stress (Fig. 105) will act in the faces of the cutoff element lengthwise. These stresses will also be maximum at the surface and will be zero at points on the axis.

Thus, if we cut the twisted shaft by a diametral plane (Fig. 109), the points on straight line  $AB$  perpendicular to the shaft axis will experience shearing stresses which change linearly. There will be no normal stresses in these planes. Normal stresses act only in inclined planes and are maximum in planes which are inclined at  $45^\circ$  to the shaft axis.

Actually, element  $ABCD$  cut near the shaft surface (Fig. 110) experiences only shearing stresses on its side faces. It is in similar conditions as the element  $abcd$  in Fig. 75, i.e. in conditions of pure shear. Therefore, there are no shearing stresses in planes inclined at  $45^\circ$  to the shaft axis; these are the principal planes which are subjected to tensile and compressive stresses  $\sigma_1$  and  $\sigma_3$  equal to  $\tau$  at each point (see Fig. 105).

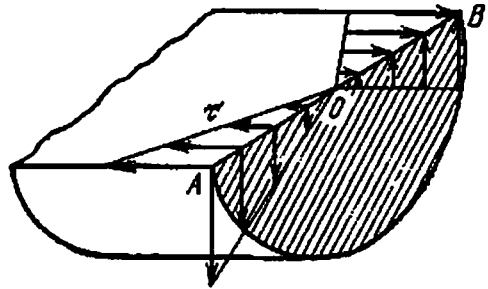


Fig. 109

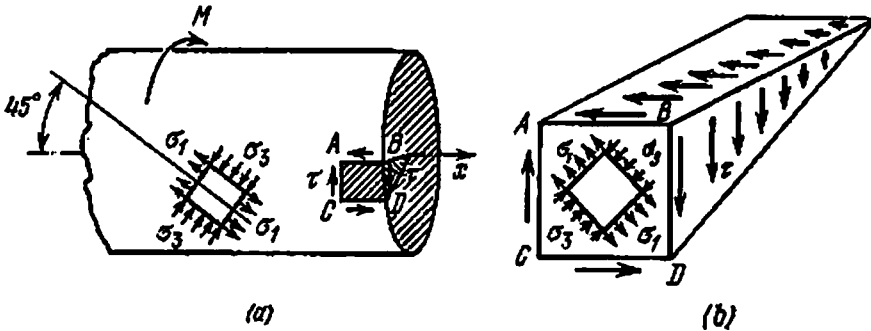


Fig. 110

The value of these stresses varies from point to point in direct proportion to their distance from the centre and is equal to  $\tau$ . Brittle materials like cast iron fail in torsion due to rupture in an inclined sec-

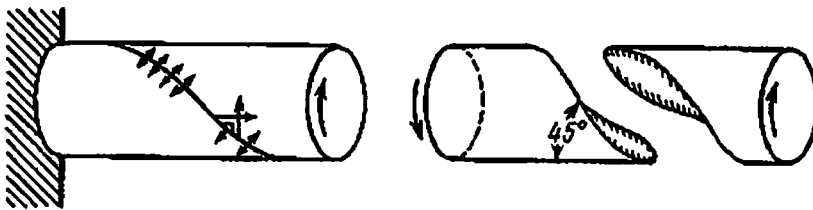


Fig. 111

tion  $BC$  (Figs. 110 and 111), i.e. in a section where the tensile stresses are maximum.

Knowing the magnitude and direction of the principal stresses at any point, we can determine the normal and shearing stresses in any

inclined plane by the stress circle or with the help of formulas (6.5) and (6.6). As the absolute values of the maximum normal and shearing stresses are equal and the permissible shearing stress is less than normal one, we can limit the strength check in torsion, as in pure shear, to analyzing shearing stresses only.

## § 52. Potential Energy of Torsion

Previously, when we were studying tension, it was shown (§ 35) that when an elastic system deforms, it accumulates energy called the potential energy of deformation.

This phenomenon occurs in torsion as well. If we twist an elastic rod within the limit of elasticity, then, when the external forces are removed, it will untwist and perform work at the expense of the potential energy it had accumulated during deformation. Neglecting the irreversible losses (heating, internal friction, etc.), we can consider that the work done by the internal forces, which is determined by the amount of accumulated potential energy  $U$ , is equal to the work  $W$  done by the external forces.

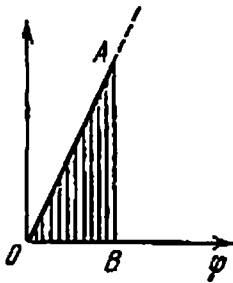


Fig. 112

result in a corresponding increase of  $\varphi$  which is related to  $M_t$  by equation (9.18):

$$\varphi = \frac{M_t l}{GJ_p}$$

If we plot the angle of twist (deformation) along the  $x$ -axis and the corresponding values of the twisting moment along the  $y$ -axis, then the relation between the two will be represented by an inclined straight line  $OA$  (Fig. 112). By the same reasoning as employed in calculating the work done by a tensile force  $P$ , we find that the work done by the force couple  $M$  may be expressed through the area of triangle  $OAB$ :

$$W = \frac{M_t \varphi}{2} \quad (9.20)$$

The constant  $1/2$  in formula (9.20) is due to the fact that the moment  $M$  has not been applied in its full magnitude at once but increased gradually, "statically" from zero to its finite value.

Replacing  $\varphi$  by its value from equation (9.18) and keeping in mind

that  $U=W$ , we get the expression for potential energy in torsion:

$$U = \frac{M_t^2 l}{2GJ_p} \quad (9.21)$$

The potential energy may also be expressed through deformation if we replace the torque in formula (9.20) by its value from formula (9.18):

$$M_t = \frac{GJ_p}{l} \varphi$$

Then

$$U = \frac{GJ_p}{2l} \varphi^2 \quad (9.22)$$

It is evident from formulas (9.21) and (9.22) that the potential energy of torsion, as of tension, is a function of the square of force or deformation.

### § 53. Stress and Strain in Close-coiled Helical Springs

Tension and compression helical springs are used in wagons, valves and other parts of mechanisms. When designing such springs, we must know how to calculate their maximum stress (for strength check) and deformation, their elongation or compression. This is essential because the load on the spring is controlled by deforming it more or less under tension or compression.

Hence, we must determine the relation between deformation and the force, acting on the spring provided its dimensions are known. It will be seen that the spring material experiences torsion when it is stretched or compressed.

We shall restrict our discussion only to close-coiled helical springs, i.e. springs in which the distance between adjacent coils (pitch) is small as compared to the diameter. If this condition is satisfied the coil inclination may be ignored and it may be assumed that any arbitrary cross section of the spring is parallel to forces  $P$  acting along the spring axis and either stretching or compressing it (Fig. 113).

Let us introduce the following notations: radius of the spring helix  $R$ ; diameter of the spring wire  $d=2r$ , number of turns in the spring  $n$  and shear modulus of the spring material  $G$ .

To determine the internal forces and stresses acting in the spring section when it is stretched (or compressed), let us cut one of the coils by a plane passing through the spring axis and consider the equilibrium of one of the cutoff portions, for example, the lower one (Figs. 113(b) and 114). External force  $P$  acting on this portion in the downward direction is balanced by an upward acting internal force  $P_1=P$  which lies in the plane of the section and is transmitted through this section from the upper portion to the lower one.

Since forces  $P$  and  $P_1$  form a couple with a moment  $M=PR$  that

rotates the portion of spring under consideration in the anticlockwise direction, it can be balanced only by a moment  $M_t = PR$  of the internal forces lying in the plane of the section and acting in the clockwise direction. Since internal forces  $P_1$  and their moment  $M_t$ , which replace the action of the upper portion of the spring on the lower, lie in the

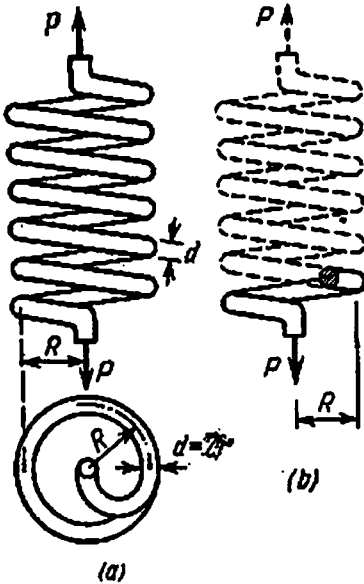


Fig. 113

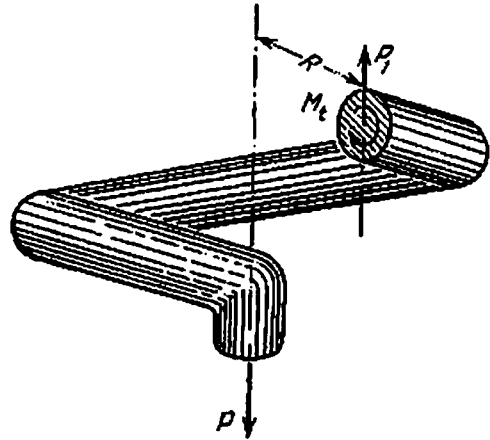


Fig. 114

plane of section, they are made up of shearing stresses. Shearing force  $P_1 = P$  is formed from elementary shearing forces  $dP_1 = \tau_1 dA$  that prevent the section from shearing downwards (Fig. 115 (a)). If the distribution of shearing stresses over the section area is assumed to be uniform, then force  $P_1$  may be expressed as  $P_1 = \tau_1 A$ , wherefrom shearing stress

$$\tau_1 = \frac{P_1}{A} = \frac{P}{\pi r^2} \tag{9.23}$$

The torque  $M_t$  that prevents the section from rotating (Fig. 114) is related to shearing stresses  $\tau_2$  in torsion by the formula

$$\tau_2 = \frac{M_t}{J_p} \rho = \frac{PR}{J_p} \rho \tag{9.24}$$

Both systems of stresses  $\tau_1$  and  $\tau_2$  that appear in the spring section when it is subjected to a tensile force  $P$  are depicted in Figs. 115 (a) and (b). At each point of the section stresses  $\tau_1$  and  $\tau_2$  are summed geometrically as their directions coincide only along radius  $AO$ .

As the shearing stresses due to torsion are maximum at the periphery of the section [formula (9.10)], i.e.

$$\tau_{2 \max} = \frac{M_t}{W_p} = \frac{2PR}{\pi r^3}$$

point *A* on the internal edge of the contour will be the critical point since here stresses  $\tau_1$  and  $\tau_2$  add up arithmetically. Hence, the maximum total shearing stress in the spring section is

$$\tau_{\max} = \frac{P}{\pi r^2} + \frac{2PR}{\pi r^3} = \frac{P}{\pi r^2} \left( 1 + \frac{2R}{r} \right) \tag{9.25}$$

From strength condition  $\tau_{\max} \leq [\tau]$ , or

$$\tau_{\max} = \frac{P}{\pi r^2} \left( 1 + \frac{2R}{r} \right) \leq [\tau] \tag{9.25'}$$

As in a majority of cases the second term inside the brackets is considerably greater than unity, the first term is usually ignored, i.e. the stresses due to pure shear are neglected and only stresses due to torsion by moment  $PR$  are considered. Therefore

$$\tau_{\max} = \frac{2PR}{\pi r^3} \tag{9.26}$$

The elongation of the spring's axis under tension, which is denoted by  $\lambda$ , can be very easily calculated on the basis of this approximation.

Let us cut from the spring a segment of length  $ds$  by two adjacent sections  $CO_1$  and  $CO_2$  passing through the spring axis (Fig. 116). As we select the sections very close to each other, it may be assumed that before deformation the radii  $R$  drawn from the spring's axis to the centres of the sections lie in the same plane and form a triangle  $O_1CO_2$ .

After deformation due to torsion of the segment  $ds$ , the second section turns w.r.t. the first by an angle  $d\varphi = \frac{M_1 ds}{GJ_p}$ . Consequently, radius  $O_2C$  turns w.r.t. radius  $O_1C$  by the same angle  $d\varphi$  and point  $C$  occupies the position  $C_1$ , which means that the end of the spring moves down by

$$d\lambda = R d\varphi = R \frac{M_1 ds}{GJ_p}$$

If we consider that all similar elements  $ds$  deform in an identical manner, then the total distance by which the lower spring end moves

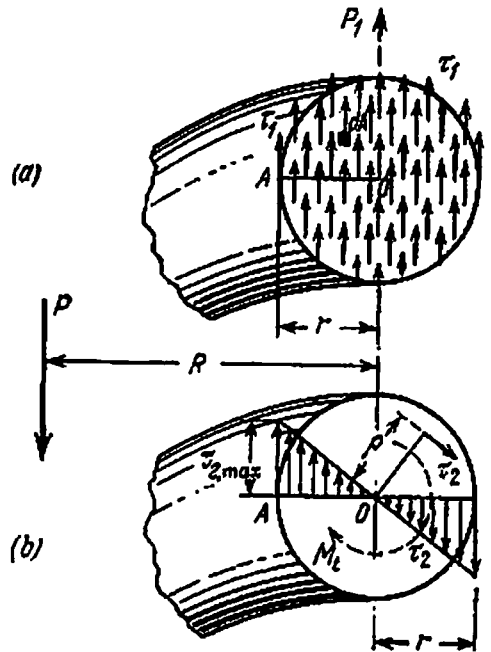


Fig. 115



down, i.e. its elongation, may be expressed as the sum of  $d\lambda$ :

$$\lambda = \sum d\lambda = \int_0^l R \frac{M_t ds}{GJ_p} = R \frac{M_t l}{GJ_p} \tag{9.27}$$

Here  $l = \int_0^l ds$  is the total length of the spring wire and  $\frac{M_t l}{GJ_p}$  is the relative angle of torsion of the ends of the spring wire, which is determined under the assumption that the spring wire has been straightened.

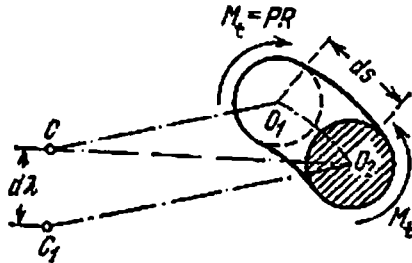


Fig. 116

Neglecting the inclination of the spring coils to the horizontal and assuming the number of turns to be  $n$  we get the total length of the spring wire equal to

$$l = 2\pi Rn$$

Therefore

$$\lambda = \frac{M_t R}{GJ_p} 2\pi Rn = \frac{4PR^3n}{Gr^3} \tag{9.28}$$

A similar formula can be derived by comparing the work done by external forces  $W = \frac{1}{2} Pl$  with the potential energy of torsion  $U = \frac{M_t^2 l}{2GJ_p}$ ; the reader is advised to do this independently.

Denoting the permissible elongation (or compression) of the spring by  $[\lambda]$ , we can write the following rigidity condition:

$$\lambda = \frac{4PR^3n}{Gr^3} \leq [\lambda] \tag{9.28'}$$

Formulas (9.25') and (9.28') enable us to check the strength and find the deformation of the spring.

The greater the permissible shearing stress  $[\tau]$ , the more flexible is the spring and the greater will be its compression under a particular load  $P$ , because it may be manufactured from a thinner wire. The wagon springs must be sufficiently flexible, therefore they are made from tempered steel with a high elastic limit. The permissible shearing

stress may be up to 40 kgf/mm<sup>2</sup> and sometimes as high as 80 kgf/mm<sup>2</sup>. The permissible stress for chromium-vanadium steel in tension springs is taken up to 70 kgf/mm<sup>2</sup> at  $r=6$  to 8 mm. The permissible shearing stress for phosphor-bronze is  $|\tau|=13$  kgf/mm<sup>2</sup> at  $G=4400$  kgf/mm<sup>2</sup> and  $r$  up to 8 mm.

These values of permissible stress are valid only under static loading; under alternating loads they reduce by about 1/3, and for springs working non-stop (valve springs) by about 2/3. In these cases an important factor is the development of fatigue cracks (see § 16). In addition, the valve springs often work at high temperatures; this also requires a reduction in the permissible stresses.

In practice, when designing springs according to formula (9.25), we introduce a correction factor  $k$  which, apart from shearing, takes into account other factors (bending of the spring wire, longitudinal deformation, etc.) that were not considered above. The greater the ratio  $\frac{r}{R}$ , i.e. the greater the torsional rigidity of the spring, the greater the value of factor  $k$ .

Formula (9.25), which in addition to torsion accounts for shear due to force  $P$ , is replaced by

$$\max \tau = k \frac{M_t}{W_p} = k \frac{PR}{2} \quad (9.29)$$

The value of correction factor  $k$  may be taken from Table 8.

Table 8

Correction Coefficients for Designing Springs

$R/r$	4	5	6	7	8	9	10	11	12	15
$k$	1.42	1.31	1.25	1.21	1.18	1.16	1.14	1.12	1.11	1.09

In design of springs, the known quantity sometimes is not the force  $P$  which stretches or compresses the spring but energy  $T$  which it must absorb. As in tension or compression of a rod, the potential energy of deformation  $U$  of the spring is measured in terms of the work done by the external forces.

As  $P$  and  $\lambda$  are linearly dependent upon each other [formula (9.28)], the potential energy of deformation of the spring may be written as

$$U = \frac{1}{2} P\lambda = \frac{2P^2 R^3 n}{Gr^4} \quad (9.30)$$

From formula (9.26) we have

$$PR = \frac{\tau \pi r^3}{2}$$

Putting this value in equation (9.30), we obtain

$$U = \frac{2\pi Rn}{4G} \pi r^3 \tau^2$$

As  $2\pi Rn$  is the length of spring wire and  $\pi r^2$  its area of cross section,

$$U = \frac{\tau^2}{4G} V \quad (9.31)$$

Here  $V$  is the volume of the spring. Keeping in mind that  $U=T$ , we can write formula (9.31) as

$$V = \frac{4GT}{[\tau]^2} \quad (9.32)$$

Thus, by assuming the limiting value of stress  $\tau=[\tau]$  we can calculate the volume of the spring required to absorb energy  $T=U$  such that the permissible stress  $[\tau]$  is not exceeded. The compression of the spring under  $[\tau]$  should be checked; it should be such that the gap between the spring turns is not completely eliminated.

As an illustration we shall calculate the maximum stress and elongation of the cylindrical spring shown in Fig. 113, if spring radius  $R=100$  mm, spring wire diameter  $d=20$  mm, number of turns  $n=10$  and tensile force  $P=220$  kgf. Shear modulus  $G=8.5 \times 10^5$  kgf/cm<sup>2</sup>.

The stresses will be calculated with the help of formula (9.29). As the ratio  $\frac{R}{r} = 10$ , the correction factor  $k=1.14$  (Table 8) and

$$\tau_{\max} = k \frac{2PR}{\pi r^3} = 1.14 \frac{2 \times 220 \times 10}{3.14 \times 1^3} = 1592 \text{ kgf/cm}^2$$

The elongation (or compression) of the spring according to formula (9.28) is

$$\lambda = \frac{4PR^3}{G r^4} = \frac{4 \times 220 \times 10^3 \times 10}{8.5 \times 10^5 \times 1^4} = 10.4 \text{ mm}$$

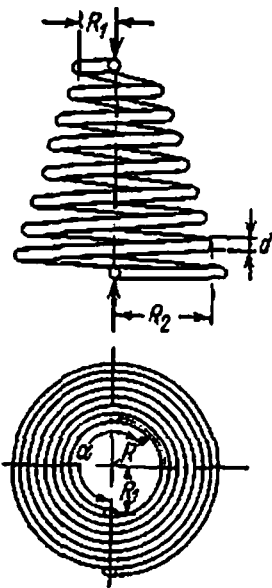


Fig. 117

In addition to cylindrical coil springs conical springs (Fig. 117) are also used in engineering practice. The radii of the top and bottom turns in Fig. 117 are denoted by  $R_1$  and  $R_2$  respectively; the average

radius  $R$  may be calculated by the formula

$$R = R_1 + \frac{R_2 - R_1}{2\pi n} \alpha$$

where  $n$  is the number of turns and  $\alpha$  is the angle formed by the radius under consideration with the top radius  $R_1$  and measured along the spring turns.

The strength of conical spring is checked with the help of formulas (9.25) or (9.26) by replacing  $R$  with its maximum value  $R_2$ . To determine  $\lambda$ , as in the previous case, we must add the elementary deformations

$$d\lambda = \frac{M_t R ds}{GJ_p}$$

$M_t = PR$  is now a variable quantity. Therefore

$$\lambda = \int \frac{M_t R ds}{GJ_p} = \frac{P}{GJ_p} \int_0^{2\pi n} \left[ R_1 + \frac{(R_2 - R_1)\alpha}{2\pi n} \right]^2 d\alpha = \frac{Pn}{r^4 G} [R_1^2 + R_2^2] [R_1 + R_2] \quad (9.33)$$

Sometimes springs are manufactured not from a round wire but a rectangular-section wire; for such springs the formulas given in § 54 (Table 9) have to be used to calculate the stresses and deformations.

### § 54. Torsion in Rods of Non-circular Section

In engineering practice we often come across rods of non-circular section subjected to torsion; these include rolled and thin-walled rods. Under torsion the cross sections of such rods do not remain planes, they warp. As depicted on the example of a rectangular section, points of the section do not remain on the plane (some get displaced inwards, others outwards) and the section undergoes *plane shift (warping)* (Fig. 118). A. When a rod of uniform section is twisted by force couples applied at its free ends, all cross sections of the rod undergo equal plane shift. Therefore the distance between equally displaced points on adjacent sections does not change, i.e. the lengths of longitudinal fibres remain unchanged. This means that the cross sections of the rod are free of normal stresses when plane shift of its sections is uniform.

Torsion is known as *pure* or *free* when cross sections of the twisted rod are free of normal stresses. It should be noted that free torsion is possible only under conditions of unconstrained (free) plane shift of all sections. In pure torsion the magnitude and distribution of shearing stresses are the same in all cross sections.

If plane shift of a single cross section of the twisted rod of non-circular section is constrained (for example, by the conditions of fixation or loading), torsion can no more be considered free: it will be ac-

accompanied by change in length of longitudinal fibres and normal stresses will begin to act in cross sections. In this case the shearing stresses have different magnitude in different sections: they are made up of shearing stresses of pure torsion and additional shearing stresses

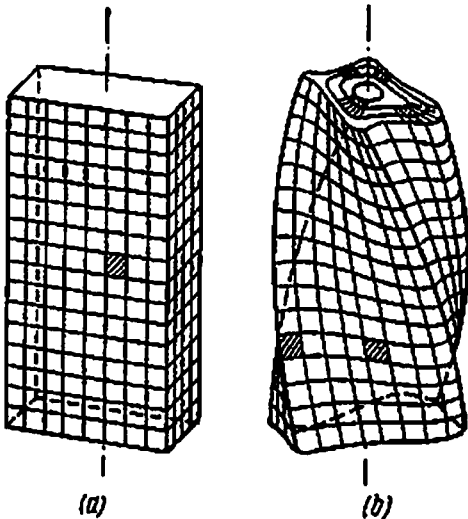


Fig. 118

connected with the non-uniform plane shift of the rod along its length. Torsion with constrained plane shift is known as *constrained torsion*.

Figures 119 and 120 depict the states of pure and constrained shear in an I-section. Figure 119 shows the deformation of I-section with free ends to which force couples with moments  $M_0$  are applied, i.e. an I-section subjected to pure torsion. Figure 120 depicts the deformation of the same I-section when same moments  $M_0$  are applied to its ends. In this case, however, one end of the rod is rigidly fixed; therefore

the fixed end remains plane, its warping is completely constrained and hinders free plane shift of adjacent sections. Torsion may be considered free only at the free right end of the rod. Hence, this is a case of constrained torsion or, as it is also known, bending torsion (the I-section flanges, like elements of thin-walled sections in general bend when the section is subjected to torsion).

The problem of constrained torsion was first formulated and solved by Prof. S. P. Timoshenko in 1905\*. However, these problems drew the attention of engineers and research workers only towards the end of twenties in connection with the developments in aircraft industry and introduction of thin-walled structures in civil engineering. Soviet scientists contributed much to the theory of design of thin-walled structures and shells, in particular Prof. V. Z. Vlasov who put forward the general theory of design of thin-walled open-profile rods (1939\*\*). This theory further developed in subsequent years and along with the theory of shell design grew into an independent branch of mechanics of structures, which is widely covered in literature.

The theory of constrained torsion is to a certain extent based on the theory of pure torsion of rods of non-circular sections; some of the results of the theory are given below.

\* *Proceedings of St. Petersburg Polytechnical Institute*, Vol. 4, 1905.

\*\* V. Z. Vlasov, *Thin-walled Elastic Rods*, Stroiizdat, 1940 (in Russian). Also see N. M. Belyaev, *Strength of Materials*, Nauka, 1965 (in Russian).

B. Since torsion of rods of non-circular sections is accompanied by warping of the sections, one of the basic hypotheses of strength of materials—the hypothesis of plane sections—becomes inapplicable. The problem of torsion of such rods requires more complicated mathematical analysis and can be solved only by the methods of the theory of elasticity.

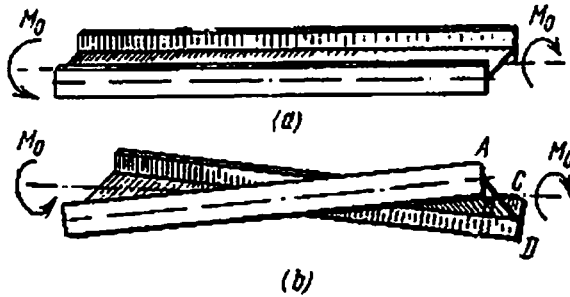


Fig. 119

The first theoretical investigation of pure torsion in rods of non-circular sections was carried out by Saint-Venant in 1864; he also presented a number of solutions of particular problems (torsion of rods of rectangular and elliptical sections). Solutions to many problems on free torsion of rods, including rods of very complex profiles, have

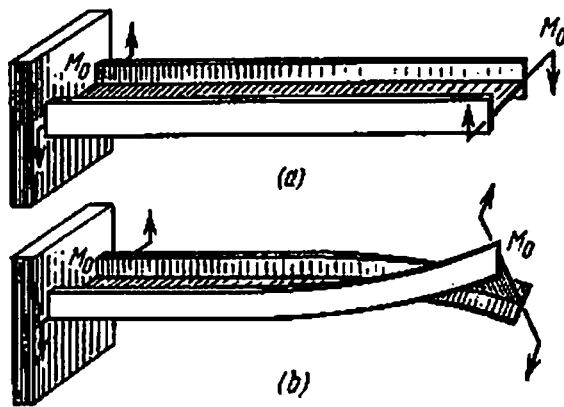


Fig. 120

been found by now on the basis of the general method of design of such rods developed by Saint-Venant. However, in spite of the complexity involved in solving these problems by the theory of elasticity, their results can be presented in a simple and convenient form for practical use. The formulas for maximum shearing stresses and strains are presented in the form of expressions which are completely identical to the formulas for maximum shearing stresses and angle of twist

of round bars in torsion:

$$\tau_{\max} = \frac{M_t}{W_t} \quad (9.34)$$

$$\varphi = \frac{M_t l}{G J_t} \quad (9.35)$$

In these formulas  $J_t$  and  $W_t$  are geometrical characteristics of the section (similar to  $J_p$  and  $W_p$  for round sections and having same units) which are conditionally called the torsional moment of inertia ( $J_t$ ) and the section modulus in torsion ( $W_t$ ). For circular and ring sections  $J_t = J_p$  and  $W_t = W_p$ .

For some sections these geometrical characteristics have been determined in closed form: for instance, for an ellipse

$$J_t = \frac{\pi a^3 b^3}{a^2 + b^2}, \quad W_t = \frac{\pi a b^3}{2} \quad (9.36)$$

Here  $a$  and  $b$  are the major and minor axes of the ellipse, respectively. The shearing stress diagram for the elliptical section is shown in Fig. 121. Along the profile of the section the stresses form a conti-

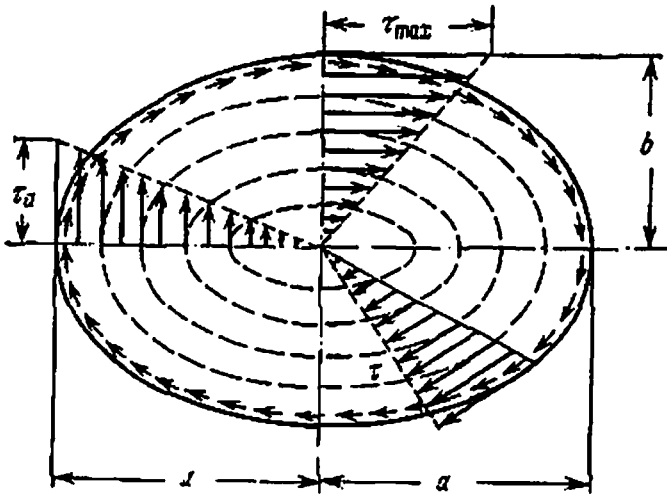


Fig. 121

nuous flux tangent to the profile, and attain maximum value at the end of the minor axis ( $\tau_{\max} = \frac{M_t}{W_t}$ ); at the end of the major axis  $\tau_a = \frac{b}{a} \tau_{\max}$ .

Identical shearing stress fluxes are directed along closed curves shown by dotted lines (shearing stress trajectories). The magnitude of shearing stress  $\tau$  increases, as we move from the centre of the ellipse towards its periphery, in direct proportion to the distance (Fig. 121).

It should be noted that when a rod of an arbitrary profile is subjected to torsion, the shearing stresses at the contour should be tangent to the section in accordance with the law of complementary shearing stresses. If the possibility of stress component  $\tau_t$  perpendicular to the periphery is conceded, this will imply that complementary shearing stresses act on the side surface free of all stresses (Fig. 122). For the same reason shearing stress  $\tau=0$  at the corners. We can see this in the example of a rectangular section (Fig. 122; top left corner).

For a rectangular section with sides  $b$  and  $h$ , the geometrical characteristics depend upon the ratio between the sides and are expressed by the following formulas:

$$J_t = \alpha b^4 \quad \text{and} \quad W_t = \beta b^3 \quad (9.37)$$

or

$$J_t = \alpha_1 h b^3, \quad W_t = \beta_1 h b^2 \quad (9.37')$$

where

$$\alpha_1 = \frac{b}{h} \alpha \quad \text{and} \quad \beta_1 = \frac{b}{h} \beta$$

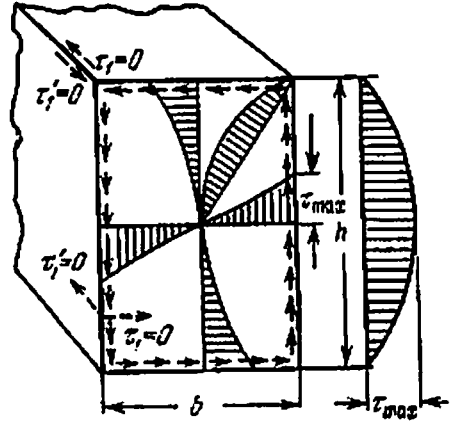


Fig. 122

The distribution of shearing stresses over a rectangular section is shown in Fig. 122. Along each side the shearing stress  $\tau$  varies according to a parabolic law and attains maximum value at the middle of the longer side ( $\tau_{max} = \frac{M_t}{W_t}$ ); at the middle of the shorter side  $\tau = \gamma \tau_{max}$ , and at the corners  $\tau=0$ .

Table 9 contains the values of coefficients  $\alpha$ ,  $\beta$  and  $\gamma$ .

Table 9

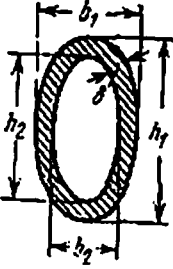
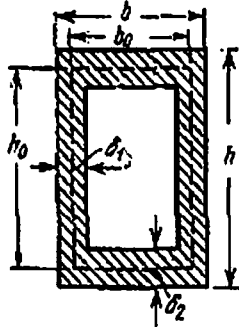
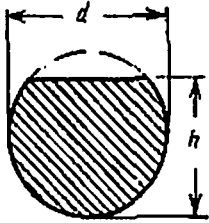
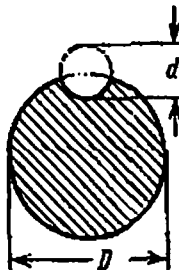
Coefficients for Designing Rectangular Bars Under Torsion

$h/b$	$\alpha$	$\beta$	$\gamma$	$h/b$	$\alpha$	$\beta$	$\gamma$
1.0	0.141	0.208	1.000	3.0	0.790	0.801	0.753
1.2	0.199	0.263	0.935	4.0	1.123	1.128	0.745
1.5	0.294	0.346	0.859	5.0	1.455	1.455	0.744
1.75	0.375	0.418	0.820	6.0	1.789	1.789	0.743
2.0	0.457	0.493	0.795	8.0	2.456	2.456	0.742
2.5	0.622	0.645	0.766	10.0	3.123	3.123	0.742



Table 10

Data on Torsion of Non-circular Sections

Shape of the section	Moment of Inertia $J_t$ (cm <sup>4</sup> )	Section modulus $W_t$ (cm <sup>3</sup> )	Remarks
	$\frac{\pi}{16} \frac{m^3}{(m^2+1)} b_1^4 (1-\alpha^4)$	$W_t = \frac{\pi b_1^3}{16} (1-\alpha^4) m$	$\frac{h_1}{b_1} = \frac{h_2}{b_2} = m > 1$ $\frac{h_2}{h_1} = \frac{b_2}{b_1} = \alpha < 1$ $\tau_{\max} = \frac{M_t}{W_t}$
	$\frac{h_0^2 b_0^2 \delta_1 \delta_2}{h \delta_2 + b \delta_1 - \delta_1^2 - \delta_2^2}$	$W_{t1} = 2h_0 h_1 \delta_1$ $W_{t2} = 2h_0 b_0 \delta_2$	At the middle of longer side $\tau_1 = \frac{M_t}{W_{t1}}$ At the middle of shorter side $\tau_2 = \frac{M_t}{W_{t2}}$
	$\frac{d^4}{16} \left( 2.6 \frac{h}{d} - 1 \right)$	$\frac{d^3}{8} \frac{\left( 2.6 \frac{h}{d} - 1 \right)}{\left( 0.3 \frac{h}{d} + 0.7 \right)}$	$\frac{h}{d} > 0.5$ $\tau_{\max} = \frac{M_t}{W_t}$
	$J_t = \alpha \frac{D^4}{16}$	$W_t = \beta \frac{D^3}{8}$	At the base of the groove $\tau_{\max} = \frac{M_t}{W_t}$

$\alpha$  and  $\beta$  from the table depending upon the ratio  $d/D$ .

$d/D$	0.0	0.05	0.10	0.20	0.40	0.60	0.80	1.0
$\alpha$	1.57	0.80	0.81	0.82	0.76	0.66	0.52	0.38
$\beta$	1.57	1.56	1.56	1.46	1.22	0.92	0.63	0.38

According to Table 9, for narrow rectangular sections ( $\frac{h}{b} \geq 10$ ) coefficients  $\alpha$  and  $\beta \geq 3.123$ , and  $\alpha_1$  and  $\beta_1$  are approximately equal to  $\frac{1}{3}$  (from 0.312 to 0.333). In accordance with formula (9.37') for such rectangular sections we obtain

$$J_t = \frac{1}{3} hb^3, \quad W_t = \frac{1}{3} hb^2 \quad (9.38)$$

Table 10 contains formulas for the geometrical characteristics of more complicated profiles and maximum shearing stresses in torsion. If we are studying torsion in a rod of complex profile which may be divided into a number of elements, then for such a section

$$J_t = J_{t1} + J_{t2} + \dots = \sum J_{tn}$$

where  $n=1, 2, 3, \dots$  are the numbers of the elementary parts into which the section is divided.

As the angle of twist is the same for the complete section and all its parts, we have

$$\varphi = \frac{M_t l}{G J_t} = \frac{M_{t1} l}{G J_{t1}} = \dots = \frac{M_{tn} l}{G J_{tn}}$$

the torque is distributed over different portions of the section in direct proportion to their rigidity:

$$M_{t1} = M_t \frac{J_{t1}}{J_t}, \quad M_{t2} = M_t \frac{J_{t2}}{J_t}, \quad \dots, \quad M_{tn} = M_t \frac{J_{tn}}{J_t}$$

Correspondingly the maximum shearing stress in each of the  $n$  portions of the section is

$$\tau_{tn} = \frac{M_{tn}}{W_{tn}} = \frac{M_t}{W_{tn}} \left( \frac{J_{tn}}{J_t} \right) = \frac{M_t}{J_t} \left( \frac{J_{tn}}{W_{tn}} \right)$$

The maximum value of  $\tau$  occurs in the element for which  $\frac{J_{tn}}{W_{tn}}$  is maximum. Hence

$$\tau_{\max} = \frac{M_t}{J_t} \left( \frac{J_{tn}}{W_{tn}} \right)_{\max} = \frac{M_t}{W_t}$$

where

$$W_t = \frac{J_t}{\left( \frac{J_{tn}}{W_{tn}} \right)_{\max}}$$

In addition to Table 10, we give here the formulas for  $J_t$  and  $\tau$  for sections composed of narrow and long rectangles, for example, L-, T-, I- and U-shaped sections.

For such sections we may take

$$J_t = \frac{1}{3} \eta \sum h \delta^3 \quad (9.38')$$

where  $\delta$  is the shorter and  $h$  the longer side of the rectangles into which the section may be divided.

Coefficient  $\eta$  depends upon the shape of the section and has the following values:

for an L-section	$\eta = 1.00$
for an I-section	$\eta = 1.20$
for a T-section	$\eta = 1.15$
for a U-section	$\eta = 1.12$

Angle  $\varphi$  is expressed as before by the formula

$$\varphi = \frac{M_t l}{G J_t}$$

The maximum shearing stress is expected to occur in the broadest of the rectangles into which the given section has been divided. It may be calculated by the following formula:

$$\tau_{\max} = \frac{M_t \delta_{\max}}{J_t} \quad (9.39)$$

where  $\delta_{\max}$  is the maximum thickness among all the portions.

We may use the formulas for round sections in the analysis on torsion of pipes with a non-circular section and small thickness of the wall. According to formula (9.16) the section modulus of a thin-walled ring is

$$W_p = 2\pi r_0^2 t = 2A_0 t$$

where  $A_0$  is the area of the circle bounded by the midline of the ring, and  $t$  its thickness. Assuming that the shearing stresses are distributed uniformly over the ring section, we get

$$\tau = \frac{M_t}{2A_0 t} \quad (9.40)$$

This formula may be employed for the analysis of thin-walled rods of non-circular closed sections.

The angle of twist may be determined by the formula

$$\varphi = \frac{M_t l r_0}{G J_p r_0} = \frac{\tau l}{G r_0}$$

Multiplying and dividing by  $2\pi r_0 = S$ , we get

$$\varphi = \frac{\tau S}{2GA_0} l \quad (9.41)$$

where  $S$  is the length of the centre line of the pipe section, and  $A_0$  is the area bounded by the midline of the given closed section.

## PART IV

# Bending. Strength of Beams

### CHAPTER 10

## Internal Forces in Bending. Shearing Force and Bending-moment Diagrams

### § 55. Fundamental Concepts of Deformation in Bending. Construction of Beam Supports

A prismatic bar with a straight axis bends if it is acted upon by forces perpendicular to its axis and lying in a plane passing through the axis.

A bar working under bending is usually called a beam. It has been shown experimentally that under the action of such forces the beam's axis takes the form of a curve, and the beam bends. Figure 123 shows

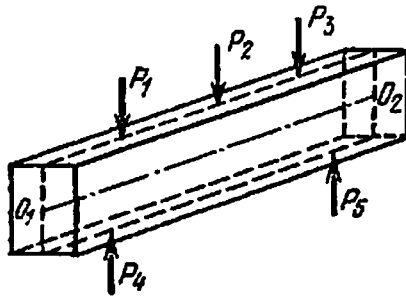


Fig. 123

a system of forces bending a rectangular beam; the forces act in the plane of symmetry of the beam. If the plane of action of the forces differs from the plane of symmetry then in addition to bending the beam is subjected to torsion.

Beams are the most commonly used element of structures and machines; they withstand the pressure of other elements of the structure (for example, forces  $P_1$ ,  $P_2$ , and  $P_3$  in Fig. 123) and transfer it to the parts supporting them (for example, forces  $P_4$  and  $P_5$  in Fig. 123).

Thus, the beam experiences the forces applied to it and the reactions of the supports. Both kinds of the forces must be known to enable us to solve the problem on strength of beams under bending.

The external applied forces may be calculated if we know the parts of the structure supported by the beam. These forces are classified as concentrated  $P$  (tf, kgf, N), force couples with moment  $M$  (tf·m, kgf·m, N·m), and loads uniformly and non-uniformly distributed over the length of the beam.

The uniformly distributed loads are measured by their intensity  $q$ , i.e. load per unit length of the beam and are expressed in tf/m, kgf/m or N/m.

The intensity of non-uniformly distributed loads varies along the length of the beam and is denoted by  $q(x)$ . In this case  $q(x)$  is the load

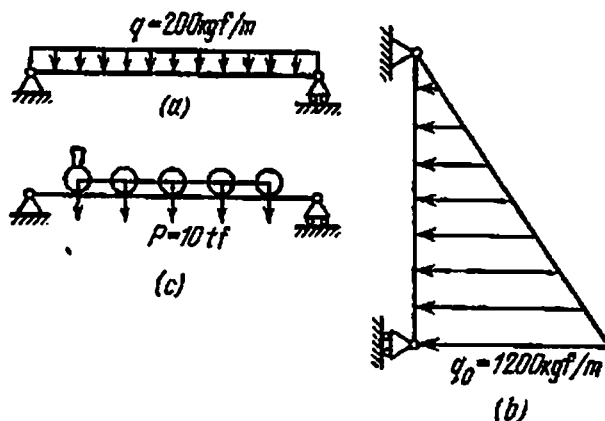


Fig. 124

per unit length of the beam at the given point \*. In other words,  $q(x)$  is equal to the limit of the ratio of load acting over a length of  $dx$  near the particular point to the length  $dx$ .

A few examples of beams are given in Fig. 124(a), (b) and (c). The first one is a joist loaded by a uniformly distributed force  $q=200$  kgf/m; the second beam is a dike support loaded by a triangular force (water pressure) of intensity  $q(x)$  varying from 0 to  $q_0=1200$  kgf/m; the third one is the main beam of a bridge, which takes the forces exerted by the engine wheels.

The wagon axle is a beam supported by the wheels and subjected to the pressure of the axle box; beams in the aeroplane wings are bent due to air pressure.

For the time being we shall study only the beams which satisfy the following two limitations:

- (1) the beam section must have at least one axis of symmetry (Fig. 125);
- (2) all external forces must lie in the plane of symmetry of the beam.

The reactions of the supports, which balance the external forces applied to the beam, must also, obviously, lie in the same plane.

\* Notation  $q(x)$  shows that the intensity of load in this case is a function of  $x$ .

To determine the reactions of the beam supports we must study their construction. The supports generally belong to one of the following three types:

- (a) fixed hinged support;
- (b) movable hinged support;
- (c) rigidly fixed support.

The fixed hinged support is schematically shown by point *A* in Fig. 126. It allows the supported section of the beam to revolve freely

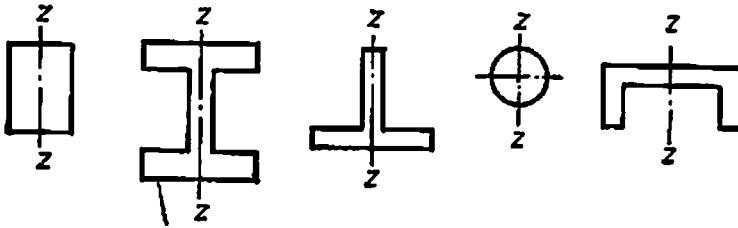


Fig. 125

round a hinge mounted at the centre of gravity *A* of the supported section, but does not permit linear displacement of this end of the beam. The resistance of such a support is expressed by the reaction which is transmitted from the support to the beam end through the hinge and which lies in the plane of acting forces.



Fig. 126

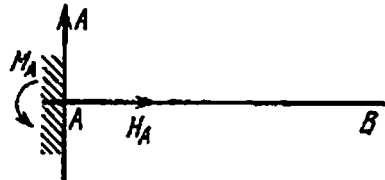


Fig. 127

We know only the point of application of the reaction—the hinge—as it is the only point at which the beam and the support come into contact, but we know neither the magnitude of reaction nor its direction. Therefore, we must always replace the support by two components:  $H_A$ , parallel to the beam axis, and  $A$ , perpendicular to it. From this reasoning a fixed hinged support gives two reactions ( $A$  and  $H_A$ ) of unknown magnitude.

A movable hinged support permits, besides rotation, free displacement in the relevant direction (Fig. 126, point *B*). Hence, this support only hinders displacement perpendicular to the particular direction. Therefore, the reaction of such a support passes through the centre of the hinge and is directed at right angles to the line of free displacement of the support (usually the beam axis). Thus a hinged movable support gives only one unknown reaction *B*.

Finally, a rigidly fixed support hinders all types of displacements of the beam end in the plane of action of the forces. It may be obtained from a fixed hinged support by removing the hinge (Fig. 127).

By removing the hinge we prevent rotation of the beam end, i.e. we introduce a new reaction that prevents such a rotation. This reaction is created by a force couple. Therefore a rigidly fixed end of the beam gives three unknown reactions: component  $H_A$  parallel to the beam axis, component  $A$  perpendicular to it, and the bearing moment  $M_A$ .

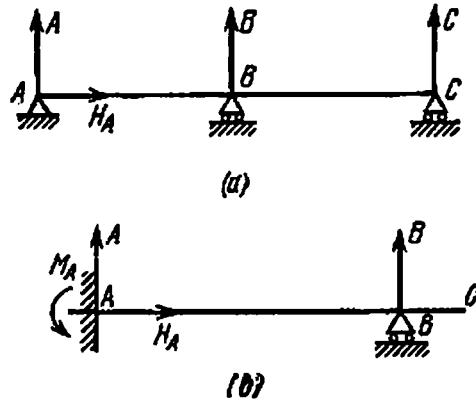


Fig. 128

A beam may rest on a number of supports of the types explained above. Figure 127, for example, shows a beam with a rigidly fixed end; in Fig. 126 the beam is supported at one end by a fixed hinged support and at the other end, by a movable hinged support; in Fig. 128 (a) the same beam is supported additionally at the centre by a movable hinged support; the beam in Fig. 128(b) is rigidly fixed at one end and supported by a movable hinged support at one of the intermediate sections.

In all these figures we have depicted the reactions of the supports of a particular construction, which may arise under the action of external forces; the forces have not been shown in the figures.

To determine the unknown reactions we shall first use the static equations expressing the condition that under the action of the forces applied to it and the reactions the beam as a whole remains in equilibrium. As all the forces lie in a single plane, we may write down three static equations. Thus, the problem of determining the reactions from conditions of statics is determinate if the number of unknown reactions is not more than three.

Hence, the beams with the construction of supports that gives three reactions (Figs. 126 and 127) are statically determinate. Multiple-support beams with intermediate hinges also belong to the group of statically determinate beams. These beams may be classified into the basic statically determinate beams (*A-1* and *2-3*) and the suspended

statically determinate (1-2 and 3-D), which are supported by the former through hinges (Fig. 129).

All other beams belong to the group of *statically indeterminate*; they will be analyzed later in special chapters.

The construction of the supports is, in fact, sometimes very much different from the construction shown in Figs. 126 and 127. Therefore, before we start analyzing a beam we must first study the design of

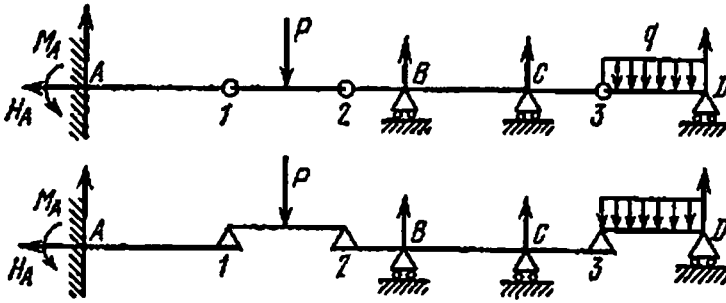


Fig. 129

its supports and establish to which group of supports shown in Figs. 126 and 127 do they belong.

As the deformation of the beams is usually very small and stresses are within the elastic limit, we must find out whether the support permits even a small rotation or displacement. If this is so, it is suf-

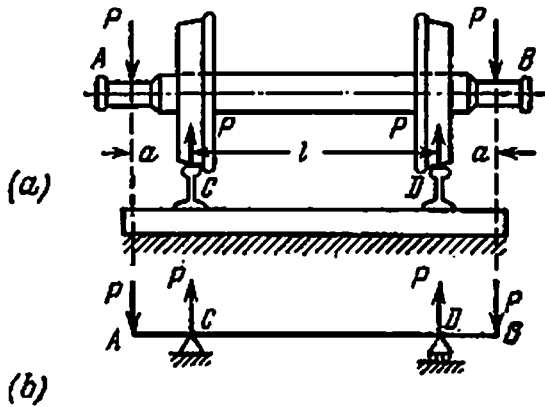


Fig. 130

ficient to consider the support hinged or movable. If the end of a metallic or wooden beam is fixed in a brick wall to a small depth, then a little rotation of this end is quite possible, and therefore the end should be considered as hinged.

Thus before determining the support reactions, we must represent the supports by schematic diagram replacing the actual construction by an equivalent approximate drawing. Thus, for instance, the wagon



axle (Fig. 130(a)) that experiences pressure  $P$  of the wagon body and transmits it to the rails may be looked upon as a beam loaded by forces  $P$  at points  $A$  and  $B$  and resting on hinged supports  $C$  and  $D$  of which one may be considered movable (Fig. 130(b)). This schematic drawing describes the actual working of the wagon axle with some approximation because the supporting sections may rotate under bending load and the distance between points  $C$  and  $D$  may also slightly change.

We shall employ the three equations of equilibrium to determine the support reactions in statically determinate beams. The axis of the beam is assumed as the  $x$ -axis and the centre of one of the hinges as the centre of coordinates; the  $y$ -axis is directed vertically upwards (it is assumed that the beam is horizontal).

To determine the horizontal component of the reaction we equate to zero the sum of projections of all the forces on the  $x$ -axis. The vertical components of the reactions and the support moment are determined by equating to zero the sum of moments of all forces about any two points of the beam, usually about the centres of gravity of the supported sections of the beam. The sum of projections of all the forces on the  $y$ -axis should be equated to zero to check the correctness of calculations; this condition must become an identity when the values already obtained are substituted in it.

In beams with intermediate hinges, we first study the equilibrium of the suspended beams as beams on two supports and find their reactions. These reactions must balance the forces transmitted from the suspended beams to the base beam through the hinges. Knowing the forces, we can determine the reactions of the base beam (see § 59).

## § 56. Nature of Stresses in a Beam.

### Bending Moment and Shearing Force

Selection of the design scheme and determination of the support reactions completes the first part of the problem of beam analysis—determination of the external forces acting on the beam.

We can now proceed with finding the stresses in beam sections; this will be the next step in solving the problems on bending. For discussion, let us consider a hinged beam (Fig. 131) which is loaded by forces  $P_1$ ,  $P_2$ , and  $P_3$ . For the given system of forces the horizontal reaction  $H_A$  is zero, the reactions  $A$  and  $B$  are determined from the equations of moments; thus all the external forces can be determined.

Before determining the stresses we must find the critical section of the beam through which the maximum stresses are transferred. This can be achieved by deriving formulas which enable us to determine the stresses in any section (for example, inclined section 3-3). Once we have derived these formulas, we shall be able to determine the critical section as well as the maximum stresses.

Let us start by determining stresses in a plane perpendicular to the axis of the beam, then in a plane parallel to the axis, and finally in any plane. Let us take a section *1-1* perpendicular to the axis of the beam with its centre of gravity  $O_1$  at a distance  $x$  from the left

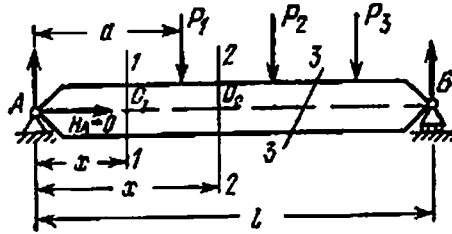


Fig. 131

support. To determine the stresses in this section we remove one portion of the beam and replace its action on the remaining portion by the unknown stress. For convenience of calculation, the equilibrium of that portion of the beam should be considered to which less number of forces are applied; in the example under consideration, the left portion. This portion must maintain equilibrium under the action of external and internal forces acting on it.

The only external force—force  $A$  acting upwards—is applied to the left of section  $1-1$  (the weight of the beam is neglected). This force can be balanced only by the internal force  $Q=A$  (or  $Q=P_2+P_3-B=A$ ) which is transmitted from the right cut-out portion of the beam and acts vertically downwards along the tangent to the section (Fig. 132(a)). Since forces  $A$  and  $Q$  lying in the vertical plane form a couple with moment  $M=Ax$  in the clockwise direction, the section must experience internal forces which also result in a moment of the same magnitude  $M=Ax$  acting in the anticlockwise direction.

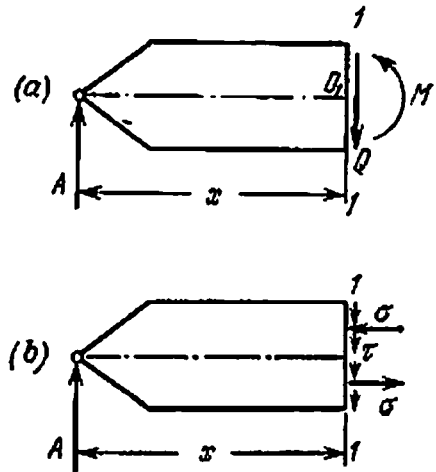


Fig. 132

Only normal stresses acting in the section are capable of creating this moment which retains the left portion of the beam in equilibrium.

Hence, the internal forces in section  $1-1$  that replace the action of the removed right portion of the beam on the left are: force  $Q=A$  parallel to the external forces and made up of shearing stresses acting in the beam cross section; a force couple of moment  $M=Ax$  that acts

in the plane of action of external forces and is made up of normal stresses.

This means that the section of the beam under consideration experiences shearing as well as normal stresses (Fig. 132(b)) that add up into internal force factors  $Q$  and  $M$  which together balance the system of external forces acting on the portion of beam being considered. It goes without saying that force factors  $Q$  and  $M$  of the same magnitude but acting in the opposite direction are transmitted across section 1-1 from the left portion of the beam to the right, and they balance the external forces applied to the right portion.

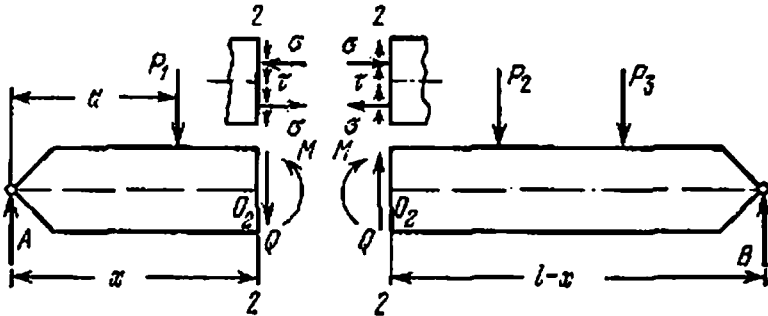


Fig. 133

To determine the stresses acting in various sections of the beam, we must learn to determine the magnitudes and directions of internal forces acting in an arbitrary section of the beam by expressing them through external forces. Let us consider, for example, an arbitrary section 2-2 (Fig. 131) and find the internal forces transmitted from the left portion of the beam to the right. In order to do this we remove the left portion and transfer the forces acting on it to the right portion—to the centre of gravity of section 2-2 (point  $O_2$ ). In the process of transfer, the forces acting in a plane are reduced to a resultant force acting at the centre of forces and a force couple. Hence, the forces transferred from the left portion to the right must be applied at point  $O_2$  in the form of force factors (Fig. 133): force

$$Q = A - P_1 \quad (10.1)$$

force couple with moment

$$M = Ax - P_1(x - a) \quad (10.2)$$

Assuming that  $A > P_1$ , we direct force  $Q$  upwards and moment  $M$ —clockwise. Identical internal force factors  $Q$  and  $M$  acting in the opposite direction are transferred from the right portion of the beam to the left (Fig. 133).

It is clear from the above discussion that in any cross section of the beam the internal forces can be reduced to force  $Q$  and force couple

of moment  $M$ , which together replace the action of one cutoff portion of the beam on the other.

Force  $Q$ , the resultant of elementary shearing forces acting in the beam section, is known as the *lateral* or *shearing force*. This force has the tendency to shear the section under consideration with respect to an adjoining section (Figs. 133 and 134). It is evident from equation (10.1) that the shearing force in each cross section is calculated as the sum of projections on the normal to the beam axis of all external forces acting to the right or left of the section. When all the forces acting on the beam are perpendicular to its axis, the shearing force

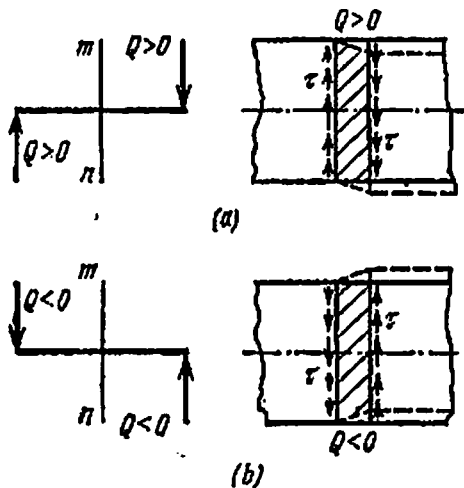


Fig. 134

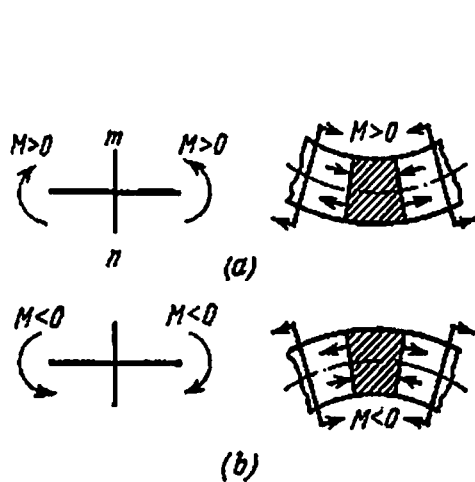


Fig. 135

may be calculated as the algebraic sum of forces acting on the portion of the beam the equilibrium of which is being considered.

The moment of internal force couple made up of elementary normal stresses acting in the beam's cross section is known as *bending moment*. The bending moment tends to rotate the section under consideration with respect to an adjacent section, which leads to deformation of the beam axis, i.e. bending (Fig. 135).

It is evident from Eq. (10.2) that the bending moment in an arbitrary section of the beam is equal to the algebraic sum of moments of all external forces acting to one side of the section about central axis  $y$  that is normal to the beam axis.

Let us establish the sign convention for  $Q$  and  $M$ . As is shown in Fig. 133, the internal force factors  $Q$  and  $M$  act in opposite directions depending on whether the section under consideration belongs to the left portion or the right. This circumstance should be taken into account when dealing with the sign convention in order to get identical values of  $Q$  and  $M$  not only in magnitude but also with the same sign irrespective of whether we consider the forces acting on the left cut-out portion or the right one.

In accordance with the above (for a horizontal beam) we shall consider shearing force  $Q$  positive if the external forces to the left of the section under consideration act upwards or the forces to the right of the section act downwards. In other words,  $Q > 0$  if the resultant of external forces acting to the left of the section is directed upwards; for forces acting to the right of the section  $Q > 0$  if their resultant is directed downwards. According to this convention the direction of  $Q$  coincides with the direction of shearing stresses  $\tau$  which constitute the shearing force (Fig. 134).

The bending moment will be considered positive if the algebraic sum of moments of forces applied to the left of the section gives a resulting moment acting in the clockwise direction; or if forces applied to the right of the section give an anticlockwise resulting moment (Fig. 135). Hence, for the left cutoff portion the bending moment due to each individual force is considered positive if the moment of this force w.r.t. the centre of gravity of the section is clockwise; on the other hand,  $M < 0$  if the force gives an anticlockwise moment w.r.t. the centre of gravity of the section. If the right cutoff portion of the beam is considered, the convention is just the reverse.\*

The accepted sign convention for  $M$  is related to the nature of deformation of the beam: if the bending moment is positive, the beam bends with its convex surface down, if the bending moment is negative, with its convex surface up (Fig. 135). In the section where  $M$  passes through zero the beam axis has an inflection point; the beam axis remains straight in the segments where  $M = 0$ .

We have seen that the expressions for shearing force and bending moment are different in different sections of the beam (1-1 and 2-2). By the very definition of internal force factors it is obvious that the shearing stresses are maximum in the section where  $Q = Q_{\max}$ , whereas the normal stresses are maximum in the section where  $M = M_{\max}$ . Therefore, for checking the strength of beams we must find those sections in which shearing force and bending moment are maximum. The search for these critical sections is greatly facilitated by plotting of bending-moment and shearing-force diagrams, i.e. diagrams that show how bending moment  $M$  and shearing force  $Q$  vary in different sections of the beam when they are plotted as a function of  $x$ .

Thus, the shearing force  $Q(x)$  and bending moment  $M(x)$  are functions of  $x$ . In future for brevity's sake we shall denote these quantities by  $Q$  and  $M$ , and use the notation  $(x)$  only when we want to emphasize that  $Q$  and  $M$  are variable quantities which depend upon  $x$ . While plotting the diagrams, the ordinates which, to a certain scale, represent the value of the bending moment or the shearing force, are

---

\* Some writers relate the signs for  $Q$  and  $M$  with the direction of the coordinate axes, which in some cases (for example, compound bending of bars with broken axis) simplifies the sign convention.

laid off under the given section from the *x*-axis parallel to the axis of the beam. Positive ordinates of the *Q*- and *M*-diagrams will be laid off upwards and negative downwards. Some books recommend plotting of the bending-moment diagram on the convex side of the bent beam, the positive ordinates downwards and negative upwards. However, this is merely a matter of liking, which is not significant.

It may become easier to plot these diagrams if we are able to establish some relation between the values of bending moment and shearing force in an arbitrary section and also the relation of *Q* and *M* with the forces acting on the beam.

In the next section we shall explain how to correlate the external forces, the shearing force and the bending moment.

**§ 57. Differential Relation Between the Intensity of a Continuous Load, Shearing Force and Bending Moment**

It was shown in § 56 that for equilibrium of the cut-out portion of a beam it is essential to apply in the section force factors *Q* and *M* that replace the action of the removed portion on the portion under consideration. Hence, if we cut from the beam (Fig. 136) an element of infinitely small length *dx*, it must remain in equilibrium under the continuous load of intensity *q* (which may be considered constant over the length *dx*), the forces *Q* and *Q<sub>1</sub>* and moments *M* and *M<sub>1</sub>*, which represent the action on the element of the left and right cutoff \* portions, respectively. Let us note that *Q<sub>1</sub>* = *Q* + *dQ* and *M<sub>1</sub>* = *M* + *dM* because the increment of these quantities in transition from section *mn* to an infinitely close section *m<sub>1</sub>n<sub>1</sub>* is also an infinitely small quantity.

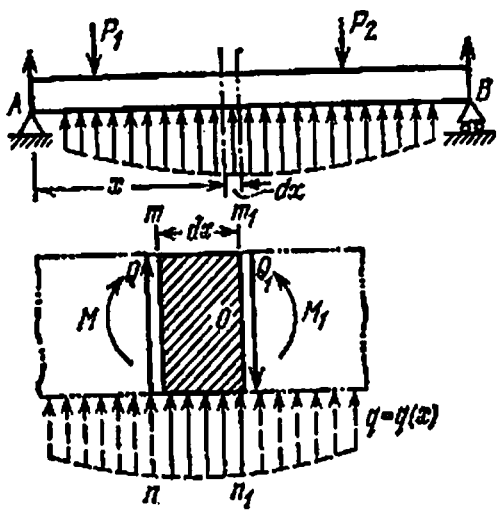


Fig. 136

The conditions of equilibrium of the isolated element may be written as

$$\sum Y = 0, \quad Q + q \, dx - (Q + dQ) = 0$$

$$\sum M_o = 0, \quad M + Q \, dx + q \, dx \frac{dx}{2} - (M + dM) = 0$$

From the first equation we get

$$q \, dx - dQ = 0$$

\* No concentrated force or moment acts over the element *dx*.

wherefrom

$$\frac{dQ}{dx} = q \quad (10.3)$$

i.e. the derivative of the shearing force w.r.t. the abscissa of the section is equal to the intensity of the continuous load in the same section.

From the second equation, neglecting the infinitesimals of the second order, we get

$$Q dx - dM = 0 \quad \text{or} \quad \frac{dM}{dx} = Q \quad (10.4)$$

i.e. the derivative of the bending moment w.r.t. the abscissa of the section is equal to the shearing force in the same section.

Differentiating both sides of Eq. (10.4), we get

$$\frac{d^2M}{dx^2} = \frac{dQ}{dx} \quad \text{or} \quad \frac{d^2M}{dx^2} = q \quad (10.5)$$

i.e. the second derivative of the bending moment w.r.t. the abscissa is equal to the intensity of the continuous load. If  $q$  is directed downwards, equations (10.5) become

$$\frac{d^2M}{dx^2} = -q \quad \text{and} \quad \frac{dQ}{dx} = -q$$

By integrating formulas (10.3) and (10.4), we get

$$Q(x) = \int_0^x q(x) dx + Q(0) \quad (10.3')$$

$$M(x) = \int_0^x Q(x) dx + M(0) \quad (10.4')$$

The arbitrary constants  $Q(0)$  and  $M(0)$  are concentrated force and moment (if they exist) in the beginning of the segment. These formulas are convenient to use while plotting diagrams for non-uniform loading  $q=q(x)$ . In the geometrical sense each integral represents area:  $\int_0^x q(x) dx = \omega_q$  is the load area (see § 59) and  $\int_0^x Q(x) dx = \omega_Q$  is the area of  $Q$ -diagram over length  $x$ . Formulas (10.3') and (10.4') may be written in the form

$$Q(x) = \omega_q + Q(0) \quad (10.3'')$$

$$M(x) = \omega_Q + M(0) \quad (10.4'')$$

The relations obtained above may be used in plotting the diagrams for  $Q$  and  $M$ , especially if we consider that the derivative of a function

geometrically represents the slope of the tangent to the curve at the given point. In other words, the shearing force in a section may be regarded as the slope of the tangent to the bending-moment diagram at the point corresponding to the given section. Therefore, it should be borne in mind that if the  $x$ -axis is directed from right to left, then  $\frac{dM}{dx} = -Q$ , because the slope of the tangent to the curve changes its sign if the direction of the axis is reversed.

It follows from Eq. (10.3) that in the section where intensity of the load  $q=0$ , the shearing force  $Q=Q_{\max}$  or  $Q=Q_{\min}$ , because if  $q=\frac{dQ}{dx}=0$  then the tangent to the shearing force diagram must be parallel to the  $x$ -axis. By the same reasoning we come to another more important conclusion from Eq. (10.4): the bending moment is maximum (or minimum) in the section where  $Q=\frac{dM}{dx}=0$ , i.e. where the shearing force passes through zero.

Although Eq. (10.4) enables us to get  $Q$  as the first derivative of  $M$ , it should be determined independently when plotting the shearing force diagram, and Eq. (10.4) should be employed only for checking its value. Similarly, for checking whether we are plotting the bending-moment diagram correctly, we can use formula (10.4') according to which the ordinate of  $M$ -diagram in an arbitrary section is equal to the area of  $Q$ -diagram to one side of the section or differs from it by a value equal to the concentrated bending moment  $M(0)$ , if the latter enters in the expression for  $M(x)$ . Likewise Eq. (10.5) may also be used to check the correctness of plotting the  $M$ -diagram, because the direction of convexity of the bending-moment diagram is determined by the sign of the second derivative of  $M$ . Instructions on checking the correctness of plotting the shearing-force and bending-moment diagrams will be given below (§ 60).

### § 58. Plotting Bending-moment and Shearing-force Diagrams \*

**Example.** Plot the bending-moment and shearing-force diagrams for a simply supported beam loaded with force  $P$  (Fig. 137).

To calculate  $M$  and  $Q$  in any section of the beam, it is first of all necessary to find the reactions. The assumed directions of the reactions  $A$ ,  $H_A$ , and  $B$  is shown in Fig. 137.

By equating to zero the sum of the projections of all forces on the axis of the beam we get

$$H_A = 0$$

---

\* A number of examples on plotting  $Q$ - and  $M$ -diagrams are given in problem books. See N. M. Belyaev, *Problems in Strength of Materials*, Pergamon Press, 1966.



This result could have been predicted beforehand, because all the forces acting on the beam are perpendicular to its axis.

By taking the sum of the moments of all the forces about point *B*, we get

$$\sum M_B = 0, \quad +Al - Pb = 0$$

or

$$A = +\frac{Pb}{l}$$

Similarly

$$\sum M_A = 0, \quad -Bl + Pa = 0$$

or

$$B = +\frac{Pa}{l}$$

To check the correctness of the results obtained, we take the sum of the projections of all forces on the vertical *y*-axis:

$$A - P + B = 0 \quad \text{or} \quad A + B = P$$

Substituting the values of the reactions found above, we get

$$\frac{Pb}{l} + \frac{Pa}{l} = \frac{P(a+b)}{l} = P$$

which is in accordance with the condition of equilibrium. Such a check is always desirable, because an error in determining the reactions will inevitably lead to errors in plotting the bending-moment and shearing-force diagrams.

The expressions giving the values of shearing force and bending moment in any section may be obtained by taking an arbitrary section 1-1 between *A* and *C* at a distance *x*<sub>1</sub> from *A*. Let us take note that the expression "taking a section" includes not only marking of the section on the drawing but also giving its distance from the selected origin of coordinates. The centre of gravity of the section is denoted by *O*<sub>1</sub>.

It is more convenient to consider the left cutoff portion to determine the shearing force *Q* in the section, because the left portion is acted upon by a less number of forces (only force *A*). Considering the portion of the beam to the left of section *O*<sub>1</sub> and projecting the forces acting on it on a plane perpendicular to its axis, we get the expression

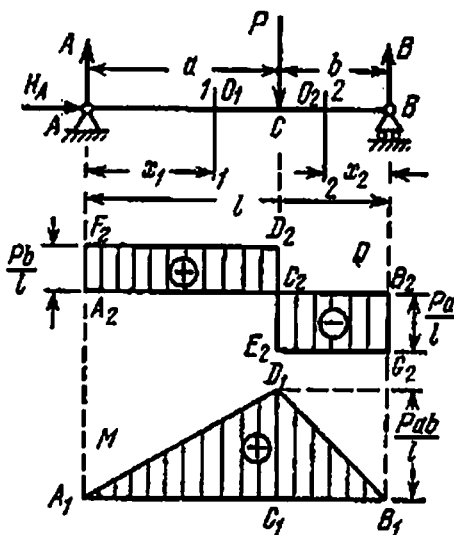


Fig. 137

the shearing force *Q* in the section, because the left portion is acted upon by a less number of forces (only force *A*). Considering the portion of the beam to the left of section *O*<sub>1</sub> and projecting the forces acting on it on a plane perpendicular to its axis, we get the expression

for shearing force  $Q_1$  in the section at a distance  $x_1$  from support  $A$ :

$$Q_1 = +A = \frac{Pb}{l} \quad (10.6)$$

The shearing force in a section having abscissa  $x_1$  does not depend upon this distance. Thus, as long as  $x_1$  varies from 0 to  $a$ , the shearing force remains constant, and its diagram in this portion is represented by a straight line  $F_2D_2$  parallel to the axis of abscissa  $A_2B_2$  (Fig. 137).

Expression (10.6) for  $Q_1$  holds good as long as the section does not go beyond point  $C$ , i.e. till  $0 \leq x_1 \leq a$ . If  $x_1 > a$ , the left portion of the beam will experience two forces  $A$  and  $P$ ; consequently, the sum of the projections of forces acting on the left cutoff portion will change.

To find the shearing force in the second portion, we shall have to take another section between points  $B$  and  $C$  with centre of gravity at  $O_2$ . Its distance  $x_2$  will be measured from the right support  $B$ . It will be convenient for us in this case to consider the equilibrium of the right portion of the beam as it is acted upon by only one force  $B$ .

Considering the right cutoff portion of the beam, we get the expression for shearing force in section 2-2:

$$Q_2 = -B = -\frac{Pa}{l} \quad (10.7)$$

The minus sign shows that force  $B$  acting on the right cutoff portion is directed upwards.

It is obvious that if we had considered the left cutoff portion, we would have obtained the same expression for  $Q_2$ :

$$Q_2 = A - P = -B \quad (\text{since } A + B = P)$$

Expression (10.7) is valid for any value of  $x_2$  not exceeding the limits of the portion  $BC$ , i.e. for  $0 \leq x_2 \leq b$ ; this expression also shows that  $Q_2$  does not depend upon  $x_2$ .

The shearing-force diagram over the length of the second portion is a straight line  $E_2G_2$  parallel to the  $x$ -axis. It has a discontinuity—a jump at the point of application of force  $P_1$ . At this point the shearing force passes through zero and is not equal to  $D_2E_2 = P$ . In a section immediately to the left of point  $C$

$$Q = +\frac{Pb}{l}$$

in a section to the right of point  $C$

$$Q = -\frac{Pa}{l}$$

Let us note that the absolute value of the jump is equal to the concentrated force  $P$  acting in this section.

Such a shape of the shearing-force diagram (Fig. 137) is possible only if we consider the concentrated force  $P$  acting at a single point  $C$ . Actually pressure  $P$  is transferred to the beam through a very small area (Fig. 138). Therefore, in this area the shearing force changes

gradually from  $+\frac{Pb}{l}$  to  $-\frac{Pa}{l}$ , passing through zero in the process.

The maximum absolute value of the shearing force in this example will be (if  $a > b$ )

$$|Q_{\max}| = \frac{Pa}{l}$$

All sections of portion  $CB$  of the beam are prone to failure due to shearing stresses.

In plotting the bending-moment diagram we shall use the same sections 1-1 (with the origin of coordinates at point  $A$ ) for the left portion of the beam and 2-2 (with

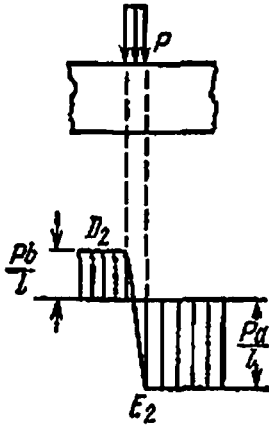


Fig. 138

the origin of coordinates at point  $B$ ) for the right portion of the beam.

Considering the left portion, we determine the moment in section 1-1 as the sum of the moments of forces acting on it about the centre of gravity of the section  $Q_1$ :

$$M_1 = Ax_1 = \frac{Pb}{l}x_1 \tag{10.8}$$

$M_1$  is a linear function in  $x_1$ . Therefore, if we move the section, i.e. change  $x_1$ , then  $M_1$  varies linearly. Expression (10.8) for  $M_1$  holds good as long as the section does not go beyond point  $C$ , i.e. till  $0 \leq x_1 \leq a$ .

As soon as  $x_1$  becomes greater than  $a$ , the left portion of the beam starts experiencing two forces:  $A$  and  $P$ , and formula (10.8) no more holds good. As the diagram is a straight line, it is sufficient to give two values to  $x_1$  to obtain the two points required for plotting the line. At  $x_1=0$ , we get  $M_1=0$ —this is the ordinate under section  $A$ . Similarly at  $x_1=a$  we get  $M_1=+\frac{Pab}{l}$ ; this is the ordinate under section  $C$ .

Laying off upwards from the  $x$ -axis (positive moment) the segment  $C_1D_1$ , which expresses to a certain scale the ordinate  $\frac{Pab}{l}$ , and joining points  $D_1$  and  $A_1$  by a straight line, we get the first portion of the bending-moment diagram. To plot the diagram for the second portion, we write down the expression for the moment about point  $O_2$

of forces acting on the right cutoff portion of the beam:

$$M_2 = Bx_2 = \frac{Pa}{l}x_2 \quad (10.9)$$

In this portion also the moment is positive, because we consider the right portion, and force  $B$  rotates it about point  $O_2$  in the anti-clockwise direction. Expression (10.9) represents the equation of a straight line and holds good for  $0 \leq x_2 \leq b$ . At  $x_2 = b$ ,  $M_2 = +\frac{Pab}{l}$  and at  $x_2 = 0$ ,  $M_2 = 0$ .

Thus, the second portion of the bending-moment diagram is represented by the straight line  $D_2B_1$ . The bending moment is positive over the whole length of the beam and is maximum in section  $C$ , the point of application of force  $P$ , where it is equal to

$$M_{\max} = \frac{Pab}{l} \quad (10.10)$$

The maximum normal stresses will act in this section.

At  $a = b = \frac{l}{2}$  (the force acts in the middle of the beam) we get

$$M_{\max} = \frac{Pl}{4} \quad (10.10')$$

In any cross section of the beam taken between the end points  $A$ - $C$  and  $C$ - $B$  the values of  $Q$  and  $M$  are graphically represented by the ordinates of the corresponding diagrams shown in Fig. 137 by vertical hatching.

We shall study a few more examples on plotting bending-moment and shearing-force diagrams for beams subjected to various types of loading.

Let us plot the  $M$ - and  $Q$ -diagrams for the beam shown in Fig. 139, loaded by a continuous uniformly distributed force of intensity  $q$  (expressed in  $\text{kgf/m}$ ,  $\text{tf/m}$ ,  $\text{N/m}$ , etc.).

It is essential to determine the support reactions before we start solving the problem.

The reaction  $H_A$  is zero, reactions  $A$  and  $B$  are equal from symmetry; each of them is equal to half of the total load on the beam:

$$A = B = \frac{ql}{2}$$

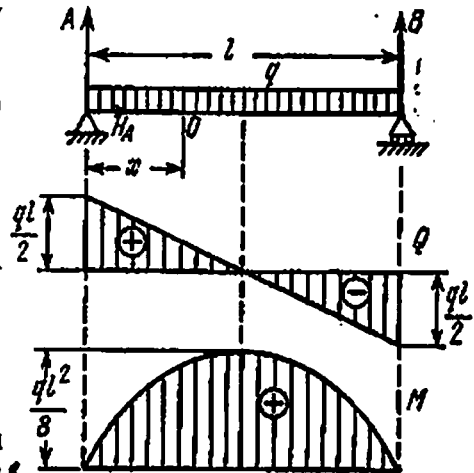


Fig. 139

Let us take a section  $O$  at a distance  $x$  from the left end of the beam. We shall consider the equilibrium of the left-hand portion to determine  $Q$  and  $M$ . It is acted upon by reaction  $A$  and load  $q$  uniformly distributed over length  $x$ .

We must take the sum of all the forces acting on the left cutoff portion to determine the shearing force in section  $O$ . To the left of the section is force  $A = \frac{ql}{2}$  directed upwards, and the resultant of the uniformly distributed load over the length  $x$ , equal to  $qx$  and directed downwards. Therefore,

$$Q = A - qx = \frac{ql}{2} - qx$$

The shearing force varies with  $x$  linearly, and the line may be plotted by taking two values of the variable  $x$ : at  $x=0$ ,  $Q = \frac{ql}{2}$  and at  $x=l$ ,  $Q = -\frac{ql}{2}$ . The shearing-force diagram is shown in Fig. 139;  $Q_{\max} = \frac{ql}{2}$ .

To plot the bending-moment diagram we take the sum of the moments of the same forces acting on the portion of beam under consideration about point  $O$ . Keeping in mind that resultant  $qx$  acts in the middle of the segment of length  $x$ , with an arm of length  $\frac{x}{2}$  about point  $O$ , we get

$$M = +Ax - qx \frac{x}{2} = \frac{ql}{2}x - \frac{qx^2}{2} = \frac{qx}{2}(l - x)$$

This equation of moments is valid for determining the bending moment in any section of the beam.

In this case the bending moment depends upon the square of abscissa  $x$ ; therefore, the diagram is of the shape of a square parabola. To plot the curve we need at least three or four points lying on it:

$$\begin{aligned} \text{at } x=0 & \quad M=0 \\ \text{at } x=\frac{l}{4} & \quad M = \frac{ql}{2 \times 4} \left( l - \frac{l}{4} \right) = \frac{3ql^2}{32} \\ \text{at } x=\frac{l}{2} & \quad M = + \frac{ql}{4} \left( l - \frac{l}{2} \right) = + \frac{ql^2}{8} \\ \text{at } x=l & \quad M=0 \end{aligned}$$

The bending-moment diagram is of the shape shown in Fig. 139.

To determine  $M_{\max}$  we find abscissa  $x_0$  of the corresponding section by equating the first derivative of  $M$  w.r.t.  $x$  to zero:

$$\frac{dM}{dx} = \frac{ql}{2} - \frac{2qx_0}{2} = 0$$

wherefrom

$$x_0 = \frac{l}{2} \quad \text{and} \quad M_{\max} = + \frac{qx_0}{2} (l - x_0) = + \frac{ql^2}{8} \quad (10.11)$$

The maximum bending moment occurs at the middle of the span, i.e. in the section where  $Q=0$ . This is a check of the relation between  $M(x)$  and  $Q(x)$  established above (in § 57).

Let us consider one more example—beam  $AB$  rigidly fixed at one end (Fig. 140). Such a beam is usually known as *cantilever*. Since the right end of the beam is free, it is essential to consider the forces acting to the right of the section while plotting the bending-moment and shearing-force diagrams. In this case it is not necessary to determine the support reactions of the rigid constraint (at the left end of the beam). Force  $P$  divides the beam into two parts:  $AC$  of length  $a$  and  $CB$  of length  $b$ .

If we consider section 1-1 at a distance  $x_1$  from the free end, we observe that there are no external forces to the right of the section and therefore it is free of internal forces. For all values of  $x_1$  between 0 and  $x_1=b$

$$Q_1=0 \quad \text{and} \quad M_1=0 \dots (a)$$

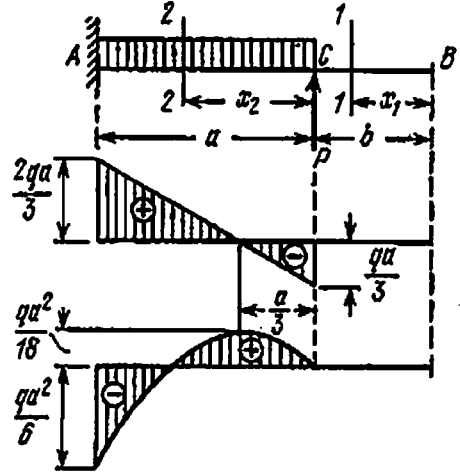


Fig. 140

The distance to section 2-2 in portion  $AC$  will be laid off from the point of application of force  $P$ . To the right of the section we will have force  $P$  acting upwards and a uniformly distributed force of intensity  $q$  acting downwards over a length  $x_2$  and having a resultant  $qx_2$ . The internal forces in section 2-2 will be

$$Q_2 = -P + qx_2 \tag{b}$$

$$M_2 = Px_2 - \frac{qx_2^2}{2} \tag{c}$$

As the abscissa is varied from  $x_2=0$  to  $x_2=a$ , shearing force  $Q_2$  changes according to linear law and bending moment  $M_2$  according to a parabolic law with a maximum in the section where  $Q_2 = \frac{dM}{dx} = 0$ , i.e. in the section where  $x_2 = \frac{P}{q}$ , as is evident from equation (b).

Let us now plot the  $Q$ - and  $M$ -diagrams. In order to calculate the ordinates in a general form we shall assume a particular ratio between  $P$  and  $q$  (this can always be done when the quantities are known numerically). Suppose, for instance, that  $P = \frac{qa}{3}$ .

It is evident from equation (a) that in the first portion of length  $b$  the ordinates of both  $Q$ - and  $M$ -diagrams are equal to zero, and the

diagrams coincide with the  $x$ -axes. In the second portion of length  $AC=a$  ( $0 \leq x_2 \leq a$ ) from equations (b) and (c) we have

$$\text{at } x_2=0, \quad Q_2 = -P = -\frac{qa}{3}, \quad M_2 = 0$$

$$\text{at } x_2 = \frac{P}{q} = \frac{a}{3}, \quad Q_2 = 0, \quad M_2 = \frac{qa}{3} \frac{a}{3} - \frac{qa^2}{2 \times 9} = \frac{qa^2}{18}$$

$$\text{at } x_2 = a, \quad Q_2 = -P + qa = \frac{2}{3} qa, \quad M_2 = Pa - \frac{qa^2}{2} = -\frac{qa^2}{6}$$

The  $Q$ - and  $M$ -diagrams are depicted in Fig. 140. It is clear from the diagrams that the absolute maximum values of  $Q$  and  $M$  occur at the fixed end and are

$$Q_{\max} = \frac{2}{3} qa, \quad M_{\max} = \left| \frac{qa^2}{6} \right|$$

### § 59. Plotting Bending-moment and Shearing-force Diagrams for More Complicated Loads

Having studied the characteristics of bending-moment and shearing-force diagrams and the general method of plotting them, we can pass over to solving more complicated problems.

Let us see how to determine  $Q$  and  $M$  when the beam is acted upon by a continuous non-uniformly distributed load whose intensity changes along the beam length with  $x$  (Fig. 141). In other words,  $q$  is a function of  $x$  or  $q=q(x)$ . The bending moment and shearing force will also be some functions of  $x$ :

$$M = M(x) \quad \text{and} \quad Q = Q(x)$$

The curve  $adceb$  representing the variation of  $q(x)$  is called the *load curve*, and the area bounded by this curve is called the *load area*.

Let us calculate  $Q$  and  $M$  in an arbitrary section at a distance  $x_1$  from the free end. Considering the shearing force as the sum of elementary forces  $q(x) dx$  acting on the left cutoff portion of the beam, and replacing the summation by integration, we find

$$Q(x_1) = - \int_0^{x_1} q(x) dx = - \int_0^{x_1} d\omega = - \omega(x_1) \quad (10.12)$$

Here  $\omega(x_1)$  represents the part of load area located to the left of section  $c-C$ . Thus, the shearing force  $Q(x_1)$  equal to resultant  $R_q$  of the continuous load over the length  $AC=x_1$  may be calculated as the load area  $\omega(x_1)$ , lying to one side of the section.

The bending moment in the same section is equal to the sum of moments of elementary forces  $q(x) dx$ , acting on the cutoff portion of the beam, about point  $C$ , and may be calculated as the moment

of resultant  $R_q$ , i.e.

$$M(x_1) = -R_q x_r = -\omega(x_1) x_r \tag{10.13}$$

In other words, the bending moment of a continuous non-uniformly distributed load is equal to the product of the load area lying to one side of the section and the distance of the centre of gravity of this area from the section under consideration (arm of the resultant).

Let us study how to plot the bending-moment and shearing-force diagrams for a beam which is acted upon by a distributed force that varies along its length as shown in Fig. 142.

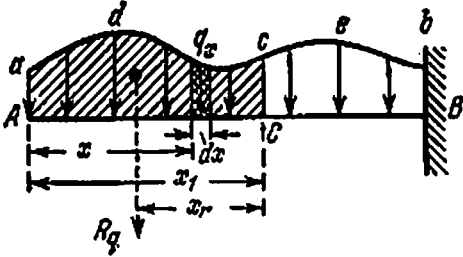


Fig. 141

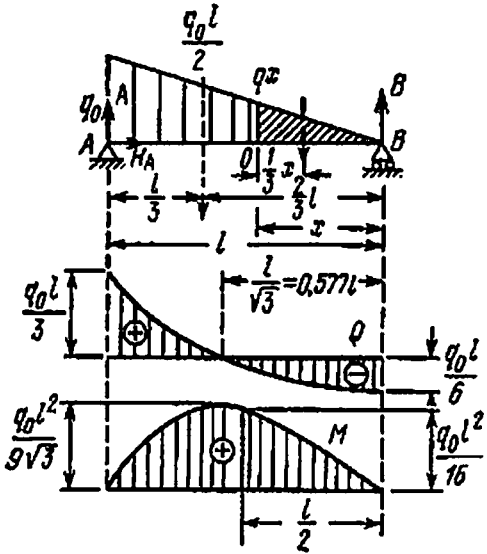


Fig. 142

Loads of this kind are applied to beams that support water and earth pressure, for example, dam supports and columns for strengthening walls of water storage reservoirs. Connecting rods of steam and internal combustion engines are subjected to similar loading by forces of inertia.

The load is characterized by the ordinate  $q_0$ , the maximum intensity of the load (in kgf/m). The reaction  $H_A=0$ ; we have to determine  $A$  and  $B$ .

For determining  $A$  we write down the equation of moments about point  $B$ . The moment of the load is equal to the moment of its resultant, i.e. moment of the load area  $\frac{q_0 l}{2}$  multiplied by the distance of its centre of gravity from point  $B$ . The resultant is shown in Fig. 142 by the dotted line; this emphasizes that the concentrated force equal to the load area  $\omega = \frac{1}{2} q_0 l$  does not actually act on the beam, but we



make use of it while taking the moment of the total load for determining the support reactions.

The equations of moments may be written as

$$\begin{aligned} \sum M_B = 0, & \quad Al - \frac{2}{3} \omega l = 0, & \quad A = \frac{2}{3} \omega = \frac{q_0 l}{3} \\ \sum M_A = 0, & \quad -Bl + \omega \frac{l}{3} = 0, & \quad B = \frac{1}{3} \omega = \frac{q_0 l}{6} \end{aligned}$$

Thus, support  $A$  takes two-thirds of the total load  $\omega = \frac{q_0 l}{2}$ , whereas support  $B$  takes only one-third.

To plot the diagrams let us take a section at a distance  $x$  from the right end of the beam. The ordinate  $q(x)$  of the load in this section is determined from similarity of triangles:

$$\frac{q(x)}{q_0} = \frac{x}{l}, \quad q(x) = q_0 \frac{x}{l}$$

While determining  $Q$  and  $M$  we shall consider the right-hand portion because it is acted upon by the concentrated force and triangular load, whereas the left-hand portion is acted upon by the concentrated force and trapezoidal load, which complicates the computations.

Shearing force  $Q$  will be the sum of the projections on the vertical of reaction  $B$  and the hatched load  $\omega(x) = \frac{1}{2} q(x)x = \frac{1}{2} q_0 \frac{x^2}{l}$ , i.e.

$$Q = -B + \omega(x) = -\frac{q_0 l}{6} + \frac{q_0 x^2}{2l} = -\frac{q_0 l}{6} \left( 1 - \frac{3x^2}{l^2} \right)$$

In this case the shearing-force diagram is represented by a quadratic curve, and

$$\text{at } x=0, \quad Q = -\frac{q_0 l}{6} = -B$$

$$\text{at } x=l, \quad Q = \frac{q_0 l}{3} = +A$$

$$\text{at } x = \frac{l}{2}, \quad Q = -\frac{q_0 l}{6} \left( 1 - \frac{3}{4} \right) = -\frac{q_0 l}{24}$$

The shearing-force diagram is given in Fig. 142. It is clear from the diagram that the maximum shearing force (in absolute value) occurs in section  $A$  (at the support):

$$Q_{\max} = +A = +\frac{q_0 l}{3}$$

The shearing force passes through zero at  $x_0$  which may be determined by the following equation:

$$Q = 0 = -\frac{q_0 l}{6} \left( 1 - \frac{3x_0^2}{l^2} \right); \quad x_0 = -\frac{l}{\sqrt{3}} = 0.577l$$

We shall use this value of  $x_0$  for determining the maximum value of  $M$ . The shearing force achieves its analytical minimum in point  $B$ , where the intensity of the continuous load is zero. As is evident from Eq. (10.3), the tangent to the shearing-force diagram in this section is parallel to the  $x$ -axis.

Let us pass over to plotting the bending-moment diagram for which we again consider the right cutoff portion of the beam. The moment of the resultant of the hatched triangular load (Fig. 142) about point  $O$  is equal to its load area multiplied by the arm  $\frac{x}{3}$ :

$$- \omega(x) \frac{1}{3} x = - \frac{x}{2} q(x) \frac{1}{3} x = - \frac{q_0 x^3}{6l}$$

The bending moment in this section is

$$M = Bx - \frac{q_0 x^3}{6l} = \frac{q_0 l}{6} x - \frac{q_0 x^3}{6l} = \frac{q_0 x l}{6} \left( 1 - \frac{x^2}{l^2} \right)$$

This expression for  $M$  holds good for the whole length of the beam. The bending-moment diagram is represented by a cubic curve. To plot the cubical parabola we must calculate a few ordinates:

$$\text{at } x=0, \quad M=0$$

$$\text{at } x = \frac{l}{2}, \quad M = \frac{q_0 l^2}{12} \left( 1 - \frac{1}{4} \right) = \frac{3q_0 l^2}{48} = \frac{q_0 l^2}{16}$$

$$\text{at } x=l, \quad M=0$$

The bending moment is maximum in the section where  $Q=0$ , i.e. at  $x_0 = \frac{l}{\sqrt{3}}$ ; it is equal to

$$M_{\max} = \frac{q_0 l}{6l \sqrt{3}} \left( l^2 - \frac{l^2}{3} \right) = \frac{q_0 l^2}{9 \sqrt{3}} = \frac{q_0 l^2}{15.58} \quad (10.14)$$

The diagram is shown in Fig. 142. It is evident from formula (10.14) that the maximum bending moment differs slightly from the moment at the middle of the span, which is equal to  $\frac{q_0 l^2}{16}$ . In actual design calculations for a beam loaded by a triangular force, the maximum bending moment  $M_{\max}$  may always be replaced by the moment in the middle of the span equal to  $\frac{q_0 l^2}{16}$ ; the error will not be more than 2.6%.

Let us analyze the plotting of shearing-force and bending-moment diagrams for a simply supported hinged beam (Fig. 143) loaded by a continuous force whose intensity varies according to the following parabolic law:

$$q(x) = 4q_0 \left( \frac{x}{l} - \frac{x^2}{l^2} \right)$$

Due to symmetry, the support reactions are

$$A = B = \frac{\omega}{2}$$

Here  $\omega$  is the load area which is determined from condition (10.12):

$$\begin{aligned} \omega &= \int_0^l q(x) dx = \frac{4q_0}{l} \left[ \int_0^l x dx - \frac{1}{l} \int_0^l x^2 dx \right] \\ &= \frac{4q_0}{l} \left[ \frac{l^2}{2} - \frac{l^3}{3} \right] = \frac{2}{3} q_0 l \end{aligned} \quad (10.15)$$

Hence the support reactions are

$$A = B = \frac{q_0 l}{3}$$

Let us now write down the expression for  $Q(x)$  and  $M(x)$  in section  $1-1$  at a distance  $x_1$  from the left-hand support  $A$ . Denoting the load area of length  $x_1$  by  $\omega(x)$ , we get

(a) The shearing force  $Q(x) = A - \omega(x)$

The load area to the left of the section is

$$\begin{aligned} \omega(x) &= \int_0^{x_1} q(x) dx \\ &= \frac{4q_0}{l} \left[ \int_0^{x_1} x dx - \frac{1}{l} \int_0^{x_1} x^2 dx \right] \end{aligned}$$

or

$$\begin{aligned} \omega(x) &= \frac{4q_0}{l} \left[ \frac{x_1^2}{2} - \frac{x_1^3}{3l} \right] \\ &= \frac{2}{3} \frac{q_0 x_1^3}{l^2} (3l - 2x_1) \end{aligned}$$

Putting the values of  $A$  and  $\omega(x)$  in the expression for  $Q(x)$ , we get

$$Q(x) = \frac{q_0 l}{3} - \frac{2}{3} \frac{q_0 x_1^3}{l^2} (3l - 2x_1) \quad (10.16)$$

(b) We shall calculate the bending moment with the help of formula (10.4):

$$M(x) = \int Q(x) dx + M(0)$$

The constant of integration  $M(0) = 0$  because there is no concentrated moment at this end of the portion. Putting the expression for

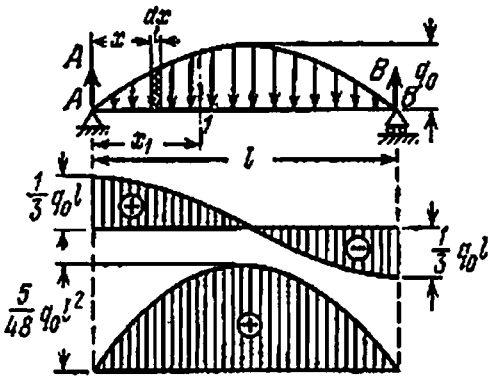


Fig. 143

$Q(x)$  under the integral sign, we obtain

$$\begin{aligned} M(x) &= \int_0^{x_1} \left[ \frac{q_0 l}{3} - \frac{2}{3} \frac{q_0 x^2}{l^2} (3l - 2x) \right] dx \\ &= \int_0^{x_1} \frac{q_0 l}{3} dx - \int_0^{x_1} \frac{2q_0 x^2}{l} dx + \int_0^{x_1} \frac{4q_0 x^3}{3l^2} dx \\ &= \frac{q_0 l}{3} x_1 - \frac{2q_0 x_1^3}{3l} + \frac{q_0 x_1^4}{3l^2} \end{aligned}$$

OR

$$M(x) = \frac{q_0 l}{3} x_1 - \frac{q_0 x_1^3}{3l^2} (2l - x) \quad (10.17)$$

It is evident from Eqs. (10.16) and (10.17) that the shearing force varies according to a cubical parabola, whereas the bending moment varies according to a fourth-degree parabola.

We shall take a few values of the variable  $x$  to find points for plotting these curves:

$$\begin{aligned} x=0, \quad Q(x) &= \frac{q_0 l}{3}, & M(x) &= 0 \\ x=\frac{l}{2}, \quad Q(x) &= \frac{q_0 l}{3} - \frac{2}{3} q_0 \frac{2l}{4} = 0, & M(x) &= \frac{q_0 l^2}{6} - \frac{q_0 l^2}{24l^2} \frac{3l}{2} = \frac{5}{48} q_0 l^2 \\ x=l, \quad Q(x) &= \frac{q_0 l}{3} - \frac{2}{3} q_0 l = -\frac{q_0 l}{3}, & M(x) &= \frac{q_0 l^2}{3} - \frac{q_0 l^2}{3} = 0 \end{aligned}$$

The corresponding shearing-force and bending-moment diagrams are shown in Fig. 143. The maximum values of  $Q$  and  $M$  are respectively equal to

$$Q_{\max} = \frac{q_0 l}{3} \quad \text{and} \quad M_{\max} = \frac{5}{48} q_0 l^2 \quad (10.18)$$

We shall now discuss the order of plotting  $Q$ - and  $M$ -diagrams for a two-span beam with an intermediate hinge; such beams are often employed in bridge design. The dimensions of the beam and the forces acting on it are shown in Fig. 144(a).

We must determine the reactions of the beam before plotting the diagrams. It is clear from Fig. 144(a) that the arrangement may have four support reactions:  $A$ ,  $H_A$ ,  $B$ , and  $D$ . However, we can write only three equations of equilibrium for the whole beam. The fourth equation is determined from the condition that hinge  $C$  (on account of its construction) cannot transmit bending moment, because it permits relative rotation of one part of the beam ( $AC$ ) about the other ( $CD$ ).

The last condition requires that the sum of moments of all forces acting either to the left or right of the hinge about point  $C$  should be zero. In other words, to maintain equilibrium the bending moment

in the hinge must be zero. This additional requirement makes the beam  $AD$  statically determinate.

First we shall determine  $H_A$ . By equating to zero the sum of projections of all the forces on the beam's axis we find that  $H_A=0$ .

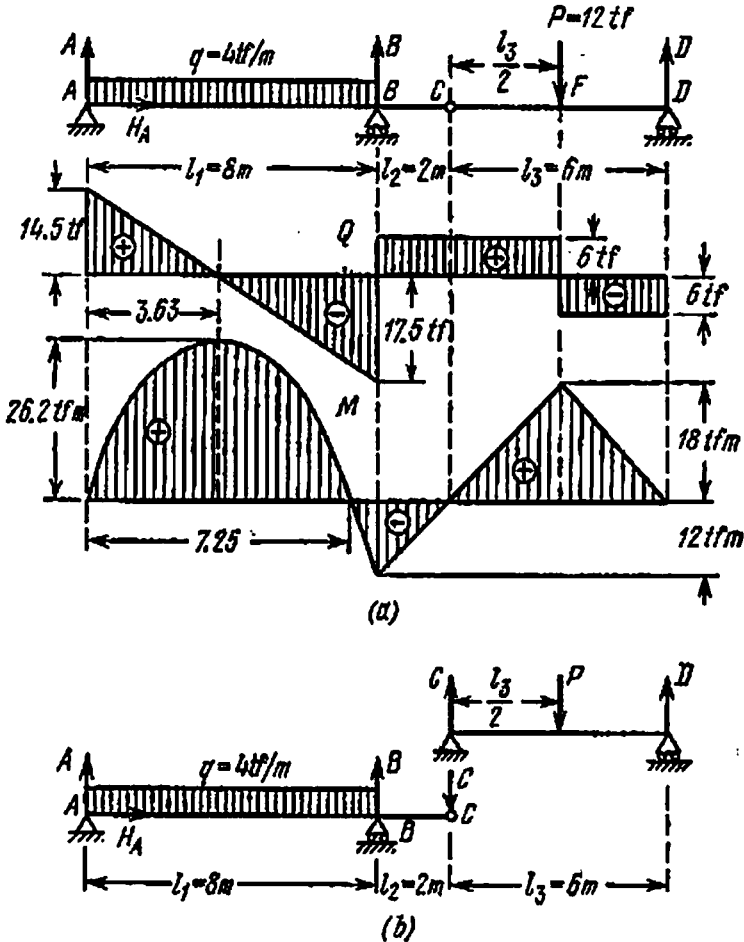


Fig. 144

Next we may write three equations for the moments as follows:

(1) by equating to zero the sum of moments of all the forces about point  $A$ ;

(2) by equating to zero the sum of moments of all the forces about point  $B$  or  $D$ ;

(3) by equating to zero the sum of moments of all the forces either to the left or right of hinge  $C$ , about point  $C$ .

By solving these three equations we can determine all the three unknown reactions  $A$ ,  $B$  and  $D$ . However, the reactions can be determined more easily by breaking the beam arrangement  $AD$  into simple beams. The suspended beam  $CD$  is supported by a hinge  $C$  at the end

of cantilever  $BC$  and by a movable hinge at point  $D$ . Therefore, we may consider the whole beam (Fig. 144(b)) as a combination of two beams. The suspended beam experiences reaction  $C$  through the hinge at the end of the cantilever and in its turn presses this end with the same force  $C$ .

By first analyzing the equilibrium of the suspended beam we find its reactions  $D$  and  $C$ , then by taking into account the already known force  $C$  acting at the end of the cantilever, we determine reactions  $A$  and  $B$ . In this example

$$C = D = \frac{P}{2} = 6 \text{ tf}, \quad A = \frac{ql_1}{2} - C \frac{l_2}{l_1} = \frac{4 \times 8}{2} - 6 \frac{2}{8} = 14.5 \text{ tf}$$

$$B = \frac{ql_1}{2} + C \frac{l_1 + l_2}{l_1} = \frac{4 \times 8}{2} + 6 \frac{10}{8} = 23.5 \text{ tf}$$

$$\text{Check: } \Sigma Y = A + B + D - ql_1 - P = 14.5 + 23.5 + 6 - 4 \times 8 - 12 = 0.$$

Having determined the reactions we again assume the beam to be a single unit with all forces and reactions and determine the moments and shearing forces as in the general case. We shall check the values by equating to zero the sum of moments about point  $C$ . It should be borne in mind that hinge  $C$  does not represent the separation point of sections of the diagrams if it is not acted upon by an external force. The bending-moment and shearing-force diagrams are shown in Fig. 144(a).

After determining the reactions it is more convenient to plot  $Q$ - and  $M$ -diagrams separately for each suspended beam and the main beam, laying the values of  $Q$  and  $M$  from a common  $x$ -axis.

### § 60. The Check of Proper Plotting of $Q$ - and $M$ -diagrams

The differential relations between the bending moment, shearing force and intensity of continuous load determine the relation between shearing-force and bending-moment diagrams for any load. This relation is of great practical importance in checking the correctness of the plotted curves. We give below some concluding remarks which may be helpful in plotting  $Q$ - and  $M$ -diagrams.

1. It has already been stated (§ 57) that the ordinate of the shearing-force diagram  $Q = \frac{dM}{dx}$  geometrically represents the slope of the tangent to the bending-moment diagram at the corresponding point. Identical geometrical relations exist between  $q$  and  $Q$  (Fig. 145).

2. If in a certain section

(a)  $Q > 0$ , i.e.  $\tan \alpha > 0$ , the moment increases;

(b)  $Q < 0$ , i.e.  $\tan \alpha < 0$ , the moment decreases;

- (c)  $Q$  passes through zero, changing its sign from plus to minus,  
 $M = M_{\max}$ ;  
 (d)  $Q = 0$ , i.e.  $\tan \alpha = 0$ ,  $M = \text{const.}$

3. If  $q = 0$ , i.e.  $\frac{dQ}{dx} = 0$ ,  $Q = \text{const.}$  Hence in portions free of continuous load, the shearing-force diagram is bounded by straight lines parallel to the  $x$ -axis; the bending-moment diagram is made up of inclined straight lines provided  $Q \neq 0$  (see item 2(d)). If  $q < 0$ , i.e.  $\tan \beta < 0$ , the shearing force decreases.

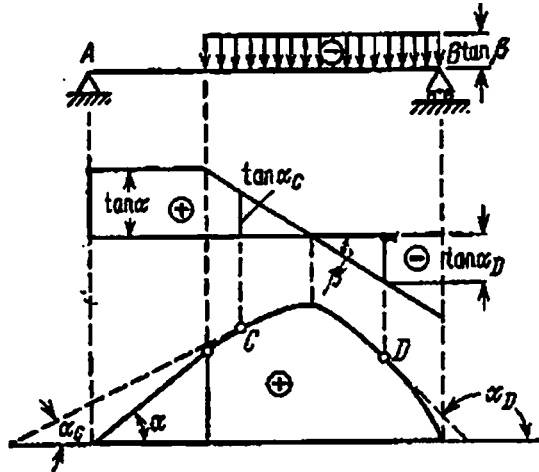


Fig. 145

4. Over portions of the beam loaded by uniformly distributed force, the bending-moment diagram is a parabola, whereas the shearing-force diagram is an inclined straight line. If the load is distributed non-uniformly, then the  $Q$ - and  $M$ -diagrams are represented by curves whose shape depend upon the type of loading.

5. In sections under concentrated force the shearing-force diagram undergoes a jump (equal to the force), and the bending-moment diagram experiences a sharp change in the angle between the adjacent regions (see, for example, section  $C$  in Fig. 137).

6. If the continuous load is directed downwards, i.e.  $\frac{d^2M}{dx^2} = q < 0$ , or, in other words, if the second derivative characterizing the curvature of the  $M$ -curve is negative, then the diagram is convex upwards. On the contrary, if  $q > 0$  (the load is directed upwards), the bending-moment diagram in the corresponding portion is convex downwards (Fig. 146).

7. In a hinged support the shearing force is equal to the reaction of the support, and if there is no external moment acting on it, the bending moment in the hinge is zero.

8. The bending moment on the free end of a cantilever is zero if the end is not acted upon by a concentrated force couple. In the ab-

sence of a concentrated force on the free end the shearing force  $Q$  is also zero.

9. At the fixed end,  $Q$  and  $M$  are equal to the reaction and moment of the support, respectively.

10. In sections where a force couple is acting, the bending-moment diagram undergoes a jump equal to the moment of this force couple. The shearing-force diagram however, remains unaffected.

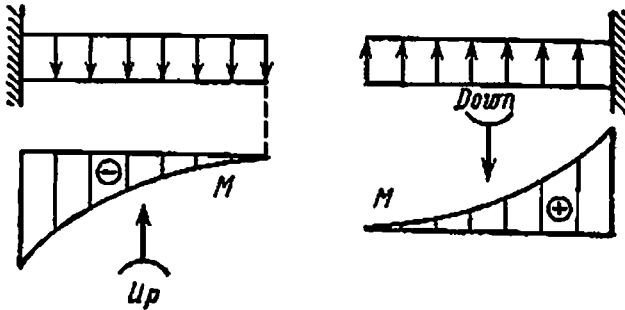


Fig. 146

The differential relations explained in § 57 and the remarks given above help not only in checking the correctness of the diagrams but will be used in future in plotting the diagrams too (Chapters 15, 16, etc.).

### § 61. Application of the Principle of Superposition of Forces in Plotting Shearing-force and Bending-moment Diagrams

Analyzing the expressions for  $Q$  and  $M$  obtained in the previous examples, we see that the external forces enter these expressions to the first power;  $M$  and  $Q$  are linearly dependent upon the load.

Analyzing, for example, equation for  $M(x)$  in the section of a cantilever (Fig. 140),

$$M(x) = Px - q \frac{x^2}{2}$$

we find that the ordinates of the bending moments in sections of this portion consist of two components,  $Px$  and  $-\frac{qx^2}{2}$ , the first component representing the bending moment in the particular section due to force  $P$ , whereas the second due to uniformly distributed load  $q$ .

We could have plotted the bending-moment diagrams for forces  $P$  and  $q$  separately, and then added their ordinates algebraically. This would be the application of the *method of superposition of forces*.

We shall illustrate with an example how to plot the total bending-moment diagram. For the beam shown in Fig. 147 we have already



plotted separately bending-moment diagrams under uniformly distributed load  $q$  ( $M_q$ ) and concentrated force  $P$  ( $M_p$ ). The absolute maximum value of the bending moments at the rigidly fixed end are

$$M_q = -\frac{ql^2}{2} \quad \text{and} \quad M_p = -Pl$$

To add the ordinates of two diagrams of similar sign, we place one above the other as shown in Fig. 148(a). The bending moment in an arbitrary section is the sum of moments:

$$M_q = -\frac{qx^2}{2}$$

and

$$M_p = -Px$$

The sign of  $M_p$  changes if force  $P$  is directed upwards. To add two diagrams having different signs, it is sufficient to superimpose one

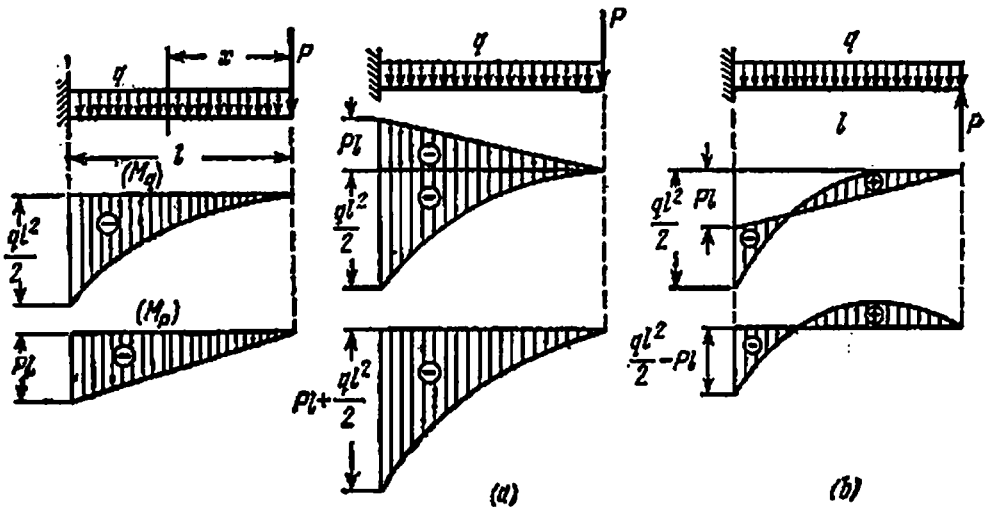


Fig. 147

Fig. 148

of them over the other (Fig. 148(b)).

Suppose that in absolute value  $\min M_q > \max M_p$ , i.e.

$$\left| \frac{ql^2}{2} \right| > |Pl|$$

Upon superposition of diagrams their ordinates get deducted automatically, and in this example we shall get a negative ordinate at the fixed end, the ordinates being positive over the span at a certain distance.

Obviously, in graphical summation both the diagrams must be drawn to the same scale. In an identical manner we can plot the shear-

ing-force diagram. The method of summation of diagrams is particularly useful in analyzing statically indeterminate solid beams (Chapter 19).

To obtain the diagram in the conventional form, we may lay off the summed ordinates from the horizontal axis (Fig. 148(a) and (b)).

## CHAPTER 11

### Determination of Normal Stresses in Bending and Strength of Beams

#### § 62. Experimental Investigation of the Working of Materials in Pure Bending

The bending-moment and shearing-force diagrams enable us to determine the internal forces in an arbitrary section of the beam; these forces are made up of normal and shearing stresses in the section as a result of bending. We shall discuss how to determine these stresses. It was earlier shown that shearing force in a section is the resultant of elementary shearing forces, and the bending moment, of the normal stresses which form force couples. If no shearing force  $Q$  acts over a certain length of the beam, i.e. the shearing stresses in sections within this length are absent, then these sections are acted upon only by normal stresses which are easier to compute in this case.

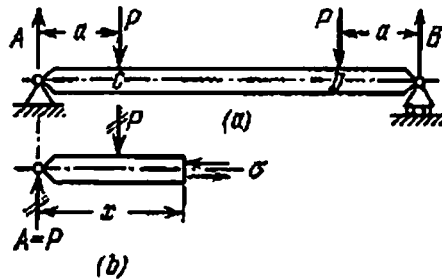


Fig. 149

The type of bending in which shearing force is zero in sections normal to the beam's axis is known as *pure bending*. Pure bending can be achieved in practice if the system of external forces acting on some portion of the beam can be reduced to force couples (see, for example, Fig. 130). Actually, however, pure bending is possible only in those cases when the dead weight of the beam is sufficiently small as compared to the external forces acting on it and may therefore be neglected.

As an example we shall consider the bending of a wagon axle (see § 55). The external forces acting on the axle (its weight is neglected) are depicted in Fig. 149. Keeping in mind that due to symmetry both

the support reactions are equal ( $A=B=P$ ), for an arbitrary section between points  $C$  and  $D$  we obtain

$$Q(x) = A - P = 0, \quad M(x) = Ax - P(x - a) = Pa = \text{const}$$

Thus, there is no shearing force in the middle portion  $CD$  of the axle, and  $M = \text{const}$  (recall that  $Q = \frac{dM}{dx}$ ); the beam experiences pure bending over the length  $CD$ .

Let us now return to finding normal stresses for this case. Let us take a section at a distance  $x$  from the left support  $A$  and consider the equilibrium conditions of the left cutoff portion (Fig. 149). This por-

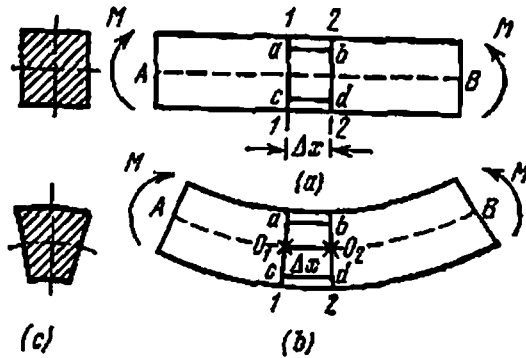


Fig. 150

tion is acted upon by a force couple with moment  $M = Pa$  and normal stresses in the section, which form force couples with a resulting moment  $M(x)$ . Our task is to find the magnitude of these stresses at every point of the cross section and determine their maximum value. However, the conditions of equilibrium between the external and internal forces expressed by the relationship  $M(x) = M$  are not sufficient for determining normal stresses  $\sigma$  because we know neither the magnitude of these stresses nor their distribution over the section. The problem is statically indeterminate, and for its solution we must study the elastic deformation of the beam on the basis of experimental investigations. Let us consider the results of experiments obtained from pure bending of a beam by moment  $M$  acting in its plane of symmetry (Fig. 150).

Lines  $1-1$  and  $2-2$  drawn on the beam surface perpendicular to its axis are traces of two adjacent cross sections located at a distance  $\Delta x$  from each other, whereas lines  $ab$  and  $cd$  joining them and parallel to the beam's axis represent longitudinal fibres of length  $\Delta x$  prior deformation (Fig. 150(a)).

Experiments reveal that after deformation (Fig. 150(b)):

(1) Lines  $1-1$  and  $2-2$  remain straight but turn with respect to one another through an angle  $\Delta\alpha$ . This leads us to the idea that the cor-

responding cross sections also remain planes but turn with respect to one another through angle  $\Delta\alpha$ .

(2) Lines  $ab$  and  $cd$  change their length: line  $ab$  gets shorter, whereas  $cd$  elongates leading to the conclusion that the upper fibres are subjected to compression and lower to tension.

(3) As shown in Fig. 150(c), the cross-sectional dimensions also change: in the upper part the width of the beam increases, which corresponds to axial compression, whereas in the lower part (stretched zone) it decreases.

As the deformation of the longitudinal fibres varies continuously over the height of the beam, there must be a layer at a certain height which does not change its length at all; this layer is called the *neutral layer* and serves as the interface between the compressed and stretched zones. In Fig. 150(b) the neutral layer is shown by dotted line; segment  $O_1O_2$  retains its initial length  $\Delta x$ .

The neutral layer is perpendicular to the plane of symmetry of the beam in which the external forces act and intersects each cross section of the beam along a straight line which is also perpendicular to the plane of action of the external forces. The line of intersection of the neutral layer with the plane of a cross section is known as the *neutral axis* of the section. The neutral layer is an aggregate of the neutral lines.

As the section is symmetrical with respect to the plane of application of the external forces, both halves of the beam width must deform symmetrically about this plane; this enables us to consider that longitudinal deformation of the fibres of an arbitrary layer parallel to the neutral one is independent of the location of the fibres along the beam width.

It has been experimentally established that deformation in the lateral direction is related to the deformation of longitudinal fibres by Poisson's ratio. This gives sufficient ground to presume that the longitudinal fibres do not press each other, and under pure bending experience only simple compression on the concave side and simple tension on the convex, i.e. on the other side of the neutral layer.

At the same time, lateral deformation is instrumental in somewhat distorting the beam section and making the neutral axis curved (Fig. 150(c)), which leads to additional deformation of the neutral layer making it doubly curved. However, as the elastic deformations are small these distortions are ignored: in each cross section of the beam the neutral axis is considered a straight line and the neutral layer, a cylindrical surface.

Since the section is symmetrical w.r.t. the plane of application of external forces, the beam axis also curves in the same plane in bending. Such bending in which after deformation the beam axis remains in the plane of application of external forces is known as *uni-planar bending*.

Experimental study of the bending of beams helps us to make a number of assumptions which have been used in deriving new conclusions:

1. In pure bending the cross sections which were planes prior deformation remain planes during deformation too (the hypothesis of plane sections).
2. Longitudinal fibres of the beam do not press on each other, and therefore due to normal stresses experience simple uniaxial tension or compression.
3. The deformation of fibres does not depend upon their position along the width of the section. Therefore, the normal stresses, though changing along the height of the section, remain constant along its width.

In addition to the assumptions made above, we shall introduce three limiting conditions:

1. The beam has at least one plane of symmetry, and all the external forces lie in this plane.
2. The beam material obeys Hooke's law, the modulus of elasticity being the same under tension as well as compression.
3. The relation between the beam's dimensions ensures that it works under pure bending without warping or twisting.

It is known from experience that beams with a small width easily lose their stability as far as the shape of the section is concerned (they warp). If in a beam of rectangular section the ratio of height to span is  $\frac{h}{l} > \frac{1}{5}$ , it works not as a beam but as a plate and it must be analyzed in a different manner. •

In general, assumptions made above are only approximately true. However, the theoretical error is so small (except in special cases) that it can be ignored.

### § 63. Determination of Normal Stresses in Bending. <sup>1</sup> Hooke's Law and Potential Energy of Bending

A. Let us consider a beam subjected to pure bending by a moment  $M$  (Fig. 151). Let us cut the beam in two parts by section  $1-1$ , and using the method of sections consider the equilibrium of one of the portions, say, the left, shown below in Fig. 151. For simplicity we consider a beam of rectangular cross section. As the curvature of the beam is practically negligible in comparison with its dimensions, the cutoff portion may be drawn in undeformed shape.

The line of intersection of the plane of symmetry of the beam with the plane of the section is taken as the  $z$ -axis (positive direction downwards); the neutral axis of the section has been taken as the  $y$ -axis, its location along the height of the beam being not yet known. The

$x$ -axis has been taken along the neutral layer perpendicular to the  $y$ - and  $z$ -axis.

Every point in the cross section is acted upon by a normal stress  $\sigma$ . Let us isolate an elementary area  $dA$  about an arbitrary point having coordinates  $y$  and  $z$ , and denote the force acting on it by  $dN = \sigma dA$ . The cutoff portion of the beam maintains its equilibrium under the action of external forces constituting a couple of moment  $M$  and

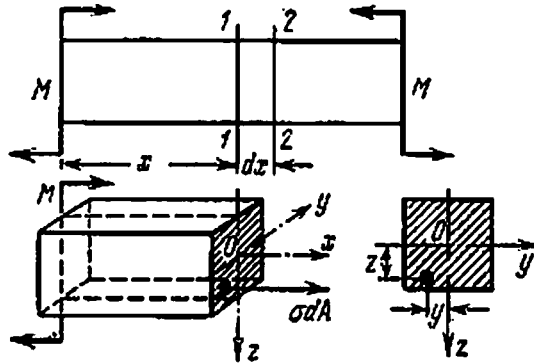


Fig. 151

the normal force  $dN$  which represents the influence of the removed portion of the beam. The beam will remain in equilibrium only if this system of forces satisfies the six static equations. Let us first write down the equations of projections on the three coordinate axes of  $x$ ,  $y$  and  $z$ .

As the projection of moment  $M$  on any axis is zero, these equations give us the condition that the sum of the projections of normal force  $dN$  on the beam's axis is zero. Replacing the summation over the whole area by integration, we get

$$\sum X = 0, \quad \int_A \sigma dA = 0 \quad (11.1)$$

Expressions  $\sum Y = 0$  and  $\sum Z = 0$  give identities of the type  $0 = 0$ , because the force  $dN = \sigma dA$  projects on these axes into a point.

Let us now write down the equations of moments about the axes  $Ox$ ,  $Oy$  and  $Oz$ . Let us note that moment  $M$  lies in the plane  $xOz$  and therefore does not give any moment about axes  $Ox$  and  $Oz$ .

Expression  $\sum M_x = 0$  gives an identity, because the force  $dN = \sigma dA$  is parallel to the  $x$ -axis:

$$\sum M_y = 0, \quad M - \sum dN z = 0 \quad \text{or} \quad M - \int_A \sigma z dA = 0$$

wherefrom

$$\int_A \sigma z dA = M \tag{11.2}$$

$$\sum M_x = 0, \quad \sum dN_y = 0 \quad \text{or} \quad \int_A \sigma y dA = 0 \tag{11.3}$$

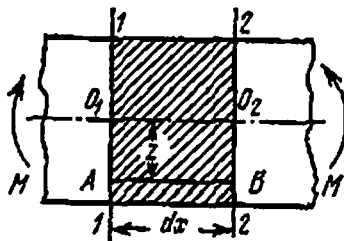
Thus, out of the six static equations we can use only three:

$$\sum X = 0 \quad \text{or} \quad \int_A \sigma dA = 0 \tag{11.1'}$$

$$\sum M_y = 0 \quad \text{or} \quad \int_A \sigma z dA = M \tag{11.2'}$$

$$\sum M_x = 0 \quad \text{or} \quad \int_A \sigma y dA = 0 \tag{11.3'}$$

However, the three static equations obtained above are not sufficient to determine the normal stresses, because  $\sigma$  varies with the distance  $z$  of area  $dA$  from the neutral axis according to a law which we yet do not know. The distance  $z$  is also unknown, because we do not know the location of the neutral axis  $Oy$ .



**B.** Let us isolate an element of length  $dx$  of the beam by two infinitely close sections 1-1 and 2-2 to study its deformation. The shape of the element before and after deformation is shown in Fig. 152.

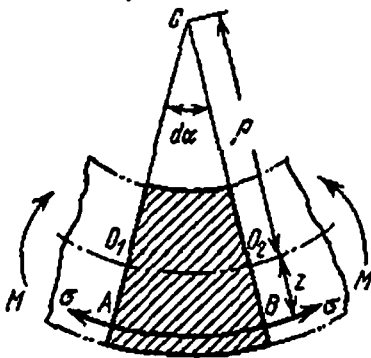


Fig. 152

For greater clarity the deformation of the element is shown in a highly magnified form. Both cross sections continue to remain planes but turn about their neutral axes (points  $O_1$  and  $O_2$  in the front view) to form an angle  $d\alpha$ . The neutral layer has been shown by a dotted line. Line  $O_1O_2$  of the neutral layer retains its initial length  $dx$  after deformation. All fibres above the neutral layer shorten, whereas those below it elongate.

We shall try to find the elongation of an arbitrary fibre  $AB$  at a distance  $z$  from the neutral layer and stretched by stress  $\sigma$ . The initial length of this layer is  $dx = O_1O_2 = \rho d\alpha$ . After deformation its length along the arc  $AB$  becomes  $AB = (\rho + z) d\alpha$ . The absolute elongation of the fibre is  $\Delta l = (\rho + z) d\alpha - \rho d\alpha = z d\alpha$ . Relative elongation is equal to

$$\epsilon = \frac{z d\alpha}{\rho d\alpha} = \frac{z}{\rho}$$

i.e. the elongation of fibres is directly proportional to their distance from the neutral layer.

Here  $\rho$  is the radius of curvature of the neutral layer, which may be considered constant for the isolated (infinitely small) element. Assuming that under bending the fibres do not press on each other and that each fibre experiences simple (uniaxial) tension or compression, we may make use of Hooke's law in determining the tensile stresses:

$$\sigma = E\varepsilon \quad \text{or} \quad \sigma = \frac{Ez}{\rho} \quad (11.4)$$

Equation (11.4) shows that the normal stresses in bending vary in direct proportion to distance  $z$  of the point of the section under consideration from the neutral layer. This means that stresses vary along the height of the beam linearly.

On the neutral axis  $z=0$  and  $\sigma=0$ . If we move into the zone of compression (above the neutral axis),  $\sigma$  along with  $z$  changes its sign to minus (compression) and continues to increase in absolute value as

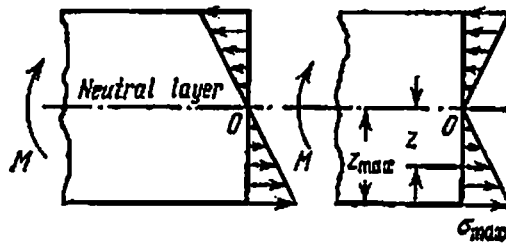


Fig. 153

we move away from the neutral axis. Hence the maximum stress occurs at the uppermost and lowermost layers of the section when  $z=z_{\max}$ . The distribution of stresses along the height is shown in Fig. 153.

Equation (11.4) only gives an idea about the nature of distribution of normal stresses over the section; it cannot be used for calculating the magnitude of the stresses because both  $\rho$  as well as  $z$  are not known since we do not know the location of the neutral layer in the height of the section.

C. To determine  $\sigma$  as a function of the bending moment, we shall simultaneously solve Eq. (11.4) obtained from deformation considerations and the static equations (11.1), (11.2), and (11.3).

Substituting the value of  $\sigma$  from expression (11.4) in Eq. (11.1), we get

$$\sum X = 0 \quad \text{or} \quad \int_A \frac{E}{\rho} z dA = 0$$



Since  $\frac{E}{\rho} = \text{const} \neq 0$ ,

$$\int_A z dA = 0 \quad (11.5)$$

This integral represents the *static moment* of the area of section about the neutral axis  $Oy$ , which becomes zero only about the central axis. Therefore the neutral axis must pass through the centre of gravity of the section. As the centre of gravity also lies on the axis of symmetry  $Oz$ , the point of intersection of these two axes  $O$  represents the centre of gravity of the section, and  $Ox$  represents the axis of the beam.

Thus, we have completely determined the location of the neutral layer and neutral axis. The centres of gravity of all sections of the beam are located on the neutral layer.

Now let us put the same expression (11.4) into Eq. (11.3):

$$\sum M_x = 0, \quad \int_A \frac{E}{\rho} zy dA = 0, \quad \text{or} \quad \frac{E}{\rho} \int_A zy dA = 0$$

wherefrom it ensues that

$$\int_A zy dA = 0 \quad (11.6)$$

The above integral, which is the sum of the products of elementary areas by their distances from the coordinate axes  $Oy$  and  $Oz$  is called the *product of inertia* of the section with respect to the axes  $Oy$  and  $Oz$ . The product of inertia of the section may be positive or negative; consequently it may also vanish, because the coordinates of elementary areas may have different signs.

According to expression (11.6), the product of inertia of the section, which is generally denoted by

$$J_{zy} = \int_A zy dA$$

should in this case be zero.

As the section is symmetrical about axis  $Oz$ , for each elementary area  $dA$  with coordinates  $(z, y)$  to the left of the  $z$ -axis we can find a similar, symmetrically located elementary area to the right of the  $z$ -axis. The  $z$ -coordinates of these areas will be the same by the magnitude and sign, while the  $y$ -coordinates will be equal in magnitude but will have opposite signs. Therefore the integral

$$\int_A zy dA$$

will consist of two integrals equal in magnitude but of opposite signs. Thus, for symmetrical sections this integral is always zero, and Eq.

(11.6) changes into an identity. In our case the condition  $J_{xy}=0$  is satisfied. Bending will be uni-planar only under the condition that the product of inertia of the section is zero about axes one of which is in the plane of application of the external forces; then all subsequent conclusions will be valid.

Finally, let us study Eq. (11.2); substituting expression (11.4) into it, we get

$$\sum M_v = 0, \quad \int_A \frac{E}{\rho} z^2 dA = M \quad \text{or} \quad \frac{E}{\rho} \int_A z^2 dA = M$$

Let us introduce the notation

$$J_y = \int_A z^2 dA \quad (11.7)$$

This integral, which is the sum of the products of elementary areas by the square of their distance from the axis, is called the *axial or equatorial moment of inertia* of the area about the  $y$ -axis and is denoted by  $J_y$ . As the  $y$ -axis is the neutral axis,  $J_y$  is the moment of inertia of the area of the section about the neutral axis\*. From the transformed expression of equation (11.2), we get

$$\frac{EJ}{\rho} = M \quad \text{or} \quad \frac{E}{\rho} = \frac{M}{J} \quad (11.8)$$

Putting this value of  $\frac{E}{\rho}$  in Eq. (11.4), we get

$$\sigma = \frac{Mz}{J} \quad (11.9)$$

Hence, the normal stresses in any point of the section are directly proportional to the bending moment and its distance from the neutral axis, and inversely proportional to the moment of inertia of the section about the neutral axis.

The neutral axis passes through the centre of gravity of the section and is perpendicular to the plane of action of the external forces.

It is obvious from formula (11.7) that the moment of inertia is measured in units of length to the fourth power and depends upon the shape and size of the section. Methods of determining the moment of inertia for various sections will be given below.

Let us modify formula (11.8) to understand the physical meaning of this quantity:

$$\frac{1}{\rho} = \frac{M}{EJ} \quad (11.10)$$

---

\* In future, when denoting the moment of inertia about the neutral  $y$ -axis, we shall often drop the index  $y$  and denote it in short by  $J$  instead of  $J_y$ .

It is clear from this formula that the greater the moment of inertia  $J$  of the section for a given bending moment, the greater will be the radius of curvature of the neutral layer and, consequently, of the beam's axis, i.e. the less will be the bending of the beam.

The value of the moment of inertia characterizes the ability of beam to resist bending depending upon the shape and dimensions of its cross-sectional area. The modulus of elasticity  $E$  also characterizes the ability of the beam to resist bending depending upon the material of the beam. The product  $EJ$  is called the *rigidity of the beam under bending*. The greater the rigidity, the less will be the bending of the beam with a given bending moment.

D. The relative rotation of the sections is connected with the bending of the beam's axis. As is clear from the drawing (Fig. 152), the length of segment  $O_1O_2=dx$  is equal to  $\rho d\alpha$ . Herefrom the angle of rotation between two adjacent sections may be written as

$$d\alpha = \frac{dx}{\rho}$$

Replacing  $\frac{1}{\rho}$  by its value  $\frac{M}{EJ}$ , we get

$$d\alpha = \frac{M dx}{EJ} \quad (11.11)$$

i.e. the deformation and displacements in bending—the angle of turning  $d\alpha$  and the curvature of the beam  $\frac{1}{\rho}$ —are directly proportional to the bending moment and inversely proportional to the rigidity of the beam.

Repeating the reasoning employed in § 52, we can easily calculate the *potential energy* accumulated by the beam during bending. If we consider the bending of an infinitely small segment of the beam of length  $dx$ , we can calculate the work done by the bending moment over the  $d\alpha$  as follows:

$$dW = \frac{1}{2} M d\alpha$$

Putting the value of  $d\alpha$  from Eq. (11.11), we get

$$dU = dW = \frac{1}{2} \frac{M^2 dx}{EJ}$$

Integrating over the whole length of the beam, we get

$$U = \int_0^l \frac{M^2 dx}{2EJ} \quad (11.12)$$

In pure bending of a beam ( $M = \text{const}$ ) with a constant cross-sectional area over the whole length ( $EJ = \text{const}$ ), the potential energy may be expressed as

$$U = \frac{M^2 l}{2EJ} \quad (11.12')$$

If bending moment along the beam's length is expressed in terms of different functions of  $x$  (for different portions), then integral (11.12) breaks up into a sum of integrals (each within the limits of the corresponding portion), and the expression for potential energy of bending becomes

$$U = \sum \int \frac{M^2 dx}{2EJ} \quad (11.12'')$$

The potential energy of deformation of the beam on account of shear (§ 36) caused by shearing forces  $Q$  is usually neglected as it is relatively small (for details, see Chapter 18).

#### § 64. Application of the Results Derived Above In Checking the Strength of Beams

Formula (11.9) solves the question about the magnitude and distribution of normal stresses over the section. It has been derived for pure bending, when the sections remain planes.

Experiments show that when  $Q$  is not zero, the sections not only turn but also slightly warp under the action of shearing stresses. This warping, however, does not alter the distribution of stresses in fibres enclosed between the two adjacent sections. Therefore, formula (11.9) may be used even when  $Q$  is not zero.

It should be noted here that as yet we can use this formula only if the sections of the beam have an axis of symmetry, and the external forces act in the symmetry plane.

The neutral axis of each section, from which  $z$  is measured, passes through its centre of gravity perpendicular to the axis of symmetry.

Figure 154 shows examples of the distribution of stresses for beams of various sections—rectangular, T-shaped, triangular. The normal stresses are the same in all points located at equal distances from the neutral axis. We get compressive stresses to one side of the neutral axis, and tensile stresses to the other. The maximum stresses occur in points which are farther from the neutral axis. For the accepted convention of signs of  $M$  and  $z$ , formula (11.9) automatically gives the proper sign of  $\sigma$ , plus for tensile stresses and minus for compressive stresses.

If the bending moment is positive, the beam bends with its convexity downwards, the upper fibres are compressed ( $z < 0$ ), whereas the lower fibres are stretched. The reverse picture occurs if the bend-

ing moment is negative. Therefore, in selecting the sign of normal stresses while solving practical problems, we may follow the following rules: if the point of the section under consideration is located in the zone of stretching,  $\sigma$  should be taken with a plus sign; if the point is located in the zone of compression,  $\sigma$  should be taken with a minus sign. Obviously, in this case the absolute values of  $M$  and  $z$  should be used in formula (11.9).

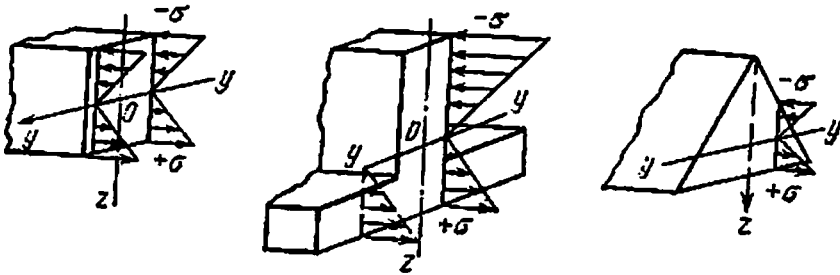


Fig. 154

To check the strength of a material w.r.t. normal stresses, it is essential to find the maximally stretched or compressed areas. This can be achieved by applying formula (11.9) to the critical section, i.e. using  $M_{\max}$  instead of  $M$  and instead of  $z$  put  $z_{\max}$ , the distance of the farthest point from the neutral axis. Then we get the following formula for the maximum normal stress:

$$\sigma_{\max} = \frac{M_{\max} z_{\max}}{J}$$

Usually, this formula is transformed by dividing both the numerator and the denominator by  $z_{\max}$ :

$$\sigma_{\max} = \frac{M_{\max}}{\frac{J}{z_{\max}}}$$

Quantity  $J/z_{\max}$  is called the axial section modulus and is denoted by the letter  $W$ . As  $J$  is measured in units of length to the fourth power,  $W$  is measured in units of length to the third power, e.g.  $\text{cm}^3$ . Hence

$$\sigma_{\max} = \frac{M_{\max}}{W} \quad (11.13)$$

where

$$W = \frac{J}{z_{\max}} \quad (11.14)$$

If the section is symmetrical about the neutral axis, for example, a rectangular section, the outer stretched and compressed fibres are

located at equal distance from the neutral axis, and such a section has a single definite value of the section modulus about the  $y$ -axis. Thus, if we consider a rectangular section of height  $h$  (Fig. 155(a)), then

$$z_{\max} = \frac{h}{2} \quad \text{and} \quad W = \frac{J}{\frac{h}{2}}$$

If the section is not symmetrical about the neutral axis, for example, a T-shaped section, we get two values of the section modulus: one for layer A (Fig. 155(b)),  $W_1 = \frac{J}{h_1}$ , and the other for layer B,  $W_2 = \frac{J}{h_2}$ .

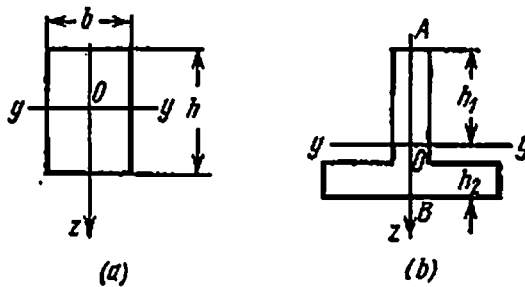


Fig. 155

Now in formula (11.13) we should introduce:  $W_1$  when calculating stresses in point A and  $W_2$  when calculating stresses in point B.

Let us write down the strength condition for tensile or compressive stresses. The condition reflects the idea that the maximum stress should not exceed the permissible:

$$\sigma_{\max} = \frac{M_{\max}}{W} \leq [\sigma] \quad (11.15)$$

From this condition we find that

$$W \geq \frac{M_{\max}}{[\sigma]} \quad (11.16)$$

i.e. the section modulus determined from strength considerations should be greater than or equal to the maximum bending moment divided by the permissible stress.

Since  $W$  depends upon the shape and size of the beam section, by selecting a particular shape (rectangular, T-shape, I-shape) we can find the dimensions of the beam such that its section modulus equals the one obtained from formula (11.16). We shall show below how this

can be done in practice. The values of  $W$  and  $J$  for rolled sections are given in specification tables (see Appendix).

We must differentiate between the following two cases when using formulas (11.15) and (11.16).

The first case is more common in bending, when the material shows equal resistance to tension and compression; in this case the permissible stress is the same for both deformations:

$$[\sigma_t] = [\sigma_c] = [\sigma]$$

In the case of a symmetrical section it becomes irrelevant whether we check the strength of the stretched or compressed fibres, because for both of them the section modulus  $W$  and the maximum actual stress have the same value. In the case of an unsymmetrical section, in formulas (11.15) and (11.16)  $W$  should be replaced either by  $W_1$  or by  $W_2$ , whichever is less; it should correspond to the farthest fibre.

The second case deals with beams whose material has different resistance to tension and compression. In this case we must write two strength conditions instead of one—one for the stretched fibres and the other for compressed:

$$\sigma_t = + \frac{M_{\max}}{W_1} \leq [\sigma_t], \quad \sigma_c = - \frac{M_{\max}}{W_2} \leq [\sigma_c] \quad (11.17)$$

Depending upon whether the material has better resistance under tension or compression, i.e. which of  $[\sigma_t]$  or  $[\sigma_c]$  is greater, we have to design the section by selecting its shape and size such that  $W_1$  and  $W_2$  satisfy the strength condition.

The physical nature of section modulus is clear from formula (11.13): the greater the section modulus  $W$ , the greater is the bending moment to which the beam can be subjected without danger of failure. Thus, section modulus characterizes the effect of shape and size of the selected section on the strength of the beam when the stresses do not exceed the limit of proportionality.

Formulas (11.13) and (11.17) cease to be valid for stresses exceeding the limit of proportionality of the material.

Formulas (11.15) and (11.17) enable us to check the strength of a given section (when the value of section modulus  $W$  is known). If the beam's material has been selected and its permissible stress is known, then with the help of formula (11.16) we can compute the necessary value of section modulus, provided the maximum bending moment  $M_{\max}$  is preliminarily calculated. Then, depending upon the beam's profile, i.e. the shape of the section, the required cross-sectional dimensions can be determined.

It was shown earlier that for this we must find the relation between the cross-sectional dimensions and the value of the section modulus. In § 73 we shall elaborate on this.

## CHAPTER 12

## Determination of Moments of Inertia of Plane Figures

### § 65. Determination of Moments of Inertia and Section Moduli for Simple Sections

While deriving the expression for normal stresses (§ 63) we had obtained expression (11.7) of the type

$$J_y = \int_A z^2 dA$$

where  $z$  is the distance of any elementary area from the central  $y$ -axis. This integral, which covers the whole area of the cross section, was called the moment of inertia of the area about the neutral axis. The ability of a beam section to resist deformation in bending depends upon the value of moment of inertia (11.10).

Apart from this, the strength condition in bending (§ 64) includes the expression for section modulus (11.14):

$$W_y = \frac{J_y}{z_{\max}}$$

It ensues from the above that we must learn to calculate the moment of inertia and section modulus for cross sections of any shape to ensure strength and rigidity of the beam. Let us start with the simplest beam section, a rectangle of width  $b$  and height  $h$  (Fig. 156). Draw axes of symmetry  $Oz$  and  $Oy$  through its centre of gravity  $O$ . If the external forces acting on the beam lie in plane  $xOz$ , then  $Oy$  is the neutral axis (axis  $Ox$  is directed along the beam). Let us first find the moment of inertia about this axis, and the section modulus of the rectangle.

Elementary areas  $dA$  into which the whole area of the section should be divided will be taken as narrow rectangles of width  $b$  and height  $dz$  (Fig. 156). Then

$$dA = b dz$$

and integral  $J_y$

$$J_y = \int_A bz^2 dz$$

If we take the integral over the total area of the rectangular section,  $z$  varies from  $-\frac{h}{2}$  to  $+\frac{h}{2}$ . Therefore

$$J_y = \int_{-h/2}^{+h/2} bz^2 dz = b \left[ \frac{z^3}{3} \right]_{-h/2}^{+h/2} = \frac{bh^3}{12} \quad (12.1)$$



We get the section modulus about the neutral axis  $Oy$  by dividing  $J_y$  by  $z_{\max} = \frac{h}{2}$ :

$$W = \frac{J_y}{z_{\max}} = \frac{bh^3/12}{h/2} = \frac{bh^2}{6} \quad (12.2)$$

If we have to calculate the moment of inertia and section modulus of the rectangular section about the axis  $Oz$ , then all that is required is to interchange  $b$  and  $h$  in the above formulas:

$$J_z = \frac{hb^3}{12}$$

and

$$W_z = \frac{hb^2}{6} \quad (12.3)$$

Let us note that the sum of the products  $z^2 dA$  does not change if we displace all the strips  $dA = b dz$  (Fig. 156) parallel to themselves in such a way that they lie within the parallelogram  $ABCD$  (Fig. 157).

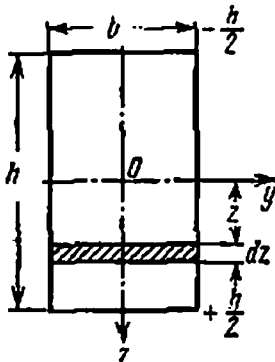


Fig. 156

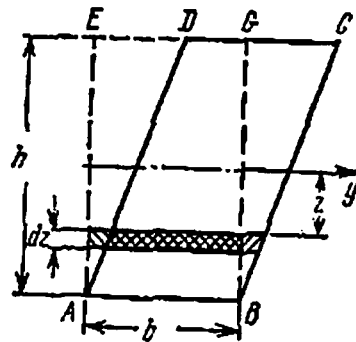


Fig. 157

Hence the moment of inertia of the parallelogram  $ABCD$  about the  $y$ -axis is equal to the moment of inertia of an equivalent rectangle  $ABGE$ :

$$J_y = \frac{bh^3}{12} \quad (12.1)$$

As the moment of inertia of an area is an integral of the type  $J_y = \int_A z^2 dA$ , we can immediately determine the moment of inertia of a rectangular box section (Fig. 158) with the help of formula (12.1):

$$J_y = \frac{BH^3}{12} - \frac{bh^3}{12} = \frac{1}{12} (BH^3 - bh^3) \quad (12.1')$$

The section modulus is

$$W_u = \frac{J_u}{z_{\max}} = \frac{BH^3 - bh^3}{12H/2} = \frac{BH^3 - bh^3}{6H} \quad (12.2')$$

Note that the section modulus cannot be calculated in the form of difference  $W = W_1 - W_2$  or  $W = BH^2/6 - bh^2/6$ , because this runs counter to the very concept of section modulus as the ratio  $J_u/z_{\max}$ .

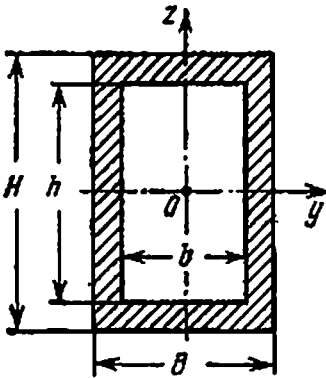


Fig. 158

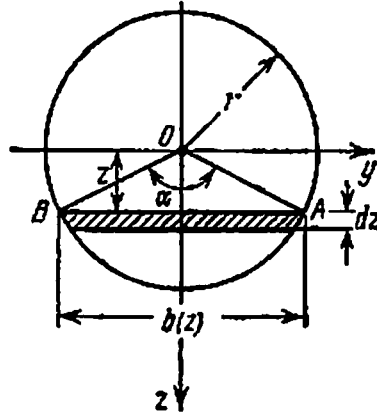


Fig. 159

While determining the *moment of inertia of a circle of radius r* (Fig. 159) we similarly divide its total area into elementary strips of thickness  $dz$  along the axis  $Oz$ ; the width of the strips  $b = b(z)$  also varies along the height of the section. The elementary area is

$$dA = b(z) dz$$

The moment of inertia is

$$J = \int_A z^2 b(z) dz$$

As the upper and lower halves of the section are identical, it is sufficient to calculate the moment of inertia for one half and double the result. The limits in which  $z$  varies are from 0 to  $r$ :

$$J = 2 \int_0^r z^2 b(z) dz$$

We introduce now a new variable of integration, angle  $\alpha$  (Fig. 159):

$$z = r \cos \frac{\alpha}{2}, \quad dz = -\frac{1}{2} r \sin \frac{\alpha}{2} d\alpha, \quad b(z) = 2r \sin \frac{\alpha}{2}$$

The limits of integration are  $\alpha=\pi$  at  $z=0$  and  $\alpha=0$  at  $z=r$ , therefore

$$J = -2 \int_{\pi}^0 2r^4 \cos^2 \frac{\alpha}{2} \sin^3 \frac{\alpha}{2} \frac{1}{2} d\alpha = \frac{r^4}{2} \int_0^{\pi} \sin^3 \alpha d\alpha \frac{\pi r^4}{4} \quad (12.4)$$

and

$$W = \frac{J}{z_{\max}} = \frac{J}{r} = \frac{\pi r^3}{4} \quad (12.5)$$

For a circle any axis passing through the centre of gravity is the axis of symmetry. Therefore formulas (12.4) and (12.5) are valid for all such axes.

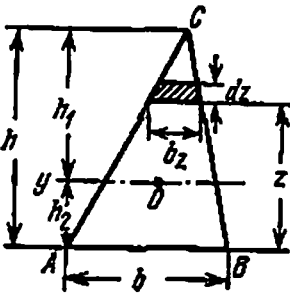


Fig. 160

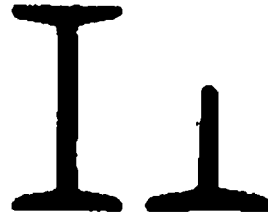


Fig. 161

Substituting  $r = \frac{d}{2}$ , we shall now express  $J$  and  $W$  through the circle's diameter:

$$J = \frac{\pi d^4}{64} \quad (12.4')$$

$$W = \frac{\pi d^3}{32} \approx 0.1d^3 \quad (12.5')$$

The moment of inertia of a triangle (Fig. 160) about  $AB$  is:

$$J_{AB} = \int_A^h z^2 b_z dz, \quad b_z = b \frac{h-z}{h} = b \left(1 - \frac{z}{h}\right)$$

$$J_{AB} = \int_0^h b z^2 \left(1 - \frac{z}{h}\right) dz = \frac{bh^3}{3} - \frac{bh^3}{4} = \frac{bh^3}{12}$$

Later (§§ 66-68) we shall explain how to calculate the moment of inertia of a section of any complex shape about an arbitrary axis.

The symmetrical sections which we generally come across in practice are: for wood—rectangular and circular, for metals—I-shaped and T-shaped (Fig. 161). For rolled sections we may use the GOST

tables \* (specifications), which contain the dimensions and the values of  $J$  and  $W$  for the sections manufactured at the rolling plants. These tables are given in Appendix.

Generally, metal beams have complex cross sections, because a more economic exploitation of the metal is possible in these sections as compared to, say, rectangular or circular sections.

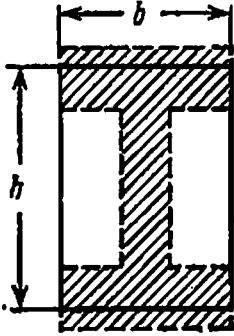


Fig. 162

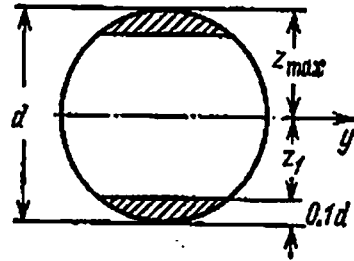


Fig. 163

We saw in § 48 that the shafts are made hollow to remove the portion of material that works under lower loading. In bending beams the material near the neutral axis experiences very small normal stresses (formula (11.9)) and is consequently not utilized fully. It is therefore more expedient to modify the rectangular section by removing the metal near the neutral axis and utilizing a part of this metal in the upper and lower zones of the beam, which work under more severe conditions, and saving the rest of it. Thus, from a rectangular section we obtain an I-shaped section (Fig. 162), which has the same strength but is lighter. The I-sections should preferably be used for materials which have equal resistance to tension and compression (in the majority of the metals).

The T-shaped sections are used in the cases when this is dictated by design considerations and when the materials, for example, cast iron and concrete, greatly differ in resistance to tension and compression. The latter condition requires that the stresses should be different in the outer fibres.

It ensues from the above discussion that the most economic design of the section should endeavour to obtain the maximum moment of inertia and section modulus for the fixed area  $A$ . In this design the greater part of the material will be located farther from the neutral axis.

However, in some sections the section modulus may be increased not by adding, but, on the contrary, by cutting off a part of the sec-

\* GOST stands for All-Union State Standard [in the USSR].

tion which is farthest from the neutral axis. If we cut off the hatched segments of the circular section (Fig. 163), its section modulus somewhat increases, because the decrease in the moment of inertia is less than that of distance  $z_{max}$  from the outer fibres.

The most effective section in bending will be that for which the ratio  $W/A$  of section modulus to the cross-sectional area is maximum. It is more convenient to assess the effectiveness of section by the dimensionless coefficient  $\alpha = W/(Ah)$ , where  $h$  is the height of the section. Table 11 contains the values of coefficient  $\alpha$  for a few sections. We see from the table that  $\alpha$  is maximum for an I-section.

Table 11

Coefficients of Profile Effectiveness

Shape of section	Coefficient $\alpha$	Shape of section	Coefficient $\alpha$
I-section (depending upon the profile No)	0.31-0.34	Rectangle	0.167
Channel section (depending upon the profile No)	0.29-0.31	Circle	0.125
T-section	0.085	Triangle	0.083
		Hollow circular section (when $r/R=0.9$ )	0.226

§ 66. General Method of Calculating the Moments of Inertia of Complex Sections

While checking the strength of elements of structures we often come across sections of complex shape for which the simple method used for calculating the moment of inertia of sections like a rectangle or circle, discussed in § 65, does not hold.

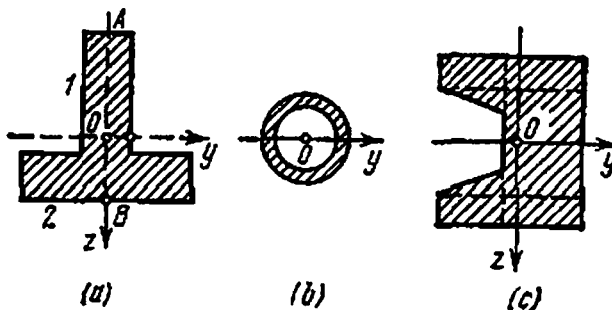


Fig. 164

Such a section may be, for example, a T-shaped section (Fig. 164(a)), a pipe section working under bending load (in aviation design) (Fig. 164(b)), a ring cross section of the neck of a shaft or a more com-

plex section (Fig. 164(c)). All these sections may be divided into simple shapes such as rectangles, triangles, circles. It can be shown that the moment of inertia of a complex section is the sum of the moments of inertia of the parts into which it is divided.

Let us take (Fig. 165) an arbitrary figure representing the cross section of a beam; the  $y$ -axis is drawn in the plane of the section. The moment of inertia of this figure about the  $y$ -axis is (11.7)

$$J_y = \int_A z^2 dA$$

where  $z$  is the distance of elementary areas  $dA$  from the  $y$ -axis.

Let us divide the area of the figure into four parts:  $A_1$ ,  $A_2$ ,  $A_3$ , and  $A_4$ . Now when calculating the moment of inertia according to formula (11.7), the terms under the integral sign should be grouped in a way such that we can carry out integration of the elementary areas separately for each portion and then add the results. The value of the integral will remain unchanged after this operation.

The integral will break into four integrals each of which covers one of the areas  $A_1$ ,  $A_2$ ,  $A_3$  or  $A_4$ :

$$J_y = \int_A z^2 dA = \int_{A_1} z^2 dA + \int_{A_2} z^2 dA + \int_{A_3} z^2 dA + \int_{A_4} z^2 dA$$

Each of these integrals represents the moment of inertia of the corresponding portion about axis  $Oy$ ; therefore

$$J_y = J_y^I + J_y^{II} + J_y^{III} + J_y^{IV} \tag{12.6}$$

where  $J_y^I$  is the moment of inertia of area  $A_1$  about the  $y$ -axis,  $J_y^{II}$  is the moment of inertia of area  $A_2$  about the same axis, and so on.

The result obtained above may be formulated in the following manner: the moment of inertia of a complex figure is equal to the sum of the moments of inertia of parts comprising it. Therefore, to calculate, for example, the moment of inertia of the section shown in Fig. 164(c) about axis  $Oy$ , we must calculate the moments of inertia of appropriate triangles and rectangles about the same axis and add the results. We must know how to calculate the moment of inertia of an arbitrary figure about an arbitrary axis lying in its plane.

The solution of this problem forms the contents of this chapter.

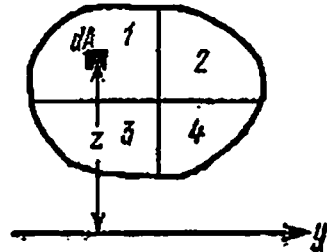


Fig. 165

### § 67. Relation Between Moments of Inertia About Two Parallel Axes One of Which Is the Central Axis

The problem of obtaining the simplest possible formulas for computing the moment of inertia of any figure about an arbitrary axis can be solved in a number of ways. If we take a number of axes parallel to one another, then the moment of inertia of the figure about any of these axes can be calculated if we know the moment of inertia of the figure about the axis passing through its centre of gravity and parallel to the selected axes.

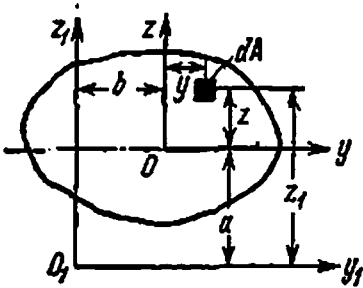


Fig. 166

We shall call the axes passing through the centre of gravity the *central axes*. Let us take (Fig. 166) an arbitrary figure. Draw the central axis  $Oy$  and denote by  $J_y$  the moment of inertia of the figure about this axis. In the plane of the figure draw axis  $O_1y_1$  parallel to the  $y$ -axis and located at a distance  $a$  from it. We shall try to establish

the relation between  $J_y$  and  $J'_{y'}$ , the moment of inertia about the  $y_1$ -axis. For this we shall have to write the expressions for  $J_y$  and  $J'_{y'}$ . Break the figure into elementary areas  $dA$ , and denote by  $z$  and  $z_1$  the distances of points lying on the elementary area from axes  $Oy$  and  $O_1y_1$ , respectively. We find that

$$J_y = \int_A z^2 dA \quad \text{and} \quad J'_{y'} = \int_A z_1^2 dA$$

But it is evident from the drawing that

$$z_1 = z + a$$

Therefore

$$\begin{aligned} J'_{y'} &= \int_A (z + a)^2 dA = \int_A (z^2 + 2az + a^2) dA \\ &= \int_A z^2 dA + 2a \int_A z dA + a^2 \int_A dA \end{aligned}$$

The first of the three integrals represents the moment of inertia about the central axis  $Oy$ . The second integral represents the static moment about the same axis. It is equal to zero, because the  $y$ -axis passes through the centre of gravity of the figure. Finally, the third

integral represents the area of the figure. Therefore

$$J'_y = J_y + a^2 A \quad (12.7)$$

i.e. the moment of inertia about an arbitrary axis is equal to the moment of inertia about the central axis parallel to the arbitrary axis plus the product of the area of the figure by the square of the distance between the axes.

Hence, our problem reduces to determining the central moments of inertia. Knowing them we can calculate the moment of inertia about any other axis with the help of formula (12.7). It is evident from formula (12.7) that the *central moment of inertia* is the minimum of the moments about parallel axes, and it may be expressed as

$$J_y = J'_y - a^2 A \quad (12.7')$$

We can similarly determine the product of inertia  $J'_{yz}$  of the section about axes  $O_1y_1$  and  $O_1z_1$  parallel to the central axes, if  $J_{yz} = \int_A yz \, dA$  is known (Fig. 166). From the definition

$$J'_{yz} = \int_A y_1 z_1 \, dA$$

where  $y_1 = y + b$ ,  $z_1 = z + a$ ; therefore

$$\begin{aligned} J'_{yz} &= \int_A (y + b)(z + a) \, dA \\ &= \int_A yz \, dA + ab \int_A dA + a \int_A y \, dA + b \int_A z \, dA \end{aligned}$$

The last two integrals are equal to zero because they represent the static moments of the area about the central axes,  $Oy$  and  $Oz$ . Therefore

$$J'_{yz} = J_{yz} + abA \quad (12.8)$$

The product of inertia of a section about two mutually perpendicular axes parallel to the central axes is equal to the product of inertia of the section about the central axes plus the product of the area of the figure by the coordinates of its centre of gravity w.r.t. the new axes.

### § 68. Relation Between the Moments of Inertia Under Rotation of Axes

We can draw any number of central axes. But the question is: Can we express the moment of inertia about an arbitrary central axis in terms of the moment of inertia about one or two definite axes?



We shall see how the moment of inertia about two mutually perpendicular axes changes when the axes rotate through an angle  $\alpha$ .

Let us take an arbitrary figure and draw two mutually perpendicular axes  $Oy$  and  $Oz$  through its centre of gravity  $O$  (Fig. 167). Suppose that the moments of inertia about these axes,  $J_y$  and  $J_z$ , and the product of inertia of the section,  $J_{yz}$ , are known. Let us draw the second system of coordinate axes  $Oy_1$  and  $Oz_1$  at an angle  $\alpha$  to the first. This angle will be considered positive if the rotation of the axes about point  $O$  is anticlockwise. The origin of coordinates  $O$  is retained. Let us express the moments about the second system of coordinate axes,  $J'_y$  and  $J'_z$ , through the known moments  $J_y$  and  $J_z$ .

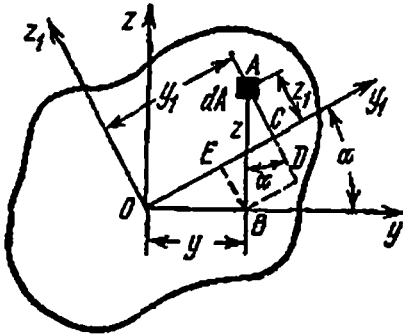


Fig. 167

The expressions for the moments of inertia about these axes are as follows:

$$\left. \begin{aligned} J_y &= \int_A z^2 dA, & J_z &= \int_A y^2 dA \\ J'_y &= \int_A z_1^2 dA, & J'_z &= \int_A y_1^2 dA \end{aligned} \right\} \quad (12.9)$$

It is clear from the drawing that the coordinates of area  $dA$  in the system of rotated axes  $Oy_1$  and  $Oz_1$  are

$$\left. \begin{aligned} y_1 &= OE + EC = OE + BD = y \cos \alpha + z \sin \alpha \\ z_1 &= AD - DC = AD - BE = z \cos \alpha - y \sin \alpha \end{aligned} \right\} \quad (12.10)$$

Putting these values of  $y_1$  and  $z_1$  in formula (12.9), we get

$$\begin{aligned} J'_y &= \int_A (z \cos \alpha - y \sin \alpha)^2 dA \\ &= \int_A (z^2 \cos^2 \alpha + y^2 \sin^2 \alpha - 2yz \sin \alpha \cos \alpha) dA \end{aligned}$$

or

$$J'_y = \cos^2 \alpha \int_A z^2 dA + \sin^2 \alpha \int_A y^2 dA - \sin 2\alpha \int_A yz dA \quad (12.11)$$

Similarly

$$J'_z = \int_A (y \cos \alpha + z \sin \alpha)^2 dA$$

or

$$J'_z = \sin^2 \alpha \int_A z^2 dA + \cos^2 \alpha \int_A y^2 dA + \sin 2\alpha \int_A yz dA \quad (12.12)$$

The first two integrals in expressions (12.11) and (12.12) represent the axial moments of inertia,  $J_y$  and  $J_z$ , whereas the third represents the product of inertia of section about the two axes,  $J_{yz}$ . Therefore

$$\left. \begin{aligned} J'_y &= J_y \cos^2 \alpha + J_z \sin^2 \alpha - J_{yz} \sin 2\alpha \\ J'_z &= J_y \sin^2 \alpha + J_z \cos^2 \alpha + J_{yz} \sin 2\alpha \end{aligned} \right\} \quad (12.13)$$

To determine the product of inertia of the section we may require formulas for passing over from one system of coordinates to the other. For the rotated axes (Fig. 167) we get

$$J'_{yz} = \int_A y_1 z_1 dA$$

where  $y_1$  and  $z_1$  are calculated according to formula (12.10). Consequently

$$\begin{aligned} J'_{yz} &= \int_A (z \sin \alpha + y \cos \alpha)(z \cos \alpha - y \sin \alpha) dA \\ &= \sin \alpha \cos \alpha \int_A z^2 dA - \sin \alpha \cos \alpha \int_A y^2 dA \\ &\quad + \cos^2 \alpha \int_A yz dA - \sin^2 \alpha \int_A yz dA \end{aligned}$$

After simplification we get

$$J'_{yz} = \frac{1}{2} (J_y - J_z) \sin 2\alpha + J_{yz} \cos 2\alpha \quad (12.14)$$

Thus, in order to determine the moment of inertia about an arbitrary central axis  $Oy_1$ , we must know the moments of inertia  $J_y$  and  $J_z$  about a system of two mutually perpendicular central axes  $Oy$  and  $Oz$ , the product of inertia of the section,  $J_{yz}$ , about the same axes, and the angle between axes  $Oy_1$  and  $Oy$ .

To calculate  $J_y$ ,  $J_z$ , and  $J_{yz}$  we must select the axes  $Oy$  and  $Oz$  and break the area of the figure into parts in such a way that the above values may be computed for each composite part by using the rule of parallel axes only. We shall show in the example below how to do this in practice. It should be noted that complex figures should be broken into elementary areas for which the central moments of inertia about a system of two perpendicular axes are known.

Let us note that the above procedure and the final results (12.13) and (12.14) would have been the same if we had taken the centre of coordinates in an arbitrary point  $O$  other than the centre of gravity of the section. Hence, formulas (12.13) and (12.14) hold true when we transfer from one system of mutually perpendicular axes to another rotated through an angle  $\alpha$ , irrespective of whether the axes pass through the centre of gravity or not.

From formula (12.13) we may obtain another relation between the moments of inertia when the axes are rotated. By adding the expressions for  $J_y'$  and  $J_z'$  (12.13), we get

$$J_y' + J_z' = J_y (\cos^2 \alpha + \sin^2 \alpha) + J_z (\sin^2 \alpha + \cos^2 \alpha) = J_y + J_z \quad (12.15)$$

i.e. the sum of the moments of inertia about any two mutually perpendicular axes  $Oy$  and  $Oz$  does not change when the axes rotate. Putting the values of  $J_y$  and  $J_z$  from (12.9) in formula (12.15), we get

$$J_y + J_z = \int_A z^2 dA + \int_A y^2 dA = \int_A (z^2 + y^2) dA = \int_A \rho^2 dA = J_p \quad (12.16)$$

where  $\rho = \sqrt{y^2 + z^2}$  is the distance of elementary area  $dA$  from point  $O$ . As we already know, the quantity  $J_p = \int_A \rho^2 dA$  is called the polar moment of inertia about point  $O$  (§ 48).

The polar moment of inertia of a section about a point is equal to the sum of the axial moments of inertia about two mutually perpendicular axes passing through this point. This explains why this sum remains constant when the axes rotate. Expression (12.16) may be utilized for simplifying the computation of the moment of inertia. Thus, for a circle we already have (§ 48)

$$J_p = \frac{\pi r^4}{2}$$

Due to symmetry in a circle  $J_y = J_z$ , therefore

$$J_z = J_y = \frac{J_p}{2} = \frac{\pi r^4}{4}$$

which is the same as obtained by integration (§ 65).

Similarly, on the basis of formula (9.15) we get the following expression for a thin-walled ring section:

$$J_y = \frac{J_p}{2} \approx \pi r_0^3 t$$

### § 69. Principal Axes of Inertia and Principal Moments of Inertia

Formulas (12.7) and (12.13) solve the problem set before us in § 66: knowing the central moments of inertia  $J_y$  and  $J_z$ , and  $J_{yz}$  for a particular figure we can calculate its moment of inertia about any other axis.

As the basic system of axes we select a system which will help simplify formulas (12.13). To be precise, we may select a system for which the product of inertia of the section is zero. Indeed, moments

of inertia  $J_y$  and  $J_z$  are always positive because they are the sum of positive terms; the product of inertia of the section

$$J_{yz} = \int_A zy dA$$

may be positive or negative, because the terms  $zy dA$  may have different signs depending upon the signs of  $y$  and  $z$  for particular elementary areas. This means that it may also be zero (§ 63, item C).

The axes about which the product of inertia of section is zero are called the *principal axes of inertia*. If the centre of this system of axes lies at the centre of gravity of the figure, then they are called the *principal central axes of inertia*. We shall denote these axes by  $Oy_0$  and  $Oz_0$ ; for these axes

$$J_{y_0z_0} = 0$$

Let us determine the angle  $\alpha_0$  between the principal axes and the central axes  $Oy$  and  $Oz$  (Fig. 168).

Fig. 168

In formula (12.14) for the product of inertia, where we pass over from axes  $yOz$  to  $y_1Oz_1$ , angle  $\alpha$  is replaced by  $\alpha_0$ ; then axes  $Oy_1$  and  $Oz_1$  coincide with the principal axes, and the product of inertia of the section vanishes:

$$\text{at } \alpha = \alpha_0 \quad J'_{yz} = J_{y_0z_0} = 0$$

or

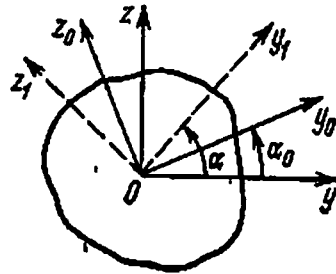
$$J_{y_0z_0} = -\frac{1}{2} \sin 2\alpha_0 (J_z - J_y) + J_{yz} \cos 2\alpha_0 = 0$$

wherefrom

$$\tan 2\alpha_0 = \frac{2J_{yz}}{J_z - J_y} \quad (12.17)$$

This equation is satisfied by two values of  $2\alpha_0$  differing by  $180^\circ$ , or two values of  $\alpha_0$  differing by  $90^\circ$ . Thus, equation (12.17) determines the location of two axes at right angles to each other. These are the principal central axes of inertia  $Oy_0$  and  $Oz_0$  for which  $J_{y_0z_0} = 0$ .

Using formula (12.17) and knowing  $J_y$ ,  $J_z$ , and  $J_{yz}$  we may obtain formulas for the principal moments of inertia  $J_{y_0}$  and  $J_{z_0}$ . For this we shall again use formulas (12.13); they give us the values of  $J_{y_0}$



and  $J_{z_0}$  if we replace  $\alpha$  by  $\alpha_0$ :

$$\left. \begin{aligned} J_{y_0} &= J_y \cos^2 \alpha_0 + J_z \sin^2 \alpha_0 - J_{yz} \sin 2\alpha_0 \\ J_{z_0} &= J_y \sin^2 \alpha_0 + J_z \cos^2 \alpha_0 + J_{yz} \sin 2\alpha_0 \end{aligned} \right\} \quad (12.18)$$

These formulas along with formulas (12.17) may be used in solving problems. We shall show in § 70 that one of the principal moments of inertia is  $J_{\max}$  and the other is  $J_{\min}$ .

Formulas (12.18) can be modified into a form which does not contain  $\alpha_0$ . Expressing  $\cos^2 \alpha_0$  and  $\sin^2 \alpha_0$  in terms of  $\cos 2\alpha_0$ , putting their values in the first formula in (12.18) and simultaneously substituting the value of  $J_{yz}$  from formula (12.17), we get

$$\begin{aligned} J_{y_0} &= \frac{J_y + J_z}{2} + \frac{J_y - J_z}{2} \cos 2\alpha_0 + \frac{J_y - J_z}{2} \frac{\sin 2\alpha_0}{\cos 2\alpha_0} \\ &= \frac{J_y + J_z}{2} + \frac{J_y - J_z}{2} \frac{1}{\cos 2\alpha_0} \end{aligned}$$

From formula (12.17), replacing the fraction

$$\frac{1}{\cos 2\alpha_0} \quad \text{by} \quad \pm \sqrt{1 + \tan^2 2\alpha_0} = \pm \sqrt{1 + \frac{(2J_{yz})^2}{(J_y - J_z)^2}},$$

we get

$$J_{\frac{\max}{\min}} = \frac{J_y + J_z}{2} \pm \frac{1}{2} \sqrt{(J_y - J_z)^2 + 4(J_{yz})^2} \quad (12.18')$$

We would have obtained the same result by a similar transformation of the second formula in (12.18).

Instead of  $Oy$  and  $Oz$  we may take the principal axes  $Oy_0$  and  $Oz_0$  as the basic system of the central axes of inertia from which we can pass over to any other system. Then the product of inertia of the section will not appear in formulas of the type (12.13) ( $J_{y_0 z_0} = 0$ ). Let us denote by  $\beta$  the angle that axis  $Oy_1$  makes with the principal axis  $Oy_0$  (Fig. 169). In calculating  $J'_y$ ,  $J'_z$ , and  $J'_{yz}$ , angle  $\alpha$  in formulas (12.13) and (12.14) should be replaced by  $\beta$  and  $J_y$ ,  $J_z$ , and  $J_{yz}$  should be replaced by  $J_{y_0}$ ,  $J_{z_0}$ , and  $J_{y_0 z_0} = 0$ . We find that

$$\left. \begin{aligned} J'_y &= J_{y_0} \cos^2 \beta + J_{z_0} \sin^2 \beta \\ J'_z &= J_{y_0} \sin^2 \beta + J_{z_0} \cos^2 \beta \\ J'_{yz} &= \frac{J_{y_0} - J_{z_0}}{2} \sin 2\beta \end{aligned} \right\} \quad (12.19)$$

The above formulas are exactly the same as the formulas for normal stresses  $\sigma_\alpha$  and shearing stresses  $\tau_\alpha$  (6.5) and (6.6) acting in two mutually perpendicular planes in an element subjected to tension in two directions (§ 30). Therefore Mohr's circle can be used in this case also. The axial moment of inertia should be laid off along the hori-

zontal axis, and the product of inertia of the section along vertical axis. It is proposed that the reader should himself plot and analyze the Mohr's circle in this case. We shall only give the formula which enables us to select that value among the two values of  $\alpha_0$  (formula (12.17)), which corresponds to deviation of the first principal axis (giving maximum  $J$ ) from the original position of the  $y$ -axis:

$$\tan \alpha_0 = \frac{J_{zy}}{J_{\min} - J_y} \quad (12.17')$$

This formula is exactly similar to formula (6.11).

We can finally state the law by which the moment of inertia of a complex figure about an arbitrary axis can be found in the simplest possible manner. It is essential to draw axes  $Oy$  and  $Oz$  through the centre of gravity of the figure so that to divide the figure in simple parts for which  $J_y$ ,  $J_z$  and  $J_{zy}$  can be easily calculated. Then we determine  $\alpha_0$  from formula (12.17) and calculate the principal central moments of inertia  $J_{y_0}$  and  $J_{z_0}$  according to formulas (12.18).

We can calculate the moment of inertia about an arbitrary central axis  $Oy_1$  (Fig. 169), inclined at an angle  $\beta$  to  $Oy_0$ , according to formula (12.19):

$$J'_{y_1} = J_{y_0} \cos^2 \beta + J_{z_0} \sin^2 \beta$$

Knowing the central moment of inertia  $J'_{y_1}$ , we can calculate the moment of inertia about any parallel axis  $y_2$  located at a distance  $a$  (Fig. 169) from the centre of gravity by formula (12.7):

$$J''_{y_2} = J'_{y_1} + a^2 A$$

In a number of cases the principal axes of a figure can be drawn straightaway. If the figure has an axis of symmetry, then this axis will be one of the principal axes. Actually, while deriving the formula  $\sigma = \frac{Mz}{J}$ , we came across the integral  $\int_A yz \, dA$ , which represents the product of inertia of the section about the axes  $Oy$  and  $Oz$ . It was proved that if  $Oz$  is the axis of symmetry, then this integral becomes zero.

This implies that in the present case  $Oy$  and  $Oz$  represent the principal central axes of inertia of the section. Hence, the axis of symmetry is always a principal axis, and the second principal central axis passes through the centre of gravity at right angles to the axis of symmetry.

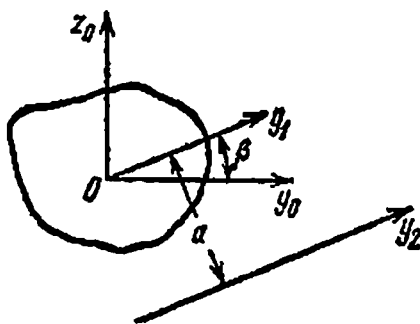


Fig. 169

### § 70. The Maximum and Minimum Values of the Central Moments of Inertia

We already know that the central moments of inertia are the minimum of all moments about a number of parallel axes.

Let us now determine the extreme (maximum and minimum) values of the central moments of inertia. If we start rotating axis  $Oy_1$ , i.e. changing the value of  $\alpha$ , there is the change in the value of

$$J'_y = J_y \cos^2 \alpha + J_z \sin^2 \alpha - J_{yz} \sin 2\alpha$$

The maximum and minimum values of this moment of inertia correspond to angle  $\alpha_1$  for which  $dJ'_y/d\alpha$  vanishes. This derivative is

$$\frac{dJ'_y}{d\alpha} = -2J_y \cos \alpha \sin \alpha + 2J_z \sin \alpha \cos \alpha - 2J_{yz} \cos 2\alpha$$

Putting  $\alpha = \alpha_1$  in the above equation and equating it to zero, we get

$$(J_z - J_y) \sin 2\alpha_1 - 2J_{yz} \cos 2\alpha_1 = 0$$

wherefrom

$$\tan 2\alpha_1 = \frac{2J_{yz}}{J_z - J_y} = \tan 2\alpha_0 \quad (\text{see (12.17)})$$

Thus, the axes about which the central moments of inertia are maximum or minimum are the principal central axes of inertia. When these axes are rotated, the sum of the corresponding moments of inertia does not change; therefore

$$J'_y + J'_z = J_y + J_z = J_p$$

When one of the central moments of inertia is maximum, the other must be minimum, i.e. if

$$J_{y_0} = J_{\max}, \quad \text{then} \quad J_{z_0} = J_{\min}$$

Thus, the principal central axes of inertia are mutually perpendicular axes passing through the centre of gravity of the section, about which the product of inertia of the section is zero and the axial moments of inertia have the maximum and minimum values.

In future we shall denote the principal axes of inertia by  $Oy$  and  $Oz$  and the principal moments of inertia by  $J_y$  and  $J_z$ . We shall continue to denote the axis of the beam by the  $x$ -axis as before.

### § 71. Application of the Formula for Determining Normal Stresses to Beams of Non-symmetrical Sections

By equating to zero the product of inertia of section about the principal axes, we can show that the formulas given in § 63 are valid under certain conditions for non-symmetrical sections as well.

While deriving the formula for normal stresses (§ 63) we introduced the limitation that the beam should be symmetrical about the plane of action of the external forces,  $xOz$ , with the primary aim of (1) establishing that the neutral axis  $Oy$  is perpendicular to the plane  $zOx$ , and (2) proving that the sum of the moments of elementary forces  $dN$  about the axis  $Oz$  is zero:

$$\sum M_z = 0, \quad \frac{E}{\rho} \int_A xy dA = 0, \quad \int_A zy dA = 0 \quad (11.6)$$

However, the conditions that the  $z$ - and  $y$ -axes be at right angles and the integral  $\int_A zy dA$  be equal to zero may also be fulfilled for a non-symmetrical section. For this it is sufficient that the  $z$ -axis lying in the plane of action of the external forces and the neutral  $y$ -axis be the principal central axes of inertia of the beam's cross section. The perpendicularity is then satisfied and the integral  $\int_A zy dA$  representing the product of inertia of the section about the principal axes is also equal to zero.

Hence, the condition that the plane of action of the external forces should coincide with the plane of symmetry may be replaced by another condition: the plane of action of the external forces should coincide with one of the two planes containing the principal axes of inertia of the cross section. In a beam these two planes are called the *principal planes of inertia*.

The second principal axis, which is perpendicular to the plane of action of the external forces, represents the neutral axis, and the condition  $\int_A zy dA = 0$  is automatically satisfied.

Since we can always find the principal central axes of inertia for a beam of any shape, formulas (11.9) and (11.13)

$$\sigma = \frac{Mz}{J} \quad \text{and} \quad \sigma_{\max} = \frac{M_{\max}}{W}$$

may be used for beams of any cross section, provided the external forces lie in one of the principal planes of inertia of the beam and  $J$  and  $W$  are taken about the other principal axis, which is perpendicular to the plane of action of the external forces and represents the neutral axis.

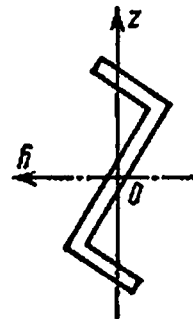


Fig. 170



A Z-shaped beam (Fig. 170) with principal axes  $Oz$  and  $Oy$  may be taken as an example. The formulas given above are applicable to this beam only if the external forces lie in plane  $xOz$  or  $xOy$ . In the first case the  $y$ -axis will be neutral, in the second the  $z$ -axis. As in this case too the neutral axes of the section are perpendicular to the plane of action of the external forces, the axis of the beam remains in this plane even after deformation. Thus, if the external forces lie in one of the principal planes of inertia, this will be the general case of uni-planar bending.

Beams of Z-section are often employed as purlins, which are laid over rusters. Under vertical pressure of the roof weight and snow the purlins bend in the plane of action of the external forces (for corresponding roof slope), i.e. they experience uni-planar bending.

It should be noted that in some cases additional normal and shearing stresses connected with extra twisting of beam are set up in beams of non-symmetrical (about the axis lying in the plane of action of external forces) sections.

## § 72. Radii of Inertia.

### Concept of the Momental Ellipse

We shall now introduce one more geometrical characteristic of section which correlates the moment of inertia of the section,  $J$ , with its area  $A$  by the following formulas:

$$J_y = i_y^2 A \quad \text{and} \quad J_z = i_z^2 A \quad (12.20)$$

Quantities  $i_y$  and  $i_z$  are known as *radii of inertia* and are respectively equal to

$$i_y = \sqrt{\frac{J_y}{A}} \quad \text{and} \quad i_z = \sqrt{\frac{J_z}{A}} \quad (12.21)$$

If  $J_y$  and  $J_z$  represent the principal moments of inertia,  $i_y$  and  $i_z$  are known as the principal radii of inertia. For example, for a rectangular section we find with the help of formulas (12.1) and (12.3)

$$i_y = \sqrt{\frac{bh^3}{12bh}} = \frac{h}{\sqrt{12}}, \quad i_z = \sqrt{\frac{hb^3}{12bh}} = \frac{b}{\sqrt{12}} \quad (12.22)$$

For a circular section formula (12.4) yields

$$i_y = i_z = \sqrt{\frac{\pi r^4}{4\pi r^2}} = \frac{r}{2} \quad (12.23)$$

The values of principal radii of inertia for rolled profiles are given in standard normal profile tables (see Appendix).

The ellipse plotted on the principal radii of inertia as its major and minor axes is known as *momental ellipse*. To plot the momental ellipse we lay off from the centre of gravity of the section the radii of inertia:  $i_y$  is normal to the central  $y$ -axis, i.e. along the  $z$ -axis, and  $i_z$  is normal to the  $z$ -axis (along the  $y$ -axis). If  $J_y = J_{max}$ , the major axis of the ellipse  $2i_y$  will lie along the  $z$ -axis (Fig. 171).

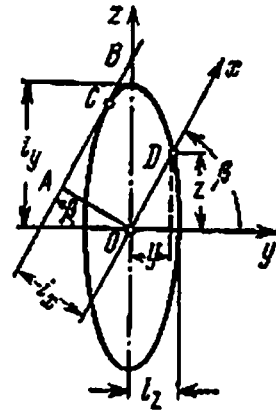


Fig. 171

The momental ellipse has the following remarkable property: the radius of inertia about an arbitrary axis  $Ox$  drawn through the centre of gravity of the section is equal to the normal dropped from the centre of ellipse to the tangent parallel to the above axis. Hence, with the help of the momental ellipse we can graphically find the radius of inertia  $i_x$  for an arbitrary axis  $Ox$  making an angle  $\beta$  with the principal axis  $Oy$ . For this it is sufficient to draw a tangent to the ellipse parallel to the  $x$ -axis and measure distance  $i_x$  between the axis and tangent (Fig. 171). Knowing the measured radius of inertia  $i_x$ , we calculate the moment of inertia about the  $x$ -axis by formula

$$J_x = i_x^2 A \tag{12.24}$$

Some sections like circle, square, etc. (Fig. 172), which are commonly used in engineering practice, have equal moments of inertia about the two principal axes of inertia. Consequently, the principal

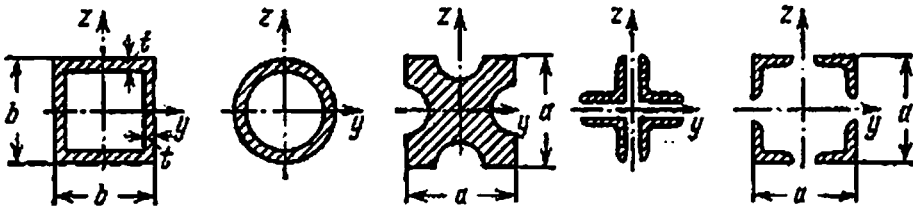


Fig. 172

radii of inertia are also equal ( $i_y = i_z$ ), and the momental ellipse changes to the momental circle. For such sections every central axis represents a principal central axis of inertia; this is also evident from formula (12.19) for the product of inertia of section, which vanishes for every value of  $\beta$  if  $J_y = J_z$  (see § 69).

A bar of such a section displays equal resistance to bending in all directions, which is particularly important in axial compression of long bars (Chapter 27).

### § 73. Strength Check, Choice of Section and Determination of Permissible Load in Bending

Formulas (11.15), (11.16), and (11.17) derived in Chapter 11 for expressing the strength condition in bending, combined with the ability to calculate the moments of inertia and section moduli (Chapter 12), enable us to solve the fundamental problems of strength of materials in bending (§ 4), namely:

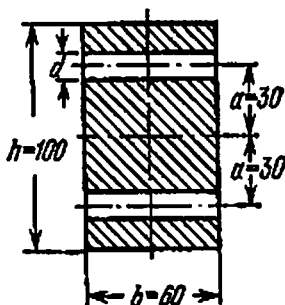


Fig. 173

(a) check the beam strength when the beam dimensions and the forces acting on it are known;

(b) determine the required cross-sectional dimensions if the axial dimensions of the beam and the forces acting on it are known;

(c) determine the permissible load which the beam can withstand if its axial and cross-sectional dimensions are known.

It is assumed that the permissible stresses are known in all the above cases.

We shall illustrate with examples how to apply the strength conditions for solving the above problems.

A. Suppose it is required to check the strength of a rectangular  $60 \times 100$  mm steel bar weakened by two symmetrical holes of diameter  $d=10$  mm (Fig. 173), if the bending moment in the critical section  $M_{\max}=1.3$  tf·m and the permissible stress  $[\sigma]=1600$  kgf/cm<sup>2</sup>.

Let us calculate the moment of inertia of the section about neutral axis  $Oy$ :

$$J_y = \frac{bh^3}{12} - 2 \left( bd a^2 + \frac{bd^3}{12} \right) = \frac{6 \times 10^3}{12} - 2 \left( 6 \times 1 \times 3^2 + \frac{6 \times 1^3}{12} \right) = 391 \text{ cm}^4$$

The section modulus is

$$W_y = \frac{J_y}{z_{\max}} = \frac{391}{5} = 78.2 \text{ cm}^3$$

The maximum stress in critical section is

$$\sigma_{\max} = \frac{M_{\max}}{W} = \frac{1.3 \times 10^6}{78.5} = 1660 \text{ kgf/cm}^2 > 1600 \text{ kgf/cm}^2$$

Overstressing of  $\frac{1660-1600}{1600} \times 100 = 3.75\%$  is permissible.

**B.** Let us now solve a problem on selecting a section. Let a hinged I-beam of span  $l=4$  m be loaded along its length by a uniformly distributed force  $q=2$  tf/m and a concentrated force  $P=6$  lf at the centre of the span. It is required to select a section for the beam if the permissible stress  $[\sigma]=1600$  kgf/cm<sup>2</sup>.

The maximum bending moment at the middle of the span can be calculated by applying the principle of superposition of forces (§ 61).

Bending moment due to the distributed load  $q$  according to formula (10.11) is

$$M_q = \frac{ql^2}{8} = \frac{2 \times 4^2}{8} = 4 \text{ tf} \cdot \text{m}$$

Bending moment due to concentrated force  $P$  (10.10') is

$$M_P = \frac{Pl}{4} = \frac{6 \times 4}{4} = 6 \text{ tf} \cdot \text{m}$$

The maximum total bending moment in the critical section is

$$M_{\max} = M_q + M_P = 4 + 6 = 10 \text{ tf} \cdot \text{m} = 10 \times 10^5 \text{ kgf} \cdot \text{cm}$$

According to strength condition (11.16) the required section modulus

$$W \geq \frac{M_{\max}}{[\sigma]} = \frac{10 \times 10^5}{1600} = 625 \text{ cm}^3$$

From standard tables (see Appendix) we find the profile No. which satisfies this condition: I-section No. 33 having section modulus  $W=597$  cm<sup>3</sup> (overstressing of about 5% is permissible).

**C.** Let us now consider an example in which we have to determine the permissible uniformly distributed load which may be safely applied to a hinged jib beam of span  $l=10$  m. The beam has I-section No. 60 strengthened by two  $200 \times 20$  mm plates welded to it (Fig. 174). Permissible stress  $[\sigma]=1400$  kgf/cm<sup>2</sup>.

The moment of inertia of the section will be found as the sum of moments of inertia of the I-section and the two plates about the neutral axis (as per standards) and it will be calculated with the help of formula for moment of inertia about parallel axes (12.7):

$$\begin{aligned} J &= J_1 + 2 \left[ \frac{bt^3}{12} + bt \left( \frac{h}{2} + \frac{t}{2} \right)^2 \right] \\ &= 76\,806 + 2 \left[ \frac{20 \times 2^3}{12} + 20 \times 2 \times (30 + 1)^2 \right] \approx 153\,700 \text{ cm}^4 \end{aligned}$$

Section modulus

$$W = \frac{J_y}{z_{\max}} = \frac{153\,700}{32} = 4820 \text{ cm}^3$$

According to strength condition (11.16) the maximum bending moment  $M_{\max} = \frac{ql^2}{8}$  must not exceed  $[\sigma]W$ , wherefrom

$$[q] \leq \frac{8[\sigma]W}{l^2} = \frac{8 \times 1400 \times 4820}{10^2 \times 100^2} \approx 54 \text{ kgf/cm}$$

or 5400 kgf/m.

If the dead weight of the beam is taken into account, then we should subtract the distributed load due to the weight of two plates,  $2 \times$

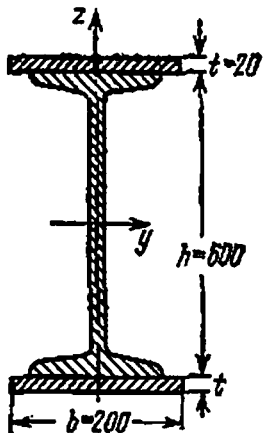


Fig. 174

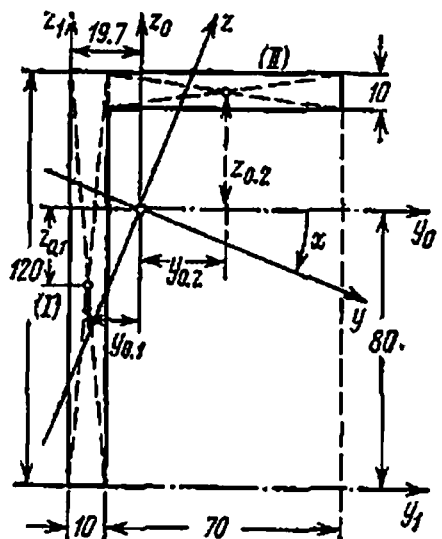


Fig. 175

$\times 20 \times 2 \times 100 \times 0.00785 = 63 \text{ kgf/m}$ , and the weight of the I-beam (see Appendix)  $108 \text{ kgf/m}$  ( $q_0 = 63 + 108 = 171 \text{ kgf/m}$  in all).

Hence, the beam may be loaded by a service load

$$q = [q] - q_0 = 5400 - 171 \approx 5230 \text{ kgf/m}$$

**D.** Finally, we shall now discuss the analysis of a composite beam of non-symmetrical section. Suppose it is required to determine the permissible bending moment for a beam fixed rigidly at one end in a wall, if a force couple is applied at the other end in the principal plane of inertia. The dimensions of the section are given in Fig. 175. The span of the beam is  $l = 0.6 \text{ m}$ . The permissible stress is  $[\sigma] = 1600 \text{ kgf/cm}^2$ .

First of all it is necessary to locate the centre of gravity of the section. For this we select an arbitrary system of coordinate axes  $y_1Oz_1$ .

It is convenient if the whole figure lies in the first quadrant. The distances of the centre of gravity from these axes may be determined by the formulas

$$y_c = \frac{S_{z_1}}{A} \quad \text{and} \quad z_c = \frac{S_{y_1}}{A}$$

where  $S_{y_1}$  and  $S_{z_1}$  are static moments of the area about axes  $Oy_1$  and  $Oz_1$ , respectively.

To determine the static moments we divide the area into two rectangles, vertical  $I$  and horizontal  $II$ . The area of the figure is  $A = 1 \times 12 + 7 \times 1 = 19.0 \text{ cm}^2$ . The static moments\* are

$$S_{z_1} = A_1 y_{1,1} + A_2 y_{1,2} = 12 \times 0.5 + 7(1 + 3.5) = 37.5 \text{ cm}^3$$

$$S_{y_1} = A_1 z_{1,1} + A_2 z_{1,2} = 12 \times 6.0 + 7 \times 11.5 = 152.5 \text{ cm}^3$$

The coordinates of the centre of gravity are

$$y_c = \frac{37.5}{19} = 1.97 \text{ cm} \approx 2.0 \text{ cm}$$

$$z_c = \frac{152.5}{19} \approx 8.00 \text{ cm}$$

Let us now choose the coordinate system of the central axes of inertia  $Oy_0$  and  $Oz_0$ . The simplest way is to direct these axes parallel to the arms of the figure; this will be helpful in calculating the moments of inertia of the section about these axes.

The moments of inertia of individual rectangles about axes  $Oy_0$  and  $Oz_0$  can be calculated from the formulas of parallel axes (12.7) and (12.8), and the moments of inertia of the rectangles about their own axes from formula (12.1).

Table 12 (see Fig. 175) contains the plan of computations with the help of which we can determine the angles between the principal axes and axis  $Oy_0$ :

$$\tan 2\alpha_0 = \frac{2J_{yz}^0}{J_z^0 - J_y^0} = \frac{2 \times 97}{100 - 278} = -1.09$$

$$2\alpha_0' = -47^\circ 40' \quad \text{and} \quad \alpha_0' = -23^\circ 50'$$

The minus sign shows that angle  $\alpha_0'$  should be laid off in the clockwise direction:

$$\sin \alpha_0' = -0.404, \quad \cos \alpha_0' = 0.915, \quad \sin 2\alpha_0' = -0.74, \quad \cos 2\alpha_0' = 0.673$$

---

\* In the indices of the coordinates the first subscript denotes the axes  $Oy_1$  or  $Oz_1$ , and the second subscript denotes the area.

Table 12

## Determination of the Moment of Inertia

Number of part	Area of the part	Coordinates of the areas (cm)		Moments of inertia of the areas (cm <sup>4</sup> )							
				$J_y^0 = \frac{bh^3}{12} + Az_0^2$		$J_z^0 = \frac{bh^3}{12} + Ay_0^2$		$J_{yz}^0 = Ay_0z_0$			
		$y_0$	$z_0$	$\frac{bh^3}{12}$	$Az_0^2$	$J_y^0$	$\frac{bh^3}{12}$	$Ay_0^2$	$J_z^0$	$\pm$	$J_{yz}^0$
1	12	-1.5	-2.0	144	48	192	1.0	27	28	+	36
2	7	2.5	3.5	0.6	85.6	86	28.6	43.8	72	+	61
$\Sigma$	19			144.6	133.6	278	29.6	70.8	100	+	97

The principal moments of inertia are

$$J_y = J_y^0 \cos^2 \alpha_0 + J_z^0 \sin^2 \alpha_0 - J_{yz}^0 \sin 2\alpha_0 \\ = 278 \times 0.915^2 + 100 \times 0.404^2 + 97 \times 0.74 = 320 \text{ cm}^4$$

$$J_z = J_y^0 \sin^2 \alpha_0 + J_z^0 \cos^2 \alpha_0 + J_{yz}^0 \sin 2\alpha_0 \\ = 278 \times 0.404^2 + 100 \times 0.915^2 - 97 \times 0.74 = 58 \text{ cm}^4$$

Let us check whether the results obtained are correct:

$$1. J_y + J_z = 320 + 58 = 378 \text{ cm}^4 = J_y^0 + J_z^0 = 278 + 100 = 378 \text{ cm}^4$$

$$2. J_{yz} = \frac{1}{2} (J_y^0 - J_z^0) \sin 2\alpha + J_{yz}^0 \cos 2\alpha \\ = -\frac{1}{2} (278 - 100) 0.74 + 97 \times 0.673 = 0$$

It is clear from the calculations that  $J_y = J_{\max}$ , and  $J_z = J_{\min}$ . Hence, it is advantageous to apply the bending couple in the plane  $xOz$  so that axis  $Oy$  becomes the neutral axis (Fig. 176).

Let us now find the section modulus. For this it is necessary to determine the distance  $z_{\max}$  of the farthest fibre from the neutral axis  $Oy$ . This can easily be done by drawing the section to a certain scale and marking the principal axes \* on it. For the section under consideration the measured distance was found to be  $z_{\max} = 8.1$  cm. Therefore the section modulus about the  $y$ -axis is

$$W_y = \frac{J_y}{z_{\max}} = \frac{320}{8.1} = 39.5 \text{ cm}^3$$

\* Formulas (12.10) may be used for analytical determination of  $z_{\max}$  or  $y_{\max}$ .

We determine the maximum permissible bending moment from the strength condition\*:

$$\sigma = \frac{\max \{M\}}{W_y} \leq [\sigma]$$

wherefrom

$$\max \{M\} \leq [\sigma] W_y$$

$$M_0 = \max \{M\} \leq 1600 \times 39.5 = 63\,200 \text{ kgf}\cdot\text{cm} \approx 0.63 \text{ tf}\cdot\text{m}$$

If the bending moment is applied in plane  $xOy$ , then the distance of the outer fibre from the axis  $Oz$  being  $y_{\max} = 4.12 \text{ cm}$ , the section

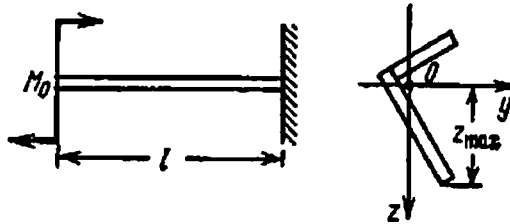


Fig. 176

modulus will be  $W_z = \frac{J_z}{y_{\max}} = \frac{58}{4.12} = 14.1 \text{ cm}^3$ , and the magnitude of the moment which can be applied safely will be

$$M_1^0 = \max \{M_1\} \leq 1600 \times 14.1 = 22\,560 \text{ kgf}\cdot\text{cm} \approx 0.226 \text{ tf}\cdot\text{m}$$

which is three times less than the moment which can be applied in plane  $xOz$ .

Let us note that if the moment is located in a plane other than the principal plane, for example, parallel to the flange of the angle section, then the bending of the beam will not be uni-planar, and the strength condition will be different (§ 120).

## CHAPTER 13

### Shearing and Principal Stresses in Beams

#### § 74. Shearing Stresses in a Beam of Rectangular Section

Let us try to determine, first of all, the shearing stresses in sections perpendicular to the beam axis when the sections are rectangles (Fig. 177).

\* In this example we do not account for the additional normal stresses which appear due to restrained torsion.



Suppose a positive shearing force  $Q$  acts in a section when the beam is subjected to bending. Let us make the following assumptions regarding shearing stresses  $\tau$  in this section:

(1) all shearing stresses in the section act parallel to the shearing force  $Q$ , which is the resultant of the former;

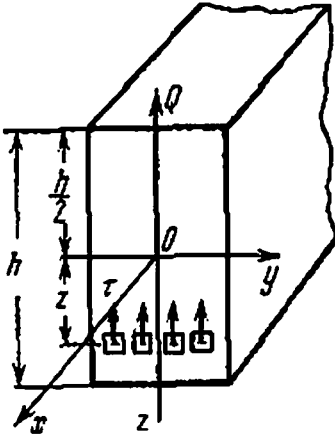


Fig. 177

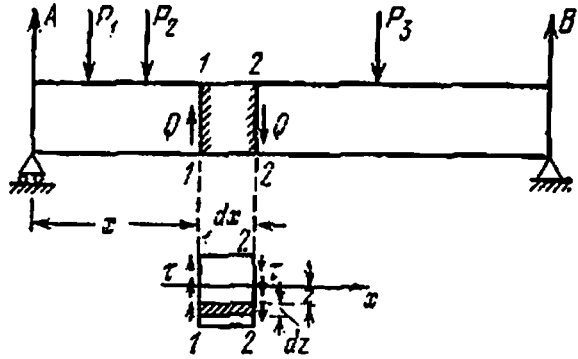


Fig. 178

(2) shearing stresses acting in planes which are located at the same distance  $z$  from the neutral axis are equal in magnitude.

Both these assumptions were put forward by D. I. Zhuravskii. The theory of elasticity reveals that the assumptions are valid for rectangular beams if the height of the beam is greater than its width.

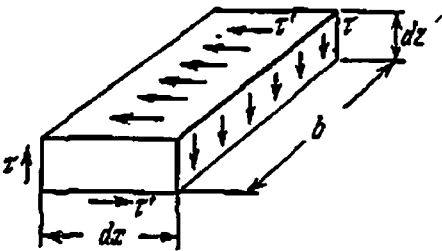


Fig. 179

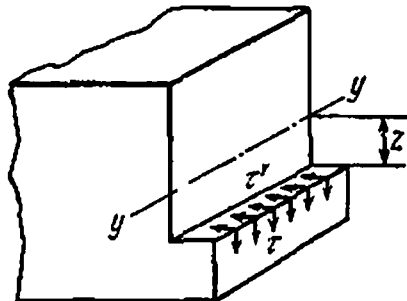


Fig. 180

We shall now try to calculate the shearing stresses and ascertain the law of distribution of shearing stresses along the height of section.

Let us consider a beam loaded by a number of forces (Fig. 178). Let us isolate a part of length  $dx$  cut out by sections 1-1 and 2-2. It will be assumed that section 2-2 on the right side of the cutout portion experiences shearing stresses  $\tau$ , which give resultant shearing force  $Q$  acting downwards. Then on the other side section 1-1 will experience shearing stresses acting upwards, which also give a resultant shearing

force  $Q$ . It is quite natural that in the absence of distributed load on the isolated part of the beam, the shearing forces should be equal in magnitude. Sections 1-1 and 2-2 will also experience normal stresses which, however, are not shown here.

According to the law of complementary shearing stresses (Chapter 6, formula (6.8)), similar shearing stresses should be expected to act in planes parallel to the neutral layer. Therefore, if we take two horizontal sections of the beam at distances  $z$  and  $z+dz$  from the neutral axis and isolate an element of sides  $b$ ,  $dx$ , and  $dz$  (Fig. 179), then the vertical faces of this element will experience shearing stresses  $\tau$ , whereas the horizontal faces will be acted upon by equal but opposite shearing stresses  $\tau'$ .

As the fibres parallel to the axis of the beam do not press on each other in the process of deformation, the sections of the beam parallel to the neutral layer do not experience any normal stresses. Therefore, instead of determining the shearing stresses  $\tau$  over the beam cross section, we shall determine equal stresses  $\tau'$  acting in a plane parallel to the neutral layer (Fig. 180).

At first it seems strange that shearing stresses appear in planes parallel to the neutral layer. However, we can explain this phenomenon with the following example.

Let us suppose that the beam consists of two identical rectangular rods placed over one another (Fig. 181(a)); the friction between the rods may be ignored. It is assumed that the beam

bends under the action of at least one force  $P$  acting in the middle of the span. The bent beam is shown in Fig. 181(b) in a highly magnified scale. The lower fibres of the upper beam  $A_1B_1$  stretch, whereas the upper fibres of the lower beam  $A_2B_2$  shorten as compared to their initial length  $AB$ .

If the beam were a single rod, it would have bent as shown in Fig. 181(c). Fibres  $AB$  would be in the neutral layer and would not have changed their lengths. Therefore in bending of a solid beam, shearing stresses  $\tau'$  preventing the upper and lower halves of the beam from shear along the neutral layer are transmitted from the upper half to the lower through the neutral layer, and vice versa (Fig. 181(d)).

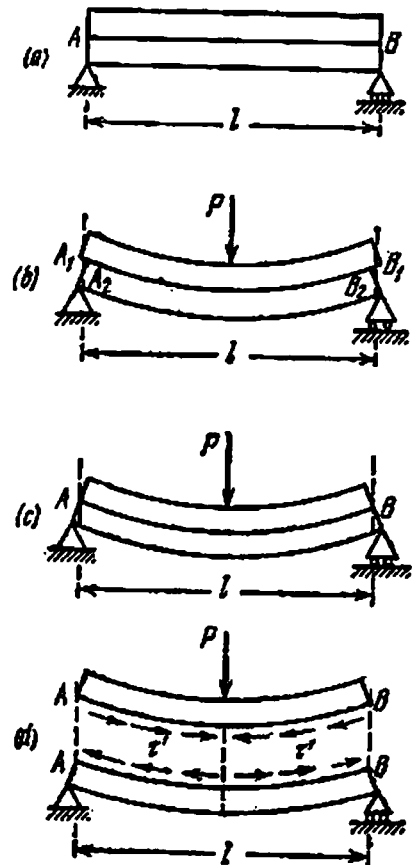


Fig. 181

Figure 182 shows a part of the façade of a rectangular beam subjected to uni-planar bending. Let us draw two very close sections 1-1 and 2-2 at a distance  $dx$  from each other. Let us also draw a horizontal section at a distance  $z$  from the neutral layer.

Thus, we shall be able to isolate from the beam an element  $ABCD$  having sides  $dx$ ,  $h/2-z$ , and  $b$ . An axonometric projection of the element is shown in Fig. 182. Let  $M$  be the bending moment in section

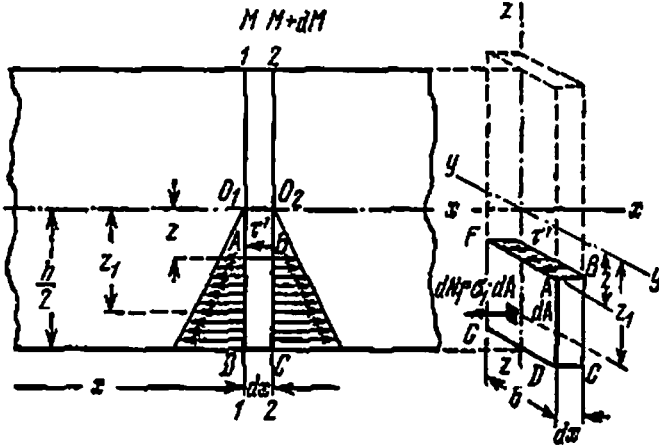


Fig. 182

1-1, and  $M+dM$  in the adjacent section 2-2. The side faces of the element will be acted upon by normal stresses  $\sigma$  which are lower to the left and greater to the right. The horizontal section will experience shearing stresses  $\tau'=\tau$ .

We have not shown in the diagram the shearing stresses  $\tau$  acting in sections 1-1 and 2-2 because they do not enter the condition of equilibrium of the isolated element, which is obtained by equating to zero the sum of the projections of all the forces on the axis of the beam.

To obtain the condition of equilibrium of the isolated element, we must calculate all those forces acting on it which are parallel to the axis of the beam. The elementary shearing force  $dT$  on the elementary area  $b dx$  is

$$dT = \tau b dx$$

The normal stresses acting on an infinitely small area  $dA$  of the side face at a height  $z_1$  from the neutral axis are

$$\sigma = \frac{Mz_1}{J}$$

The force  $dN_1$  acting on this area is

$$dN_1 = \frac{Mz_1}{J} dA$$

The whole of the side face  $AD$  is acted upon by a force  $N_1$  (Fig. 183):

$$N_1 = \int_{A_1} \frac{Mz_1}{J} dA = \frac{M}{J} \int_{A_1} z_1 dA$$

Integral  $\int_{A_1} z_1 dA$  is the static moment about the neutral  $y$ -axis of the part of section  $GFAD$  enclosed between the section at a height  $h$  and the edge of the beam (Fig. 184). Let us denote it by  $S_y^0$ . Thus,

$$N_1 = \frac{MS_y^0}{J_y} \tag{13.1}$$

Identically face  $BC$  of the element is acted upon by a force

$$N_2 = \frac{(M+dM) S_y^0}{J_y} \tag{13.2}$$

The difference of the normal forces

$$N_2 - N_1 = \frac{dM S_y^0}{J_y}$$

when projected on axis  $Ox$  (Fig. 183) is balanced by the shearing force  $dT$ . Therefore

$$\tau = \frac{dM}{dx} \frac{S_y^0}{J_y b}$$

But  $\frac{dM}{dx} = Q$ , therefore

$$\tau = \frac{QS_y^0}{J_y b} \tag{13.3}$$

implying thereby that this formula represents the shearing stress at height  $z$  in a section perpendicular to the axis of the beam.

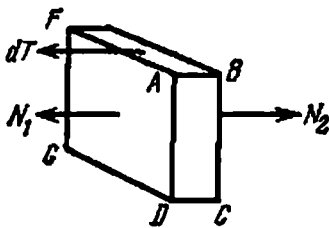


Fig. 183

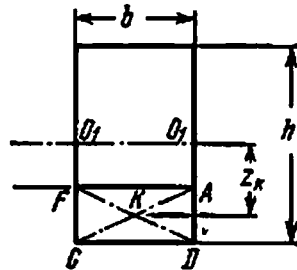


Fig. 184

Let us derive the formula for  $S_y^0$  for a rectangular beam (Fig. 184) of height  $h$  and width  $b$ . The static moment of area  $GFAD$  about axis  $O_1O_1$  is equal to the area multiplied by distance  $z_h$  of its centre of gra-

vity from axis  $O_1O_1$ . The area of  $GFAD$  is equal to

$$b \left( \frac{h}{2} - z \right)$$

and distance  $z_k$  is

$$z_k = \left( \frac{h}{2} - \frac{\frac{h}{2} - z}{2} \right) = \frac{1}{2} \left( \frac{h}{2} + z \right)$$

Hence,

$$S_y^0 = b \left( \frac{h}{2} - z \right) \frac{1}{2} \left( \frac{h}{2} + z \right) = \frac{bh^2}{8} \left( 1 - \frac{4z^2}{h^2} \right) \quad (13.4)$$

While computing the static moment of the area of a section it is immaterial whether we take the portion of section which is below the level  $z$  or the bigger portion, because both the static moments are

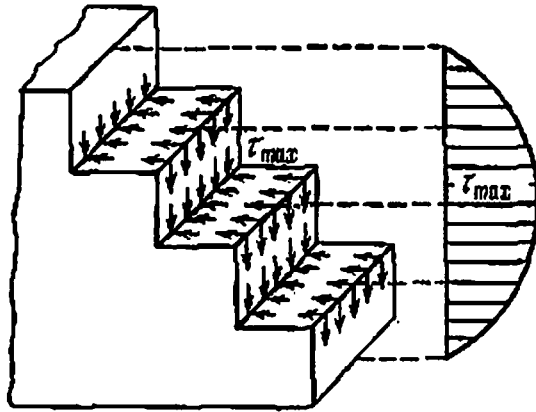


Fig. 185

equal in magnitude. Generally, we take the static moment of the portion which is easier to compute. Since for a rectangle  $J_y = \frac{bh^3}{12}$ , formula (13.3) takes the form

$$\tau = \frac{Qbh^2}{bh^3} \frac{12}{8} \left( 1 - \frac{4z^2}{h^2} \right) = \frac{3}{2} \frac{Q}{bh} \left( 1 - \frac{4z^2}{h^2} \right) \quad (13.5)$$

Hence, shearing stress  $\tau$  changes along the height of the rectangular section according to a parabolic law. The shearing stress vanishes at the lower and upper ends of the section where  $z = \pm \frac{h}{2}$ ; this is in strict conformity with the law of complementary shearing stresses. It attains maximum value on the neutral axis (where the normal stress is zero) where  $z=0$ , and in the section where  $Q(x) = Q_{\max}$ :

$$\tau_{\max} = \frac{3}{2} \frac{Q_{\max}}{bh} \quad (13.6)$$

Thus, the maximum shearing stress in a rectangular section is 1.5 times greater than its average value. Figure 185 shows the distribution of shearing stresses when the shearing force is positive.

Shearing stresses somewhat distort the accepted picture of deformation of a beam. We had assumed that under the action of bending moments the cross sections of a beam turn w.r.t. each other, although they continue to remain planes (Fig. 186(a)). Due to shearing stresses the elements of the material enclosed between two sections warp.

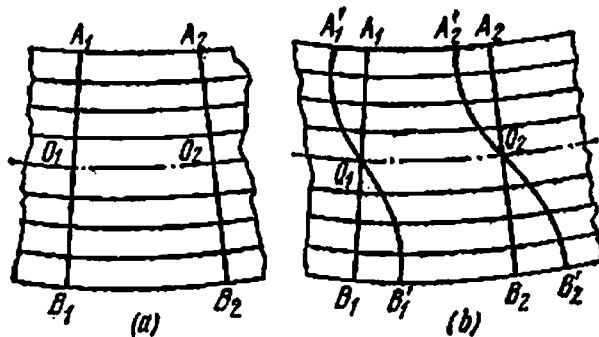


Fig. 186

In accordance with the variation in the value of the shearing stress, the warping increases from the edges of the beam towards the neutral axis. Therefore the sections are deformed (Fig. 186(b)). However, warping has almost no effect on the deformation of the fibres along the beam, therefore formula  $\sigma = \frac{Mz}{J}$  can be used even if a shearing force is acting on the beam.

Thus, in addition to the strength check for maximum normal stresses (11.15)

$$\sigma_{\max} = \frac{M_{\max}}{W} \leq [\sigma]$$

we must check the strength of the material for maximum shearing stresses

$$\tau_{\max} = \frac{Q_{\max} S_{\max}}{J_{\nu} b} \leq [\tau] \tag{13.7}$$

We shall solve a numerical example to get an idea of the order of the magnitude of  $\tau$  in rectangular beams.

Let us determine the maximum normal and shearing stresses for a rectangular beam with the following data: the beam lies on two supports and over its total length  $l=4$  m takes a uniform load of intensity  $q=1.2$  tf/m;  $M_{\max}=2.4$  tf·m;  $Q_{\max}=2.4$  tf;  $h=27$  cm;  $b=$

=18 cm;  $[\sigma]=110 \text{ kgf/cm}^2$ ;  $[\tau]=22 \text{ kgf/cm}^2$ .

$$\sigma_{\max} = \frac{M_{\max}}{W} = \frac{240\,000 \times 6}{18 \times 27^2} = 109.5 \text{ kgf/cm}^2 < 110 \text{ kgf/cm}^2$$

$$\tau_{\max} = \frac{3Q_{\max}}{2bh} = \frac{3 \times 2400}{2 \times 27 \times 18} = 7.5 \text{ kgf/cm}^2 < 22 \text{ kgf/cm}^2$$

We see that a rectangular beam designed to take the maximum normal stress equal to the permissible remains highly understressed as far as the shearing stresses are concerned.

However, in practice we may come across just the reverse case; it may occur when the shearing force is large whereas the bending moment is small. In such cases of loading, even in a rectangular section the decisive part in determining the dimensions of the beam is played by the shearing stresses.

The formula for shearing stresses in a rectangular section was first derived by the Russian engineer D. I. Zhuravskii when he was designing wooden bridges for the St. Petersburg-Moscow railway line in 1885. Zhuravskii employed a slightly different and more complicated method in obtaining this formula without using the relation  $\frac{dM}{dx} = Q$ .

### § 75. Shearing Stresses in I-beams

As the sections of I- and T-beams may be considered as consisting of rectangles, then with a certain degree of approximation the formulas derived for rectangular sections in § 74 may be applied to these sections too. The shearing stresses in a point at a distance  $z$  from the neutral axis may, for an I-section (Fig. 187), be expressed by the same formula

$$\tau = \frac{QS_y^0}{J_y b(z)} \quad (13.3)$$

Here  $S_y^0$  is the static moment of the area enclosed between level  $z$  and the edge of the beam about the neutral  $y$ -axis. As for the quantity  $b(z)$ , the width of the section, it has been written as a function of  $z$  to emphasize that in the denominator of formula (13.3) the width at level  $z$  should be used. If we examine the derivation of formula (13.3), we see that  $b$  is the multiplier in the term  $\tau b dx$ , i.e. it is the lateral dimension of the area which is being acted upon by the stress  $\tau$ . Thus  $b$  is the width of the beam at level  $z$ . Therefore, when applying formula (13.3) to an I-section for calculating the shearing stresses in web sections, instead of  $b(z)$  web thickness  $b_w$  should be used. Static moment  $S_y^0$  may be computed as the sum of static moments of the two rectangles hatched in Fig. 187(a). Upon computation we get

$$\tau_w = \frac{Q}{8b_w J_y} \left[ b_f h^2 \left( 1 - \frac{h_f^2}{h^2} \right) + b_w h_f^2 \left( 1 - \frac{4z_w^2}{h_f^2} \right) \right] \quad (13.8)$$

It is evident from the formula that along the web height the shearing stresses vary by a parabolic law (Fig. 187(b)) and become maximum on the neutral axis of the section.

Formula (13.3) cannot be used for calculating shearing stresses in the portions lying in the flanges of the I-section, because these stresses are far from being equal along the flange width. In the area around the  $z$ -axis they may be assumed to vary approximately as shown by dotted lines in Fig. 187(b). However, in the remaining area of the

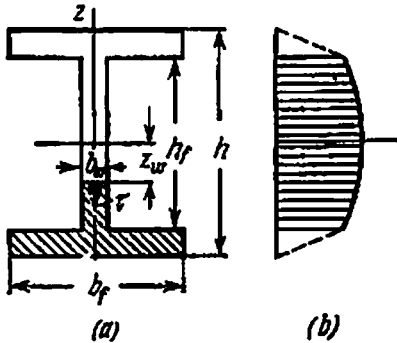


Fig. 187

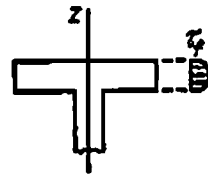


Fig. 188

flange, i.e. along almost the whole of flange width, they vary as shown in Fig. 188 and do not achieve large magnitudes due to the conditions on the flange surface and the law of complementary shearing stresses.

Knowing now the laws of distribution of normal and shearing stresses along the height of I-section, we can draw the following conclusion about the working of an I-section.

The flanges of an I-section, being located at a considerable distance from the neutral axis, experience over their whole area normal stresses that are maximum or close to maximum. Shearing stresses in the flanges of an I-section are negligible.

As we move towards the neutral axis, the normal stresses in the web of the I-section tend to zero. Within web limits the static moment  $S_y^0$  does not change much for various values of  $z$ . Therefore shearing stresses along the web height are sufficiently large (see the curve in Fig. 187(b)). In short, it may be summarized that the flanges of an I-section bear normal stresses, and the web bears shearing stresses.

Let us check the shear strength of a beam acted upon by a shearing force  $Q=2.4$  tf, assuming the permissible shearing stress  $[\tau]=1000$  kgf/cm<sup>2</sup>. The section is shown in Fig. 189. From Table I of Appendix we find  $J=1290$  cm<sup>4</sup>. The static moment of half of the section is  $S_{\max}=81.4$  cm<sup>3</sup>= $S_y$ . For calculating the stresses at point 2 the static moment can be found by subtracting the static moment of half of the web from  $S_{\max}$ :

$$S_2 = 81.4 - 0.5 \times 0.51 \times 8.19^2 = 81.4 - 17.1 = 64.3 \text{ cm}^3$$



The shearing stresses are

$$\tau_1 = 0, \quad \tau_2 = \frac{2400 \times 64.3}{1290 \times 0.51} = 236 \text{ kgf/cm}^2$$

$$\tau_3 = \frac{2400 \times 81.4}{1290 \times 0.51} = 297 \text{ kgf/cm}^2$$

The diagram of distribution of shearing stresses along the I-section height is shown in Fig. 189. It can be seen from the diagram that the

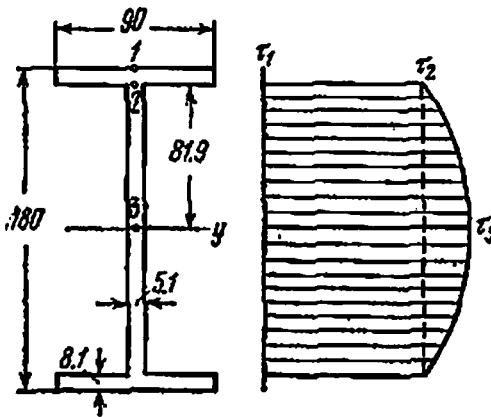


Fig. 189

maximum shearing stress is considerably less than the permissible which may be attributed to the large thickness of the web in the rolled profile. Much better utilization of metal can be achieved in composite beams (see § 80), riveted and welded.

Let us determine that fraction of the shearing force which is taken up by the web. For this we multiply the ordinates of the shearing-stress diagram by the area of the web of I-section:  $236 \times 0.51 \times$

$\times 16.38 \times \frac{2}{3} = 2312 \text{ kgf}$ , which comprises 96% of the total shearing force.

The method of determining shearing stresses in an I-beam which has been explained here may also be used for other sections made of rectangles: hollow rectangular section, T-section, etc.

### § 76. Shearing Stresses in Beams of Circular and Ring Sections

Let us consider a beam of circular section. In this beam the shearing stresses can no more be parallel to the shearing force. If there are no forces acting on the side surface of the beam, the shearing stresses on elementary areas 1 and 2 in the vicinity of section contour must act along the tangent to the section contour (Fig. 190(a)). These tangents will intersect the line of action of the shearing force at point C. Since shearing force  $Q$  is the resultant of shearing stresses (Fig. 190), the shearing stresses on arbitrary elementary areas 3 and 4 at the same distance  $z$  from the horizontal diameter act along the line passing through the same point C. Each of these shearing stresses  $\tau$  may be broken into two components: vertical  $\tau_1$  and horizontal  $\tau_2$ . The horizontal components in the left and right halves of the section balance each other, whereas the vertical components add up into

shearing force  $Q$ . Hence, in round beams vertical stress components  $\tau_1$  play the same role as the total stresses  $\tau$  in rectangular beams.

We can thus apply formula (13.3) to round sections too, but it will

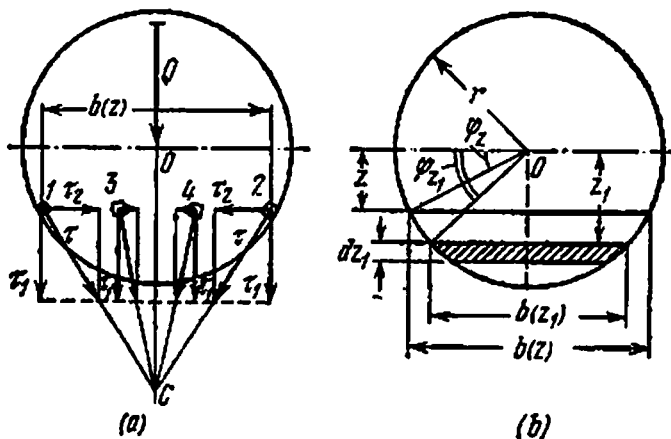


Fig. 190

give us only the vertical component of shearing stress at an arbitrary point. In subsequent discussion we shall write  $\tau$  instead of  $\tau_1$ :

$$\tau = \frac{QS_y^0}{J_y b(z)} \quad (13.3)$$

Here, as in the previous case,  $S_y^0$  is the static moment of the area between the edge of the section and level  $z$  and is expressed by the formula

$$S_y^0 = \int_A z_1 dA = \int_A z_1 b(z_1) dz_1$$

It is more convenient to introduce a new variable, angle  $\varphi_{z1}$ , in computing the static moment; if  $r$  is the radius of the section, then

$$z = r \sin \varphi_z, \quad z_1 = r \sin \varphi_{z1}, \quad b(z_1) = 2r \cos \varphi_{z1} \\ dz_1 = r \cos \varphi_{z1} d\varphi_{z1}, \quad b(z) = 2r \cos \varphi_z$$

We shall limit ourselves to determining  $\tau_{\max}$ :

$$\tau_{\max} = \frac{Q_{\max} S_{\max}}{J_y b} \quad (13.7)$$

$$S_{\max} = \int_0^{\pi/2} 2r \cos \varphi_{z1} r \sin \varphi_{z1} r \cos \varphi_{z1} d\varphi_{z1} \\ = \frac{2r^3}{3} \left[ -\cos^3 \varphi_{z1} \right]_0^{\pi/2} = \frac{2r^3}{3} \quad (13.9)$$

Since  $J = \frac{\pi r^4}{4}$  and  $b_{z=0} = d = 2r$ , we get

$$\tau_{\max} = \frac{Q \times 2r^3 \times 4}{3 \times 2r\pi r^4} = \frac{4Q}{3\pi r^2}$$

Thus, for a circular section

$$\tau_{\max} = \frac{4}{3} \frac{Q}{\pi r^2} \quad (13.10)$$

i.e.  $\tau_{\max}$  is 1.33 times greater than the mean value of  $\tau$ .

Even in rectangular sections, where  $\tau_{\max}$  is 1.5 times greater than the mean value, check for shear strength is often not required and this is all the more so for circular sections. It should, however, be noted that shearing stresses may be of a considerably higher magnitude in pipe-section beams.

**Example.** Find the maximum shearing stress in an iron pipe of external diameter  $d=10$  cm and wall thickness  $t=1$  cm;  $Q_{\max}=2$  tf.

Maximum shearing stress occurs in points of the neutral layer and is expressed by the formula

$$\tau_{\max} = \frac{Q_{\max} S_{\max}}{J_y b} \quad (13.7)$$

here  $J_y$  is the moment of inertia of the pipe section;  $S_{\max}$  is the static moment of the semicircular ring,  $b=2t$  is the double thickness of the pipe wall.

$$J_y = \frac{\pi}{4} \left[ \left( r_0 + \frac{t}{2} \right)^4 - \left( r_0 - \frac{t}{2} \right)^4 \right] = \pi r_0^3 t \left( 1 + \frac{t^2}{4r_0^2} \right) \approx \pi r_0^3 t \quad (13.11)$$

where  $r_0$  is the mean pipe radius.

The static moment of a semicircular ring is equal to the difference of the static moments about the diameter of the inner and outer semicircles; the static moment of a semicircle is expressed by the formula

$$S(r) = \frac{2r^3}{3} \quad (13.9)$$

The required static moment of the semicircular ring is

$$S_{\max} = \frac{2}{3} \left[ \left( r_0 + \frac{t}{2} \right)^3 - \left( r_0 - \frac{t}{2} \right)^3 \right] = 2r_0^2 t \left[ 1 + \frac{t^2}{12r_0^2} \right] \approx 2r_0^2 t \quad (13.12)$$

Therefore

$$\tau_{\max} = \frac{Q \times 2r_0^2 t}{2t \times \pi r_0^3 t} = \frac{Q}{\pi r_0 t} = \frac{2Q}{\pi d t} = \frac{2 \times 2000}{\pi \times 9 \times 1} = 141.4 \text{ kgf/cm}^2$$

The maximum shearing stress in a semicircular ring is twice the mean stress. Let us recapitulate that this ratio is 1.5 for a rectangular section and 1.33 for a solid circular section.

§ 77. Strength Check for Principal Stresses

In the previous discussion we worked out two criteria for checking the strength of beams under bending under normal stresses (11.15) and shearing stresses (13.7):

$$\sigma_{max} = \frac{M_{max}}{W} \leq [\sigma] \tag{11.15}$$

$$\tau_{max} = \frac{Q_{max} S_{max}}{J_y b(z)} \leq [\tau] \tag{13.7}$$

We shall consider the elements of beams whose strength may be checked by these formulas.

Figure 191 shows a part of the front view of the beam being analyzed in the sections of maximum bending moment and maximum shearing force. The diagram shows the elements whose strength is checked by

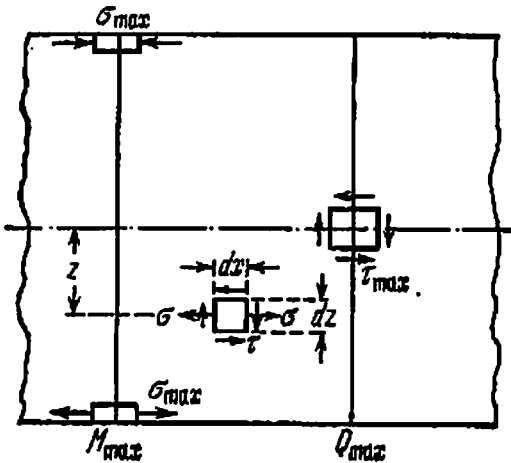


Fig. 191

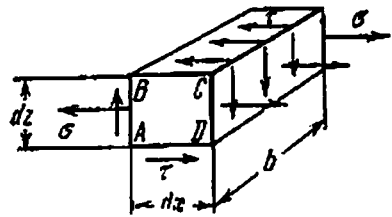


Fig. 192

conditions (11.15) and (13.7). The first formula is used for elements located near the top and bottom edges of the section with  $M_{max}$ . These elements are subjected to simple tension or compression. The second condition, (13.7), applies to an element located near the neutral axis with  $Q_{max}$ ; this element experiences pure shear.

Thus, when checking the strength of the beam under normal and shearing stresses according to the universally accepted method of stress analysis, we actually check the strength of material in three elements shown in Fig. 191.

Generally speaking, it cannot be said with certainty that these three elements are the maximally loaded. Therefore, we must learn how to check the strength of every element of the beam taken in an arbitrary section at a distance  $z$  from the neutral axis. Only then can we be sure of defining the maximally loaded element and check its strength.

Let us take an element of the material (Fig. 192) in an arbitrary section at a distance  $z$  from the neutral layer. The faces of this element perpendicular to the axis of the beam will be acted upon by normal stresses  $\sigma$ , whereas shearing stresses  $\tau$  will act on all the four side faces. The front faces of the element will be free of stresses.

Stresses  $\sigma$  and  $\tau$  may be expressed by the following formulas:

$$\sigma = \frac{Mz}{J}, \quad \tau = \frac{QS(z)}{Jb}$$

where  $M$  is the bending moment, and  $Q$  the shearing force in the isolated element.

Let us consider the case when both  $\sigma$  and  $\tau$  are positive. We shall have to take recourse to the theories of strength to check the strength of the element because it is in a compound stressed state; the computations must be started by calculating the principal stresses.

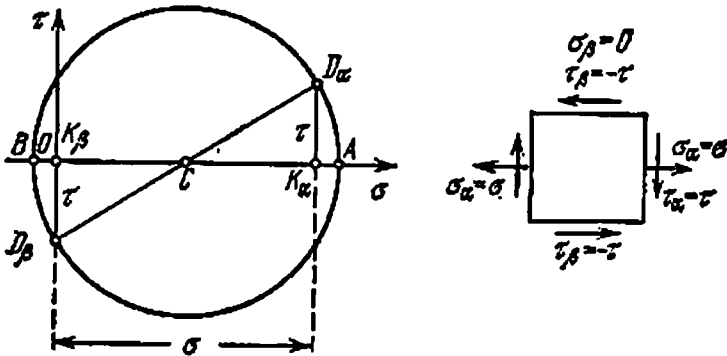


Fig. 193

As the front face  $ABCD$  of the element (Fig. 192) and faces parallel to it do not experience shearing stresses, they must lie in one of the principal planes. The principal stress acting in this plane is zero, because the plane is free of normal stresses. Thus, we are to study a problem of plane stressed state.

Our aim now is to determine the remaining two principal stresses knowing the normal and shearing stresses in two mutually perpendicular planes, one of which is parallel and the other perpendicular to the axis of the beam (Fig. 191). We solved an identical problem in § 32 by plotting the stress circle. There the method was applied to the more general case of a stressed state, where two mutually perpendicular planes with normals  $\alpha$  and  $\beta$  are acted upon by stresses  $\sigma_\alpha$ ,  $\sigma_\beta$ ,  $\tau_\alpha$ , and  $\tau_\beta = -\tau_\alpha$ . In this problem we shall attribute index  $\alpha$  to the face of the element perpendicular to the axis of the beam, and index  $\beta$  to the face parallel to the axis (Fig. 193).

Let us lay off from point  $O$  the segment  $OK_\alpha$ , representing  $\sigma_\alpha = \sigma$ , in the positive direction and another segment  $K_\alpha D_\alpha$  equal to  $\tau$  on

the perpendicular to the  $\sigma$ -axis at point  $K_\alpha$ . Point  $D_\alpha$  on the stress circle corresponds to the plane perpendicular to the axis of the beam.

In a plane parallel to the axis of the beam  $\sigma_\beta=0$ ; this means that point  $K_\beta$  coincides with point  $O$ . Segment  $K_\beta D_\beta$  laid off downwards represents the shearing stress  $\tau_\beta=-\tau$  and gives the second point on the circle,  $D_\beta$ . Joining the two points we get the centre of the circle, point  $C$ , and the radii  $CD_\alpha$  and  $CD_\beta$ . After plotting the circle we get segments  $OA$  and  $OB$  representing the principal stresses, which remain to be determined. It is evident from the drawing that these stresses have different signs. Therefore, the numbering of principal stresses may be done as follows:

$$\sigma_1 = \overline{OA} > 0, \quad \sigma_2 = 0, \quad \sigma_3 = \overline{OB} < 0$$

Making use of formula (6.13) given in § 32, we get

$$\begin{aligned} \sigma_1 &= \frac{\sigma}{2} + \frac{1}{2} \sqrt{\sigma^2 + 4\tau^2} = \frac{1}{2} [\sigma + \sqrt{\sigma^2 + 4\tau^2}] \\ \sigma_3 &= \frac{\sigma}{2} - \frac{1}{2} \sqrt{\sigma^2 + 4\tau^2} = \frac{1}{2} [\sigma - \sqrt{\sigma^2 + 4\tau^2}] \\ \sigma_2 &= 0 \end{aligned}$$

The formulas for  $\sigma_1$  and  $\sigma_3$  may be written in an integrated form as

$$\left. \begin{array}{l} \sigma_1 \\ \sigma_3 \end{array} \right\} = \frac{1}{2} |\sigma \pm \sqrt{\sigma^2 + 4\tau^2}| \quad (13.13)$$

We have plotted the stress circle and computed the stresses on the assumption that both  $\sigma$  and  $\tau$  are positive. If any of the stresses is negative, then the corresponding sign in formula (13.13) should be changed. A similar change would also have been essential in graphic determination of  $\sigma_1$  and  $\sigma_3$  by plotting the stress circle.

Knowing all the three principal stresses, we can write down the conditions of analysis for all the theories of strength.

According to the first theory, the theory of maximum normal stresses,

$$\sigma_1 \leq [\sigma], \quad \text{or} \quad \frac{1}{2} [\sigma + \sqrt{\sigma^2 + 4\tau^2}] \leq [\sigma] \quad (13.14)$$

According to the second theory, the theory of maximum strain,

$$[\sigma_1 - \mu(\sigma_2 + \sigma_3)] \leq [\sigma]$$

Putting the values of  $\sigma_1$ ,  $\sigma_2$ , and  $\sigma_3$  we get

$$\left[ \frac{1}{2} (\sigma + \sqrt{\sigma^2 + 4\tau^2}) - \frac{1}{2} \mu (\sigma - \sqrt{\sigma^2 + 4\tau^2}) \right] \leq [\sigma]$$

Assuming  $\mu=0.3$ , we find

$$[0.35\sigma + 0.65 \sqrt{\sigma^2 + 4\tau^2}] \leq [\sigma] \quad (13.15)$$

According to the third theory, the theory of maximum shearing stresses,

$$[\sigma_1 - \sigma_3] \leq [\sigma]$$

or

$$\frac{1}{2} [\sigma + \sqrt{\sigma^2 + 4\tau^2} - \sigma + \sqrt{\sigma^2 + 4\tau^2}] \leq [\sigma]$$

which yields

$$\sqrt{\sigma^2 + 4\tau^2} \leq [\sigma] \quad (13.16)$$

Finally, according to the fourth theory, the theory of maximum potential energy of distortion, we have

$$[(\sigma_1 - \sigma_2)^2 + (\sigma_2 - \sigma_3)^2 + (\sigma_3 - \sigma_1)^2] \leq 2[\sigma]^2$$

wherefrom

$$\frac{1}{4} [(\sigma + \sqrt{\sigma^2 + 4\tau^2})^2 + (\sigma - \sqrt{\sigma^2 + 4\tau^2})^2 + (2\sqrt{\sigma^2 + 4\tau^2})^2] \leq 2[\sigma]^2$$

After simplification we get

$$[\sigma^2 + 3\tau^2] \leq [\sigma]^2, \quad \sqrt{\sigma^2 + 3\tau^2} \leq [\sigma] \quad (13.17)$$

Now we shall try to find the points of the beam in which its strength for principal stresses should be checked.

As the reduced stress depends both upon  $\sigma$  and  $\tau$ , the strength check should be carried out for those elements of the beam which simulta-

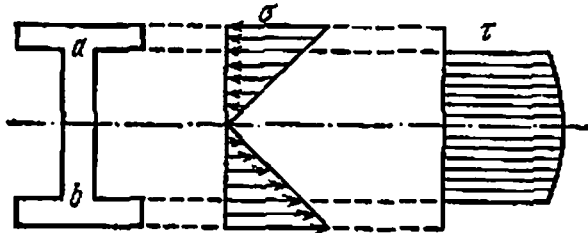


Fig. 194

neously experience maximum  $\sigma$  and  $\tau$ . This is possible if the following two conditions are fulfilled for the element:

(1) Bending moment and shearing force are maximum in the same section.

(2) Beam width changes sharply near the edges of the section (for example in an I- or a box section). The bending-moment and shearing-force diagrams for such a section (Fig. 194) reveal that the shearing and normal stresses near the region where the flange becomes the web are close to maximum (points *a* and *b*).

Thus, the two above conditions determine whether an additional strength check is necessary and also determine the element where this check should be carried out. In the cases where these conditions are not satisfied, we limit ourselves to selecting a few points where the maximum reduced stresses can occur. As for selecting the proper formula for analysis, the best, of course, is the one based on the theory of maximum distortion energy (13.17).

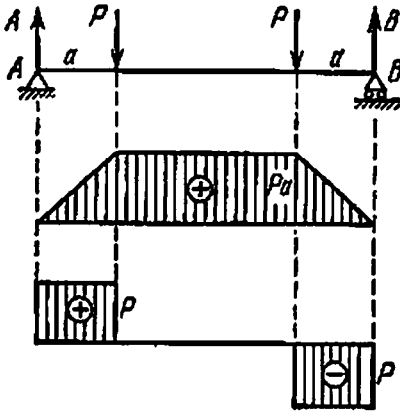


Fig. 195

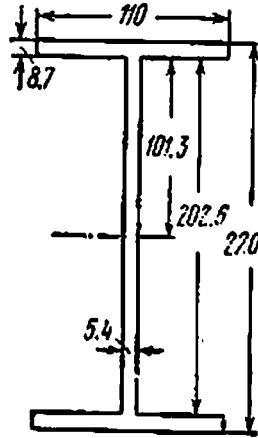


Fig. 196

In practice, however, the theory of maximum normal stresses (13.14) is still used in the analysis of beams, because it often gives smaller dimensions of the section.

**Example.** A simply supported beam  $AB$  (Fig. 195) is loaded by symmetrically acting forces  $P=6.4$  tf located at distances  $a=50$  cm from the supports; the permissible stress is  $[\sigma]=1400$  kgf/cm<sup>2</sup>. Select an I-section and check its strength in the region of transition from flange to web.

The maximum values of  $M$  and  $Q$  occur in the same section under the load:

$$M_{\max} = Pa = 0.5 \times 6.4 = 3.2 \text{ tf} \cdot \text{m}$$

$$Q_{\max} = P = 6.4 \text{ tf}$$

The required section modulus is

$$W = \frac{M_{\max}}{[\sigma]} = \frac{320\,000}{1400} = 229 \text{ cm}^3$$

We should take an I-beam No. 22 having  $W=232$  cm<sup>3</sup>;  $J=2550$  cm<sup>4</sup>. The dimensions of the cross section have been schematically shown in Fig. 196. For the selected section

$$\sigma_{\max} = \frac{320\,000}{232} = 1380 \text{ kgf/cm}^2$$





enough for materials which have equal resistance to tension and compression. For materials like reinforced concrete, however, it is extremely important to know the direction of tensile stresses in every point so that we can place the reinforcement rods in this direction.

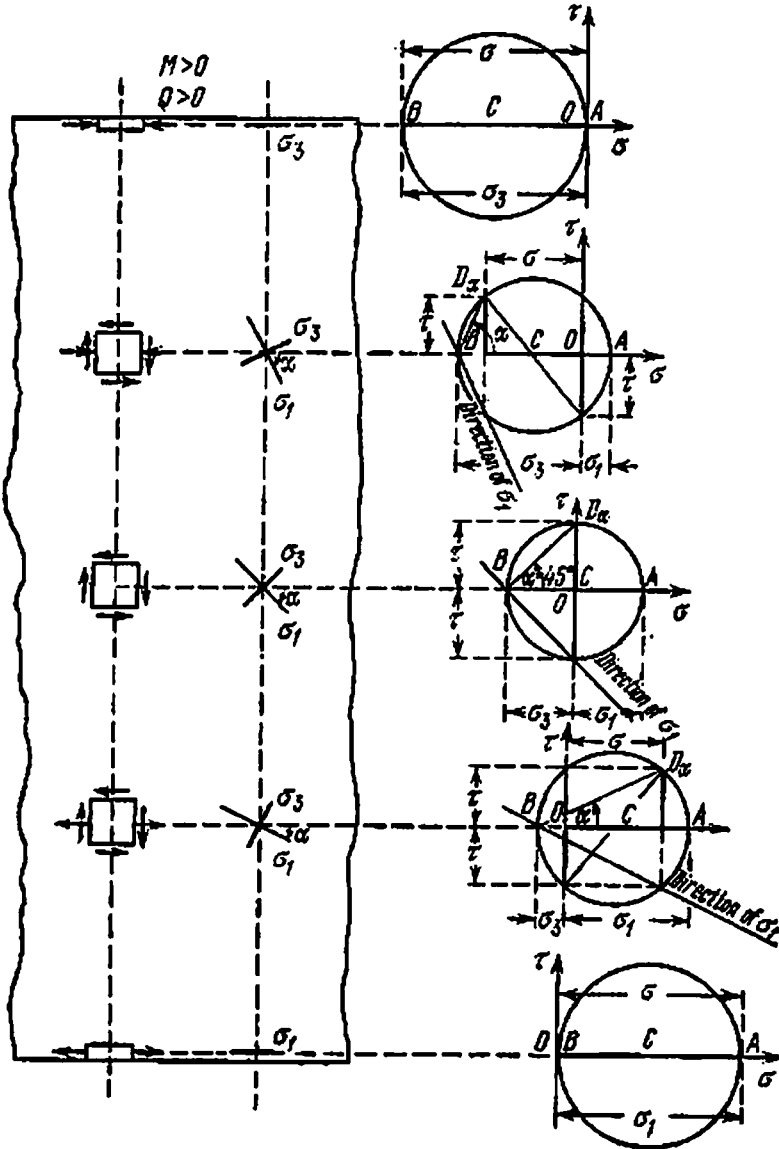


Fig. 198

The direction of the principal stresses may be determined with the help of the stress circle (Fig. 197). Suppose  $\sigma_\alpha$  and  $\tau_\alpha$ , acting in a plane perpendicular to the axis of the beam, are positive:

$$\sigma_\alpha = +\sigma = \frac{Mz}{J}$$

and

$$\tau_{\alpha} = +\tau = \frac{QS_y^0}{Jb}$$

After plotting the stress circle we see that the relative position of the lines of action of stress  $\sigma_{\alpha}$  and the maximum (algebraically) principal stress  $\sigma_1$  is the same as the relative position of line  $BD_{\alpha}$  and the  $x$ -axis; the latter two make an angle  $\alpha$  in the stress circle (Fig. 197). To mark the direction of  $\sigma_1$  on the drawing we must lay off angle  $\alpha$  from the direction of  $\sigma_{\alpha}$  clockwise.

The principal stresses change their direction within the limits of the section. Near the edges of the beam one of the principal stresses

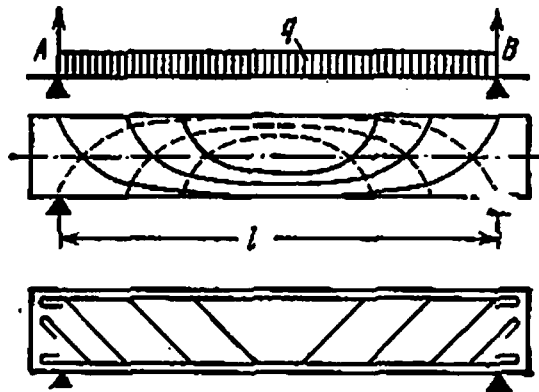


Fig. 199

is zero, whereas the other is directed parallel to the axis of the beam; at the neutral layer the principal stresses make an angle of  $45^{\circ}$  with the axis of the beam.

Figure 198 shows the stress circles and directions of the principal stresses in various points of the section. It is assumed that the bending moment and shearing force in the section are positive.

Having obtained the directions of the principal stresses in an arbitrary point of the given section, we continue one of the lines till it intersects the adjacent section. We determine the direction of the principal stress in this new point and continue the line till it intersects the next section. We thus obtain a broken line which in the limit changes into a curve the tangent to which coincides with the direction of the principal stress in the point under consideration. This curve is known as the *trajectory of the principal stress*. The directions of the trajectories of principal stresses depend upon the type of loading and the working conditions of the beam. We can draw two trajectories of principal stresses through every point of the beam—one for the tensile stresses and the other for compressive stresses. The tra-

jectories for compressive stresses are shown by dotted lines and those for the tensile stresses by solid lines (Fig. 199, the middle drawing).

The reinforcement in reinforced concrete beams should be placed in such a way that it is located approximately in the direction of the trajectory of the principal tensile stresses (Fig. 199, the lower drawing).

Theoretical investigations on principal stresses in bending that give the present-day design formulas were first carried out by N. A. Belilyubskii in connection with the design of bridge beams (his results were published in 1870-76). In his works principal stresses were called "oblique stresses".

## CHAPTER 14

### Shear Centre. Composite Beams

#### § 79. Shearing Stresses Parallel to the Neutral Axis. Concept of Shear Centre

A. Beams of thin-walled sections experience shearing stresses parallel to the  $y$ -axis in addition to shearing stresses parallel to shearing force  $Q$ , i.e. perpendicular to the neutral axis ( $y$ ) that were discussed in §§ 74-76. The validity of this statement can be easily confirmed by considering the parallelepiped having sides  $AH=y$ ,  $AB=l$ , and  $BC=dx$  (Fig. 200(a) and (b)) which is isolated from, say, the flange of an I-section by sections 1-1 and 2-2 and plane  $ABCD$  parallel to plane  $xz$ .

Let us assume that bending moment  $M_1=M$  in section 1-1 is less than the bending moment  $M_2=M+dM$  in section 2-2. The resultant  $N_1$  of internal normal forces acting on the front face ( $ABGH$ ) of the parallelepiped will be less than the resultant  $N_2$  of the normal forces on the rear face (Fig. 200(c)). The difference between  $N_2$  and  $N_1$  (see formulas (13.1) and (13.2)) is calculated by the formula

$$dN = N_2 - N_1 = \frac{dM}{J_y} S_y^0 \quad (14.1)$$

where  $S_y^0$  is the static moment about the neutral axis of area  $ABGH$  of the front face or a similar rear face where the internal normal stresses are summed up. The difference between  $N_2$  and  $N_1$  can be balanced only by internal shearing stresses acting on face  $ABCD$  because the top, bottom and side faces of the parallelepiped, being external surfaces, are free from forces and there is no possibility of any additional forces appearing on the front and rear faces which could counterbalance the difference (Fig. 200(b) and (c)).

Hence, on face  $ABCD$  of the parallelepiped we have shearing stresses  $\tau_f$ , and in accordance with the law of complementary shearing stresses similar stresses  $\tau_f$  appear on face  $ABGH$ , i.e. in the cross section of the beam (Fig. 200(b) and (c)). On account of the fact that flange thickness  $t_f$  and length  $dx$  of the isolated element are small quantities, these shearing stresses can be considered to be uniformly

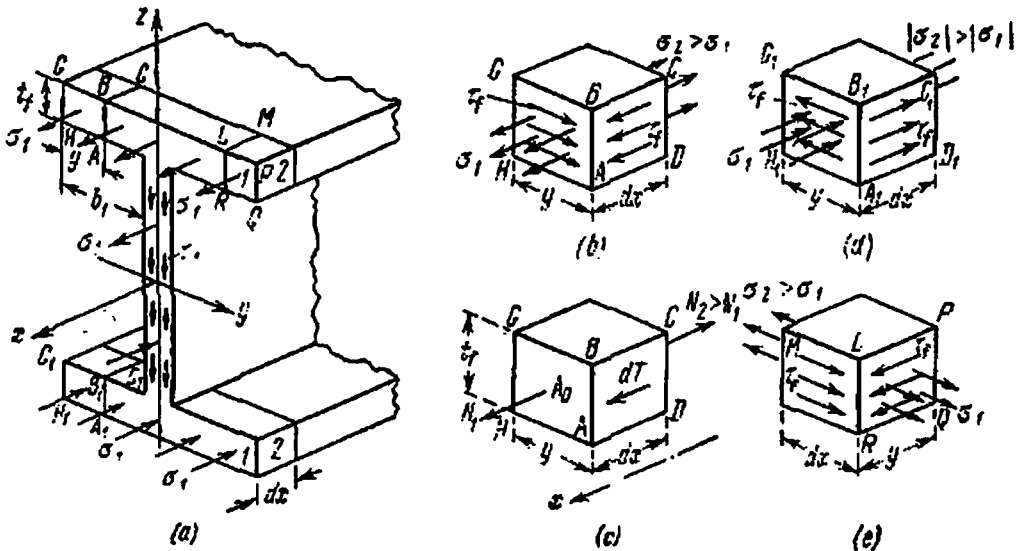


Fig. 200

distributed over the area of face  $ABCD$ . Consequently, the sum of elementary internal shearing forces acting here will be

$$dT = \tau_f t_f dx$$

The equilibrium condition of the isolated parallelepiped can be written as follows:

$$\sum x = 0, \quad N_1 + dT - N_2 = dT - dN = 0$$

or

$$\tau_f t_f dx = \frac{dM}{J_y} S_y^0$$

wherefrom

$$\tau_f = \frac{QS_y^0}{J_y t_f} \tag{14.2}$$

Thus, Zhuravskii's formula (13.3) can also be employed for shearing stresses parallel to the neutral axis in thin-walled sections if quantity  $b$  in the denominator is taken as the width of the layer in which shearing stress is calculated, irrespective of whether the thin-walled section is assumed to be cut parallel or perpendicular to the neutral axis.

In our case (with the assumption that  $N_2 > N_1$ ) shearing stresses  $\tau_1$  in the left half of the top flange act in the cross section from left to right. It can be easily seen that in the left half of the lower flange, where the normal stresses are compressive and as before  $|\sigma_2| > |\sigma_1|$ , shearing stresses  $\tau_1$  act in the opposite direction (Fig. 200(d)); in the right half of the top flange they act from right to left (Fig. 200(e)), whereas in the right half of the lower flange from left to right.

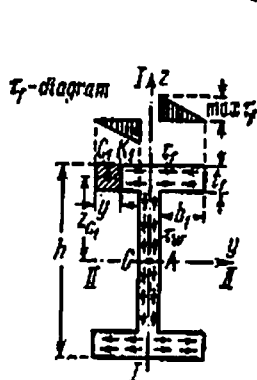


Fig. 201

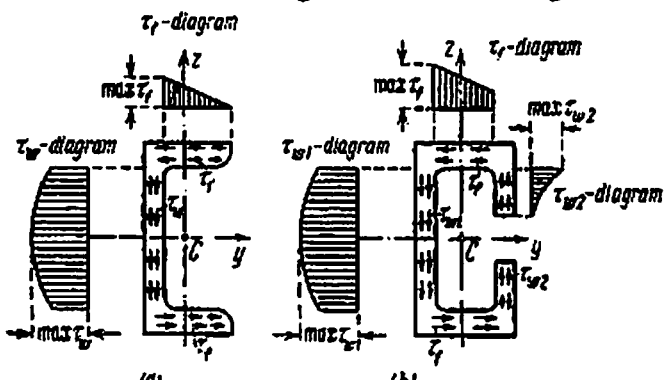


Fig. 202

The shearing stresses in the flanges and web of the thin-walled section form the so-called shearing stress "streamlines"; the streamlines for an I-section are depicted in Fig. 201.

Let us write the expression for shearing stresses  $\tau_1$ . One of the quantities in formula (14.2) is the static moment of the flange area hatched in Fig. 201:

$$S_y^0 = A_0 z_c = y t_f \frac{h - t_f}{2}$$

Therefore

$$\tau_1 = \frac{QS_y^0}{J_y t_f} = \frac{Q(h - t_f)y_1}{2J_y} \tag{14.3}$$

i.e. shearing stress  $\tau_1$  varies linearly along the flange length (in formula (14.3) the  $y$ -coordinate is to the first power). This stress becomes maximum when  $y = b_1$ :

$$\tau_{1 \max} = \frac{Q(h - t_f)b_1}{2J_y} \tag{14.4}$$

When  $b_1 < y < b_1 + t_w$ , the whole web of the I-section lies in the vertical section. The shearing stress is not distributed uniformly along the web height, therefore Zhuravskii's formula cannot be employed for its calculation. The shearing-stress ( $\tau_1$ ) diagram for I-section is shown in Fig. 201. The diagrams of shearing-stress distribution in the flanges and web of a channel section are depicted in Fig. 202(a); for a

C-section, in Fig. 202(b). The shearing-stress streamlines are shown in the cross section for each of these profiles.

When the shearing stresses have to be determined in the flange of a closed thin-walled profile symmetrical about the axis of loading (z-axis), for instance, at point  $K$  of the flange of a box section (Fig. 203), then one imaginary section must pass through point  $K$  and the

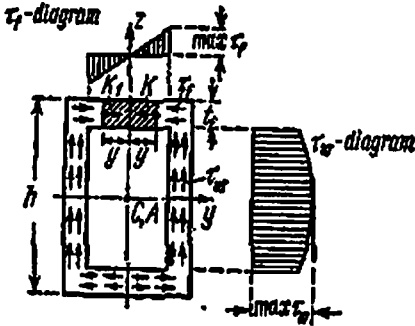


Fig. 203

other through a symmetrically located (with respect to the axis of loading) point  $K_1$ . In the numerator of formula (14.2) we introduce the static moment of the area of flange bounded by these two sections (the area is hatched in Fig. 203), and in the denominator the double thickness of the web (due to two sections). We obtain a formula for determining  $\tau_f$ , which is similar to formula (14.3). Figure 203 shows the shearing-stress diagrams in the flange and the web and also the shearing-stress streamlines in the profile.

If the web or flange of the thin-walled section is inclined to the plane of loading at an angle  $\alpha$ , then this circumstance must be taken into account while computing shearing stress by formulas (13.3) and/or (14.2) by introducing a factor  $\cos \alpha$  in the denominator of these formulas. Let us assume that an equal leg angle section beam is loaded in the plane of symmetry  $zOx$  (Fig. 204). The sum of projections on the z-axis of internal shearing forces, replaced in Fig. 204(a) by forces  $T$ , will be equal to  $2T \cos \alpha$ . As this sum of projections of the internal forces is equal to the shearing force  $Q$ ,

$$T = \frac{Q}{2 \cos \alpha}$$

Hence, shearing stress  $\tau_f$ , which may be considered uniformly distributed over the flange thickness, may be determined at some point  $K$  of the angle flange by the formula

$$\tau_f = \frac{QS_y^0}{J_y t_f \cos \alpha} = \frac{Qu t_f z_c}{J_y t_f \cos \alpha} = \frac{Qu \left( b - 2a - \frac{t_f}{2} - \frac{u}{2} \right)}{J_y}$$

where  $S_y^0$  is the static moment of the hatched area of the flange. Shearing stress  $\tau_f$  is maximum at point  $N$  on the  $y$ -axis where  $u = u_{\max} =$

$$= b - 2a - \frac{t_f}{2} :$$

$$\tau_{f \max} = \frac{Q}{2J_y} \left( b - 2a - \frac{t_f}{2} \right)^2 \tag{14.5}$$

B. If we consider Figs. 201-203, we note that when the I- and box beams are loaded in the plane coinciding with the principal central plane of inertia  $xOy$  (or  $xOz$ ), which is also the plane of symmetry of the beam, the internal shearing forces give a resultant equal to shearing force  $Q$  and directed along the axis of symmetry of the section (the shearing-stress streamlines are, so to say, in equilibrium).

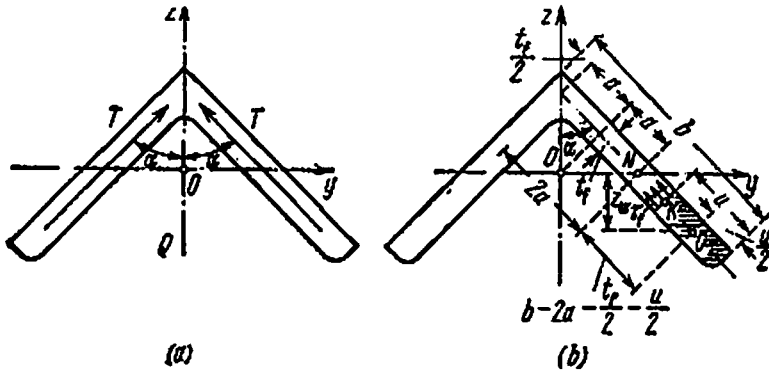


Fig. 204

However, if we consider channel, C- (Fig. 202(a) and (b)), T- (Fig. 207), equal leg and unequal leg angle (Figs. 208 and 209) sections also loaded in the plane coinciding with the principal central plane of inertia,  $xOz$ , but which is not the plane of symmetry of the beam, the internal shearing forces in the sections give the aforementioned resultant and a force couple about the  $x$ -axis of the beam. This implies that the resultant of internal shearing forces of the section equal to the shearing force  $Q$  passes not through the centre of gravity  $C$  along the principal central axis of inertia  $Oz$ , but parallel to this axis through some other point in the section. The beam consequently experiences torsion in addition to uni-planar bending.

The point through which the resultant of all internal shearing forces of the section passes (the moment of all internal shearing forces of the section about this point is zero) is known as *shear centre* or *flexural centre*, and the line parallel to the  $x$ -axis and joining the shear centres of all sections of the beam is called the *shear-centre line*. Obviously, for the beam to experience only uni-planar bending without torsion of the thin-walled section, the plane of application of external forces must pass through the shear-centre line parallel to one of the principal central planes of inertia of the beam. This ensures fulfilment of the condition of equilibrium according to which the product



of inertia of the section about the line of loading and a perpendicular neutral line must be zero, i.e. the beam experiences uni-planar bending. At the same time, the moment of external forces as well as the moment of internal shearing forces about the shear centre will be zero, i.e. the beam will not be subjected to torsion.

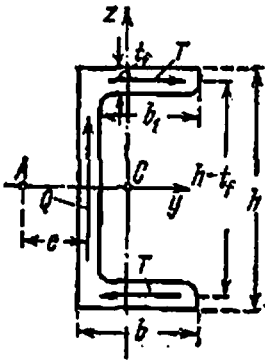


Fig. 205

Let us take the channel section (Fig. 205 and 206) as an example and explain how to determine the shear centre, point A. Neglecting the shearing stresses parallel to the axis in the flanges, we assume that internal shearing forces in the walls of a channel section give a resultant approximately equal to shearing force Q and directed along the middle line of the wall. The resultants of internal shearing forces in the flanges, acting parallel to the neutral line of the section, will be denoted by T and assumed to be applied at the middle of flange thickness

ness. Keeping in mind that shearing stress  $\tau_f$  in the flange varies linearly, with a maximum value according to formula (14.4) equal to

$$\tau_{f \max} = \frac{Q(h-t_f)b_f}{2J_y}$$

we may write the following expression for resultant T:

$$T = \tau_{f, \max} A_f = \frac{\tau_{f \max} \cdot 0}{2} t_f b_f = \frac{Q(h-t_f)b_f^2 t_f}{4J_y}$$

The condition according to which the moment of all internal shearing forces in the channel section about the shear centre is equal to zero may be written as follows:

$$Qe - T(h-t_f) = 0$$

wherefrom

$$e = \frac{T(h-t_f)}{Q} = \frac{(h-t_f)^2 b_f^2 t_f}{4J_y} \quad (14.6)$$

In the more complex cases the shear centre location can be determined by special methods which are discussed in the theory of bending and torsional deformations of thin-walled bars.

Let us note that the shear centre coincides with the centre of gravity of the section if the latter has two axes of symmetry (Figs. 201, 203). If the section has one axis of symmetry, the shear centre lies on this axis (Figs. 202, 207, 208). If the section consists of rectangles

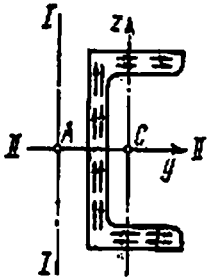


Fig. 206

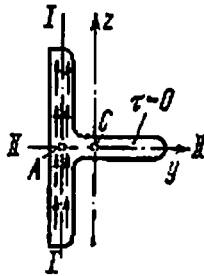


Fig. 207

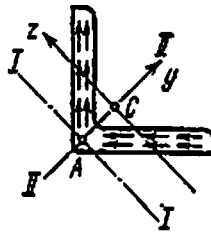


Fig. 208

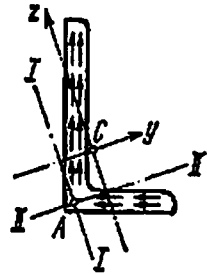


Fig. 209

whose middle lines intersect at one point, the shear centre lies at this point (Figs. 207, 208, 209). In these figures the shear centre is denoted by  $A$ , while  $I$  and  $II$  show the directions along which the loading leads to uni-planar bending of the beam without torsion.

§ 80. Riveted and Welded Beams

In the examples of selection of cross-sectional dimensions of beams which were discussed in preceding sections the required values of section moduli of I-beams were such that we were able to select rolled profiles in all the cases. The biggest rolled profile manufactured in the Soviet Union, the I-section No. 60, has a section modulus of about  $2560 \text{ cm}^3$ .

In practice, however, we often require profiles of considerably bigger size. In such cases we use composite beam sections by riveting plates and angles or by welding plates.

A riveted beam (Fig. 210) consists of a vertical plate 1, a number of pairs of horizontal plates 2 and angles 3. The angles and plates are joined by rivets. A welded beam (Fig. 211) consists of vertical and horizontal plates joined by welds.

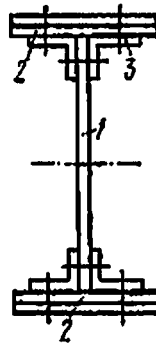


Fig. 210

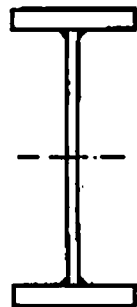


Fig. 211

The design of welded and riveted beams is treated in the courses on metal structures. There it is pointed out how to determine beam dimensions if the maximum bending moment is known.\* Given below is an example on checking the strength of a welded beam.

A schematic diagram of the beam, the forces acting on it, and the bending-moment and shearing-force diagrams are shown in Fig. 212.

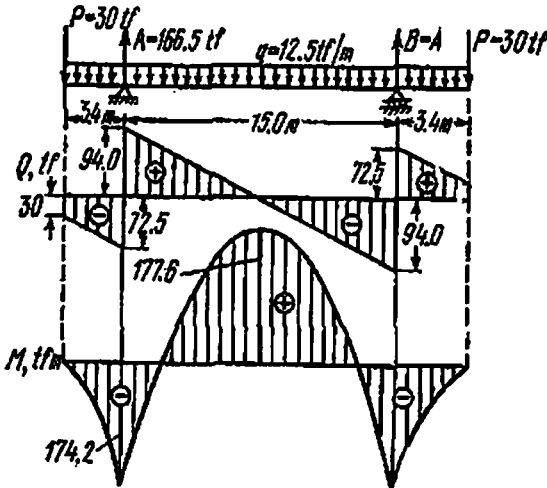


Fig. 212

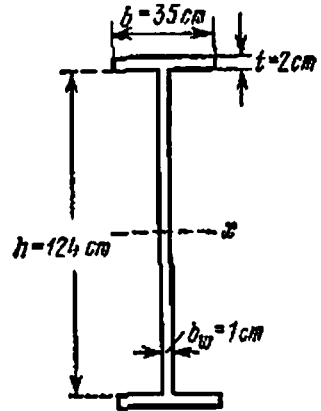


Fig. 213

The cross-sectional dimensions of the beam are given in Fig. 213. We have to check the strength of the beam as a whole and of the welded joints.

Let us calculate the moment of inertia of the whole section, working as a rigid one, about the principal  $x$ -axis:

$$J_x = \frac{1 \times 124^3}{12} + 2 \times 35 \times 2 \times 63^2 = 159\,000 + 555\,600 = 714\,600 \text{ cm}^4$$

The section modulus

$$W_x = \frac{J_x}{z_{\max}} = \frac{714\,600}{64} = 11\,160 \text{ cm}^3$$

The maximum normal stress in the beam at the middle of its span

$$\sigma_{\max} = \frac{M_{\max}}{W_x} = \frac{177.6 \times 10^5}{11\,160} = 1592 \text{ kgf/cm}^2$$

is less than the permissible stress which is 1600 kgf/cm<sup>2</sup>.

The shearing stresses at the upper or lower ends of the web

$$\tau_j = \frac{QS_y^0}{J_x b_w} = \frac{94 \times 10^3 \times 35 \times 2 \times 63}{714\,600 \times 1} = 580 \text{ kgf/cm}^2$$

\* The design of riveted and welded beams has been treated in detail in the previous editions of this book. See N. M. Belyaev, *Strength of Materials*, Nauka, Editions 7-14 (in Russian).

These shearing stresses will be taken up by a pair of welded seams (one on each side of the web) along planes  $I-I$  of dimension  $m$  each (Fig. 214). Therefore, while calculating shearing stresses in the seams, thickness  $2m$  of the two seams must be substituted in the denominator of the formula instead of  $b_w$ . The minimum design thickness of the seams is taken equal to 0.4 cm. For this value of  $m$  the shearing stresses in the seams are

$$\tau_s = \frac{QS_y^0}{J_x 2m} = \frac{94 \times 10^3 \times 35 \times 2 \times 63}{714600 \times 2 \times 0.4} = 725 \text{ kgf/cm}^2$$

or, what is the same

$$\tau_s = 580 \frac{b_w}{2m} = 580 \frac{1}{0.8} = 725 \text{ kgf/cm}^2$$

These stresses do not exceed the permissible shearing stress for welded joints.

The joint may also be made by intermittent seams (Fig. 215). The shearing force acts over length  $a$  and is taken up by seams of

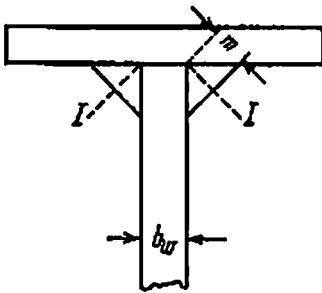


Fig. 214

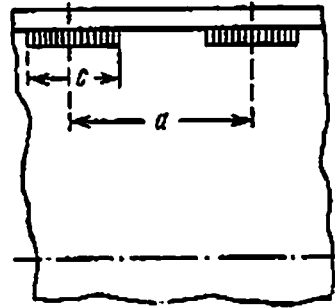


Fig. 215

length  $c$ . Therefore, everything else remaining the same, the stresses in intermittent seams (welded keys) will be  $\frac{a}{c}$  times greater than stresses in continuous seams of the same size. Now automatic welding of parts with continuous seams is generally used. Therefore, joints made with the help of intermittent seams are gradually becoming obsolete. The intermittent seams have the additional shortcoming that the beginning and end of each seam are pockets of local stress concentration, which is not taken into account by the design formulas.

The strength of the web should be checked against principal stresses at the base of the weld seam. This area will experience normal stresses of a considerable magnitude (from  $M=174.2$  tf·m) and shearing stresses which are just slightly less than  $580 \text{ kgf/cm}^2$ . The combination of these two stresses may considerably raise the principal and reduced stresses at this level.

# PART V

## Deformation of Beams Due to Bending

### CHAPTER 15

#### Analytical Method of Determining Deformations

##### § 81. Deflection and Rotation of Beam Sections

When external forces act in one of the principal planes of inertia of a beam, its axis is observed to bend in the same plane and uniplanar bending occurs.

In Fig. 216 the deformation of a beam rigidly fixed at one end and loaded at the other by a concentrated force is shown in an enlarged scale. The centre of gravity  $O$  of a section having abscissa  $x$  moves to  $O_1$ .

Displacement  $OO_1$  of the centre of gravity of a section in a direction perpendicular to the axis of the beam is called the *deflection of beam in the particular section* or the *deflection of the particular section of the beam*. We shall denote deflection by  $y$ .

Strictly speaking, since the beam axis lies in the neutral layer it does not change its length and the displaced point  $O_1$  must be slightly

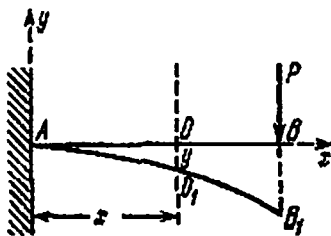


Fig. 216

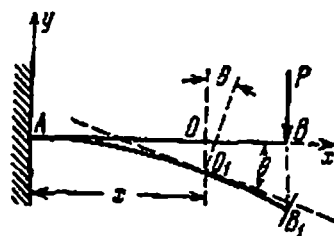


Fig. 217

to a side from the perpendicular to the beam axis. However, deflection  $y$  is usually small as compared to the length of the beam and the displacement of the perpendicular to a side represents a small quantity in comparison with deflections; it is therefore neglected.

During deformation sections of the beam remain plane and turn w.r.t. their original position. In Fig. 217 sections  $O-O_1$  and  $B-B_1$  are shown before and after deformation.

Angle  $\theta$  by which each section turns w.r.t. its original position is called the *angle of rotation of the section*. We must learn to calculate the deflection and angle of rotation in each section for practical application.

Maximum deflection can serve as a measure of the degree of distortion of the structure when it is acted upon by external forces. Generally, to prevent the beam joints from loosening and to reduce vibrations under a dynamic load the value of maximum deflection is restricted for a loaded beam. Thus, in steel beams, depending upon their designation, the maximum deflection should not exceed 1/1000-1/250 of the span.

Besides, we also require the value of deformation when solving statically indeterminate problems, in which the number of reactions is more than the number of equations of statics. The additional equations can be written only by studying the deformation of the structure. We must know how to calculate deflection  $y$  and angle of rotation  $\theta$  for every section in order to be able to determine the deformation completely. Both  $y$  and  $\theta$  are functions of  $x$ —the distance of the section from the centre of coordinates; there is a definite relation between  $y$  and  $\theta$  in each section.

Let us decide upon a coordinate system, which we shall use in future. The centre of coordinates will be a point on the original position of the beam axis, which we shall always select as the  $x$ -axis, and the  $y$ -axis shall be directed upwards, perpendicular to the beam axis before deformation. Under these conditions the equation

$$y = f(x) \quad (15.1)$$

represents the equation of a curve along which the beam bends when it is loaded; it is the *equation of the deflected axis of the beam*.

The tangent to the deflected axis of the beam (Fig. 217) at point  $O_1$  makes an angle  $\theta$  with the  $x$ -axis, i.e. an angle equal to the angle of rotation of the section about its original position. On the other hand we know that the tangent of the angle between the tangent to the curve  $y=f(x)$  and the  $x$ -axis is

$$\tan \theta = \frac{dy}{dx} \quad (15.2)$$

Since in actual practice the deflection of a beam is generally small as compared to its span, angle  $\theta$  is also very small and generally does not exceed  $1^\circ$ . For such a small value of the angle we may consider that the tangent of the angle is equal to the angle expressed in radians. It ensues that

$$\theta = \frac{dy}{dx} \quad (15.3)$$

i.e. the angle of rotation of a section is equal to the first derivative of the deflection in this section w.r.t.  $x$ .

Thus, the problem of studying the deformation of a beam narrows down to obtaining the equation of the deflected axis  $y=f(x)$ ; knowing the equation, we can calculate the angle of rotation in any section by differentiation.

## § 82. Differential Equation of the Deflected Axis

In order to obtain  $y$  as a function of  $x$ , we must establish a relation between the deformation of a beam due to external forces and its size and material. We had obtained such a relation before in § 63.

Let us make use of formula (11.10), which we had obtained while studying pure bending. Extending the formula over the general case of bending, i.e. neglecting the effect of the shearing force on deformation, we get the relation

$$\frac{1}{\rho(x)} = \frac{M(x)}{EJ}$$

where  $\rho(x)$  is the radius of curvature of the deflected axis between two adjacent sections at a distance  $x$  from the centre of coordinates,  $M(x)$  is the bending moment in the same section, and  $EJ$  is the rigidity of the beam. Generally, the effect of  $Q(x)$  on the deformation of beam is not large; the method of taking into account its effect is given in § 108.

Figure 218 depicts the change in the radii of curvature as the bending moment is increased. In order to obtain the equation of the deflected axis we shall employ the mathematical relation between the radius of curvature of the axis and its coordinates  $x$  and  $y$ :

$$\frac{1}{\rho(x)} = \pm \frac{\frac{d^2y}{dx^2}}{\sqrt{\left[1 + \left(\frac{dy}{dx}\right)^2\right]^{3/2}}} \quad (15.4)$$

Putting this value of curvature  $\frac{1}{\rho(x)}$  in formula (11.10), we get a differential equation which relates  $y$ ,  $x$ ,  $M(x)$  and  $EJ$ :

$$\pm \frac{\frac{d^2y}{dx^2}}{\sqrt{\left[1 + \left(\frac{dy}{dx}\right)^2\right]^{3/2}}} = \frac{M(x)}{EJ} \quad (15.5)$$

This is known as the *differential equation of the deflected axis* or quite often *differential equation of the elastic curve*.

In a vast majority of practical cases we find that  $\frac{dy}{dx}$ , representing the angle of rotation of a section of the beam, is a very small quantity. Therefore, its square may be neglected in comparison to unity; consequently, equation (15.5) may be written in a simpler way:

$$\pm \frac{d^2y}{dx^2} = \frac{M(x)}{EI}, \quad \text{or} \quad \pm EJ \frac{d^2y}{dx^2} = M(x) \quad (15.6)$$

This relation is known as the approximate differential equation of the deflected axis.

The convention for the sign of bending moments is decided irrespective of the direction of the coordinate axes; it is known that the second differential is positive if the concave side of the curve faces

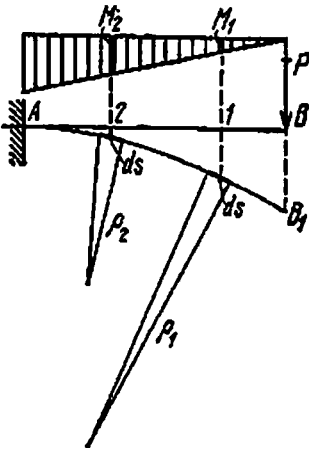


Fig. 218

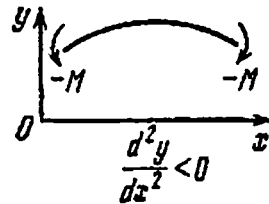
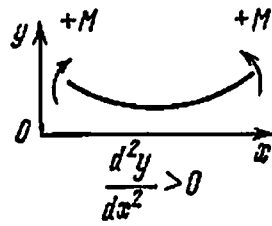


Fig. 219

the positive direction of the  $y$ -axis and negative if the convex side faces it (Fig. 219). Hence, the sign of the bending moment does not depend upon the location of the coordinate axes but the sign of the second differential does.

If the  $y$ -axis is directed upwards, then the positive sign should be used in equation (15.6); the negative sign should be used if the  $y$ -axis is directed downwards.

In the future we shall always direct the  $y$ -axis upwards, and the differential equation (15.6) may be written as:

$$EJ \frac{d^2y}{dx^2} = M(x) \quad (15.7)$$

The sign of the bending moment shall be selected according to the above convention.



The deflection may be obtained from the differential equation of the deflected axis by integrating equation (15.7). Bending moment  $M(x)$  is a function of  $x$ ; therefore, upon integration we get

$$EJ \frac{dy}{dx} = \int M(x) dx + C$$

Integrating once again,

$$EJy = \int dx \int M(x) dx + Cx + D$$

Thus we get the following equation for the angle of rotation:

$$\theta = \frac{dy}{dx} = \frac{1}{EJ} \left[ \int M(x) dx + C \right] \quad (15.8)$$

and the following equation for deflection:

$$y = \frac{1}{EJ} \left[ \int dx \int M(x) dx + Cx + D \right] \quad (15.9)$$

These equations have two constants of integration  $C$  and  $D$ . The method of calculating these constants will be shown in examples below.

Before we take up practical problems, we deem it necessary once again to emphasize that equation (15.7) is approximate; the error that we allow by neglecting the quantity  $\left(\frac{dy}{dx}\right)^2$  in comparison to unity is small only in those cases when the deformation of the beam is small in comparison with its size. If this condition is not satisfied, then the angles of rotation are found to be large enough so that their square cannot be ignored anymore; in such cases it becomes essential to integrate the whole of equation (15.5).

Examples of such cases are the deformation of thin springs and thin veneer and, generally, bending of flexible beams.

### § 83. Integration of the Differential Equation of the Deflected Axis of a Beam Fixed at One End

Consider a beam fixed at end  $A$  and loaded by a concentrated force  $P$  at the other end and a uniformly distributed force  $q$  along the whole length of the beam (Fig. 220); let  $l$  be the span of the beam. We shall designate point  $A$  as the centre of coordinates, direct the  $y$ -axis upwards and the  $x$ -axis towards the right. The differential equation of the deflected axis is:

$$EJy'' = M(x)$$

The bending moment in an arbitrary section at a distance  $x$  from the centre of coordinates is

$$M(x) = -P(l-x) - q \frac{(l-x)^2}{2} \quad (15.10)$$

$$EJy'' = -P(l-x) - q \frac{(l-x)^2}{2} \quad (15.11)$$

We integrate this equation twice:

$$EJy' = -P \left( lx - \frac{x^2}{2} \right) - \frac{q}{2} \left( l^2x - lx^2 + \frac{x^3}{3} \right) + C \quad (15.12)$$

$$EJy = -P \left( \frac{lx^2}{2} - \frac{x^3}{6} \right) - \frac{q}{2} \left( \frac{l^2x^2}{2} - \frac{lx^3}{3} + \frac{x^4}{12} \right) + Cx + D \quad (15.13)$$

To determine  $C$  and  $D$  we must locate such sections of the beam where the deflection as well as the angle of rotation are known. One of these sections lies over support  $A$ ; in this section at  $x=0$ ,  $y'=0$  and  $y=0$ . Putting these values first in equation (15.12) and then in (15.13), we get  $C=0$  and  $D=0$ . It is evident from the expressions of deflection and angle of rotation that constants  $C$  and  $D$ , when divided by rigidity  $EJ$  of the beam, give the corresponding values of angle of rotation and deflection in a section which lies at the origin of coordinates  $A$ . The constants  $C$  and  $D$  have the following dimensions:

$$[C] = \text{force} \times (\text{length})^2 \text{ and}$$

$$[D] = \text{force} \times (\text{length})^3$$

The fact that the constants of integration are found to be zero is a direct outcome of selecting the fixed end of the beam as the origin of coordinates. In plotting bending moment and shearing force diagrams we measured abscissa  $x$  from the loaded end of the beam; here it is more expedient to measure  $x$  from the fixed end to reduce the amount of calculations required to determine  $C$  and  $D$ ; this somewhat complicates the expression for  $M(x)$  but simplifies the determination of deformations. Having determined  $C$  and  $D$ , we can now transform the expressions for  $y$  and  $\theta$  in such a manner so that the brackets contain only dimensionless numbers, which is helpful in calculating the deflection and angle of rotation:

$$\theta = \frac{dy}{dx} = -\frac{Plx}{2EJ} \left( 2 - \frac{x}{l} \right) - \frac{ql^2x}{6EJ} \left( 3 - \frac{3x}{l} + \frac{x^2}{l^2} \right) \quad (15.14)$$

$$y = -\frac{Plx^2}{6EJ} \left( 3 - \frac{x}{l} \right) - \frac{ql^2x^2}{24EJ} \left( 6 - \frac{4x}{l} + \frac{x^2}{l^2} \right) \quad (15.15)$$

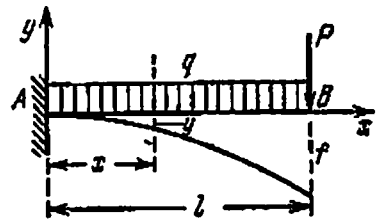


Fig. 220

With the help of these expressions we can determine the maximum values of  $y$  and  $\theta$ . From the designer's point of view the maximum absolute value of deflection  $y$  is of greater interest; therefore, besides the analytical maximum of function  $y$  at  $\theta = \frac{dy}{dx} = 0$ , we must also find its value at the ends of the span. In the example under consideration the maximum deflection  $y$  occurs at point  $B$ , where  $\theta$  is not zero. The analytical maximum of function  $y$  is equal to zero at point  $A$ .

We shall denote the deflections in various sections by letter  $f$  with an index showing the section in which it occurs. Thus at  $x=l$

$$f_B = -\frac{Pl^3}{3EJ} - \frac{ql^3}{8EJ} \quad (15.16)$$

The minus sign shows that the deflection is in the downward direction. Obviously, the maximum angle of rotation will occur in the same section; it will be

$$\theta_B = -\frac{Pl^2}{2EJ} - \frac{ql^2}{6EJ} \quad (15.17)$$

The minus sign indicates that the section turns in the clockwise direction.

Both expressions (15.16) and (15.17) show the separate effect of  $P$  and  $q$  on the deflection and angle of rotation, respectively. When one of the forces is absent, the corresponding part of expression becomes zero.

To have an idea about the magnitude of deformation let us take  $P=2$  tf,  $q=0.5$  tf/m,  $l=2$  m,  $E=2 \times 10^6$  kgf/cm<sup>2</sup>, permissible stress  $[\sigma]=1400$  kgf/cm<sup>2</sup>, and select an I-beam from the specification table. The strength condition for the beam may be written as:

$$W = \frac{M_{\max}}{[\sigma]} = \frac{(2 \times 2 + 0.5 \frac{2 \times 2}{2}) 10^6}{1400} = 357 \text{ cm}^3$$

From the standard table for I-beams (see Appendix) we find I-beam No. 27 having  $W=371$  cm<sup>3</sup>,  $J=5010$  cm<sup>4</sup>. The angle of rotation and deflection may be calculated as

$$\theta_B = -\left(\frac{2 \times 2^2}{2} + 0.5 \frac{2^3}{6}\right) \frac{10^7}{2 \times 10^6 \times 5010} = \frac{1}{215} \text{ radian}$$

$$f_B = -\left(\frac{2 \times 2^3}{3} + 0.5 \frac{2^4}{8}\right) \frac{10^9}{2 \times 10^6 \times 5010} = -0.63 \text{ cm}$$

The maximum deflection constitutes  $(0.63/200) = \frac{1}{320}$  of the beam span, while the square of the maximum angle of rotation  $\left(\frac{1}{215}\right)^2 = 1.46 \text{ 000}$ , i.e. it is negligibly small as compared to unity in formula (15.5).

### § 84. Integrating the Differential Equation of the Deflected Axis of a Simply Supported Beam

Let us find the deformation of a simply supported beam, loaded uniformly by a continuous force  $q$  (Fig. 221). The origin of coordinates lies at the left support and the  $x$ -axis is directed towards the right. A distinguishing feature of this problem as compared to the previous

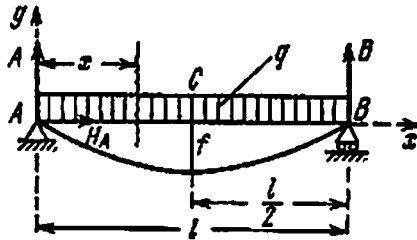


Fig. 221

one is that the support reactions must be determined in order to find an expression for  $M(x)$ .

From symmetry  $A=B=\frac{ql}{2}$  and  $H_A=0$ . We calculate in the following order:

$$EJ \frac{d^2y}{dx^2} = M(x), \quad M(x) = +\frac{ql}{2}x - \frac{qx^2}{2} = +\frac{q}{2}(lx - x^2)$$

$$EJ \frac{d^2y}{dx^2} = \frac{q}{2}(lx - x^2)$$

$$EJ \frac{dy}{dx} = \frac{q}{2} \left( \frac{lx^2}{2} - \frac{x^3}{3} \right) + C \quad (15.18)$$

$$EJy = \frac{q}{2} \left( \frac{lx^3}{6} - \frac{x^4}{12} \right) + Cx + D \quad (15.19)$$

We know the following values of deflection: at support  $A$ , i.e. at  $x=0$ , deflection  $y=0$ , and at support  $B$ , i.e. at  $x=l$ , deflection  $y=0$ .

Applying formula (15.19) to section  $A$  first, we get:

$$D = 0$$

Then applying it to section  $B$ , we get the following equation:

$$0 = \frac{q}{2} \left( \frac{l^3}{6} - \frac{l^4}{12} \right) + Cl$$

wherefrom

$$C = -\frac{ql^3}{24}$$

The formulas for  $y$  and  $\frac{dy}{dx}$  may now be written as follows:

$$EJ \frac{dy}{dx} = \frac{q}{2} \left( \frac{lx^2}{2} - \frac{x^3}{3} \right) - \frac{ql^3}{24} = -\frac{ql^3}{24} \left( 1 - \frac{6x^2}{l^2} + \frac{4x^3}{l^3} \right) \quad (15.20)$$

$$EJy = \frac{q}{2} \left( \frac{lx^3}{6} - \frac{x^4}{12} \right) - \frac{ql^3}{24} x = -\frac{ql^3x}{24} \left( 1 - \frac{2x^2}{l^2} + \frac{x^3}{l^3} \right) \quad (15.21)$$

In order to find the maximum deflection we must determine the section in which  $\theta=0$ ; from symmetry this must be the middle section. By putting  $\frac{x}{l} = \frac{1}{2}$  in formula (15.20) we find that  $\theta = \frac{dy}{dx}$  becomes zero; under these conditions:

$$f_{\max} = -\frac{5ql^4}{384EJ}$$

The maximum values of  $\theta$  occur at  $x=0$  and  $x=l$ :

$$\theta_{\max} = \mp \frac{ql^3}{24EJ}$$

In this example also we find that  $\frac{D}{EJ}$  is the deflection of the beam at the origin of coordinates and  $\frac{C}{EJ}$  is the angle of rotation of the section at support  $A$ , which coincides with the origin of coordinates.

In all the above examples, if we direct the  $y$ -axis upwards and the  $x$ -axis towards the right, then a negative value of  $\theta$  corresponds to

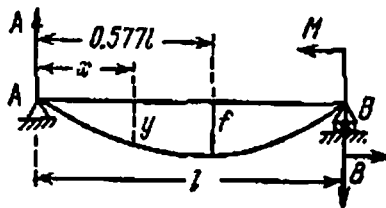


Fig. 222

clockwise and a positive value corresponds to anticlockwise rotation of the section.

Let us determine the deformation in one more case of a simply supported beam. Assume that the beam is acted upon by a moment  $M$  at the right-hand support (Fig. 222). Reactions  $A$  and  $B$  give a moment  $M$  and are equal to

$$A = B = \frac{M}{l}$$

We assume the left-hand support to be the origin of coordinates; therefore

$$EJ \frac{d^2y}{dx^2} = M(x) = + Ax = + \frac{M}{l} x$$

$$EJ \frac{dy}{dx} = \frac{Mx^2}{2l} + C, \quad EJy = \frac{Mx^3}{6l} + Cx + D$$

The constants of integration are determined from the condition that the deflection at supports *A* and *B* is zero: at  $x=0$  deflection  $y=0$ , wherefrom  $D=0$ ; at  $x=l$  deflection  $y=0$ , wherefrom  $C = -\frac{Ml}{6}$ . Therefore

$$\theta = \frac{dy}{dx} = -\frac{Ml}{6EJ} \left( 1 - \frac{3x^2}{l^2} \right) \quad (15.22)$$

$$y = -\frac{Mlx}{6EJ} \left( 1 - \frac{x^2}{l^2} \right)$$

The maximum deflection occurs in the section where  $\frac{dy}{dx} = 0$ , therefore

$$1 - 3 \frac{x_0^2}{l^2} = 0$$

The abscissa of this section is

$$x_0 = \frac{l}{\sqrt{3}} = 0.577l \quad (15.23)$$

Maximum deflection is

$$f = -\frac{Ml \times l}{6 \sqrt{3} EJ} \left( 1 - \frac{l^2}{3l^2} \right) = -\frac{Ml^3}{9 \sqrt{3} EJ} = -\frac{Ml^3}{15.6EJ}$$

and deflection at the middle of the span is

$$f_{l/2} = -\frac{Ml^3}{12EJ} \left[ 1 - \frac{l^2}{4l^2} \right] = -\frac{Ml^3}{16EJ}$$

The deviation from the maximum deflection is of the order of 2.5%; thus even for such a highly unsymmetric loading as this we can with sufficient accuracy assume that the maximum deflection in a simply supported beam occurs at the middle of the span.

### § 85. Method of Equating the Constants of Integration of Differential Equations When the Beam Has a Number of Differently Loaded Portions

In the examples discussed above the beams were identically loaded along the whole length and there were two constants of integration, *C* and *D*. Every portion of new loading adds two constants of integra-

tion and complicates solution of the problem if we do not follow the rules which reduce the number of constants of integration to two, irrespective of the number of differently loaded portions.

Let us consider a beam with three differently loaded portions (Fig. 223). Let us decide to have a common origin of coordinates for

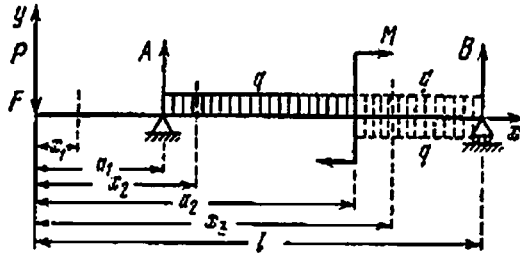


Fig. 223

all the portions—at the left or right end of the beam—and while writing the bending moment expression consider that portion which includes the origin of coordinates.

Let  $F$  be the origin of coordinates. We write the equation of the deflected beam axis in the first portion and integrate it twice:

$$EJy_1'' = -Px_1$$

$$EJy_1' = -\frac{Px_1^2}{2} + C_1 \quad (15.24)$$

$$EJy_1 = -\frac{Px_1^3}{6} + C_1x_1 + D_1 \quad (15.25)$$

The bending moment expression for the second portion should be written in such a way so that summands  $EJy''$ ,  $EJy'$  and  $EJy$  coincide with identical quantities of the equations of the first portion in the boundary section (over support  $A$ ). This will take place if  $(x-a)$ , which represents the arm of the force that is absent in the first portion, is integrated with respect to  $d(x-a)$  or, in other words, without opening the brackets. Let us point out that  $x$  is the abscissa of an arbitrary section of the portion under consideration;  $a$  is the abscissa of the starting point of this portion.

Let us now write three equations for the second portion:

$$EJy_2'' = -Px_2 + A(x_2 - a_1) - \frac{q(x_2 - a_1)^2}{2}$$

$$EJy_2' = -\frac{Px_2^2}{2} + \frac{A(x_2 - a_1)^2}{2} - \frac{q(x_2 - a_1)^3}{6} + C_2 \quad (15.26)$$

$$EJy_2 = -\frac{Px_2^3}{6} + \frac{A(x_2 - a_1)^3}{6} - \frac{q(x_2 - a_1)^4}{24} + C_2x_2 + D_2 \quad (15.27)$$

In the section at support  $A$  the angles of rotation computed from equations (15.24) and (15.26) must be equal, i.e. the beam axis must

bend smoothly over support  $A$ . The deflections at the support, calculated from equations (15.25) and (15.27), must also be equal. In other words,  $y'_1=y'_2$  and  $y_1=y_2$  when  $x_1=x_2=a_1$ . From these conditions we find  $C_1=C_2=C$  and  $D_1=D_2=D$ .

Let us now pass over to the third portion. There is no distributed load on this portion. In order to retain the bending moment expressions due to distributed load in their previous form, it is necessary to extend the distributed load of the second portion to the end of the beam and for compensating this extra load apply an identical load of opposite sign. These transformations will not disturb the equilibrium of the beam nor will they change the support reactions.

To ensure that the new load in the form of a concentrated moment  $M$  does not change the structure of the three equations of the third portion as compared to the second, moment  $M$  should be multiplied by  $(x-a)$  to the power zero; this affects neither the units of the force, nor the conditions of equilibrium.

In the light of the above, let us now write the equation of the deflected beam axis and integrate it twice:

$$EJy_3'' = -Px_3 + A(x_3 - a_1) - \frac{q(x_3 - a_1)^2}{2} + \frac{q(x_3 - a_2)^2}{2} + M(x_3 - a_2)^0$$

$$EJy_3' = -\frac{Px_3^2}{2} + \frac{A(x_3 - a_1)^2}{2} - \frac{q(x_3 - a_1)^3}{6} + \frac{q(x_3 - a_2)^3}{6} + M(x_3 - a_2) + C_3 \quad (15.28)$$

$$EJy_3 = -\frac{Px_3^3}{6} + \frac{A(x_3 - a_1)^3}{6} - \frac{q(x_3 - a_1)^4}{24} + \frac{q(x_3 - a_2)^4}{24} + \frac{M(x_3 - a_2)^2}{2} + C_3x_3 + D_3 \quad (15.29)$$

At the boundary section (where  $M$  is applied) we have the following conditions for equating the constants of integration:  $y_2'=y_3'$  and  $y_2=y_3$  when  $x_2=x_3=a_2$ . Substituting the first of these conditions in equations (15.26) and (15.28), we find that  $C_2=C_3=C$ . Substituting the second condition in equations (15.27) and (15.29) we find  $D_2=D_3=D$ .

The constants of integration are reduced to two:  $C$  and  $D$ . For determining these constants we employ the following conditions: deflection of beam at supports  $A$  and  $B$  is equal to zero, i.e. at  $x_1=a_1$ ,  $y_1=0$  and at  $x_3=l$ ,  $y_3=0$ . After substituting these conditions in equations (15.25) and (15.29) we get the following two equations:

$$-\frac{Pa_1^3}{6} + Ca_1 + D = 0 \quad (15.30)$$

$$-\frac{Pl^3}{6} + \frac{A(l - a_1)^3}{6} - \frac{q(l - a_1)^4}{24} + \frac{q(l - a_2)^4}{24} + \frac{M(l - a_2)^2}{2} + Cl + D = 0 \quad (15.31)$$



The values of  $C$  and  $D$  are obtained by simultaneous solution of equations (15.30) and (15.31).

We considered all the three portions and wrote three equations for each of them to show how to reduce the number of constants of integration to two:  $C$  and  $D$ . While solving other problems it is not at all necessary to again write all equations for each portion, it is sufficient to write three equations only for the portion which is farthest from the origin of coordinates. All summands of the right-hand side of the equations will pertain to this portion. At this stage it is desirable to mark the summands which pertain to the previous portions. One of the ways of marking is shown in the next lines:

$$EJy' = \underbrace{-\frac{Px^2}{2}}_1 + \underbrace{\frac{A(x-a_1)^2}{2} - \frac{q(x-a_1)^3}{6}}_2 + \underbrace{\frac{q(x-a_2)^3}{6} + M(x-a_2)}_3 + C \quad (15.32)$$

$$EJy = \underbrace{-\frac{Px^3}{6}}_1 + \underbrace{\frac{A(x-a_1)^3}{6} - \frac{q(x-a_1)^4}{24}}_2 + \underbrace{\frac{q(x-a_2)^4}{24} + \frac{M(x-a_2)^2}{2}}_3 + Cx + D \quad (15.33)$$

Here  $C$  and  $D$  pertain to all the portions. Sometimes  $C$ ,  $Cx$  and  $D$  are written in the beginning of the right-hand side of equations (15.32) and (15.33).

The method of equating the constants of integration was first proposed by R.F.A. Clebsch.

### § 86. Method of Initial Parameters for Determining Displacements in Beams

If we take a careful look at the equations for angle of rotation (15.32) and deflection (15.33), obtained by Clebsch's method and discussed in the preceding section, we can note that load in the form of concentrated moment  $M$  was respectively reflected in these equations as

$$M(x-a) \quad \text{and} \quad \frac{M(x-a)^2}{2}$$

The significance of the parentheses was earlier explained in § 85. Let us recall that  $x$  is the abscissa of an arbitrary section in the portion of beam under consideration and  $a$  is the abscissa of the starting point of this portion.

Concentrated force  $P$  and support reaction  $A$  were reflected in the same equations as

$$\frac{P(x-a)^2}{2} \quad \text{and} \quad \frac{P(x-a)^3}{6}$$

Uniformly distributed force  $q$  entered the equations as

$$\frac{q(x-a)^3}{6} \quad \text{and} \quad \frac{P(x-a)^4}{24}$$

It was mentioned in § 83 that the constants of integration  $C$  and  $D$  are angle of rotation ( $\theta_0$ ) and deflection ( $y_0$ ) at the origin of coordinates, respectively, multiplied by  $EJ$ . We may, therefore, write  $C = EJ\theta_0$  and  $D = EJy_0$ .

Keeping in mind that in a beam having a number of differently loaded portions there may be a number of concentrated moments  $M$ , a number of concentrated forces  $P$  and the uniformly distributed force  $q$  may be acting on a number of portions, the equations for angle of rotation (15.32) and deflection (15.33) may be written in the following general form:

$$EJy' = EJ\theta_0 + \sum M(x-a) + \sum P \frac{(x-a)^2}{2} + \sum q \frac{(x-a)^3}{6} \quad (15.34)$$

$$EJy = EJy_0 + EJ\theta_0 x + \sum M \frac{(x-a)^2}{2} + \sum P \frac{(x-a)^3}{6} + \sum q \frac{(x-a)^4}{24} \quad (15.35)$$

This method of writing the displacement equations is known as the *method of initial parameters*, while the equations are called the *general equations of the method of initial parameters*.

This method was first mentioned in the works of Prof. N. P. Puzyrevskii and Academician A. N. Krylov.

The application of this method will be illustrated in an example in the next section.

### § 87. Simply Supported Beam Unsymmetrically Loaded by a Force

Let us write the displacement equations (15.34) and (15.35) for the beam shown in Fig. 224 by the method of initial parameters:

$$EJy' = EJ\theta_0 + A \frac{x^2}{2} - P \frac{(x-a)^2}{2} \quad (15.36)$$

$$EJy = EJy_0 + EJ\theta_0 x + A \frac{x^3}{6} - P \frac{(x-a)^3}{6} \quad (15.37)$$

According to the first condition (at  $x=0$ ,  $y_A=0$ ) equation (15.37) changes into an identity:  $0=0$ . The second condition (at  $x=l$ ,  $y_B=0$ ) applied to equation (15.37) yields the following:

$$EJ\theta_0 l + A \frac{l^3}{6} - P \frac{(l-a)^3}{6} = 0$$

After substituting  $A = \frac{Pb}{l}$  and  $(l-a) = b$ , we obtain the following expression for the initial parameter, the angle of rotation at support A:

$$\theta_A = -\frac{Pb}{6EJl}(l^2 - b^2)$$

Knowing now the angle of rotation and deflection at the origin of coordinates and keeping in mind the above two substitutions, we rewrite equations (15.36) and (15.37) in the final form:

$$EJy' = -\frac{Pb}{6l}(l^2 - b^2) + \frac{Pbx^2}{2l} - \frac{P(x-a)^2}{2} \quad (15.38)$$

$$EJy = -\frac{Pbx}{6l}(l^2 - b^2) + \frac{Pbx^3}{6l} - \frac{P(x-a)^3}{6} \quad (15.39)$$

As it has been assumed in Fig. 224 that  $a > b$ , the maximum deflection will occur in the first portion between the middle of beam and point of application of force  $P$ . We shall therefore not include in further

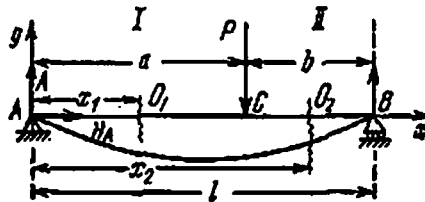


Fig. 224

calculations the last summands having the factor  $(x-a)$  as they pertain to the second portion.

The angle of rotation is zero in the section of maximum deflection (at  $x = x_c$ ); therefore

$$EJy' = -\frac{Pb}{6l}(l^2 - b^2) + \frac{Pbx_c^2}{2l} = 0$$

wherfrom

$$x_c = \sqrt{\frac{l^2 - b^2}{3}} \quad (15.40)$$

Let us now calculate the maximum deflection in this section:

$$EJf_{\max} = -\frac{Pb(l^2 - b^2)\sqrt{l^2 - b^2}}{6l\sqrt{3}} + \frac{Pb(l^2 - b^2)\sqrt{l^2 - b^2}}{6l3\sqrt{3}}$$

$$f_{\max} = -\frac{Pb\sqrt{(l^2 - b^2)^3}\sqrt{3}}{27EJl} = -\frac{Pbl^2\sqrt{3}\sqrt{\left(1 - \frac{b^2}{l^2}\right)^3}}{27EJ} \quad (15.41)$$

If force  $P$  is shifted to the centre of the beam, i.e. if we take  $a=b=0.5l$ , the deflection in the section of application of force  $P$  becomes

$$f_{l/2} = -\frac{Pl^3 \sqrt{3} \times 3\sqrt{3}}{54EJ \times 8} = -\frac{Pl^3}{48EJ} \quad (15.42)$$

If, on the other hand, force  $P$  is shifted towards the right support so that in the limit  $b$  tends to zero, then for  $b \rightarrow 0$

$$x_c = \frac{l}{\sqrt{3}} = 0.577l$$

Thus, when force  $P$  is shifted from the middle of the beam to support  $B$ , the point of maximum deflection changes its abscissa merely from  $0.5l$  to  $0.577l$  (Fig. 225) (see also formula (15.23)).

If force  $P$  acts as shown in Fig. 224, the deflection at the middle of span is

$$f_{l/2} = -\frac{Pb}{48EJ} (3l^2 - 4b^2) \quad (15.43)$$

By substituting the numerical values of all the quantities in formulas (15.41) and (15.43) we can confirm that the difference between the magnitudes of the two deflections is very small, which makes it

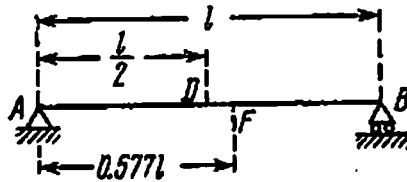


Fig. 225

possible to calculate the deflection for practical purposes at the middle of span without determining the location and magnitude of maximum deflection. This is valid in all those cases in which the bending moment diagram is unique.

### § 88. Integrating the Differential Equation for a Hinged Beam

In the preceding examples the portions into which the beam was divided for writing the equation of the deflected axis corresponded to similar portions of the bending moment diagram. The continuity of the beam axis is broken by the hinge. Therefore, while integrating the equation of the deflected axis, the portion containing the hinge should be divided into two, although the bending moment equation is the same on both sides of the hinge. Only the deflections of the ele-

ments joined by a hinge are equal at the joint; the angles of rotation of the sections are different. Therefore the equation of the deflected axis is different for parts of the beam which are joined by a hinge.

Let us consider the beam shown in Fig. 226; there is a hinge in section C. To keep the calculations simple we shall load the beam only by a moment  $M$  acting in section B. The reaction  $B$  can be found

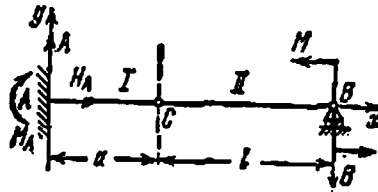


Fig. 226

easily by equating to zero the sum of the moments of all forces (i.e.  $B$  and  $M$ ) to the right of the hinge with respect to point C. We get  $B = \frac{M}{l}$ .

Reaction  $A$  may be determined by taking the projection on the vertical axis of all the forces acting on beam  $ACB$  (i.e. forces  $A$  and  $B$ ). We get  $A = \frac{M}{l}$ . The reactive moment  $M_A$  is equal to the sum of moments of forces  $M$  and  $B$  about point  $A$ :

$$M_A = -M \frac{a}{l}$$

Let us select point  $A$  as the origin of coordinates. The bending moment in any section of the beam between  $A$  and  $B$  can be expressed by the formula:

$$M(x) = \frac{M}{l}x - \frac{M}{l}a = \frac{M}{l}(x-a)$$

To obtain the equation of the deflected axis we must consider two portions,  $AC$  and  $CB$ . The differential equations and their integrals may be written as follows:

First Portion	Second Portion
$EJ \frac{d^2 y_1}{dx^2} = \frac{M}{l}(x-a)$	$EJ \frac{d^2 y_2}{dx^2} = \frac{M}{l}(x-a)$
$EJ \frac{dy_1}{dx} = \frac{M}{l} \left( \frac{x^2}{2} - ax \right) + C_1$	$EJ \frac{dy_2}{dx} = \frac{M}{l} \left( \frac{x^2}{2} - ax \right) + C_2$
$EJ y_1 = \frac{M}{l} \left( \frac{x^3}{6} - \frac{ax^2}{2} \right) + C_1 x + D_1$	$EJ y_2 = \frac{M}{l} \left( \frac{x^3}{6} - \frac{ax^2}{2} \right) + C_2 x + D_2$

We have the following four conditions from which to determine the constants of integration:

$$\text{in section } A: \frac{dy_1}{dx} = 0 \quad \text{and} \quad y_1 = 0 \quad \text{at} \quad x = 0$$

$$\text{in section } C: y_1 = y_2 \quad \text{at} \quad x = a$$

$$\text{in section } B: y_2 = 0 \quad \text{at} \quad x = a + l$$

From the first two conditions we get:

$$C_1 = 0, \quad D_1 = 0$$

From the last two conditions we get:

$$\frac{M}{l} \left( \frac{a^3}{6} - \frac{a^2}{2} \right) = \frac{M}{l} \left( \frac{a^3}{6} - \frac{a^2}{2} \right) + C_2 a + D_2$$

$$\frac{M}{l} \left[ \frac{(a+l)^3}{6} - \frac{a(a+l)^2}{2} \right] + C_2 (a+l) + D_2 = 0$$

wherefrom

$$C_2 = - \frac{M(a+l)^2(l-2a)}{6l^2}, \quad D_2 = \frac{M(a+l)^2(l-2a)a}{6l^3}$$

We shall explain the outlines of the solution for determining the deflection of the beam shown in Fig. 227.

The beam has six portions, therefore we get 12 constants of integration when we write down equations for determining the deformations.

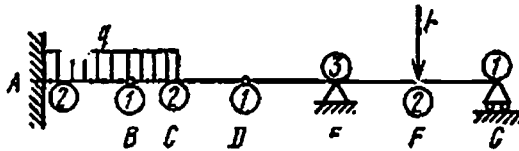


Fig. 227

It is evident that sections separating the different loaded portions, the supports and the hinges will give us the required 12 equations. The fixed end *A* gives two equations: the deflection equal to zero and angle of rotation equal to zero. The hinged end *G* gives one equation: deflection equal to zero. Hinges *B* and *D* give one equation each: the portions to the left and right of the hinge have equal deflection at the hinge.

Sections separating the differently loaded portions (section *C*, where the distributed load finishes, and section *F*, where the concentrated force *P* is applied) give two equations each: the deflections of portions to the left and right of the section are equal and the angles of rotation of these portions are also equal. The hinged intermediate support *E* gives three equations: equality of the deflections, equality

of the angles of rotation and that both the deflections are zero in this section.

In Fig. 227 the number of equations that each section gives has been circumscribed.

### § 89. Superposition of Forces

Hooke's law is true not only for the beam material but for the beam as a whole; the deflections and angles of rotation are directly proportional to the external forces. This is a direct outcome of the linear relation between the bending moment and load, and the curvature and the bending moment. For a beam fixed rigidly at one end and loaded with a distributed force  $q$  and a concentrated force  $P$  acting at the free end the bending moment in a section at a distance  $x$  from the fixed end can be written as a function of force according to the following formula:

$$M(x) = -P(l-x) - q \frac{(l-x)^2}{2} \quad (15.10)$$

The relationship between curvature and bending moment is also linear:

$$EJ \frac{d^2y}{dx^2} = M(x) = - \left[ P(l-x) + \frac{q(l-x)^2}{2} \right] \quad (15.11)$$

Therefore upon integration w.r.t.  $x$  we get an expression for  $y$  as a linear function of external forces:

$$y = - \frac{Plx^2}{6EJ} \left[ 3 - \frac{x}{l} \right] - \frac{ql^2x^2}{24EJ} \left[ 6 - \frac{4x}{l} + \frac{x^2}{l^2} \right]$$

In cases of compound loading this result enables us to obtain the equation of the deflected axis by adding the ordinates of curves corresponding to individual forces. This simplifies the computation of maximum deflection in some cases.

Let us study the application of the method of superposition of forces in determining the deformation of a cantilever's end  $A$  of a single-span beam  $ABC$  (Fig. 228). By replacing the effect of the distributed force  $q$  of cantilever  $AB$  on portion  $BC$  by a moment  $M_0 = -\frac{qa^2}{2}$ , we can calculate the angle of rotation of the beam in section  $B$  by using formula (15.22) given in § 84:

$$\theta_B = \frac{M_0 l}{3EJ} = \frac{qa^2 l}{6EJ}$$

When section  $B$  rotates, the straight axis of cantilever  $AB$  also bends by an angle  $\theta_B$  and the deflection of the cantilever's end  $A$  will be

$$f'_A = \overline{AA_1} = -\theta_B a = -\frac{M_0 l a}{3EJ} = -\frac{q l a^3}{6EJ}$$

Under the action of distributed force  $q$  the cantilever does not remain straight; it bends and acquires position  $A_2B$  (without, however, changing the angle of rotation  $\theta_B$  in section  $B$ ), and the deflection at

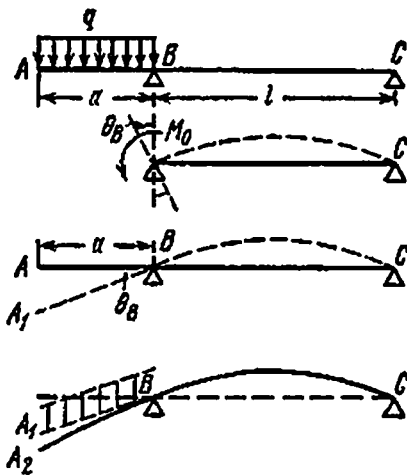


Fig. 228

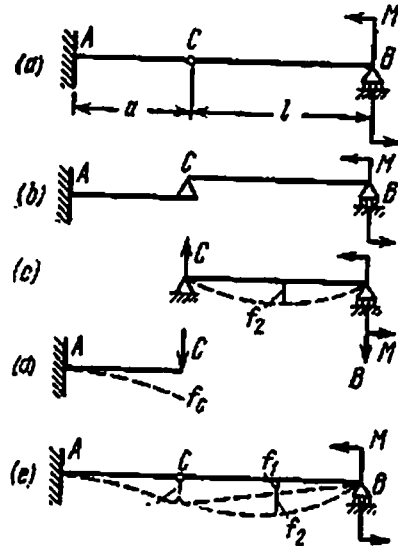


Fig. 229

end  $A$  of the cantilever can be expressed by the same formula which is employed for deflection of cantilever beams under bending (see § 83, formula (15.16))

$$f''_A = \overline{A_1A_2} = -\frac{q a^4}{8EJ}$$

the total deflection of cantilever end  $A$  will be:

$$f_A = f'_A + f''_A = -\frac{q l a^3}{6EJ} - \frac{q a^4}{8EJ} = -\frac{q a^3 (4l + 3a)}{24EJ}$$

The displacements of hinged beams can also be determined by using the method of superposition of forces. For this the beam should be divided into the number of beams comprising it, each of these beams should be studied separately and then the individual displacements should be added up.

Thus, for example, the schematic diagram of the beam discussed in § 88 (Fig. 229(a)) may be replaced by the diagram shown in Fig. 229(b). In this diagram the "suspended" beam  $CB$  is supported at its left end  $C$  by the right end  $C$  of the main beam  $AC$ . The effect of the hinge may be replaced by forces  $C$  (Fig. 229(c) and (d)).



Force  $C$  can be determined by studying the equilibrium of beam  $CB$ ; for this beam, force  $C$  is a passive force as it is the reaction of beam  $AC$ . An active force  $C$  of the same magnitude will act on beam  $AC$ —this force is the pressure of beam  $CB$  on beam  $AC$ .

The deflection of beam  $CB$ , shown separately in Fig. 229(c), can be determined at any point. The deflection of beam  $AC$  may be determined as shown in Fig. 229(d). Both these cases were discussed in §§ 83 and 84.

The deformation of beam  $ACB$  is shown in Fig. 229(e). Portion  $AC$  of beam  $ACB$  experiences the same deflection over its whole length, as beam  $AC$  separately. The deflection of portion  $CB$  of beam  $ACB$  consists of two deflections: deflection  $f_1$ , which is a component of deflection  $f_C$  (directly proportional to the distance from point  $B$ ), and deflection  $f_a$ , calculated for beam  $CB$  according to the schematic diagram in Fig. 229(c).

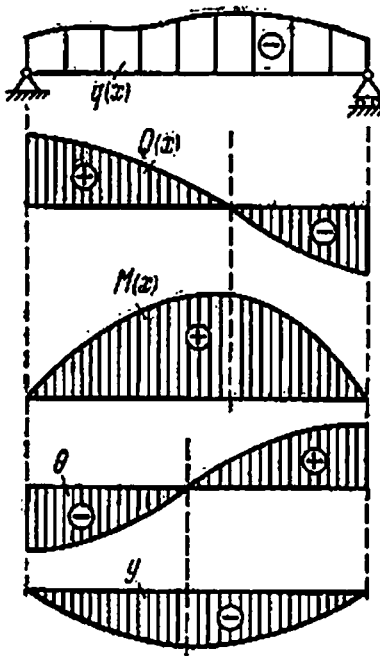


Fig. 230

### § 90. Differential Relations in Bending

In §§ 57 and 82 we obtained differential relations for continuous load  $q(x)$ , shearing force  $Q(x)$ , bending moment  $M(x)$ , angle of rotation  $\theta$  and deflection  $y$ :

$$\frac{dM(x)}{dx} = Q(x), \quad \frac{dQ(x)}{dx} = q(x)$$

$$EJ \frac{d^2y}{dx^2} = M(x), \quad \frac{dy}{dx} = \theta$$

After certain transformations these relations can be written in the following sequence:

$$\frac{d}{dx} (EJy) = EJ\theta$$

$$\frac{d^2}{dx^2} (EJy) = \frac{d}{dx} (EJ\theta) = M(x)$$

$$\frac{d^3}{dx^3} (EJy) = \frac{d^2}{dx^2} (EJ\theta) = \frac{d}{dx} M(x) = Q(x)$$

$$\frac{d^4}{dx^4} (EJy) = \frac{d^3}{dx^3} (EJ\theta) = \frac{d^2}{dx^2} M(x) = \frac{d}{dx} Q(x) = q(x)$$

From the equations it is evident that knowing force  $q(x)$  and the types of supports, we can obtain  $Q(x)$ ,  $M(x)$ ,  $EJ\theta$  and  $EJy$  by successive integration: conversely, knowing the equation of the deflected

axis, by successive differentiation of  $EJy$  w.r.t.  $x$  we can obtain  $EJ\theta$ ,  $M(x)$ ,  $Q(x)$  and  $q(x)$ . In graphic representation of these relations we shall lay off the positive values of the above quantities upwards and the negative values downwards; the positive direction of the  $x$ -axis will be towards the right, rotation of the section in the clockwise direction will be considered negative and in the anticlockwise direction positive. Figure 230 contains diagrams depicting the law of variation of all quantities, which characterize the bending of a hinged beam loaded with a non-uniform distributed force  $q(x)$  (the load is negative as it is acting downwards).

## CHAPTER 16

## Graph-analytic Method of Calculating Displacement in Bending

## § 91. Graph-analytic Method

The method of integrating the differential equation of the deflected axis gives us equations of deflections and angles of rotation, with the help of which we can calculate the deflection and angle of rotation in any section of the beam.

In a number of problems (statically indeterminate beams, determination of maximum deflection) it is sufficient to determine the deflection and angle of rotation for a few definite sections. In such cases it is more appropriate to use the *graph-analytic method*. This method is based on the resemblance of differential relations between deflection, bending moment and intensity of continuous load.

Imagine a beam with an arbitrarily loading (Fig. 231). The differential equation of the deflected axis of this beam may be written (§ 82) as:

$$\frac{d^2(EJy)}{dx^2} = M(x) \quad (16.1)$$

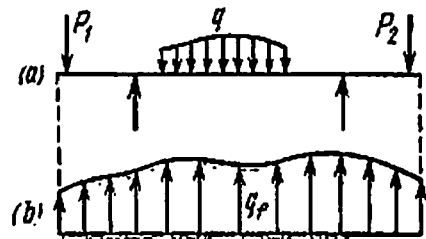


Fig. 231

Below the beam we draw another beam of the same length loaded by an, as yet unknown, continuous force  $q_f$ , the positive direction of which is taken upwards; we shall refrain from specifying the type of supports also and shall only point out that the support reactions must balance the external force  $q_f$ . The second beam will be hereafter

mentioned as the *fictitious beam*; all quantities relating to this beam will be denoted with a symbol  $f$ . For this fictitious beam we shall determine the bending moment  $M_f$  in each section by integration, using the differential equation that correlates the bending moment with the intensity of the continuous force (§§ 57 and 90):

$$\frac{d^2 M_f}{dx^2} = q_f \quad (16.2)$$

Let us compare equations (16.1) and (16.2). If we assume that

$$q_f = M(x)$$

i.e. if we load the fictitious beam with a fictitious force, which changes according to the bending moment of the real beam, then

$$\frac{d^2 (EJy)}{dx^2} = \frac{d^2 M_f}{dx^2}$$

If in integration we can achieve equality of the constants of integration on the left- and right-hand sides of the equation, i.e.  $C_l = C_r$ , and  $D_l = D_r$ , we shall obtain

$$\frac{d(EJy)}{dx} = \frac{dM_f}{dx}, \quad EJy = M_f$$

Considering that  $\frac{dM_f}{dx} = Q_f$  and solving these equations for  $y$  and  $\theta$ , we get the following formulas:

$$y = \frac{M_f}{EJ} \quad (16.3)$$

$$\theta = \frac{Q_f}{EJ} \quad (16.4)$$

Thus, deflection in the section of the real beam (due to the given load) is equal to the bending moment in the same section of the fictitious beam (from the fictitious load), divided by the rigidity of the real beam. Similarly, the angle of rotation of the real beam (due to the given load) is equal to the shearing force in the same section of the fictitious beam (from the fictitious load), divided by the rigidity of the real beam.

In the analytical method of determining deformations, the constants of integration were found from boundary conditions, i.e. by equating to zero the deflections at the supports and equating the deformations in sections common to two adjoining portions of the beam.

In the method under discussion the equality of constants of integration, while integrating equations (16.1) and (16.2), can be achieved by fixing the ends (or intermediate sections) of the fictitious beam in

such a way so as to satisfy the following conditions, which directly ensue from expressions (16.3) and (16.4):

(1) if deflection  $f$  of the real beam is zero, then the bending moment in the corresponding section of the fictitious beam must be zero;

(2) if the angle of rotation  $\theta$  of the real beam is zero, then the shearing force in the corresponding section of the fictitious beam must be zero;

(3) if the deflection and angle of rotation of the real beam are not equal to zero, then the corresponding bending moment  $M_f$  and shearing force  $Q_f$  must also not be zero.

Table 13 contains conditions for all types of supports of the real beam and gives the constraints in corresponding sections of the fictitious beam, which satisfy the conditions of constraint of the real beam. In Fig. 232 are depicted the widely prevalent combinations of real and fictitious beams for statically determinate structures. In each pair any beam may be taken as the real, then the second automatically becomes fictitious; this can be easily checked with the help of Table 13.

Table 13

### Conditions for Obtaining the Proper Fictitious Beam

Real beam		Fictitious beam	
Type of support	Conditions for $y$ and $\theta$	Required conditions for $M_f$ and $Q_f$	Constraints of the fictitious beam satisfying these conditions
Hinged support (no deflection; rotation of section is possible)	$y=0$ $\theta \neq 0$	$M_f=0$ $Q_f \neq 0$	Hinged support (no moment; support reaction is possible)
Fixed end of the beam (no deflection and no rotation)	$y=0$ $\theta=0$	$M_f=0$ $Q_f=0$	Free end of the beam (no moment and no concentrated force)
Free end of the beam (both deflection and rotation are possible)	$y \neq 0$ $\theta \neq 0$	$M_f \neq 0$ $Q_f \neq 0$	Fixed end of the beam (both support reaction and reactive moment occur)
Intermediate support (no deflection; rotation of section is possible)	$y=0$ $\theta \neq 0$	$M_f=0$ $Q_f \neq 0$	Intermediate hinge (no moment; hinge transmits force)
Intermediate hinge (both deflection and rotation of section is possible)	$y \neq 0$ $\theta \neq 0$	$M_f \neq 0$ $Q_f \neq 0$	Intermediate support (both moment and support reaction are possible)

In multispans beams with intermediate hinges the fictitious beam may be selected according to the method explained for the beam in Fig. 233.

It must be noted that the fictitious beam corresponding to a statically determinate real beam must also be statically determinate.

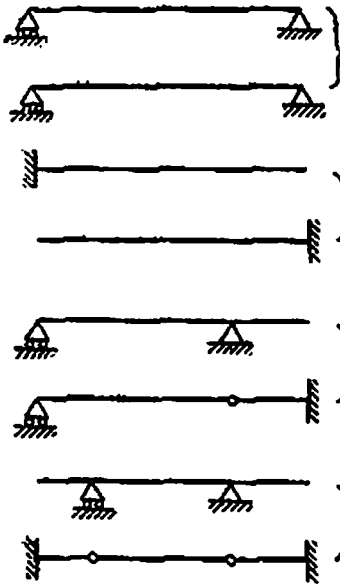


Fig. 232

Thus, in order to determine deflection  $y$  and angle of rotation  $\theta$  in a section of the given (real) beam, we must follow the procedure explained below:

(a) draw the given beam alongwith the forces;

(b) draw the bending moment diagram  $M(x)$ ;

(c) assume the zero axis of the bending moment diagram as the axis of the fictitious beam and the bending moment diagram  $M(x)$  as the fictitious load  $q_i$ ; if the bending moment is positive the ordinates of force  $q_i$  must be directed upwards, if it is negative  $q_i$  must be directed downwards;

(d) draw the supports of the fictitious beam in accordance with the conditions given in Table 13 and Figs. 232 or 233;

(e) calculate the reactions of the fictitious beam due to the fictitious load (i.e. the fictitious support reactions); for cantilever beams this step may be bypassed;

(f) calculate bending moment  $M_f$  in that section of the fictitious beam which has the same abscissa as the section of the real beam in which deflection  $f$  is required to be determined;

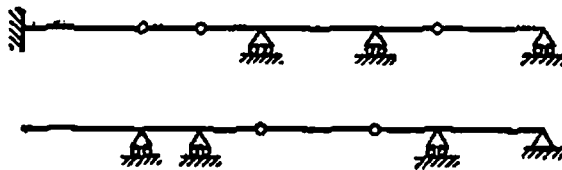


Fig. 233

(g) calculate shearing force  $Q_f$  in that section of the fictitious beam which has the same abscissa as the section of the real beam in which the angle of rotation  $\theta$  is required to be determined;

(h) calculate  $f$  and  $\theta$  according to formulas (16.3) and (16.4).

The graph-analytic method of determining deformations relieves us from calculating the constants of integration in each particular case and with the help of data given in Table 13 and Figs. 232 or 233 offers a direct solution, which is in agreement with the given initial conditions.

Fictitious moments have the dimensions of force  $\times$  (length)<sup>3</sup>, fictitious shearing forces have the dimensions of force  $\times$  (length)<sup>2</sup>, and intensity of the fictitious load is measured in units of force  $\times$  length.

## § 92. Examples of Determining Deformations by the Graph-analytic Method

Let us find the deflection at point  $B$  of beam  $AB$  shown in Fig. 234. The bending moment diagram for the above beam is a triangle with the maximum ordinate in section  $A$  equal to  $Pl$ . We shall take the axis of the bending-moment diagram as the axis of the fictitious beam and

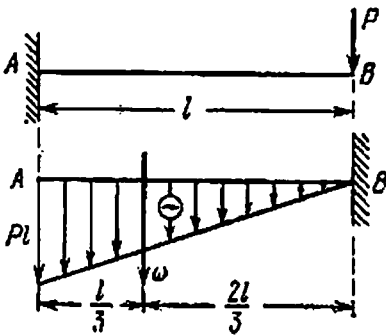


Fig. 234

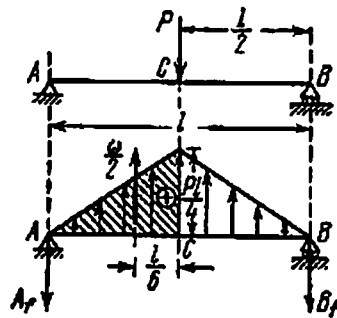


Fig. 235

consider the bending-moment diagram as the fictitious load (this can be done by putting downward arrows at the ends of the ordinates as the ordinates are negative).

Following the instructions given in Table 13 we take point  $B$  as the rigidly fixed end of the fictitious beam and point  $A$  as its free end.

Now we have to calculate the bending moment in section  $B$  of the fictitious beam. The moment of the triangular load about point  $B$  will be equal to the product of the area of the load,  $\omega$ , with the distance of its centre of gravity from section  $B$ :

$$M_{fB} = -\frac{1}{2} Pl \times l \times \frac{2l}{3} = -\frac{Pl^3}{3}$$

Dividing this expression by  $EJ$  we get the deflection at point  $B$ :

$$f_B = -\frac{Pl^3}{3EJ}$$

The formula is exactly similar to the result obtained in § 83.

The shearing force in section  $B$  of the fictitious beam is numerically equal to the area of the triangle:

$$Q_f = -\frac{1}{2} Pl \times l = -\frac{Pl^2}{2}$$

Therefore the angle of rotation in section  $B$  of the real beam is

$$\theta_B = \frac{Q_f}{EJ} = -\frac{Pl^2}{2EJ}$$

Let us find the deflection at the point of application of the force for a simply supported beam loaded in the middle of the span by force  $P$  (Fig. 235).

The bending-moment diagram of the real beam is a triangle with the ordinate at the point of application of the force equal to  $+\frac{Pl}{4}$ . Consider the bending-moment diagram as the fictitious load, with the arrows pointing upwards, as the ordinates of the diagram are positive in this example.

The supports of the fictitious beam can be determined according to Table 13 so as to satisfy the conditions of constraint of the real beam. From symmetry the reactions of the fictitious beam must be equal, and each must be equal to half of the total load:

$$A_f = B_f = \frac{1}{2} \times \frac{1}{2} \times \frac{Pl}{4} \times l = \frac{Pl^2}{16}$$

Bending moment in section  $C$  is equal to the sum of the moment of reaction (with a minus sign) and the moment of half of the triangular load (with arm  $l/6$ ):

$$\begin{aligned} M_{fC} &= -A_f \times \frac{l}{2} + \frac{1}{2} \times \frac{1}{2} \times \frac{Pl}{4} \times l \times \frac{l}{6} \\ &= -\frac{Pl^2}{16} \times \frac{l}{2} + \frac{Pl^2}{16} \times \frac{l}{6} = -\frac{Pl^3}{48} \end{aligned}$$

wherefrom

$$f_C = -\frac{Pl^3}{48EJ}$$

The angle of rotation at the left support is

$$\theta_A = \frac{Q_{fA}}{EJ} = -\frac{A_f}{EJ} = -\frac{Pl^2}{16EJ}$$

because the shearing force at the support is equal to the support reaction (in this example with a minus sign because  $A_f$  is directed downwards). At support  $B$

$$\theta_B = +\frac{Pl^2}{16EJ}$$

It is evident from the above examples that for the convention of signs of fictitious load, bending moment and shearing force decided earlier, the minus sign in the formula for deflection corresponds, as before, to deflection downwards and in the formula for the angle of

rotation to rotation in a clockwise direction; positive sign corresponds to the reverse directions.

Let us find by the graph-analytic method the deflection in the middle of the span and at the ends of cantilevers for the beam shown in Fig. 236.

The bending-moment diagram is a trapezium with maximum ordinates  $M = -Pa$ . Let us change the bending-moment diagram to a fictitious load acting downwards. The fictitious beam consists of two small

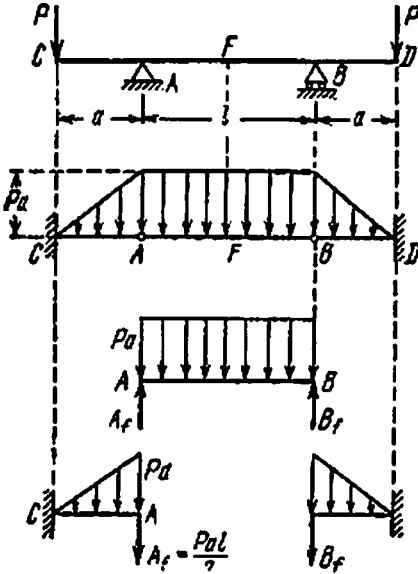


Fig. 236

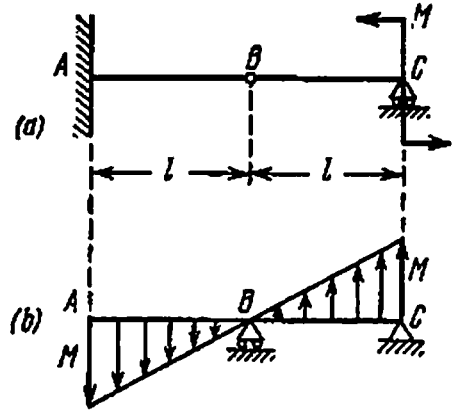


Fig. 237

cantilevers supporting the suspended beam  $AB$ . Deflection in the middle of the span (point  $F$ ) is equal to the fictitious moment at this point due to the distributed load divided by the rigidity of the beam:

$$f_F = \frac{q_f l^2}{8EJ} = \frac{Pa l^2}{8EJ}$$

The deflection at point  $C$  can be determined by first calculating the fictitious bending moment in the section; the deflection is caused by the triangular force acting on beam  $CA$  and the reaction of the suspended beam equal to  $A_f = \frac{Pa l}{2}$  (Fig. 236):

$$M_{fC} = -A_f a - \frac{Pa \times a}{2} \frac{2}{3} a = -\frac{Pa^2 l}{2} - \frac{Pa^3}{3}$$

wherefrom the deflection in section  $C$  is

$$f_C = \frac{M_{fC}}{EJ} = -\frac{Pa^3}{6EJ} (3l + 2a)$$



In the last example we shall determine deflection in section  $B$  of the beam shown in Fig. 237.

Let us first draw the bending moment diagram. The moment is  $+M$  in section  $C$  and zero in section  $B$ . The moment changes linearly over the whole length of the beam. We change the bending moment diagram to the fictitious load and draw the fictitious beam according to the conditions given in Table 13. Considering the cantilever  $AB$ , we determine the fictitious bending moment at point  $B$ :

$$M_{fB} = -\frac{1}{2} Ml \times \frac{2}{3} l = -\frac{Ml^2}{3}$$

The corresponding deflection is

$$f_B = -\frac{Ml^2}{3EJ}$$

### § 93. The Graph-analytic Method Applied to Curvilinear Bending-moment Diagrams

The bending-moment diagram of a uniformly distributed load is a parabola.

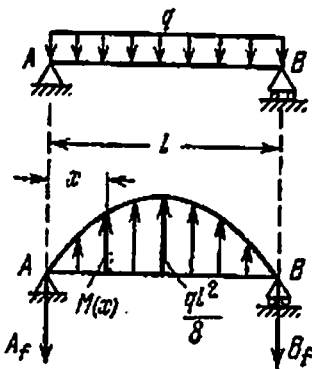


Fig. 238

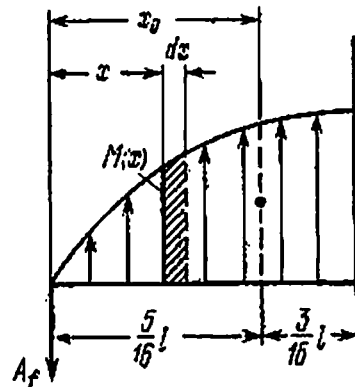


Fig. 239

The convex parabola (Fig. 238) is characteristic of simply supported beams. The ordinates of this parabola are given by the expression

$$M(x) = \frac{ql}{2} x - \frac{q}{2} x^2$$

The area of this parabola can be found from the expression

$$\omega = \int_0^l M(x) dx = \int_0^l \left( \frac{ql}{2} x - \frac{q}{2} x^2 \right) dx = \frac{ql^3}{12}$$

This area may also be found as two-thirds of the area of the circumscribed rectangle:

$$\omega = \frac{2}{3} \frac{ql^2}{8} l = \frac{ql^3}{12}$$

Abscissa  $x_0$  of the centre of gravity of half of the parabola area (Fig. 239) is calculated as follows:

$$x_0 = \frac{\int_0^{l/2} xM(x) dx}{\frac{\omega}{2}} = \frac{\frac{5}{384} ql^4}{\frac{1}{24} ql^3} = \frac{5}{16} l$$

The distance between the centre of gravity of half of the parabola area and the centre of the whole parabola is

$$\frac{l}{2} - x_0 = \frac{3}{16} l$$

The concave parabola represents the bending moment diagram of a beam rigidly fixed at one end (Fig. 240). The ordinate of any point on this parabola is found from the expression  $M(x) = -qx^2/2$ .

The area of the parabola is found as

$$\omega = \int_0^l M(x) dx = \int_0^l \frac{qx^2}{2} dx = \frac{ql^3}{6}$$

This area is also equal to one-third of the circumscribed rectangle

$$\omega = \frac{1}{3} \frac{ql^2}{2} l = \frac{ql^3}{6}$$

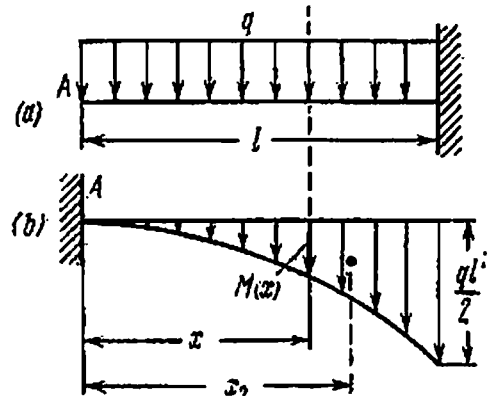


Fig. 240

Ordinate  $x_0$  of the centre of gravity of the parabola is

$$x_0 = \frac{\int_0^l xM(x) dx}{\omega} = \frac{\frac{1}{8} ql^4}{\frac{1}{6} ql^3} = \frac{3}{4} l$$

The distance between the centre of gravity of the parabola and the section of maximum bending moment (rigidly fixed end) is equal to one-fourth of the beam span.

Let us solve the following examples using the relations derived here.

Find the deflection at the middle of the beam shown in Fig. 238. The area of the bending-moment diagram is taken as the fictitious load. The diagram is positive, therefore the fictitious load is directed upwards. The fictitious support reactions are

$$A_f = B_f = \frac{\omega}{2} = \frac{ql^3}{24}$$

These reactions are directed downwards (Fig. 238).

The fictitious bending moment in the middle of the span is equal to the sum of static moments of the fictitious forces located on one side of the middle section, say, on the left-hand side. The forces located to the left of the section are  $A_f$  and the left half of the parabola. The arm of force  $A_f$  is equal to half of the span; arm of the half parabola is  $\frac{3l}{8}$ . Therefore, the fictitious bending moment in the middle of the span is

$$\begin{aligned} M_f &= -A_f \times \frac{l}{2} + \frac{\omega}{2} \times \frac{3}{16}l \\ &= -\frac{ql^3}{24} \times \frac{l}{2} + \frac{ql^3}{24} \times \frac{3}{16}l = -\frac{5}{384}ql^4 \end{aligned}$$

and the deflection in the middle of the span is

$$f_{l/2} = -\frac{5}{384} \frac{ql^4}{EJ}$$

Consider a beam rigidly fixed at one end and loaded by a uniformly distributed force  $q$  (Fig. 240(a)). Let us find the deflection of the free end. The bending-moment diagram of the real and the fictitious beams is shown in Fig. 240(b).

The bending moment at the fixed end  $A$  of the fictitious beam is equal to the product of the area  $\omega$  of the complete diagram with the distance between  $A$  and its centre of gravity, i.e.

$$M_f = \omega x_0 = \frac{ql^3}{6} \frac{3}{4}l = -\frac{ql^4}{8}$$

and the deflection in section  $A$  is

$$f_A = -\frac{ql^4}{8EJ}$$

Consider beam  $ABC$  with one cantilever as shown in Fig. 241(a). Using the method of breaking the diagrams and the method of superposition of forces, find the deflection and angle of rotation in section  $C$ . The beam is loaded all along its length by a uniformly distributed force.

The possible bending moment diagram is in Fig. 241(b). Replace this diagram by its components: from force  $q$  over length  $l$  (Fig. 241(c)) and from force  $q$  on the cantilever of length  $a$  (Fig. 241(d)). The ordinates of the last two diagrams can be taken from the problems solved earlier. The important ordinates have been written in Fig. 241(c) and (d). The fictitious beam is shown in Fig. 241(e).

Let us isolate the fictitious beam  $BC$ : it is acted upon by pressure  $B_f$  from the suspended beam  $AB$  and the parabolic force of maximum ordinate  $\frac{qa^2}{2}$  (Fig. 241(f)).

In the fictitious beam  $AB$ , taking the sum of moments of all fictitious forces about support  $A$ , we find (Fig. 241(g)) that

$$B_f = \frac{2}{3} \frac{1}{2} \frac{qa^2}{2} l - \frac{1}{2} \frac{ql^3}{12}$$

$$= \frac{1}{6} qa^2 l - \frac{ql^3}{24}$$

Returning to Fig. 241(f) we calculate

$$Q_{fC} = -B_f - \frac{1}{3} \frac{qa^2}{2} a$$

$$= -\frac{1}{6} qa^2 l + \frac{ql^3}{24} - \frac{qa^3}{6}$$

$$M_{fC} = -B_f a - \frac{1}{3} \frac{qa^2}{2} a \frac{3}{4} a$$

$$= -\frac{1}{6} qa^2 l + \frac{qal^3}{24} - \frac{qa^4}{8}$$

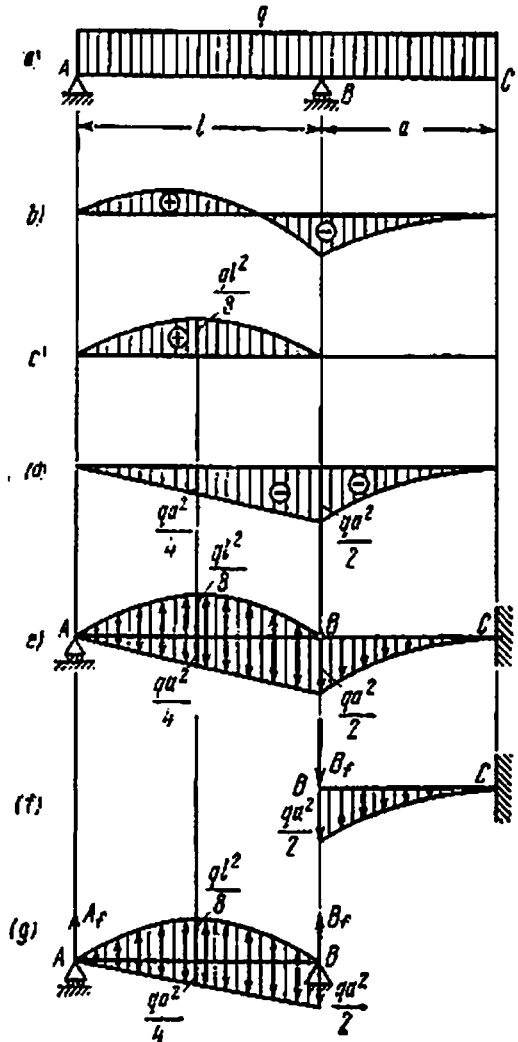


Fig. 241

The required values of deflection and angle of rotation in section  $C$  are:

$$\theta_C = \frac{Q_{fC}}{EJ} = -\frac{q}{24EJ} (4a^2 l - l^3 + 4a^3)$$

$$\bar{f}_C = \frac{M_{fC}}{EJ} = -\frac{qa}{24EJ} (4a^2 l - l^3 + 3a^2)$$

## CHAPTER 17

## Non-uniform Beams

## § 94. Selecting the Section in Beams of Uniform Strength

All preceding discussions were on beams of uniform section. In practice, however, we often have to deal with beams in which the cross-sectional dimensions change either gradually or sharply.

We give below a few examples on selecting the dimensions of the cross section and determining the deformation of non-uniform beams.

We know that bending moment usually varies along the length of the beam; therefore, by determining the cross-sectional dimensions from the condition of maximum bending moment we provide an extra margin in all sections of the beam except the one which corresponds to  $M_{\max}$ . Beams of uniform strength are used to achieve greater economy of metal and in some cases also to increase flexibility. Under this term come beams in which the maximum normal stress is the same in all sections and equal to the permissible stress (or less than it).

The dimensions of such a beam are calculated for the following condition:

$$\sigma_{\max} = \frac{M(x)}{W(x)} = [\sigma] \quad (17.1)$$

and

$$W(x) = \frac{M(x)}{[\sigma]} \quad (17.2)$$

Here  $M(x)$  and  $W(x)$  are the bending moment and section modulus in any arbitrary section of the beam; in each section  $W(x)$  must vary in direct proportion to the bending moment.

Conditions (17.1) and (17.2) are true also for the section with the maximum bending moment; if we denote the section modulus in the section of maximum bending moment  $M_{\max}$  by  $W_0$ , then

$$\frac{M_{\max}}{W_0} = \frac{M(x)}{W(x)} = [\sigma] \quad (17.3)$$

We shall explain the order of computations with the help of the following example. Consider a beam of span  $l$  rigidly fixed at end  $A$  and loaded at the other end by a force  $P$  (Figs. 242 and 243). Assume the beam to be of rectangular section. The problem of obtaining a varying section modulus can be solved by changing either the height or the width of the beam or both simultaneously.

Suppose the height of the beam is fixed,  $h=h_0$ , and the width varies,  $b=b(x)$ . The section modulus at a distance  $x$  from the free end will be  $W(x) = \frac{b(x)h^2}{6}$ , and the bending moment will be  $-Px$ ; the section

modulus in the support section is  $W_0 = \frac{b_0 h^2}{6}$ , and the maximum bending moment at the support is  $M_{\max} = |Pl|$ . Only the absolute values of  $M(x)$  and  $M_{\max}$  are required for computations. From formula (17.3) we get

$$\frac{Pl \times 6}{b_0 h^2} = \frac{Px \times 6}{b(x) h^2}$$

wherefrom

$$b(x) = b_0 \frac{x}{l} \tag{17.4}$$

i.e. width varies linearly as a function of  $x$ . At  $x=l$  the width is  $b_0$ . The front view and plan of the beam are shown in Fig. 242. This shape is obtained if we consider the strength of the beam only w.r.t. the normal stresses; in section  $B$  the width of the beam is zero.

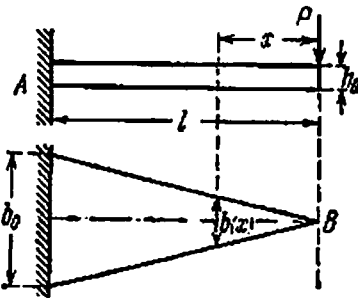


Fig. 242

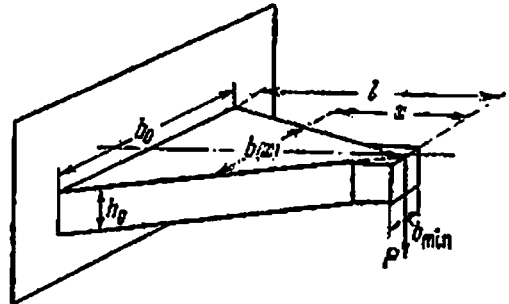


Fig. 243

However, we must ensure sufficient strength of the beam under shearing stresses also. The minimum width of the beam according to this condition is determined from the following equation

$$\tau_{\max} = \frac{3Q_{\max}}{2hb_{\min}} = [\tau]$$

and, since  $Q_{\max} = P$ ,

$$b_{\min} = \frac{3P}{2h[\tau]}$$

The corrected shape of the beam is shown in Fig. 243.

### § 95. Practical Examples of Beams of Uniform Strength

The example discussed above finds practical application in design of springs. If we ignore its small curvature, a spring may be looked upon as a simply supported beam (Fig. 244(a)) loaded with a force  $P$  in the middle of its span and having reactions  $\frac{P}{2}$  at its ends.

We design such a bar by the same principles as a beam of uniform

strength of constant height  $h_0$  and variable width  $b(x)$ ; as the loading is symmetric it is sufficient to study just one half of the span.

The section moduli  $W(x)$  and  $W_0$  can be expressed by the same formulas as in the preceding example. The maximum bending moment in the middle of the span is:

$$M_{\max} = \frac{Pl}{4}$$

Bending moment in any arbitrary section is:

$$M(x) = \frac{Px}{2}$$

Solving, as in the preceding example, we get:

$$b(x) = b_0 \frac{2x}{l} \quad (17.5)$$

The maximum width required to successfully resist the shearing force  $\frac{P}{2}$  can be determined from the following formula:

$$b_{\min} = \frac{3}{4} \frac{P}{h_0 [\tau]}$$

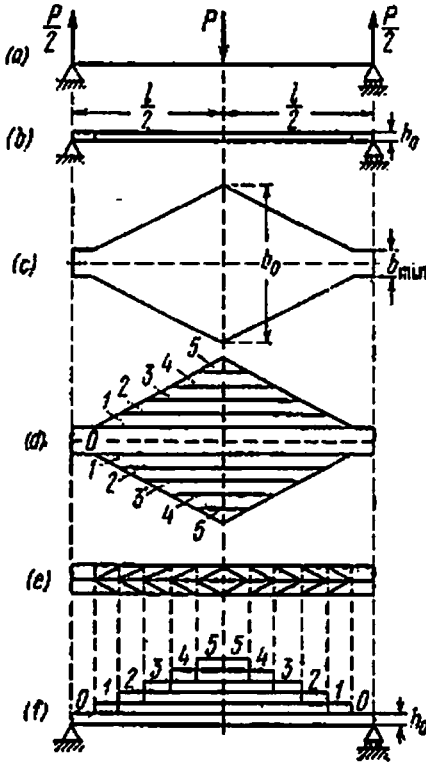


Fig. 244

The front and top views of the spring are shown in Fig. 244(b) and (c). However, such a shape of the spring is highly inconvenient from the practical point of view; therefore the shape is slightly modified without affecting the performance of the spring. Imagine that the spring is divided into thin strips when seen from the top, as shown in Fig. 244(d). If we place these strips not adjacent to each other but one over the other and neglect the friction between them, then without affecting its working the spring may be given a shape the top and front views of which are shown in Fig. 244(e) and (f), respectively.

Obviously, in actual practice each spring plate, the 1st, 2nd, etc., is manufactured in one piece and not in two halves.

Non-uniform beams are often used in mechanical engineering. For example, shafts are often designed as beams of uniform strength.

### § 96. Displacements in Non-uniform Beams

When determining the deflection and angle of rotation of a non-uniform beam, it should be borne in mind that the rigidity of such a beam is a function of  $x$ . Therefore, the differential equation of the de-

flected axis may be written as

$$EJ(x) \frac{d^2y}{dx^2} = M(x)$$

where  $J(x)$  is the variable moment of inertia in different beam sections.

Before integrating this equation we must express  $J(x)$  in terms of  $J$ , i.e. the moment of inertia of the section in which the maximum bending moment acts. Having done this, we can carry out the computations in the same manner as for a beam of uniform section (§ 82).

Let us show this through the example discussed earlier. We shall determine the deflection in a beam of uniform strength (Fig. 242), which is fixed at one end, loaded at the other by a force  $P$  and has a fixed height. Let the free end of the beam be the origin of coordinates. Then

$$M(x) = -Px, \quad J(x) = \frac{b(x)h^3}{12} = \frac{b_0h^3}{12} \frac{x}{l} = J \frac{x}{l} \quad (17.6)$$

$$EJ \frac{x}{l} \frac{d^2y}{dx^2} = -Px$$

The differential equation may be written as

$$EJ \frac{d^2y}{dx^2} = -\frac{Px l}{x} = -Pl \quad (17.7)$$

Integrating twice,

$$EJ \frac{dy}{dx} = -Plx + C, \quad EJy = -Pl \frac{x^2}{2} + Cx + D$$

We have the following conditions for determining the constants of integration: at point  $A(x=l)$  deflection  $y=0$  and angle of rotation  $\frac{dy}{dx}=0$ . Therefore

$$0 = -Pl^2 + C \quad \text{and} \quad 0 = -\frac{Pl^3}{2} + Cl + D$$

wherefrom

$$C = Pl^2 \quad \text{and} \quad D = -\frac{Pl^3}{2}$$

The expressions for  $y$  and  $\theta$  may be written as follows:

$$\theta = \frac{dy}{dx} = -\frac{Pl}{EJ} x + \frac{Pl^2}{EJ} = \frac{Pl^2}{EJ} \left(1 - \frac{x}{l}\right)$$

$$y = -\frac{Pl}{2EJ} x^2 + \frac{Pl^2}{EJ} x - \frac{Pl^3}{2EJ} = -\frac{Pl^3}{2EJ} \left(1 - 2\frac{x}{l} + \frac{x^2}{l^2}\right)$$

Maximum deflection at the free end is obtained by putting  $x=0$ :

$$f_{\max} = -\frac{Pl^3}{2EJ}$$



If we had a beam of uniform section with a moment of inertia  $J$ , then the maximum deflection would be

$$f_{\max} = -\frac{Pl^3}{3LJ}$$

or two-thirds greater.

Hence, non-uniform beams are more flexible than beams of uniform section of the same strength. It is because of this property and not due to saving of metal that non-uniform strength beams are used in the manufacture of elements such as springs.

Equation (17.7) indicates that in this example the curvature of the beam is constant, i.e. the beam axis deflects along a circle. But upon integration the equation obtained was that of a parabola. It is suggested that the reader should explain the reason for this.

When the graph-analytic method is used for determining the deformation of non-uniform beams, it does not present any difficulties. Instead of dividing the bending moment and shearing force in the fictitious beam by  $EJ$  to compute  $f$  and  $\theta$ , we obtain the fictitious load by dividing the ordinates of the bending moment diagram of the real beam by rigidity  $EJ$ . Then

$$q'_i = \frac{M(x)}{EJ} \quad \text{and} \quad f = M'_f, \quad \theta = Q'_f$$

When applying this method to non-uniform beams, we assume that

$$q'_f = \frac{M(x)}{EJ(x)}$$

Then we load the fictitious beam by this force and obtain the required deflection and angle of rotation as the bending moment and shearing force in sections of the fictitious beam.

In the example discussed above  $q'_f = -\frac{Px}{EJ_x} = -\frac{Pl}{EJ}$ , i.e. the fictitious beam should be loaded not by a triangular force but by a uniformly distributed force (Fig. 245). The deflection of section  $B$ , which is equal to the bending moment in the fixed end of the fictitious beam, can be expressed by the formula

$$f = M'_f = \frac{q'_f l^2}{2} = -\frac{Pl^3}{2EJ}$$

We could have obtained the same result by assuming that the beam has constant rigidity  $EJ$  and its bending moment diagram is obtained by multiplying each ordinate by the ratio  $\frac{J}{J(x)}$ ; the ordinates of the bending moment diagram thus obtained are

$$-Px \frac{J}{J(x)} = -Px \frac{Jl}{Jx} = -Pl$$

(Fig. 246). Then according to the general principle of the graph-analytic method

$$M_f = -Pl \times l \frac{1}{2} = -\frac{Pl^2}{2} \quad \text{and} \quad y = -\frac{Pl^3}{2EI}$$

Thus, deformation of non-uniform beams can be calculated by the same method as that for beams of uniform rigidity. The only difference is that the bending moment diagram used in this case is obtained by multiplying with the ratio  $\frac{J}{J(x)}$ .

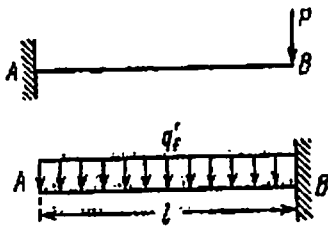


Fig. 245

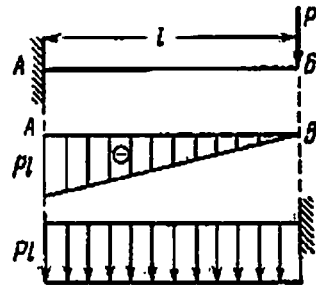


Fig. 246

Let us determine by the graph-analytic method the deflection under force  $P$  for a simply supported beam loaded at the middle of the span by the above force  $P$  (Fig. 247(a)). The moment of inertia of the sec-

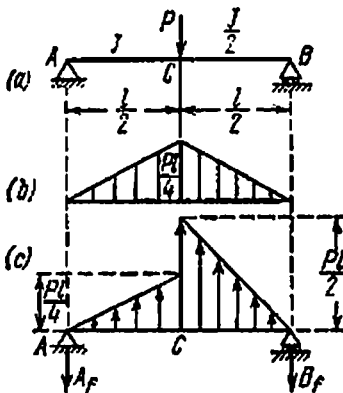


Fig. 247

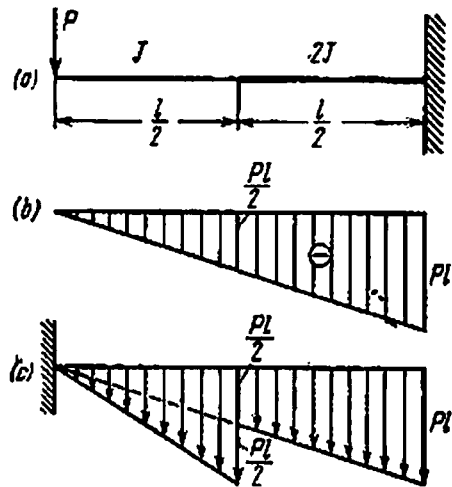


Fig. 248

tion is  $J$  in the left half and  $0.5J$  in the right half. Let us obtain the new bending moment diagram by multiplying the ordinates of the right half of the real bending moment diagram (Fig. 247(b)) with the ratio  $J/0.5J=2$ ; the fictitious beam with the new loading is shown

in Fig. 247(c). The reaction of the left-hand fictitious support is:

$$A_f = \frac{1}{2} \frac{Pl}{4} \frac{l}{2} \frac{2}{3} + \frac{1}{2} \frac{Pl}{2} \frac{l}{2} \frac{1}{3} = \frac{Pl^2}{12}$$

The fictitious bending moment in section C and the deflection of point C are:

$$\begin{aligned} M_{fC} &= -A_f \frac{l}{2} + \frac{1}{2} \frac{l}{2} \frac{Pl}{4} \frac{l}{6} \\ &= -\frac{Pl^2}{24} + \frac{Pl^2}{96} = -\frac{Pl^2}{32} \end{aligned}$$

and

$$f_c = -\frac{Pl^3}{32EJ}$$

Let us determine the deflection of a beam rigidly fixed at one end and loaded at the other by a concentrated force (Fig. 248(a)). The cross-sectional area of one half of the beam is greater, and  $J_2 > J_1$ . In order to transform the bending moment diagram (Fig. 248(b)) into the fictitious load, we must multiply the ordinates of the left-hand portion of the diagram by  $\frac{J_2}{J_1}$  (Fig. 248(c)).

Deflection under force  $P$  may be calculated as follows (for  $J_2 = 2J_1$ ):

$$\begin{aligned} M_f &= -\frac{1}{2} P \frac{l}{2} \frac{l}{2} \frac{2}{3} \frac{l}{2} - Pl \frac{2l}{3} \frac{l}{2} = -\frac{3}{8} Pl^2 \\ f_P &= -\frac{3Pl^3}{8EJ_2} \end{aligned}$$

## PART VI

# Potential Energy. Statically Indeterminate Beams

### CHAPTER 18

## Application of the Concept of Potential Energy in Determining Displacements

### § 97. Statement of the Problem

Besides the methods of determining deflection and angle of rotation discussed above, there is a more general method, which can be used for determining deformation of any elastic structure. It is based on the law of conservation of energy.

When a static tensile or compressive force is applied to an elastic bar, transformation of potential energy from one form to another takes place; a part of the potential energy of the force acting on the bar changes into potential energy of strain. If we load the bar by successive addition of small loads  $dP$  at its end (Fig. 249), then each addition will be accompanied by a decrease in the level of the load and the potential energy of strain will correspondingly increase.

This phenomenon is true for all types of deformation of an elastic structure provided the loading is static. Such a construction may be looked upon as a machine which converts one type of potential energy into another.

We have agreed (§ 2) that a load will be called static if it increases gradually, so that acceleration in the elements may be ignored; transmission of pressure (force) from one part of the structure to another does not affect the motion of these parts, i.e. their velocity remains constant and acceleration is zero.

Under these conditions deformation of the structure is not accompanied by any change in kinetic energy of the system; only conversion of one form of potential energy into another takes place. In making this statement we neglect the magnetic, electric and thermal effects, which do not alter the deformation considerably.

As the motion of the elements of the structure does not change with time, at each instant every part of the structure will be in equilibrium under the action of external forces and forces of reaction, and each element of a part will be in equilibrium under the external forces

and stresses acting on it. Deformation of the structure, stresses in the various parts, and reactions transferred from one part to another, all follow the increase in load.

Thus, we may say that total conversion of one form of potential energy into another takes place if deformation occurs without violating the equilibrium of the system. Work done by the forces acting on the structure serves as a measure of the energy transformed into another form.

Let us denote the accumulated potential energy of strain by  $U$  and the decrease in potential energy of the external forces by  $U_p$ . The quantity  $U_p$  is determined as the positive work  $W_p$  done by these forces; on the other hand, the accumulated potential energy of strain  $U$  is equal to the negative work  $W$  done by the internal intermolecular forces (negative because the direction of displacement of points of the body due to deformation is opposite to the internal forces).

The law of conservation of energy for elastic systems may be expressed as follows:

$$U_p = U \quad (18.1)$$

In this formula, replacing  $U_p$  and  $U$  by the corresponding values of work  $W_p$  and  $W$ , we get a modified form of the same law:

$$W_p = -W \text{ or } W_p + W = 0 \quad (18.2)$$

This formulation of the law of conservation of energy coincides with

the *principle of virtual work* as applied to elastic systems: equation (18.2) states that the sum of work of all forces acting on a body is zero if deformation of the body occurs without violating the equilibrium of the system.

Thus, the principle of virtual work as applied to elastic systems is a corollary of the law of conservation of energy.

It ensues from formula (18.1) that the potential energy of strain  $U$  is numerically equal to work  $W_p$  done by the external forces in causing this strain:

$$U = W_p \quad (18.3)$$

The following interpretation of this equation sometimes given in books on structural mechanics is erroneous: "Work done by the external forces in deforming a body changes into potential energy of strain." Actually, only a different form of energy can change into potential

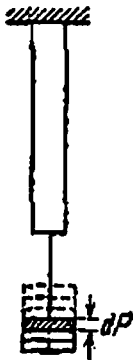


Fig. 249

energy of strain. As a rule, this is the potential energy of the external forces. Work done by the external forces during this conversion is only a numerical measure of the converted energy.

### § 98. Potential Energy in the Simplest Cases of Loading

We have already derived the expressions for computing potential energy in tension and compression (§ 10), shear (§ 36), torsion (§ 52), and also in pure bending (§ 63 (D)).

Let us write all the above-mentioned formulas in Table 14.

Table 14

#### Potential Energy of Strain in Simplest Cases

Type of deformation	Potential energy of deformation
Tension or compression	$\frac{1}{2} P \Delta l = \frac{P^2 l}{2EA} = \frac{\Delta l^2 EA}{2l}$
Shear	$\frac{1}{2} Q \Delta s = \frac{Q^2 a}{2GA} = \frac{\Delta s^2 GA}{2a}$
Torsion	$\frac{1}{2} M_t \varphi = \frac{M_t^2 l}{2GJ_p} = \frac{\varphi^2 GJ_p}{2l}$
Pure bending	$\frac{1}{2} M \theta = \frac{M^2 l}{2EJ} = \frac{\theta^2 EJ}{2l}$

Let us have a look at the contents of the right half of the table. The potential energy of strain is equal to half of the product of force or moment of force couple with the displacement of the section in which the force or force couple is applied. Let us use the term *generalized force* for every load that causes displacement, i.e. it may be a concentrated force or the moment of a force couple. The displacement corresponding to the generalized force will be known as *generalized displacement*. The word "corresponding" implies that we are talking of displacement of the section in which the force under consideration is acting. Elaborating further, we are talking of displacement which when multiplied by the force gives us the work done. For a concentrated force this displacement will be linear in the direction of the force (deflection or elongation). For the moment of a force couple it will be the angle of rotation of the section in the direction of the moment. The formulas in the first column may be stated in a general manner as follows: the potential energy of strain is numerically equal to half of the product of the generalized force with the generalized displacement.

The second column in these formulas shows that the potential energy of strain is a second order function of the independent external forces. Potential energy is always positive.

The third column shows that the potential energy of strain is a second order function of the finite values of generalized displacements—elongations, angles of rotation, deflections—and is completely determined by the latter.

Consequently, although these formulas have been derived on the assumption that the load increases statically without violating the equilibrium of the structure during the process of loading, they are valid for all types of forces provided the force and displacement are linearly related and are considered at an instant when the structure has attained equilibrium.

### § 99. Potential Energy for the Case of Several Forces

Imagine a beam acted upon by several forces:  $P_1, P_2, P_3, \dots$ . Let  $\delta_1, \delta_2, \delta_3, \dots$  denote the displacements of the beam in the sections of application of the forces and in the direction of their action. In Fig. 250 the solid line shows the straight axis of the beam while the dotted line shows it after deflection. We will assume that the following conditions are satisfied: (a) all forces are applied statically (their magnitude increases gradually from zero to a finite value  $P_i$ ); (b) all deformations are within the elastic limit and are linearly related to the external forces; and (c) a decrease in the potential energy of the applied force is accompanied by an increase in the potential energy of strain of the beam.

Any of the forces  $P_i$  shown in Fig. 250 can be considered a generalized force. Here, the generalized force  $P_i$  will not be just the active force but a balanced force system (including support reactions) which produces displacement  $\delta_i$  at the point of application of the force in the direction of its action.

All the forces and displacements are related to each other by the following expressions:

$$\left. \begin{aligned} \delta_1 &= a_{11}P_1 + a_{12}P_2 + a_{13}P_3 + \dots \\ \delta_2 &= a_{21}P_1 + a_{22}P_2 + a_{23}P_3 + \dots \\ \delta_3 &= a_{31}P_1 + a_{32}P_2 + a_{33}P_3 + \dots \\ &\dots \dots \dots \dots \dots \dots \dots \end{aligned} \right\} \quad (18.4)$$

Here,  $a$  denotes constants and the subscripts must be interpreted as follows: the first is the serial number of the displacement, or the "point of displacement" (for instance, number 1 as the first subscript denotes the displacement in the section of application of force  $P_1$ ); the second is the serial number of the force causing the displacement, or the "cause

of displacement" (number 2 as the second subscript denotes that the displacement has been caused by force  $P_2$ ).

The system of equations (18.4) is known as the *generalized Hooke's law for a deformable body*. The basic idea behind each line is that any displacement represents the sum of displacements of the given point due to each of forces  $P_i$ .

The generalized Hooke's law (18.4) may also be called the law of cumulative action of forces, or the law (principle) of superposition of

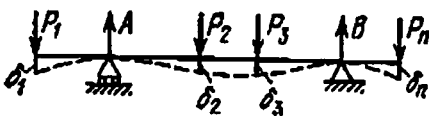


Fig. 250

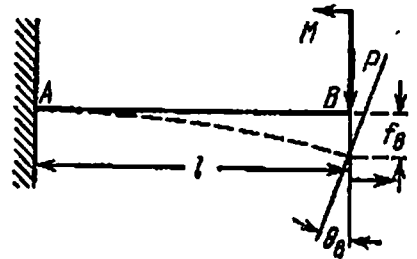


Fig. 251

forces. We have used these formulas on more than one occasion for deriving design equations (for example, equations (6.18) in § 33).

When a number of forces are acting, the potential energy should be calculated by *Clapeyron's theorem*:

$$U = W = \frac{1}{2} P_1 \delta_1 + \frac{1}{2} P_2 \delta_2 + \frac{1}{2} P_3 \delta_3 \dots \quad (18.5)$$

the notations here are the same as in formula (18.4).

Clapeyron's theorem may be stated as follows: the strain energy of an elastic system due to a number of generalized forces is equal to one-half of the sum of the products of the generalized forces and generalized displacements caused by the simultaneous action of the former.

In conclusion, it should be pointed out that in principle any group of acting force factors that can be defined by one parameter can be taken as the generalized force. However, from the practical point of view, it is convenient to partition the complicated load acting on the structure into simple generalized forces.

Let us consider an example. A beam that is rigidly fixed at one end is loaded at the free end by a concentrated force  $P$  and a force couple of moment  $M$  (Fig. 251). We shall calculate the potential energy of strain of the beam.

Clapeyron's theorem in this case can be written thus:

$$U = W = \frac{1}{2} (P f_B + M \theta_B) \quad (18.6)$$



The displacements may be taken from examples solved earlier or from a handbook:

$$f_B = \frac{Pl^3}{3EJ} - \frac{Ml^2}{2EJ}, \quad \theta_B = \frac{Ml}{EJ} - \frac{Pl^2}{2EJ} \quad (18.7)$$

The minus sign shows that the direction of displacement does not coincide with that of the corresponding force. Let us substitute the displacements into Clapeyron's theorem

$$\begin{aligned} U = W &= \frac{1}{2} P \left( \frac{Pl^3}{3EJ} - \frac{Ml^2}{2EJ} \right) + \frac{1}{2} M \left( \frac{Ml}{EJ} - \frac{Pl^2}{2EJ} \right) \\ &= \frac{P^2 l^3}{6EJ} + \frac{M^2 l}{2EJ} - \frac{PMl^2}{2EJ} \end{aligned} \quad (18.8)$$

The reader's attention is drawn to the fact that while calculating potential energy due to a number of forces it is wrong to calculate the potential energy due to each force separately and then sum them up.

### § 100. Calculating Bending Energy Using Internal Forces

In general, the bending moment  $M(x)$  is a variable quantity. It has a corresponding shearing force  $Q(x)$  in every section. Therefore, it is expedient to consider the equilibrium of a small element of length

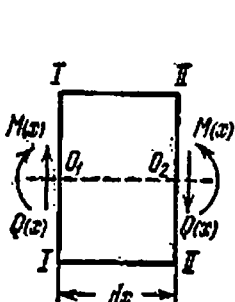


Fig. 252

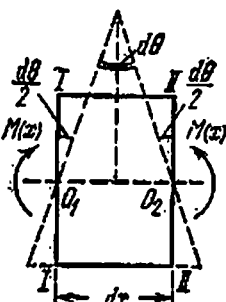


Fig. 253

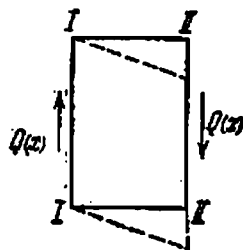


Fig. 254

$dx$  instead of the whole beam (Fig. 252). Due to the bending action of forces, the sections of the element turn and make an angle  $d\theta$  with one another (Fig. 253). The shearing forces tend to shear (Fig. 254) the element; thus the displacement due to the normal stresses is perpendicular to the direction of the shearing stresses, and vice versa. This enables us to calculate independently the work done by the normal and shearing forces.

Usually the work done by the shearing forces is small in comparison to the work done by the normal forces; therefore, we shall not take it into consideration for the time being. Elementary work done by the

normal forces (as in simple bending) is:

$$dW_p = dU = \frac{1}{2} M(x) d\theta = \frac{1}{2} M(x) \frac{M(x) dx}{EJ} \quad (18.9)$$

or 
$$dU = \frac{M^2(x) dx}{2EJ} \quad (18.10)$$

Total potential energy of bending can be obtained by integrating this expression over the whole length of the beam:

$$U = \int_l \frac{M^2(x) dx}{2EJ} = \frac{1}{2EJ} \int_l M^2(x) dx \quad (18.11)$$

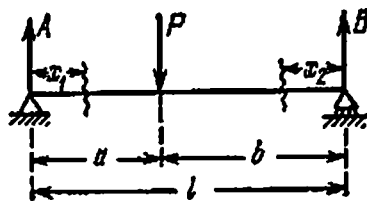
The limit of integration indicates that integration should cover the whole length of the beam; if there are a number of zones for  $M(x)$ , then integral (18.11) must be divided into a sum of integrals.

We end this section by calculating the potential energy of a simply supported beam loaded by force  $P$  (Fig. 255). The bending moment diagram has two zones; therefore

$$U = \int_0^a \frac{M_1^2 dx}{2EJ} + \int_0^b \frac{M_2^2 dx}{2EJ} \quad (18.12)$$

$$M_1 = +Ax_1 = +\frac{Pb}{l}x_1,$$

$$M_2 = +Bx_2 = +\frac{Pa}{l}x_2$$



$$U = \frac{1}{2EJ} \left[ \int_0^a \left( \frac{Pb}{l} \right)^2 x_1^2 dx + \int_0^b \left( \frac{Pa}{l} \right)^2 x_2^2 dx \right] = \frac{P^2 a^2 b^2}{6EJl}$$

Fig. 255

### § 101. Castigliano's Theorem

Let us now explain the method of determining displacements via the potential energy of strain. We shall determine the displacement of the points of an elastic system in the direction of the forces acting on it.

We shall solve this problem in a number of stages, starting with the simple case (Fig. 256) when concentrated forces  $P_1, P_2, P_3, \dots$  act in sections 1, 2, 3,  $\dots$  of the beam. Due to these forces the beam bends into curve  $I$  and there retains its equilibrium.

Let us denote by  $y_1, y_2, y_3, \dots$  the deflection of sections 1, 2, 3,  $\dots$  in which forces  $P_1, P_2, P_3, \dots$  are acting. We shall calculate one of these deflections, say,  $y_1$  (the deflection of the section in which force  $P_1$  is acting).

Let us shift the beam from position *I* into an adjacent portion *II*, shown in Fig. 256 by a dotted line, without disturbing its equilibrium. This may be achieved by various methods: by adding a new force, by increasing the existing forces, etc.

Let us assume that an infinitesimal increment  $dP_1$  (Fig. 256) is applied, in addition to force  $P_1$ , to shift the beam from position *I* to deformed state *II*. In order to retain the equilibrium of the beam

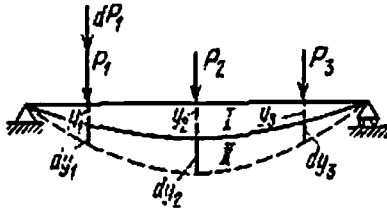


Fig. 256

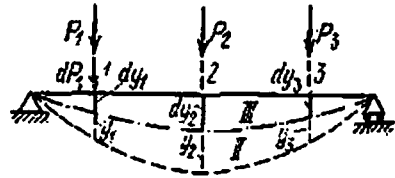


Fig. 257

during this shift we assume that the increment is applied statically, i.e. increases from zero to the final value slowly and gradually.

As the beam shifts from position *I* to position *II* all forces fall in level, meaning thereby that the potential energy decreases. Since the equilibrium of the beam remains undisturbed, the decrease in potential energy  $dU_p$  of the forces may be considered to be completely transformed into the potential energy of strain  $dU$  of the beam;  $dU_p$  is measured by the work of the external forces in shifting the beam from position *I* to position *II*:

$$dU = dW_p \tag{18.13}$$

The change in the potential energy of strain, the energy being a function of forces  $P_1, P_2, P_3, \dots$ , occurred due to an infinitesimal increment in one of the independently applied forces,  $P_1$ . Therefore, the differential of this composite function will be

$$dU = \frac{\partial U}{\partial P_1} dP_1 \tag{18.14}$$

Quantity  $dW_p$ , in its turn, represents the difference in the work done by all the forces in position *II* and in position *I*:

$$dW_p = W_2 - W_1$$

If all the forces increase simultaneously and gradually, then work  $W_1$  can be calculated as follows:

$$W_1 = \frac{1}{2} P_1 y_1 + \frac{1}{2} P_2 y_2 + \frac{1}{2} P_3 y_3 + \dots$$

While calculating  $W_2$  we must consider that it depends entirely upon the final shape of the deformed beam (§ 100) and not upon the order in which the forces are applied.

Suppose we first load the beam by force  $dP_1$ ; the beam bends slightly (Fig. 257, position *III*) and its deflections in sections 1, 2, 3 are  $dy_1$ ,  $dy_2$ ,  $dy_3$ , respectively. The work accomplished by the static force  $dP_1$  is  $\frac{1}{2} dP_1 dy_1$ . We now start loading the beam gradually and simultaneously by increasing forces  $P_1$ ,  $P_2$ ,  $P_3$ .

Deflections  $y_1$ ,  $y_2$ ,  $y_3$  will be added to the original deflections  $dy_1$ ,  $dy_2$ , and  $dy_3$  (Fig. 257). In this stage of loading, forces  $P_1$ ,  $P_2$ ,  $P_3$  will accomplish work  $\frac{1}{2} P_1 y_1 + \frac{1}{2} P_2 y_2 + \frac{1}{2} P_3 y_3 = W_1$ . In addition, force  $dP_1$ , which is already acting on the beam, will also accomplish work (it traverses a distance  $y_1$ ; since it remains constant during the second stage of loading, the work done is  $dP_1 y_1$ ). The beam occupies position *II* shown in Fig. 257 by a dotted line.

Hence, the total work done by the external forces in shifting the beam from the undeformed state into position *II* is (Fig. 257):

$$W_2 = \frac{1}{2} dP_1 dy_1 + W_1 + dP_1 \times y_1$$

Now we can calculate

$$dU = dW_p = W_2 - W_1 = \frac{1}{2} dP_1 dy_1 + dP_1 \times y_1$$

Neglecting the second-order term, we get

$$dW_p = dP_1 \times y_1 \quad (18.15)$$

Putting the values of  $dU$  (18.14) and  $dW_p$  (18.15) in equation (18.13), we get

$$dP_1 \times y_1 = \frac{\partial U}{\partial P_1} dP_1$$

or

$$y_1 = \frac{\partial U}{\partial P_1} \quad (18.16)$$

Hence, in this example the deflection at the point of application of the concentrated force  $P_1$  is equal to the partial derivative of the potential energy of strain with respect to this force.

The result obtained above can be generalized. Suppose moments  $M$  act in various sections of the beam besides the concentrated forces (Fig. 258). We may repeat the preceding discussion for the case when the beam is shifted from position *I* to position *II* due to the addition of an infinitesimally small moment  $dM_1$  to the original moment  $M_1$ . The reasoning remains unchanged. However, when calculating the work done by the moments, the latter should be multiplied not by the deflections but by the angles of rotation  $\theta_1$ ,  $\theta_2$ , . . . , etc. of the sections,

where the above moments are applied. Then  $dU$  will be equal to  $\frac{\partial U}{\partial M_1} \times dM_1$ ,  $dW_p$  will be equal to  $\theta_1 dM_1$  and formula (18.16) will take the form

$$\theta_1 = \frac{\partial U}{\partial M_1} \quad (18.17)$$

As  $y_1$  is the displacement corresponding to force  $P_1$  and  $\theta_1$  the displacement corresponding to moment  $M_1$ , the conclusions arrived at can

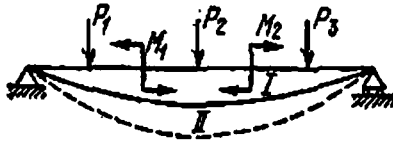


Fig. 258

be formulated more broadly as follows: the derivative of strain energy with respect to a generalized force is equal to the generalized displacement.

This result is known as *Castigliano's theorem*. It was published in 1875.

We note that if the beam were acted upon by a distributed force, the preceding derivations would still remain valid because every distributed force can be considered as consisting of a large number of concentrated forces.

The above discussion pertains to a beam, but it should be absolutely clear that it can be repeated for any structure in which deformation follows Hooke's law.

For bending we obtained a formula which correlates the potential energy with the bending moment:

$$U = \int \frac{M^2(x) dx}{2EJ} \quad (18.11)$$

Let us calculate the partial derivative of  $U$  w.r.t. one of the external forces, for example,  $P_1$ :

$$\frac{\partial U}{\partial P_1} = \frac{\partial}{\partial P_1} \left[ \int_l \frac{M^2(x) dx}{2EJ} \right]$$

We have to deal in this case with differentiation of a definite integral w.r.t. parameter, as  $M(x)$  is a function of both  $P_1$  and  $x$ ; we integrate w.r.t.  $x$  and differentiate w.r.t.  $P_1$ . We know also that if the limits of integration are constant, then it is sufficient to differentiate the function under the sign of integration.

Thus, deflection at the point of application of concentrated force  $P_1$  will be:

$$y_1 = \frac{\partial U}{\partial P_1} = \int_l \frac{M(x) dx}{EJ} \frac{\partial M(x)}{\partial P_1} \tag{18.18}$$

and the angle of rotation in the section under moment  $M_1$  will be:

$$\theta_1 = \frac{\partial U}{\partial M_1} = \int_l \frac{M(x) dx}{EJ} \frac{\partial M(x)}{\partial M_1} \tag{18.19}$$

The limit of integration,  $l$ , shows that integration is over the whole length of the beam.

### § 102. Examples of Application of Castigliano's Theorem

Let us calculate (Fig. 259) the deflection of the free end  $B$  of a beam which is rigidly fixed at its other end  $A$ . The beam is loaded by a concentrated force acting at point  $B$ . In this case we can directly apply

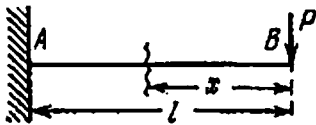


Fig. 259

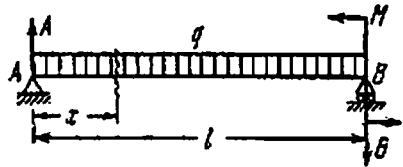


Fig. 260

Castigliano's theorem, because we are required to find the deflection of the section where concentrated force  $P$  is applied:

$$y_B = \frac{\partial U}{\partial P} = \int_l \frac{M(x) dx}{EJ} \frac{\partial M(x)}{\partial P} \tag{18.18}$$

The origin for abscissa  $x$  may be selected arbitrarily, the only consideration to be kept in mind being that the formula for  $M(x)$  should be as simple as possible. Measuring  $x$  from point  $B$ , we get the following expression for the bending moment in an arbitrary section:

$$M(x) = -Px \quad \text{and} \quad \frac{\partial M(x)}{\partial P} = -x$$

Substituting these values in the formula for  $y_B$  and integrating over the whole length of the beam from 0 to  $l$ , we obtain:

$$y_B = \int_0^l \frac{(-Px) dx}{EJ} (-x) = \frac{P}{EJ} \int_0^l x^2 dx = + \frac{Pl^3}{3EJ}$$

We have obtained the same formula as before, with the only difference that  $y_B$  is positive. We have determined the displacement corresponding to the force with respect to which the equation was differentiated. By the term "corresponding" we mean that the product of the force and corresponding displacement gives us the work done by the above force. If the displacement is positive, the work will also be positive, which implies that the displacement is in the direction of the force. If, however, the deflection or angle of rotation is negative, then displacement occurs in a direction opposite to that of the force. Thus, in this problem point  $B$  deflects downwards.

Let us consider an example in which it is essential to calculate the reactions prior to calculating the bending moment  $M(x)$ .

Let us calculate the angle of rotation at support  $B$  of a simply supported beam of span  $l$  (Fig. 260) loaded with a moment  $M$  acting at the above support and a uniformly distributed force  $q$  over its whole length.

The required angle of rotation is:

$$\theta_B = \frac{\partial U}{\partial M} = \int \frac{M(x) dx}{EJ} \frac{\partial M(x)}{\partial M} \quad (18.19)$$

Bending moment (Fig. 260) is expressed by the equation

$$M(x) = + Ax - \frac{qx^2}{2}$$

When we calculate the derivative of  $M(x)$  w.r.t.  $M$  the expression for  $M(x)$  must contain only the independent external forces, which are considered in Castigliano's theorem. Therefore, reaction  $A$  must be expressed through  $M$  and  $q$ ; if this is not done there is a chance of making a mistake during differentiation by overlooking the fact that  $A$  is a function of  $M$  and  $q$ . Reaction  $A$  is:

$$A = \frac{ql}{2} + \frac{M}{l}$$

Therefore

$$M(x) = \frac{ql}{2} x - \frac{qx^2}{2} + \frac{Mx}{l}$$

and the derivative is:

$$\frac{\partial M(x)}{\partial M} = + \frac{x}{l}$$

The limits of integration are determined from the condition that the formula for the bending moment must be valid for the total length of the beam. The required angle of rotation can be calculated as follows:

$$\theta_B = \frac{\partial U}{\partial M} = \int_0^l \frac{1}{EJ} \left( \frac{ql}{2} x - \frac{qx^2}{2} + \frac{Mx}{l} \right) \frac{x}{l} dx = \frac{ql^3}{24EJ} + \frac{Ml}{3EJ}$$

If the bending moment is expressed by different functions of  $x$  in different portions, then the integral should be divided into separate integrals for each portion. The total displacement will then be equal to the sum of all the integrals, which will be equal in number to the number of different portions in the beam. When solving such a problem it is extremely important to select the proper limits of integration.

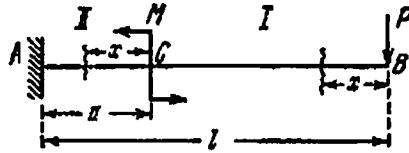


Fig. 261

Let us consider a beam of span  $l$  rigidly fixed at one end (Fig. 261), loaded by moment  $M$  acting at point  $C$  at a distance  $a$  from the support, and a force  $P$  acting at the free end. We have to determine the angle of rotation in section  $C$ .

The point of application of moment  $M$  divides the beam into two portions:  $BC$  and  $AC$ . Therefore the angle of rotation of section  $C$  is:

$$\theta_c = \frac{\partial U}{\partial M} = \int \frac{M_1 dx}{EJ} \frac{\partial M_1}{\partial M} + \int \frac{M_2 dx}{EJ} \frac{\partial M_2}{\partial M}$$

where  $M_1$  and  $M_2$  are bending moments in the sections of the first and second portions, respectively. The limits of integration can be written only after we decide the point of reference from which to measure abscissa  $x$  for each section in the two portions.

Let us consider an arbitrary section in the first portion at a distance  $x$  from the free end  $B$ . The bending moment in this section is:

$$M_1 = -Px \quad \text{and} \quad \frac{\partial M_1}{\partial M} = 0$$

the limits of integration in this portion being 0 and  $l-a$ .

When calculating the bending moment in sections of the second portion, we shall continue to measure  $x$  from the free end  $B$ ; then

$$M_2 = -Px + M \quad \text{and} \quad \frac{\partial M_2}{\partial M} = +1$$

the limits of integration being  $l-a$  and  $l$ . However, it is better to measure  $x$  for the second portion in such a way that the lower limit becomes zero (this simplifies calculations). Obviously, point  $C$ —the initial point of the second portion—should be taken as the origin. In this case we get:

$$M_2 = -P(x+l-a) + M \quad \text{and} \quad \frac{\partial M_2}{\partial M} = +1$$

the limits of integration being 0 and  $a$ .



Considering the second version, we get:

$$\theta_c = \int_0^{l-a} \frac{M_1 dx}{EJ} \frac{\partial M_1}{\partial M} + \int_0^a \frac{M_2 dx}{EJ} \frac{\partial M_2}{\partial M}$$

The first integral is zero; therefore

$$\theta_c = \frac{1}{EJ} \int_0^a [-P(x+l-a) + M] dx = -\frac{P(2l-a)a}{2EJ} + \frac{Ma}{EJ}$$

The required angle of rotation is the sum of two terms: one due to force  $P$  in the clockwise direction (against the direction of  $M$ ) and the other due to moment  $M$  in the anticlockwise direction.

### § 103. Method of Introducing an External Force

Let us consider a beam of span  $l$  fixed rigidly at end  $A$  and loaded at the free end  $B$  by a force  $P$ . Our aim is to determine the angle of rotation of section  $B$ .

Direct application of Castigliano's theorem is not possible, because in this case the force does not correspond to the nature of deformation.

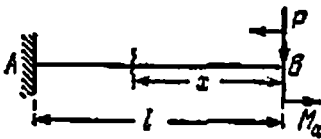


Fig. 262

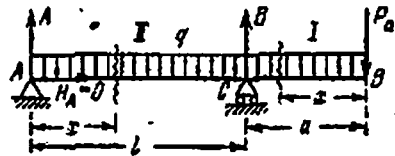


Fig. 263

We have a concentrated force acting in section  $B$  instead of a moment. To solve the problem we apply an additional moment at point  $B$  (Fig. 262) in an arbitrary direction, say, for example, in the anticlockwise direction. For a beam loaded in this manner the angle of rotation of section  $B$  can now be found by applying Castigliano's theorem.

The angle of rotation can be expressed by a formula consisting of two terms: one depending on  $P$  and the other on  $M_a$ . This formula is true for all numerical values of  $P$  and  $M_a$  including  $M_a=0$ . Therefore, by assuming that  $M_a=0$  in the final expression, we obtain the expression for angle of rotation due only to force  $P$ . The calculations are as follows:

$$\theta_B = \frac{\partial U}{\partial M_a} = \int \frac{M dx}{EJ} \frac{\partial M}{\partial M_a}$$

$$M = +M_a - Px \quad \text{and} \quad \frac{\partial M}{\partial M_a} = +1$$

The limits of integration are 0 and  $l$ ; therefore

$$\theta_B = \frac{1}{EJ} \int_0^l (M_a - Px)(+1) dx \quad (18.20)$$

We may put  $M_a=0$  after integrating the above expression. But the result will be the same if we put  $M_a=0$  in equation (18.20) and then integrate. We require the additional force only to calculate the partial derivative of the bending moment w.r.t. this additional force. Having found the partial derivative, we can safely equate the additional force to zero.

Hence, the angle of rotation of section  $B$  due to force  $P$  is:

$$\theta = \frac{1}{EJ} \int_0^l (-Px) dx = -\frac{Pl^2}{2EJ}$$

The minus sign indicates that rotation occurs against the direction of moment  $M_a$ , i.e. in the clockwise direction.

If it is required to calculate the deflection in a section of the beam where no concentrated force is acting, we must similarly apply an additional force  $P_a$  in the above section and after obtaining the expression for deflection equate the force to zero.

Let us determine the deflection of free end  $B$  of the cantilever shown in Fig. 263. The beam is loaded by a uniformly distributed force. We apply an additional force  $P_a$  in section  $B$  in order to calculate its deflection. The beam has two distinct portions:  $BC$  and  $CA$ . The deflection of  $B$  will be a sum of two integrals:

$$y_B = \frac{\partial U}{\partial P_a} = \int \frac{M_1 dx}{EJ} \frac{\partial M_1}{\partial P_a} + \int \frac{M_2 dx}{EJ} \frac{\partial M_2}{\partial P_a}$$

The reactions at the supports will be

$$A = -P_a \frac{a}{l} + \frac{q(l+a)(l-a)}{2l} = -P_a \frac{a}{l} + \frac{q(l^2 - a^2)}{2l}$$

$$B = P_a \frac{a+l}{l} + \frac{q(l+a)^2}{2l}$$

The additional force should in no case be ignored while calculating the reactions. We solve the problem by considering the additional force as one of the active forces.

The way  $x$  coordinates are measured is shown in Fig. 263 for both the portions.

In the first portion:

$$M_1 = -P_a x - \frac{qx^2}{2}, \quad \frac{\partial M_1}{\partial P_a} = -x$$

the limits of integration being  $x=0$  and  $x=a$ .

In the second portion:

$$M_2 = + Ax - \frac{qx^2}{2} = -P_a \frac{a}{l} x + \frac{q(l^2 - a^2)}{2l} x - \frac{qx^2}{2}$$

$$\frac{\partial M_2}{\partial P_a} = -\frac{a}{l} x$$

the limits of integration being  $x=0$  and  $x=l$ . Hence

$$y_B = \frac{1}{EJ} \int_0^a \left( -P_a x - \frac{qx^2}{2} \right) (-x) dx$$

$$+ \frac{1}{EJ} \int_0^l \left[ -P_a \frac{a}{l} x + \frac{q(l^2 - a^2)}{2l} x - \frac{qx^2}{2} \right] \left( -\frac{a}{l} x \right) dx$$

Assuming  $P_a=0$ , we get

$$y_B = \frac{1}{EJ} \int_0^a \frac{qx^3}{2} dx - \frac{1}{EJ} \int_0^l \left[ \frac{q(l^2 - a^2)a}{2l^2} x^2 - \frac{qx^3 a}{2l} \right] dx$$

$$= + \frac{qa^4}{8EJ} - \frac{qa^3 l}{24EJ} (l^2 - 4a^2)$$

The first factor represents the deflection due to the load on the cantilever and the second the deflection due to the load between the supports.

### § 104. Theorem of Reciprocity of Works

With the help of the concept of potential energy we may derive the following relation between deformations in various sections of a beam.

If we apply a static force  $P_2$  in section 2 of a beam already loaded by force  $P_1$ , then to deflection  $y_{11}$  of the point of application of force  $P_1$  due to this force will be added a deflection  $y_{12}$ , due to force  $P_2$  (Fig. 264). The first number in the subscript of  $y$  indicates the point the deflection of which is required to be determined; the second number indicates the force causing this deflection.

The total work done by the external forces will consist of three terms: work done by force  $P_1$  in causing deflection  $y_{11}$ , i.e.  $\frac{1}{2} P_1 y_{11}$ ; work done by force  $P_2$  in deflecting the point of its application by  $y_{22}$ , i.e.  $\frac{1}{2} P_2 y_{22}$ ; and, finally, work done by force  $P_1$  over deflection  $y_{12}$  caused by the force  $P_2$ , i.e.  $P_1 y_{12}$ .

Therefore, the total accumulated energy due to the two forces is:

$$U = \frac{1}{2} P_1 y_{11} + \frac{1}{2} P_2 y_{22} + P_1 y_{12} \quad (18.21)$$

(the potential energy of strain depends only upon the final values of forces and deflections and not upon the order of applying the external forces).

Now, if we apply force  $P_1$  to a beam already loaded by force  $P_2$ , then reasoning in the same way we obtain

$$U = \frac{1}{2} P_2 y_{22} + \frac{1}{2} P_1 y_{11} + P_2 y_{21} \quad (18.22)$$

Comparing the two expressions for  $U$ , we get

$$P_1 y_{12} = P_2 y_{21} \quad (18.23)$$

i.e. the work done by force  $P_1$  (or the first group of forces) over displacements caused by force  $P_2$  (the second group of forces) is equal to the work done by force  $P_2$  over displacements caused by force  $P_1$ .

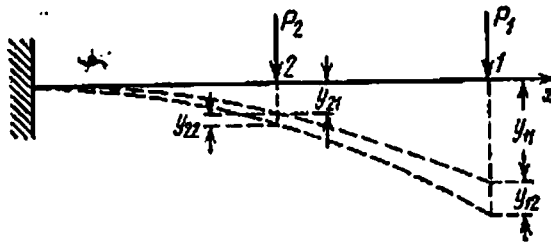


Fig. 264

This is known as the *theorem of reciprocity of works*. It can be stated in another way: work done by the first force ( $P_1$ ) under the action of the second force ( $P_2$ ) is equal to the work done by the second force under the action of the first.

By taking a particular case when  $P_1 = P_2$ , we obtain the *theorem of reciprocity of displacements*:  $y_{12} = y_{21}$ , i.e. deflection of point 1 due to the force acting at point 2, is equal to the deflection of point 2 due to the force acting at point 1.

### § 105. The Theorem of Maxwell and Mohr

Deflection of a beam at the point of application of concentrated force  $P$  is:

$$y = \int_0^l \frac{M(x) dx}{EJ} \frac{\partial M(x)}{\partial P} \quad (18.18)$$

a similar expression can be obtained for the angle of rotation by replacing  $\frac{\partial M(x)}{\partial P}$  with  $\frac{\partial M(x)}{\partial M}$ . Let us elucidate the physical meaning of these derivatives.

If a beam is acted upon by an arbitrary number of concentrated forces  $P_1, P_2, \dots$ , moments  $M_1, M_2, \dots$ , and distributed forces  $q_i$ ,

$q_2, \dots$ , then moment  $M(x)$  in any section of the beam is a linear function of all these factors:

$$M(x) = a_1 P_1 + a_2 P_2 + \dots + b_1 M_1 + b_2 M_2 + \dots + c_1 q_1 + c_2 q_2 \dots \quad (18.24)$$

Coefficients  $a_1, a_2, \dots, b_1, b_2, \dots, c_1, c_2, \dots$  are functions of the beam span, the distances of the points of application of the various forces and moments from the supports, and the abscissa  $x$  of the section in which the bending moment is required to be calculated. Suppose

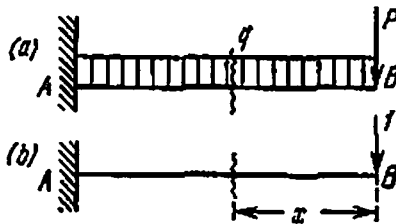


Fig. 265

we have to find the deflection of the point of application of force  $P_1$ . Then  $\frac{\partial M(x)}{\partial P_1} = a_1$ , because in this differentiation  $P_2, P_3, \dots, M_1, M_2, \dots, q_1, q_2, \dots, a_1, a_2, \dots, b_1, b_2, \dots, c_1, c_2, \dots$  are all constant quantities. However,  $a_1$  may be taken as the numerical value of moment  $M$  in an arbitrary section due to a unit force, i.e.  $P_1 = 1$ : it is evident that by putting  $P_1 = 1$  and equating all other forces to zero in equation (18.24) we get  $M = a_1$ .

For example, for the beam shown in Fig. 265(a) the bending moment is:

$$M(x) = -Px - \frac{qx^2}{2}$$

The derivative  $\frac{\partial M(x)}{\partial P} = -x$ , which is also the expression of the bending moment for the beam, if we load it by a unit force acting at point B—the point of application of force  $P$  (Fig. 265(b))—in the same direction.

Similarly, the derivative of  $M(x)$  w.r.t. force couple  $M_1$  is numerically equal to the bending moment due to a unit force couple acting in the same section as  $M_1$ .

Hence the calculation of derivatives of a bending moment may be replaced by the calculation of the bending moment due to a unit force. We shall denote such moments by  $M^0$ .

Thus, to determine displacement  $\delta$  (deflection or angle of rotation) of an arbitrary section, irrespective of whether the corresponding force acts in this section or not, we must write down the expressions for the bending moment  $M(x)$  due to the given load (we shall denote it simply

by  $M$ ) and for  $M^0$  due to a corresponding unit force acting in the section in which displacement  $\delta$  is required to be found. Then this displacement will be given by the formula

$$\delta = \int_0^l \frac{MM^0}{EJ} dx \quad (18.25)$$

This formula was first derived by J. C. Maxwell in 1864 and applied in design practice by O. Mohr in 1874.

If in formula (18.25) we want to define deflection as  $\delta$ , then moment  $M^0$  should be calculated for a unit concentrated force applied in the section where the deflection is required. If, however, we want to calculate the angle of rotation, then a unit moment should be applied.

For the example considered in Fig. 265 we have:

$$M = -Px - \frac{qx^2}{2} \quad (\text{Fig. 265(a)})$$

$$M^0 = -1 \times x = -x \quad (\text{Fig. 265(b)})$$

$$y_p = \frac{1}{EJ} \int_0^l \left( -Px - \frac{qx^2}{2} \right) (-x) dx = \frac{ql^4}{8EJ} + \frac{Pl^3}{3EJ}$$

The plus sign indicates that the direction of displacement coincides with the direction of the unit force; a minus sign would indicate the opposite direction.

If the beam has to be divided into a number of portions to calculate the bending moment in a section, then the integral in formula (18.25) will also break into a sum of the respective integrals.

### § 106. Vereshchagin's Method

Pirlet and A. N. Vereshchagin and before them H.F.B. Müller-Breslau proposed a simplification in calculations according to formula (18.25). As the unit load is usually either a concentrated force or a force couple (moment), the  $M^0$ -diagram is bounded by straight lines. In such cases, for any shape of the bending moment diagram, integral  $\int MM^0 dx$  can be calculated as follows. Suppose the bending moment diagram (Fig. 266) is represented by a curve, whereas the diagram for  $M^0$  is a straight line. The product  $M dx$  may be considered as the area element  $d\omega$ , which is shaded on the bending moment diagram.

As the ordinate  $M^0 = x \tan \alpha$ , the product  $M dx M^0 = d\omega x \tan \alpha$ . Hence integral  $\int MM^0 dx = \tan \alpha \int x d\omega$  represents the static moment of the area of the bending moment diagram about point  $A$  multiplied by  $\tan \alpha$ . However, the static moment is equal to the total area  $\omega$

of the bending moment diagram multiplied by the distance  $x_c$  of its centre of gravity from point A. Therefore

$$\int MM^0 dx = \omega x_c \tan \alpha$$

But  $x_c \tan \alpha$  is the ordinate  $M_c^0$  of the  $M^0$ -diagram under the centre of gravity of the bending moment diagram. Therefore

$$\int MM^0 dx = \omega M_c^0$$

and the required displacement is

$$\delta = \frac{\omega M_c^0}{EJ} \tag{18.26}$$

Hence, in order to determine displacement  $\delta$ , we must calculate area  $\omega$  of the bending moment diagram, multiply it by ordinate  $M_c^0$  of the unit bending moment diagram under the centre of gravity of area  $\omega$ , and divide it by the rigidity of the beam,  $EJ$ .

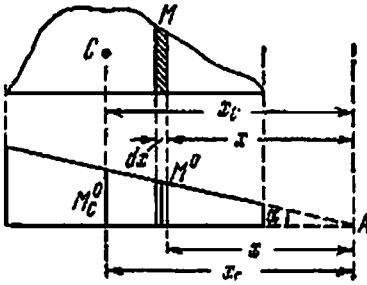


Fig. 266

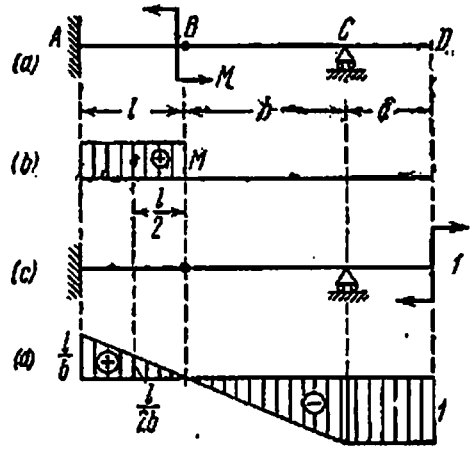


Fig. 267

Let us determine by this method the angle of rotation of section D of the beam shown in Fig. 267(a). The beam is loaded by a moment  $M$  acting at the end B of the cantilever AB. The bending moment diagram is shown in Fig. 267(b). Let us apply a unit moment in section D in an arbitrary direction (Fig. 267(c)). The bending moment diagram due to the unit load is shown in Fig. 267(d). As  $M$  is zero in portions DC and CB, we are left with only one integral for portion AB.

Area  $\omega$  is equal to  $+Ml$ , and the ordinate of the  $M^0$ -diagram under the centre of gravity of area  $\omega$  is equal to  $+\frac{l}{2b}$ . Therefore the required

angle of rotation  $\theta_D$  is:

$$\theta_D = \frac{1}{EJ} (+Ml) \left( +\frac{l}{2b} \right) = +\frac{Ml^2}{2bEJ}$$

The plus sign indicates that rotation is in the direction of the unit moment, i.e. in the clockwise direction.

### § 107. Displacements in Frames

Let us calculate the angle of rotation  $\theta$  of section  $C$  and horizontal displacement  $\Delta$  of point  $D$  of the frame shown in Fig. 268(a) with the help of Mohr's theorem.

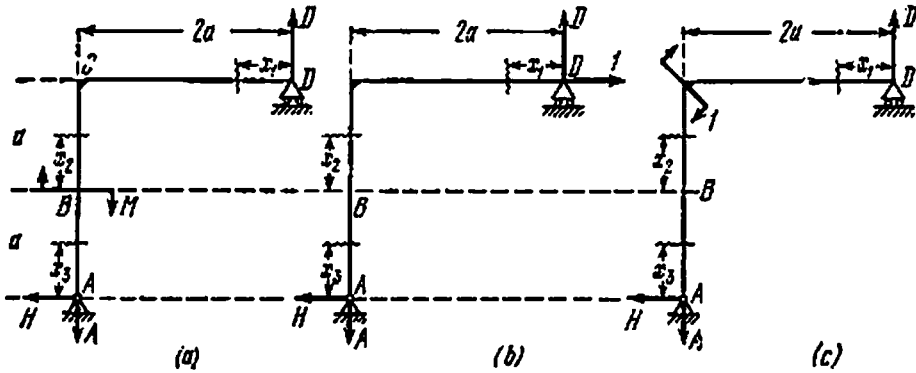


Fig. 268

Let us calculate the reactions and bending moments for all the three states in Fig. 268(a), (b), and (c), respectively;

(a) due to the given load:

$$H = 0, \quad D = \frac{M}{2a} = A, \quad M_1 = +\frac{M}{2a}x_1, \quad M_2 = +M, \quad M_3 = 0$$

(b) due to unit force:

$$H = 1, \quad D = 1 = A, \quad M_1^0 = +x_1, \quad M_2^0 = a + x_2, \quad M_3^0 = +x_2$$

(c) due to unit moment:

$$H = 0, \quad D = \frac{1}{2a} = A, \quad M_1^0 = +\frac{x_1}{2a}, \quad M_2^0 = 0, \quad M_3^0 = 0$$

The deformations are:

(a) and (b)

$$\begin{aligned} \Delta &= \frac{1}{EJ} \left[ \int_0^{2a} M_1 M_1^0 dx + \int_0^a M_2 M_2^0 dx + \int_0^a M_3 M_3^0 dx \right] \\ &= \frac{1}{EJ} \left[ \int_0^{2a} \frac{M}{2a} x_1^2 dx + \int_0^a M (a + x_2) dx \right] = \frac{17}{6} \frac{Ma^2}{EJ} \end{aligned}$$



(a) and (c)

$$\begin{aligned}\theta &= \frac{1}{EJ} \left[ \int_0^{2a} M_1 M_1^0 dx + \int_0^a M_2 M_2^0 dx + \int_0^a M_3 M_3^0 dx \right] \\ &= \frac{1}{EJ} \int_0^{2a} \frac{M}{2a} x_1 \frac{x_1}{2a} dx = \frac{2Ma}{3EJ}\end{aligned}$$

In solving the same problem by Vereshchagin's method we must plot bending moment diagrams for all the three loading arrangements in

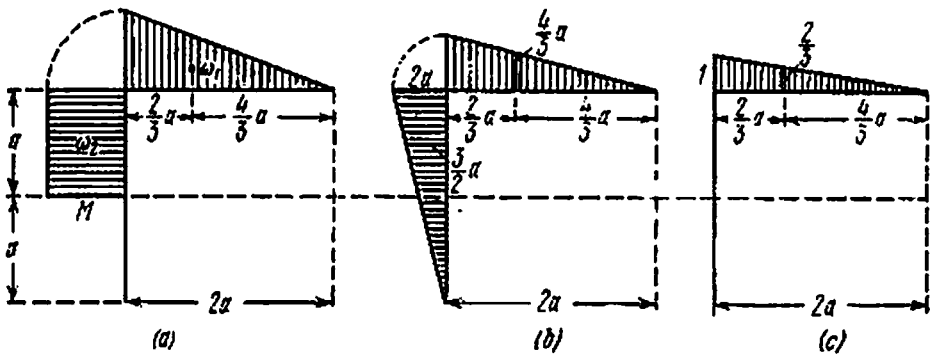


Fig. 269

Fig. 268. The diagrams, which are shown in Fig. 269(a), (b), and (c), enable us to determine the following quantities:

$$\omega_1 = Ma, \quad \omega_2 = Ma, \quad \omega_3 = 0 \quad (a)$$

$$M_{C_1}^0 = \frac{4}{3} a, \quad M_{C_2}^0 = \frac{3}{2} a \quad (b)$$

$$M_{C_1}^0 = \frac{2}{3}, \quad M_{C_2}^0 = 0, \quad M_{C_3}^0 = 0 \quad (c)$$

If there are three zones of loading, formula (18.26) can be written as

$$\delta = \frac{1}{EJ} (\omega_1 M_{C_1}^0 + \omega_2 M_{C_2}^0 + \omega_3 M_{C_3}^0)$$

The required displacements are:

$$\Delta = \frac{1}{EJ} \left( Ma \frac{4}{3} a + Ma \frac{3}{2} a \right) = \frac{17}{6} \frac{Ma^2}{EJ}$$

$$\theta = \frac{1}{EJ} Ma \frac{2}{3} = \frac{2}{3} \frac{Ma}{EJ}$$

§ 108. Deflection of Beams Due to Shearing Force

In calculating deformations we have considered only the bending moment. However, shearing forces also cause deflection. The Russian scientist Prof. I.G. Bubnov was the first to determine the deformation of a beam by considering the shearing forces.

Let us consider a beam rigidly fixed at one end and loaded at the other by a force  $P$ . Due to shearing stresses two adjacent sections  $a_1b_1$  and  $a_2b_2$  (Fig. 270(a)) separated by a distance  $dx$  will warp. Maximum distortion will occur near the neutral axis; elements locat-

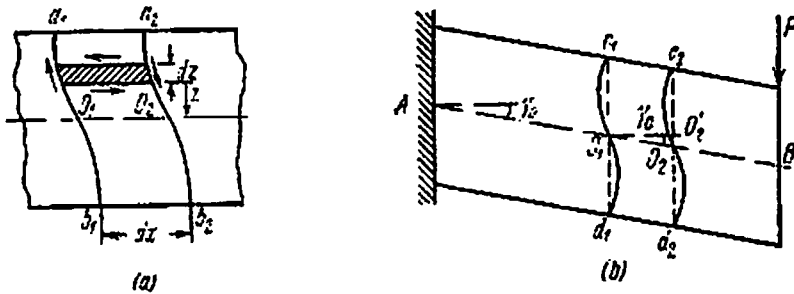


Fig. 270

ed at the top and bottom surfaces of the beam will not warp. The planes will occupy certain intermediate positions (dotted lines  $c_1O_1d_1$  and  $c_2O_2d_2$ ) making an angle  $\gamma_0$  with the original (Fig. 270(b)). As in this case the shearing stresses are the same in all sections, they will all turn by the same angle  $\gamma_0$  and due to exclusive effect of shearing stresses occupy the position shown in Fig. 270(b); end  $B$  will lower w.r.t. support  $A$ . The deformation due to bending moment, which is in the form of rotation of adjacent sections, is not shown in the figure.

Absolute deflection of the second section w.r.t. the first will be equal to segment  $O_2O_2'$ , i.e.

$$|dy_Q| = O_2O_2' \tag{18.27}$$

In the general case, when the shearing force  $Q(x)$  is not constant but varies along the length of the beam, angle  $\gamma_0$  will also vary. However, the overall picture of deformation will remain unaffected; only  $dy_Q$  will be different for different elements of length  $dx$ .

Absolute deflection of the second section w.r.t. the first,  $|dy_Q|$ , may be calculated from the condition that potential energy of strain accumulated in the element of length  $dx$  during shearing is equal to the work of external forces acting on the element:  $dU_Q = dW_P$ .

For the beam under consideration the external forces will be the shearing stresses (the shearing force  $Q(x)$ ). If the increase in load and deformation is gradual, then the work done by these forces over a rela-

tive displacement  $|dy_Q|$  is

$$dW_p = \frac{1}{2} Q(x) |dy_Q| \quad (18.28)$$

As the shearing stresses are not uniformly distributed over the section, we have to take recourse to the method of differentiation in order to determine the potential energy accumulated by the beam due to these stresses.

Let us cut a small element of dimensions  $dx$ ,  $dz$ ,  $b(z)$  at a distance  $x$  from the origin of coordinates and at a distance  $z$  from the neutral axis (Fig. 270(a)) out of a rectangular beam (or a beam made of rectangular beams). In addition to the normal stresses, the sides of this element will also be subjected to shearing stresses

$$\tau = \frac{Q(x) S(z)}{J b(z)}$$

For this element the potential energy of shear will be expressed by the formula

$$\frac{[b(z) \tau dz]^2 dx}{2b(z) G dz} = \frac{1}{2G} \tau^2 b(z) dx dz$$

Energy in the element of length  $dx$  and height  $h$  will be

$$dU_Q = \int \frac{1}{2G} \tau^2 b(z) dz dx = \frac{1}{2G} \frac{Q^2(x) dx}{J^2} \int \frac{S^2(z) dz}{b(z)}$$

Integration is carried out w.r.t.  $z$ , and the limits of integration are selected so as to cover the whole section.

The above expression may be modified by multiplying and dividing it with the cross-sectional area  $A$ :

$$dU_Q = \frac{Q^2(x) dx}{2GA} \frac{A}{J^2} \int \frac{S^2(z) dz}{b(z)} = \frac{kQ^2(x) dx}{2GA} \quad (18.29)$$

where  $k$  is a dimensionless number which depends only upon the shape and size of the beam and is:

$$k = \frac{A}{J^2} \int \frac{S^2(z) dz}{b(z)} \quad (18.30)$$

Equating the values of  $dU_Q$  and  $dW_p$ , we get

$$\frac{kQ^2(x) dx}{2GA} = \frac{1}{2} Q(x) |dy_Q|$$

wherefrom

$$|dy_Q| = k \frac{Q(x) dx}{GA}$$

The sign of deflection may be determined as follows. If the shearing force  $Q(x)$  is positive and the  $y$ -axis is positive upwards, then the relative deflection  $dy_Q$  will be negative if we move from the left-hand section towards the right (Fig. 270 (b)). Consequently,

$$dy_Q = -\frac{kQ(x)}{GA} dx \quad (18.31)$$

Total deflection of any section having abscissa  $x$  is obtained by integrating expression (18.31):

$$y_Q = -\int \frac{kQ(x)}{GA} dx + C_Q \quad (18.32)$$

The constant of integration  $C_Q$  depends upon the type of constraints. Since  $Q(x) = dM(x)/dx$ , we have

$$y_Q = \frac{-kM(x)}{GA} + C_Q \quad (18.33)$$

i.e. the deflection of the beam due to the shearing force is directly proportional to the ordinate of the bending moment diagram with the opposite sign; the ordinates are measured from a definite axis of abscissas.

Constant  $k$  may be calculated for all types of sections. For a rectangular section

$$S(z) = \frac{bh^2}{8} \left( 1 - \frac{4z^2}{h^2} \right), \quad J = \frac{bh^3}{12}, \quad b(z) = b, \quad A = bh$$

Therefore

$$k = \frac{A}{J^2} \int_{-h/2}^{h/2} \frac{S^2(z) dz}{b(z)} = \frac{9}{2h} \int_0^{h/2} \left( 1 - \frac{4z^2}{h^2} \right) dz = \frac{6}{5}$$

Let us use the above result in determining the deflection of a beam of span  $l$ , fixed at its left end  $A$  and loaded at the free end  $B$  by a concentrated force  $P$ . Assuming point  $A$  as the origin of coordinates, we get:

$$M(x) = -P(l-x) \quad \text{and} \quad y_Q = +\frac{kP(l-x)}{GA} + C_Q = \frac{6P(l-x)}{5GA} + C_Q$$

At  $x=0$  the deflection  $y_A=0$ ; therefore  $C_Q = -\frac{6Pl}{5GA}$ . Deflection  $y_Q$  may be written as

$$y_Q = -\frac{6Px}{5GA}$$

Maximum deflection occurs at point  $B$ , i.e. at the end of the beam (where  $x=l$ ):

$$f_Q = -\frac{6Pl}{5GA}$$

Total deflection of point  $B$  is:

$$f = -\frac{Pl^3}{3EJ} - \frac{6}{5} \frac{Pl}{GA} = -\frac{Pl^3}{3EJ} \left( 1 + \frac{18EJ}{5l^3GA} \right)$$

As  $\frac{J}{A} = \frac{h^2}{12}$  for a rectangular section, we get

$$f = -\frac{Pl^3}{3EJ} \left( 1 + \frac{3h^2}{10l^2} \frac{E}{G} \right)$$

Assuming  $\frac{E}{G}$  equal to  $\frac{5}{2}$  for metals and 20 for wood, we obtain:

$$f = -\frac{Pl^3}{3EJ} \left( 1 + \frac{3}{4} \frac{h^2}{l^2} \right) \quad (\text{for metals})$$

$$f = -\frac{Pl^3}{3EJ} \left( 1 + 6 \frac{h^2}{l^2} \right) \quad (\text{for wood})$$

Thus we see that additional deflection due to the shearing force depends upon  $\left(\frac{h}{l}\right)^2$ . Therefore in comparatively short beams, especially in wooden beams, it may acquire a high value. For example, if  $\frac{h}{l} = \frac{1}{4}$ , then for a wooden beam  $1 + 6 \frac{h^2}{l^2} = 1.375$ , i.e. deflection due to the shearing force is 37.5% of the deflection due to the bending moment.

It should be noted that in a number of courses  $h$  is taken as 1.5 and not as 1.2 (for a rectangular section). This result is obtained by assuming that the deflection of the beam due to a shearing force depends upon the shearing strain at the neutral surface, but this assumption is erroneous.

It should be further noted that the displacements described above will not occur over some length near the fixed end (Fig. 270), but this reduces the calculated deflection of the beam by a very small amount.

## CHAPTER 19

### Statically Indeterminate Beams

#### § 109. Fundamental Concepts

Until now we have been considering only statically determinate beams, in which the three support reactions can be determined from equations of equilibrium. Very often the conditions in which the structure works require that the number of supports be increased; the beams in these cases become *statically indeterminate*.

For example, to decrease the span of a simply supported beam (Fig. 271(a)), we may put an additional support at the middle

(Fig. 271(b)); to reduce the deflection of the beam rigidly fixed at one end (Fig. 272(a)), we may prop its free end (Fig. 272(b)).

The cross-sectional dimensions of these beams, as of the beams discussed earlier, are obtained by plotting the shearing force and bending moment diagrams (obviously after determining the support reactions).

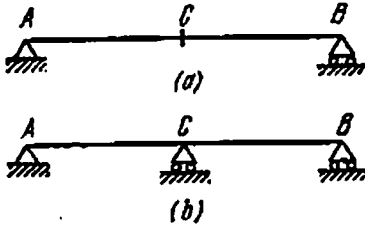


Fig. 271

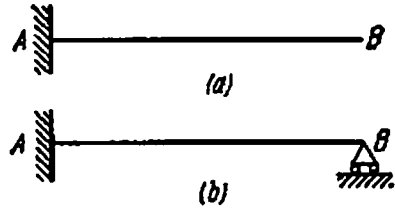


Fig. 272

In all such cases the number of possible support reactions exceeds the number of static equations.

If the number of support reactions exceeds the number of static equations by one, the beam is known as *single-degree statically indeterminate*. If the difference is greater, the beam becomes *statically indeterminate by two degrees, three degrees* and so on. In this book we have considered mostly *single-degree statically indeterminate beams* and also *multiple-degree statically indeterminate continuous beams*.

The basic method employed for removing the static indeterminacy of beams was proposed by C.-L.-M. Navier in 1826 and is based upon integration of the differential equation of the deflected beam axis. This method will be discussed in the next section.

### § 110. Removing Static Indeterminacy Via the Differential Equation of the Deflected Beam Axis

If one hinged support is added to a statically determinate beam, it makes the beam *single-degree statically indeterminate* and simultaneously creates one new condition for determining the unknowns: the deflection of the beam at the support is equal to zero. Therefore, when the differential equation of the deflected beam axis is integrated twice, the overall number of equations and unknowns is found to be equal.

Let us consider the beam shown in Fig. 273. The static equations for the beam are:  $H_A=0$  (1),  $A+B=ql$  (2); and  $B l - q \frac{l^2}{2} + M_A=0$  (3). One reaction is immediately known. We are left with two equations, (2) and (3), and three unknown support reactions:  $A$ ,  $B$ , and  $M_A$ . The beam is thus *single-degree statically indeterminate*.

Let us now write the differential equation of the deflected beam axis and integrate it twice:

$$EJy'' = Bx - q\frac{x^2}{2} \quad (19.1)$$

$$EJy' = B\frac{x^2}{2} - q\frac{x^3}{6} + C \quad (19.2)$$

$$EJy = \frac{Bx^3}{6} - \frac{qx^4}{24} + Cx + D \quad (19.3)$$

On account of  $C$  and  $D$  the number of unknowns has increased to five, but now the two static equations are supplemented by three constraint conditions: (1)  $y=0$  at  $x=0$ , (2)  $y'=0$  at  $x=l$ , and (3)  $y=0$  at  $x=l$ .

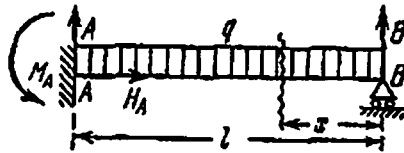


Fig. 273

It ensues from (1) that  $D=0$ . Conditions (2) and (3) when substituted into equations (19.2) and (19.3), respectively, give

$$\frac{Bl^2}{2} - \frac{ql^3}{6} + C = 0 \quad (19.4)$$

$$\frac{Bl^3}{6} - \frac{ql^4}{24} + Cl = 0 \quad (19.5)$$

Dividing (19.5) by  $l$  and subtracting (19.5) from (19.4)

$$\frac{Bl^2}{2} - \frac{ql^3}{6} - \frac{Bl^2}{6} + \frac{ql^3}{24} = 0$$

From this equation we find

$$B = \frac{3}{8} ql \quad (19.6)$$

From the equation of statics (2) we find  $A = \frac{5}{8} ql$ . Next we determine from equation (3) the moment in the rigidly fixed end,  $M_A = \frac{ql^3}{8}$ . The fact that the support reactions are positive indicates that their directions shown in Fig. 273 are correct.

Substituting  $B$  in expression (19.4), we obtain

$$C = -\frac{3}{8} ql \frac{l^2}{2} + q \frac{l^3}{6} = -\frac{ql^3}{48}$$

Now, substituting  $B$  and  $C$  in equations (19.2) and (19.3) we get the final equations for angles of rotation and deflections:

$$EJy' = \frac{3}{16} qx^2l - q \frac{x^3}{6} - q \frac{l^3}{48} \quad (19.7)$$

$$EJy = \frac{3}{48} qx^3l - q \frac{x^4}{24} - \frac{ql^3x}{48} \quad (19.8)$$

Having determined support reactions  $B$ ,  $A$ , and  $M_A$ , we can now plot the bending moment and shearing force diagrams by the usual method.

With the help of equations (19.7) and (19.8) we can determine the angle of rotation and vertical displacement of an arbitrary section of the beam in the same manner as for statically determinate beams.

If the beam has a number of differently loaded zones, the static indeterminacy may be removed either by using the method of equating the integration constants (Clebsch's method, § 85) or by the general equations of the method of initial parameters (§ 86).

### § 111. Concepts of Redundant Unknown and Base Beam

After considering the beam shown in Fig. 273 we established that the number of equations of statics was one less than the number of the unknown support reactions. One of the reactions is a superfluous or, as it is sometimes called, a "redundant" unknown. This term has taken deep roots in technical literature although it can be applied only with certain reservations. Obviously, the extra reaction and the corresponding support constraint are redundant only from the point of view of their necessity in the equilibrium of the beam as one rigid body. From the engineer's point of view in a number of cases the extra support is not redundant but is actually a helpful tool in designing structures.

In a number of methods employed for removing static indeterminacy of beams, we write down conditions expressing the compatibility of displacements in that section, where the "redundant" reaction is acting. These conditions along with the usual equations of statics enable us to determine all the unknown support reactions.

In § 110 for the beam shown in Fig. 273 we had two equations of statics for determining three unknown support reactions  $A$ ,  $B$ , and  $M_A$ . Any of the three can be taken as the redundant reaction. Let us choose the reaction of support  $B$  as redundant. In this case we can argue that the given beam is obtained from the statically determinate beam  $AB$  with end  $A$  rigidly fixed (Fig. 274); end  $B$  is later propped up by an additional support.

The statically determinate beam obtained from the statically indeterminate beam by removing the "redundant" constraint is known as the



base beam. By selecting one of the reactions as redundant we at the same time select the base beam.

Let us now try to transform the base beam (Fig. 274) into a beam which is completely identical to the given statically indeterminate beam (Fig. 273). For this we load the base beam with the distributed force  $q$  and apply a "redundant" reaction  $B$  at its end  $B$  (Fig. 275).



Fig. 274

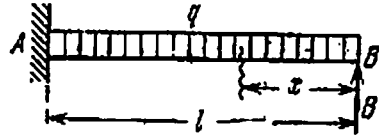


Fig. 275

However, this is not sufficient. In the beam shown in Fig. 275, point  $B$  may move vertically under the action of forces  $q$  and  $B$ , whereas in the actual statically indeterminate beam (Fig. 273) point  $B$  does not have this freedom: it must remain attached to the supporting hinge. Therefore, to make Figs. 273 and 275 identical, we must add the condition that the deflection of point  $B$  due to forces  $q$  and  $B$  must be zero:

$$f_B = 0 \quad (19.9)$$

This is the additional equation which enables us to determine reaction  $B$ . It represents the condition of joint deformation as applied to this case: end  $B$  does not detach from the support. This additional equation can be solved by a number of methods.

## § 112. Method of Comparison of Displacements

Equation (19.9)  $f_B = 0$ , which was obtained in § 111 and which expresses the condition of joint deformation, may be solved as follows.

The total deflection of point  $B$  of the base beam due to forces  $q$  and  $B$  is made up of two deflections:  $f_{Bq}$  due to force  $q$  and  $f_{BB}$  due to force  $B$ . Therefore

$$f_B = f_{Bq} + f_{BB} = 0 \quad (19.10)$$

We have to calculate these deflections. First load the base beam only by force  $q$  (Fig. 276(a)). The deflection of point  $B$  will be

$$f_{Bq} = -\frac{ql^4}{8EJ}$$

Let us load the base beam by "redundant" reaction  $B$  (Fig. 276(b)). The deflection of point  $B$  in this case will be

$$f_{BB} = +\frac{Bl^3}{3EJ}$$

Substituting these values in equation (19.10) we get

$$-\frac{ql^3}{8EJ} + \frac{Bl^3}{3EJ} = 0$$

wherefrom  $B = \frac{3ql}{8}$ , i.e. the same as obtained earlier in § 110 (19.6).

In this method we first allow the base beam to deform under force  $q$ , and then select a force  $B$  which returns point  $B$  to its original position. Thus we select the unknown reaction  $B$  such that the deflections

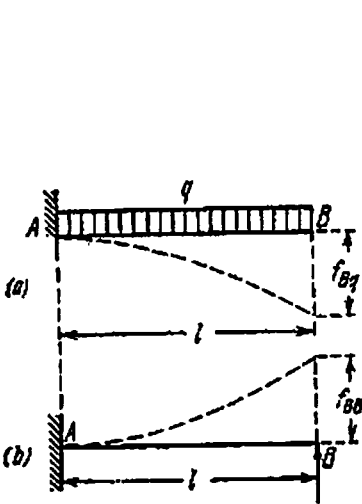


Fig. 276

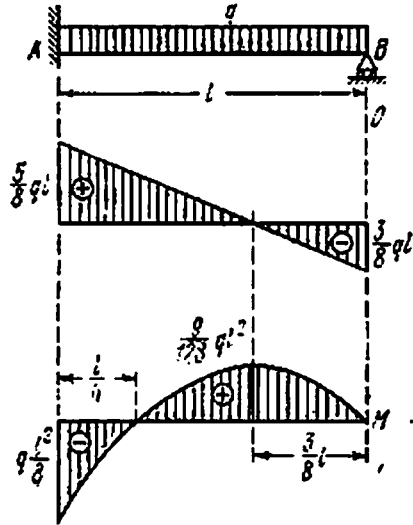


Fig. 277

due to  $q$  and  $B$  neutralize each other. This method is known as the *method of comparison of displacements*.

The remaining reactions are (see § 110)

$$A = 5 \frac{ql}{8}, \quad M_A = \frac{ql^2}{8}$$

The bending moment expression is obtained by considering the right-hand side of the beam (Fig. 275) and substituting the value of  $B$  calculated above (19.6):

$$M = \frac{3ql}{8} x - \frac{qx^2}{2} = \frac{qx}{2} \left( \frac{3l}{4} - x \right)$$

Shearing force  $Q$  is expressed by the formula

$$Q = -B + qx = -q \left( \frac{3l}{8} - x \right)$$

The bending moment and shearing force diagrams are shown in Fig. 277. The section of maximum bending moment corresponds to

abscissa  $x_0$ , which may be obtained from the following relation:

$$\frac{dM}{dx} = 0, \quad \text{i.e.} \quad \frac{3ql}{8} - qx_0 = 0$$

wherefrom  $x_0 = \frac{3l}{8}$ . The corresponding ordinate of the bending moment diagram is:

$$M_{\max} = M_{x_0} = \frac{3ql}{8} \frac{3l}{8} - \frac{q}{2} \frac{9l^2}{64} = + \frac{9}{128} ql^2$$

§ 113. Application of the Theorems of Castigliano and Mohr and Vereshchagin's Method

The indeterminacy of the beam discussed in §§ 110-112 can also be removed by Castigliano's theorem (§ 101).

The "redundant" reaction  $B$  (Fig. 278 (a)) is replaced by a redundant unknown force  $B$ , which acts on the statically determinate beam  $AB$  (Fig. 278 (b)) along with the given force  $q$ .

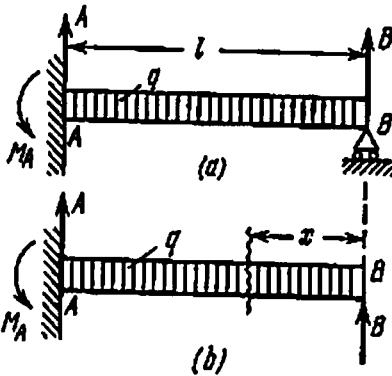


Fig. 278

By differentiating the expression for potential energy w.r.t.  $B$  and equating the deflection  $f_B$  thus obtained to zero we may write equation (19.9) as follows:

$$\int_0^l \frac{M}{EJ} \frac{\partial M}{\partial B} dx = 0 \quad (19.11)$$

We now have to calculate  $M$  and  $\frac{\partial M}{\partial B}$  and integrate within the appropriate limits

$$M = + Bx - \frac{qx^2}{2}, \quad \frac{\partial M}{\partial B} = x \quad (19.12)$$

We assume that the beam has a uniform section all along its length; after dividing by  $EJ$  equation (19.11) may be written as

$$\int_0^l \left( Bx - \frac{qx^2}{2} \right) x dx = 0 \quad (19.13)$$

wherefrom

$$B = \frac{3ql}{8} \quad (19.6)$$

After this the solution is the same as in the method of displacement comparison.

After the indeterminacy of the beam has been removed, displacements in statically indeterminate beams are determined in a manner exactly similar to that used for statically determinate beams. If an additional force has to be applied for determining displacements (§ 103), the force should be assumed to act on the base beam. Under these circumstances the additional force only affects the main reactions and the redundant reaction must be regarded as an active force, as before.

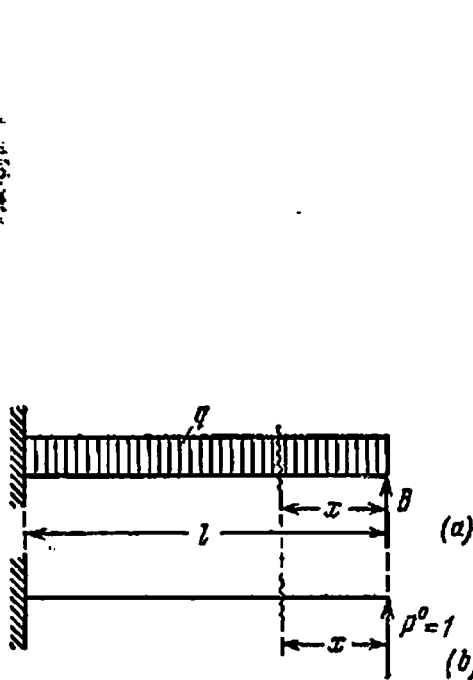


Fig. 279

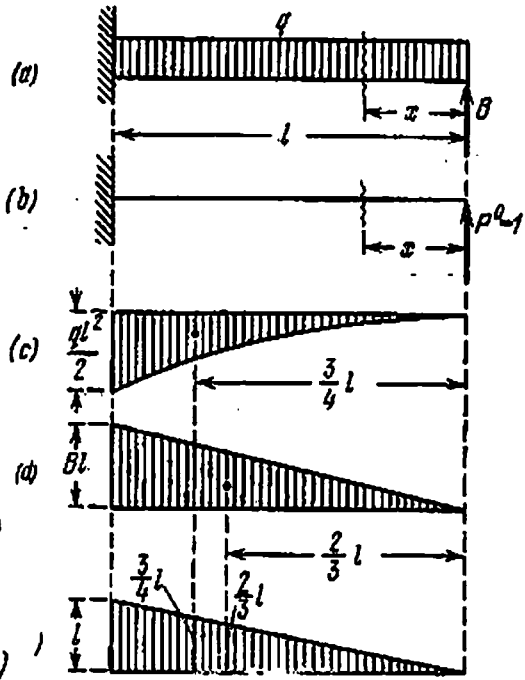


Fig. 280

If the same problem (Fig. 273) is solved by Mohr's method, then in addition to the first state when it is loaded by the given forces and the redundant unknown force (Fig. 279 (a)) we must show the beam in the second state to be loaded by force \$P^0\$ (Fig. 279 (b)). Using the notations of Fig. 279, we obtain

$$M = Bx - q \frac{x^2}{2}, \quad M^0 = x \tag{19.14}$$

i.e. the same as obtained by applying Castigliano's theorem.

When solving the same problem by Vereshchagin's method, in addition to the two loading diagrams used above (Fig. 280 (a) and (b)) we must also plot bending moment diagrams due to force \$q\$ (Fig. 280 (c)), force \$B\$ (Fig. 280 (d)) and force \$P^0 = 1\$ (Fig. 280 (e)).

The areas of the bending moment diagrams are:

$$\text{for force } q: \quad \omega_q = -\frac{1}{3} \frac{ql^2}{2} l = -\frac{ql^3}{6}$$

$$\text{for force } B: \quad \omega_B = \frac{1}{2} Bl \times l = \frac{Bl^2}{2}$$

The corresponding ordinates of the bending moment diagram of unit force are:

$$\text{multiplication factor for } \omega_q: \quad M_C^q = \frac{3l}{4}$$

$$\text{multiplication factor for } \omega_B: \quad M_C^B = \frac{2l}{3}$$

Deflection of point  $B$  is:

$$f_B = \frac{1}{EJ} \left( \frac{Bl^2}{2} \frac{2l}{3} - \frac{ql^3}{6} \frac{3l}{4} \right) = 0$$

wherefrom

$$B = \frac{3}{8} ql$$

After this the solution is the same as explained in §§ 110 and 112.

#### § 114. Solution of a Simple Statically Indeterminate Frame

Plot the bending moment diagram for the given frame (Fig. 281). The elements of the frame have uniform rigidity, which is constant

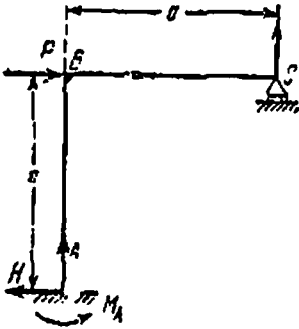


Fig. 281

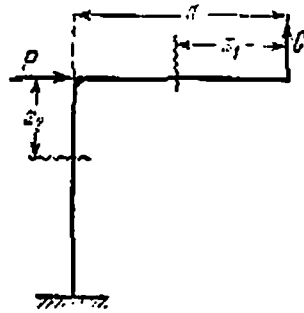


Fig. 282

along their length. Denoting the reactions by  $A$ ,  $H$ ,  $M_A$ , and  $C$ , we write the following equations of statics:

$$H = P, \quad A + C = 0, \quad Pa - Ca - M_A = 0$$

There is one redundant unknown; let this be reaction  $C$ . The base beam with the force  $P$  and the redundant unknown is shown in Fig. 282.

Let us solve the problem by applying Castigliano's theorem. In the equation of joint deformation

$$f_c = \frac{\partial U}{\partial C} = 0$$

potential energy  $U$  is the sum of the energies of the first portion,  $CB$ , and the second portion,  $BA$ . Consequently, equation  $f_c = 0$  can be written as

$$\frac{1}{EJ} \int_0^a M_1 \frac{\partial M_1}{\partial C} dx + \frac{1}{EJ} \int_0^a M_2 \frac{\partial M_2}{\partial C} dx = 0$$

The moments and their derivatives are:

$$M_1 = +Cx_1, \quad \frac{\partial M_1}{\partial C} = x_1$$

$$M_2 = +Ca - Px_2, \quad \frac{\partial M_2}{\partial C} = +a$$

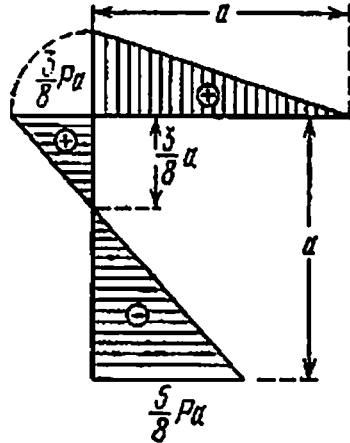


Fig. 283

Substituting these values in the equation of joint deformation, we get

$$\int_0^a Cx_1^2 dx + \int_0^a (Ca - Px_2) a dx = 0$$

After integrating we get

$$\frac{Ca^3}{3} + Ca^3 - \frac{Pa^3}{2} = 0, \quad C = \frac{3}{8} P$$

The bending moments are: in the first portion  $M_1 = \frac{3}{8} Px_1$  and in the second portion  $M_2 = \frac{3}{8} Pa - Px_2$ . The bending moment diagram is shown in Fig. 283.

In solving the above problem by Vereshchagin's method we depict two states of loading of the beam: with the given forces and reaction  $C$  (Fig. 284 (a)) acting on the beam, and with a unit force acting in the direction of reaction  $C$  (Fig. 284 (d)). Next we plot the bending moment diagrams  $M$  and  $M^0$ . Areas of the bending moment diagrams (Fig. 284 (b) and (c)) for the given load are:

$$\omega_1 = \frac{1}{2} Ca \times a = + \frac{Ca^2}{2}$$

$$\omega_2 = +Ca \times a = Ca^2 \quad \text{and} \quad \omega_2^0 = -\frac{1}{2} Pa \times a = -\frac{Pa^2}{2}$$

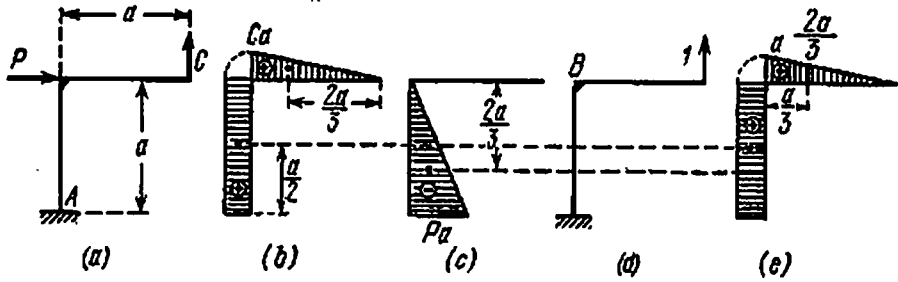


Fig. 284

The ordinates of the unit bending moment diagrams corresponding to the centres of gravity of the bending moment diagrams for the given loads are (Fig. 284 (b) and (c)):

$$M_{C_1}^0 = +\frac{2}{3}a, \quad M_{C_2}^0 = +a, \quad M_{C_3}^0 = +a$$

The condition of joint deformation (after factoring out  $EJ$ ) is:

$$\frac{Ca^2}{2} \frac{2}{3}a + Ca^2a - \frac{Pa^2}{2}a = 0$$

wherefrom  $C = \frac{3}{8}P$ , which is the result obtained earlier by applying Castigliano's theorem.

### § 115. Analysis of Continuous Beams

From a practical point of view a very important category of indeterminate beams are the *continuous beams*, which lie on a number of intermediate supports to which they are hinged. The ends of such beams may be either hinged or rigidly fixed. Let us first discuss a case when



Fig. 285

the beam has hinged supports. In continuous beams one of the end supports is usually fixed whereas all others are capable of moving. The numbering of supports and spans will be from left to right, the extreme left support will be denoted by  $O$  and the extreme left span by  $l$ . Lengths of the spans will be denoted by letter  $l$  with the number of the corresponding span as a subscript. We shall assume that the beam is of uniform section and consequently its rigidity  $EJ$  is constant. Figure 285 shows a continuous beam with appropriate notations, and also the support reactions. It can be easily seen that the number of

redundant support reactions is equal to the number of intermediate supports.

If we were to follow the method discussed above, we would take the reactions of the intermediate supports as redundant unknowns and a beam simply supported at points  $O$  and  $n+2$  as the base beam. Additional equations would be obtained by equating to zero the deflections of the points of intermediate supports of the base beam. However, there is a simpler and more popular method which makes use of a different type of base beam and redundant unknowns; in this method there are not more than three unknowns in each equation.

Selection of the redundant unknowns and base beam is closely interlinked. The statically determinate base beam is obtained from the statically indeterminate beam by removing constraints that are the redundant unknowns.

The problem can also be approached in a different manner. Convert by some method the statically indeterminate beam into a statically determinate beam and study which of the reactions and constraints must be removed to achieve this. These reactions will constitute the redundant unknowns in the statically indeterminate beam.

Thus, in the two-span continuous beam (Fig. 286(a)), the reaction of intermediate support  $B$  may be taken as the redundant unknown. Then the base beam will be a beam simply supported at points  $A$  and  $C$ ; the beam can, however, be made statically determinate by introduction of a hinge at point  $D$  (Fig. 286(b)). The base beam system will consist of cantilever  $CBD$  and suspended beam  $AD$ . By introducing a hinge we impose the condition that the bending moment and hence the normal stresses in section  $D$  should be zero. Thus, when we consider the base beam system we actually equate to zero the normal stresses in section  $D$  acting from the left portion on the right and vice versa. These stresses give resultant moments equal in magnitude to the bending moment in section  $D$ . These moments reapplied to the base beam are shown in Fig. 286(c).

While transforming our statically indeterminate beam into statically determinate by introducing hinge  $D$ , we select the bending moment in section  $D$  as the redundant unknown instead of one of the support reactions.

Point  $D$  may be selected arbitrarily. However, the computations are simplified considerably if we select point  $D$  in the section of the

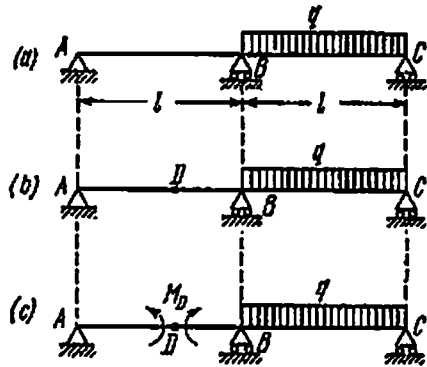


Fig. 286



beam just above the intermediate support, point  $B$ , i.e. if we consider the moment at support  $B$  as the redundant unknown. Now the base beam system will consist of two simply supported beams hinged at points  $A$ ,  $B$ , and  $C$  and having a common support at point  $B$ .

This precisely is how the base beam system is selected in continuous beams. The bending moments  $M_1, M_2, \dots, M_{n-1}, M_n, M_{n+1}$  at the intermediate supports are taken as the redundant unknowns.

Such a selection of the redundant unknowns simplifies the equations from which the former are calculated. The equations may be written in general form with the help of the theorem of three moments.

### § 116. The Theorem of Three Moments

To derive the theorem of three moments let us consider a continuous beam having a number of spans of different lengths,  $l_1, l_2$ , etc., and loaded by vertical forces acting arbitrarily (Fig. 287 (a)). Let us first show all the reactions which may occur in this case. From the equilibrium of the beam it is evident that the horizontal reaction  $H_0=0$ .

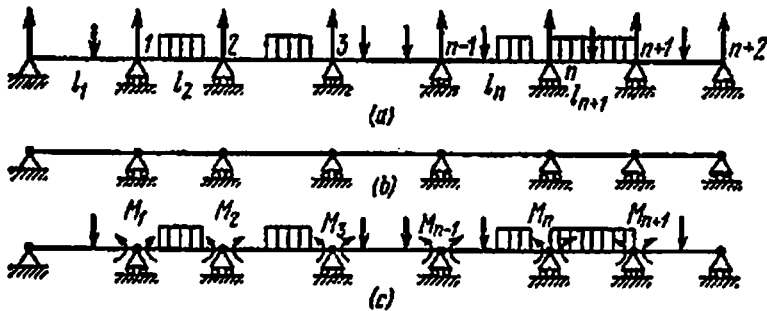


Fig. 287

The base beam (Fig. 287 (b)) is obtained by introducing hinges at all the intermediate supports. Then the redundant unknowns are the bending moments  $M_1, M_2$ , etc., acting at the intermediate supports. Moments at the end supports must be zero. Let us load the base beam by the external forces and the moments acting at the supports (Fig. 287 (c)). As the direction of support moments is not known, we consider them positive. After the solution is completed the sign of the result will show whether the assumed direction is correct or not.

The next step is to write down the condition which imposes the same restrictions on the deformation of the base beam as are present in the continuous beam. In the base beam the spans on both sides of the  $n$ th hinge which separates them may rotate (Fig. 288) due to the external load independent of each other. Let us denote by  $\theta'_n$  the angle of rotation of the span to the left of the  $n$ th hinge, and by  $\theta''_n$  the angle of rotation of the span to the right of the  $n$ th hinge. These possible angles of rotation of two adjacent spans are shown in Fig. 288. In a continuous

beam both sections coincide and simply represent two sides of the same section. Therefore, the condition of joint deformation may be written as

$$\theta'_n - \theta''_n = 0 \tag{19.15}$$

This is the condition which must be satisfied by adjacent spans at support  $n$  of the base beam loaded by the external forces and support moments. Such a condition may be written for all intermediate supports and, consequently, the number of additional equations that we obtain is equal to the number of redundant unknowns.

Let us take an example to elucidate how condition (19.15) can be expressed mathematically. Consider a two-span continuous beam (Fig. 289(a)) loaded by different distributed forces  $q_1$  and  $q_2$ , acting on the two spans.

The base beam loaded only by the external forces is shown in Fig. 289(b). For clarity the two adjacent spans have been shown slightly separated at support  $1$ ; actually, hinges  $1'$  and  $1''$  coincide.

Both sides of section  $1$  of the support will turn as shown in the diagram. The deformations must be the same in a continuous beam; this can be achieved by loading the base beam by a negative support moment  $M_1$  (Fig. 289(c)) of such magnitude that the deformations become equal. It follows from the above discussion that the deformations will be equal only when the following condition is satisfied:

$$\theta'_1 - \theta''_1 = 0 \tag{19.15'}$$

Returning to the analysis of statically indeterminate beams by strain comparison and considering Fig. 287, we must expand equation (19.15) by calculating the deformations involved in it.

In the base beam the angles of rotation at support  $n$  depend only upon the deformation of two adjacent spans  $l_n$  and  $l_{n+1}$ . Let us isolate these two spans together with the forces acting on them (Fig. 290). Span  $l_n$  is acted upon by the external forces applied to it as well as support moments  $M_{n-1}$  and  $M_n$ , and span  $l_{n+1}$  is acted upon by support moments  $M_n$  and  $M_{n+1}$  in addition to the external forces applied to it. For clarity the two adjacent spans have been shown slightly separated at support  $n$ ; actually, hinges  $n'$  and  $n''$  coincide.

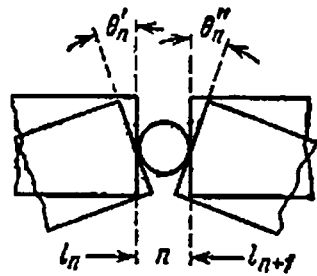


Fig. 288

We shall determine  $\theta_n^*$  and  $\theta_n^*$  by the graph-analytic method. The fictitious beams, shown below their respective spans, are also hinged. The fictitious load of the left span is made up of:

(a) the bending moment diagram of the external forces, obtained by multiplying load area  $\omega_n$  with the distance  $a_n$  of its centre of gra-

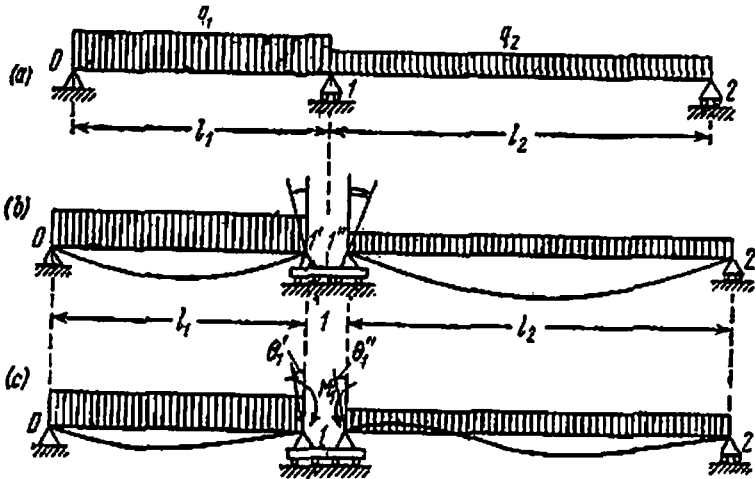


Fig. 289

vity from the left support (as the bending moment diagram is positive, the load ordinates are drawn with arrows pointing vertically upwards; if the ordinates of the bending moment diagram are negative, area  $\omega_n$  is used in calculations with a minus sign);

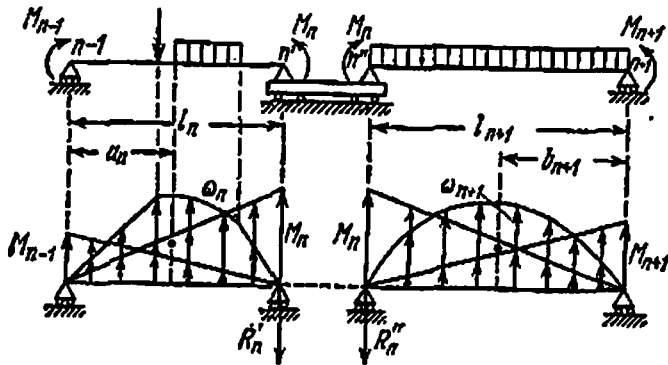


Fig. 290

(b) the triangular bending moment diagram from positive support moment  $M_{n-1}$ ;

(c) the triangular bending moment diagram from positive support moment  $M_n$ .

The right-hand fictitious beam corresponding to span  $l_{n+1}$  is acted upon by the following forces:

(a) the bending moment diagram of the external forces, obtained by multiplying load area  $\omega_{n+1}$  with the distance  $b_{n+1}$  of its centre of gravity from the right support;

(b) the triangular bending moment diagram from positive support moment  $M_n$ ;

(c) the triangular bending moment diagram from positive support moment  $M_{n+1}$ .

The angle of rotation of section  $n'$  is equal to the shearing force of the fictitious beam in this section divided by the rigidity of the beam:

$$\theta'_n = \frac{Q'_n}{EJ}$$

The shearing force at the support is equal to the support reaction  $R'_n$  of the fictitious beam.

Let us calculate this reaction. Load area  $\omega_n$  is distributed between the supports of the fictitious beam as in a lever arrangement, exerting a force of  $\omega_n \frac{a_n}{l_n}$  at support  $n'$ . The triangular load with the maximum ordinate  $M_n$  gives a reaction at the support which is two-thirds of its total value, whereas the triangular load with the ordinate  $M_{n-1}$  gives a reaction which is one-third of its total value. Hence

$$\begin{aligned} R'_n &= \omega_n \frac{a_n}{l_n} + \frac{2}{3} \frac{1}{2} M_n l_n + \frac{1}{3} \frac{1}{2} M_{n-1} l_n \\ &= \omega_n \frac{a_n}{l_n} + \frac{1}{3} M_n l_n + \frac{1}{6} M_{n-1} l_n \end{aligned}$$

The fictitious shearing force  $Q'_n$  is equal to this reaction taken with a positive sign:

$$Q'_n = R'_n$$

The angle of rotation  $\theta'_n$  is:

$$\theta'_n = \frac{Q'_n}{EJ} = \frac{1}{6EJ} \left( 6\omega_n \frac{a_n}{l_n} + 2M_n l_n + M_{n-1} l_n \right)$$

In a similar manner we obtain reaction  $R''_n$  for the right span:

$$R''_n = \omega_{n+1} \frac{b_{n+1}}{l_{n+1}} + \frac{1}{3} M_n l_{n+1} + \frac{1}{6} M_{n+1} l_{n+1}$$

The shearing force in this case is equal to the support reaction taken with a negative sign:

$$Q''_n = -R''_n$$

The angle of rotation  $\theta''_n$  is:

$$\theta''_n = -\frac{1}{6EJ} \left( 6\omega_{n+1} \frac{b_{n+1}}{l_{n+1}} + 2M_n l_{n+1} + M_{n+1} l_{n+1} \right)$$

Substituting the values of  $\theta'_n$  and  $\theta''_n$  in equation (19.15) and cancelling out  $6EJ$ , we obtain:

$$\left(6\omega_n \frac{a_n}{l_n} + 2M_n l_n + M_{n-1} l_n\right) + \left(6\omega_{n+1} \frac{b_{n+1}}{l_{n+1}} + 2M_n l_{n+1} + M_{n+1} l_{n+1}\right) = 0$$

or

$$M_{n-1} l_n + 2M_n (l_n + l_{n+1}) + M_{n+1} l_{n+1} = -6 \left( \frac{\omega_n a_n}{l_n} + \frac{\omega_{n+1} b_{n+1}}{l_{n+1}} \right) \quad (19.16)$$

which is the *equation of three moments*.

We can write as many equations of this type as the number of intermediate supports, i.e. as the number of unknown support moments. Once the support moments are known the problem becomes one of analyzing a number of simply supported beams loaded by the external forces and known support moments.

The brackets on the right-hand side of equation (19.16) contain the sum of fictitious reactions at the middle support due to the given load acting on the adjoining spans. Consequently, the theorem of three moments (19.16) may be formulated in short as follows:

$$M_{n-1} l_n + 2M_n (l_n + l_{n+1}) + M_{n+1} l_{n+1} = -6R'_n \quad (19.17)$$

Here  $R'_n$  represents the fictitious reaction of support ( $n$ ) due to bending moment diagrams  $M(x)$  of the given load on the two adjoining spans.

### 117. An Example on Application of the Theorem of Three Moments

Let us consider a three-span continuous beam of uniform section which is loaded as shown in Fig. 291(a). Start numbering the supports from left to right. The equation of three moments should be written twice: for supports 1 and 2.

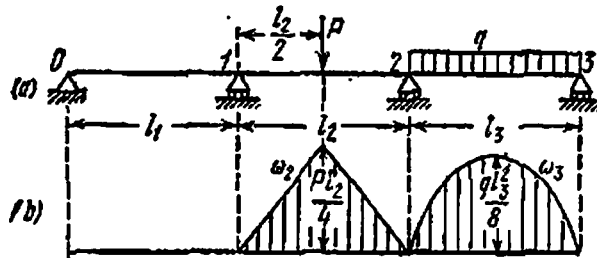


Fig. 291

We shall need the areas of the bending moment diagrams of external forces acting on the base beam. These diagrams are shown in Fig. 291(b). Let us write the equation of three moments (19.17) for support 1. Assum-

ing  $n=1$ , we obtain

$$M_{n-1} = M_0 = 0, \quad \omega_n = \omega_1 = 0$$

$$\omega_{n+1} = \omega_2 = +\frac{1}{2} \frac{Pl_2}{4} l_2 = +\frac{Pl_2^3}{8}, \quad b_{n+1} = b_2 = \frac{l_2}{2}$$

The equation can be written

$$2M_1(l_1 + l_2) + M_2l_2 = -\frac{3}{8}Pl_2^3 \quad (19.18)$$

Let us pass over to support 2 now. Assuming  $n=2$ , we get

$$M_{n+1} = M_2 = 0, \quad \omega_n = \omega_2 = +\frac{Pl_2^3}{8}$$

$$\omega_{n+1} = \omega_3 = +\frac{2l_2}{3} \frac{ql_2^3}{8} = +\frac{ql_2^3}{12}$$

$$a_n = a_2 = \frac{l_2}{2}, \quad b_{n+1} = b_3 = \frac{l_2}{2}$$

The second equation of three moments is:

$$M_1l_2 + 2M_2(l_2 + l_3) = -\frac{3}{8}Pl_2^3 - \frac{ql_2^3}{4} \quad (19.19)$$

The redundant unknowns  $M_1$  and  $M_2$  can be calculated by solving equations (19.18) and (19.19).

If we consider a particular case and assume  $l_1 = l_2 = l_3 = l$  and  $ql = P$  (Fig. 292 (a)), we obtain

$$M_1 = -\frac{7}{120}Pl \quad \text{and} \quad M_2 = -\frac{17}{120}Pl$$

Knowing the support moments, we can easily plot the bending moment diagram of the continuous beam without any additional calculations. To do this we first draw the bending moment diagrams of the base beam system due to the given load (Fig. 292 (b)). The bending moment diagrams due to support moments  $M_1$  and  $M_2$  are shown in Fig. 292 (c). The resultant diagram with the characteristic ordinates is shown in Fig. 292 (d). The bending moment diagram may also be plotted without moving the sections apart at the support; in the given problem this was done for the sake of clarity.

The support reactions may be calculated for each span separately. The two reactions determined separately for each intermediate support may then be algebraically summed up.

The support reactions can be computed in another way. The sum of the moments of all forces to the left of support 1 about the point of support is equated to the support moment  $M_1$ :

$$Al = M_1 = -\frac{7}{120}Pl$$

which implies that

$$A = -\frac{7}{120}P$$

(the minus sign means that reaction  $A$  acts vertically downwards). We now consider the two left spans. The sum of the moments of all

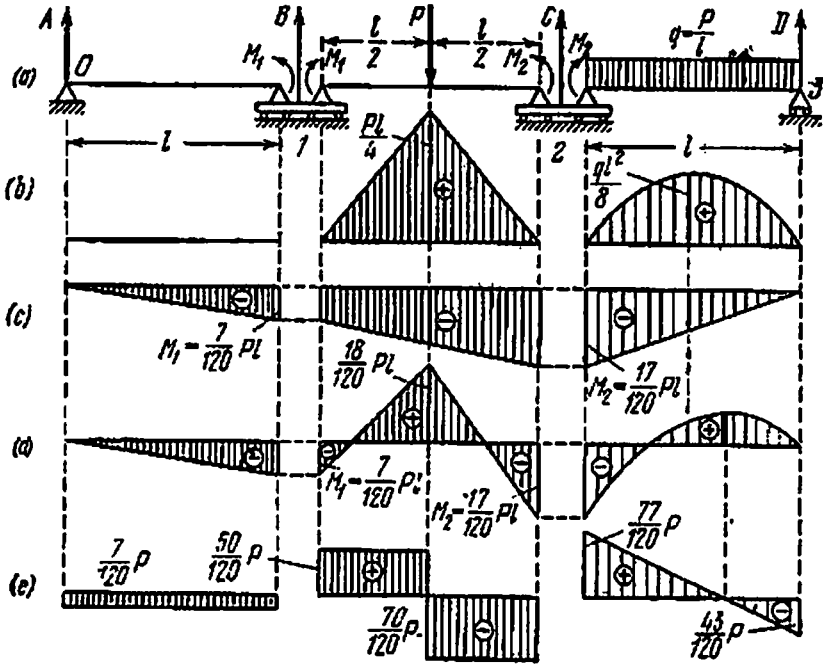


Fig. 292

forces about point 2 is equated to the support moment  $M_2$ :

$$A2l + Bl - P \times 0.5l = M_2 = -\frac{17}{120}Pl$$

After substituting the value of  $A$  and certain computations we obtain  $B = -\frac{57}{120}P$  (directed upwards). Next we consider the extreme left span:

$$Dl - 0.5Pl = M_2 = -\frac{17}{120}Pl, \quad D = \frac{43}{120}P$$

And, finally, we determine  $C$  after considering the two right spans:

$$D2l - \frac{3}{2}Pl + Cl - \frac{1}{2}Pl = M_1 = -\frac{7}{120}P, \quad C = \frac{147}{120}P$$

Let us finally check whether the calculations were correct:

$$\begin{aligned} \sum y &= 0, & A + B + C + D &= 2P \\ -\frac{7}{120}P + \frac{57}{120}P + \frac{147}{120}P + \frac{43}{120}P &= 2P \end{aligned}$$

We see that they are. With all the reactions calculated the shearing force diagrams for all the spans can be plotted without any difficulty (Fig. 292 (d)).

**§ 118. Continuous Beams with Cantilevers.**  
**Beams with Rigidly Fixed Ends**

The theorem of three moments can be easily applied to situations when the beam has cantilevers or when the ends (one or both) of the beam are rigidly fixed.

Let us consider a two-span beam with a cantilever (Fig. 293 (a)), which works under the following conditions:

$$l_1 = 6 \text{ m}, \quad l_2 = 5 \text{ m}, \quad a = 2 \text{ m}, \quad q = 4 \text{ tf/m}$$

The moment  $M_C$  may be considered as known and equal to the bending moment in section C due to the load acting on the cantilever.

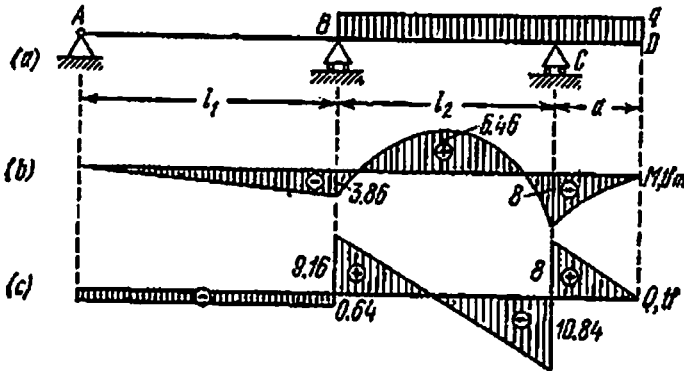


Fig. 293

Thus, we have the following data to write the equation of three moments:

$$\begin{aligned} M_{n-1} = M_0 &= 0, & M_n = M_1 &= ?, & M_{n+1} = M_2 &= -\frac{qa^2}{2} \\ n &= 1, & \omega_1 &= 0, & \omega_2 &= \frac{ql_2^3}{12} \end{aligned}$$

The equation is:

$$2M_1(l_1 + l_2) - \frac{qa^2}{2}l_2 = -6\frac{ql_2^3}{12}\frac{1}{2} \tag{19.20}$$



or

$$2M_1(l_1 + l_2) = \frac{qa^2l_2}{2} - \frac{ql_2^2}{4}$$

wherefrom

$$M_1 = -3.86 \text{ tf} \cdot \text{m}$$

When determining the support reactions, it is recommended to study beam  $AB$  and the beam with cantilever  $BCD$  separately. The bending moment and shearing force diagrams are shown in Fig. 293 (b) and (c).

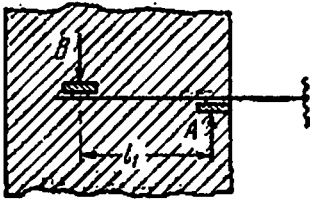


Fig. 294

In order to explain how to solve the problem when one end of the beam is rigidly fixed, we must first study the design of the constraint (Fig. 294).

The fixed end may be considered as propped from below at point  $A$  and above at point  $B$  or vice versa. Such a construction cannot be considered absolutely rigid, because the portion of length  $l_1$  between points  $A$  and  $B$  is capable of undergoing deformation, and the beam section which coincides with the front face of the wall can turn as a consequence. The smaller the length  $l_1$  and the greater the moment of inertia of the portion and the lower the pliability of the wall, the more rigid is the constraint. We shall get an absolutely rigid fixation by assuming that in the limit  $l_1=0$  (or  $J_1=\infty$ ). While analyzing continuous beams with fixed ends, we must replace the fixation by an additional span, write the equation of three moments and then obtain the conditions for the actual beam by substituting

$$l_1=0 \quad \text{or} \quad J_1=\infty$$

Let us consider a beam rigidly fixed at both ends and loaded by a force  $P$  acting at distances  $a$  and  $b$  from the left and right supports respectively (Fig. 295(a)). We assume that supports  $A$  and  $B$  do not impede longitudinal deformation of the beam. We remove the constraints and add a span on each side thus reducing our problem to the analysis of a three-span continuous beam (Fig. 295(b)).

We have the following data for writing the equation of three moments at support  $I$ :

$$M_{n-1} = M_0 = 0, \quad \omega_n = \omega_1 = 0, \quad \omega_{n+1} \frac{b_{n+1}}{l_{n+1}} = \frac{Pab}{6} \left( 1 + \frac{b}{l_2} \right)$$

The equation is:

$$2M_1(l_1 + l_2) + M_2l_2 = -6 \frac{Pab}{6} \left(1 + \frac{b}{l_2}\right) \quad (19.21)$$

The data for writing the equation of three moments at support 2 ( $n=2$ ) is as follows:

$$M_{n+1} = M_3 = 0, \quad \omega_n \frac{a_n}{l_n} = \frac{Pab}{6} \left(1 + \frac{a}{l_2}\right)$$

$$\omega_{n+1} = \omega_3 = 0$$

Therefore

$$M_1l_2 + 2M_2(l_2 + l_2) = -6 \frac{Pab}{6} \left(1 + \frac{a}{l_2}\right) \quad (19.22)$$

Now we substitute  $l_1=l_3=0$  and  $l_2=l$  in the above equations of three moments (19.21) and (19.22). We obtain the following set of equations:

$$2M_1l + M_2l = -Pab \left(1 + \frac{b}{l}\right)$$

$$M_1l + 2M_2l = -Pab \left(1 + \frac{a}{l}\right)$$

Solving the equations, we get

$$M_1 = -\frac{Pab^2}{l^2}, \quad M_2 = -\frac{Pa^2b}{l^2}$$

The moment in the section under force  $P$  is:

$$M_P = P \frac{ab}{l} + \frac{M_1b}{l} + \frac{M_2a}{l} = \frac{2Pa^2b^2}{l^3}$$

The bending moment diagram plotted for this data is shown in Fig. 295(e).

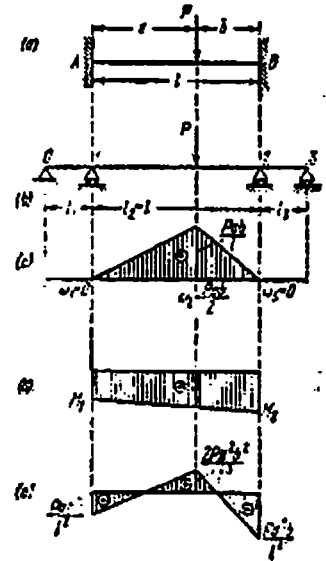


Fig. 295

# PART VII

## Resistance Under Compound Loading

### CHAPTER 20

## Unsymmetric Bending

### § 119. Fundamental Concepts

Until now we have studied problems in which the elements of a structure are subjected to only one of the fundamental deformations: simple tension or compression, torsion, or planar bending. In actual practice a majority of the elements of structures and machines are acted upon by forces which give rise to two or more types of deformations simultaneously.

Shafts in machines are subjected to torsion as well as bending. Besides tension or compression bars of trusses (rafters, bridges and cranes) also experience bending, because of welded and riveted joints at corners instead of hinges for which the trusses are actually designed. All such cases in which we have a combination of fundamental deformations are cases of *compound loading*.

Analysis of compound loading is usually based on the principle of superposition of forces, i.e. it is assumed that the effect of deformation caused by one of the forces on the deformation caused by the rest of the forces is negligible. Experiments confirm that this principle can be applied when deformations are small (exceptional situations when it is not applicable at all will be discussed later). Hence the principle of superposition of forces may be applied to determine total stresses and deformations in an elastic system subjected to compound loading of an arbitrary nature, i.e. stresses and strains corresponding to the various types of fundamental deformations may be added geometrically.

Let us first study the particular cases of compound loading and then the case when the elastic system is subjected to the most general compound loading.

### § 120. Unsymmetric Bending. Determination of Stresses

Till now we have been using the formula  $\sigma = \frac{Mz}{J_y}$  for calculating the normal stresses in bending. However, normal stresses in a section of the beam can be completely determined by this formula only in case of uni-planar bending\*, when the beam bends in the plane of action of the forces and the neutral axis is perpendicular to the plane of loading and represents the principal axis of inertia.

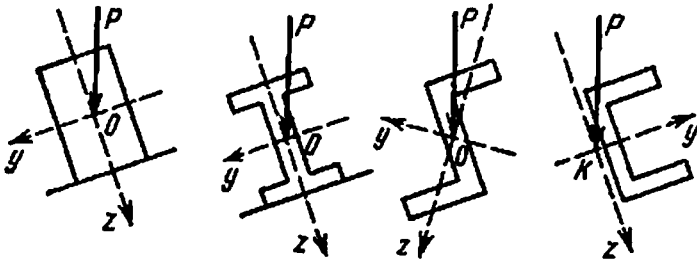


Fig. 296

In actual practice we often come across cases when the plane of application of the forces does not coincide with any of the two principal axes of inertia of the section. Experiments show that under such loading the axis of the bent beam does not lie in the plane of application of the forces; this is known as *unsymmetric bending*.

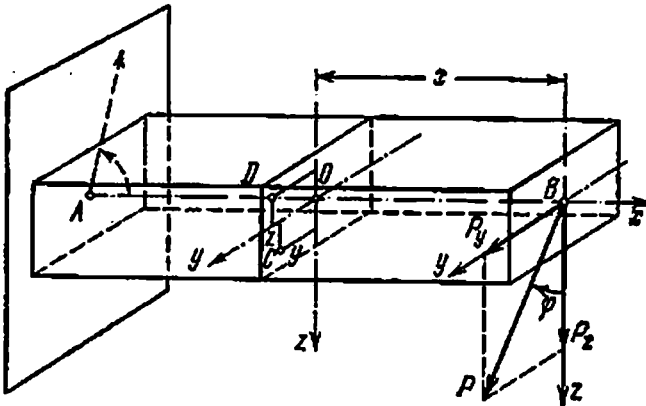


Fig. 297

Roof beams are usually acted upon by forces the plane of application of which makes a considerably large angle with the principal axes

\* Speaking more accurately, this will occur when all the forces lie in one of the principal planes of inertia of the section passing through the bending centre; in a number of cases the bending centre coincides with the centre of gravity of the cross section (§ 79).

(Fig. 296). We also often come across cases when the plane of application of forces is only slightly inclined to the principal axes of inertia.

We shall explain the method of checking the strength and calculating the deformation in case of unsymmetric bending with the help of the following example.

Consider a beam rigidly fixed at one end and loaded at the other by a force  $P$  which acts on the face of the beam and makes an angle  $\varphi$  with the principal axis  $Bz$  (Fig. 297). The second principal axis  $By$  is perpendicular to the first; let us select the direction of the coordinate axes such that force  $P$  lies in the first quadrant.

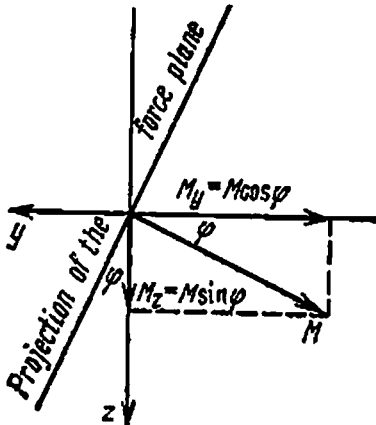


Fig. 298

For checking the strength of the beam we must first find the point which experiences the maximum normal stress. Let us derive an expression for the normal stress at any point of an arbitrary section at a distance  $x$  from the free end of the beam.

Let us divide force  $P$  into components,  $P_z$  and  $P_y$ , which are directed along the principal axes  $Bz$  and  $By$ . The values of these components may be calculated by the following formulas:

$$P_z = P \cos \varphi \quad \text{and} \quad P_y = P \sin \varphi$$

Thus, we have reduced unsymmetric bending to a combination of two planar bendings caused by forces  $P_z$  and  $P_y$ , which act in the principal planes of inertia of the beam. Adding the stresses and deformations for each of these bendings, we find their total values in unsymmetric bending.

The bending moments due to forces  $P_z$  and  $P_y$  in the section having abscissa  $x$  are:

$$\left. \begin{aligned} |M_y| &= P_z x = Px \cos \varphi = M \cos \varphi \\ |M_z| &= P_y x = Px \sin \varphi = M \sin \varphi \end{aligned} \right\} \quad (20.1)$$

The subscripts  $y$  and  $z$  of  $M$  denote the principal axes about which the moments have been calculated;  $M$  denotes the bending moment in the plane of application of force  $P$ , and its value in the given section is  $Px$ . If we depict the moments in vector form, we notice that we can obtain  $M_y$  and  $M_z$  by directly resolving the total bending moment  $M$  along the principal axes (Fig. 298).

To determine the signs of the bending moments in a three-dimensional problem like this, it is necessary to find additional conditions (we

shall explain this point below). Let us restrict ourselves to finding the magnitude of the bending moments only; the effect of the direction of bending moments on the sign of stresses will be taken into account when the latter are calculated.

We determine the stresses at point  $C$  (having coordinates  $y$  and  $z$ ) lying in the first quadrant (Fig. 297). We can separately calculate the normal stresses at this point caused by moments  $M_y$  and  $M_z$  which bend the beam in principal planes  $xz$  and  $xy$  respectively. The formulas derived for planar bending are valid in this case too.

The normal stress at point  $C$  due to bending moment  $M_y$  is compressive (negative) and may be expressed by the formula

$$-\frac{M_y z}{J_y} = -\frac{M_z}{J_y} \cos \varphi$$

where  $J_y$  is the moment of inertia of the section about the  $y$ -axis which is also the neutral axis for bending due to moment  $M_y$ . Moment  $M_z$  will also give rise to compressive stresses at point  $C$  equal to

$$-\frac{M_z y}{J_z} = -\frac{M_y}{J_z} \sin \varphi$$

where  $J_z$  is the moment of inertia of the section about the  $z$ -axis. Total stress at point  $C$  is obtained as the algebraic sum of the stresses calculated above:

$$\sigma = -\frac{M_y z}{J_y} - \frac{M_z y}{J_z} = -M \left( \frac{z \cos \varphi}{J_y} + \frac{y \sin \varphi}{J_z} \right) \quad (20.2)$$

The above formula may be used for calculating the stresses at any point in any section of the beam. As the formula has been derived for a point with positive coordinates  $y$  and  $z$ , we shall always get the stresses with their proper signs if we substitute  $y$  and  $z$  with proper signs in formula (20.2).

Thus, at point  $D$  (Fig. 297)  $y$  is positive but  $z$  is negative. Consequently, the first term in formula (20.2) will become positive whereas the second will remain negative as before.

Although formula (20.2) has been obtained by considering a particular case of a beam rigidly fixed at one end and loaded at the other, it is not difficult to notice that it is a general formula for calculating stresses in unsymmetric bending. Only the rules for finding the proper sign of the stresses will be different for beams which are loaded or constrained in a different manner. If the positive direction of the principal axes of inertia passing through the centroid is always selected in such a way that the plane of application of forces always passes through the first quadrant, then the sign before the right-hand side of formula (20.2) should be in accordance with the nature of deformation which takes place due to the bending moment (or its components) at any point in the first quadrant (a positive sign in case of tension and

a negative sign in case of compression). Now it would suffice to use the proper signs of  $y$  and  $z$  to obtain the proper signs of the stresses within the elastic limits at any point from formula (20.2).

In order to determine the maximum normal stresses we must first locate the critical section of the beam and then the maximum stressed point of this critical section. It is evident from formula (20.2) that the critical section is the section in which the bending moment  $M$  is maximal.

While finding the maximum stressed point we must bear in mind that in uni-planar bending the deformation due to normal stresses is rotation of the sections about their respective neutral axes. In unsymmetric bending, which is a combination of two uni-planar bendings, there is simultaneous rotation of the sections about two axes which intersect at the centre of gravity of the section.

We know from kinematics that rotation of a body about two axes may be replaced by rotation about an axis passing through the point of intersection of the two axes. Hence, in unsymmetric bending also in every section we have a line which passes through its centre of gravity and about which the section rotates during deformation of the beam. This axis will be the neutral axis: the fibres of the beam material lying in its plane will neither elongate nor shorten and the normal stresses at points on the neutral axis will be zero. In relative rotation of two sections the maximum deformation (tension or compression) occurs in the fibres which are farthest from the neutral axis.

Hence, the problem of determining the maximum stressed points in unsymmetric bending is reduced to locating the neutral axis and the points farthest from it.

Equation of the neutral axis can be written from the condition that normal stresses are zero at points lying on the neutral axis. Let us denote the coordinates of a point on the neutral axis by  $y_0$  and  $z_0$ ; substituting these values for  $y$  and  $z$  in formula (20.2), we get the value of  $\sigma$  equal to zero:

$$0 = -\frac{M \cos \varphi \times z_0}{J_y} - \frac{M \sin \varphi \times y_0}{J_z}$$

Dividing by  $-M$ , we get

$$\frac{\cos \varphi \times z_0}{J_y} + \frac{\sin \varphi \times y_0}{J_z} = 0 \quad (20.3)$$

This is the equation of the neutral axis. It represents a straight line passing through the centre of gravity of the section (at  $y_0=0$  and  $z_0=0$ ).

Figure 299 shows two beam sections; the  $y$ - and the  $z$ -axis are the principal axes of inertia. Assuming that the beams are loaded as in Fig. 297, the projection of force  $P$  has been shown in both the sections and the proper signs of the normal stresses have been given for each quadrant; the signs above and below the section are for stresses due

to moment  $M_y$ , whereas the signs to the right and left of the section are for moment  $M_z$ . For a beam which is loaded and constrained in a different way (Fig. 300), the signs of the stresses will also change accordingly.

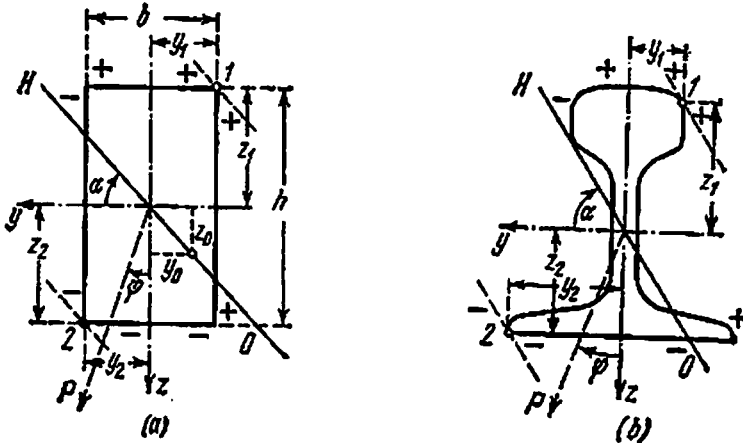


Fig. 299

Approximate location of the neutral axis is shown in Fig. 299. As the neutral axis passes through the centre of gravity, it is sufficient to know angle  $\alpha$  which it makes with the  $y$ -axis in order to locate it fully. It is evident from Fig. 299 that the tangent of this angle is equal to the absolute value of the ratio of  $z_0$  to  $y_0$ :

$$\tan \alpha = \left| \frac{z_0}{y_0} \right|$$

From equation (20.3) we obtain

$$\tan \alpha = \left| \frac{z_0}{y_0} \right| = \tan \varphi \frac{J_y}{J_z} \quad (20.4)$$

Hence, the location of the neutral axis does not depend upon the magnitude of force  $P$ , but only upon the angle which the plane of application of external forces makes with the  $z$ -axis and upon the shape of the section.

After calculating angle  $\alpha$  from formula (20.4), we plot the neutral axis on the diagram, and by drawing tangents to the section parallel to the neutral axis we find the maximum stressed points, which are the points farthest from the neutral axis (points 1 and 2 in Fig. 299).

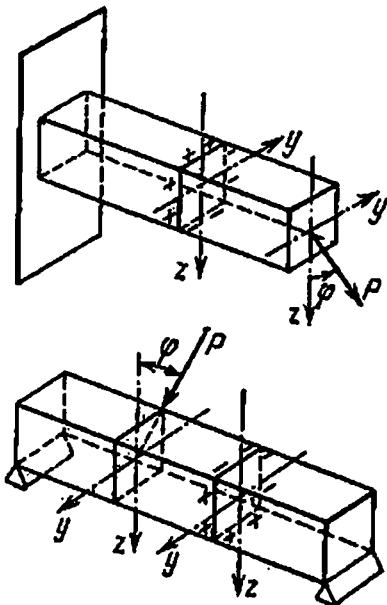


Fig. 300



Substituting the coordinates of these points ( $y_1, z_1$ , or  $y_2, z_2$ ) with their proper signs in formula (20.2), we calculate the maximum tensile or compressive stresses. The strength condition for the beam may be written as

$$|\sigma_{\max}| = M_{\max} \left( \frac{\cos \varphi}{J_y} z_1 + \frac{\sin \varphi}{J_z} y_1 \right) \leq [\sigma] \quad (20.5)$$

where  $y_1$  and  $z_1$  (or  $y_2$  and  $z_2$ ) are the coordinates of the point (in the coordinate system of principal axes passing through the centroid) farthest from the neutral axis.

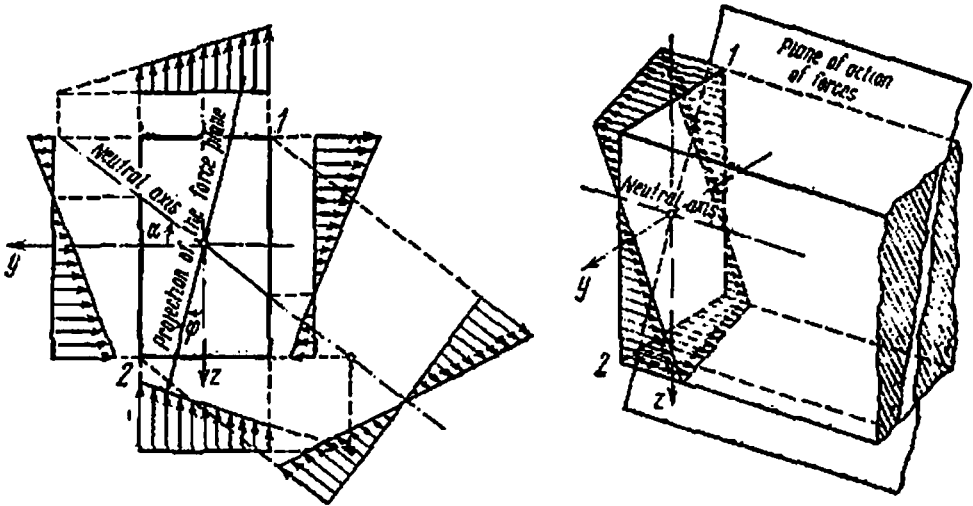


Fig. 301

For section with corners in which both the principal axes of inertia are the axes of symmetry (rectangle, I-beam), i.e.

$$|y_1| = |y_2| = |y_{\max}| \quad \text{and} \quad |z_1| = |z_2| = |z_{\max}|$$

formula (20.5) may be simplified and the expression for  $\sigma_{(1,2)}$  may be written as follows:

$$\sigma_{(1,2)} = \pm M \left( \frac{\cos \varphi}{W_y} + \frac{\sin \varphi}{W_z} \right) = \pm \frac{M}{W_y} \left( \cos \varphi + \frac{W_y}{W_z} \sin \varphi \right) \quad (20.6)$$

The strength condition for such sections is as follows:

$$|\sigma_{\max}| = \frac{M_{\max}}{W_y} \left( \cos \varphi + \frac{W_y}{W_z} \sin \varphi \right) \leq [\sigma] \quad (20.7)$$

While selecting the section we set the value of  $\frac{W_y}{W_z}$ , and knowing  $[\sigma]$ ,  $M_{\max}$ , and angle  $\varphi$  we find by trial and error the values of  $W_y$  and  $W_z$  which satisfy the strength condition (20.7). In unsymmetric sections without corners, i.e. when we use strength condition (20.5), the loca-

tion of neutral axis and the coordinates of the farthest point ( $y_1, z_1$ ) must be determined every time beforehand. For a rectangular section,  $\frac{W_y}{W_z} = \frac{h}{b}$ . Therefore assuming the ratio  $\frac{h}{b}$  known we can easily find  $W_y$  and the dimensions of the section from condition (20.7).

The diagrams showing the distribution of stresses in a rectangular section are given in Fig. 301.

It is clear from equation (20.4) that angles  $\alpha$  and  $\varphi$  are not equal, i.e. the neutral axis is not perpendicular to the plane of application of external forces as was the case in uni-planar bending. The perpendicularity can be achieved only if

$$J_y = J_z \quad (20.8)$$

but then all axes become the principal axes, and unsymmetric bending becomes impossible; irrespective of the plane of loading we shall have uni-planar bending. This will be true for square, circular and all other sections which satisfy equation (20.8).

The shearing stresses may also be calculated by a method similar to the one adopted for determining the normal stresses; the total shearing stress will be equal to the geometric sum of the stresses due to bending in each of the principal planes. Usually the value of the shearing stresses has no practical importance.

### § 121. Determining Displacements in Unsymmetric Bending

We shall again apply the principle of superposition of forces to determine the deflection in various sections of a beam subjected to unsymmetric bending. Considering the same example discussed in the preceding section, we shall first find the deflection of point  $B$  (free end of the beam) only due to force  $P_z$ ; the deflection is in the direction of the  $z$ -axis and is

$$f_z = \frac{P_z l^3}{3EJ_y} = \frac{l^3 P \cos \varphi}{3EJ_y}$$

where  $l$  is the span of the beam. Similarly, the deflection of point  $B$  due to a single force  $P_y$  is in the direction of the  $y$ -axis and may be expressed

$$f_y = \frac{P_y l^3}{3EJ_z} = \frac{l^3 P \sin \varphi}{3EJ_z}$$

Total deflection  $f$  of the free end of the beam is equal to the geometric sum of the two deflections:

$$f = \sqrt{f_y^2 + f_z^2} \quad (20.9)$$

Also

$$\frac{f_y}{f_z} = \frac{\sin \varphi}{\cos \varphi} \frac{J_y}{J_z} = \tan \varphi \frac{J_y}{J_z} = \tan \alpha \quad (20.10)$$

and

$$f = \frac{f_y}{\sin \alpha} = \frac{f_z}{\cos \alpha}$$

It follows from this relation that the angle between total deflection  $f$  and the  $z$ -axis is equal to  $\alpha$ , i.e. deflection  $f$  is perpendicular to the neutral axis. The beam bends not in the plane of application of forces, but in a plane perpendicular to the neutral axis (Fig. 302).

We shall consider the  $y$ -axis the principal axis with the maximum moment of inertia, then plane  $xOz$  will be the *plane of maximum rigidity*, because the deflection of the beam is minimal in this plane. If,

as in the examples discussed above,  $J_y > J_z$  and hence  $\alpha > \varphi$ , the *plane of bending* deflects from the plane of maximum rigidity more than the *plane of application of external forces*.

The greater the ratio  $\frac{J_y}{J_z}$  the greater the difference. Hence, in narrow and high sections in which the ratio of the principal moments of inertia may be quite great, even a small deviation of the plane of application of forces from the plane of maximum rigidity will give rise to considerable deviation of the plane of bending of the beam.

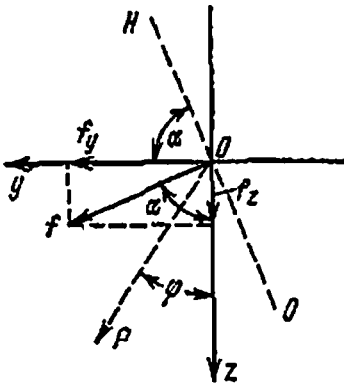


Fig. 302

As long as the external forces acting on the beam of such a section

lie in the plane of maximum rigidity  $xOz$ , the beam deflects in the same plane and the magnitude of deflections is small because of the moment of inertia  $J_y$  being large. But as soon as the plane of application of forces deviates from axis  $Oz$  by a small angle  $\varphi$ , there is a large increase in the deflections in the direction of  $y$ -axis (the designer very often overlooks this factor). The deflections in the direction of the  $z$ -axis are, however, almost unaffected. Let us take a numerical example to study this phenomenon. Consider a timber beam (Fig. 297)  $h=20$  cm high and  $b=6$  cm wide. Then

$$J_y = \frac{20^3 \times 6}{12} = 4000 \text{ cm}^4, \quad J_z = \frac{6^3 \times 20}{12} = 360 \text{ cm}^4$$

Ratio of the moments of inertia is:

$$\frac{J_y}{J_z} = \frac{4000}{360} \approx 11$$

When the plane of application of forces deflects by  $5^\circ$  from the  $z$ -axis, we obtain

$$\tan \alpha = \tan \varphi \frac{J_y}{J_z} = 0.0875 \times 11 = 0.963, \quad \alpha \approx 44^\circ$$

Deflections in the direction of the  $y$ -axis will almost be equal to the deflections in the direction of the  $z$ -axis:

$$f_y = f_z \tan \alpha = 0.963 f_z$$

Moreover, the deviation of the plane of application of forces from the plane of maximum rigidity is accompanied by a considerable increase in the normal stresses. In the example discussed above the maximum normal stresses (as compared to uni-planar bending when  $\varphi=0$ ) increase in the ratio (see formula (20.6))

$$\frac{\frac{M}{W_y} \left( \cos \varphi + \frac{W_y}{W_z} \sin \varphi \right)}{\frac{M}{W_y}} = \left( 1 + \frac{h}{b} \tan \varphi \right) \cos \varphi \approx \left( 1 + \frac{20}{6} 0.0875 \right) 1 = 1.29$$

Fig. 303 shows the relative location of the neutral surface, the plane of bending and the plane of loading.

Beams in which the principal moments of inertia of sections differ considerably from one another, work satisfactorily if bending occurs

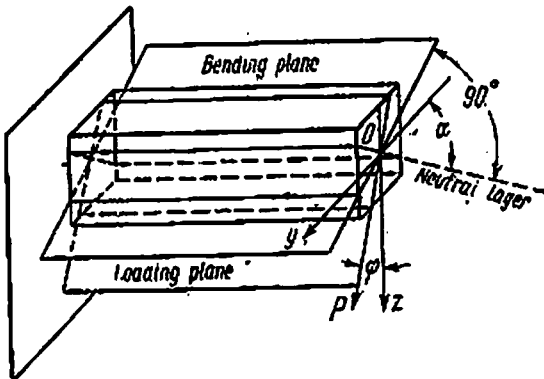


Fig. 303

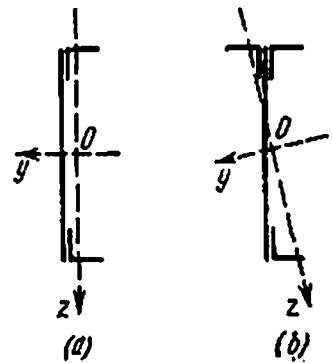


Fig. 304

in the plane of maximum rigidity (high rectangular sections, I-beams, channel bars). They, however, fail under unsymmetric bending. Therefore in situations where the designer is not very sure of a sufficiently accurate coincidence of the plane of loading with the principal plane, he should avoid using such sections or make additional provisions (by putting constraints) to prevent lateral deformation, which might occur during unsymmetric bending.

However, careless reinforcement of the existing structures may be extremely harmful. We know a case when a beam of channel section

consisting of a plate and two angles (Fig. 304(a)), working under a load acting in plane  $xOz$  was reinforced by welding to it an extra angle (Fig. 304(b)). This resulted in deviation of the principal axes from the plane of loading and gave rise to deformation in the lateral direction, which was completely unforeseen.

**Example.** Select the section for a wooden lath of height  $h$  and width  $b$  and determine the deflection of its middle point. Assume that  $\frac{h}{b} = 2$ ; the length of the beam (distance between the two supporting trusses) is  $l = 4$  m and the roof is inclined at  $23^\circ$  to the horizontal; the load due to the lath's weight and the weight of snow on the roof may be considered as uniformly distributed and having the intensity  $q = 400$  kgf/m. The lath is simply supported. Permissible stress is  $100$  kgf/cm<sup>2</sup>, and the modulus of elasticity is  $E = 10^5$  kgf/cm<sup>2</sup>.

Maximum bending moment will occur at the middle of the span; it will be

$$M_{\max} = \frac{ql^2}{8} = \frac{400 \times 16}{8} = 800 \text{ kgf} \cdot \text{m}$$

As angle  $\varphi$  is equal to the angle of slant of the roof, i.e.  $25^\circ$ , it follows from formula (20.7) and condition  $\frac{h}{b} = 2$  that

$$\begin{aligned} W_y = \frac{bh^2}{6} = \frac{h^3}{12} &\geq \frac{M_{\max}}{[\sigma]} \left( \cos \varphi + \frac{h}{b} \sin \varphi \right) \\ &= \frac{80\,000}{100} (0.906 + 2 \times 0.423) = 1402 \text{ cm}^3 \end{aligned}$$

wherefrom  $h \geq \sqrt[3]{12 \times 1402} = 25.6 \approx 26$  cm and  $b = 13$  cm.

Maximum deflection of the beam occurs at the middle of the span. Moments of inertia of the section are:

$$J_y = \frac{bh^3}{12} = \frac{13 \times 26^3}{12} = 19\,050 \text{ cm}^4, \quad J_z = \frac{b^3h}{12} = \frac{13^3 \times 26}{12} = 4760 \text{ cm}^4$$

The angle of inclination,  $\alpha$ , of the neutral axis can be determined as follows:

$$\tan \alpha = \tan \varphi \frac{J_y}{J_z} = \tan 25^\circ \frac{19\,050}{4760} = 1.865$$

wherefrom  $\alpha = 61^\circ 50'$ , and the angle made by the plane of bending with the plane of loading is:

$$\alpha - \varphi = 61^\circ 50' - 25^\circ = 36^\circ 50'$$

The deflection in the plane of maximum rigidity is:

$$f_z = \frac{5ql^4 \cos \varphi}{384 J_y E} = \frac{5 \times 4 \times 4^4 \times 0.906 \times 10^8}{384 \times 19\,050 \times 10^5} = 0.64 \text{ cm}$$

Total deflection is:

$$f = \frac{f_z}{\cos \alpha} = \frac{0.64}{0.472} = 1.35 \text{ cm}$$

Deflection in the direction of the  $y$ -axis (parallel to the arm of width  $b$ ) is:

$$f_y = f_z \tan \alpha = 0.64 \times 1.865 = 1.19 \text{ cm}$$

Hence, in this example the deflection in the direction of axis  $Oy$  is much greater than in the direction of  $Oz$  and is almost equal to the total deflection.

## CHAPTER 21

### Combined Bending and Tension or Compression

#### § 122. Deflection of a Beam Subjected to Axial and Lateral Forces

In engineering practice we often come across cases when a beam is subjected to combined bending and tension or compression. Deformation of this type may occur either by the simultaneous action of axial and lateral forces or by the action of axial forces only.



Fig. 305

The first of these cases is shown in Fig. 305. Beam  $AB$  is acted upon by a uniformly distributed force  $q$  and an axial compressive force  $P$ . If we assume that the deflection of the beam is negligible as compared to its cross-sectional dimensions, we can also assume with sufficient accuracy that after deformation force  $P$  will give rise to axial compression only.

Applying the method of superposition of forces, we can find the normal stresses at any point of an arbitrary section as the algebraic sum of stresses caused by forces  $P$  and  $q$ .

Compressive stress  $\sigma_P$  due to force  $P$  is uniformly distributed over the cross-sectional area,  $S$ , and is equal in all sections:

$$\sigma_P = -\frac{P}{S}$$

In a section with abscissa  $x$  the normal stresses due to bending in the vertical plane are given by the formula

$$\sigma_q = \frac{M(x)z}{J_y}$$

where  $x$  is measured, say, from the left end of the beam.

Hence, at a point of this section having coordinate  $z$  (measured from the neutral axis) the total stress is:

$$\sigma = \sigma_p + \sigma_q = -\frac{P}{S} + \frac{M(x)z}{J_y}$$

Figure 306 shows the diagrams of stress distribution in the given section due to forces  $P$  and  $q$  and also the resultant diagram. Maximum stress occurs in the uppermost fibres, where both deformations are

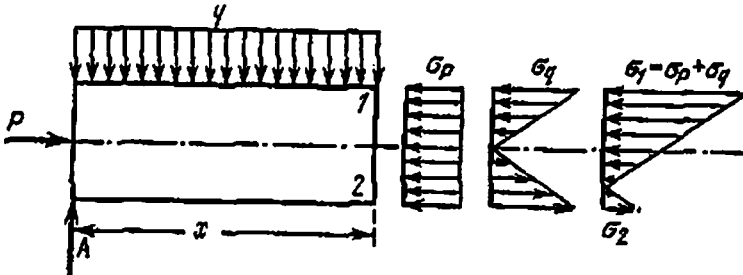


Fig. 306

compressive; the fibres below the neutral axis experience either tension or compression depending upon the numerical values of  $\sigma_p$  and  $\sigma_q$ . In order to write the strength condition let us determine the maximum normal stress.

As the stresses due to forces  $P$  are equal in all sections and uniformly distributed, the critical fibres are those which experience the maximum bending stresses. These fibres are the outer fibres of the section in which the maximum bending moment occurs; for them

$$\sigma_{q \max} = \pm \frac{M_{\max}}{W}$$

Thus, stresses in the outer fibres 1 and 2 (Fig. 306) of the middle section of the beam may be expressed

$$\left. \begin{matrix} \sigma_1 \\ \sigma_2 \end{matrix} \right\} = -\frac{P}{S} \mp \frac{M_{\max}}{W} \tag{21.1}$$

and the design stress

$$|\sigma_{\max}| = |\sigma_1| = \left| \frac{P}{S} + \frac{M_{\max}}{W} \right| \tag{21.2}$$

If forces  $P$  were tensile, the sign of the first factor would be reversed and the lowermost fibres would be the critically loaded ones.

By denoting the compressive or tensile forces by  $N$  we can write the general expression for checking the strength of such beams:

$$\sigma_{\max} = \pm \left( \frac{N}{S} + \frac{M_{\max}}{W} \right) \leq [\sigma] \quad (21.3)$$

In writing equation (21.3) we have assumed that the section is symmetric about the neutral axis and the beam material has equal resistance to tension and compression.

The above method can also be applied to beams subjected to inclined loading (Fig. 307). The inclined force can be decomposed into

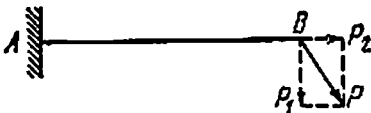


Fig. 307

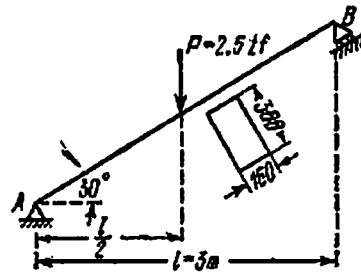


Fig. 308

a normal component, which bends the beam, and an axial component, which stretches or compresses it.

**Example.** An inclined beam (Fig. 308) is loaded at the middle of its span by a force  $P = 2.5$  tf. Find the maximum compressive stress in the beam.

The upper half of the beam only bends; the lower half is bent as well as compressed. Bending is caused by the force  $P \cos 30^\circ$ , whereas compression by the force  $P \sin 30^\circ$ . Maximum bending moment

$$M_{\max} = \frac{P \cos 30^\circ \left( \frac{l}{\cos 30^\circ} \right)}{4} = \frac{Pl}{4} = \frac{2.5 \times 3}{4} = 1.875 \text{ tf} \cdot \text{m}$$

The section modulus and the cross-sectional area are, respectively,

$$W = \frac{bh^3}{6} = \frac{16 \times 30^3}{6} = 2400 \text{ cm}^3, \quad S = 16 \times 30 = 480 \text{ cm}^2$$

The maximum compressive stress (in the uppermost fibre of the beam in a section to the left of the applied force) is:

$$\begin{aligned} \sigma &= - \frac{P \sin 30^\circ}{S} - \frac{M_{\max}}{W} = - \frac{2500}{2 \times 480} - \frac{187500}{2400} \\ &= -2.6 - 78.1 = -80.7 \text{ kgf/cm}^2 \end{aligned}$$



### § 123. Eccentric Tension or Compression

A second situation in which the bending and axial deformations are added up is *eccentric tension or compression*, which results from axial forces only. This type of deformation occurs when the bar is acted upon by two equal and opposite forces  $P$  which act along  $AA$  parallel to its axis (Fig. 309). The distance of point  $A$  from the centre of gravity of section  $O$  is  $OA=e$  and is known as the *eccentricity*.

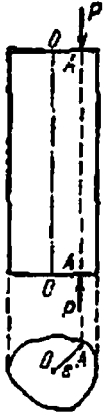


Fig. 309

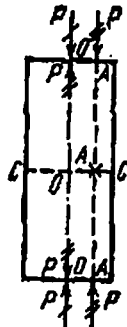


Fig. 310

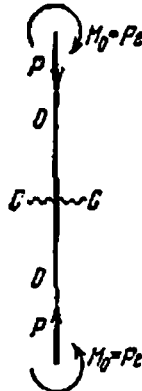


Fig. 311

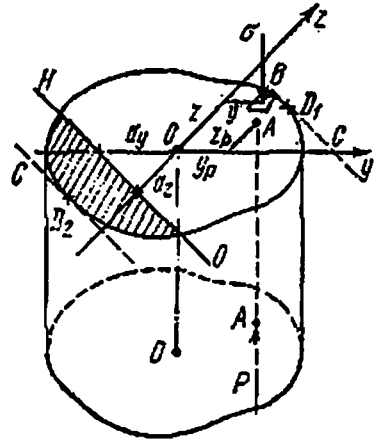


Fig. 312

Let us first consider eccentric compression, because it is of greater practical importance. Our task is to calculate the maximum stresses in the material of the bar and check its strength. To solve the problem let us apply two equal and opposite forces  $P$  at points  $O$  (Fig. 310). This will not violate the equilibrium of the bar as a whole and will not affect the stresses acting in its sections.

Forces  $P$  crossed by a single stroke will cause axial compression, whereas the pairs of forces  $P$  crossed by two strokes will give rise to pure bending of moments  $M_0 = Pe$ . The design scheme of the bar is given in Fig. 311. Since plane  $OA$  of the bending moment may not coincide with any of the principal planes of inertia of the bar, the deformation, in general, will be a combination of axial compression and pure unsymmetric bending.

As the stresses are equal in all sections in axial compression and pure bending, we may check the strength of the bar in any section, say section  $C-C$  (Fig. 311).

Let us remove the upper portion and consider the equilibrium of the lower portion (Fig. 312). Assume  $Oy$  and  $Oz$  to be the principal axes of inertia of the section. Let  $y_p$  and  $z_p$  be the coordinates of point  $A$ , the point of intersection of the line of action of force  $P$  with the cross section. We shall select the positive direction of axes  $Oy$  and  $Oz$  in such a way that point  $A$  always remains in the first quadrant. Then both  $y_p$  and  $z_p$  will be positive.

In order to find the maximum stressed point of the section, we write the expression for normal stress  $\sigma$  at an arbitrary point  $B$  having coordinates  $y$  and  $z$ . The stresses in section  $C-C$  are made up of axial compressive stress due to force  $P$  and bending stress due to pure unsymmetric bending by moment  $Pe$ , where  $e=OA$ . The compressive stress due to force  $P$  is equal to  $\frac{P}{S}$  at every point, where  $S$  is the cross-sectional area of the bar; unsymmetric bending may be replaced by bending moments in the principal planes. Moment  $P y_P$  bends the bar in plane  $xOy$  about the neutral axis  $Oz$  and gives rise to normal compressive stress  $\frac{P y_P y}{J_z}$  at point  $B$ . Similarly, the normal stress at point  $B$  due to bending in plane  $xOz$  caused by moment  $P z_P$  is also compressive and is equal to  $\frac{P z_P z}{J_y}$ .

Summing the stresses due to axial compression and bending in two planes and considering the compressive stresses to be negative, we get the following formula for the stress at point  $B$ :

$$\sigma = -\frac{P}{S} - \frac{P y_P y}{J_z} - \frac{P z_P z}{J_y} = -P \left( \frac{1}{S} + \frac{y_P y}{J_z} + \frac{z_P z}{J_y} \right) \quad (21.4)$$

This formula is valid for calculating the stresses at any point of an arbitrary section, only the coordinates of the point in the system of principal axes should be substituted for  $y$  and  $z$  with proper signs.

In the case of eccentric tension, the signs of all the terms in the expression for the normal stress at point  $B$  will be reversed. Therefore, in order to obtain the stress with the proper sign from formula (21.4), regardless of whether it is eccentric tension or compression, we must consider the sign of force  $P$  in addition to the signs of coordinates  $y$  and  $z$ ; in eccentric tension there should be a positive sign before the expression

$$P \left( \frac{1}{S} + \frac{y_P y}{J_z} + \frac{z_P z}{J_y} \right)$$

and in eccentric compression a negative sign.

The above formula may be modified somewhat. Let us factor out  $\frac{P}{S}$ ; we obtain

$$\sigma = -\frac{P}{S} \left( 1 + \frac{y_P y}{i_z^2} + \frac{z_P z}{i_y^2} \right) \quad (21.5)$$

Here  $i_z$  and  $i_y$  are the radii of gyration of the section about the principal axes (recall that  $J_z = i_z^2 S$  and  $J_y = i_y^2 S$ ).

To find the maximum stressed point we must select the  $y$ - and the  $z$ -axis in such a way that  $\sigma$  attains the maximum value. The varying terms in formulas (21.4) and (21.5) are the last two, which reflect the

influence of bending. Also, since the maximum stresses in bending occur at points which are farthest from the neutral axis, it is essential, as in unsymmetric bending, to locate the neutral axis first.

Let us denote the coordinates of points on the neutral axis by  $y_0$  and  $z_0$ . As the normal stresses are zero at points on this axis, after substituting  $y_0$  and  $z_0$  in formula (21.5) we get

$$0 = -\frac{P}{S} \left( 1 + \frac{y_P y_0}{i_z^2} + \frac{z_P z_0}{i_y^2} \right)$$

or

$$1 + \frac{y_P y_0}{i_z^2} + \frac{z_P z_0}{i_y^2} = 0 \quad (21.6)$$

This is the equation of the neutral axis; it is the equation of a straight line not passing through the centre of gravity of the section.

The simplest way of plotting this line is to calculate the segments it cuts on the coordinate axes. Let us denote these segments by  $a_y$  and  $a_z$ . In order to find segment  $a_y$  cut on the  $y$ -axis, we put in equation (21.6)

$$z_0 = 0, \quad y_0 = a_y$$

and obtain

$$1 + \frac{y_P a_y}{i_z^2} = 0, \quad \text{hence} \quad a_y = -\frac{i_z^2}{y_P} \quad (21.7)$$

Similarly, assuming that

$$y_0 = 0, \quad z_0 = a_z$$

we obtain

$$a_z = -\frac{i_y^2}{z_P} \quad (21.8)$$

If  $y_P$  and  $z_P$  are positive, segments  $a_y$  and  $a_z$  will be negative, i.e. the neutral axis will be located on the other side of the centre of gravity than point  $A$  (Fig. 312).

The neutral axis divides the section into two parts, compressed and stretched. In Fig. 312 the stretched part has been shaded. Drawing tangents to the contour of the section, tangents parallel to the neutral axis, we obtain two points  $D_1$  and  $D_2$  which are subjected to the maximum compressive and tensile stresses.

Measuring the coordinates  $y$  and  $z$  of these points and substituting them in formula (21.4), we calculate the maximum stresses at points  $D_1$  and  $D_2$  by the formula

$$\sigma_{(1,2)} = -P \left( \frac{1}{S} + \frac{y_P y_{(1,2)}}{J_z} + \frac{z_P z_{(1,2)}}{J_y} \right) \quad (21.9)$$

If the bar's material has equal resistance to tension and compression, then the strength condition may be written as

$$|\sigma_{\max}| = P \left( \frac{1}{S} + \frac{y_P y_1}{J_z} + \frac{z_P z_1}{J_y} \right) \leq [\sigma] \quad (21.10)$$

For sections with corners in which both principal axes of inertia are also the axes of symmetry (rectangle, I-beam, etc.),  $y_1 = y_{\max}$  and  $z_1 = z_{\max}$ . Therefore formula (21.10) may be simplified and written as follows:

$$|\sigma_{\max}| = P \left( \frac{1}{S} + \frac{y_p}{W_z} + \frac{z_p}{W_y} \right) \leq [\sigma] \quad (21.11)$$

If the material of the bar has unequal resistance to tension and compression, then its strength must be checked in the stretched as well as compressed zone.

However, in some cases one check may suffice for these materials also. It is evident from formulas (21.7) and (21.8) that the location of point  $A$  of application of force and that of the neutral axis are inter-related; the nearer point  $A$  is to the centre of gravity the smaller the coordinates  $y_p$  and  $z_p$  and the greater the segments  $a_y$  and  $a_z$ . Thus, as point  $A$  approaches the centre of gravity of the section, the neutral axis moves away from it, and vice versa. Therefore, in certain positions of point  $A$  the neutral axis will pass outside the section and the whole section will experience either tensile or compressive stress. Obviously, in such cases it is always sufficient to check the strength of the material at point  $D_1$  only.

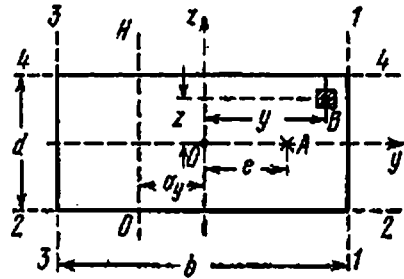


Fig. 313

Let us analyze a case of practical importance, when a bar of rectangular section (Fig. 313) is eccentrically loaded by force  $P$  at point  $A$  on the principal axis  $Oy$ . The eccentricity  $OA$  is equal to  $e$ , and the dimensions of the section are  $b$  and  $d$ . Applying the formulas obtained above, we get

$$y_p = +e, \quad z_p = 0$$

The stress at point  $B$  is

$$\sigma = \frac{P}{S} \left( 1 + \frac{y_p y S}{J_z} \right) = \frac{P}{bd} \left( 1 + \frac{12ey}{b^2} \right) \quad (21.12)$$

because

$$\frac{S}{J_z} = \frac{12bd}{b^2 d} = \frac{12}{b^2}$$

The stresses are equal at all points on a line parallel to axis  $Oz$ . Location of the neutral axis is determined by the segments

$$a_y = -\frac{l_z^2}{e} = -\frac{b^2}{12e}, \quad a_z = \infty \quad (21.13)$$

The neutral axis is parallel to the  $z$ -axis; the points which experience maximum tensile and compressive stresses are located on the sides 1-1 and 3-3.

The values of  $\sigma_{\max}$  and  $\sigma_{\min}$  may be obtained by substituting  $y = \pm \frac{b}{2}$  in formula (21.12):

$$\left. \begin{array}{l} \sigma_{\max} \\ \sigma_{\min} \end{array} \right\} = \frac{P}{bd} \left( 1 \pm \frac{6e}{b} \right) \quad (21.14)$$

### § 124. Core of Section

In designing elements from materials which have poor strength under tension (concrete, stone), it is highly desirable that the whole section should work under compression. This can be achieved by limiting the value of eccentricity, i.e. not shifting the point of application of force  $P$  too far from the centre of gravity.

It is desirable that the designer should know beforehand the value of eccentricity which may be permitted for a particular section without the risk of stresses of two types occurring in it. Here we require the concept of *core of section*. The term core of section defines an area about the centre of gravity within which force  $P$  may be applied at any point without giving rise to stresses of different types.

As long as point  $A$  remains within the core, the neutral axis does not intersect the contour of the section, the complete section lies to one side of the neutral axis and hence works only in compression. As we move point  $A$  away from the centre of gravity, the neutral axis approaches the contour. The core boundary is determined from the condition that when point  $A$  lies on the boundary, the neutral axis passes close to the contour just touching it.

Thus, if we move point  $A$  in such a way that the neutral axis rolls along the contour without intersecting it (Fig. 314), then the locus of points  $A$  will form the core of section. If there are "depressions" in the contour, then the neutral axis should roll along the envelope of the contour.

To plot the core of section we must draw the neutral axis in a number of positions touching the contour, determine the segments  $a_y$  and  $a_z$  and calculate  $y_p$  and  $z_p$ —the coordinates of the point of application of force—with the help of relations (21.7) and (21.8):

$$y_p = -\frac{i_z^2}{a_y}, \quad z_p = -\frac{i_y^2}{a_z} \quad (21.15)$$

They represent  $y_c$  and  $z_c$ —the coordinates of points on the core's boundary.

If the contour of the section is a polygon (Fig. 315), we can find the coordinates  $y_c$  and  $z_c$  of points on the core's boundary by successively

drawing the neutral axis coinciding with the sides of the polygon and calculating the segments  $a_y$  and  $a_z$  for the corresponding sides.

In the transition from one side of the contour to another the neutral axis will rotate about the apex between the two sides; the point of application of force will move on the core's boundary between the

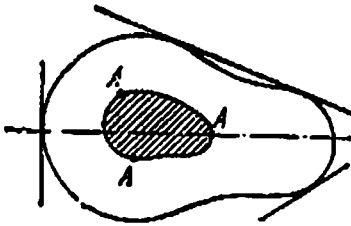


Fig. 314

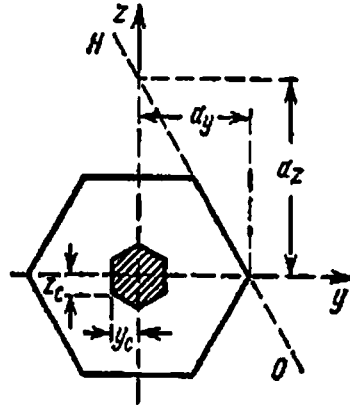


Fig. 315

points already obtained. Let us establish how the point of application of force  $P$  should move so that the neutral axis always pass through one and the same point  $B(y_B, z_B)$  and rotate about it (Fig. 316). Substituting the coordinates of this point of the neutral axis in equation (21.6)

$$1 + \frac{y_P y_B}{i_z^2} + \frac{z_P z_B}{i_y^2} = 0$$

we see that coordinates  $y_P$  and  $z_P$  of point  $A$ , the point of application of force  $P$ , are related to each other linearly. Thus, if the neutral axis rotates about a fixed point  $B$ , the point of application of force moves along a straight line. Conversely, the motion of force  $P$  along a straight line is consistent with the rotation of the neutral axis about a fixed point.

Figure 316 shows three positions of the point of application of force on this line and three corresponding positions of the neutral axis. Hence, if the contour of the section is a polygon, the core's boundary between points corresponding to the sides of the polygon consists of straight-line segments.

If the contour of the section is made up of curved lines either partially or fully, the core's boundary will be drawn with the help of points (formula (21.15)). Let us study a few simple examples on plotting the cores of sections.

For plotting the core of a rectangular section (Figs. 313 and 317) we shall employ the formulas derived at the end of the preceding section.

For plotting the core's boundary when point  $A$  moves along axis  $Oy$  we must find that value of eccentricity  $e=e_0$  corresponding to which the neutral axis occupies the position  $H_1O_1$  (Fig. 317). From formula (21.13) we find that

$$a_y = -\frac{b}{2} = -\frac{b^2}{12e_0}$$

wherefrom

$$e_0 = \frac{b}{6} \tag{21.16}$$

Hence, along axis  $Oy$  the core's boundary will lie at a distance of  $\frac{b}{6}$  from the centre of gravity (Fig. 317, points 1 and 3). Along axis  $Oz$  the core's boundary will be determined by a distance of  $\frac{d}{6}$  (points 2 and 4).

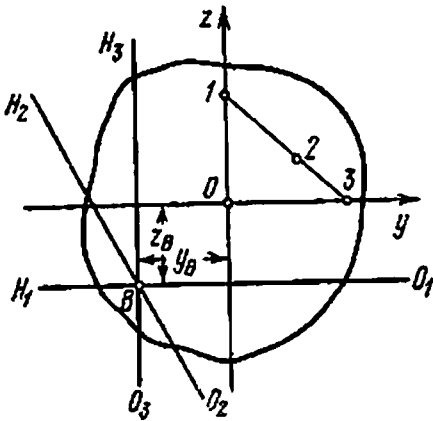


Fig. 316

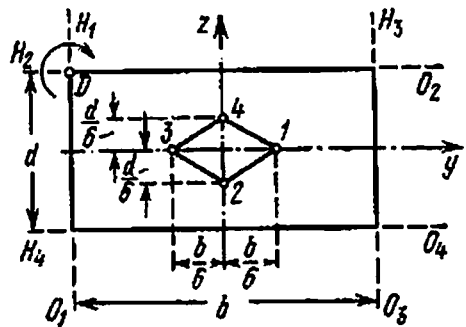


Fig. 317

To draw the core's boundary completely, let us plot the neutral axis in positions  $H_1O_1$  and  $H_2O_2$  corresponding to the extreme points 1 and 2.

As the force moves from point 1 to point 2 along the core's boundary, the neutral axis must pass from position  $H_1O_1$  to  $H_2O_2$  all the time touching the section, i.e. rotating about point  $D$ . For this to occur, the force must move along the straight line 1-2. It can be similarly proved that lines 2-3, 3-4, and 4-1 will form the other boundary lines of the core.

Thus, for a rectangular section the core is a rhombus with diagonals equal to one-third of the corresponding sides of the section. Hence, if the force is applied on the principal axes, the whole section experiences stresses of a particular sign, provided the point of application of the force does not lie beyond one-third of the distance of the corresponding side from the centre of gravity.

Figure 318 shows the distribution of normal stresses along the height of a rectangular section when the eccentricity is equal to zero, less than, equal to and more than one-sixth of the width of the section. It

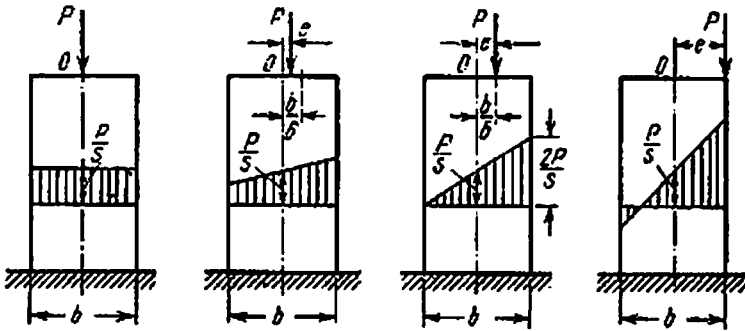


Fig. 318

should be noted that for all locations of force  $P$  the stress at the centre of gravity of the section (point  $O$ ) is the same and equal to  $\frac{P}{S}$ , and force  $P$  does not have any eccentricity along the second principal axis.

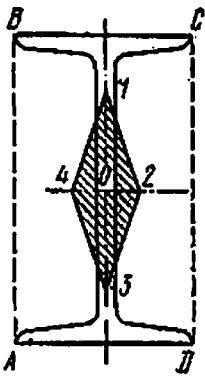


Fig. 319

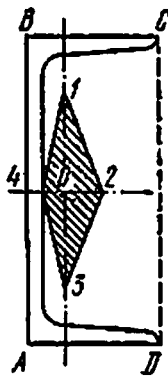


Fig. 320

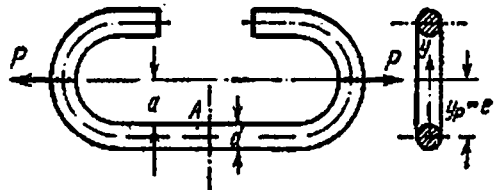


Fig. 321

From symmetry considerations the core of a circular section of radius  $r$  will also be a circle of radius  $r_0$ . Let us consider an arbitrary position of the neutral axis tangent to the contour. We shall direct axis  $Oy$  perpendicular to this tangent. Then

$$a_y = r, \quad a_z = \infty, \quad z_c = 0$$

$$y_c = r_0 = -\frac{I_z^2}{a_y} = -\frac{\frac{\pi r^4}{4}}{\pi r^2} = -\frac{r}{4}$$

Hence, the core is a circle of radius four times less than the radius of the section.



In an I-beam the neutral axis will not intersect the section while moving round it, if it remains tangential to rectangle  $ABCD$  described around the I-beam (Fig. 319). Therefore, in an I-beam the core is a rhombus, as in a rectangular section, but only with different dimensions.

In a channel bar, as in an I-beam, points 1, 2, 3, 4 of the core's boundary (Fig. 320) correspond to positions of the neutral axis when it coincides with the sides of rectangle  $ABCD$ . The distances may be found from formulas (21.15).

**Example 1.** A cutout element of a chain (Fig. 321) is made of steel wire of diameter  $d=50$  mm;  $a=60$  mm. Find the maximum permissible value of force  $P$  if the permissible tensile stress in section  $A$  is  $[\sigma]=1200$  kgf/cm<sup>2</sup>.

In the given section the wire material is subjected to eccentric tension. Eccentricity  $e$  is equal to  $a + \frac{d}{2}$ . Selecting axis  $Oy$  in the plane passing through force  $P$  and the axis of the straight part of the wire as the other axis, we get

$$z_p = 0, \quad y_p = e = a + \frac{d}{2}$$

Stress at an arbitrary point of the section is given by the expression

$$\sigma = +\frac{P}{S} + \frac{P \left( a + \frac{d}{2} \right) y}{J_z}$$

Substituting the limiting values  $y = \pm \frac{d}{2}$ , we find the maximum and minimum stresses:

$$\left. \begin{array}{l} \sigma_{\max} \\ \sigma_{\min} \end{array} \right\} = \frac{4P}{\pi d^2} \pm \frac{64Pde}{2\pi d^4} = \frac{4P}{\pi d^2} \left[ 1 \pm \frac{8e}{d} \right] = \frac{4P}{\pi d^2} \left[ 1 \pm \frac{8 \left( a + \frac{d}{2} \right)}{d} \right]$$

The strength condition may be written as

$$\frac{4P}{\pi d^2} \left[ 1 + \frac{8 \left( a + \frac{d}{2} \right)}{d} \right] = \frac{4P}{\pi d^2} (8a + 5d) \leq [\sigma]$$

wherefrom

$$P = \frac{\pi d^2 [\sigma]}{4(8a + 5d)} = \frac{3.14 \times 5^2 \times 1200}{4(8 \times 6 + 5 \times 5)} \approx 1610 \text{ kgf}$$

**Example 2.** A long bulkhead  $h=3$  m high and  $b=2$  m wide (Fig. 322) supports an earth mound. Earth pressure per metre length of the bulkhead is  $H=3$  tf and acts at a height of  $\frac{h}{3}$  from the foundation. Specific weight of brickwork is  $\gamma=2$  tf/m<sup>3</sup>. Find the limiting values of stresses in a section taken through the foundation.

If we isolate a portion one metre long from the wall (Fig. 322), we can consider it as a bar fixed at one end and subjected to bending due to earth pressure and compression due to its own weight. As the maximum stresses occur at the fixed end, it is sufficient to check the strength of the cutoff portion in this section only. The problem of determining stresses in this section is equivalent to analyzing a bar subjected to simultaneous compression and bending. The forces transmitted through this section are the weight of the cutoff portion  $N=1 \times 2 \times 3 \times 2=12$  tf and earth pressure  $H=3$  tf. The bending moment in this section due to force  $H$  is equal to  $M=H \frac{h}{3}=3$  tf·m. We shall employ formula (21.3) for calculating the maximum normal stresses at the edge of the foundation. The section which is being checked is a rectangle with dimensions  $b=2$  m and  $d=1$  m; therefore the maximum compressive stress on side 1-1 of this section is

$$\begin{aligned}\sigma_{\max} &= -\frac{H}{S} - \frac{M}{W} = -\frac{12}{2 \times 1} - \frac{6 \times 3}{1 \times 2^2} \\ &= -6 - 4.5 \\ &= -10.5 \text{ tf/m}^2 = -1.05 \text{ kgf/cm}^2\end{aligned}$$

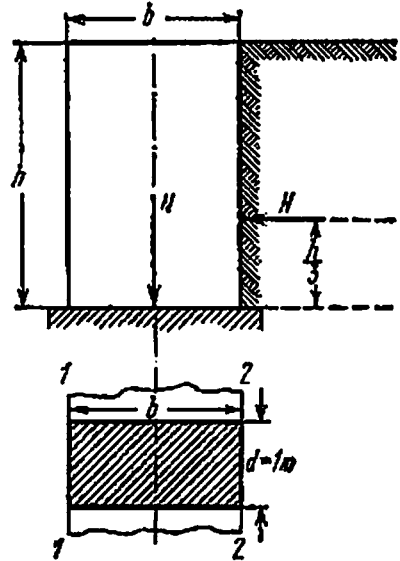


Fig. 322

The compressive stress at points on side 2-2 of the section is

$$\begin{aligned}\sigma_{\min} &= -\frac{N}{S} + \frac{M}{W} = -6 + 4.5 \\ &= -1.5 \text{ tf/m}^2 = -0.15 \text{ kgf/cm}^2\end{aligned}$$

## CHAPTER 22

## Combined Bending and Torsion

## § 125. Determination of Twisting and Bending Moments

In Chapter 9 we discussed a problem on checking the strength of a shaft under torsion. However, machine parts such as shafts rarely work under pure torsion. Even a straight shaft working under torsion bends due to its own weight, weight of the pulleys and the pressure exerted by the belts. Hence, a majority of machine parts working under torsion are actually subjected to combined bending and torsion. Crankshafts belong to this group.

In the analysis of elements subjected to combined bending and torsion the first thing to do is to find the design values of the bending moment  $M_b$  and twisting moment  $M_t$ .

Let us consider a straight circular shaft with a pulley and crank. The loading diagram of the shaft is shown in Figs. 323 and 324. A pulley of weight  $Q$  is mounted at its left end, the belt pressures on the tight and slack sides of the pulley are  $T$  and  $t$ , respectively ( $T > t$ ),

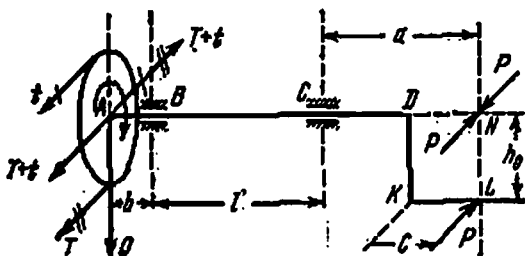


Fig. 323

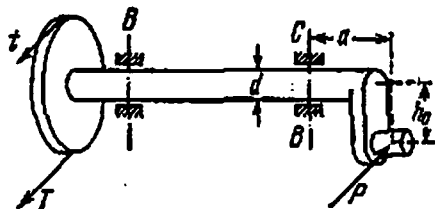


Fig. 324

and a horizontal force  $P$  acts at the crank pin at the right end of the shaft. Let us consider the instant when the crank is vertical. All dimensions are given on the diagrams.

We have to calculate the bending and twisting moments for shaft  $AD$ . Forces  $T$  and  $t$  (pull of the belt) acting on the pulley may be replaced by a force  $T+t$  acting at the centre of the pulley and a moment  $(T-t)R_0$ , where  $R_0$  is the radius of the pulley. Force  $T+t$  along with the weight of pulley,  $Q$ , bends the shaft; moment  $(T-t)R_0$ , which twists the shaft, is balanced by the moment applied to its right end.

Let us replace force  $P$  acting at the crank pin by an identical force  $P$  acting on the shaft at point  $N$  of its extension and a moment  $Ph_0$ . Thus, the ends of the shaft are acted upon by moments  $Ph_0$  and  $(T-t)R_0$ . In equilibrium, when the machine runs uniformly, these two moments are equal to the twisting moment  $M_t = Ph_0 = (T-t)R_0$ . If we know the number of revolutions of the shaft per unit time,  $n$ , and the transmitted power,  $N$ , then the twisting moment can be found from formula (9.3) of § 46:

$$M_t = \frac{716.2N}{n}, \quad \text{hence} \quad P = \frac{M_t}{h_0}$$

and

$$T = \frac{M_t}{R_0(1-m)}, \quad \text{where} \quad m = \frac{t}{T}$$

As far as bending is concerned, the shaft is acted upon by vertical force  $Q$  and horizontal forces  $T+t$  and  $P$ . Therefore, we must plot the bending-moment diagrams for the horizontal as well as the vertical forces (Fig. 325 (a) and (b)), considering the shaft to be simply support-

ed at the bearings *B* and *C* (one of the bearings permits horizontal displacement).

Having plotted the bending-moment diagrams for the vertical and horizontal forces, we can find the total bending moment  $M_b$  in a section as the geometric sum of the two. The geometric addition of the vectors representing the bending moments in section *B* is shown in Fig. 326. The total bending moment in section *B* may be written as

$$M_b = b \sqrt{Q^2 + (T + t)^2}$$

Each section will have its own plane of bending. However, since the section moduli of a circular body is the same about all axes passing through its centre of gravity, we can superpose the bending-moment

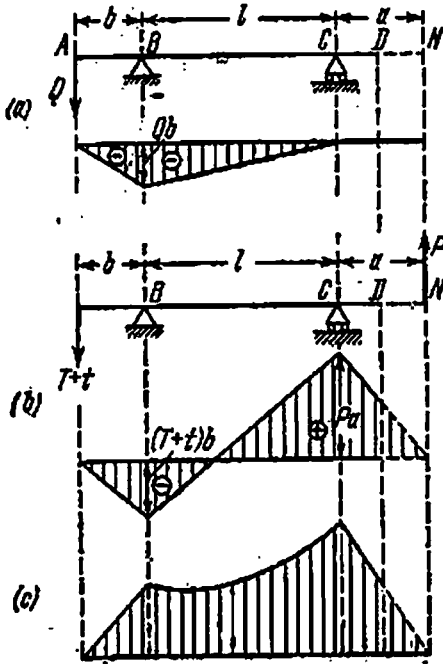


Fig. 325

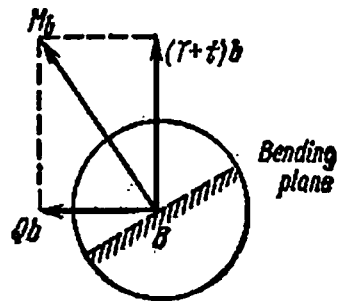


Fig. 326

planes of all sections in the plane of the diagram and then plot the resultant bending-moment diagram, without in any way affecting the final results. This precisely has been done in Fig. 325 (c). We wish to point out without a formal proof that between sections *B* and *C* the resultant bending-moment diagram does not have a maximum.

It is evident from the shape of the diagram that critical loading occurs either in bearing *B* or in bearing *C*, depending on the numerical values.

### § 126. Determination of Stresses and Strength Check in Combined Bending and Torsion

Having calculated the maximum bending moment  $M_b$  and the maximum twisting moment  $M_t$ , we can now find the maximum stresses in the shaft material and write the strength condition. Let us assume the shaft to be cut in the critical section  $C$  (Fig. 327) and analyze it with the help of the principle of superposition of forces. We shall calculate the stresses in the cross section due to the bending moment and add to them the stresses due to torsion.

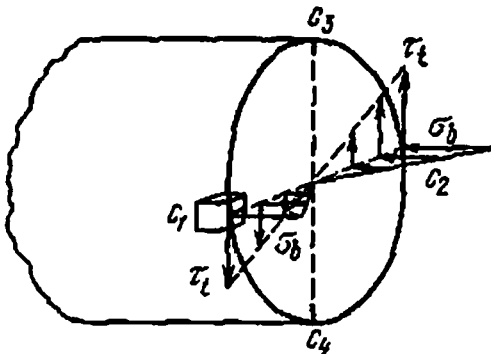


Fig. 327

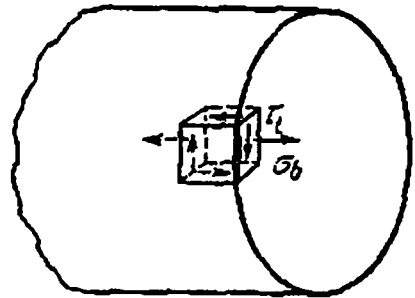


Fig. 328

The bending moment acts in the horizontal plane, the neutral axis will be vertical, and the maximum normal stresses  $\sigma_b$  will occur at points  $c_1$  and  $c_2$  at the endpoints of the horizontal diameter. Torsion will give rise to shearing stresses only, which will be maximal at points on the contour.

Thus, points  $c_1$  and  $c_2$  in the sectional plane will experience maximum normal as well as maximum shearing stresses. At points  $c_3$  and  $c_4$  on the vertical diameter the shearing stresses due to torsion will be substantiated by shearing stresses due to bending. However, these stresses are small in magnitude and experimental studies show that points  $c_1$  and  $c_2$  are the critically loaded points. Let us isolate cubic elements of the shaft's material around these points (Fig. 327). Four faces of these elements will be subjected to shearing stresses  $\tau_t$  (two of these four faces will experience normal stresses too) and the other two faces of the cube will be completely free of stresses (Fig. 328). Hence, the element is in a two-dimensional stressed state. It is known (§§ 39 and 77) that in order to check the strength of a material in two-dimensional stressed state, we must find the principal stresses  $\sigma_1$  and  $\sigma_2$  and substitute their values in the strength condition written on the basis of one of the theories of failure.

An element of a bent beam cut at a distance  $z$  from the neutral axis is also in a similar two-dimensional state of stress. We discussed how to check the strength of such an element (§ 77) while studying the

strength of beams that experience both a bending moment and a shearing force. The only difference was that both the normal stress  $\sigma$  and the shearing stress  $\tau$  were caused by bending in that case.

For checking the strength of an element cut from the shaft, we can directly apply the formulas derived in § 77 by substituting  $\sigma_b$  and  $\tau_t$  in place of  $\sigma$  and  $\tau$ , respectively. Then we obtain the following strength conditions according to four different theories of failure:

the theory of maximum normal stresses:

$$\frac{1}{2}(\sigma_b + \sqrt{\sigma_b^2 + 4\tau_t^2}) \leq [\sigma]$$

the theory of maximum strain:

$$(0.35\sigma_b + 0.65 \sqrt{\sigma_b^2 + 4\tau_t^2}) \leq [\sigma]$$

the theory of maximum shearing stresses:

$$\sqrt{\sigma_b^2 + 4\tau_t^2} \leq [\sigma]$$

the theory of distortion energy:

$$\sqrt{\sigma_b^2 + 3\tau_t^2} \leq [\sigma]$$

(22.1)

We must calculate  $\sigma_b$  and  $\tau_t$  to correlate the strength check with the numerical value of moments  $M_b$  and  $M_t$  and the dimensions of the shaft. Stress  $\sigma_b$ , which is the maximum normal stress due to bending moment  $M_b$ , is

$$\sigma_b = \frac{M_b}{W}$$

For a circular shaft  $W = \frac{\pi r^3}{4}$ , where  $r$  is the radius of the circular section. On the other hand, the maximum stress  $\tau_t$  due to torsion is

$$\tau_t = \frac{M_t}{W_p} = \frac{M_t}{\frac{\pi r^3}{2}} = \frac{M_t}{2 \frac{\pi r^3}{4}} = \frac{M_t}{2W}$$

Substituting these values in the first expression of formula (22.1), we obtain

$$\frac{1}{2} \left( \frac{M_b}{W} + \sqrt{\frac{M_b^2}{W^2} + 4 \frac{M_t^2}{4W^2}} \right) = \frac{M_b + \sqrt{M_b^2 + M_t^2}}{2W} = \frac{M_d}{W} \leq [\sigma]$$

We can similarly obtain design formulas for the other theories of failure. It is evident that all these formulas can be represented by a single general formula of the type

$$\frac{M_d}{W} \leq [\sigma] \quad (22.2)$$

where  $M_d$  is the design moment whose value depends not only upon the moments  $M_b$  and  $M_t$  but also upon the theory of failure applied. According to

the theory of maximum normal stresses:

$$M_{d1} = \frac{1}{2} (M_b + \sqrt{M_b^2 + M_t^2})$$

the theory of maximum strain:

$$M_{d2} = 0.35M_b + 0.65\sqrt{M_b^2 + M_t^2}$$

the theory of maximum shearing stresses:

$$M_{d3} = \sqrt{M_b^2 + M_t^2}$$

the theory of distortion energy:

$$M_{d4} = \sqrt{M_b^2 + 0.75M_t^2}$$

(22.3)

Formula (22.2) is similar to the formula by which we check the strength under normal stresses due to bending by a moment  $M_d$ . Therefore, the strength check of a round shaft under combined bending and torsion may be replaced by a check due to bending only by the bending moment  $M_d$ .

In some constructions the shafts are subjected to tension or compression due to an axial load  $N$  in addition to bending and torsion. The effect of the axial forces on the strength of the shaft may be taken into account by the addition of stresses  $\sigma_a$  caused by them to the maximum bending stresses  $\sigma_b$ :  $\sigma_a = \frac{N}{A}$ , where  $A$  is the cross-sectional area of the shaft.

From formula (22.2) we obtain

$$W = \frac{\pi r^3}{4} \geq \frac{M_d}{[\sigma]}$$

wherefrom the radius of the shaft

$$r \geq \sqrt[3]{\frac{4M_d}{\pi[\sigma]}}, \quad d = 2r \quad (22.4)$$

For using this formula all we have to do is to establish which of the theories of failure should be used and, consequently, which of the expression in formulas (22.3) should be employed for calculating the design moment.

We can straightaway reject the theory of maximum normal stresses (see § 39), because shafts are usually made from steel and from ductile materials in general. Until recent times, shafts in machine tool industry were designed by the formula based on the second theory (the theory of maximum strain). The formula is sometimes also referred to as

*Saint-Venant's formula:*

$$\frac{1}{W} (0.35M_b + 0.65 \sqrt{M_b^2 + M_t^2}) \leq [\sigma]$$

It was used despite the fact that the hypothesis underlying it is definitely not true for ductile materials. For some time now shafts are designed by formulas which are based either on the third theory (theory of maximum shearing stresses) or on the fourth theory (distortion energy theory):

$$\frac{1}{W} \sqrt{M_b^2 + M_t^2} \leq [\sigma] \quad \text{and} \quad \frac{1}{W} \sqrt{M_b^2 + 0.75M_t^2} \leq [\sigma]$$

Table 15 compares the values of shaft diameters for different ratios of  $M_b$  and  $M_t$ , using the same permissible stress in all the theories of failure. The diameter obtained by the theory of maximum strain (Saint-Venant's formula) is taken as unity.

Table 15

Comparison of the Shaft Diameters

	Shaft diameter according to		
	II theory	III theory	IV theory
$M_b = 0$	1	1.15	1.10
$M_b = \frac{1}{2} M_t$	1	1.07	1.03
$M_b = M_t$	1	1.03	1.01

It is evident from the table that, firstly, the difference in the dimensions of the shaft is not large regardless of the theory used and, secondly, the diameter by Saint-Venant's formula is in all cases less than the diameter obtained by the other two theories. This helps to explain the fact that Saint-Venant's formula is still used sometimes in engineering practice, although it is based on a hypothesis which has been proved inapplicable to ductile materials.

A designer must remember that transition to the new design formulas based on more accurate theories would have been practically impossible if the old values of permissible stresses had been retained. This would have led to the use of shafts of bigger diameters, where old shafts of smaller size designed according to Saint-Venant's formula were working satisfactorily.

The idea is that when we change over to a new formula we cannot retain the previous factor of safety and the previous permissible stress.



More accurate design and deeper knowledge about the working of materials must, as a rule, be accompanied by a reduction in the factor of safety and consequently an increase in the permissible stress,  $[\sigma]$ .

Therefore, when we are calculating the design moment by the new formulas, we must increase the permissible stress  $[\sigma]$  by such a value so that we can justify the dimensions of shafts already working satisfactorily on the basis of the new theories and reliable experimental investigations.

## CHAPTER 23

### General Compound Loading

#### § 127. Stresses in a Bar Section Subjected to General Compound Loading

The methods of finding stresses and deformations used in solving particular problems of compound loading may also be employed in situations of more complex loading of the body. Limiting our discussion to prismatic bars, in which the centre of bending coincides with the centre of gravity of the section, we assume that such a bar (Fig. 329 (a)) is in equilibrium under the forces acting on it; the orientation of these forces in space is arbitrary. To simplify the diagram, only concentrated forces have been shown in Fig. 329 (a). However, distributed loads and moments may also be applied. This will not affect our discussion.

For finding the stresses at an arbitrary point  $A$  of the bar, let us draw a section  $mn$  perpendicular to the bar's axis; the section cuts the bar into two parts ( $I$  and  $II$ ). Let us remove one part, say, the right one, and transfer all forces acting on it to the centre of gravity of section  $mn$ , to point  $C$ . In the future discussion we shall use a right-hand rectangular coordinate system with the  $x$ -axis passing through the centre of gravity of section  $mn$  and normal to it and the other two axes coinciding with the principal axes of inertia of the section passing through the centroid.

When a force  $P_k$  is transferred to point  $C$  (Fig. 329 (b)), we obtain a force  $P_h$  acting at the centre of gravity in general and not coinciding with any of the coordinate axes and a moment  $M_k = P_k a_k$  acting in general in a plane which is inclined to all the coordinate planes. Projecting force  $P_h$  on the  $x$ -,  $y$ - and  $z$ -axes, we find the components  $P_{hx}$ ,  $P_{hy}$  and  $P_{hz}$ ; similarly, projecting  $M_k$  on the  $x$ -,  $y$ -, and  $z$ -axes, we obtain the components  $M_{hx}$ ,  $M_{hy}$  and  $M_{hz}$  (Fig. 329 (c) shows the resolution of vector  $L_h$  representing moment  $M_h$  into the components  $L_{hx}$ ,  $L_{hy}$  and  $L_{hz}$ ). By doing the same operation with all the forces  $P_h$  acting on the right part of the bar, we can replace the force system  $P_h$  by a statically equivalent system consisting of six components: three forces

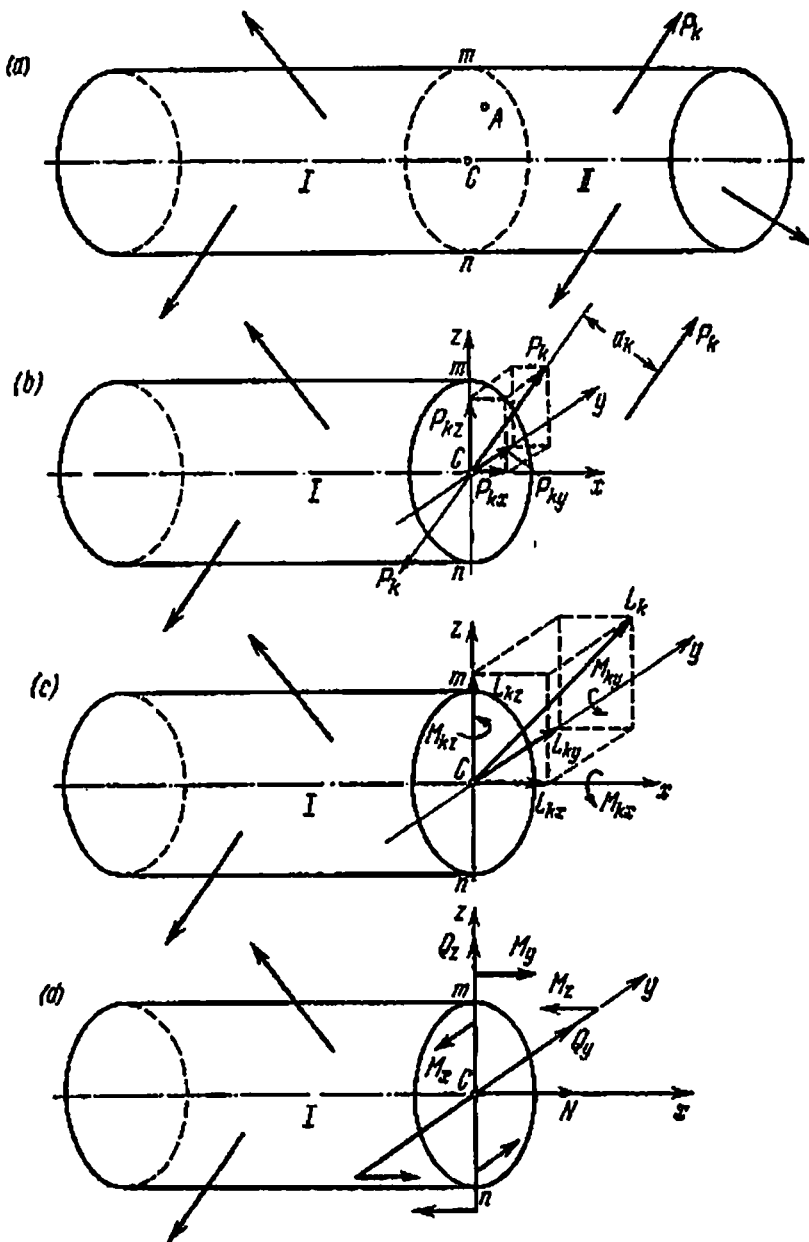


Fig. 329

along the coordinate axes acting at the centre of gravity of the section,

$$N = \sum_{k=1}^n P_{kx}, \quad Q_y = \sum_{k=1}^n P_{ky}, \quad Q_z = \sum_{k=1}^n P_{kz}$$

and three moments about these axes,

$$M_x = \sum_{k=1}^n M_{kx}, \quad M_y = \sum_{k=1}^n M_{ky}, \quad M_z = \sum_{k=1}^n M_{kz}$$

(Fig. 329 (d)). Forces  $N$ ,  $Q_y$ , and  $Q_z$  will be considered positive if they coincide with the positive directions of the coordinate axes, while moments  $M_x$ ,  $M_y$ , and  $M_z$  will be considered positive if they act in the anticlockwise direction about the corresponding axes (all the force and moment components shown in Fig. 329 (d) are positive).

From the earlier discussion we know the simple forms of deformation which result from the action of each of these components. It should be borne in mind that these forces transferred from the right cutout part to the left reflect the action of the right part on the left and therefore in section  $mn$  are manifested as stresses. Thus,  $N$  is the sum of normal stresses distributed over the section,  $M_x$  is the sum of moments about the  $x$ -axis of all shearing stresses acting in section  $mn$ , and so on. It is evident that  $N$  gives rise to tension or compression,  $Q_y$  and  $Q_z$  to shear in the direction of the  $y$ - and the  $z$ -axis, respectively,  $M_x$  to torsion, and  $M_y$  and  $M_z$  to pure uni-planar bending about the  $y$ - and the  $z$ -axis, respectively. Thus, in the most general case of loading of the bar, the latter experiences four simple deformations: tension or compression ( $N$ ), torsion ( $M_x$ ) and uni-planar bending about two axes, ( $M_y$  and  $Q_z$ ) and ( $M_z$  and  $Q_y$ ). Three force factors,  $N$ ,  $M_y$ , and  $M_z$ , give rise to normal stresses in section  $mn$  while the remaining three,  $Q_y$ ,  $Q_z$ , and  $M_x$ , to shearing stresses (Fig. 330 (a) and (c)).

Let us first study the case when only normal stresses appear in the bar section. It can be easily seen that this is a particular case of compound loading—tension or compression with pure bending in two principal inertia planes passing through the centroid.

### § 128. Determination of Normal Stresses

Let us assume that the forces acting on the removed part of the bar can be reduced in section  $mn$  to three components: the normal force  $N$  and two bending moments  $M_y$  and  $M_z$ ; we shall assume all the components to be positive (Fig. 330 (a)). Let us derive a formula for determining normal stress at a point  $A$  located in the first quadrant of section  $mn$  and having coordinates  $y$  and  $z$ .

The positive normal force  $N$  gives rise to the uniformly distributed tensile stress,  $\sigma' = \pm N/S$ , the positive bending moment  $M_y$  gives in the first quadrant tensile stress  $\sigma'' = +M_y z/J_y$ , while the positive bending moment  $M_z$  gives compressive stress  $\sigma''' = -M_z y/J_z$  (see Fig. 330 (b)). Summing up these components of normal stress we get the following expression for calculating the total normal stress at point  $A$ :

$$\sigma = \sigma' + \sigma'' + \sigma''' = \frac{N}{S} + \frac{M_y z}{J_y} - \frac{M_z y}{J_z} \quad (23.1)$$

For calculating the total normal stress at any other point of the bar's cross section, it is sufficient to substitute in formula (23.1) the values of  $N$ ,  $M_y$ , and  $M_z$  and coordinates  $y$  and  $z$  with the proper signs; this gives us the total normal stress with the proper sign.

It is obvious from formula (23.1) that the normal stresses are linear functions of coordinates  $y$  and  $z$ ; they must attain maximum at those points of the section which are farthest from the neutral axis (at the

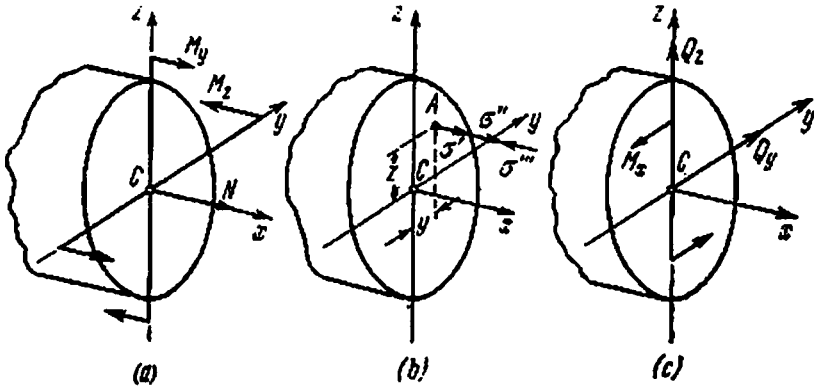


Fig. 330

neutral axis the normal stresses are zero). Figure 331 (a) depicts a section of the bar; in all the quadrants the signs of normal stresses, (1)  $\sigma'$ , (2)  $\sigma''$  and (3)  $\sigma'''$ , are shown in the assumption that  $N$ ,  $M_y$  and  $M_z$  are positive. It is obvious that the neutral axis will intersect the quadrants with normal stresses of different signs and in the given case will not pass through the centre of gravity and the top left quadrant.

Assuming that in formula (23.1) stress  $\sigma$  is equal to zero and denoting the coordinates of a point on the neutral axis by  $y_n$  and  $z_n$ , we get the following equation of the neutral axis:

$$\frac{N}{S} + \frac{M_y}{J_y} z_n - \frac{M_z}{J_z} y_n = 0$$

Equating to zero first  $z_n$  and then  $y_n$ , we find the intercepts cut by the neutral axis on the axes of  $y$  and  $z$ , respectively (Fig. 331 (b)):

$$a_y = \frac{NJ_z}{SM_z} \quad \text{and} \quad a_z = -\frac{NJ_y}{SM_y} \quad (23.2)$$

As the presence or absence of factor  $N/S$  in formula (23.1) does not affect the inclination of the neutral axis with respect to the coordinate axes, the inclination may be determined from the equation

$$\frac{M_y}{J_y} z_n - \frac{M_z}{J_z} y_n = 0$$

wherefrom it ensues that

$$\tan \alpha = \frac{z_n}{y_n} = \frac{J_y}{J_z} \frac{M_z}{M_y} \tag{23.3}$$

By geometrically summing the moments  $M_y$  and  $M_z$  acting in section  $mn$  in planes  $xz$  and  $xy$ , we obtain the resultant bending moment

$$M_b = \sqrt{M_y^2 + M_z^2} \tag{23.4}$$

Angle  $\varphi$  between the plane in which  $M_b$  acts and the vertical plane  $xz$  may be found from the expression

$$\tan \varphi = \frac{M_z}{M_y} \tag{23.5}$$

This expression enables us to write formula (23.3) in the following form:

$$\tan \alpha = \frac{J_y}{J_z} \tan \varphi \tag{23.6}$$

Angles  $\alpha$  and  $\varphi$  will be considered positive if they are laid in the anti-clockwise direction from the corresponding axes ( $\alpha$  from the  $y$ -axis and  $\varphi$  from the  $z$ -axis).

It is clear from (23.3) that in general the neutral axis in the section is not perpendicular to the trail of the resultant bending moment

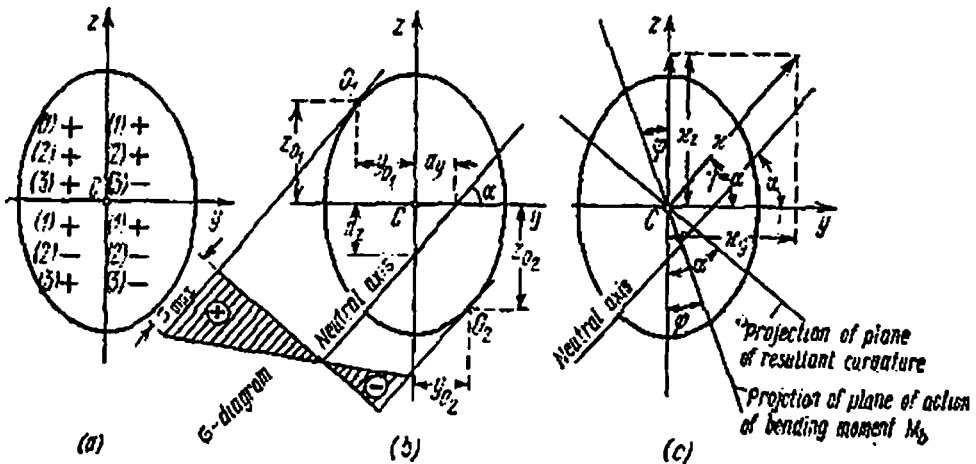


Fig. 331

(Figs. 331 and 332) acting in the same section. The neutral axis will be perpendicular only when angles  $\alpha$  and  $\varphi$  are equal. This, in turn, is possible only under the following conditions: (1)  $\varphi=0$ , i.e.  $M_z=0$ ; (2)  $\varphi=\frac{\pi}{2}$ , i.e.  $M_y=0$ ; and (3)  $J_y=J_z$ . In the first two cases the bar

experiences uni-planar bending in one of the principal planes of inertia irrespective of the magnitude of the principal moments of inertia; in the third case all the axes of inertia are principal central axes of inertia (circle, square, etc.) and therefore bending is uni-planar in all directions. The whole discussion leads to the following general conclusion: bending is uni-planar and the neutral axis is perpendicular to the projection of the plane of action of the resultant bending moment if this plane intersects the section perpendicular to one of the principal central axes of inertia at right angles.

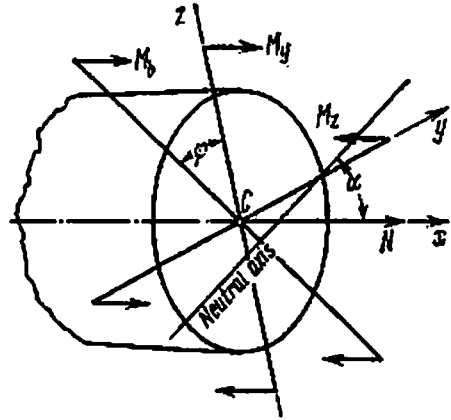


Fig. 332

In general the neutral axis divides the cross section into two zones: a stretched zone and a compressed zone. Drawing lines parallel to the neutral axis and tangent to the contour of the cross section, we find the points  $O_1$  and  $O_2$  of maximum tensile and compressive stresses which lie farthest from the neutral axis (Fig. 331(b)) for both zones. Substituting the coordinates of these points ( $y_{O_1}$  and  $z_{O_1}$ , or  $y_{O_2}$  and  $z_{O_2}$ ) with their proper signs in formula (23.1), we find the maximum tensile and compressive stresses:

$$\sigma_{\max} = \frac{N}{S} + \frac{M_y}{J_y} z_0 - \frac{M_z}{J_z} y_0 \tag{23.7}$$

While solving practical problems it is sometimes more convenient to replace general formula (23.7) by the following formula:

$$\sigma_{\max} = \pm \frac{|N|}{S} \pm \frac{|M_y z_0|}{J_y} \pm \frac{|M_z y_0|}{J_z} \tag{23.8}$$

in which the absolute values of  $N$ ,  $M_y$ ,  $M_z$ ,  $y_0$  and  $z_0$  are substituted, and the signs of the terms are ascertained in each particular case from the actual direction of force factors and location of the points in the section.

### § 129. Determination of Shearing Stresses

Shearing stresses in a bar's section occur due to torsion of the bar about the  $x$ -axis,  $M_x$ , and shear in planes  $xy$  and  $xz$  ( $Q_y$  and  $Q_z$ ); see Fig. 330(c). For a bar of circular or ring section the shearing stresses  $\tau_t$  due to twisting moment  $M_x$  can be calculated by the well-known

formula

$$\tau_t = \frac{M_x \rho}{J_p} \quad (23.9)$$

For a bar of any other cross section the maximum shearing stresses may be determined by the formula

$$\max \tau_t = \frac{M_x}{W_t} \quad (23.10)$$

using the data for  $W_t$  given in the section on twisting of bars of non-circular section. In all the cases the maximum shearing stresses (torsion) occur at the contour of the section and act along the tangent to it.

The shearing stresses due to forces  $Q_y$  and  $Q_z$  are, as a rule, of secondary importance; they are determined by Zhuravskii's formula

$$\tau_y = \frac{Q_y S_z^0}{J_z b(y)} \quad \text{and} \quad \tau_z = \frac{Q_z S_y^0}{J_y b(z)} \quad (23.11)$$

In rectangular and round sections these shearing stresses attain their maximum on the corresponding principal axes of inertia:  $\tau_y$  on the  $z$ -axis and  $\tau_z$  on the  $y$ -axis. At those points of the contour where the direction of maximum shearing stresses due to shearing forces ( $\max \tau_y$  or  $\max \tau_z$ ) coincides with the direction of maximum shearing stress due to torsion, the two are arithmetically summed up and the maximum total stress is used for strength analysis:

$$\tau_{\max} = \max \tau_t + \max \tau_y, \quad \text{or} \quad \tau_{\max} = \max \tau_t + \max \tau_z$$

Since the normal stresses due to bending and the total shearing stresses due to shear and torsion are both maximum at the contour of the section, it is logical to search for the maximally stressed points and also to check the strength of the bar's material on the contour. The points experiencing maximum shearing stresses do not always coincide with the points subjected to maximum normal stresses. In such cases the strength of the bar's material should be checked at those points on the contour where the combined effect of normal and shearing stresses is most unfavourable.

### § 130. Determination of Displacements

If we recall that in the general case of compound loading the bar experiences, besides other types of elementary deformations, two planar bendings in the principal planes of inertia, it becomes clear that in general the deflected axis of the bar must be represented by a curve in space. The curvature of the axis in plane  $xy$  is

$$\kappa_z = \frac{1}{\rho_{xy}} = \frac{M_x}{EJ_z} \quad (23.12)$$

and in plane  $xz$  it is

$$\kappa_y = \frac{1}{\rho_{xz}} = -\frac{M_y}{EJ_y} \quad (23.13)$$

If the curvature vectors,  $\kappa_z$  and  $\kappa_y$ , are laid on the corresponding coordinate axes, vector  $\kappa$  of the total curvature of the deflected axis, which represents the geometrical sum

$$\kappa = \sqrt{\kappa_y^2 + \kappa_z^2} \quad (23.14)$$

makes an angle  $\gamma$  with the  $z$ -axis, and the tangent of this angle (see Fig. 331(c)) is found from the formula

$$\tan \gamma = \frac{\kappa_z}{\kappa_y} = -\frac{M_z J_y}{M_y J_z} \quad (23.15)$$

A comparison of formuläs (23.15) and (23.3) assures us that angles  $\alpha$  and  $\gamma$  are equal, i.e. the total curvature vector is parallel to the neutral axis, and if there is no normal force the two coincide. Hence, the resultant curvature plane, which is perpendicular to the total curvature vector and tangent to the deflected axis of the bar in the given section, is always perpendicular to the neutral axis. The centre of gravity of the given section gets displaced perpendicular to the neutral axis only when the bar is subjected to bending in one plane (when  $\varphi = \text{const}$  and  $\alpha = \text{const}$  along the whole length of the bar, for instance, in uni-planar and unsymmetric bending).

If  $J_y > J_z$ , as in the example depicted in Fig. 331, then according to (23.3)  $\tan \alpha > \tan \varphi$  and  $\alpha > \varphi$ , i.e. the centre of gravity gets displaced in a direction which is inclined to the plane of action of bending moment  $M_b$  and tends towards the  $y$ -axis. It can be easily noticed that the centre of gravity always deflects from the plane of the resultant bending moment towards the axis about which the moment of inertia is maximum.

It follows from the above that the deflected axis of the bar can be represented by a curve in a plane only if the total curvature vector makes a constant angle  $\gamma = \alpha$  with the  $y$ -axis along the whole length of the bar; i.e. (see (23.15)) if the product  $\frac{J_y}{J_z} \frac{M_z}{M_y}$  is independent from the  $x$ -coordinate. The last may occur, for instance, when a bar of uniform section is loaded by forces that act in a single plane.

Applying the principle of superposition of forces, we can use the differential equations obtained from (23.12) and (23.13) for finding the total displacement of the centre of gravity of an arbitrary section. After integrating and finding the constants of integration from the boundary conditions and then determining for the given section two displacement components  $f_y$  and  $f_z$  in the direction of the principal axes of inertia  $y$  and  $z$ , we can determine the total displacement as



the geometric sum:

$$f = \sqrt{f_y^2 + f_z^2} \quad (23.16)$$

Besides the analytical method, the displacement can also be found by the graph-analytic method and Castigliano's theorem, which is particularly useful when dealing with crank rods (see below). When Castigliano's theorem is employed for determining displacements under compound loading, the potential energy of deformation,  $U$ , must be expressed as a function of all the six force components:  $N$ ,  $Q_y$ ,  $Q_z$ ,  $M_x$ ,  $M_y$ , and  $M_z$ . Neglecting the energy of shearing stress due to shearing forces, we may write

$$U = U(N) + U(M_x) + U(M_y) + U(M_z)$$

Assuming that in general normal force  $N$  and twisting moment  $M_x$  do not remain constant over the whole length of the bar, we can write the following expressions for the energy stored in an element of length  $dx$ :

$$dU(N) = \frac{N^2 dx}{2EA} \quad \text{and} \quad dU(M_x) = \frac{M_x^2 dx}{2GJ_t}$$

and the following expressions for the energy stored in a segment of length  $l$  of the bar:

$$U(N) = \int \frac{N^2 dx}{2EA} \quad \text{and} \quad U(M_x) = \int \frac{M_x^2 dx}{2GJ_t}$$

We have the following expressions for the energy due to normal stresses in uni-planar bending (see § 100):

$$U(M_y) = \int \frac{M_y^2 dx}{2EJ_y} \quad \text{and} \quad U(M_z) = \int \frac{M_z^2 dx}{2EJ_z}$$

Keeping the above expressions in mind, we can write the formula for  $U$  as follows:

$$U = \int \left( \frac{N^2}{2EA} + \frac{M_x^2}{2GJ_t} + \frac{M_y^2}{2EJ_y} + \frac{M_z^2}{2EJ_z} \right) dx \quad (23.17)$$

where subscript  $l$  shows that the expression is integrated over a length  $l$  of the bar for which the functions of the  $x$ -coordinate, i.e.  $N$ ,  $M_x$ ,  $M_y$ , and  $M_z$ , are continuous. If the bar contains a number of such segments, then separate integrals should be calculated for each of them and then summed up.

Applying Castigliano's theorem, we can find the displacement in the direction of any of the forces  $P$  from the following expression:

$$\delta = \frac{\partial U}{\partial P} = \sum_{i=1}^n \int_{l_i} \left( \frac{N}{EA} \frac{\partial N}{\partial P} + \frac{M_x}{GJ_t} \frac{\partial M_x}{\partial P} + \frac{M_y}{EJ_y} \frac{\partial M_y}{\partial P} + \frac{M_z}{EJ_z} \frac{\partial M_z}{\partial P} \right) dx \quad (23.18)$$

By  $P$  and  $\delta$  we denote here a general force and the displacement corresponding to it. The formulas used in the methods of Mohr and Vereshchagin can be derived in a similar manner.

§ 131. Design of a Simple Crank Rod

Crank rods are often used in engineering practice as parts of crank gear and other mechanisms, crankshafts, etc. The design of crank rods is a little more difficult than that of straight rods. As an example, we shall explain how to design the crank rod shown in Fig. 333. The rod consists of two parts: a vertical part (of rectangular section) and a horizontal part (of circular section), rigidly connected at right angles to each other. The following loads are applied to the crank rod. In section  $A$ :  $P_1=1200$  kgf,  $P_2=1000$  kgf,  $P_3=400$  kgf and a moment  $M_0=800$  kgf·m; in section  $B$ :  $P_4=6000$  kgf and  $P_5=300$  kgf. The first part is  $l_1=120$  cm long, the second  $l_2=80$  cm,  $b=8$  cm,  $h=15$  cm. The rod is made of carbon steel:  $E=2 \times 10^6$  kgf/cm<sup>2</sup>,  $G=8 \times 10^5$  kgf/cm<sup>2</sup> and  $[\sigma]=800$  kgf/cm<sup>2</sup>. It is required to check the strength of the rod in the first part, determine the diameter of the second part, the total displacement of centre of gravity of section  $A$ , and the angle of rotation of this section about the longitudinal axis of the first part.

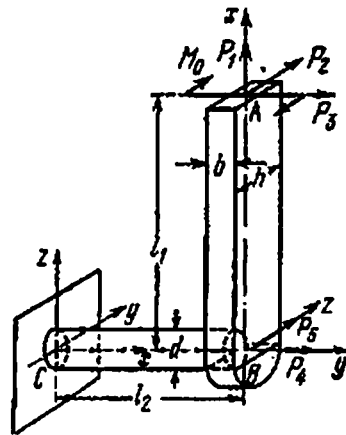


Fig. 333

The analysis starts by plotting diagrams that show the variation of all force factors on each part of the crank rod. Each may be assigned its own system of rectangular coordinates, choosing the axes in such a way that force  $N$  is always a normal force,  $M_x$  a twisting moment, and  $M_y$  and  $M_z$  bending moments. In Fig. 334 such diagrams for the first part are shown to the right of the crank rod (Fig. 334(a)), and for the second part below the crank rod. On these diagrams the values of force factors at the beginning and end of each part are written in arithmetic form. After plotting the diagrams for all the parts we are in a position to locate the critical sections, in which the combined effect of all the force factors is most unfavourable. In our example the critical sections are: horizontal section 1-1 in the first part and vertical section 2-2 in the second part, both in the vicinity of section  $B$  (see Fig. 334(a)). These sections and the forces acting on them are shown in Fig. 334(b) and (c).

Let us check the strength of the rod in section 1-1. The forces acting on this section may be reduced to the force  $N = P_1 = 1200$  kgf, twisting moment  $M_x = M_0 = -80\,000$  kgf·cm, and two bending moments:

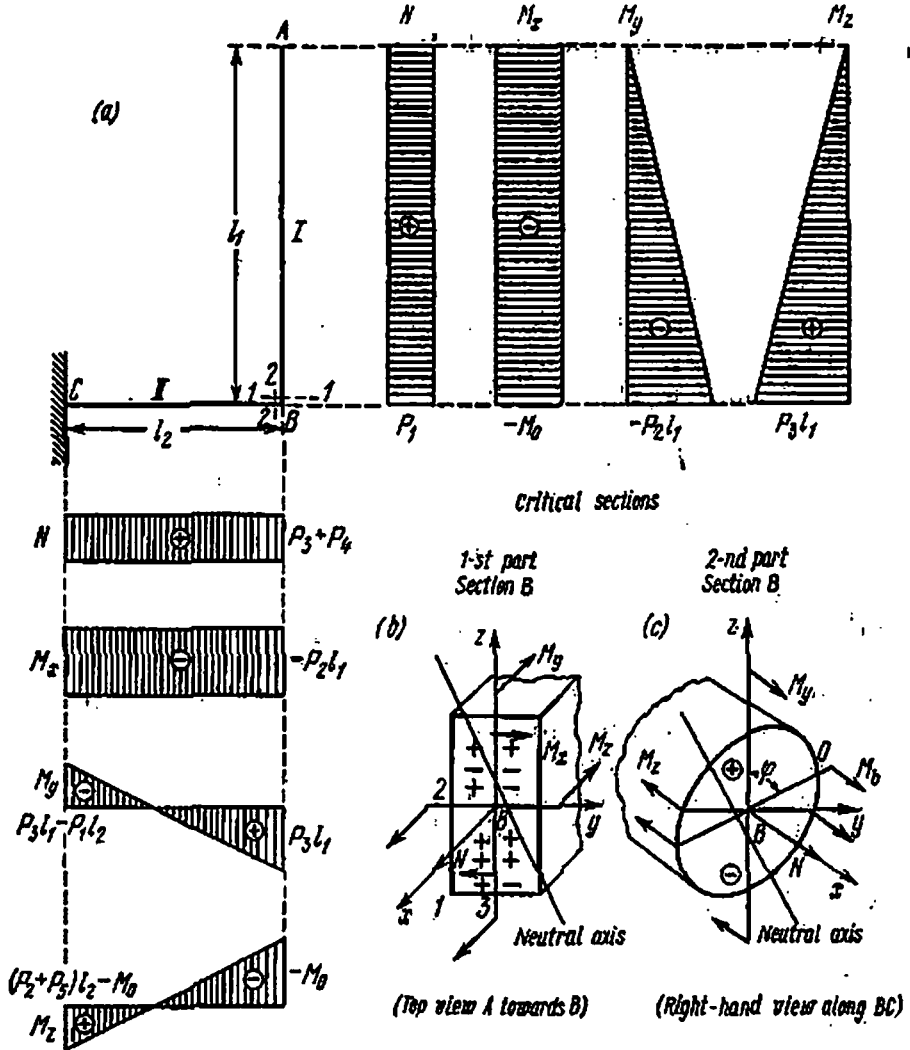


Fig. 334

$M_y = -P_2 l_1 = -1000 \times 120 = -120\,000$  kgf·cm and  $M_z = P_3 l_1 = 400 \times 120 = 48\,000$  kgf·cm. Normal stresses at any point of this section may be calculated by the formula (see (23.1))

$$\sigma = \frac{N}{S} + \frac{M_y z}{J_y} - \frac{M_z y}{J_z} = \frac{1200}{120} - \frac{120\,000}{2250} z - \frac{48\,000}{640} y = 10 - \frac{160}{3} z - 75y$$

since  $S = bh = 8 \times 15 = 120$  cm<sup>2</sup>,  $J_y = bh^3/12 = 8 \times 15^3/12 = 2250$  cm<sup>4</sup>, and  $J_z = hb^3/12 = 15 \times 8^3/12 = 640$  cm<sup>4</sup>. The neutral axis cuts the following

intercepts on the  $y$ - and the  $z$ -axis:

$$a_y = \frac{NJ_z}{SM_z} = \frac{1200 \times 640}{120 \times 48000} = \frac{2}{15} = 0.133 \text{ cm}$$

$$a_z = -\frac{NJ_y}{SM_y} = \frac{1200 \times 2250}{120 \times 120000} = \frac{3}{16} = 0.1875 \text{ cm}$$

Maximum normal stresses occur at point 1 which is farthest from the neutral axis and has coordinates  $y_1 = -4$  cm and  $z_1 = -7.5$  cm (this is a case of uniaxial stressed state):

$$\begin{aligned} \sigma_{\max} = \sigma_{(1)} &= 10 + \frac{160}{3} \times 7.5 + 75 \times 4 = 710 \text{ kgf/cm}^2 < [\sigma] \\ &= 800 \text{ kgf/cm}^2 \end{aligned}$$

Hence, the rod's material at point 1 is sufficiently strong. We must now check the strength of the rod's material at points 2 and 3, which experience torsional shearing stresses in addition to the normal stresses. The normal stresses at these points are

$$\sigma_{(2)} = \frac{N}{S} - \frac{M_z}{J_z} y_2 = 10 + 75 \times 4 = 310 \text{ kgf/cm}^2$$

$$\sigma_{(3)} = \frac{N}{S} + \frac{M_y}{J_y} z_3 = 10 + \frac{160}{3} \times 7.5 = 410 \text{ kgf/cm}^2$$

To find the shearing stresses we determine  $J_t = \alpha b^4$  and  $W_t = \beta b^3$ . From the ratio  $n = h/b = \frac{15}{8} = 1.875$  we find from Table 9 (§ 54) by linear interpolation the coefficients  $\alpha = 0.416$ ,  $\beta = 0.406$ , and  $\gamma = 0.808$ . Hence  $J_t = 0.416 \times 8^4 = 2506 \text{ cm}^4$  and  $W_t = 0.406 \times 8^3 = 233 \text{ cm}^3$ . At point 2

$$\tau_{(2)} = \tau_{\max} = \frac{M_x}{W_t} = \frac{80000}{233} = 343 \text{ kgf/cm}^2$$

and at point 3

$$\tau_{(3)} = \gamma \tau_{\max} = 0.808 \times 343 = 277 \text{ kgf/cm}^2$$

We will check the strength of the rod at these points by the third strength theory:

$$\begin{aligned} \sigma_{\text{des}(2)}^{\text{III}} &= \sqrt{\sigma_{(2)}^2 + 4\tau_{(2)}^2} = \sqrt{310^2 + 4 \times 343^2} \\ &= 753 \text{ kgf/cm}^2 < 800 \text{ kgf/cm}^2 \end{aligned}$$

$$\begin{aligned} \sigma_{\text{des}(3)}^{\text{III}} &= \sqrt{\sigma_{(3)}^2 + 4\tau_{(3)}^2} = \sqrt{410^2 + 4 \times 277^2} \\ &= 689 \text{ kgf/cm}^2 < 800 \text{ kgf/cm}^2 \end{aligned}$$

Hence, at these points too the rod is sufficiently strong.

Let us now undertake the analysis of the second part. In critical section 2-2 the force factors are

$$\begin{aligned} N &= P_3 + P_4 = 400 + 6000 = 6400 \text{ kgf} \\ M_x &= -P_2 l_1 = -1000 \times 120 = -120\,000 \text{ kgf} \cdot \text{cm} \\ M_y &= P_3 l_1 = 400 \times 120 = 48\,000 \text{ kgf} \cdot \text{cm} \\ M_z &= -M_0 = -80\,000 \text{ kgf} \cdot \text{cm} \end{aligned}$$

As the section is a circle and has equal moments of inertia for bending about the two principal axes of inertia, i.e.

$$J_y = J_z = J_b = \frac{\pi r^4}{4} \quad \text{and} \quad J_t = J_p = \frac{\pi r^4}{2} = 2J_b$$

bending moments  $M_y$  and  $M_z$  can be geometrically summed up into the resultant bending moment

$$M_b = \sqrt{M_y^2 + M_z^2} = \sqrt{48\,000^2 + 80\,000^2} = 93\,280 \text{ kgf} \cdot \text{cm}$$

The projection of the plane of action of the resultant bending moment passes through the centre of gravity making an angle  $\varphi$  with the  $z$ -axis such that

$$\tan \varphi = \frac{M_z}{M_y} = \frac{80\,000}{48\,000} = \frac{5}{3} \quad \text{and} \quad \varphi = 59^\circ 2'$$

The critical point of the section is point  $O$ , which lies at the intersection of the projection of the  $M_b$ -plane with the contour. At this point the normal stress is

$$\sigma_{(O)} = \sigma_{\max} = \frac{N}{S} + \frac{M_b}{W_b} = \frac{N}{\pi r^2} + \frac{4M_b}{\pi r^3} = \frac{6400}{3.14r^2} + \frac{4 \times 93\,280}{3.14r^3} = \frac{2037}{r^2} + \frac{118\,770}{r^3}$$

and the shearing stress is

$$\tau_{(O)} = \tau_{\max} = \frac{M_x}{W_p} = \frac{2M_x}{\pi r^3} = \frac{2 \times 120\,000}{3.14r^3} = \frac{76\,300}{r^3}$$

To determine the radius of the section for this part of the crank rod we shall again use the third strength theory:

$$\begin{aligned} \sigma_{\text{des}}^{\text{III}}(O) &= \sqrt{\sigma_{(O)}^2 + 4\tau_{(O)}^2} \\ &= \sqrt{\left(\frac{2037}{r^2} + \frac{118\,770}{r^3}\right)^2 + 4\left(\frac{76\,300}{r^3}\right)^2} \\ &\leq [\sigma] = 800 \text{ kgf/cm}^2 \end{aligned}$$

Taking the square of both sides of this equation and multiplying the result by  $r^6$ , we obtain

$$2037^2 r^2 + 2 \times 2037 \times 118\,770 r + 118\,770^2 + 152\,600^2 \leq 64 \times 10^6 r^6$$

or

$$\Phi = r^6 - 6.485r^3 - 756.1r - 58516 \geq 0 \tag{*}$$

While solving equation  $\Phi=0$  by trial and error we neglect the factors containing  $r^2$  and  $r$  in the first approximation (i.e. we neglect the relatively small normal stress  $N/S$ ). This gives

$$r \geq \sqrt[6]{58516} = 6.24 \text{ cm}$$

If we substitute a slightly larger value of  $r=6.3$  cm in the equation  $\Phi=0$ , we get

$$\begin{aligned} \Phi &= 6.3^6 - 6.485 \times 6.3^3 - 756.1 \times 6.3 - 58516 \\ &= -1013 \text{ kgf} \cdot \text{cm}^6 \end{aligned}$$

We thus see that the selected value of  $r$  is not sufficient for satisfying the inequality (\*); let us try  $r=6.4$  cm. In this case  $\Phi = +5099$  kgf  $\times$   $\text{cm}^6$ . By interpolation we find that  $r=6.32$  cm. This corresponds to

$$\begin{aligned} S &= \pi r^2 = 3.14 \times 6.32^2 = 125.5 \text{ cm}^2 \\ J_b &= \frac{\pi r^4}{4} = \frac{3.14 \times 6.32^4}{4} = 1253 \text{ cm}^4 \\ J_t &= J_p = 2J_b = 2 \times 1253 = 2506 \text{ cm}^4 \end{aligned}$$

We shall apply Castigliano's theorem to calculate the displacements. In Table 16 force factors  $N$ ,  $M_x$ ,  $M_y$ , and  $M_z$  and their derivatives  $P_1$ ,  $P_2$ ,  $P_3$ , and  $M_0$  are expressed for each of the crank rod parts as func-

Table 16

Force Factors and Their Derivatives

First part ( $0 < x < l_1$ )				
Force factors	$N$	$M_x$	$M_y$	$M_z$
Formulas for them	$P_1$	$-M_0$	$-P_2x$	$P_3x$
$\partial/\partial P_1$	1			
$\partial/\partial P_2$			$-x$	
$\partial/\partial P_3$				$x$
$\partial/\partial M_0$		$-1$		
Second part ( $0 < x < l_2$ )				
Formulas for force factors	$P_3 + P_4$	$-P_2l_1$	$Pl_1 - P_1x$	$P_2x + P_6x - M_0$
$\partial/\partial P_1$			$-x$	
$\partial/\partial P_2$		$-l_1$		$x$
$\partial/\partial P_3$	1		$l_1$	
$\partial/\partial M_0$				$-1$

tions of  $x$ . Using the data of the table, we easily find that

$$\begin{aligned} f_1 &= \frac{\partial U}{\partial P_1} = \int_0^{l_1} \frac{N_1}{ES_1} \frac{\partial N_1}{\partial P_1} dx + \int_0^{l_2} \frac{M_{y2}}{EJ_{y2}} \frac{\partial M_{y2}}{\partial P_1} dx \\ &= \int_0^{l_1} \frac{P_1 \times 1}{ES_1} dx + \int_0^{l_2} \frac{(P_3 l_1 - P_1 x)(-x)}{EJ_{y2}} dx \\ &= \frac{1}{2 \times 10^8} \left( \int_0^{120} \frac{1200}{120} dx + \int_0^{80} \frac{1200x^2 - 48\,000x}{1253} dx \right) \\ &= \frac{42\,060}{2 \times 10^8} = 0.21 \text{ cm} \end{aligned}$$

$$\begin{aligned} f_2 &= \frac{\partial U}{\partial P_2} = \int_0^{l_1} \frac{M_{y1}}{EJ_{y1}} \frac{\partial M_{y1}}{\partial P_2} dx + \int_0^{l_2} \frac{M_{x2}}{GJ_{t2}} \frac{\partial M_{x2}}{\partial P_2} dx + \int_0^{l_2} \frac{M_{z2}}{EJ_{z2}} \frac{\partial M_{z2}}{\partial P_2} dx \\ &= \frac{1}{E} \left( \int_0^{l_1} \frac{-P_2 x(-x)}{J_{y1}} dx + \int_0^{l_2} \frac{-P_2 l_1(-l_1)}{0.4J_{t2}} dx + \int_0^{l_2} \frac{(P_2 + P_3)x - M_0}{J_{z2}} x dx \right) \\ &= \frac{1}{2 \times 10^8} \left( \int_0^{120} \frac{1000x^2}{2250} dx + \int_0^{80} \frac{1000 \times 120 \times 120}{0.4 \times 2506} dx + \int_0^{80} \frac{(1300x^2 - 80\,000x) dx}{1253} \right) \\ &= \frac{1\,278}{2} = 0.639 \text{ cm} \end{aligned}$$

$$\begin{aligned} f_3 &= \frac{\partial U}{\partial P_3} = \int_0^{l_1} \frac{M_{z1}}{EJ_{z1}} \frac{\partial M_{z1}}{\partial P_3} dx + \int_0^{l_2} \frac{N_2}{ES_2} \frac{\partial N_2}{\partial P_3} dx + \int_0^{l_2} \frac{M_{y2}}{EJ_{y2}} \frac{\partial M_{y2}}{\partial P_3} dx \\ &= \frac{1}{E} \left( \int_0^{l_1} \frac{P_3 x^2}{J_{z1}} dx + \int_0^{l_2} \frac{P_3 + P_4}{S_2} dx + \int_0^{l_2} \frac{P_3 l_1 - P_1 x}{J_{y2}} l_1 dx \right) \\ &= \frac{1}{2 \times 10^8} \left( \int_0^{120} \frac{400x^2}{640} dx + \int_0^{80} \frac{6400}{125.5} dx + \int_0^{80} \frac{(120\,000 - 1200x) 120 dx}{1253} \right) \\ &= \frac{0.9167}{2} = 0.408 \text{ cm} \end{aligned}$$

$$\begin{aligned} \varphi &= \frac{\partial U}{\partial M_0} = \int_0^{l_1} \frac{M_{x1}}{GJ_{t1}} \frac{\partial M_{x1}}{\partial M_0} dx + \int_0^{l_2} \frac{M_{z2}}{EJ_{z2}} \frac{\partial M_{z2}}{\partial M_0} dx \\ &= \frac{1}{E} \left( \int_0^{l_1} \frac{M_0}{0.4J_{t1}} dx + \int_0^{l_2} \frac{[(P_2 + P_3)x - M_0](-1)}{J_{z2}} dx \right) \end{aligned}$$

$$\begin{aligned}
 &= \frac{1}{2 \times 10^6} \left( \int_0^{120} \frac{80\,000 \, dx}{0.4 \times 1704} + \int_0^{80} \frac{(1300x - 80\,000)(-1)}{1253} \, dx \right) \\
 &= \frac{15\,870}{2 \times 10^6} = 0.00794 = 0.455^\circ
 \end{aligned}$$

The total displacement is

$$\begin{aligned}
 f &= \sqrt{f_1^2 + f_2^2 + f_3^2} = \sqrt{0.21^2 + 0.639^2 + 0.408^2} \\
 &= 0.787 \text{ cm}
 \end{aligned}$$

## CHAPTER 24

### Curved Bars

#### § 132. General Concepts

Besides straight-axis bars in structures we often come across bars in which the axis, i.e. the line passing through the centres of gravity of successive cross sections, is a curved line. Chain links, lugs, hooks, arches, vaults, hoisting crane frames, etc., all belong to this group of elements (Fig. 335). Strictly speaking, no bar has an absolutely straight axis. All bars, which we design as straight bars, have a slight curvature. Therefore, a study of the effect of curvature of the bar's axis on the distribution of stresses will, on the one hand, enable us to check the strength of bars having appreciable curvature and, on the other hand, judge the influence of a slight deviation of the axis from a straight line on the strength of a straight bar.

We introduce the following restrictions for checking the strength of curved bars:

(a) sections of the bar have an axis of symmetry;

(b) the axis of the bar is a flat curve which lies in the plane of symmetry;

(c) all external forces also lie in the same plane.

On account of symmetry, deformation of the bar will also occur in the same plane, the bar's axis will remain a flat curve lying in the plane of external forces and the picture will be identical to that of uni-planar bending of beams.

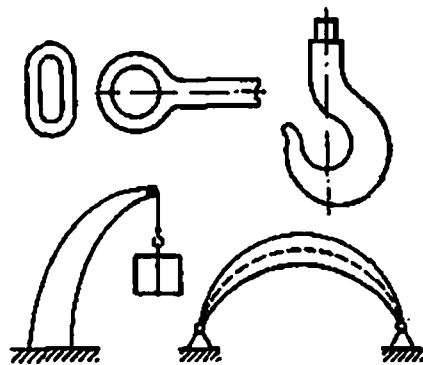


Fig. 335



By writing the above restrictions we cover almost all situations of the working of curved bars. Our task is to find the maximum stresses, check the strength and determine the deformation of curved bars.

The solution will be similar to the case of bending of straight beams.

### § 133. Determination of Bending Moments and Normal and Shearing Forces

Imagine a curved bar (Fig. 336) loaded by external forces  $P_1, P_2, P_3,$  and  $P_4$  acting in the plane of symmetry of the cross sections. The support reactions, not shown in the figure, lie in the same plane.

To determine the stresses in sections perpendicular to the bar's axis we draw a section  $mn$  which divides the bar into two parts, *I* and *II*.

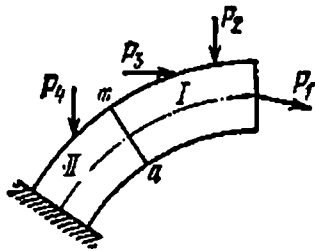


Fig. 336

Let us remove part *I* and consider the equilibrium of part *II* (Fig. 337(a)). Part *II* is acted upon by force  $P_4$ , the reactions at the fixed end (not shown in the figure) and stresses in section  $mn$  which appear because of the action of the removed part on the part under consideration. What are the stresses in section  $mn$ ?

The section will experience normal as well as shearing stresses (not shown in Fig. 337(a)). With the restrictions of § 132 the normal stresses will give the following resultants: the bending moment  $M$  and the normal force  $N$ . The shearing stresses in the section will yield a resultant shearing force  $Q$ . These three forces are shown in Fig. 337(a).

Let us now consider part *I* of the curved bar (Fig. 337(b)). All external forces acting on this part of the curved bar may be reduced in general to a resultant force  $R$  and a moment  $M_y$ . Resultant  $R$  may be resolved into two components,  $R_x$  and  $R_z$ . These three resultants are depicted in Fig. 337(c). They also represent the action of part *I* of the curved bar on part *II*.

A comparison of Figs. 337(a) and 337(c) immediately reveals that bending moment  $M$  in section  $mn$  will be equal to  $M_y$ , normal force  $N$  will be equal to  $R_x$  and shearing force  $Q$  to  $R_z$ .

The internal forces in curved bars—the bending moment, normal force and shearing force—can be calculated as in the bending of straight bars through external forces acting on one side of the cross section. Their computation amounts to solving the equations of statics.

The internal forces in curved bars—the bending moment, normal force and shearing force—can be calculated as in the bending of straight bars through external forces acting on one side of the cross section. Their computation amounts to solving the equations of statics.

The bending moment is equal to the algebraic sum of the moments of all the forces located on one side of the section about the centre of gravity of the section.

The normal force is equal to the algebraic sum of the projections of all the forces located on one side of the section on the tangent to the bar's axis drawn through the given section.

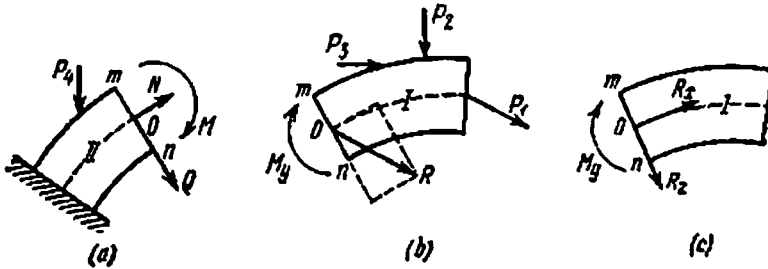


Fig. 337

The shearing force is equal to the algebraic sum of the projections of all forces located to one side of the section on the vertical axis of the section.

The bending moment will be considered positive if it increases the curvature of the bar. The normal force will be considered positive if it tends to detach the portion under consideration from the removed

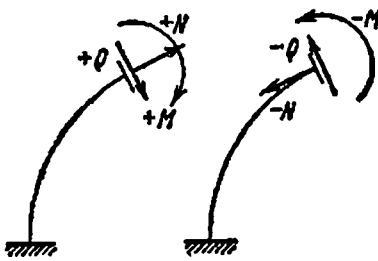


Fig. 338

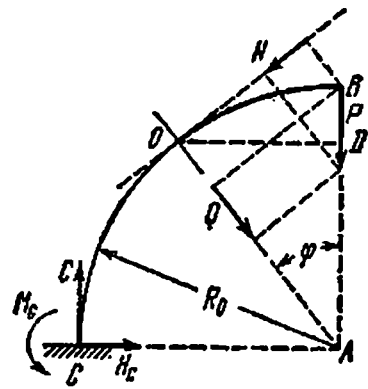


Fig. 339

portion. The shearing force will be considered positive if it is obtained by rotating the positive direction of the normal force through 90° clockwise (Fig. 338).

As in a beam, while determining  $M$ ,  $N$ , and  $Q$  we may consider the equilibrium of either the left or the right portion of the bar, into which it is divided by the particular section; the selection is arbitrary and depends upon the convenience of computations.

The sign conventions decided above for the bending moment, normal force and shearing force are independent of whether the left or the right portion is considered.

Let us study an example for determining  $M$ ,  $N$ , and  $Q$ . Consider a bar representing one quadrant of a circle of radius  $R_0$ , fixed rigidly at one end and loaded at the other by a force  $P$  (Fig. 339). Draw an arbitrary plane with the centre of gravity at  $O$ . Location of the plane is de-

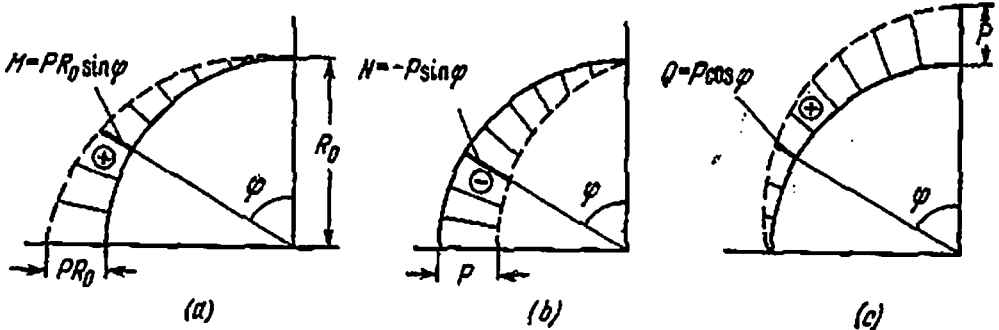


Fig. 440

termined by angle  $\varphi$  which it makes with the vertical. We consider the right portion of the bar to determine  $M$ ,  $N$ , and  $Q$ . This spares us the trouble of determining the reactions in section  $C$ .

The bending moment is equal to the moment of force  $P$  about point  $O$ :

$$M = + P \times \overline{OD} = + PR_0 \sin \varphi \quad (24.1)$$

Projecting force  $P$  on the normal to the section and on the plane of the section itself, we obtain

$$N = -P \sin \varphi, \quad Q = + P \cos \varphi \quad (24.2)$$

Hence the maximum bending moment and normal force occur at  $\varphi=90^\circ$ , i.e. at the fixed end. Figure 340 shows the  $M$ -,  $N$ -, and  $Q$ -diagrams. The axis of the bar has been taken as the zero line. Ordinates have been cut along the radii of curvature of the bar.

### § 134. Determination of Stresses Due to Normal and Shearing Forces

The shearing stresses acting in a section of the curved bar add up to form the shearing force,  $Q$ . We can derive precise formulas for calculating shearing stresses in curved bars using the same approach that was employed in calculating shearing stresses in straight beams. However, theoretical investigations reveal that the distribution of shearing stresses in curved bars closely resembles their distribution in straight beams. It is therefore permissible to calculate shearing stresses in

curved bars by Zhuravskii's formula, which was derived for straight beams:

$$\tau \approx \frac{QS_y^0}{J_y b} \quad (13.3)$$

The strength condition for shearing stresses in curved bars may consequently be written as

$$\tau_{\max} = \frac{Q_{\max} S_{\max}}{J_y b} \leq [\tau] \quad (13.7)$$

Let us now determine the normal stresses due to the two resultant internal forces: bending moment  $M$  and normal force  $N$ . Let us first consider the normal force.

Considering an element of length  $ds$  of the curved bar which is acted upon by forces  $N$  (Fig. 341), we notice that these forces acting at the

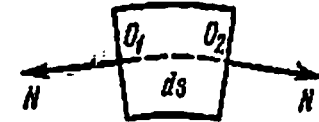


Fig. 341

centres of gravity of the sections result in simple axial tension or compression of the element under consideration. Therefore, the corresponding stresses must be normal to the sections and uniformly distributed over the cross-sectional area,  $A$ :

$$\sigma = \frac{N}{A} \quad (24.3)$$

The sign of the stress is determined by the sign of force  $N$ .

### § 135. Determination of Stresses Due to Bending Moment

The task of finding the law of distribution of normal stresses due to the bending moment over the section and deriving appropriate formulas for computing them is statically indeterminate and, as in straight beams, requires that besides writing and solving the static equations we must consider the corresponding deformations and write down additional equations. While determining stresses due to  $Q$  and  $N$  we could manage without similar computations, because we made use of known solutions; to determine the normal stresses due to the bending moment  $M$  we propose to carry out all the computations, which, incidentally, we have already given while deriving the formula for normal stresses in straight beams.

Under the action of external moment  $M$  the curved bar  $AB$  (Fig. 342) experiences pure bending over its whole length.

Figure 343 depicts the part  $DC$  of the bar which is acted upon by internal forces transmitted from the removed parts  $AD$  and  $CB$ . Bending moment  $M$  is shown on the left and the elementary normal force  $\sigma dA$  on the right.

The location of the neutral layer along the height of the section is not known and has to be determined; we shall assume that it does not pass through the centres of gravity of the sections. Let the origin of

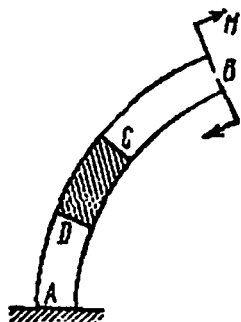


Fig. 342

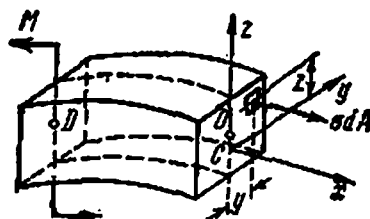


Fig. 343

coordinates be located at point  $C$ , which lies on the neutral axis,  $y$ , but does not coincide with the centre of gravity  $O$ ; moreover, distance  $OC$  is as yet to be determined. The  $z$ -axis is the axis of symmetry, and the  $x$ -axis is perpendicular to the plane of the section. Bending moment  $M$  lies in the plane of symmetry  $x Cz$ , and each elementary area  $dA$  with coordinates  $y$  and  $z$  is acted upon by a force  $\sigma dA$ . We can write six equations of equilibrium for the portion, which retains its equilibrium under the influence of  $M$  and  $\sigma dA$ .

The projection of the external forces on the  $x$ -axis is zero; the sum of projections of forces  $\sigma dA$  may be represented by an integral over the whole cross-sectional area:

$$\sum X = 0, \quad \int_A \sigma dA = 0 \quad (24.4)$$

Equations that represent the projections of all the forces on the  $y$ - and the  $z$ -axis,

$$\sum Y = 0 \quad \text{and} \quad \sum Z = 0$$

become identities, because the  $\sigma$ 's are perpendicular to the  $y$ - and the  $z$ -axis. We similarly get an identity from the equation of moments about the  $x$ -axis:

$$\sum M_x = 0$$

because neither force  $\sigma dA$ , which is parallel to the  $x$ -axis, nor bending moment  $M$ , which lies in plane  $x Cz$ , give a moment about the  $x$ -axis.

By similar logic the moment  $M$  about the  $z$ -axis must also be zero; as for elementary forces  $\sigma dA$ , their moment about the above axis is given by the integral  $\int_A \sigma dA y$ .

The fifth equation of equilibrium will therefore be

$$\sum M_z = 0, \quad \int_A \sigma dA y = 0 \tag{24.5}$$

The last integral is zero on account of the symmetry of the section about the  $z$ -axis.

Now we equate to zero the sum of moments of all the external forces about the  $y$ -axis. The equation may be written thus:

$$\sum M_y = 0, \quad M - \int_A \sigma dA z = 0 \tag{24.6}$$

Hence we get the following two equations by considering the static equilibrium of the portion:

$$\int_A \sigma dA = 0 \tag{24.4}$$

$$M - \int_A \sigma dA z = 0 \tag{24.6}$$

We still do not know the law of distribution of normal stresses over the height of the section. For this reason let us first study the deformation of the bar.

As in uni-planar bending of straight bars, we shall make use of the hypothesis of plane sections, which has been experimentally found

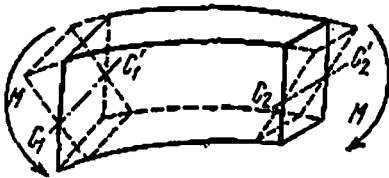


Fig. 344

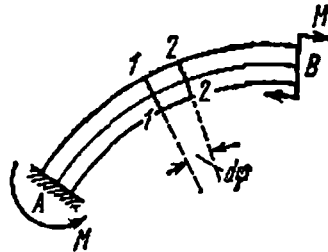


Fig. 345

applicable for curved bars also. We shall assume that, under the influence of bending moment, sections perpendicular to the axis of the bar remain flat and simply turn w.r.t. one another (Fig. 344). The fibres of the neutral layer  $C_1C_2-C'_1C'_2$  retain their original length, and fibres located at equal distances from the neutral axis elongate and

shorten by an equal amount and hence experience equal stresses over the width of the section. Let us establish a relation between the relative angle of rotation and deformation of fibres for two adjacent sections. Let us cut from the curved bar which is being acted upon by only a bending moment (Fig. 345) an element by two close sections making an angle  $d\varphi$  with one another. This element is depicted in Fig. 346:  $O_1-O_2$  is the axis of the bar, and  $C_1-C_2$  is its neutral layer.

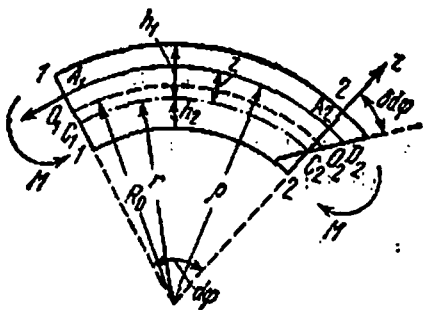


Fig. 346

The normal stresses acting in the cut planes form couples; due to these force couples the angle between adjacent sections 1-1 and 2-2 changes by  $\delta d\varphi$  on account of relative rotation of these sections.

Let us determine the normal stresses in these sections at points  $A_1$  and  $A_2$ , which lie at a distance  $z$  from their respective neutral axes. We select the positive direction of the  $z$ -axis towards the outer fibres. Fibre  $A_1A_2$  elongates by  $A_2D_2$ ; the corresponding stress is

$$\sigma = \varepsilon E$$

where  $\varepsilon$  is the relative elongation of fibre  $A_1A_2$ . It is equal to the ratio of absolute elongation  $A_2D_2$  to the initial length of the fibre  $A_1A_2$ :

$$\varepsilon = \frac{A_2D_2}{A_1A_2}$$

Denoting the radius of curvature of fibre  $A_1A_2$  by  $\rho$ , we obtain

$$\begin{aligned} A_2D_2 &= z \delta d\varphi, & A_1A_2 &= \rho d\varphi \\ \varepsilon &= \frac{z}{\rho} \frac{\delta d\varphi}{d\varphi}, & \sigma &= \frac{z}{\rho} \frac{\delta d\varphi}{d\varphi} E \end{aligned} \quad (24.7)$$

Formula (24.7) gives the distribution of normal stresses due to bending moment  $M$  over the height of the section.

As  $\frac{\delta d\varphi}{d\varphi}$  and  $E$  are constants for each section,  $\sigma$  depends only upon the  $z$ -coordinate and the radius of curvature of fibre  $A_1A_2$  ( $\rho = r + z$ , where  $r$  is the radius of curvature of the neutral layer).

For a straight beam we had obtained a linear law of distribution of normal stresses; in a curved bar  $\sigma$  varies according to a hyperbolic law (Fig. 347). It is also evident from formula (24.7) that in fibres which are on the outside w.r.t. the neutral layer the increase of stresses

is slower than that of  $z$ , whereas in fibres which are on the inside w.r.t. the neutral layer stresses increase faster than  $z$ , because  $z$  changes sign from positive to negative.

Hence in a curved bar the normal stresses at the "inside" outer fibre are greater, and at the "outside" outer fibre are less than the stresses for the same fibres of a straight bar. This is quite understandable since the initial length of the inside fibre of a curved bar is much less than that of the outside fibre; in a straight bar these lengths are equal. This explains the difference in relative deformation and hence the difference in stress for these fibres.

Let us proceed with the solution of equations of statics (24.4) and (24.6) with the help of relation (24.7) obtained by considering the deformation of the bar. Substitute expression (24.7) in equation (24.4):

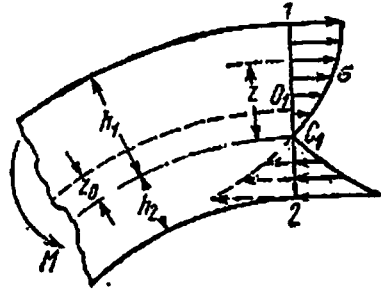


Fig. 347

$$\int_A \sigma dA = \int_A E \frac{\delta d\varphi}{d\varphi} \frac{z}{\rho} dA = 0$$

Factoring out the constant quantities, we obtain

$$\int_A \frac{z}{\rho} dA = 0 \tag{24.8}$$

This equation enables us to determine the location of the neutral axis.

Equation (24.8) implies that in the case of a curved bar it is not the static moment about the neutral axis,  $\int z dA$ , that is zero. This clearly shows that in bending of curved bars, the neutral axis really does not pass through the centre of gravity of the section. Substituting in equation (24.8)  $z = \rho - r$  (Fig. 346), we find

$$\int_A \frac{\rho - r}{\rho} dA = \int_A dA - r \int_A \frac{dA}{\rho} = 0$$

wherefrom it ensues that

$$r = \frac{A}{\int_A \frac{dA}{\rho}} \tag{24.9}$$



The method for computing  $r$  will be different for each particular section. Substituting now expression (24.7) in equation (24.6), we get

$$M - E \frac{\delta d\varphi}{d\varphi} \int_A \frac{z^2}{\rho} dA = 0 \quad (24.10)$$

where  $M$  is the bending moment; integration is over the whole cross-sectional area. The integral in the above equation may be modified as follows:

$$\int_A \frac{z^2}{\rho} dA = \int_A \frac{\rho - r}{\rho} z dA = \int_A z dA - r \int_A \frac{z}{\rho} dA$$

On the basis of equation (24.8) the second of the last two integrals is equal to zero, whereas the first is equal to the static moment of the cross-sectional area about the neutral axis. This integral may be computed as the product of the cross-sectional area by the distance of its centre of gravity from the neutral axis,  $z_0$  (Fig. 347):

$$S = A z_0 \quad (24.11)$$

Hence, equation (24.10) may be written

$$M - E \frac{\delta d\varphi}{d\varphi} S = 0 \quad (24.12)$$

wherefrom

$$\frac{\delta d\varphi}{d\varphi} = \frac{M}{ES} \quad (24.13)$$

and the formula for normal stresses, (24.7), becomes

$$\sigma = \frac{M}{S} \frac{z}{\rho} \quad (24.14)$$

Equation (24.12) confirms that the static moment  $S$  of the cross-sectional area about the neutral axis is not zero, i.e. in bending of curved bars the neutral axis does not pass through the centre of gravity but is slightly (by  $z_0$ ) displaced. In Fig. 347 we depicted this displacement towards the centre of curvature of the bar. After actually determining  $r$  from equation (24.9) for a number of sections we find that the neutral axis really gets displaced towards the centre of curvature.

This displacement occurs on account of the equality of the total compressive and tensile forces acting in the section. Since the stresses due to bending moment are less at the "outside" fibre and greater at the "inside" fibre, as compared to stresses in the corresponding fibres of an identical section of a straight bar (Fig. 347), the neutral axis must get displaced towards the inside fibres in order to maintain an equality of the total tensile and compressive forces.

Adding to these stresses the stresses due to the normal force obtained in the preceding section, we get the following formula for total normal stresses in a curved bar:

$$\sigma = \frac{N}{A} + \frac{M}{S} \frac{z}{\rho} \tag{24.15}$$

The maximum tensile and compressive stresses will occur at the outer fibres 1 and 2 (Fig. 347).

§ 136. Computation of the Radius of Curvature of the Neutral Layer in a Rectangular Section

Equation (24.9) is the expression for determining  $r$ :

$$r = \frac{A}{\int_A \frac{dA}{\rho}}$$

Let us solve this equation for a bar of rectangular cross section. Let  $h$  be the height and  $b$  the width of the section,  $R_0$  the radius of curvature of the bar,  $R_1$  the radius of curvature of the outer fibres,  $R_2$  the

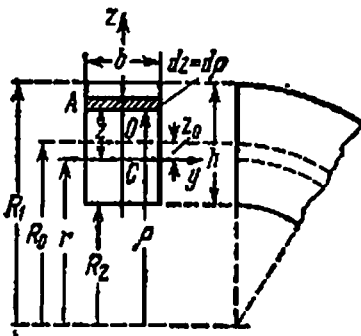


Fig. 348

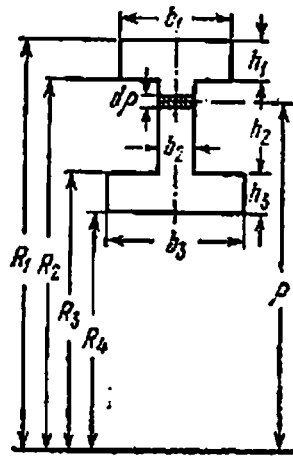


Fig. 349

radius of curvature of the inner fibres and  $r$  the radius of curvature of the neutral layer (Fig. 348). If we divide the section into elementary strips of area  $dA = b \, d\rho$ , then equation (24.9) may be written

$$r = \frac{bh}{\int_A \frac{b \, d\rho}{\rho}} = \frac{h}{\int_{R_2}^{R_1} \frac{d\rho}{\rho}} = \frac{h}{\ln \frac{R_1}{R_2}} \tag{24.16}$$

wherfrom

$$z_0 = R_0 - \frac{h}{\ln \frac{R_1}{R_2}} \tag{24.17}$$

Formulas (24.16) and (24.17) enable us to determine  $r$  and  $z_0$  and, hence,  $S$  for a rectangular section.

Location of the neutral layer in sections consisting of a number of rectangles is determined by the same method as in the rectangular section of a curved bar; only formula (24.16) becomes more complicated.

Let us consider an I-beam having flanges of different sizes (Fig. 349). The denominator in equation (24.9) is calculated as follows:

$$\int_A \frac{dA}{\rho} = \int_{R_1}^{R_2} \frac{b_1 d\rho}{\rho} + \int_{R_2}^{R_3} \frac{b_2 d\rho}{\rho} + \int_{R_3}^{R_4} \frac{b_3 d\rho}{\rho}$$

$$= b_1 \ln \frac{R_1}{R_2} + b_2 \ln \frac{R_2}{R_3} + b_3 \ln \frac{R_3}{R_4}$$

The radius of curvature of the neutral layer is determined from the expression

$$r = \frac{b_1 h_1 + b_2 h_2 + b_3 h_3}{b_1 \ln \frac{R_1}{R_2} + b_2 \ln \frac{R_2}{R_3} + b_3 \ln \frac{R_3}{R_4}} \tag{24.18}$$

§ 137. Determination of the Radius of Curvature of the Neutral Layer for Circle and Trapezoid

To determine the radius of curvature of the neutral layer for a circular section of diameter  $d$ , we cut the disc into elementary strips of area  $dA$  by lines drawn parallel to the neutral axis (Fig. 350).

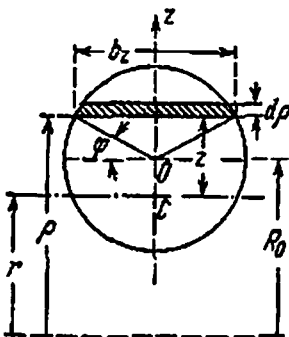


Fig. 350

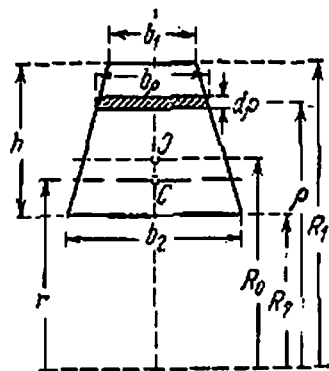


Fig. 351

Let us express  $dA$  and  $\rho$  as functions of angle  $\varphi$  subtended at the centre. It is clear from the diagram that

$$\rho = R_0 + \frac{d}{2} \sin \varphi, \quad dA = b_z d\rho$$

But

$$b_z = d \cos \varphi \quad \text{and} \quad d\rho = \frac{d}{2} \cos \varphi d\varphi$$

which implies that  $dA = \frac{d^2}{2} \cos^2 \varphi d\varphi$ . The denominator in equation (24.9) may be written

$$\int_A \frac{dA}{\rho} = \int_{-\pi/2}^{+\pi/2} \frac{d^2 \cos^2 \varphi d\varphi}{2R_0 + d \sin \varphi}$$

After integration we get

$$d^2 \int_{-\pi/2}^{+\pi/2} \frac{\cos^2 \varphi d\varphi}{2R_0 + d \sin \varphi} = \pi (2R_0 - \sqrt{4R_0^2 - d^2})$$

Putting this value in equation (24.9) and substituting  $\pi d^2/4$  for  $A$ , we obtain

$$r = \frac{d^2}{4(2R_0 - \sqrt{4R_0^2 - d^2})} \quad (24.20)$$

For a trapezoid (Fig. 351) we again use equation (24.9). The area of the trapezoid is

$$A = \frac{b_1 + b_2}{2} h$$

The width of the trapezoid at a distance  $\rho$  from the centre of curvature is

$$b(\rho) = b_1 + (b_2 - b_1) \frac{R_1 - \rho}{R_1 - R_2}, \quad dA = b(\rho) d\rho$$

The integral  $\int_A \frac{dA}{\rho}$  has the following value (dropping the intermediate operations):

$$\int_A \frac{dA}{\rho} = \left( b_1 + R_1 \frac{b_2 - b_1}{h} \right) \ln \frac{R_1}{R_2} - (b_2 - b_1)$$

Now from equation (24.9) we get

$$r = \frac{h \frac{b_1 + b_2}{2}}{\left( b_1 + R_1 \frac{b_2 - b_1}{h} \right) \ln \frac{R_1}{R_2} - (b_2 - b_1)} \quad (24.21)$$

When  $b_2 = b_1$ , i.e. when the trapezoid becomes a rectangle, the above formula becomes identical to formula (24.16).

When  $b_1=0$ , we obtain the formula for determining the neutral axis of a triangular section:

$$r = \frac{hb}{2R_1 \frac{b}{h} \ln \frac{R_1}{R_2} - 2b} \quad (24.22)$$

### § 138. Determining the Location of Neutral Layer from Tables

With the reasoning of §§ 136 and 137 for rectangular, circular and trapezoidal sections, we can calculate  $r$  and  $z_0$  for an arbitrary section. The results for a few shapes are given in Table 17. In this table the values of  $z_0$  are given as fractions of the radius  $R_0$  depending upon the ratio  $\frac{R_0}{c}$ , where  $c$  is the distance of the inner fibres from the centre of gravity of the section. In the extreme left columns are given values of  $R_0/c$ . At the top of all the other columns is given the shape of the particular curved bar. The quantity  $z_0$  is obtained by multiplying the corresponding tabulated value,  $k$ , with  $R_0$ , i.e.

$$z_0 = kR_0$$

It is evident from this table that when the ratio  $\frac{R_0}{c}$  increases, the ratio  $\frac{z_0}{R_0}$  rapidly approaches zero, i.e. the neutral axis approaches the centre of gravity. This means that the difference in the working of material in a curved and a straight bar diminishes to the point of becoming immaterial. It follows that in the limit the neutral axis passes through the centre of gravity of the section. Hence, when  $\frac{R_0}{c}$  is large, the location of the neutral axis and the stresses in the curved bar are determined, with a small error, by the same formulas which are used for straight bars.

For a ratio of  $\frac{R_0}{c}$  equal to ten, the quantity  $z_0$  may be considered equal to zero for all practical purposes.

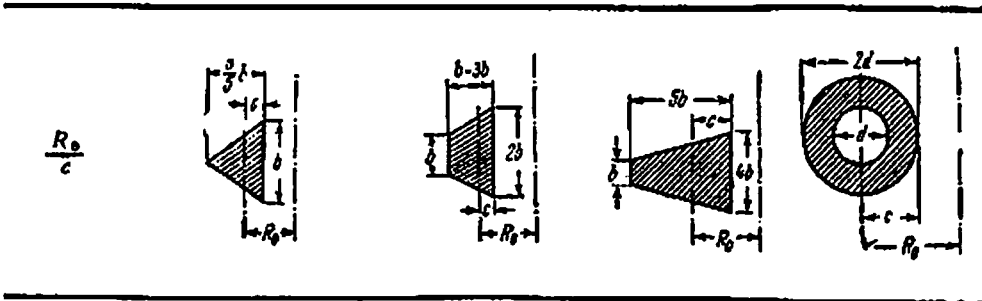
### § 139. Analysis of the Formula for Normal Stresses in a Curved Bar

Substituting the coordinates of the farthest points of the section in the formula for normal stresses (24.15),

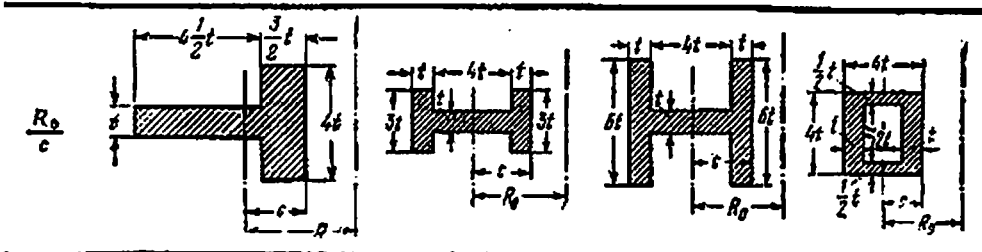
$$\begin{array}{ll} \text{for point 1,} & z_1 \text{ and } R_1 \text{ (outside fibres)} \\ \text{for point 2,} & -z_2 \text{ and } R_2 \text{ (inside fibres)} \end{array}$$

Table 17

Locating the Neutral Layer from Tables



$\frac{R_0}{c}$				
1.2	0.361	0.336	0.352	0.269
1.4	0.251	0.229	0.243	0.182
1.6	0.186	0.168	0.179	0.134
1.8	0.144	0.128	0.138	0.104
2.0	0.116	0.102	0.110	0.083
2.2	0.096	0.084	0.092	0.068
2.4	0.082	0.071	0.078	0.057
2.6	0.070	0.061	0.067	0.049
2.8	0.060	0.053	0.058	0.043
3.0	0.052	0.046	0.050	0.038
3.5	0.038	0.033	0.037	0.028
4.0	0.029	0.024	0.028	0.020
6.0	0.013	0.011	0.012	0.0087
8.0	0.0060	0.0060	0.0060	0.0049
10.0	0.0039	0.0039	0.0039	0.0031



$\frac{R_0}{c}$				
1.2	0.418	0.408	0.453	0.399
1.4	0.299	0.285	0.319	0.280
1.6	0.229	0.208	0.236	0.205
1.8	0.183	0.160	0.183	0.159
2.0	0.149	0.127	0.147	0.127
2.2	0.125	0.104	0.122	0.104
2.4	0.106	0.088	0.104	0.088
2.6	0.091	0.077	0.090	0.077
2.8	0.079	0.067	0.078	0.067
3.0	0.069	0.058	0.067	0.058
3.5	0.052	0.041	0.048	0.042
4.0	0.040	0.030	0.036	0.031
6.0	0.018	0.013	0.016	0.014
8.0	0.010	0.0076	0.0089	0.0076
10.0	0.0065	0.0048	0.0057	0.0048

we may write down the following strength condition of a curved bar:

$$\left. \begin{aligned} \sigma_1 &= \frac{N}{A} + \frac{M}{S} \frac{z_1}{R_1} \leq [\sigma] \\ \sigma_2 &= \frac{N}{A} - \frac{M}{S} \frac{z_2}{R_2} \leq [\sigma] \end{aligned} \right\} \quad (24.23)$$

If the material has unequal strength under tension and compression, then  $[\sigma]$  will have two different values. On account of the fact that two factors,  $M$  and  $N$ , give rise to normal stresses, it is more complicated to determine the critical section for a curved bar than for a straight one. In some cases (see § 133)  $M$  and  $N$  attain maximum values in the same section, which obviously is the critical section. If the situation is different, the strength of the material has to be checked in a number of sections and the critical section can be determined only after appropriate calculations.

If the radius of curvature  $R_0$  of the bar is large as compared to the height of the section  $h$  (precisely, when  $R_0 > 5h$ ), then the ratios  $\frac{z}{\rho}$  ( $\frac{z_1}{R_1}$  or  $\frac{z_2}{R_2}$ ) become negligibly small and the normal stresses which depend upon the bending moment differ only slightly from the normal stresses calculated by using the formula for a straight bar. This statement can be easily verified from the data given in §§ 135 and 136. Let us take, for example, equations (24.10) and (24.7). Eliminating  $E \frac{\delta d\varphi}{d\varphi}$  and substituting  $r+z$  for  $\rho$ , we obtain

$$\sigma = \frac{Mz}{(r+z) \int_A \frac{z^2}{r+z} dA} = \frac{Mz}{\left(1 + \frac{z}{r}\right) \int_A \frac{z^2 dA}{1+z/r}} \quad (24.24)$$

If we neglect  $\frac{z}{r}$ , then formula (24.24) becomes the same as the formula for calculating normal stresses in a straight bar:

$$\sigma = \frac{Mz}{J}$$

Let us determine the error that is made if we determine the maximum normal stresses due to the bending moment in a curved rectangular bar from the formula for straight bars

$$R_0 = 5h$$

The radius of curvature of the neutral layer is

$$r = \frac{h}{\ln \frac{R_0 + 0.5h}{R_0 - 0.5h}} = \frac{h}{\ln \frac{5.5}{4.5}} = \frac{h}{0.20067} = 4.9833h$$

and consequently

$$z_0 = R_0 - r = 0.0167h, \quad \text{or} \quad z_0 = 0.00334R_0$$

i.e. the neutral axis passes from the centre of gravity at a distance which is only  $\frac{1}{60}$  of the height of the section.

The normal stresses due to bending, when calculated from the formulas for curved bars, are found to be

$$\sigma_1 = \frac{M}{S} \frac{z_1}{R_1} = \frac{M \times 0.5167h}{bh \times 0.0167h \times 5.5h} = \frac{0.5167 \times M \times 6}{0.5511bh^2} = 0.935 \frac{M}{W}$$

$$\sigma_2 = \frac{M}{S} \frac{z_2}{R_2} = \frac{M \times 0.4833h}{bh \times 0.0167h \times 4.5h} = \frac{0.4833 \times M \times 6}{0.4509bh^2} = 1.071 \frac{M}{W}$$

i.e. the values of stresses differ by  $\pm 7\%$  from those calculated by the formula for straight bars.

This is the main reason why curved bars are divided into two groups for purposes of strength check. Bars with a large curvature ( $\frac{R_0}{h} \leq 5$ ) fall in the first group. In such bars the normal stresses should be calculated by the following formula:

$$\sigma_{1,2} = \frac{N}{A} \pm \frac{M}{S} \frac{z_{1,2}}{R_{1,2}} \leq [\sigma] \quad (24.23)$$

Practical examples of this group of bars are machine parts like hooks, chain links and rings. To the second group belong bars with a small curvature, in which the radius of curvature of the axis is large as compared to the dimensions of the cross section ( $\frac{R_0}{h} > 5$ ). In such bars the normal stresses due to bending may be calculated according to the formula for straight bars:

$$\sigma_{1,2} = \frac{N}{A} \pm \frac{M}{W_{1,2}} \leq [\sigma] \quad (24.25)$$

This group generally consists of curved bars used in various structures: arches, domes, etc.

#### § 140. Additional Remarks on the Formula for Normal Stresses

While checking the strength of curved bars, we often obtain considerably high stresses at the inside fibres. These stresses (Fig. 347) start decreasing fairly sharply at a small distance from the edge of the section. Thus, they bear strong resemblance to local stresses and their effect on the strength of a material must be taken into account according to the recommendations given in § 15: ductile materials (mild steel) do



not face danger of failure because of these stresses exceeding the yield stress, if the loading is static.

The fundamentals of the theory of analysis of curved bars, discussed in § 135, were first put forward by the Russian Academician A. V. Gadin between 1856 and 1860. The accurate theory of bending of curved rectangular bars was formulated in 1880 by Kh. S. Golovin; results obtained by him prove that sections of curved rectangular bars remain planes after bending. Experiments conducted for the verification of this theory show satisfactory concurrence of the results with the theoretically computed values.

The hyperbolic law of distribution of stresses can be distinctly seen by beaming monochromatic polarized light on a transparent model of a deformed curved bar. We notice rows of dark and light strips in the model; the sharper the change of stresses the narrower and more frequent are these strips. Figure 352 shows the distribution of strips un-

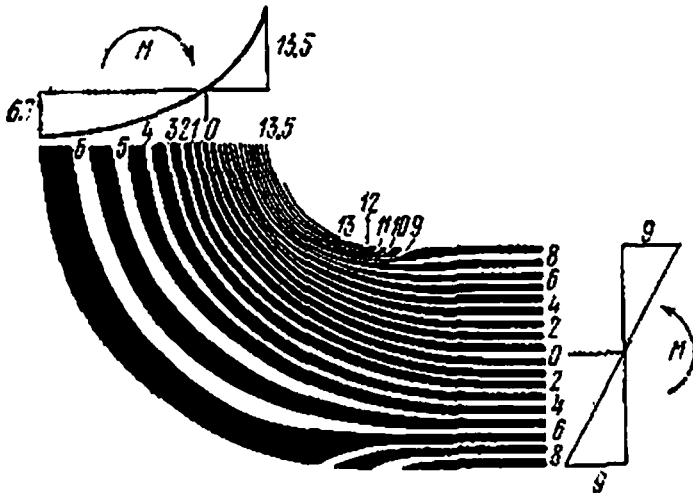


Fig. 352

der pure bending for a model which has a straight as well as a curved portion. The strips are spaced uniformly in the straight portion because the stresses change linearly, i.e. uniformly. In the curved portion we notice a concentration of the strips on the concave side and an opposite picture on the convex side, which corresponds to sharp and non-uniform increase of stresses in the former zone and a considerably slower change in the latter.

While studying the distribution of normal stresses in curved bars we ignored the radial normal stresses which occur due to mutual compression of fibres of the bar material. These stresses have much greater importance for curved bars than for straight bars, as is seen from experiments on gypsum (brittle) models. These stresses are particularly high in sections in which the width changes suddenly (I-beams).

### § 141. An Example on Determining Stresses in a Curved Bar

A bent frame is acted upon by two forces  $P$  of 800 kgf each. Find the maximum stresses in section  $AB$ . The radius of the axis is  $R_0=80$  mm, and the cross section is a rectangle  $80 \times 30$  mm in size (Fig. 353).

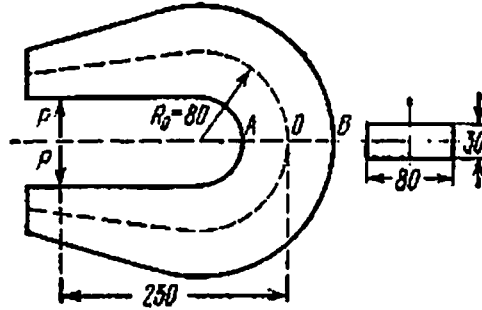


Fig. 353

As  $\frac{R_0}{h} < 5$ , we must use the formula applicable to bars with large curvature. Let us determine radius  $r$  of the neutral layer:

$$r = \frac{h}{\ln \frac{R_1}{R_2}}$$

In our example  $h=80$  mm,  $R_1=120$  mm, and  $R_2=40$  mm; therefore

$$r = \frac{80}{\ln \frac{120}{40}} = \frac{80}{1.099} = 72.8 \text{ mm}$$

Now we calculate the quantities necessary for analysis:

$$z_0 = R_0 - r = 80 - 72.8 = 7.2 \text{ mm} = 0.72 \text{ cm}$$

$$S = Az_0 = 8 \times 3 \times 0.72 = 17.3 \text{ cm}^3$$

$$z_1 = \frac{h}{2} + z_0 = 4 + 0.72 = 4.72 \text{ cm}$$

$$z_2 = \frac{h}{2} - z_0 = 4 - 0.72 = 3.28 \text{ cm}$$

Bending moment about the centre of gravity of the section is

$$M = -800 \times 25 = -20\,000 \text{ kgf} \cdot \text{cm}$$

Normal force  $N = +800$  kgf. The cross-sectional area  $A = 24 \text{ cm}^2$ . The normal stresses at point  $A$  ( $\sigma_1$ ) and  $B$  ( $\sigma_2$ ) are

$$\sigma_1 = +\frac{800}{24} - \frac{20\,000}{17.3} \times \frac{4.72}{12} = +33 - 455 = -422 \text{ kgf/cm}^2$$

$$\sigma_2 = +\frac{800}{24} + \frac{20\,000}{17.3} \times \frac{3.28}{4} = +33 + 948 = +981 \text{ kgf/cm}^2$$

Had we ignored the curvature of the bar and computed the stresses by the formula

$$\sigma = \frac{N}{A} \pm \frac{M}{W}$$

we would have obtained

$$\left. \begin{matrix} \sigma_1 \\ \sigma_2 \end{matrix} \right\} = + \frac{800}{24} \mp \frac{20\,000}{\frac{3 \times 8^3}{6}} = +33 \mp 625 = \left\{ \begin{matrix} -592 \\ +658 \end{matrix} \right\} \text{ kgf/cm}^2$$

The stresses in the inside fibres would have been

$$\frac{981 - 658}{981} 100 = 33\%$$

less, which is beyond the provided factor of safety. Hence, we may conclude that considerable overstressing may occur if the cross section of a curved bar is designed without taking into consideration its curvature.

### § 142. Determination of Displacements in Curved Bars

Analysis and experiments show that though the curvature must be accounted for while determining stresses in bars of large curvature, the same may be ignored in majority of cases when deformation is being determined. Let us study how to calculate potential energy expended in bending of a curved bar.

Let us cut from the bar an element of length  $ds$  by two cross sections (Fig. 354). Both faces of the element will be acted upon by shearing stresses, which give a resultant force  $Q$ , and normal stresses, which give a normal force  $N$  and a bending moment  $M$ .

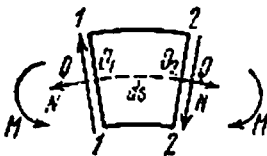


Fig. 354

For determining the potential energy accumulated in the element, we must compute the work done by all the forces acting on the element. While determining the potential energy of a beam we neglected the

work done by the shearing forces. This simplification is all the more justified in case of curved bars because the effect of shearing forces is still less.

Now all we have to do is to calculate  $N$  and  $M$ . If we neglect the curvature of the bar, then this is equivalent to assuming that the

deformation of the element under force couple  $M$  is identical to that of a beam. The potential energy due to this deformation is equal to  $\frac{M^2 ds}{2EJ}$ ; the only difference when compared to the expression for potential energy of a beam lies in a different notation of the length of the element,  $ds$  instead of  $dx$ .

On account of the fact that we ignore the curvature of the bar, the neutral axis must pass through the centre of gravity of the section. Therefore, when the section rotates under the action of  $M$ , the centres of gravity  $O_1$  and  $O_2$  do not move and  $N$  does not do any work. Consequently, we may calculate the work done by  $N$  independent of  $M$  and then add to it the value obtained from the expression given above.

Forces  $N$  acting on the element produce simple tension or compression; the potential energy accumulated during tension or compression is given by the expression  $\frac{N^2 ds}{2EA}$ . The potential energy accumulated in the element is

$$dU = \frac{M^2 ds}{2EJ} + \frac{N^2 ds}{2EA}$$

The potential energy accumulated in the whole of the bar is obtained by integrating the above expression over its total length:

$$U = \int_s \frac{M^2 ds}{2EJ} + \int_s \frac{N^2 ds}{2EA} \quad (24.26)$$

According to Castigliano's theorem, the first derivative of this expression w.r.t. concentrated force  $P$  gives us the linear displacement of the centre of gravity of the section in which force  $P$  is applied. Similarly, the first derivative of  $U$  w.r.t.  $M_0$  gives us the angle of rotation of the corresponding section:

$$f = \frac{\partial U}{\partial P} = \int_s \frac{M ds}{EJ} \frac{\partial M}{\partial P} + \int_s \frac{N ds}{EA} \frac{\partial N}{\partial P} \quad (24.27)$$

$$\theta = \frac{\partial U}{\partial M_0} = \int_s \frac{M ds}{EJ} \frac{\partial M}{\partial M_0} + \int_s \frac{N ds}{EA} \frac{\partial N}{\partial M_0} \quad (24.28)$$

Mohr's method may also be used for determining displacements in a curved bar. Formulas (24.27) and (24.28) are replaced by

$$\delta = \int_s \frac{M(x) M^0 ds}{EJ} + \int_s \frac{N(x) N^0 ds}{EA} \quad (24.29)$$

Let us apply this formula for calculating the vertical displacement of end  $B$  of the curved bar whose axis is described by radius  $R_0$ . The bar must be drawn in two states:

(a) when it is loaded by the given force,  $P$  (Fig. 355(a));

(b) when it is loaded by a unit force  $P^0=1$  acting on section  $B$  in the direction of the required displacement (Fig. 355(b)).

Let us calculate  $M(x)$ ,  $M^0$ ,  $N(x)$ , and  $N^0$ :

$$\begin{aligned} M &= +PR_0 \sin \varphi, & M^0 &= R_0 \sin \varphi \\ N &= -P \sin \varphi, & N^0 &= -\sin \varphi, & ds &= R_0 d\varphi \end{aligned}$$

Substituting the above values in formula (24.29), we obtain:

$$\begin{aligned} f &= \frac{1}{EJ} \int_0^{\pi/2} P \sin^2 \varphi R_0^3 d\varphi + \frac{1}{EA} \int_0^{\pi/2} P \sin^2 \varphi R_0 d\varphi \\ &= \left( \frac{PR_0^3}{EJ} + \frac{PR_0}{EA} \right) \int_0^{\pi/2} \sin^2 \varphi d\varphi = \left( \frac{PR_0^3}{EJ} + \frac{PR_0}{EA} \right) \frac{\pi}{4} \\ &= \frac{\pi PR_0^3}{4EJ} \left( 1 + \frac{J}{AR_0^2} \right) = \frac{\pi PR_0^3}{4EJ} \left( 1 + \frac{i^2}{R_0^2} \right) \end{aligned}$$

where  $i$  is the radius of gyration of the section.

The first term in the parentheses shows the effect of the bending moment on deflection, the second term shows the effect of normal force. Since in the majority of cases  $\frac{i^2}{R_0^2}$  is a small quantity, the effect of normal force on the deformation of curved bars is in a number of cases comparatively small.

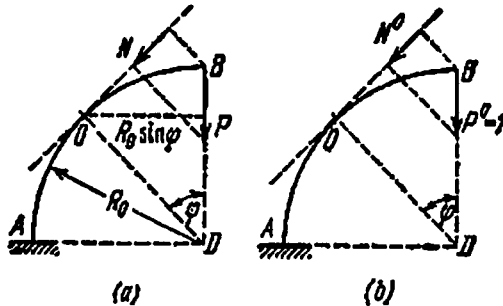


Fig. 355

If we want to find the horizontal displacement of point  $B$ , we should apply a unit horizontal force  $P^0=1$  at the above point. We can similarly find the angle of rotation of this section by applying  $M^0=1$ .

If it is required to break the bar into a number of portions for calculating  $M$  and  $N$ , then each of the corresponding integrals in formula (24.29) becomes a sum of integrals with appropriate limits.

### § 143. Analysis of a Circular Ring

Let us find the stresses in the critical section of a circular ring (Fig. 356) subjected to two tensile forces  $P$ . The radius of the ring is  $R_0$  and its rigidity  $EJ$ . The problem is statically determinate as far as the external forces are concerned. However, with respect to internal forces it is statically indeterminate.

Let us cut the ring by a horizontal section into two parts; the upper part is shown in Fig. 357. The sectioning plane will experience inter-

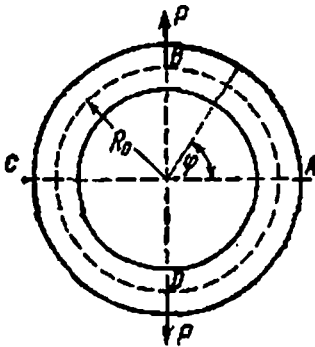


Fig. 356

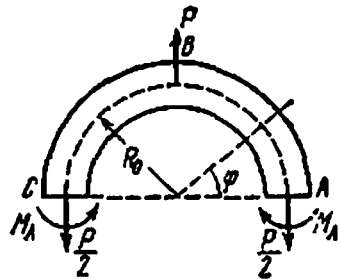


Fig. 357

nal forces transmitted from the lower (removed) part: normal force  $N=0.5P$  and bending moment  $M_A$  drawn arbitrarily as shown in the figure (there is no shearing force in the horizontal sections). We have exhausted all equations of statics in drawing these conclusions from the symmetry of the ring, but moment  $M_A$  still remains unknown. Let us now consider a section making an angle  $\varphi$  with the sectioning plane (see Figure). The following forces will act in this section:

$$M_\varphi = M_A + 0.5PR_0(1 - \cos \varphi) \quad (24.30)$$

$$N_\varphi = 0.5P \cos \varphi \quad (24.31)$$

$$Q_\varphi = 0.5P \sin \varphi \quad (24.32)$$

Since the section is symmetric, the angles of rotation of horizontal sections to which moments  $M_A$  are applied will be zero; therefore the partial derivative of potential energy with respect to  $M_A$  will also be zero:

$$\begin{aligned} \frac{\partial U}{\partial M_A} &= \frac{1}{EJ} \int_s M_\varphi \frac{\partial M_\varphi}{\partial M_A} ds \\ &= \frac{1}{EJ} \int_0^{\pi/2} [M_A + 0.5PR_0(1 - \cos \varphi)] R_0 d\varphi = 0 \end{aligned}$$

The equation is solved as follows:

$$\int_0^{\pi/2} (M_A + 0.5PR_0 - 0.5PR_0 \cos \varphi) d\varphi = M_A \frac{\pi}{2} + 0.5PR_0 \frac{\pi}{2} - 0.5PR_0 = 0$$

$$M_A = -0.5PR_0 \left(1 - \frac{2}{\pi}\right) = -0.182PR_0$$

Hence, moment  $M_A$  acts in the opposite direction to the one shown in the figure.

With the help of formulas (24.30)-(24.32) we can determine the internal forces in any section of the ring. The section that evokes maximum interest is section  $B$ . In this section at  $\varphi = \pi/2$  we have

$$\begin{aligned} M_B &= -0.182PR_0 + 0.5PR_0 = 0.318PR_0 \\ Q_B &= 0.5P, \quad N_B = 0 \end{aligned}$$

Thus, we see that for a ring section  $B$ , where force  $P$  is applied, is critical although the normal force in this section is zero.

The reader is advised to plot the bending-moment, normal-force and shearing-force diagrams for the ring section using formulas (24.30) and (24.32).

## CHAPTER 25

### Thick-walled and Thin-walled Vessels

#### § 144. Analysis of Thick-walled Cylinders

We were perfectly justified in considering the distribution of stresses as uniform over the thickness of the wall in a thin-walled cylindrical reservoir subjected to internal pressure (§ 29). This assumption has minimal effect on the accuracy of design.

However, such an assumption in the case of cylinders having considerable wall thickness as compared to their radius is sure to result in large errors. The analysis of such cylinders was worked out by G. Lamé and A. V. Gadolin in 1852-4. The latter gained worldwide fame thanks to his works on analysis of curved bars in application to strength analysis of artillery guns. Figure 358 shows the cross section of a thick-walled cylinder of external radius  $r_1$  and internal radius  $r_2$ ; the cylinder is subjected to external pressure  $p_1$  and internal pressure  $p_2$ .

Let us consider a very thin ring of radius  $r$  in the cylinder wall. Let  $dr$  be the thickness of the ring and let  $AB$  (Fig. 359) depict a small element of this ring subtending an angle  $d\theta$  at the centre.

Suppose the element has unit thickness in a plane perpendicular to the plane of the figure and suppose  $\sigma_r$  and  $\sigma_r + d\sigma_r$  are the stresses acting

at the inner and outer faces of element  $AB$ ; also suppose  $\sigma_t$  is the stress at its side faces. It is obvious from the symmetry of the section and the load that element  $AB$  will not warp and that no shearing stresses will act on its faces. Faces of the element which lie in the plane of the

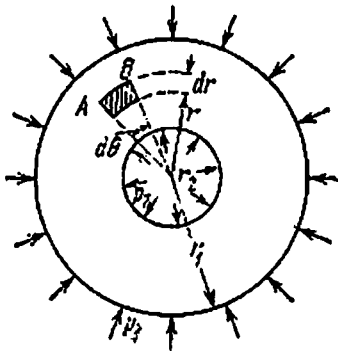


Fig. 358

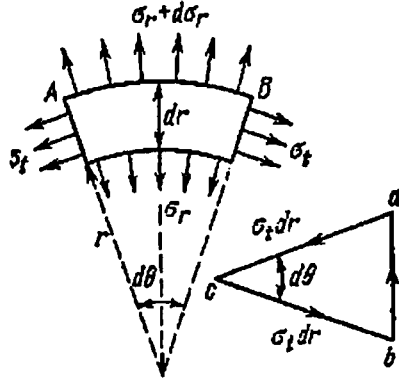


Fig. 359

figure will experience the third principal stress,  $\sigma_z$ , caused by the pressure on the cylinder base. This stress may be considered constant over the cylinder's cross section.

In the plane of the figure, element  $AB$  is acted upon by two forces  $\sigma_t dr \times l$ , making an angle  $d\theta$  between themselves, and a radial force

$$(\sigma_r + d\sigma_r)(r + dr) d\theta \times l - \sigma_r r d\theta \times l$$

This force is directed towards the outer surface. In equilibrium the three forces constitute a closed triangle  $abc$ . It is evident then that the radial force represented by segment  $ab$  is connected with force  $\sigma_t dr$  (segment  $ca$ ) by the following relation:

$$\overline{ab} = \overline{ca} d\theta$$

or

$$[(\sigma_r + d\sigma_r)(r + dr) - \sigma_r r] d\theta = \sigma_t dr d\theta$$

Neglecting the small quantities of higher order, we get

$$\sigma_r dr + d\sigma_r r = \sigma_t dr$$

wherefrom

$$\sigma_r - \sigma_t + \frac{d\sigma_r}{dr} r = 0 \tag{25.1}$$

The equilibrium conditions give us only one equation for determining two unknown stresses. The problem is statically indeterminate and we must consider the deformation of the cylinder.

Deformation of the cylinder consists in its elongation and in radial displacement of all points of its cross sections. Let us denote the radial



displacement of points of the internal surface of the element by  $u$  (Fig. 360). Points on the outer surface will get radially displaced by  $u+du$ . Thus, thickness  $dr$  of the element will increase by  $du$  and the relative elongation of the cylinder material in the radial direction will be  $\epsilon_r = \frac{du}{dr}$ .

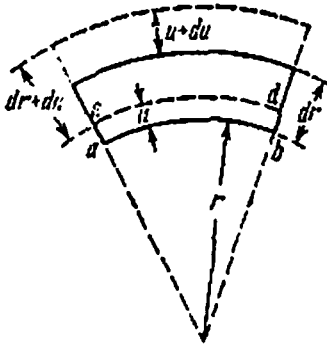


Fig. 360

In the direction of stresses  $\sigma_t$  the relative elongation  $\epsilon_t$  will be equal to the relative elongation of arc  $ab$  when it occupies position  $cd$ . As the relative elongation of the arc is the same as the relative elongation of radius  $r$ ,  $\epsilon_t = \frac{u}{r}$ . From Hooke's law (formulas (6.21), § 34),

$$\left. \begin{aligned} \epsilon_r &= \frac{1}{E} (\sigma_r - \mu\sigma_t - \mu\sigma_z) = \frac{du}{dr} \\ \epsilon_t &= \frac{1}{E} (\sigma_t - \mu\sigma_r - \mu\sigma_z) = \frac{u}{r} \end{aligned} \right\} \quad (25.2)$$

As both  $\epsilon_t$  and  $\epsilon_r$  are functions of  $u$ , they must be compatible. Differentiating  $\epsilon_t$  w.r.t.  $r$ , we get

$$\epsilon_t = \frac{u}{r}, \quad \frac{d\epsilon_t}{dr} = \frac{\frac{du}{dr} r - u}{r^2} = \frac{1}{r} \left( \frac{du}{dr} - \frac{u}{r} \right) = \frac{1}{r} (\epsilon_r - \epsilon_t) \quad (25.3)$$

This is the condition of joint deformation. Substituting in it the values of  $\epsilon_r$  and  $\epsilon_t$  from (25.2), we obtain the second equation correlating  $\sigma_t$  and  $\sigma_r$ :

$$\frac{d}{dr} \left[ \frac{1}{E} (\sigma_t - \mu\sigma_r - \mu\sigma_z) \right] = \frac{1}{r} \frac{1+\mu}{E} (\sigma_r - \sigma_t)$$

or

$$\frac{d\sigma_t}{dr} - \mu \frac{d\sigma_r}{dr} = \frac{1+\mu}{r} (\sigma_r - \sigma_t) \quad (25.4)$$

Substituting in this equation the value of  $\sigma_r - \sigma_t$  from (25.1), we get

$$\frac{d\sigma_t}{dr} - \mu \frac{d\sigma_r}{dr} = - (1 + \mu) \frac{d\sigma_r}{dr}$$

or

$$\frac{d\sigma_t}{dr} + \frac{d\sigma_r}{dr} = 0 \quad (25.5)$$

For simultaneous solution of equations (25.1) and (25.5) we differentiate the first w.r.t.  $r$  and substitute in it the value of  $\frac{d\sigma_t}{dr}$  from the

second. This gives us

$$\frac{d\sigma_r}{dr} - \frac{d\sigma_t}{dr} + r \frac{d^2\sigma_r}{dr^2} + \frac{d\sigma_r}{dr} = 0$$

The differential equation may be rewritten as

$$\frac{d^2\sigma_r}{dr^2} + \frac{3}{r} \frac{d\sigma_r}{dr} = 0 \quad (25.6)$$

The solution of this equation is

$$\sigma_r = A + \frac{B}{r^2} \quad (25.7)$$

which can be checked. Constants  $A$  and  $B$  are calculated from the boundary conditions at the internal and external surfaces of the cylinder:

$$(\sigma_r)_{r=r_1} = -p_1, \quad (\sigma_r)_{r=r_2} = -p_2 \quad (25.8)$$

The negative sign in the right-hand sides of these expressions signifies that the positive direction of  $\sigma_r$  corresponds to tensile stresses (Fig. 359).

From the expression (25.8) we get

$$A = \frac{p_2 r_2^2 - p_1 r_1^2}{r_1^2 - r_2^2}, \quad B = - \frac{(p_2 - p_1) r_1^2 r_2^2}{r_1^2 - r_2^2}$$

The values of the constants and equation (25.7) give us the final formulas for  $\sigma_r$  and  $\sigma_t$ :

$$\left. \begin{aligned} \sigma_r &= \frac{p_2 r_2^2 - p_1 r_1^2}{r_1^2 - r_2^2} - \frac{(p_2 - p_1) r_1^2 r_2^2}{r^2 (r_1^2 - r_2^2)} \\ \sigma_t &= \frac{p_2 r_2^2 - p_1 r_1^2}{r_1^2 - r_2^2} + \frac{(p_2 - p_1) r_1^2 r_2^2}{r^2 (r_1^2 - r_2^2)} \end{aligned} \right\} \quad (25.9)$$

It is obvious from these formulas that the sum  $\sigma_r + \sigma_t$  does not depend upon  $r$ , i.e. the strain along the axis of the cylinder is the same at all points of the section (as  $\sigma_z$  is the same for all points), and the section remains a plane.

A situation in which only internal pressure  $p_2$  acts on the cylinder is of considerable practical importance. Here

$$\left. \begin{aligned} \sigma_r &= \frac{p_2 r_2^2}{r_1^2 - r_2^2} \left( 1 - \frac{r_1^2}{r^2} \right) \\ \sigma_t &= \frac{p_2 r_2^2}{r_1^2 - r_2^2} \left( 1 + \frac{r_1^2}{r^2} \right) \end{aligned} \right\} \quad (25.10)$$

Figure 361 shows the distribution of stresses over the thickness of the cylinder walls when  $p_1 = 0$ . As  $\sigma_z$  is usually much less than  $\sigma_r$  and  $\sigma_t$  in

magnitude, only the latter two are considered in checking the strength of the cylinder. From the third theory of failure (theory of maximum shearing stresses) we find that the maximum difference of principal stresses,

$$(\sigma_t - \sigma_r)_{\max} = \frac{2p_2 r_1^3}{r_1^3 - r_2^3} \quad (25.11)$$

occurs at points of the internal surface of the cylinder and is always considerably greater in magnitude than the internal pressure.

Thus, permanent deformation begins at the internal surface of the cylinder when  $(\sigma_t - \sigma_r)_{\max}$  becomes equal to the yield stress of its material; any attempt to curb the appearance of permanent deformation

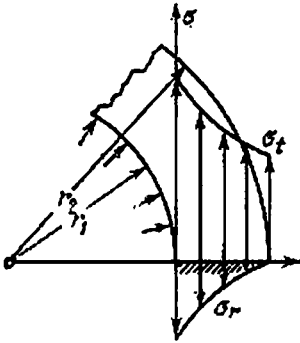


Fig. 361

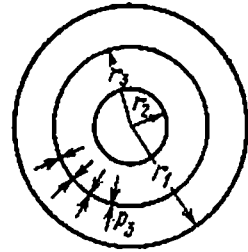
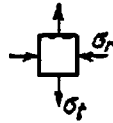


Fig. 362

by increasing the external radius  $r_1$  is accompanied by an increase of the numerator as well as denominator in formula (25.11). Therefore, although the difference of principal stresses  $(\sigma_t - \sigma_r)_{\max}$  becomes less, the decrease is very slow. However, when permanent deformation begins at the internal surface of the cylinder, this does not mean that the maximum lifting capacity of the structure has been exhausted; we can properly evaluate the strength of the cylinder only by analysis based on the method of permissible loads.

Lifting capacity of thick cylinders in the elastic range may be improved by creating initial stresses. For this the cylinder must be made of two cylinders, one fitted into the other. The external diameter of the internal cylinder is made a little more than the internal diameter of the outer cylinder. The outer cylinder is put on the internal one in heated state and upon cooling gives rise to reactions at the surface of contact; the reactions compress the internal cylinder and stretch the outer. The analysis given below will show that these initial stresses improve the working of the composite cylinder which is subjected to internal pressure.

Figure 362 shows a composite cylinder after it has cooled. Stresses in a tangential direction will be: for the outer cylinder (tensile)

$$\sigma'_t = \frac{p_3 r_3^2}{r_1^2 - r_3^2} + \frac{p_3 r_1^2 r_3^2}{r_1^2 (r_1^2 - r_3^2)}$$

and for the inner cylinder (compressive)

$$\sigma''_t = - \frac{p_3 r_3^2}{r_3^2 - r_2^2} - \frac{p_3 r_3^2 r_2^2}{r_3^2 (r_3^2 - r_2^2)}$$

Figure 363 shows the distribution curves of these initial stresses for the following numerical data:

$$r_1 = 11.50 \text{ cm}, \quad r_2 = 5.70 \text{ cm}, \quad r_3 = 8.25 \text{ cm}, \quad p_3 = 280 \text{ kgf/cm}^2$$

For the outer cylinder stresses at the external surface are

$$\sigma'_{t_1} = + p_3 \frac{2r_3^2}{r_1^2 - r_3^2} = + 613 \text{ kgf/cm}^2$$

and stresses at the internal surface are

$$\sigma'_{t_2} = + p_3 \frac{r_1^2 - r_3^2}{r_1^2 - r_3^2} = + 895 \text{ kgf/cm}^2$$

For the inner cylinder stresses at the internal surface are

$$\sigma''_{t_2} = - p_3 \frac{2r_3^2}{r_3^2 - r_2^2} = - 1080 \text{ kgf/cm}^2$$

and stresses at the external surface are

$$\sigma''_{t_3} = - p_3 \frac{r_3^2 + r_2^2}{r_3^2 - r_2^2} = - 800 \text{ kgf/cm}^2$$

Let us now assume that the cylinder is subjected to an internal pressure of  $p_2 = 3400 \text{ kgf/cm}^2$ . The distribution of  $\sigma_t$  without considering the initial stresses  $p_3$  will be given by formula (25.10):

$$\sigma_t = \frac{p_2 r_3^2}{r_1^2 - r_3^2} \left( 1 + \frac{r_1^2}{r^2} \right)$$

The limiting values of these stresses are:

at the external surface  $\sigma_{t_1} = +2245 \text{ kgf/cm}^2$

at the internal surface  $\sigma_{t_2} = +5620 \text{ kgf/cm}^2$

The corresponding curve is depicted in Fig. 363. When internal pressure and initial stresses act simultaneously, the total stress may be

taken as the sum of ordinates of curves  $\sigma_t + \sigma'_t$  and  $\sigma_t + \sigma''_t$ ; the curve of total stresses has the shape of a tooth, as is shown in Fig. 363.

The shape of the resultant curve shows that when initial stresses  $p_3$  are acting, the stresses in the outer cylinder increase whereas the stresses in the inner cylinder decrease. As a consequence, the material works more uniformly—the maximum stress comes down to  $5620 - 1080 = +4540 \text{ kgf/cm}^2$  and the minimum stress grows up to  $2245 + 613 = 2858 \text{ kgf/cm}^2$ . Of course, this distribution holds well only when the material is working within the elastic limit.

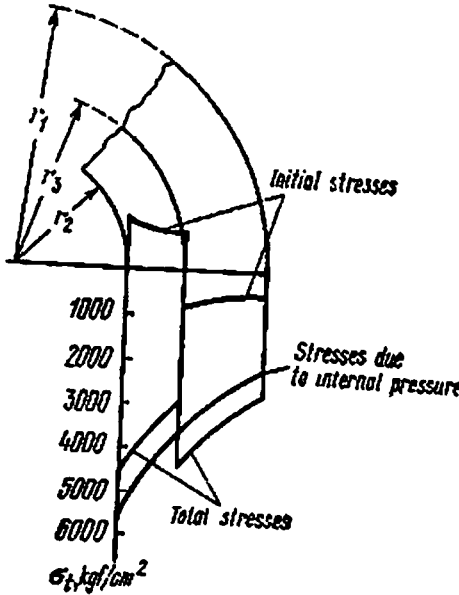


Fig. 363

Let us determine the difference of radii,  $\Delta r_3 = r_3'' - r_3'$ , which is essential to create the required initial stress  $p_3$  (here  $r_3'$  is the initial external radius of the inner cylinder, and  $r_3''$  is the initial internal radius of the outer cylinder).

As the outer cylinder cools, these radii tend to become equal due to a decrease in  $r_3''$  by  $\Delta r_3'$  and an increase in  $r_3'$  by  $\Delta r_3''$ ; the sum of absolute values of these deformations must be  $\Delta r_3$ :

$$|\Delta r_3'| + |\Delta r_3''| = \Delta r_3$$

Relative tangential elongation of the material at the internal surface of the outer cylinder is

$$e'_t = \frac{1}{E} (\sigma'_t - \mu \sigma'_{r_3}) = \frac{p_3}{E} \left( \frac{r_1^2 + r_3^2}{r_1^2 - r_3^2} + \mu \right)$$

In this formula for  $r_3$  we substituted the radius  $r_3 = r_3' - \Delta r_3$  common to both cylinders; this is possible because  $\Delta r_3$  is a small quantity and the error committed by it is very small. Relative elongation of radius  $r_3$  will also be  $e'_t$ ; therefore

$$\Delta r_3' = e'_t r_3 = \frac{p_3 r_3}{E} \left( \frac{r_1^2 + r_3^2}{r_1^2 - r_3^2} + \mu \right)$$

Relative tangential compression of the material at the external surface of the inner cylinder is

$$e''_t = \frac{1}{E} (\sigma''_t - \mu \sigma''_{r_3}) = - \frac{p_3}{E} \left( \frac{r_3^2 + r_3^2}{r_3^2 - r_3^2} - \mu \right)$$

and the shortening of radius  $r_3^*$  is

$$\Delta r_3^* = -\frac{p_3 r_3}{E} \left( \frac{r_3^2 + r_2^2}{r_3^2 - r_2^2} - \mu \right)$$

The sum of absolute values of  $\Delta r_3'$  and  $\Delta r_3^*$  will as before be

$$\frac{p_3 r_3}{E} \left( \frac{r_1^2 + r_3^2}{r_1^2 - r_3^2} + \mu \right) + \frac{p_3 r_3}{E} \left( \frac{r_3^2 + r_2^2}{r_3^2 - r_2^2} - \mu \right) = \frac{2p_3 r_3^2}{E} \frac{r_1^2 - r_2^2}{(r_1^2 - r_3^2)(r_3^2 - r_2^2)} = \Delta r_3$$

Hence, in order to create the desired initial stress  $p_3$ , we must provide a difference of diameters

$$\Delta d_3 = \frac{4p_3 r_3^2}{E} \frac{r_1^2 - r_2^2}{(r_1^2 - r_3^2)(r_3^2 - r_2^2)}$$

The minimum temperature  $t^0$  up to which the outer cylinder must be heated before it is put on the inner cylinder can be determined from the following relation:

$$\alpha_t r_3 t^0 = \Delta r_3$$

wherefrom

$$t^0 = \frac{2p_3 r_3^2}{E \alpha_t} \frac{r_1^2 - r_2^2}{(r_1^2 - r_3^2)(r_3^2 - r_2^2)} = 66^\circ \text{C}$$

(We have assumed the following numerical values:  $\alpha = 125 \times 10^{-7}$ ,  $E = 2 \times 10^6 \text{ kgf/cm}^2$ ,  $\Delta d_3 = 0.0137 \text{ cm}$ .)

### § 145. Stresses In Thick Spherical Vessels

Figure 364 shows an element cut from the wall of a thick spherical vessel. The element has internal radius  $r$  and external radius  $r + dr$ ; stresses acting on the element are also shown in the figure. From the equations of equilibrium and joint deformation we get

$$\sigma_r = A + \frac{B}{r^3}, \quad \sigma_t = A - \frac{B}{r^3} \tag{25.12}$$

Constants  $A$  and  $B$  may be determined from the boundary conditions at the internal and external surfaces of the vessel at  $r = r_2$  and  $r = r_1$ , respectively, where  $r_1$  and  $r_2$  are the external and internal radii of the vessel.

For example, if the vessel is subjected to an external pressure  $p_1$  and an internal pressure  $p_2$ , constants  $A$  and  $B$  may be determined from

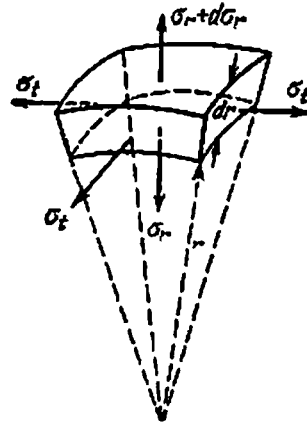


Fig. 364

the following conditions:

$$\sigma_r = A + \frac{B}{r^3} = -p_2 \quad \text{at the internal surface}$$

$$\sigma_r = A + \frac{B}{r^3} = -p_1 \quad \text{at the external surface}$$

wherefrom

$$B = -(p_2 - p_1) \frac{r_1^3 r_2^3}{r_1^3 - r_2^3}, \quad A = + \frac{p_2 r_2^3 - p_1 r_1^3}{r_1^3 - r_2^3}$$

Therefore

$$\left. \begin{aligned} \sigma_r &= + \frac{p_2 r_2^3 - p_1 r_1^3}{r_1^3 - r_2^3} - (p_2 - p_1) \frac{r_1^3 r_2^3}{r^3 (r_1^3 - r_2^3)} \\ \sigma_t &= + \frac{p_2 r_2^3 - p_1 r_1^3}{r_1^3 - r_2^3} + (p_2 - p_1) \frac{r_1^3 r_2^3}{2r^3 (r_1^3 - r_2^3)} \end{aligned} \right\} \quad (25.13)$$

### § 146. Analysis of Thin-walled Vessels

If the thickness of the cylinder wall,  $t=r_1-r_2$ , is small compared to radii  $r_1$  and  $r_2$ , then from formula (25.10) we get

$$\sigma_t = \frac{p_2 r}{t}$$

which is the same as obtained earlier (§ 29).

A general formula can be derived for calculating stresses in thin-walled vessels which represent surfaces of rotation and are subjected to internal pressure  $p$  symmetrical about the axis of rotation.

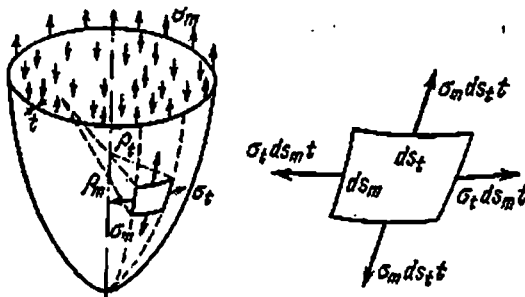


Fig. 365

Let us cut from the vessel (Fig. 365) an element by two meridian sections and two sections perpendicular to the meridian. Let  $ds_m$  and  $ds_t$  be the dimensions of the element along the meridian and perpendicular to it, and let us denote by  $\rho_m$  and  $\rho_t$  the radii of curvature of the meridian and of the section perpendicular to it; let  $t$  be the wall thickness.

From symmetry, the faces of the element will be acted upon by normal stresses  $\sigma_m$  in the direction of meridian and  $\sigma_t$  in the perpendicular direction. The corresponding forces acting on the faces of the element will be  $\sigma_m ds_t t$  and  $\sigma_t ds_m t$ . Since a thin shell, just like a flexible string, has resistance only against tensile loading, these forces act along the tangents to the meridian and to a section normal to the meridian.

Along the normal to the surface of the element forces  $\sigma_t ds_m t = ac = bc$  (Fig. 366) give resultant  $ab$ , which is equal to

$$\overline{ab} = \overline{bc} d\theta_t = \sigma_t ds_m t \frac{ds_t}{\rho_t}$$

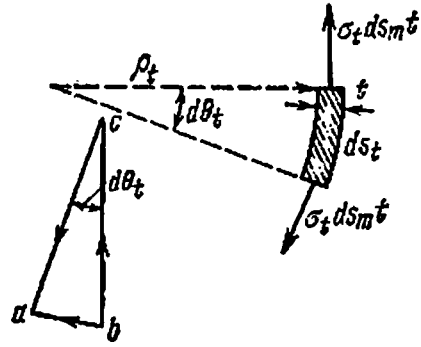


Fig. 366

Similarly force  $\sigma_m ds_t t$  gives a resultant  $\sigma_m ds_t ds_m \frac{t}{\rho_m}$  in the same direction. The sum of these forces must balance the normal pressure acting on the element:

$$p ds_m ds_t = \sigma_m ds_t ds_m \frac{t}{\rho_m} + \sigma_t ds_m ds_t \frac{t}{\rho_t}$$

wherefrom

$$\frac{\sigma_m}{\rho_m} + \frac{\sigma_t}{\rho_t} = \frac{p}{t} \tag{25.14}$$

This basic equation, correlating  $\sigma_m$  and  $\sigma_t$  in thin-walled vessels having a surface of rotation, was derived by Laplace.

As we had assumed that the stresses are distributed (uniformly) over the section, the problem is statically determinate; the second equilibrium equation can be obtained by considering the equilibrium of the lower portion of the vessel cut by a parallel circular section.

Let us consider a vessel subjected to hydrostatic loading (Fig. 367). Let us describe the meridian curve in the system of  $x$  and  $y$  coordinate axes with the origin at the apex of the curve. Assume that the sectioning plane passes at a height  $y$  from point  $O$ . Radius of the corresponding parallel circle is  $x$ .

Each force couple  $\sigma_m ds_t t$  acting on diametrically opposite elements  $ds_t$  of the section will give resultant  $bc$  equal to

$$\overline{bc} = 2\overline{ab} \cos \theta = 2\sigma_m ds_t t \cos \theta$$

The sum of these forces acting on the whole circular section will be  $2\pi x \sigma_m t \cos \theta$ ; it will balance the liquid's pressure  $p = \gamma(h - y)$  at



this level and weight  $P_y$  of the liquid in the cutoff portion:

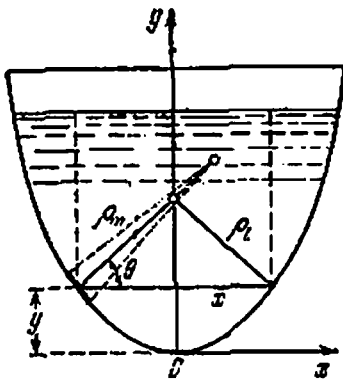
$$2\pi x \sigma_m t \cos \theta = \pi x^2 \rho + P_y$$

wherefrom

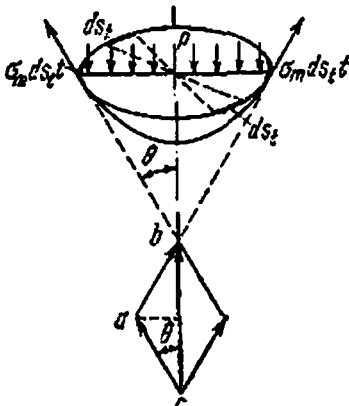
$$\sigma_m = \frac{\rho x}{2t \cos \theta} + \frac{P_y}{2\pi x t \cos \theta} \tag{25.15}$$

Knowing the equation of the meridian curve, we can find  $\theta$ ,  $x$ , and  $P_y$  for all values of  $y$  and, consequently, determine  $\sigma_m$ . We can then determine  $\sigma_t$  from equation (25.14).

For instance, for a conical reservoir having apex angle  $2\alpha$  and filled with a liquid of specific weight  $\gamma$  to a height  $h$  we have



$$\begin{aligned} \rho_m &= \infty, & x &= y \tan \alpha \\ P_y &= \frac{1}{3} \gamma \pi x^2 y = \frac{1}{3} \gamma \pi y^3 \tan^2 \alpha \\ \rho &= \gamma (h - y), & \theta &= \alpha \\ \rho_t &= \frac{x}{\cos \alpha} = \frac{y \tan \alpha}{\cos \alpha} \end{aligned}$$



Therefore

$$\begin{aligned} \sigma_m &= \frac{\gamma (h - y) y \tan \alpha}{2t \cos \alpha} + \frac{\gamma \pi y^3 \tan^2 \alpha}{6\pi y \tan \alpha t \cos \alpha} \\ &= \frac{\gamma (h - y) y \tan \alpha}{2t \cos \alpha} + \frac{y^2 \gamma \tan \alpha}{6t \cos \alpha} \\ &= \frac{\gamma y \tan \alpha}{2t \cos \alpha} \left( h - \frac{2}{3} y \right) \\ \sigma_t &= \frac{\rho \rho_t}{t} = \frac{\gamma (h - y) y \tan \alpha}{t \cos \alpha} \end{aligned}$$

Fig. 367

For a spherical vessel of radius  $r_0$  subjected to internal pressure  $p_0$ , from symmetry we have  $\sigma_t = \sigma_m = \sigma$ . Now as  $\rho_m = \rho_t = r_0$ , equation (25.14) gives

$$\frac{2\sigma}{r_0} = \frac{p_0}{r} \quad \text{or} \quad \sigma = \frac{p_0 r_0}{2t}$$

If the meridian curve has a discontinuity of angle  $\theta$ , the equilibrium of the thin shell at the point of discontinuity can be achieved only if a reaction acts at this point of the shell. Such a reaction can be made to appear with the help of special rings capable of taking the load that occurs due to unbalanced stresses  $\sigma_m$  on both sides of the point of discontinuity.

## CHAPTER 26

## Design for Permissible Loads. Design for Limiting States

### § 147. Design for Permissible Loads.

#### Application to Statically Determinate Systems

In the methods explained above for designing under tension or compression statically determinate as well as indeterminate structures we proceeded from the fundamental strength condition  $\sigma_{\max} \leq [\sigma]$  (§§ 4 and 18). According to this condition, the dimensions of the structure should ensure that the maximum stress in the critical section does not exceed the permissible value.

Let us view the problem from a different angle (§ 4). We require that the load acting on the whole structure should not exceed a permissible value. This condition may be expressed as follows:

$$P_{\max} \leq [P]$$

The permissible load is the  $k$ th part of the load at which the structure ceases to function properly and no longer serves the purpose for which it has been designed. The latter is generally called the *ultimate load* and sometimes the *breaking load* in the broader sense of the word (destruction of the structure means that it stops functioning properly).

Let us consider a system consisting of two steel rods  $AB$  and  $AC$  (Fig. 368) loaded with a force  $P$ . By the conventional method of design we determine forces  $N_1$  and  $N_2$  according to the formula

$$N_1 = N_2 = \frac{P}{2 \cos \alpha} = N$$

(from the equilibrium of point  $A$ ). Hence the cross-sectional area of each rod must be

$$S \geq \frac{N}{[\sigma]} = \frac{P}{2[\sigma] \cos \alpha}$$

By the method of permissible loads we have

$$P \leq [P]$$

Taking for the whole structure the same factor of safety  $k$  which we had assumed in the method of permissible stresses, we get  $[P] = \frac{P_u}{k}$ .

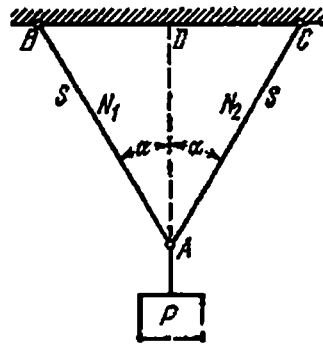


Fig. 368

The ultimate critical load,  $P_u$ , is the load at which the stresses in the rods reach the yield stress:

$$P_u = 2S\sigma_y \cos \alpha \quad (a)$$

Thus, the permissible load is

$$[P] = \frac{2S\sigma_y \cos \alpha}{k}$$

The strength condition (a) takes the form

$$P \leq \frac{2S\sigma_y \cos \alpha}{k}$$

Keeping in mind that  $\frac{\sigma_y}{k} = [\sigma]$ , we have

$$P \leq 2S[\sigma] \cos \alpha$$

wherefrom

$$S \geq \frac{P}{2[\sigma] \cos \alpha}$$

Hence, design for permissible loads gives the same results as the design for permissible stresses. This is always true of statically determinate structures with uniform stress distribution, when the material is utilized fully over the whole section.

#### § 148. Design of Statically Indeterminate Systems Under Tension or Compression by the Method of Permissible Loads

We get entirely different results if we apply the method of permissible loads for designing statically indeterminate systems in which the rods are made of a material capable of large plastic deformations, for example mild steel.

Let us consider as an example a system consisting of three rods loaded with force  $Q$  (Fig. 369). The rods are all assumed to be made of mild steel having yield stress  $\sigma_y$ . Let us denote the lengths of the side bars by  $l_1$ , and that of the middle bar by  $l_3$ . The permissible stress  $[\sigma] = \frac{\sigma_y}{k}$ . As in the previous case, we assume the ratio of the cross-sectional areas of all the bars to be known; let all the rods be of equal cross-sectional areas  $S$ . Solving the problem in the same way as in § 18, we get

$$N_3 = \frac{Q}{1 + 2 \cos^3 \alpha}, \quad N_1 = \frac{Q \cos^3 \alpha}{1 + 2 \cos^3 \alpha} = N_2$$

As  $N_2 > N_1$ , the middle rod is stressed more than the side rods; therefore  $S$  should be determined from the formula

$$S \geq \frac{N_2}{[\sigma]} = \frac{Q}{(1 + 2 \cos^3 \alpha) [\sigma]}$$

The side rods have the same cross-sectional area; they will have a slightly greater reserve.

Let us apply the method of permissible loads; the strength condition may be written as

$$Q \leq [Q] = \frac{Q_u}{k}$$

What is the ultimate load of the structure in this case? As the structure is made of a material having a yield plateau, in analogy with simple tension of a rod of the same material, the ultimate load is the load at which the whole structure starts yielding. Let us denote this load by  $Q_y^s$ . Until force  $Q$  is less than this value, the deformation (lowering of point  $A$ ) is possible only by increasing the load. As soon

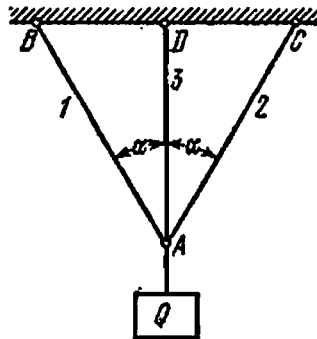


Fig. 369

as  $Q$  attains the value  $Q_y^s$ , further deformation occurs without any increase of the load and the structure gets out of order.

Let us study the process of deformation of the system to determine  $Q_y^s$ . As the middle rod is stressed more than the side rods, it attains the yield stress earlier than the side rods. Let us denote the load corresponding to this instant by  $Q_y$ , it will be

$$Q_y = (1 + 2 \cos^3 \alpha) N_y^s$$

where  $N_y^s = S \sigma_y$  is the force on the middle rod corresponding to its yield stress.

The stresses in the side rods, having the same cross-sectional area, will not have reached the yield stress as yet, and they will continue to be subjected to elastic deformation. For this deformation to occur, it is necessary that the load on the side rods be increased until the

stresses do not attain the yield stress. Only then will the maximum lifting capacity,  $Q_y^s$ , of the structure be reached.

As the yield stress  $\sigma_y$  has been already attained in the middle rod at load  $Q_y$ , further increase of the load does not affect it and, consequently, force  $N_3$  remains unchanged. Our statically indeterminate system is

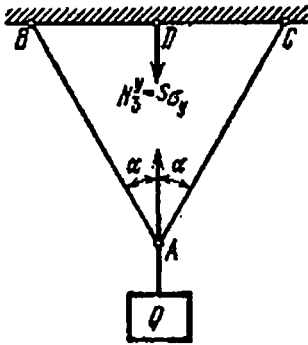


Fig. 370

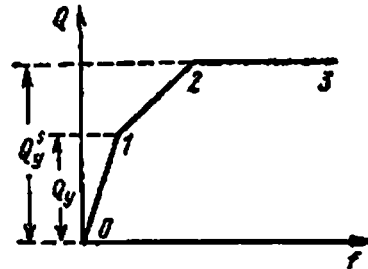


Fig. 371

transformed into a statically determinate one consisting of two rods  $AB$  and  $AC$  and loaded with the force  $Q$  acting at point  $A$  vertically downwards and the known force  $N_3^y$  equal to  $S\sigma_y$  (Fig. 370). The structure will continue to work in this way until

$$Q_y \leq Q \leq Q_y^s$$

Let us plot the graph of force  $Q$  versus displacement  $f$  to illustrate the course of deformation of the given structure (Fig. 371). As long as  $Q \leq Q_y$ , the distance by which point  $A$  lowers is equal to the elongation of the middle rod and is determined by the formula

$$f_{01} = \Delta l_3 = \frac{Q l_3}{(1 + 2\cos^2 \alpha) ES}$$

When  $Q$  falls in the interval  $Q_y \leq Q \leq Q_y^s$ , the displacement of point  $A$  has to be calculated as the lowering of the joint of the system of two rods  $AB$  and  $AC$  loaded at point  $A$  with force  $(Q - S\sigma_y)$ . From § 18 one knows that the lowering of point  $A$  is

$$f = \frac{\Delta l_1}{\cos \alpha}$$

In its turn

$$\Delta l_1 = \frac{N_1 l_1}{ES}, \quad N_1 = \frac{Q - S\sigma_y}{2\cos \alpha}$$

whence

$$\Delta l_1 = \frac{(Q - S\sigma_y) l_1}{2ES \cos \alpha}, \quad f_{12} = \frac{(Q - S\sigma_y) l_1}{2ES \cos^2 \alpha} = \frac{(Q - S\sigma_y) l_3}{2ES \cos^3 \alpha}$$

For  $f_{12}$  (in the second segment) we again get the equation of a straight line, but in this case not passing through the origin of coordinates. When force  $Q$  attains the value  $Q_y^s$ , the stresses in the side rods reach the yield stress, and further deformation of the system occurs without increase in load. The displacement curve is now parallel to the  $x$ -axis.

To determine the ultimate lifting capacity  $Q_y^s$  of the whole system we must, for a system of two rods loaded with force  $(Q - S\sigma_y)$ , find the value of  $Q$  for which the stresses in the side rods reach the yield stress (the same problem was solved in the previous section). Substituting  $Q - S\sigma_y$  for  $P$  in equation (a) of § 147, we get

$$(Q - S\sigma_y)_a = Q_y^s - S\sigma_y = 2S\sigma_y \cos \alpha$$

whencefrom

$$Q_y^s = S\sigma_y (1 + 2 \cos \alpha)$$

The permissible load will be

$$[Q] = \frac{Q_y^s}{k} = \frac{S\sigma_y (1 + 2 \cos \alpha)}{k}$$

Taking into account that

$$\frac{\sigma_y}{k} = [\sigma]$$

we get

$$[Q] = S[\sigma](1 + 2 \cos \alpha)$$

Finally

$$Q \leq [Q] = S[\sigma](1 + 2 \cos \alpha) \quad \text{and} \quad S \geq \frac{Q}{[\sigma](1 + 2 \cos \alpha)}$$

This value is less than the value obtained by the conventional method, i.e. less than

$$\frac{Q}{[\sigma](1 + 2 \cos^2 \alpha)}$$

At  $Q=4$  tf,  $\alpha=30^\circ$ ,  $[\sigma_s]=1000$  kgf/cm<sup>2</sup> (steel) we get:

(1) by the conventional method

$$S = \frac{4000}{1000(1 + 2 \cos^2 30^\circ)} = 1.74 \text{ cm}^2$$

(2) by the method of permissible loads

$$S = \frac{4000}{1000(1 + 2 \cos 30^\circ)} = 1.46 \text{ cm}^2$$

Thus, in designing a statically indeterminate system from a material having a yield plateau, the method of permissible loads is more econo-

mical than the method of permissible stresses. This is quite obvious: in the method of permissible stresses we take as the breaking load the force  $Q_y$  at which only the middle rod attains the yield stress (the side rods remaining understressed). In the method of permissible loads the ultimate lifting capacity is determined from the condition  $Q_y^s > Q_y$ . The material of all the three rods is fully employed at the load  $Q_y^s$ .

Hence, the method of permissible loads helps us to discover the latent sources of reducing the safety factor of statically indeterminate structures, increasing their design lifting capacity and achieving greater uniformity of strength of all their parts. Without any difficulty the method can be applied to the case when the cross-sectional areas of the middle and side rods are not equal.

The theoretical considerations discussed above were experimentally verified a number of times, and the calculated and experimental values of the ultimate load were found to be in good agreement with each other. This assures that the theoretical premises on which the method of permissible loads is based are correct.

#### § 149. Determination of Limiting Lifting Capacity of a Twisted Rod

The method of designing for permissible loads may also be applied to torsion. As already explained in § 148 the result obtained by this method in tension and compression differs from the one obtained by designing for permissible stresses only for a statically indeterminate system of bars, because the stresses are distributed uniformly over the cross sections of each bar. The situation is different in torsion: the stresses are not distributed uniformly over the cross sections.

In § 49 we determined the required dimensions of a twisted shaft from the condition that the maximum shearing stress at points on the contour of the cross section should not exceed the permissible shearing stress  $[\tau]$ . We conducted the analysis on the basis of permissible stresses without considering the inhomogeneity of stress distribution in the section.

In this method of analysis, as in the analysis of statically indeterminate systems, under tension or compression, we do not utilize the ultimate lifting capacity of the rod to the full. In § 49 we considered as critical the state of the material when the shearing stresses  $\tau$  equal the yield stress (for steel) only at the contour of the section (Fig. 372(a)). According to the distortion energy theory of strength,  $\tau_y$  should be equal to  $0.6 \sigma_y$ . The twisting moment in this case will be:

$$M_t = \frac{\pi r^3 \tau_y}{2}$$

and the angle of twist will be

$$\varphi_t = \frac{M_t l}{GJ_p} = \frac{\pi r^2 \tau_y l}{2G \frac{\pi r^4}{2}} = \frac{\tau_y l}{Gr}$$

To further increase of the angle of twist we must increase the twisting moment, because the material inside the rod is still in an elastic state. While the deformation increases, the increase in stress at the

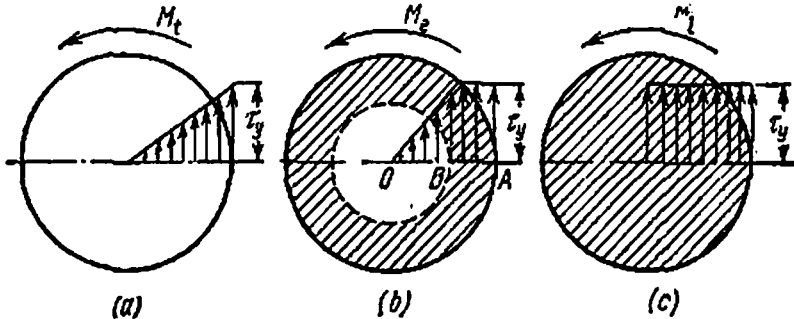


Fig. 372

edge of the section will stop (yielding), and at a certain value  $M > M_1$ , the distribution of stresses will correspond to the diagram shown in Fig. 372(b). The material inside the non-hatched circle of radius  $OB$  will continue to be in an elastic state as before.

The limiting state corresponding to complete utilization of the lifting capacity of the rod will be the state in which the elastic zone within the shaft is completely absent; in such a state the stress all over the section will be equal to the yield stress  $\tau_y$  (Fig. 372(c)).\*

The limiting twisting moment  $M_1$  may in this case be calculated as the sum of moments of all internal forces about the centre of the circle. For this we divide the area of the given section by concentric circles into a number of infinitesimal rings.

In the limiting state the stresses acting at each point of the section have a constant value equal to  $\tau_y$  (Fig. 372(c)). The internal force acting on an elementary area of radius  $\rho$  will be equal to (Fig. 373)  $\tau_y dS$ , and the moment of the internal force will be  $\rho \tau_y dS$ . By summing the elementary moments of the internal forces over the area of the whole circle, we get

$$dM_{in} = \tau_y \rho \sum dS = \tau_y \rho 2\pi \rho d\rho$$

\* This manner of working in the limiting state is only approximate. Actually, although the stresses at the centre change sharply, they do not increase in jumps, and at the surface they do not remain constant but increase due to work hardening of the material.



If we now write the equilibrium condition for the limiting twisting moment, we find that

$$M_t = \int_0^r 2\pi\tau_v \rho^2 d\rho = 0$$

wherefrom

$$M_t = \frac{2}{3} \pi r^3 \tau_v \quad (26.1)$$

The maximum permissible twisting moment for safety factor  $k$  is:

$$[M_t] = \frac{M_t}{k} = \frac{2\pi}{3} r^3 \frac{\tau_v}{k} = \frac{2\pi}{3} r^3 [\tau] \quad (26.2)$$

Therefore

$$r \geq \sqrt[3]{\frac{3M_t}{2\pi [\tau]}}$$

Simultaneously, from conventional analysis we have (§ 50)

$$r \geq \sqrt[3]{\frac{2M_t}{\pi [\tau]}}$$

Hence, the design on the basis of limiting lifting capacity enables us to reduce the shaft diameter in the ratio

$$\sqrt[3]{\frac{3}{2 \times 2}} = 0.91$$

Due to non-uniform stress distribution over the section in elastic state, the transition to design on the basis of limiting lifting capacity helps reduce the consumption of materials.

It should, however, be borne in mind that the above analysis holds true only under static loading, when the failure occurs due to yielding. A vast majority of the shafts under torsion, however, work under varying loads, when the failure occurs due to the appearance of fatigue cracks; therefore the analysis should be based on this factor. Obviously, the above analysis cannot be applied in the design of shafts in a majority of the cases. As we shall see later, the analysis of beams under bending will be entirely different.

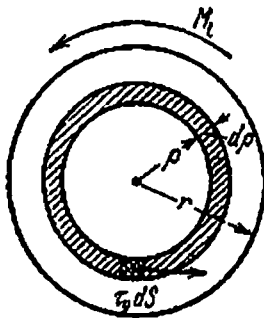


Fig. 373

The results obtained are of interest because they can be checked in

practice. It has been established experimentally that  $\tau_y$  obtained from formula (26.1) in terms of the limiting twisting moment, also determined experimentally, is sufficiently close to  $0.6\sigma_y$ , which it ought to be according to the distortion energy theory of strength.

### § 150. Selecting Beam Section for Permissible Loads

We have seen in torsion of shafts that, if the stresses are not distributed uniformly over the section, then the dimensions of the sections obtained for permissible stresses and permissible loads are different. A similar phenomenon is observed in the bending of beams.

In the analysis based on the method of permissible stresses we determine the size of the section from the condition

$$\sigma_{\max} = \frac{M_{\max}}{W} \leq [\sigma]$$

For materials having a yield zone (mild steel),  $[\sigma]$  is taken as

$$[\sigma] = \frac{\sigma_y}{k_y}$$

where  $\sigma_y$  is the yield stress, and  $k_y$  the corresponding safety factor.

Thus, we consider the material of the beam in critical state when the maximum stress in the critical section reaches the yield stress.

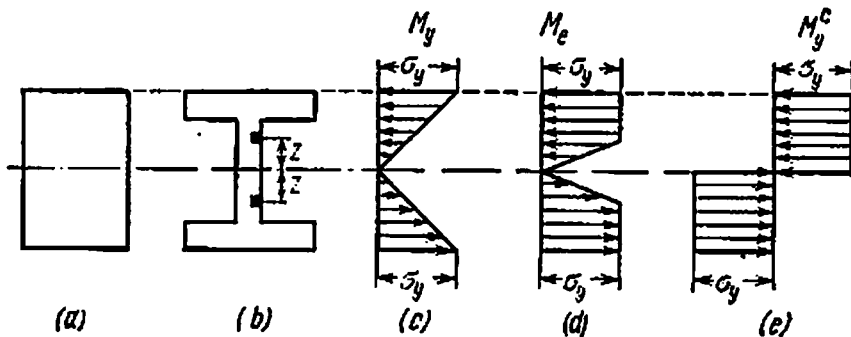


Fig. 374

Let us denote the bending moment giving rise to this state by  $M_y$ ; it corresponds to the attainment of maximum carrying capacity of the material in the maximum stressed layers of the critical section. However, this state does not mean that the maximum carrying capacity of the whole beam, as a structure, has been exhausted.

Let us consider a steel beam of symmetrical (for example, rectangular or I-section) section (Fig. 374(a) and (b)). The distribution of stresses in the critical section for a moment  $M_y$  is shown in Fig. 374(c); the yield stress is reached only in the boundary layers, and all the remaining portion of the beam remains in an elastic state. Therefore,

for further deformation of the beam we must increase the load and the bending moment: the lifting capacity of the beam remains to be exploited fully.

As we increase the moment the yield zone spreads towards the inside of the beam, the stress diagram appears as in Fig. 374(d) and in the limit, when the material begins to flow along the complete height of the section and the lifting capacity of the beam is exhausted, it takes the form of two rectangles (Fig. 374(e)). The bending moment in this state of the beam will be the limiting one for it as a whole. Further deformation of the beam will occur without any increase in the moment; a so-called *ductile hinge* will be formed in the critical section.

Let us determine this limiting moment  $M_y^c$ . It is equal to the sum of moments of forces about the neutral axis, as is evident from Fig. 374(e). A force  $\sigma_y dA$  acts on the elementary area  $dA$  at a distance  $z$  from the neutral axis; the moment of this force about the neutral axis is  $z\sigma_y dA$ . As the section is symmetric, it is sufficient to calculate the sum of moments of these forces for the upper or lower half of the section and double the result. Thus

$$M_y^c = 2 \int_{A/2} \sigma_y z dA$$

where  $A$  is the area of the whole section. As  $\sigma_y$  is constant for all points of the section, we have

$$M_y^c = 2\sigma_y \int_{A/2} z dA = 2\sigma_y S_{\max}$$

because the integral

$$\int_{A/2} z dA = S_{\max}$$

represents the static moment of one half of the section about the neutral axis.

The strength condition may be written as

$$M_{\max} \leq [M]$$

For a safety factor of  $k_y$  we get

$$[M] = \frac{M_y^c}{k_y} = \frac{2S_{\max}\sigma_y}{k_y} = 2S_{\max} [\sigma]$$

Hence the strength condition becomes

$$M_{\max} \leq 2S_{\max} [\sigma] \quad \text{or} \quad 2S_{\max} \geq \frac{M_{\max}}{[\sigma]} \quad (26.3)$$

Therefore, when analyzing a beam of symmetrical section for permissible load, its dimensions should be calculated not from the section modulus  $W$  but from the static moment of its half-section multiplied by two. For a rectangular section of height  $h$  and width  $b$

$$2S_{\max} = 2b \frac{h}{2} \frac{h}{4} = \frac{bh^2}{4} = 1.5 \frac{bh^2}{6} = 1.5W$$

Putting this value in formula (26.3), we get

$$W \geq \frac{M_{\max}}{1.5[\sigma]}$$

Thus, when designed for permissible load the required section modulus of a rectangular beam is 1.5 times less than when it is designed for permissible stresses.

For any symmetrical section the quantity  $2S_{\max}$  may be taken as a product of the section modulus and a constant  $n$  which depends upon the shape of the section:

$$2S_{\max} = nW$$

Therefore formula (26.3) takes the form

$$W \geq \frac{M_{\max}}{n[\sigma]} \quad (26.4)$$

For a rectangular section  $n=1.5$ , for I-sections of the type which we are considering  $n$  varies between 1.15 and 1.17; the mean value of  $n$  may be taken as 1.16. Thus, if we start designing steel beams of the commonly used sections by the method of permissible loads, we may increase their carrying capacity by 16%, which is equivalent to increasing their permissible stress. Such an increase in the permissible stress must be thoroughly investigated (during strength check) in conjunction with other possible factors which may cause failure of the beam.

It has been experimentally established that I-section steel beams never fail solely as a result of the yield stress appearing over the whole section. More commonly the failure is due to the loss of stability of the flange (Fig. 375) or the web. Therefore, special attention should be paid to checking the stability of the elements of the beam when higher permissible stress is used upon analyzing by the method of permissible loads.

If a repeated load acts on the beam, the possibility of failure due to the appearance of fatigue cracks should be taken into consideration. This requires an additional check against a failure of this nature occurring in the structure.

The analysis based on permissible loads is somewhat more complicated in the case of beams having one axis of symmetry, for example in T-section beams.

Figure 376 shows such a section and the diagram of normal stress distribution when the carrying capacity of the beam is reached. In such beams we must first determine the location of the neutral axis; even at this stage of working of the beam it does not pass through the centre of gravity of the section.

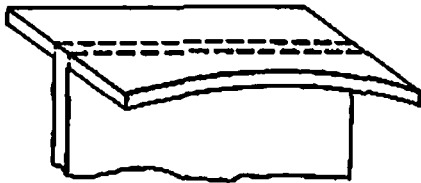


Fig. 375

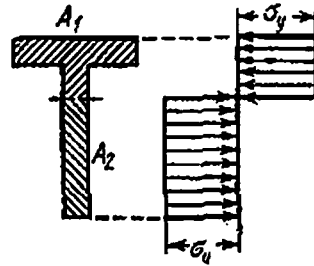


Fig. 376

Let us denote the area of the compressed portion of the section by  $A_1$  and the stretched portion by  $A_2$ . The condition that the sum of the tensile and compressive stresses should be equal gives

$$\sigma_y A_1 = \sigma_y A_2 \quad \text{or} \quad A_1 = A_2$$

The neutral axis divides the area of the section into two equal portions. In bending within the elastic limits the same condition brought us to the conclusion that the static moments of the compressed and stretched portions of the section should be equal and, therefore, the neutral axis should pass through the centre of gravity of the section. Here it divides the area of the section into two equal parts.

Having determined the location of the neutral axis, we see that

$$[M] = \frac{\sigma_y (S_1 + S_2)}{k_y}$$

where  $S_1$  and  $S_2$  are the static moments of the upper and lower halves of the area of the section about the neutral axis. The strength condition takes the form

$$(S_1 + S_2) \geq \frac{M_{max}}{[\sigma]} \tag{26.5}$$

The above discussion is valid for pure bending; the presence of shearing forces complicates the analysis.

**§ 151. Design of Statically Indeterminate Beams for Permissible Loads. The Fundamentals.**  
**Analysis of a Two-span Beam**

It was established in the preceding section that the formation of a ductile hinge is necessary to cause breakdown of a statically determinate beam.

In statically indeterminate beams the formation of one ductile hinge is not enough for full utilization of their bending capacity; it is essential that at least one more ductile hinge be formed. We shall explain this with the help of an example.

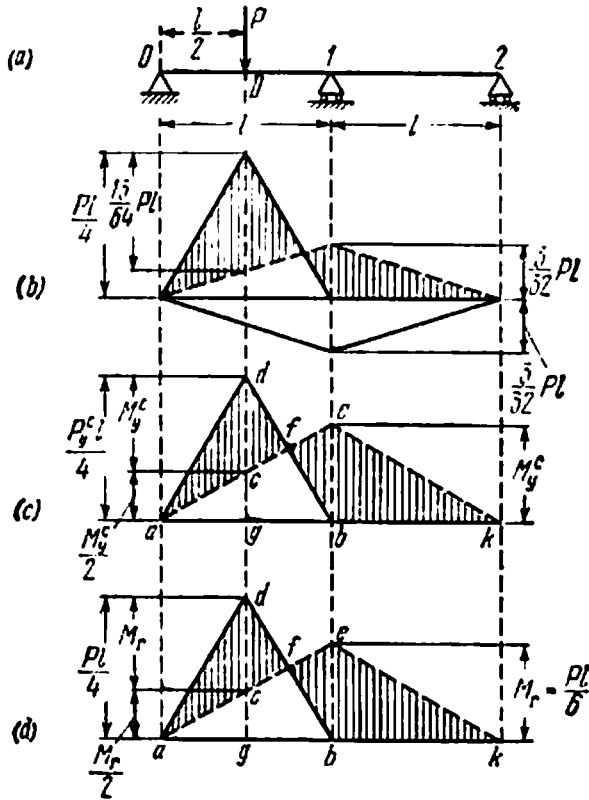


Fig. 377

Let us consider a two-span continuous beam of uniform section (Fig. 377(a)). Its bending moment diagram for work within the elastic limits (Fig. 377(b)) is the difference of the bending moment diagrams for force  $P$  and support moment  $M_1 = -\frac{3}{32}Pl$ . Graphic subtraction of the diagrams is shown by dotted lines. The resultant bending moment diagram is hatched. The maximum stressed sections are the section of application of the load with a moment  $M_p = \frac{Pl}{4} - \frac{3}{64}Pl = \frac{13}{64}Pl$  and the middle support with moment  $M_1 = \left| \frac{3}{32}Pl \right| < \frac{13}{64}Pl$ . When the load is increased, stresses in the beam become equal to the yield stress  $\sigma_y$  first of all in the top and bottom layers of the section under load  $P_y$  and may be expressed by the relation

$$\frac{13P_y l}{64W} = \sigma_y, \quad \text{wherefrom} \quad P_y = \frac{64W\sigma_y}{13l}$$

If the load is further increased, a ductile hinge is formed in this section when the bending moment (§ 150) becomes equal to:

$$M_y^c = 2\sigma_y S_{\max} = \sigma_y nW$$

However, under such a load the beam does not exhaust its maximum lifting capacity. It transforms into a statically determinate beam with a hinge at point  $D$  through which moment  $M_y^c$  is transmitted

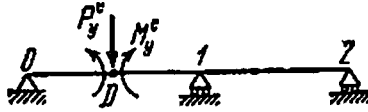


Fig. 378

(Fig. 378)—this beam is still capable of taking more load. When the load is further increased, the moment at point  $D$  remains constant whereas the moment at the support increases until it also becomes equal to  $M_y^c$ ; another ductile hinge is formed at the support, the left span transforms into a movable system and full lifting capacity of the beam is utilized as the load increases to  $P_y^c$ . The bending moment diagram of the beam for this state of loading, which is shown in Fig. 377(c), is the diagram for breaking moments. It is the difference of the ordinates of triangle  $adb$  with maximum ordinate  $\frac{P_y^c l}{4}$  in the section of load application and triangle  $ae k$  with an ordinate  $M_y^c$  at the support  $1$  and  $\frac{M_y^c}{2}$  in the section of load application. The breaking load  $P_y^c$  is determined from the condition that segment  $cd$  equal to  $\frac{P_y^c l}{4} - \frac{M_y^c}{2}$  must also be equal to  $M_y^c$ :

$$\frac{P_y^c l}{4} - \frac{M_y^c}{2} = M_y^c$$

wherefrom

$$M_y^c = \frac{P_y^c l}{6} = nW\sigma_y, \quad P_y^c = \frac{6M_y^c}{l} = \frac{6nW\sigma_y}{l} \quad (26.6)$$

The strength condition may be written as follows (§ 147):

$$P \leq [P] \quad (26.7)$$

where  $P$  is the load acting on the beam, and  $[P]$  is the permissible load.

To obtain  $[P]$  we divide both sides of equation (26.6) by the safety factor  $k$  and get

$$[P] = \frac{P_y^c}{k} = \frac{6M_y^c}{kl} = \frac{6nW\sigma_y}{kl} = \frac{6nW[\sigma]}{l} \quad (26.8)$$

Substituting this value of  $|P|$  in equation (26.7), we obtain

$$P \leq \frac{6nW|\sigma|}{l}$$

wherefrom

$$W \geq \frac{Pl}{6n|\sigma|} = \frac{M_r}{n|\sigma|} \quad (26.9)$$

where  $M_r = \frac{Pl}{6}$  is the *reduced bending moment* in sections  $I$  and  $D$ . Consequently, the beam section in this example may be selected in accordance with the reduced moment  $M_r = \frac{Pl}{6}$  and the permissible stress  $n|\sigma|$ .

It is evident from the formulas  $M_r = \frac{Pl}{6}$  and  $M_y^c = \frac{P_y^c l}{6}$  that the ordinates of the diagram of reduced moments (Fig. 377(d)) are proportional to the ordinates of the diagram of breaking moments and are obtained from them by replacing the breaking load  $P_y^c$  by the actual load  $P$ .

If we design the beam for permissible stress, we should take  $M_{\max} = \frac{13}{64}Pl > \frac{Pl}{6}$  (Fig. 377(b)) as the reduced moment and  $|\sigma|$  as the permissible stress. Hence, designing statically indeterminate beams for permissible loads has a double advantage—the permissible stress increases as in statically determinate beams, and the diagram of reduced moments “shrinks”, i.e. its ordinates in corresponding sections become smaller.

The increase in the lifting capacity of the beam is given by the ratio

$$\frac{P_y^c}{P_y} = \frac{6n\sigma_y W \times 13l}{l \times 64W^2 \sigma_y} = \frac{78}{64}n$$

Assuming that  $n=1.16$  (for I-beams, § 150), we find that the lifting capacity of the beam increases by 40% if it is designed according to the new method.

In the example discussed above the diagram of reduced moments (Fig. 377(c)) is obtained from the condition that in the two maximum stressed sections the bending moments are equal. Therefore in the design of beams of uniform section this method is sometimes referred to as the *method of equal moments*.

Keeping this in mind, we can plot the diagram of reduced moments (for permissible loads) graphically: first we plot the bending moment diagram of force  $P$  for span  $l$  of the beam ( $adb$ ) and then plot diagram  $ack$  of support moments such that  $be=cd$  (this can be done by dividing



If another force  $P$  were acting at the middle of the second span, the diagram of reduced moments would remain unaffected (Fig. 379), i.e. no reinforcement of the beam would be required even if an addi-

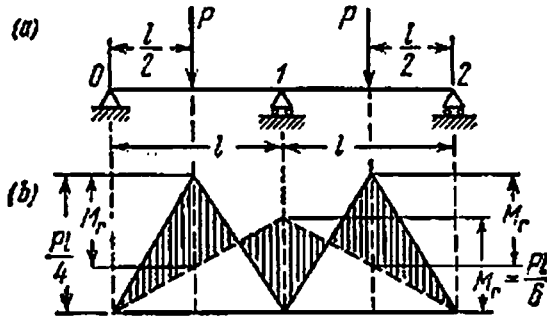


Fig. 379

tional force were applied. There would only be a change in the order of appearance of the ductile hinges: a hinge would first be formed at the middle support and then in the sections where the two forces act.

### § 152. Analysis of a Three-span Beam

Let us now consider a beam having an additional span in the middle (Fig. 380(a)). The bending moment diagram of this beam for work within the elastic region is shown in Fig. 380(b). When the load is gradually increased, ductile hinges are first formed at the intermediate support 1 and the centre (approximately) of the middle span (Fig. 380(c)). However, the beam is still capable of taking further loads until a third hinge forms at support 2. The final diagram of breaking moments is shown in Fig. 380(d). The limiting value of the moment is:

$$M_y^c = \frac{1}{2} \frac{q_y^c l^2}{8} = \frac{q_y^c l^2}{16}$$

and the reduced moment is:

$$M_r = \frac{q l^2}{16}$$

The required section modulus is:

$$W \geq \frac{M_r}{n [\sigma]} = \frac{q l^2}{16n [\sigma]}$$

Thus, three ductile hinges must be formed before the middle span fails, and the moments in all the three hinges will be equal. If all the spans of the beam were loaded, it would be essential to check the possibility of failure for each span by plotting the corresponding diagrams of reduced moments (by equating their values in the critical sections)

and select  $W$  for the maximum value of  $M_r$ , thus obtained. As a concrete example let us load the three-span beam (Fig. 381) by a uniformly distributed force  $q$  in the middle span and concentrated forces  $P=2ql$

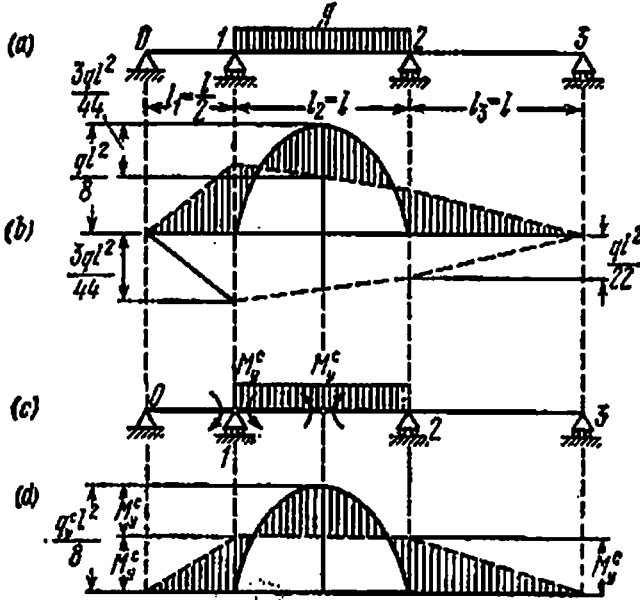


Fig. 380

acting at the centre of each side span. The reduced moments  $M_r$  for all three spans are shown in the diagram with dotted lines; their values are as follows:

$$M_r = \frac{ql^2}{6}, \quad M_r = \frac{ql^2}{16}, \quad M_r = \frac{ql^2}{3}$$

The section should be selected for the moment  $M_r = \frac{ql^2}{3}$ ; the section modulus should be  $W \geq \frac{ql^2}{3n[\sigma]}$ .

Similarly, we can analyze a beam with any number of spans by assessing the possibility of failure in each span separately.

The method of designing continuous beams explained above employs a number of approximations and restrictions. Firstly, it is valid only for static loads. Secondly, the physical picture of failure of the beam is much more complicated even for static loads than the highly simplified concept of ductile hinge formation, which we employed in the above discussion. Plastic deformation is not limited to a particular section but covers the whole beam length. In addition, the maximum lifting capacity of the beam can be restricted not only by its plastic deformation, but also by the violation of its stability as a whole or the

flange plates and web separately. Therefore, if this method is applied in actual design, greater attention should be paid to the stability of the beam even though the loading may be static.

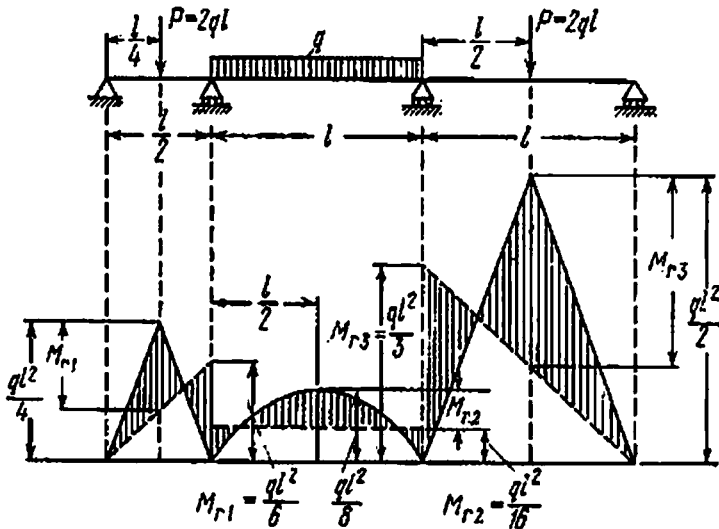


Fig. 38t

Experiments on the failure of statically indeterminate beams under static loading reveal that, if failure due to lack of stability is prevented, the breaking load calculated theoretically by the above method concurs well with the experimentally determined value.

### § 153. Fundamentals of Design by the Method of Limiting States

Design by the method of limiting states is outside the scope of the basic course on strength of materials. It is compulsory only in design of building structures and is not yet used in mechanical engineering. However, keeping in mind that the method is ultimately based upon strength of materials, we give below the fundamental concepts of design of building structures by the method of limiting states to enable those studying this method to coordinate its methods and terminology with that of the strength of materials.

Two groups of limiting states are considered below. The first group deals with limiting states that appear due to loss of load carrying capacity or because the structure is not fit for working. The second group deals with those that appear because the structure is not fit for normal functioning.

The main limiting states of the first group are failure, loss of stability, excessive opening of cracks, etc.

The limiting states of the second group include conditions that hin-

der normal functioning of the structure or reduce its service life due mainly to impermissibly large displacements (deflections, angles of rotation, etc.).

The *rated strength*,  $R^r$ , which is specified by design standards on the basis of control conditions and statistical variation of strength, is the main parameter characterizing the resistance of materials to the action of external forces. We may choose as rated strength the yield stress, ultimate strength, fatigue strength, critical stress and other similar characteristics of the material, which in the course of strength of materials are called *critical* and are denoted by  $p^{cr}$ .

The possible harmful deviation of strength characteristics from the rated strength is taken into account by the *safety factor of material*,  $k$ , by which the rated strength is divided.

The numerical value of  $k$  depends on the properties of materials and their statistical variation. When calculating the load carrying capacity of structures, the value of  $k$  is not taken less than 1.1.

By the *design strength of material*,  $R$ , we mean the strength which is considered while designing a structure and is obtained by dividing  $R^r$  by  $k$ :

$$R = \frac{R^r}{k} \quad (26.10)$$

The *coefficient of operating conditions*,  $m$ , takes care of the special features of a systematic nature that arise during actual functioning of materials, elements and joints and structures, but which are not directly reflected in the design procedure.

Coefficient  $m$  takes into account the effect of temperature, humidity and corroding effect of the atmosphere, length of time during which forces act and some other factors.

The reliability and capital investment factors in design of buildings and structures are accounted for in a number of cases by the *coefficient of reliability*,  $k_r$ . The numerical values of coefficients  $k$ ,  $m$ , and  $k_r$  are established by standards.

Thus, formula (26.10) for design strength  $R$  with suitable coefficients  $m$  and  $k_r$  when necessary may be written as follows:

$$R = m \frac{R^r}{k_r k} \quad (26.11)$$

In the courses of strength of materials design strength  $R$  is known as permissible stress and is denoted by  $[\sigma]$  or  $[\tau]$ . However,  $R$  contains a more detailed break-up of the safety factors and does not provide for safety against overloading. When a structure is designed by the method of limiting states, the safety factor against overloading is calculated by a special method, which will be discussed later.

The loads are defined mainly by their *rated* values, denoted by  $P^r$ . These are specified by standards for various structures.

The probable harmful deviation of loads from the rated values due to variation of loads or changes in conditions of normal functioning is taken account of by the *coefficient of overloading*,  $n$ . Coefficient  $n$  is the safety factor against overloading. The overloading coefficients may be different for different loads even if the latter are applied to the structure simultaneously, for instance, for permanent and temporary loads. This is the difference between this design method and the one in strength of materials in which the safety factor against overloading is the same for all loads simultaneously acting on a structure and is taken into account by a common safety factor.

The loads used in actual design are obtained by multiplying the rated values with the corresponding overloading coefficients  $n$ , and are known as *design loads*.

If the different values of the overloading coefficient for permanent and temporary loads are taken into account, then, for instance, the design bending moment  $M$  due to simultaneous action of permanent and temporary forces on a beam may be defined as

$$M = n_1 M'_{\text{perm}} + n_2 M'_{\text{temp}} \quad (26.12)$$

Structures should be designed by considering the possible unfavourable combinations of loads (for example, simultaneous loading of a bridge by a train, breaking forces and wind, or simultaneous loading of power transmission line towers by wind and one-sided tension due to snapping of wire in the adjacent span). The probability of such combinations is taken into account by the *coefficient of combination*,  $n_c$ . The values of coefficients  $n$  and  $n_c$  and the recommendations regarding their application are available in standards.

Thus, if the standards require that a coefficient of combination for temporary loads be included in the design of a structure, formula (26.12) for the design moment becomes

$$M = n_1 M'_{\text{perm}} + n_c n_2 M'_{\text{temp}} \quad (26.13)$$

If the standards do not contain instructions for the accounting of inelastic deformations, it is permitted to determine forces in statically indeterminate systems on the assumption that deformations of the structure remain in the elastic region. The strength condition, for instance, in bending, can then be written as follows:

$$\frac{M}{W} \leq R$$

Taking into account formulas (26.11) and (26.13), we get

$$\frac{n_1 M'_{\text{perm}} + n_c n_2 M'_{\text{temp}}}{W} \leq m \frac{R^r}{k_r k}$$

If the strength is to be checked for limiting states of the second group, we must determine the elastic deformation or displacement (elongation, twist angle, deflection) due to normal load. The deformation thus found must not exceed the permissible value laid down in the standards.

# PART VIII

## Stability of Elements of Structures

### CHAPTER 27

## Stability of Bars Under Compression

### § 154. Introduction. Fundamentals of Stability of Shape of Compressed Bars

In all previous discussions we determined the cross-sectional dimensions of bars from their strength condition. However, a bar may fail not because of insufficient strength but because it does not retain its designed shape. This changes the nature of stressed state of the bar.

The most typical example is that of a bar compressed by axial forces  $P$ . Until now we have checked the strength of bars by the following condition:

$$\sigma = \frac{P}{A} \leq [\sigma], \quad \text{where} \quad [\sigma] = \frac{\sigma_y}{k_y} \quad \text{or} \quad [\sigma] = \frac{\sigma_u}{k_u}$$

This condition is based on the assumption that the bar works under axial compression right up to the moment of its failure due to  $\sigma_y$  or  $\sigma_u$ . However, even the simplest of experiments shows that it is not always possible to load the bar up to its yield stress or ultimate strength.

If we subject a thin wooden scale to axial compression, it may fail due to bending. At the time of failure the compressive force acting on the scale will be considerably less than the force which the scale can withstand before its ultimate strength is reached. The scale fails because it does not retain its designed shape of a rectangle but bends, giving rise to bending moments due to forces  $P$  and, consequently, to additional bending stress: the scale loses its stability.

Therefore, for safe working of a structure it is not enough for it to have sufficient strength; it is essential that all its elements are stable and their deformation under the action of external forces is within such limits that the nature of their work remains unaffected. Hence, in a number of cases, in particular in bars under compression, the strength check must be substantiated by a check of stability. Before we carry out such a check it is necessary to get closely acquainted with the conditions which lead to the bar losing its stability.

Let us consider a bar sufficiently longer than its cross-sectional size, hinged at both ends (Fig. 382) and loaded by a gradually increasing axial force  $P$ . We notice that the bar remains straight as long as  $P$  is small. If we try to bend it to one side by applying a momentary horizontal force, it comes back to its original shape upon the removal of the external force causing deflection after doing a few oscillations.

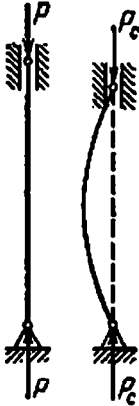


Fig. 382

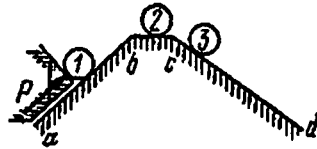


Fig. 383

As force  $P$  increases, the bar takes longer to return to its original stable position; finally force  $P$  may attain a value at which the bar fails to straighten when it is slightly bent to one side. If we try to straighten the bar without removing force  $P$ , we find that it is incapable of remaining straight. In other words, at a particular value of  $P$ , called *critical force*  $P_c$ , the straight-line shape ceases to be stable for a bar under compression.\*

The transition to critical value is sudden; a small decrease of the compressive force from the critical value is enough to make the straight-line shape stable again.

On the other hand, if the compressive force  $P$  is slightly higher than the critical value, the straight-line shape becomes extremely unstable. In this case a small eccentricity of the applied force or the non-uniformity of the bar material is enough not only to bend the bar but also to increase the curvature of bent bar due to a continuously increasing bending moment; the process of bending comes to a stop either when a new position of equilibrium is achieved or when the bar completely breaks down.

Thus, for all practical purposes we can consider critical force  $P_c$  equivalent to a load which "cripples" the compressed bar and creates a condition in which normal working of the bar becomes impossible.

\* Investigations reveal that instability begins at values of  $P$  which exceed the critical force only by a second-order quantity.

It must be kept in mind that "failure" of the bar due to a force greater than the critical occurs only when there is no obstacle to bending. Therefore failure may be avoided if buckling is prevented by a side support which restricts further bending.

Usually such a possibility is remote—the critical compressive force should practically be considered as the lower limit that causes "failure" of the bar.

The loss of stability under compression may be explained by the analogy following from mechanics of solid bodies (Fig. 383). Let us roll a cylinder on an inclined plane  $ab$  which changes into a small horizontal platform  $bc$  and then an inclined plane  $cd$  of opposite inclination. The cylinder remains stable as long as we lift it along plane  $ab$  holding it with a support perpendicular to the inclined plane. Equilibrium of the cylinder is immaterial when it rolls on platform  $bc$ . As soon as it reaches point  $c$  its equilibrium becomes unstable—the slightest push to the right is enough to make it go rolling down.

The physical picture of loss of stability in the compressed bar described above can be actually reproduced in any laboratory with very elementary equipment \*. This description is not a theoretical or ideal picture of working of a compressed bar, but a real one showing how actually a bar works when it is acted upon by compressive forces.

The loss of straight-line stable state by a compressed bar is sometimes referred to as *axial bending*, because it manifests itself in the form of considerable bending of the bar under axial compression. Therefore, instead of check on stability the term "check on axial bending" is still quite prevalent, although it is not very appropriate, because we are basically interested not in the check on bending but in the check on stability of the straight-line shape of the bar.

Having established the concept of critical force as a "crippling" load which puts an end to the normal functioning of the bar, we can easily derive a condition for checking the stability of bars identical to the strength condition.

Critical force  $P_c$  gives rise to "critical stresses" in the bar, which are denoted by  $\sigma_c = \frac{P_c}{A}$ . Critical stresses in the compressed bar are stresses at which the bar fails. Therefore, to ensure stability of a straight bar compressed by forces  $P$ , it is essential that the strength check ( $\sigma = \frac{P}{A} \leq [\sigma]$ ) should be accompanied by a stability check

$$\sigma = \frac{P}{A} \leq [\sigma_s] \quad (27.1)$$

---

\* See N. M. Belyaev, *Laboratory Experiments on Strength of Materials*, Gos-tekhnizdat, Moscow, 1951 (in Russian), § 85.



where  $[\sigma_s]$  is the permissible stress for stability equal to critical stress divided by a factor of stability:

$$[\sigma_s] = \frac{\sigma_c}{k_s}$$

Before we explain how stability is to be checked, we must show how to determine  $\sigma_c$  and how to select  $k_s$ .

### § 155. Euler's Formula for Critical Force

For determining critical stress  $\sigma_c$  we must first calculate the critical force,  $P_c$ , i.e. the minimum axial compressive force which a slightly bent compressed bar can withstand and yet remain in equilibrium. This problem was first solved by Leonhard Euler in 1774.

Let us point out that the problem is entirely different from all problems discussed in previous sections of this book. Until now we have determined deformation of a bar when the external forces acting on it

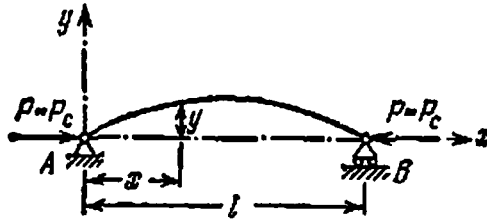


Fig. 384

are known. Our problem is just the opposite: we assume a certain deflection of the bar's axis and then determine the axial compressive force  $P$  at which the assumed deflection occurs.

Consider a uniform straight bar hinged at both ends. One of the supports permits axial displacement of the corresponding end of the bar (Fig. 384). The dead weight of the bar is negligible. Let us load the bar with an axial compressive force  $P = P_c$  and impart to it a slight deflection in the plane of minimum rigidity; the bar remains in equilibrium in the bent state because  $P = P_c$ .

The imparted deflection is assumed to be very small. Therefore, the problem may be solved by using the approximate differential equation of the deflected axis of the bar (§ 82). Selecting the origin of coordinates at point A and directing the coordinate axes as shown in Fig. 384, we get from equation (15.7)

$$EJ \frac{d^2 y}{dx^2} = M(x)$$

Consider a section at a distance  $x$  from the origin of coordinates. The ordinate of the deflected axis in this section is  $y$  and the bending mo-

ment is:

$$M(x) = -Py$$

When compared with Fig. 384 the bending moment is found to be negative although the ordinates are positive for the selected direction of the  $y$ -axis\*. (Had the bar been bent with its convexity downwards, the moment would have been positive, the  $y$ -ordinate would have been negative and  $M(x) = -Py$ .)

Consequently, differential equation (15.7) may be written as follows:

$$EJ \frac{d^2y}{dx^2} = -Py \quad (27.2)$$

Dividing both sides of the equation by  $EJ$  and denoting  $\frac{P}{EJ}$  by  $k^2$ , we may rewrite the above equation as follows:

$$\frac{d^2y}{dx^2} + k^2y = 0 \quad (27.3)$$

The general solution of this equation is:

$$y = a \sin kx + b \cos kx \quad (27.4)$$

This solution contains three unknowns: constants of integration  $a$  and  $b$  and  $k = \sqrt{\frac{P}{EJ}}$ , because the critical force is not known.

The boundary conditions of the bar give us two equations:

$$\text{at point } A: \quad x=0 \quad \text{deflection } y=0$$

$$\text{at point } B: \quad x=l \quad \text{deflection } y=0$$

It ensues from the first condition (since  $\sin kx=0$  and  $\cos kx=1$ ) that

$$0 = b$$

Thus, the bent axis is a sine curve having equation

$$y = a \sin kx \quad (27.5)$$

Upon substituting the second equation

$$y=0 \quad \text{and} \quad x=l$$

we obtain

$$0 = a \sin kl \quad (27.6)$$

It follows that either  $a$  or  $kl$  must be zero.

If  $a$  is equal to zero, then from equation (27.5) we see that the deflection of the bar is zero in all sections, i.e. the bar remains straight.

\* If the  $y$ -axis is directed downwards, a positive bending moment  $M(x)$  will correspond to a positive deflection  $y$ . However, in this case the curvature will be negative and  $d^2y/dx^2 < 0$ . Hence, the signs in equation (27.2) will remain the same.

This contradicts the assumptions made at the very beginning of this derivation. Hence,  $\sin kl=0$ , and  $kl$  may have the following values

$$kl = 0, \pi, 2\pi, 3\pi, \dots, n\pi \tag{27.7}$$

where  $n$  is an arbitrary integer.

This yields  $k = \frac{\pi n}{l}$ , and since  $k = \sqrt{\frac{P}{EJ}}$ ,

$$\frac{P}{EJ} = \frac{\pi^2}{l^2} n^2 \quad \text{or} \quad P = \frac{\pi^2 EJ}{l^2} n^2 \tag{27.8}$$

In other words, a load capable of holding a slightly deflected bar in equilibrium can, in theory, have a number of values. However, as we are interested in determining the minimum axial compressive force at which axial bending may occur, we must take  $n = n_{\min}$ .

According to the first root,  $n=0$ , the critical force  $P_c$  must be zero, but this contradicts the given data. Therefore this root is ruled out and the minimum value of  $n$  is taken as  $n=1$ . This gives

$$P_c = \frac{\pi^2 EJ}{l^2} \tag{27.9}$$

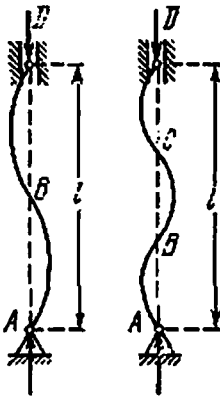


Fig. 385

(Here  $J$  is the minimum moment of inertia of the bar cross section.)

This is known as Euler's formula for compressed bars hinged at the

ends. This value of the critical force (27.9) corresponds to bending of the bar along a sine curve with one half-wave (formula (27.5)):

$$y = a \sin \frac{\pi x}{l} \tag{27.10}$$

Higher values of the critical force correspond to bending the bar along a sine curve with two, three, etc. half-waves (Fig. 385):

$$\left. \begin{aligned} P_c &= \frac{4\pi^2 EJ}{l^2}, & k &= \frac{2\pi}{l}, & y &= a \sin \frac{2\pi x}{l} \\ P_c &= \frac{9\pi^2 EJ}{l^2}, & k &= \frac{3\pi}{l}, & y &= a \sin \frac{3\pi x}{l} \end{aligned} \right\} \tag{27.11}$$

Hence, the greater the number of inflection points in the sine curve of the deflected axis of the bar, the greater the critical force must be. Intensive investigations show that the equilibrium modes determined by formula (27.11) are not stable; stable equilibrium modes can be

achieved only if we place intermediate supports at points  $B$  and  $C$  (Fig. 385).

Thus, we have solved the problem which we had set before ourselves: the critical force for our bar is calculated by the formula

$$P_c = \frac{\pi^2 EJ}{l^2}$$

and the deflected axis is represented by the sine curve

$$y = a \sin \frac{\pi x}{l}$$

The constant of integration,  $a$ , has remained undetermined; its physical nature will become clear if we substitute  $x = \frac{l}{2}$  in the equation of the sine curve. The condition  $y_{x=l/2}$  (deflection at the middle of the bar) yields

$$y_{\max} = f = a$$

This means that  $a$  is the deflection of the bar at its middle point. Deflection  $f$  remains undetermined, because the deflected bar can remain in equilibrium in various deflected positions from the straight-line shape for a single value of critical force  $P$ , provided the deflections are small.

Deflection  $f$  should be small enough to enable us to use the approximate differential equation of the deflected axis, i.e.  $\left(\frac{dy}{dx}\right)^2$  should be negligible as compared to unity (§ 82).

Having found the critical force, we can immediately determine critical stress  $\sigma_c$  by dividing  $P_c$  by the cross-sectional area,  $A$ . As the critical force was determined by considering the deformation of the bar which is not much affected by local weakenings in the section, the moment of inertia used in the expression for  $P_c$  is  $J_t = i^2 A_t$ . Thus while calculating critical stress or writing the condition of stability we must consider not the weakened but the total area  $A_t$  of unweakened section. Then

$$\sigma_c = \frac{P_c}{A_t} = \frac{\pi^2 EJ_t}{l^2 A_t} = \frac{\pi^2 E i^2}{l^2} = \frac{\pi^2 E}{(l/i)^2} = \frac{\pi^2 E}{\lambda^2} \quad (27.12)$$

We find that critical stress in a bar of a given material is inversely proportional to the square of the ratio of its length to the minimum radius of gyration of its section. This ratio,  $\lambda = \frac{l}{i}$ , is called the *flexibility* of the bar and plays an important part in all stability checks of compressed bars.

It is evident from formula (27.12) that the critical stress may be extremely small in long and thin bars; it may be less than the permissi-

ble stress  $[\sigma]$ . For steel with ultimate strength of  $4000 \text{ kgf/cm}^2$  the permissible stress may be assumed equal to  $[\sigma] = 1600 \text{ kgf/cm}^2$ ; for a bar having flexibility  $\lambda = 150$  and modulus of elasticity of the material  $E = 2 \times 10^6 \text{ kgf/cm}^2$  the critical stress will be

$$\sigma_c = \frac{\pi^2 \times 2 \times 10^6}{150^2} = 877 \text{ kgf/cm}^2 < 1600 \text{ kgf/cm}^2$$

Had the cross-sectional area of the compressed bar of given flexibility been determined from the strength condition, the bar would have failed due to loss of stability of its straight-line shape.

### § 156. Effect of Constraining the Bar Ends

Euler's formula was obtained by integrating the approximate differential equation of the deflected axis of the bar with ends constrained by a particular method (hinged). This implies that the expression for determining the critical force is valid only for bars with hinged ends,



Fig. 386

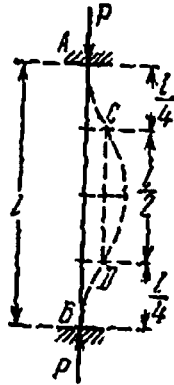


Fig. 387



Fig. 388

and changes when the method of constraint is different. If the ends of the bar are hinged this type of fixation will be referred to as the *basic method of constraint*. All other methods of constraint will be discussed by comparing them to the basic method.

If we repeat the derivation for a bar rigidly fixed at one end and loaded at the other by an axial compressive force  $P$  (Fig. 386), we shall obtain a different expression for the critical force and, consequently, for the critical stress. Leaving it to the reader to derive such an expression himself, we proceed to explain how the expression for the critical force can be obtained in this case with the help of the following simple considerations.

Suppose the bar retains its equilibrium under critical force  $P$  when it bulges slightly along the curve  $AB$ . Comparing Figs. 382 and 386, we observe that the deflected axis of the bar rigidly fixed at one end is in the same conditions as the upper half of a bar of double length hinged at both ends.

This means that the critical force in a bar of length  $l$  which is fixed at one end and free at the other is the same as in a bar of length  $2l$  hinged at both ends:

$$P_c = \frac{\pi^2 EJ}{(2l)^2} = \frac{\pi^2 EJ}{4l^2} \quad (27.13)$$

If we consider a bar in which both ends are rigidly fixed and are incapable of rotation (Fig. 387), we observe that the middle portion of length  $\frac{l}{2}$  of the deflected bar works under the same conditions as a bar which is hinged at both ends (points of inflection  $C$  and  $D$  may be considered as hinges, because the bending moment at these points is zero).

Thus, the critical force in a bar of length  $l$  which is fixed at both ends is equal to the critical force in a bar of length  $\frac{l}{2}$  in which the ends are fixed by the basic method of constraint:

$$P_c = \frac{\pi^2 EJ}{(l/2)^2} = \frac{4\pi^2 EJ}{l^2} \quad (27.14)$$

Formulas (27.13) and (27.14) may be combined with the formula for critical force in the basic method of constraint  $P_c = \frac{\pi^2 EJ}{l^2}$ , and the generalized formula may be written as follows:

$$P_c = \frac{\pi^2 EJ}{(\mu l)^2} \quad (27.15)$$

Here  $\mu$  is the *coefficient of length* with the following values:

when both ends are hinged (basic case)	$\mu = 1$
when one end is free and the other rigidly fixed	$\mu = 2$
when both ends are rigidly fixed	$\mu = 1/2$

For the bar shown in Fig. 388 which is rigidly fixed at one end and hinged at the other, coefficient  $\mu$  is approximately found to be equal to  $\frac{1}{\sqrt{2}} \approx 0.7$ , and the critical force is:

$$P_c \approx \frac{\pi^2 EJ}{(0.7l)^2} \approx 2 \frac{\pi^2 EJ}{l^2} \quad (27.16)$$

The product  $\mu l$  is called the *reduced (free) length*; with the help of the coefficient of length a bar with arbitrarily constrained ends can be reduced to a bar in which the ends are constrained by the basic method: while calculating flexibility the actual length of the bar must be replaced by the reduced length  $\mu l$ . The concept of reduced length was first

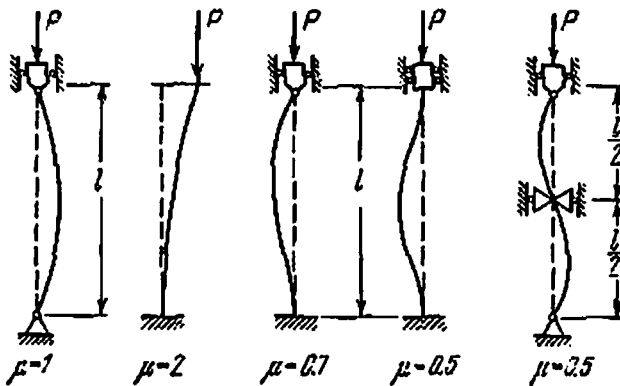


Fig. 389

introduced by Prof. F. Yasinskii \* of the St. Petersburg Institute of Railway Engineers.

Formula (27.12) for critical stresses in bars with hinged ends may be generalized for other types of constraints by introducing in the denominator the reduced flexibility

$$\lambda = \frac{\mu l}{i} \quad \text{and} \quad \sigma_c = \frac{\pi^2 E}{\lambda^2} \quad (27.12')$$

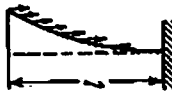
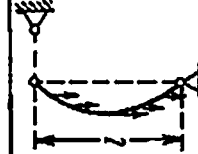

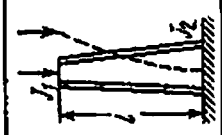
The values of coefficient  $\mu$  for some types of constraints are given in Fig. 389.

In practice, however, we rarely find constraints exactly in the form as they have been considered here (Fig. 389). Cylindrical hinges are generally used instead of hinged supports. Such bars may be considered as simply hinged if they buckle in a plane perpendicular to the axis of the hinges. If, however, the bar bends in the plane of axes, then the ends should be considered rigidly fixed (with the reservations, discussed below for rigidly fixed ends).

In structures we often find compressed bars, which are riveted or welded at the ends to other elements quite often with the help of cover plates. Such a constraint cannot, however, be considered rigid, because the elements to which the compressed bars are secured are themselves not absolutely rigid. Incidentally, even a slight rotation of the fixed end in the fixation is enough to render it more close to a hinged con-

\* *Proceedings of the Conference of Railway Engineers, St. Petersburg, 1892 (in Russian).*

Table 18

Values of Critical Force	Type of load	Type of bar	Critical force	Coefficient of length																																
Uniformly distributed over the bar length (dead weight) $q$			$(q l)_c = \frac{\pi^2 E J}{(\mu l)^2}$ $= 0.79 \frac{\pi^2 E J}{l^2}$	$\mu = 1.12$																																
Ditto			$(q l)_c = \frac{\pi^2 E J}{(\mu l)^2}$ $= 1.9 \frac{\pi^2 E J}{l^2}$	$\mu = 0.725$																																
Two forces $P_1$ and $P_2$ $\frac{P_1 - P_2}{P_1} = m$ $J_2 \div J_1 = n$			$(P_1 + P_2)_c = \frac{\pi^2 E J}{(\mu l)^2}$ $\mu \text{ from the table}$	<table border="1"> <tr> <td><math>n</math></td> <td><math>m</math></td> <td>1.00</td> <td>1.25</td> <td>1.50</td> <td>1.75</td> <td>2.00</td> <td>3.00</td> </tr> <tr> <td>1.00</td> <td>1.00</td> <td>0.95</td> <td>0.91</td> <td>0.89</td> <td>0.87</td> <td>0.82</td> <td></td> </tr> <tr> <td>1.50</td> <td>1.12</td> <td>1.06</td> <td>1.02</td> <td>0.99</td> <td>0.96</td> <td></td> <td></td> </tr> <tr> <td>2.00</td> <td>1.24</td> <td>1.16</td> <td>1.12</td> <td>1.08</td> <td>1.05</td> <td></td> <td></td> </tr> </table>	$n$	$m$	1.00	1.25	1.50	1.75	2.00	3.00	1.00	1.00	0.95	0.91	0.89	0.87	0.82		1.50	1.12	1.06	1.02	0.99	0.96			2.00	1.24	1.16	1.12	1.08	1.05		
$n$	$m$	1.00	1.25	1.50	1.75	2.00	3.00																													
1.00	1.00	0.95	0.91	0.89	0.87	0.82																														
1.50	1.12	1.06	1.02	0.99	0.96																															
2.00	1.24	1.16	1.12	1.08	1.05																															
Concentrated force at the free end $J_1 \div J_2 = n$ Uniform section ( $A = \text{const}$ ) (4 corners, etc.)			$P_c = \frac{\pi^2 E J}{(\mu l)^2}$ $\mu \text{ from the table}$	<table border="1"> <tr> <td><math>n</math></td> <td>0.0</td> <td>0.1</td> <td>0.2</td> <td>0.4</td> <td>0.8</td> <td>1.0</td> </tr> <tr> <td><math>\mu</math></td> <td>6.25</td> <td>2.71</td> <td>2.42</td> <td>2.28</td> <td>2.07</td> <td>2.0</td> </tr> </table>	$n$	0.0	0.1	0.2	0.4	0.8	1.0	$\mu$	6.25	2.71	2.42	2.28	2.07	2.0																		
$n$	0.0	0.1	0.2	0.4	0.8	1.0																														
$\mu$	6.25	2.71	2.42	2.28	2.07	2.0																														



straint rather than to a rigidly fixed one. Therefore, it is inadmissible to consider such a bar as one with rigidly fixed ends. Only when we are quite sure about the reliability of the fixation can a small (about 10-20%) decrease of the free length of the bar be permitted.

Finally, we have bars which rest on adjoining elements with the whole area of their end faces. Such bars include wooden posts, independently standing metal columns which are secured to the foundation by bolts, etc. If the end face is properly designed and secured to the foundation, such bars may be considered rigidly fixed at the end. This group of bars also includes large columns with cylindrical hinges when they are designed for buckling in the plane of the hinge axis. Generally, it is difficult to ensure uniform contact between the end face of the compressed column and the supporting foundation. Therefore, the load carrying capacity of such columns is only marginally greater than that of columns with hinged ends.

The formula for critical loads may be obtained in a form close to that of Euler's formula (27.15) even for bars of non-uniform sections and bars being acted upon by several forces. Derivations for a few cases of practical interest, which have been obtained by the theory of elasticity, are given in Table 18.

## § 157. Limits of Applicability of Euler's Formula.

### Plotting of the Diagram of Total Critical Stresses

It would seem that the results obtained in the preceding section were enough to check the stability of compressed bars; the coefficient of stability,  $k_s$ , remains to be determined. This, however, is far from true. The very first study of numerical values obtained by Euler's formula confirms that the formula gives proper results only within certain limits.

For example, if we calculate the critical stress according to formula (27.12) for a steel bar ( $E=2 \times 10^6$  kgf/cm<sup>2</sup>) of flexibility  $\lambda=50$ , we obtain

$$\sigma = \frac{\pi^2 E}{\lambda^2} = \frac{3.14^2 \times 2 \times 10^6}{50^2} = 8000 \text{ kgf/cm}^2$$

This is almost twice the ultimate strength of steel; the bar will cease to work even before the critical stress is achieved. We thus see that for low flexibility bars Euler's formula gives exaggerated values of critical stresses and forces. What are the reasons for this? Figure 390 shows the relation between  $\sigma_c$  and  $\lambda$ . The curve is a hyperbola, which is known as "*Euler's hyperbola*". While using this curve, it should be kept in mind that formula (27.12), which it represents, was obtained by integrating the differential equation of the deflected axis, i.e. it was derived on the assumption that the stresses in the bar are less than the limit of proportionality when it loses its stability.

Consequently, we cannot use the critical stresses calculated by Euler's formula if they exceed the limit of proportionality of the given material. In other words, Euler's formula is valid only when it satisfies the following conditions:

$$\sigma_c \leq \sigma_p \quad \text{or} \quad \frac{\pi^2 E}{\lambda^2} \leq \sigma_p \quad (27.17)$$

If we express  $\lambda$  through equation (27.17), the limit of applicability of Euler's formula will change:

$$\lambda_p \geq \sqrt{\frac{\pi^2 E}{\sigma_p}} \quad (27.17')$$

By substituting the values of modulus of elasticity and limit of proportionality of the given material, we can find the minimum flexi-

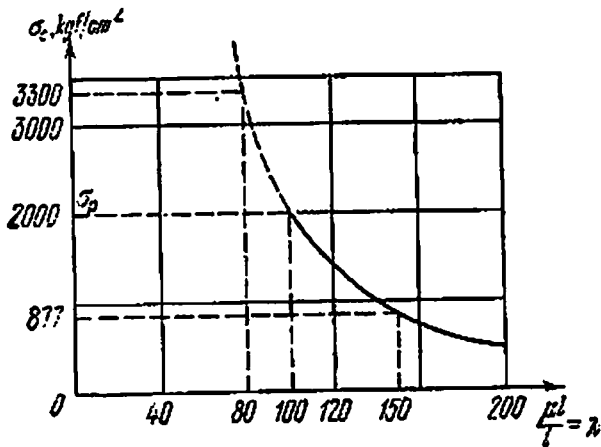


Fig. 390

bility at which Euler's formula can still be applied. For steel the limit of proportionality is  $\sigma_p = 2000$  kgf/cm<sup>2</sup>; therefore, as is evident from formula (27.17'), Euler's formula can be used for bars of this material only when

$$\lambda_p \geq \sqrt{\frac{\pi^2 \times 10^8}{2000}} \approx 100$$

i.e. when  $\lambda_p$  is greater than 100.

For another type of steel,  $\sigma_p \approx 3000$  kgf/cm<sup>2</sup> and Euler's formula is applicable when  $\lambda \geq 85$ ; Euler's formula is applicable for cast iron when  $\lambda \geq 80$ , for pine wood when  $\lambda \geq 110$ , etc. If we draw a horizontal line in Fig. 390 with an ordinate  $\sigma_p = 2000$  kgf/cm<sup>2</sup>, it will cut Euler's hyperbola into two parts; only the lower portion of the diagram, which is valid for thin and long bars, can be used, because such bars become unstable at stresses less than the limit of proportionality.

The theoretical solution obtained by Euler can be applied to a very limited category of bars, namely thin and long bars having high flexibility. In structures we often find bars having low flexibility. Attempts to apply Euler's formula for calculating critical stresses in such bars led to catastrophic results, and experiments on compression of bars also show that, if the critical stresses exceed the limit of proportionality, the actual critical force is considerably less than the value obtained by Euler's formula.

Let us note that for  $\sigma_c > \sigma_p$ , axial compression of the bar is accompanied not only by elastic but also by plastic deformation; additional bending stresses appear at the instant when the bar loses its stability (when the bar axis becomes curved). When the load is removed, the bar fails to straighten, as it does when compressed within the elastic limits.

Keeping in mind all these factors, we see that it is necessary to find methods for calculating critical stresses in those cases when they exceed the limit of proportionality, i.e. for bars which have a flexibility less than that determined by equation (27.17'), for example, for low carbon steel bars with flexibility  $\lambda=0$  to  $\lambda=100$ .

A. A theoretical solution of the problem of stability of compressed bar subjected to critical stresses exceeding the limit of proportionality of the bar material was first attempted by F. Engesser (1889), who obtained the following formula identical to Euler's, (27.12):

$$\sigma_c = \frac{\pi^2 E_1}{\lambda^2} \quad (27.18)$$

Here  $E_1$  is a variable modulus of elasticity, which is determined as the tangent of the angle of slope which the tangent at a point beyond the proportionality limit makes with the compression test diagram (Fig. 391(a)). The *tangential modulus*  $E_1 = \frac{\Delta\sigma}{\Delta\epsilon}$  depends upon the type of diagram as well as on the magnitude of critical stress  $\sigma_c$  at the instant when the bar loses stability.

It was Yasinskii who pointed out that formula (27.18) was incorrect as it did not take into account the fact that when a bar lost stability and its axis became curved it experienced additional stresses not only of compressive but also of tensile nature. Conceding to the validity of the critical remarks of Yasinskii, who pointed out the necessity of accounting for load relaxation on the convex side of a bent bar, Engesser (1895) and independently Th. Karman (1909) came to the conclusion that in formula (27.18) the tangential modulus should be replaced by *reduced modulus*  $E^*$ , which took into account load addition on the concave side with modulus  $E_1$  and load relaxation on the convex side with modulus  $E$  (load relaxation, as is well known, follows Hooke's law). The formula for critical stresses exceeding the limit of proportionality

(for bars having flexibility  $\lambda > \lambda_p$ ) may be rewritten as

$$\sigma_c = \frac{\pi^2 E^*}{\lambda^2} \tag{27.18'}$$

The reduced modulus of elasticity may be calculated from the following expression derived from the conditions of equilibrium of addi-

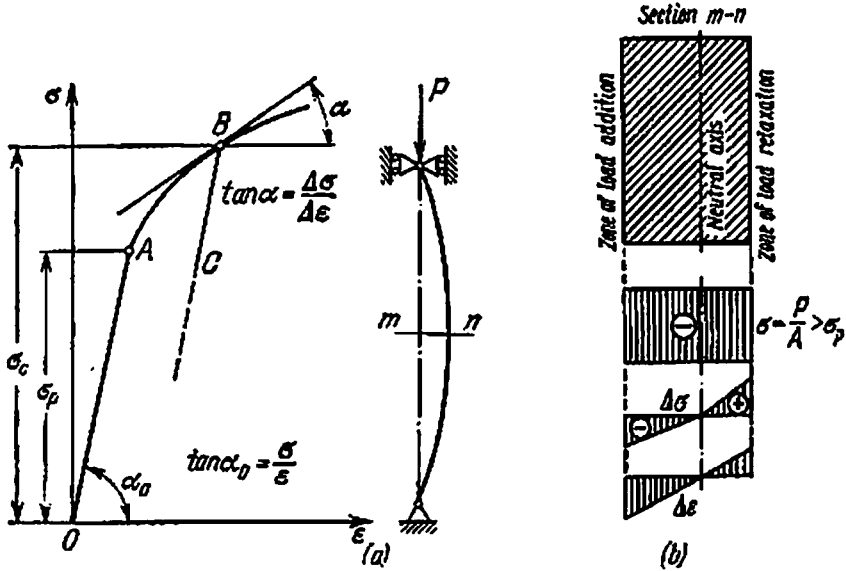


Fig. 391

tional stresses (load addition—load relaxation) and on the basis of the hypothesis of plane sections:

$$E^* = \frac{E_1 J_1 + E J_2}{J} \tag{27.19}$$

where  $J_1$  is the moment of inertia of the concave half of the section about the neutral axis,  $J_2$  is the moment of inertia of the convex half of the section and  $J$  is the moment of inertia of the whole section about the central axis.

On account of the difference between moduli  $E$  and  $E_1$  in expression (27.19), the neutral axis dividing the concave half of the section from the convex half does not pass through the centre of gravity of the section (Fig. 391(b); its location (and this means that the areas that experience additional loading and load relaxation) depends upon the shape of the section as well as upon the critical stress, which we want to determine. For different sections, assuming a particular value of  $E_1$  and using the method of successive approximations, we can find the location of the neutral axis and calculate the moments of inertia  $J_1$  and  $J_2$  and then the reduced modulus of elasticity  $E^*$  as a function of

moduli  $E$  and  $E_t$ . For a rectangular section, for instance,

$$E^* = \frac{4EE_t}{(\sqrt{E} + \sqrt{E_t})^2} \quad (27.19')$$

It is evident from equations (27.19) and (27.19') that when the critical stress does not exceed the limit of proportionality of the material (i.e. when the deformation is within the elastic limits and  $E_t = E$ ), the reduced modulus of elasticity  $E^* = E$ .

For materials having a well defined yield plateau  $E_t$  and  $E^*$  tend to zero as the critical stress approaches the yield stress. This implies that in such cases the critical stresses cannot exceed the yield stress of the material.

The Engesser-Karman formula did not find application in practical design since the determination of  $E^*$ , which depends upon the critical stress, raises serious difficulties in computation and also because it gives exaggerated values of critical stresses as compared to experimental results.

The application of Euler's formula to the inelastic region of deformation became possible only after F. Shenly published his work in which he suggested a new approach to the analysis of stability of compressed bars (1946) subjected to elasto-plastic deformation. Looking upon the loss of stability as a dynamic process under the action of a continuously increasing compressive force, Shenly, in fact, returned to the original formula of Engesser (27.18) with tangential modulus of elasticity  $E_t$ , which had earlier been rejected (if the curvature is small at the moment when the bar loses its stability, an increase of force  $P$  by  $\Delta P$  balances the load relaxation on the convex side due to additional compression).

The transition to generalized formula (27.18) considerably simplified the calculation of critical stresses for bars in which loss of stability is accompanied by plastic deformation. At present, theoretical values of critical stresses for low and medium flexibility of different materials have been calculated on the basis of experimental data on  $E_t$  corresponding to different values of critical stresses  $\sigma_c$  greater than  $\sigma_p$ , and with the help of modern computational techniques. These values are in good agreement with the results obtained from experimental research.

**B.** The first experimental investigations on stability of compressed bars were conducted with the aim of checking Euler's formula. It was found perfectly valid for long (flexible) bars but was observed to give a large discrepancy with experimental results for short bars (as is evident from theoretical considerations). On the basis of these experiments, often not conducted with due care, various empirical formulas were proposed for determining critical stresses, though without sufficient justification in most of the cases. However, the quality of experimental investigations improved as new apparatus was developed.

Extensive experiments that covered a wide range of materials and were distinguished by an extreme thoroughness were conducted in 1896 by L. Tetmajer. The results of these experiments were processed by Yasinskii who compiled a table of "breaking" (critical) stresses depending upon flexibility for bars from commonly used structural materials.

All experiments show that short bars having stability  $\lambda=30-40$  lost their load carrying capacity not due to insufficient strength but because of the compressive stresses rising to a dangerous value  $\sigma_d$  which was critical for the given material (recall that  $\sigma_d=\sigma_y$  for ductile state of material and  $\sigma_d=\sigma_u$  for brittle state). It may therefore be assumed that for bars with low flexibility critical stresses for ductile materials are practically equal to the yield stress  $\sigma_y$  and for brittle materials to the ultimate strength  $\sigma_u$ .

For medium flexibility bars, which find maximum application in structures, it was experimentally established that they lose their load

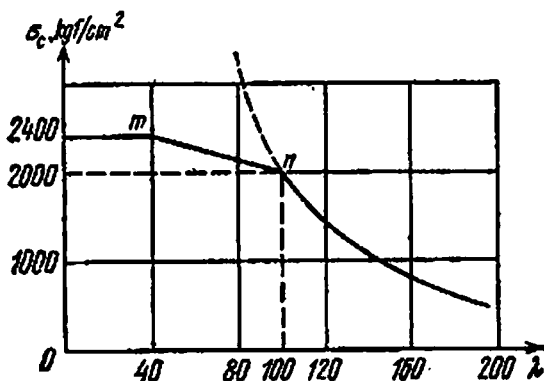


Fig. 392

carrying capacity due to loss of stability of straight-line form under stress  $\sigma_c$  greater than the limit of proportionality  $\sigma_p$  but less than  $\sigma_d$ .

In such bars, the variation of critical stresses as a function of flexibility follows an almost linear law. For instance, the empirical formula of Tetmajer-Yasinskii is:

$$\sigma_c = a - b\lambda \quad (27.20)$$

where  $a$  and  $b$  are coefficients that depend upon the material and are selected such that for flexibility  $\lambda=\lambda_{lim}$ ,  $\sigma_c=\sigma_p$  and for low flexibility  $\sigma_c$  is close to  $\sigma_d$ .

This data is used for plotting the total critical stress diagram shown in Fig. 392 for low-carbon steel having a limit of proportionality  $\sigma_p=2000$  kgf/cm<sup>2</sup> and yield stress  $\sigma_y=2400$  kgf/cm<sup>2</sup>. The diagram consists of three parts: Euler's hyperbola when  $\lambda>\lambda_{lim}=100$  (on the right), horizontal line for  $\lambda\leq 40$  when  $\sigma_c\approx\sigma_y$  (on the left) and an inclined

straight line (27.20) when  $40 \leq \lambda \leq 100$  (joining points  $m$  and  $n$ ). In order to avoid sharp inflections in the  $\sigma_c$  versus  $\lambda$  curve at points  $m$  and  $n$ , we may use the empirical formula due to Johnson which recommends a parabolic variation of critical stress in the inelastic zone

$$\sigma_c = \sigma_d - \alpha \lambda^2 \tag{27.20'}$$

Here, when  $\lambda=0$  then  $\sigma_c = \sigma_d$ , and when  $\lambda = \lambda_{lim}$ , then  $\sigma_c \approx \sigma_T$ ; moreover, coefficient  $\alpha$  is selected such so as to ensure smooth conjunction of the parabola (27.20') with Euler's hyperbola (a common tangent). For example, for structural steel having yield stress  $\sigma_y = 2800 \text{ kgf/cm}^2$ ,  $\alpha = 0.09$ .

Hence, either by using the general theoretical formula (27.19) or combining Euler's formula with experimental results, we can plot the total critical stress diagram for bars of different materials and determine critical stress  $\sigma_c$  for any flexibility.

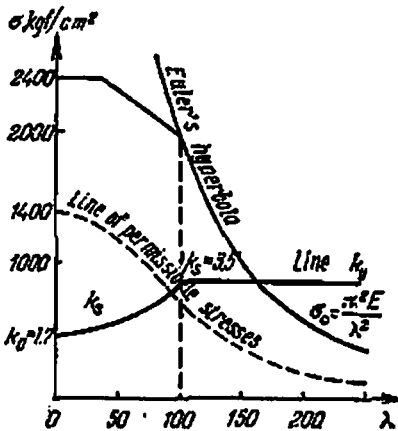


Fig. 393

### § 158. The Stability Check of Compressed Bars

We noted in § 154 that the following two checks should be carried out for bars under compression: the strength check

$$\sigma = \frac{P}{A} \leq [\sigma], \text{ where } [\sigma] = \frac{\sigma_0}{k_0}$$

the stability check

$$\sigma = \frac{P}{A} \leq [\sigma_s] \text{ where } [\sigma_s] = \frac{\sigma_c}{k_s}$$

Having plotted the total critical stress diagram for bars of any flexibility (§ 157), we can also plot the permissible stress diagram for stability for the given material by reducing the  $\sigma_c$ -ordinates  $k_s$  times:

$$[\sigma_s] = \frac{\sigma_c}{k_s}$$

We only have to choose a proper value for coefficient  $k_s$ . Bearing in mind a number of errors, which are unavoidable in axial compression (initial curvature, eccentricity, etc.) and seriously influence the load carrying capacity of the bar, the factor of safety for stability is taken greater than the safety factor for strength,  $k_0$ . For steel this coefficient varies between 1.8 and 3.5, for iron between 5.0 and 5.5 and for timber between 2.8 and 3.2.

Figure 393 shows the diagram of permissible stresses for stability

and the safety factor for stability for low-carbon steel having yield stress  $\sigma_y=2400$  kgf/cm<sup>2</sup>.

In order to establish a relation between the permissible stress for stability,  $[\sigma_s]$ , and permissible stress for strength,  $[\sigma]$ , let us take their ratio:

$$\frac{[\sigma_s]}{[\sigma]} = \frac{\sigma_c k_0}{k_y \sigma_0} \quad \text{or} \quad [\sigma_s] = \frac{\sigma_c k_0}{\sigma_0 k_y} [\sigma]$$

Denoting

$$\varphi = \frac{\sigma_c k_0}{\sigma_0 k_y} \tag{27.21}$$

we get

$$[\sigma_s] = \varphi [\sigma] \tag{27.22}$$

where  $\varphi$  is the *reduction coefficient* of the permissible stress for compressed bars.

If we have the  $\sigma_c$  versus  $\lambda$  curve for a given material, know  $\sigma_0=\sigma_y$  or  $\sigma_0=\sigma_u$  and select the safety factors for strength,  $k_0$ , and stability,  $k_s$ , we can put together a table for  $\varphi$  as a function of flexibility.

Table 19

Coefficient  $\varphi$

Flexibility $\lambda = \frac{\mu l}{i}$	Structural steels			Steel C1K	Cast iron	Wood
	C-38/23	C-44/29	C-46/33			
0	1.00	1.00	1.00	1.00	1.00	1.00
10	0.988	0.987	0.986	0.97	0.97	0.99
20	0.970	0.968	0.965	0.95	0.91	0.97
30	0.943	0.935	0.932	0.91	0.81	0.93
40	0.905	0.892	0.888	0.87	0.69	0.87
50	0.867	0.843	0.837	0.83	0.57	0.80
60	0.820	0.792	0.780	0.79	0.44	0.71
70	0.770	0.730	0.710	0.72	0.34	0.60
80	0.715	0.660	0.637	0.65	0.26	0.48
90	0.655	0.592	0.563	0.55	0.20	0.38
100	0.582	0.515	0.482	0.43	0.16	0.31
110	0.512	0.440	0.413	0.35		0.25
120	0.448	0.383	0.350	0.30		0.22
130	0.397	0.330	0.302	0.26		0.18
140	0.348	0.285	0.256	0.23		0.16
150	0.305	0.250	0.226	0.21		0.14
160				0.19		0.12
170				0.17		0.11
180				0.15		0.10
190				0.14		0.09
200				0.13		0.08



Table 19 contains data on coefficient  $\varphi$  for structural steels recommended by the latest Soviet standards for designing metal structures. The table also contains the reduction coefficients of main permissible stresses\* for improved quality steels, iron and timber (pine). The design standards used in construction recommend that coefficient  $\varphi$  for timber should be calculated by the following formulas:

$$\text{if flexibility } \lambda \leq 75, \text{ then } \varphi = 1 - 0.8 \left( \frac{\lambda}{100} \right)^2$$

$$\text{if flexibility } \lambda > 75, \text{ then } \varphi = \frac{3100}{\lambda^2}$$

The values of  $\varphi$  obtained from these formulas are quite close to the tabulated values.

This table helps us to select the cross-sectional area of the compressed bar. The cross-sectional area depends upon  $[\sigma_s]$ , which in its turn depends upon  $\varphi$  and flexibility  $\lambda$ , i.e. upon the area and shape of the cross section. Therefore, the cross-sectional area is determined by successive approximations in the following order.

We select the shape of the section and define its dimensions. Next, we calculate the minimum radius of gyration and the flexibility. We find coefficient  $\varphi$  from the table and calculate the permissible stress for stability  $[\sigma_s] = \varphi[\sigma]$ . We now compare the actual stress  $\sigma = \frac{P}{A}$  with  $[\sigma_s]$ ; if the condition

$$\sigma = \frac{P}{A} \leq \varphi[\sigma] \quad (27.23)$$

is not satisfied, or is satisfied with a big margin, we change the dimensions and repeat the calculations. Obviously, the section finally selected must also satisfy the strength condition

$$\sigma \leq [\sigma]$$

In actual calculations the stability condition is sometimes written as follows:

$$\sigma_r = \frac{P}{\varphi A} \leq [\sigma] \quad (27.23')$$

In the left-hand side  $\sigma_r$  represents the design (reduced) stress.

The order of calculations will be elaborated on in the following example.

---

\* The steels accepted in the standards are characterized by ultimate strength (numerator) and yield stress (denominator) in  $\text{kgf}/\text{mm}^2$ . Standards do not permit the use of steel bars having flexibility  $\lambda > 150$  in structures as load carrying elements subjected to compression. In design by the method of limiting states (see Chapter 26) coefficient  $\varphi$  is considered a coefficient by which the rated load should be reduced.

Find the cross-sectional dimensions of an iron pipe column hinged at both ends and subjected to a compressive force  $P=85$  tf, if the ratio of internal diameter to the external is  $d/D=0.6$ . The column is  $l=4.8$  m long. The main permissible stress under compression for iron is  $[\sigma]=1200$  kgf/cm<sup>2</sup>.

Let us express area  $A$  of the section and its radius of inertia  $i$  through diameter  $D$ :

$$A = \frac{\pi(D^2 - d^2)}{4} = \frac{\pi}{4}(D^2 - 0.36D^2) = 0.503D^2 \quad (a)$$

$$i = \sqrt{\frac{J}{A}} = \sqrt{\frac{\frac{\pi(D^4 - d^4)}{64}}{\frac{\pi}{4}(D^2 - d^2)}} = \sqrt{\frac{D^2 + d^2}{16}} = 0.291D \quad (b)$$

In stability condition (27.23) we know neither the cross-sectional area,  $A$ , nor the reduction coefficient for permissible stress,  $\varphi$ . Therefore it is essential to assume a value for one of these quantities. In the first approximation let us assume  $\varphi=0.5$ . We get

$$A \geq \frac{P}{\varphi[\sigma]} = \frac{85\,000}{0.5 \times 1200} = 142 \text{ cm}^2$$

In the first approximation the diameter is (a)  $D_1 = \sqrt{142/0.503} = 19$  cm. The radius of inertia is (b)  $i_1 = 0.291D_1 = 0.291 \times 19 = 5.5$  cm. Flexibility  $\lambda_1 = \mu l/i_1 = \frac{480}{5.5} = 87.5$ . For flexibility between  $\lambda=80$  and  $\lambda=90$  we find from the table by interpolation that  $\varphi=0.215$ . The design stresses from formula (27.23') are

$$\sigma_r = \frac{P}{\varphi A} = \frac{85\,000}{0.215 \times 142} = 2800 \text{ kgf/cm}^2 > [\sigma]$$

The section does not satisfy the stability condition. Therefore, in the second approximation let us assume that diameter  $D_2=25$  cm. Cross-sectional area  $A_2=0.503D_2^2=0.503 \times 25^2=314$  cm<sup>2</sup>. Radius of inertia  $i_2=0.291 \times 25=10.2$  cm. Flexibility  $\lambda_2=l/i_2=480/10.2=47$  and  $\varphi=0.654$ . Thus

$$\sigma_r = \frac{P}{\varphi A} = \frac{85\,000}{0.654 \times 314} = 410 \text{ kgf/cm}^2 \ll 1200 \text{ kgf/cm}^2$$

When diameter is  $D_1=19$  cm the stresses are considerably greater than the permissible, and when it is  $D_2=25$  cm they are much less. Let us try in the third approximation a section of diameter  $D=22$  cm. In this case  $A=0.503 \times 22^2=245$  cm<sup>2</sup>,  $i=0.291 \times 22=6.4$  cm,  $\lambda=$

$=480/6.4=75$ ,  $\varphi=0.30$  and the design stresses are:

$$\sigma_r = \frac{85\,000}{0.30 \times 245} = 1150 \text{ kgf/cm}^2 < 1200 \text{ kgf/cm}^2$$

The calculations may be terminated here as understressing is less than 5%.

### § 159. Selection of the Type of Section and Material

A. As the flexibility of the bar and consequently the minimum radius of gyration plays the most important part in resistance to axial bending (loss of stability), it is important to take into account not only the cross-sectional area but also its shape.

The most economic solution of the problem is obtained if the section of a certain cross-sectional area has the minimum radius of gyration of the maximum possible magnitude. To achieve this, we try to select a section in which the minimum and maximum radii of gyration are equal, i.e. a section in which the moments of inertia about all central axes are zero and consequently the inertia ellipse transforms into an inertia circle. Such a bar will have uniform resistance to buckling in all directions.

If the free length of the bar (§ 156) is different for deflection in the two principal planes, then the principal moments of inertia should be such that coefficient  $\varphi$  is the same in both the cases.

It is now essential to obtain the maximum possible central moments of inertia for the given cross-sectional area. This is possible if the material of the section is located as far away from the centre of gravity as possible. Both these conditions are, for example, fully satisfied by a pipe section (Fig. 394(a)), which is therefore often used in compressed bars and columns.

The lower limit of wall thickness of such sections is determined either by casting limitations (as in cast iron) or by the condition that local deformation (warping) of the section should not occur when the bar is working.

To prevent such local deformations and to ensure that the bar retains its designed shape, the pipe-section is reinforced with the help of plates placed at a particular distance from one another, which increase the rigidity of the thin-walled section (Fig. 394(b)). As a matter of fact, proper use of reinforcing plates is extremely important in designing compressed bars.

Some sections which have excellent bending resistance in one plane, for example beams, are found to be of no use as compressed bars. Examples are: an I-beam, a section consisting of two channel sections placed in such a way that their webs touch each other (Fig. 394(c)).

These sections are disadvantageous when used as compressed bars on account of the large difference in the values of their principal moments of inertia. This drawback may be overcome by moving apart the channel sections, as shown in Fig. 395(c). To ensure that the sections work together as a single unit, they are joined by means of a network (Fig. 395) of fixing plates.

Trouble-free working of such composite sections can be guaranteed only by providing a sufficiently strong fixation (by network of plates and angles), which ensures that all load carrying elements function simultaneously. Thus, if we join two strong channel sections weakly, they will not work as a single unit.\* Each half of the sections will work independently and its stability will be considerably less than that of a section in which both halves operate as a single unit.

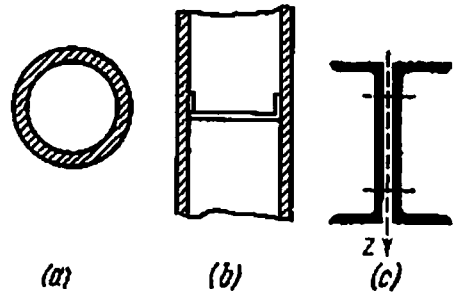


Fig. 394

Insufficient attention paid to the design of reliable fixation of composite sections has been the cause of serious catastrophes in the past.

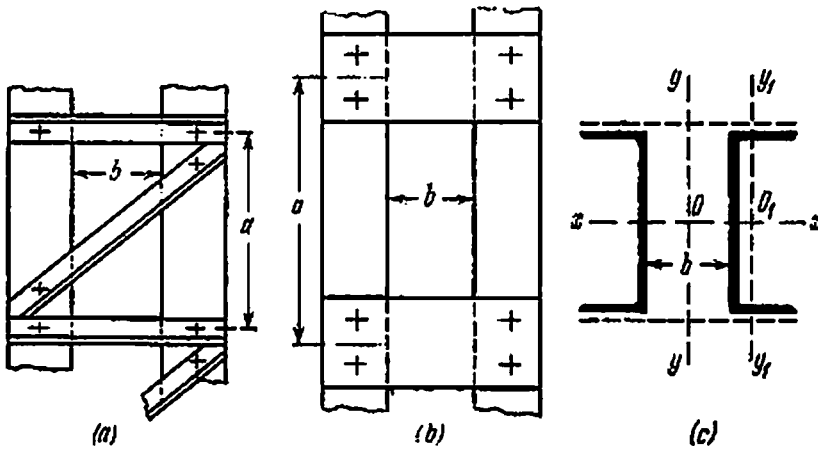


Fig. 395

In designing a composite section, distance  $b$  by which the two halves of the section should be moved apart is determined from the condition that the moments of inertia about principal axes  $y$  and  $z$  be almost

\* The analysis and methods of determining the dimensions of network plates for composite compressed bars are given in the course on metal structures. Also see N. M. Belyaev, *Strength of Materials*, Nauka, 1965 (in Russian), § 212.

equal. Usually, however, the moment of inertia about the axis perpendicular to the network plane is taken a little higher, because the network cannot ensure simultaneous working of the two halves as well as of a section which is one rigid unit.

We will show below how the stability of a composite bar subjected to compression can be improved by rationally placing the elements of

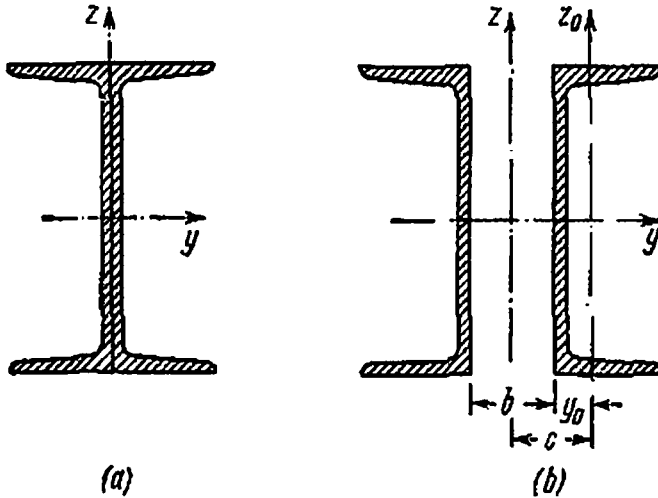


Fig. 396

section. Suppose we have to design a section from two channel sections (steel C-38/23) for a 4-m long column that is hinged at both ends and is subjected to compression.

We shall compare the maximum permissible (from the point of view of stability) compressive force acting on the column made up of two channel sections No. 30 (see Appendix). Let us consider two versions: in the first the two channel sections are attached along their height back to back so as to form an I-section (Fig. 396(a)); in the second version the two channel sections are attached by a network and placed in such a way that the section has identical moments of inertia about the two principal axes of inertia (Fig. 396(b)). The main permissible stress under compression is assumed to be  $[\sigma]=1600 \text{ kgf/cm}^2$ .

For the first version (channel sections attached without any gap) the minimum moment of inertia of the section is:

$$J_{\min} = J_z = 2(327 + 40.5 \times 2.52^2) = 1168 \text{ cm}^4$$

The area of the composite section is  $A = 2 \times 40.5 = 81 \text{ cm}^2$ . Radius of inertia of the section is  $i = \sqrt{J_z/A} = \sqrt{1168/81} = 3.8 \text{ cm}$ . Flexibility of the bar  $\lambda = \mu l/i = 400 \cdot 3.8 = 105$ .

Interpolating from Table 19 the value of  $\varphi$  between  $\lambda = 100$  and  $\lambda = 110$ , we obtain  $\varphi = 0.547$ . The maximum compressive force which can

be safely applied to the column is:

$$P_1 = [\sigma] A \varphi = 1600 \times 81 \times 0.547 = 70\,800 \text{ kgf} \approx 71 \text{ tf}$$

For the second version (when the channel sections are apart) the moment of inertia of the composite section (Fig. 396(b)) is:

$$J_y = J_z = 2 \times 5810 = 11\,620 \text{ cm}^4$$

The radius of inertia  $i = \sqrt{11620/81} = 12 \text{ cm}$ , the flexibility  $\lambda = l/i = 400/12 = 33.3$  and the coefficient  $\varphi = 0.931$ .

The permissible load on the bar may in this version be taken  $P_2 = [\sigma] A \varphi = 1600 \times 81 \times 0.931 = 120\,900 \text{ kgf} \approx 121 \text{ tf}$ , i.e. 1.7 times greater than in the first. Hence, a rational approach in selecting the shape of a section enabled us to raise the load carrying capacity of the compressed bar by 70%.

Simultaneous functioning of both halves (channel sections) of the composite section is possible only if they are reliably secured to each other by a network or plates (Fig. 395(a) and (b)). Distance  $a$  between the securing elements should ensure that neither of the channel sections bend in the plane of its minimum flexibility. This condition can be satisfied only if the flexibility of each half (in this example each channel section) does not exceed the flexibility of the column over length  $a$ :

$$\lambda_{c.s} = \frac{a}{i_{\min}} \leq \lambda_c$$

For one channel section the minimum radius of gyration is  $i_{\min} = 2.84 \text{ cm}$ . Therefore

$$a = \lambda_y i_{\min} = 33.3 \times 2.84 = 94.6 \text{ cm}$$

This means that the distance between the securing plates should not be more than 94.6 cm.

Distance  $b$  between the channel sections (Fig. 396(b)) may be determined from the condition  $J_z \geq J_y$ , where

$$J_z = 2(J_z^0 + A_0 c^2) \geq 2J_y^0$$

Here  $J_y^0$  and  $J_z^0$  are moments of inertia of one channel section about the axes passing through its centre of gravity, and  $A_0$  is the cross-sectional area of one channel section. Therefore

$$c = \sqrt{\frac{J_y^0 - J_z^0}{A_0}} = \sqrt{\frac{5810 - 327}{40.5}} = 11.6 \text{ cm}$$

Since  $b = 2(c - y_0)$  and from the specifications  $y_0 = 2.52 \text{ cm}$ , we get  $b = 2(11.6 - 2.52) = 18.2 \text{ cm}$ .

**B.** The material of compressed bars is selected from the following considerations. As long as the critical stress does not exceed the

limit of proportionality, the resistance of a bar to buckling is determined by only one mechanical property, the modulus of elasticity,  $E$ . In bars of medium and particularly low flexibility the critical stress depends to a considerable extent upon the yield stress or ultimate strength of the material. These considerations should be taken into account while selecting a material for compressed bars of high as well as low flexibility.

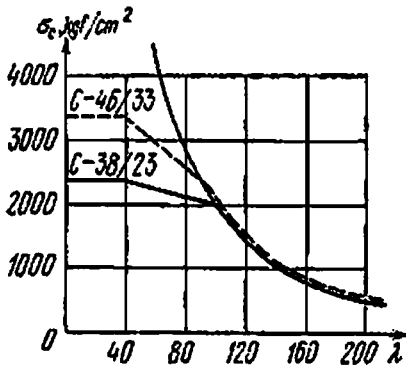


Fig. 397

For example, there is no sense in using special high-strength steels for long and thin-walled bars, because the modulus of elasticity is approximately the same for all grades of steel. On the other hand, it is advantageous to use high-grade steels in bars having critical stress higher than the limit of proportionality, because in such bars the increase of yield stress results in an increase of the critical stress,

thus improving the resistance of the bar against buckling.

Figure 397 shows approximate diagrams depicting critical stress as function of flexibility for structural steels: low-carbon steel C-38/23 and stronger steel C-46/33, which have yield stresses equal to 2300 and 3300 kgf/cm<sup>2</sup>, respectively.

It is evident from the diagrams that for highly flexible bars ( $\lambda$  greater than 100) the critical stresses, which are limited by Euler's hyperbola (27.12), are the same for both steels, as the latter have identical moduli of elasticity  $E$  upon which  $\sigma_c$  depends; the permissible stresses for stability are considerably higher for steel C-46/33 in comparison with steel C-38/23.

It follows from the above discussion that there is no advantage in using high-strength steels for bars of high strength subjected to compression in structures. Also, considerable saving of material can be achieved by using stronger steels for bars of low flexibility.

## § 160. Practical Importance of Stability Check

The check on stability is of great importance for an engineer. It can be said with authority that sudden failure of most of the structures occurs only due to loss of stability of its compressed elements. Engineers know about a large number of cases of catastrophic failure of structures in the past; yet, somehow, they fail to appreciate the actual reasons of this. This clearly shows that often engineers do not

pay sufficient attention to seemingly unimportant but actually very important aspects in the working of compressed bars.

Loss of stability is all the more dangerous because it occurs suddenly. Deformation is not noticeable and fails to arouse suspicion right up to the moment when the compressive force becomes critical. In addition, as mentioned earlier, a number of factors—eccentricity of loading, initial curvature, local overstressing of the material—can further considerably reduce the resistance of compressed bars to buckling, although the same factors have almost no effect on the working of other elements of the structure.

Special attention should be paid to the reliability of joints of parts in compressed bars made of composite sections. Neglect of this factor was the cause of tragic accidents in the past, especially in case of large bridges.

At present, an engineer has at his disposal all means to prevent such mistakes provided he designs properly and the designed structure is manufactured accurately. The theory of analysis of stability check has been worked out quite soundly, as has been already discussed (§§ 154-159).

The stability check of machine parts is slightly different. Here particular attention must be paid to the value of permissible stress  $[\sigma]$ . While selecting its value, it should be borne in mind that such machine parts as connecting rods, plungers, etc., are subjected to dynamic loading. Therefore in the formula of permissible stress for stability, namely

$$[\sigma_s] = \eta [\sigma]$$

$[\sigma]$  should imply the permissible stress for strength under dynamic loading (see Part IX, Chapter 29).

In § 154 there was a mention about the analogy between sudden increase in deformation when stresses exceed the critical stress. This analogy leads to the idea that in statically indeterminate structures failure may not occur despite the stresses achieving critical value, especially if the stresses are below the limit of elasticity.

Examples of such situations are lattice trusses of old bridges which are still working under present conditions although the load they have to take now is considerably higher. Part of the bars in these trusses may find themselves loaded up to the critical stress limit and yet remain in the elastic state of deformation. The load of these bars is taken up by the opposite bars working under tension. When the load is removed, the bars return to their original positions.

Other instances of such loading can be found in aviation engineering and ship building, where we have to cope with buckling of not only bars but also beams, plates and shells. Thus in exceptional cases we may allow the stresses in a compressed element to reach the critical limit provided that the stresses do not exceed the elastic limit, the



structure is statically indeterminate and the load of elements thus overstressed is taken up by other elements.

We shall discuss below a few more complicated problems on stability check.

## CHAPTER 28

### More Complicated Questions of Stability in Elements of Structures

#### § 161. Stability of Plane Surface in Bending of Beams

Buckling occurs not only in axial compression of bars. For example, buckling may occur in an I-beam under bending (Fig. 398).

The lower flange of such a beam represents a bar rigidly fixed to the web and subjected to axial compression. The constraint does not permit the flange to buckle in the web plane. However, for particular

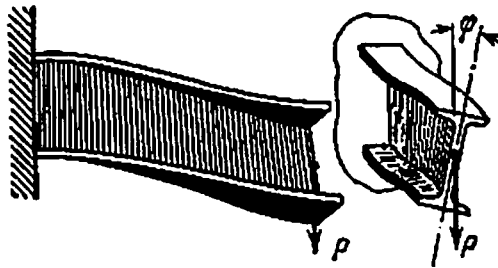


Fig. 398

beam dimensions the flange may buckle on one side, causing rotation of the sections w.r.t. one another and giving rise to torsion of the beam (Fig. 398). Instead of bending in the plane of maximum rigidity, as intended by designer, the beam starts working in unsymmetric bending, which results in a sharp increase in deformation ultimately leading to total failure.

Stability of the beam depends upon its cross-sectional dimensions and its free length. This length is restricted by providing constraints between the beams. Serious accidents may occur if insufficient attention is paid to these side constraints in long beams, although their height may be small (for example, failure of the Tarbes bridge in France).

Buckling is also dangerous for thin shells under compression, i.e. for elements in which one dimension is considerably less than the other. A thin and wide flange in an I-section will warp under compression; a web which is not sufficiently strengthened by stiffening angle will buckle.

Let us determine for a beam the approximate critical load at which the plane shape of the beam becomes unstable leading to complete failure due to side buckling if the load is further increased. Let us consider a simply supported beam of thin rectangular section (Fig. 399) acted upon by a lateral force  $P$ .

Let us assume that force  $P$  has reached its critical value and the beam is buckling slightly to one side, as shown in the top view as

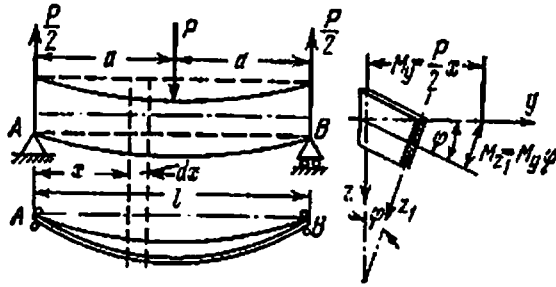


Fig. 399

well as the section in Fig. 399; only ends  $A$  and  $B$  remain in the original positions due to the constraints applied to them.

With buckling the potential energy of the deformed beam should increase due to bending on one side and torsion (the energy of bending in the vertical plane remaining constant). The potential energy of the external force should decrease, because of the lowering of its point of application.

Let us denote the potential energy of side bending by  $U_1$ , of torsion by  $U_2$ , and the work done by the load in lowering by  $U_p$ . As at the critical force the transition from plane shape to buckled shape is accompanied by transformation of energy of the load into potential energy of deformation of the beam, we may assume that

$$U_1 + U_2 = U_p \tag{28.1}$$

Potential energy of buckling (w.r.t. axis  $z_1$ ) is (§ 63):

$$U_1 = \int_0^l \frac{M^2(x) dx}{2EJ_z}$$

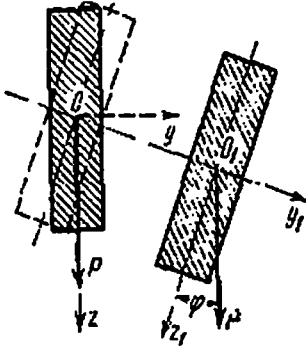
Here the bending moment in an arbitrary section at a distance  $x$  from the left support will be (assuming the angle of rotation,  $\varphi$ , to be small)

$$M(x) = \frac{P}{2} x \sin \varphi \approx \frac{P}{2} x \varphi$$

Substituting the expression for bending moment, we get

$$U_1 = \frac{P^2}{8EJ_z} \int_0^{l/2} x^2 \varphi^2 dx = \frac{P^2}{4EJ_z} \int_0^{l/2} x^2 \varphi^2 dx \quad (28.2)$$

The potential energy of torsion may also be expressed through  $\varphi$ . The work done by the twisting moment over a length  $dx$  is:



$$dU_2 = \frac{M_t d\varphi}{2}, \quad \text{where} \quad d\varphi = \frac{M_t dx}{GJ_t}$$

Keeping in mind that

$$M_t = GJ_t \frac{d\varphi}{dx} \quad \text{and} \quad d\varphi = \frac{d\varphi}{dx} dx$$

we obtain

$$dU_2 = \frac{GJ_t}{2} \frac{d\varphi}{dx} \frac{d\varphi}{dx} dx = \frac{GJ_t}{2} \left( \frac{d\varphi}{dx} \right)^2 dx$$

Fig. 400

The total potential energy of torsion due to buckling of the beam is:

$$U_2 = \frac{GJ_t}{2} \int_0^{l/2} \left( \frac{d\varphi}{dx} \right)^2 dx = GJ_t \int_0^{l/2} \left( \frac{d\varphi}{dx} \right)^2 dx \quad (28.3)$$

Let us first determine the vertical displacement of the point of application of force  $P$  (Fig. 400) in order to calculate the work done by force  $P$  in lowering. Here, it is relevant to point out that there are two reasons for the displacement of point  $O$  to  $O_1$ : rotation of the section about point  $O$  by an angle  $\varphi$  and displacement in the direction of axis  $Oy_1$ .

Since lowering of point  $O$  is not possible due to rotation, obviously the cause of lowering of the point of application of force  $P$  is buckling of the beam from plane  $xOz$ .

The vertical displacement of point  $O$  can be found by Castigliano's theorem from expression (28.2):

$$\delta = \frac{\partial U_1}{\partial P} = \frac{P}{2EJ_z} \int_0^{l/2} x^2 \varphi^2 dx \quad (28.4)$$

Wherefrom work done by force  $P$  (which is equal to critical force  $P_c$  when buckling starts) in causing displacement  $\delta$  is:

$$U_p = P\delta = \frac{P^2}{2EJ_z} \int_0^{l/2} x^2 \varphi^2 dx$$

Now substituting the values of  $U_1$ ,  $U_2$  and  $U_p$  in the original equation (28.1), we get

$$\frac{P^2}{4EJ_z} \int_0^{l/2} x^2 \varphi^2 dx + GJ_t \int_0^{l/2} \left( \frac{d\varphi}{dx} \right)^2 dx = \frac{P^2}{2EJ_z} \int_0^{l/2} x^2 \varphi^2 dx$$

wherefrom

$$\frac{P^2}{4EJ_z} \int_0^{l/2} x^2 \varphi^2 dx = GJ_t \int_0^{l/2} \left( \frac{d\varphi}{dx} \right)^2 dx$$

Denoting rigidity in bending by  $EJ_z = C_1$ , and torsional rigidity by  $GJ_t = C_2$ , we get the following expression for critical force:

$$P_c^2 = 4C_1 C_2 \frac{\int_0^{l/2} \left( \frac{d\varphi}{dx} \right)^2 dx}{\int_0^{l/2} x^2 \varphi^2 dx} \quad (28.5)$$

Under the integral sign we have two variables,  $\varphi$  and  $x$ , which are interrelated because  $\varphi$  changes along length  $x$ , i.e.  $\varphi = \varphi(x)$ . The law of variation of  $\varphi$  as a function of  $x$  is not known. Using the method of approximate solution, we assume a value of  $\varphi$  which relates it to  $x$  in such a way that the conditions of constraint at the ends are satisfied. Let us assume that

$$\varphi = k \sin \frac{\pi x}{l} \quad (28.6)$$

We see that  $\varphi = 0$  at  $x = 0$ , that  $\varphi = \varphi_{\max}$  at  $x = \frac{l}{2}$  and that  $\varphi = 0$  at  $x = l$ . Thus, the function vanishes at the supports and is maximum at the middle of the span. In other words, the function satisfies the boundary conditions.

Substituting the values of  $\varphi$  and its first derivative in the integral in equation (28.5), we obtain

$$P_c^2 = 4C_1 C_2 \frac{k^2 \pi^2 \int_0^{l/2} \cos^2 \frac{\pi x}{l} dx}{k^2 l^3 \int_0^{l/2} x^2 \sin^2 \frac{\pi x}{l} dx}$$

Upon integration we get

$$P_c = \frac{17.2}{l^2} \sqrt{C_1 C_2} \quad (28.7)$$

The exact value of critical force for a simply supported rectangular beam (Fig. 399) is given by the formula \*

$$P_c = \frac{16.93}{l^2} \sqrt{C_1 C_2}$$

The error of approximate solution is about 1.5%. The critical force depends upon the product of rigidity under bending  $C_1 = EJ_z$  and torsional rigidity  $C_2 = GJ_t$ .

If the load is uniformly distributed along the axis, then the critical value of the distributed force will be

$$(ql)_c = \frac{28.3}{l^2} \sqrt{C_1 C_2} \quad (28.8)$$

For a cantilever of length  $l$  which is loaded by a uniformly distributed force we get

$$(ql)_c = \frac{12.85}{l^2} \sqrt{C_1 C_2} \quad (28.9)$$

For a cantilever being acted upon by a concentrated force at its free end we have

$$P_c = \frac{4.01}{l^2} \sqrt{C_1 C_2} \quad (28.10)$$

The formulas for critical force in an I-beam are the same as for a rectangular. The difference is that the coefficient before  $\sqrt{C_1 C_2}$  is not a constant quantity but depends upon the resistance of flanges to buckling and is determined by the ratio

$$\alpha = \frac{C_2}{C_1} \left( \frac{l}{h} \right)^2$$

where  $h$  is the height of the I-beam. Thus, for an I-beam

$$P_c = \frac{\beta}{l^2} \sqrt{C_1 C_2} \quad (28.11)$$

where  $\beta$  has to be determined individually for each value of  $\alpha$ . The values of coefficient  $\beta$  have been determined for various types of loads and are given below in Table 20.

It is evident from the table that the values of coefficient  $\beta$  approach its values for a rectangular section as  $l/h$  is increased. At  $\alpha = 100$ ,  $\beta$  almost coincides with its numerical value for a rectangular beam.

While studying the stability of plane shape during bending it is essential that the normal stresses due to bending should not exceed

\* S. Timoshenko, *Theory of Elastic Stability*, Toronto, 1961.

Table 20

Coefficient  $\beta$  in Formula (28.11)

$\alpha = \frac{C_2}{C_1} \left( \frac{l}{h} \right)^2$				$\alpha = \frac{C_2}{C_1} \left( \frac{l}{h} \right)^2$			
$\beta_1$	$\beta_2$	$\beta_3$	$\beta_4$	$\beta_1$	$\beta_2$	$\beta_3$	$\beta_4$
1	2	3	4	1	2	3	4
0.1	31.6	86.4	143.0	16	5.08	18.3	30.5
1.0	9.76	31.9	53.0	20	4.85	18.1	30.1
2.0	8.03	25.6	42.6	32	4.50	17.9	29.4
4.0	6.73	21.8	36.3	50	4.35	17.5	29.0
6.0	6.19	20.3	33.8	70	4.10	17.4	28.8
8.0	5.87	19.6	32.6	90	4.04	17.2	28.6
12.0	5.36	18.8	31.5	100	4.04	17.2	28.6

Column 2 is for a cantilever loaded at the free end.

Column 3 is for a simply supported beam with a force acting at the middle of its span.

Column 4 is for a simply supported beam loaded with a uniformly distributed force.

the permissible stress for stability,  $[\sigma_s] = \frac{\sigma_c}{k_s}$ , where  $k_s$  is the safety factor.

Knowing the critical force for each type of load on the beam, we can easily determine the critical stress:

$$\sigma_c = \frac{M_{\max}^c}{W_y}$$

where  $M_{\max}^c$  is the maximum bending moment due to the critical force and  $W_y$  is the section modulus in the web plane.

The results obtained above hold good only when the critical stress under buckling does not exceed the limit of proportionality of the material.

If  $\sigma_c > \sigma_p$ , then the formulas derived above give exaggerated values of the critical stresses, just as Euler's formula gives overstated values for compressed bars of low flexibility. Data collected by experimental studies should be used for determining the actual critical stresses under buckling of beams when  $\sigma_c > \sigma_p$ . Prof. Yasinskii suggests that the analogy with compressed bars can be successfully employed by assuming that the ratio between the actual stresses and the stresses determined by the formulas derived in this section is the same as between the actual stresses and critical stresses in compressed bars when  $\sigma_c > \sigma_p$ .

Let us consider the following example. A simply supported I-beam No. 60 (see Appendix) with a span  $l=6$  m is loaded by a uniformly

distributed force of intensity  $q=9$  tf/m. Check the strength and stability of plane shape of the beam if the permissible stress  $[\sigma]=1600$  kgf/cm<sup>2</sup> and the safety factor for strength and stability are both equal to  $k=1.7$ .

The dimensions of the section (Fig. 401) and its geometrical characteristics, as obtained from the specifications, are:  $h=60$  cm,  $b=19$  cm,  $\delta_1=1.2$  cm,  $\delta_2=t=17.8$  mm  $\approx 1.8$  cm,  $h_1=60-2 \times 1.8=56.4$  cm,  $J_y=76\,800$  cm<sup>4</sup>,  $J_z=1725$  cm<sup>4</sup>,  $W_y=2560$  cm<sup>3</sup>.

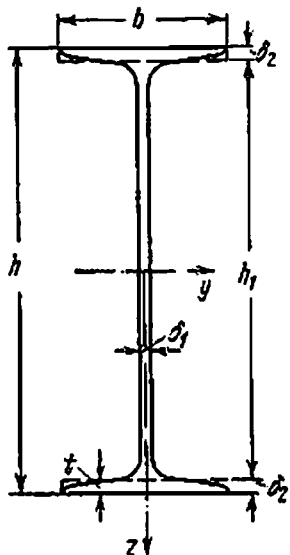


Fig. 401

The torsional moment of inertia has been calculated from formula (9.38'):  $J_t = \frac{1}{3} \eta \sum h \delta^3$ , where  $\eta=1.2$  for an I-beam. Substituting the numerical values, we obtain

$$J_t = \frac{1.2}{3} (h_1 \delta_1^3 + 2b \delta_2^3) \\ = 0.4 (56.4 \times 1.2^3 + 2 \times 19 \times 1.8^3) = 127 \text{ cm}^4$$

Let us check the beam section for strength and stability of plane form.

(a) *Strength check:*

$$M_{\max} = \frac{ql^2}{8} = \frac{9 \times 6^2}{8} = 40.5 \text{ tf} \cdot \text{m} \\ = 405 \times 10^4 \text{ kgf} \cdot \text{cm}$$

$$\sigma_{\max} = \frac{M_{\max}}{W_y} = \frac{405 \times 10^4}{2560} \\ = 1590 \text{ kgf/cm}^2 < 1600 \text{ kgf/cm}^2$$

(b) *Check for stability.* The critical load that leads to instability of the uniplanar state of bending may be calculated from formula (28.11):

$$Q_c = (ql)_c = \frac{\beta}{l^2} \sqrt{C_1 C_2}$$

where  $C_1 = EJ$ , is the rigidity under bending,  $C_2 = GJ_t$  is the torsional rigidity, and  $\beta$  is a coefficient that depends upon the ratio of rigidities and  $l/h$ .

Assuming that the modulus of elasticity for steel  $E=2 \times 10^6$  kgf/cm<sup>2</sup> and shearing modulus from formula (6.38)  $G = \frac{E}{2(1-\mu)} = \frac{E}{2.6}$ , we get

$$Q_c = (ql)_c = \frac{\beta}{l^2} \sqrt{C_1 C_2} = \frac{\beta E}{l^2} \sqrt{\frac{1725 \times 127}{2.6}} \\ = \beta \frac{2 \times 10^6}{600^2} \sqrt{84\,100} = \beta \times 5.56 \times 290 = 1610 \beta$$

As coefficient  $\beta$  depends upon the ratio

$$\alpha = \frac{C_2}{C_1} \left( \frac{l}{h} \right)^2 = \frac{GJ_1}{LJ_z} \left( \frac{l}{h} \right)^2 = \frac{127}{2.6 \times 1725} \left( \frac{600}{60} \right)^2 = 2.84$$

by using Table 20 (Column 4) and interpolating between  $\alpha=2$  and  $\alpha=4$  we find  $\beta=39.4$ , and the critical load is:

$$Q_c = (ql)_c = 1610 \times 39.4 = 63\,400 \text{ kgf}$$

In order to avoid buckling the permissible load should be taken as

$$[Q] = \frac{Q_c}{k} = \frac{63\,400}{1.7} = 37\,300 \text{ kgf}$$

For the chosen value of  $k=1.7$  the intensity of the uniformly distributed load should not exceed

$$q = \frac{[Q]}{l} = \frac{37\,300}{6} = 6250 \text{ kgf/m}$$

Hence, reliable functioning of the beam can be ensured only if the given intensity of 9 tf/m is reduced by about one and a half or by providing side supports which prevent buckling of the beam (if the beam design permits this).

Let us see how the value of critical force changes when side constraints are applied. Applying side constraints is equivalent to reducing the free length of the beam by two and using other values of coefficients  $\alpha$  and  $\beta$ :

$$\alpha = \frac{C_2}{C_1} \left( \frac{0.5l}{h} \right)^2 = \frac{GJ_1}{EJ_z} 0.25 \left( \frac{l}{h} \right)^2 = \frac{127 \times 0.25}{2.6 \times 1725} \left( \frac{600}{60} \right)^2 = 0.71$$

From Table 20 we obtain  $\beta=0.57$  by graphic interpolation between  $\alpha=0.1$  and  $\alpha=1.0$ . The critical load is:

$$Q_c = \beta \frac{E}{(0.5l)^2} \sqrt{C_1 C_2} = 0.57 \frac{E}{0.25l^2} \sqrt{\frac{J_z J_1}{2.6}} = 0.57 \frac{2 \times 10^6 \times 290}{0.25 \times 600^2} = 367\,000 \text{ kgf}$$

This corresponds to critical stress

$$\sigma_c = \frac{Q_c l}{8W_y} = \frac{367\,000 \times 600}{8 \times 2560} = 10\,300 \text{ kgf/cm}^2$$

The value of  $\sigma_c$  is considerably greater than the limit of proportionality of the material; therefore, formula (28.11) cannot be applied. The value of critical stress obtained above actually corresponds to the yield stress of the material. Therefore, in this case it is sufficient to carry out the strength check only.



### § 162. Design of Compressed-bent Bars

While studying the combined effect of axial and lateral forces in Chapter 21 we used the principle of superposition of forces and added the stresses due to tension or compression to the stresses due to bending. The strength condition in this case is:

$$\sigma_{\max} = \frac{N}{S} + \frac{M_{\max}}{W} \leq [\sigma] \quad (21.1)$$

Assuming that the axial force  $N = \pm P$  does not participate in bending, in the formula we used bending moment  $M_{\max}$  caused only by lateral forces. However, we have already seen while studying the stability of bars by Euler's method (§ 155) that in the case of buckling the axial compressive force  $P$  creates an additional bending moment  $M' = Pf$ , which gives rise to additional stresses and displacements due to additional bending of the bar (Fig. 402). The maximum stress in the critical section may be determined by the formula

$$\sigma_{\max} = \left| \frac{P}{S} + \frac{M_{\max}}{W} + \frac{Pf}{W} \right| \quad (28.12)$$

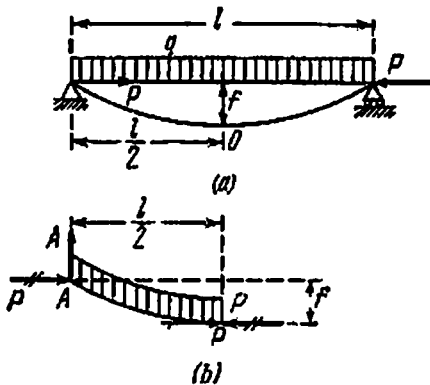


Fig. 402

where  $f$  is the maximum deflection due to the lateral and axial compressive forces. If the axial force is tensile, it decreases the curvature of the buckled bar and reduces stress  $\sigma_{\max}$ ; this case is of little interest (the third term in formula (28.12) will be deducted).

From a comparison of formulas (21.1) and (28.12) we see that by applying the principle of superposition of forces (Chapter 21) we neglect the additional bending moment  $Pf$  due to axial forces and the stress  $Pf/W$ . Strictly speaking, the principle of superposition of forces cannot be applied at all if both axial and lateral forces act on the bar. By neglecting the third term in formula (28.12) we introduce a serious error except when the bar is sufficiently rigid and deflection  $f$  is small in magnitude. However, if we ignore the bending caused by axial forces in flexible bars, this may lead to serious errors while determining the stresses.

In order to avoid such errors it is essential to take into account the bending moment due to axial forces  $P$  by determining deflection  $f$  caused by the combined action of both axial and lateral forces.

For the compressed-bent bar shown in Fig. 402 the differential

equation of the elastic curve is:

$$EJ''_y = M_0 - Py \quad (28.13)$$

Here  $M_0 = \frac{ql}{2}x - \frac{qx^2}{2}$  is the bending moment due to the lateral forces. Dividing (28.13) by  $EJ$  and substituting  $\frac{P}{EJ} = k^2$ , we obtain

$$y'' + k^2y = \frac{1}{EJ} \left( \frac{ql}{2}x - \frac{qx^2}{2} \right)$$

The general solution of this equation may be expressed

$$y = C_1 \sin kx + C_2 \cos kx + y^*$$

After choosing the particular solution  $y^*$  (here  $y^* = \frac{q}{2k^2 EJ} \times \left( \frac{2}{k^2} + lx - x^2 \right)$ ) and determining the constants of integration  $C_1$  and  $C_2$  from constraint conditions at the bar ends ( $y=0$  at  $x=0$  and  $y=0$  at  $x=l$ ) we may calculate  $y$  and find deflection  $f$  at  $x=l/2$ .

However, if several forces are acting on the bar, this approach leads to cumbersome calculations, because for different portions  $M_0$  has different expressions and the elastic curve consists of a number of conjugated curves. In such cases it is simpler to solve the problem by an approximate method. The idea lying at the root of this method is that the shape of the elastic curve is defined beforehand with the condition that it must satisfy the boundary conditions; this makes it much easier to solve the problem.

Suppose a beam is loaded by lateral forces  $P_1, P_2, P_3$  and axial compressive force  $P$  (Fig. 403). Bearing in mind that a sinusoidal elastic curve was obtained while solving Euler's problem, we assume that in our problem also the elastic curve due to lateral forces is sinusoidal:

$$y_0 = f_0 \sin \frac{\pi x}{l} \quad (28.14)$$

It can be easily seen that this equation for the elastic curve satisfies the boundary conditions: at both supports, at  $x=0$  and  $x=l$ , deflection  $y_s=0$ . At the supports the bending moments are also zero ( $M_0 = EJy''_s = -EJ\frac{\pi^2}{l^2} \sin \frac{\pi x}{l}$  becomes zero for  $x=0$  and  $x=l$ );  $f_0$  is the maximum deflection of the beam due to lateral forces acting at right angles to its axis.

Let us rewrite equation (28.13) by substituting  $EJy''_s$  for  $M_0$ :

$$EJy'' = EJy''_s - Py$$

or

$$EJy'' + Py = -EJ\frac{\pi^2}{l^2} f_0 \sin \frac{\pi x}{l}$$

Dividing by  $EJ$  and substituting  $\frac{P}{EJ} = k^2$ , we get

$$y'' + k^2 y = -\frac{\pi^2}{l^2} f_0 \sin \frac{\pi x}{l} \quad (28.15)$$

It will be easiest to look for the solution in the form  $y = f \sin \frac{\pi x}{l}$ , i.e. assume that under the combined action of axial and lateral

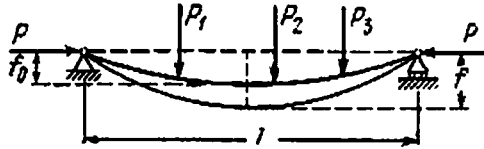


Fig. 403

forces the beam bends along the same sine curve. After substituting in equation (28.15), we obtain

$$-\frac{\pi^2}{l^2} f \sin \frac{\pi x}{l} + k^2 f \sin \frac{\pi x}{l} = -\frac{\pi^2}{l^2} f_0 \sin \frac{\pi x}{l}$$

or

$$f - \frac{k^2 l^2}{\pi^2} f = f_0$$

wherefrom

$$f = \frac{f_0}{1 - \frac{k^2 l^2}{\pi^2}} \quad (28.16)$$

Substituting  $k^2 = P/(EJ)$  and keeping in mind that expression  $\frac{\pi^2 EJ}{l^2}$  may be represented as Euler's critical force, we get

$$f = \frac{f_0}{1 - \frac{P}{P_c}} = C f_0 \quad (28.17)$$

Coefficient  $C$  accounts for the effect of axial forces on deflection:

$$C = \frac{1}{1 - \frac{P}{P_c}} = \frac{P_c}{P_c - P} \quad (28.18)$$

It is clear from formula (28.18) that deflection  $f$  should theoretically become infinite when compressive force  $P$  attains its critical value. Note that critical force  $P_c$  enters the formula formally as a substitution for  $\pi^2 EJ/l^2$ , where  $J$  is the moment of inertia of the section about the neutral axis when the beam is acted upon by lateral forces. This means that  $J$  is not  $J_{\min}$ , as the beam is usually placed in such a way that the moment of inertia of its section is maximum about the neutral axis.

Let us apply the solution obtained here to particular examples, for instance to a simply supported beam subjected to bending by a uniformly distributed force  $q$  and compressed by forces  $P$  (Fig. 402). As already established,

$$M_{\max} = M_0 + Pf = \frac{ql^2}{8} + Pf_0 C \quad (28.19)$$

where  $f_0 = \frac{5ql^4}{384EJ}$  (see Chapter 15); therefore

$$M_{\max} = \frac{ql^2}{8} + P \frac{5ql^4}{384EJ} C = \frac{ql^2}{8} \left( 1 + \frac{5Pl^4}{48EJ} C \right)$$

Multiplying and dividing the fraction inside the parentheses by  $\pi^2$ , we obtain for this fraction

$$\frac{5\pi^2 Pl^4}{48\pi^2 EJ} = \frac{1.028P}{P_c}$$

and the expression for  $M_{\max}$  becomes

$$M_{\max} = \frac{ql^2}{8} \left( 1 + \frac{1.028P}{P_c} C \right) = \frac{ql^2}{8} C_1 \quad (28.20)$$

For practical purposes we may assume that  $1.028P = P$ , and after substituting coefficient  $C = \frac{P_c}{P_c - P}$  in formula (28.20) we get

$$M_{\max} = \frac{ql^2}{8} \left( 1 + \frac{P}{P_c} \frac{P_c}{P_c - P} \right) = \frac{ql^2}{8} \frac{P_c}{P_c - P} \quad (28.20')$$

For the assumed approximation ( $1.028 \approx 1$ ) coefficient  $C_1 = \alpha C$  is found to be equal to  $C$ , i.e. the same as in deflection. Some authors suggest that we can always assume that  $C_1 = C$  on the basis of the assumption that bending moments are proportional to deflections.

Formula (28.12) for normal stresses acquires the form

$$\sigma_{\max} = \frac{P}{S} + \frac{M_0}{W} \frac{1}{1 - \frac{P}{P_c}} = \frac{P}{S} + \frac{M_0}{W} C_1 \quad (28.21)$$

When  $\frac{P}{P_c}$  is small, coefficient  $C_1$  is close to unity and formula (28.21) coincides with (21.1).

Let us note that when the beam is symmetrically loaded by lateral forces, approximate formulas (28.17) and (28.21) give results that are very close to the exact solution. The results in the case of unsymmetric loading are slightly poorer, yet they are quite acceptable for practical calculations (discrepancy does not exceed 5-7%). If all forces act in one direction, the deflection  $f_0$  may be considered maximum at the middle of the span.

It is evident from the formulas derived above that there exists a non-linear relationship between deflections and stresses and the forces applied: if all the forces are increased, say,  $n$  times, the stresses increase more than  $n$  times due to the increase in the value of coefficient  $C_1$ . This means that the strength condition  $\sigma_{\max} \leq [\sigma]$  ceases to be valid.

Therefore, in order to ensure sufficient strength the compressed-bent bars should be designed for permissible loads. Let us derive the strength condition for the beam discussed above.

Let us assume that in our beam the maximum stresses become equal to yield stress when all the forces are raised  $k_0$  times. Formula (28.21) may be rewritten as follows:

$$\frac{k_0 P}{S} + \frac{k_0 q l^2}{8W} \frac{1}{1 - \frac{k_0 P}{P_c}} = \sigma_y$$

where  $k_0 P$  and  $k_0 q$  are limiting loads. To go over to permissible loads we divide this equation by the safety factor  $k_0$ . The equation then becomes

$$\frac{P}{S} + \frac{q l^2}{8W} \frac{1}{1 - \frac{k_0 P}{P_c}} = \frac{\sigma_y}{k_0}$$

Here  $\frac{\sigma_y}{k_0} = [\sigma]$  is the main permissible stress under compression. The strength condition may be written as follows:

$$\sigma_{\max} = \frac{P}{S} + \frac{q l^2}{8W} \frac{1}{1 - \frac{k_0 P}{P_c}} \leq [\sigma] \quad (28.22)$$

The effect of axial forces on stress in the given bar is taken into account by coefficient

$$C_0 = \frac{1}{1 - \frac{k_0 P}{P_c}} = \frac{P_c}{P_c - k_0 P} \quad (28.23)$$

We now impose a restriction on deflection by writing the rigidity condition:

$$f_{\max} = f_0 \frac{1}{1 - \frac{k_f P}{P_c}} = f_0 \frac{P_c}{P_c - k_f P} \leq [f] \quad (28.24)$$

where  $[f]$  is the permissible deflection and  $k_f$  is the safety factor against deflection.

Besides checking the strength and rigidity of the bar in the plane of bending it is necessary to check its stability in the plane of mini-

imum rigidity when it is subjected only to compressive forces  $P$  (§ 158) and also check the stability for plane surface in bending (§ 161).

Let us consider one more example. Suppose that a simply supported beam is subjected to bending by a force  $P_0$ , acting at the middle of its span and is compressed by an axial force  $P$ . From formulas (28.17) and (28.18) the deflection at the middle of the span is:

$$f = f_0 C, \quad \text{or} \quad f = \frac{P_0 l^3}{48 E J} \frac{1}{1 - \frac{P}{P_c}} \quad (28.25)$$

The maximum absolute normal stresses in the critical section are:

$$\sigma_{\max} = \frac{P}{S} + \frac{M_0 + P f}{W} \quad (28.26)$$

or

$$\sigma_{\max} = \frac{P}{S} + \frac{P_0 l}{4 W} + \frac{P}{W} \frac{P_0 l^3}{48 E J} C = \frac{P}{S} + \frac{P_0 l}{4 W} \left( 1 + \frac{P l^2}{12 E J} \frac{1}{1 - \frac{P}{P_c}} \right)$$

Substituting

$$\frac{12 E J}{l^2} = \frac{\pi^2 E J}{0.822 l^2} = \frac{P_c}{0.822}$$

we obtain

$$\sigma_{\max} = \frac{P}{S} + \frac{P_0 l}{4 W} \left( 1 + \frac{0.822 P}{P_c} \frac{P_c}{P_c - P} \right) \quad (28.27)$$

After transformations, we get

$$\sigma_{\max} = \frac{P}{S} + \frac{P_0 l}{4 W} \frac{P_c - 0.178 P}{P_c - P} \quad (28.28)$$

or

$$\sigma_{\max} = \frac{P}{S} + \frac{M_0}{W} C_1$$

Here  $C_1$  is slightly less than  $C$ . For example, when  $P = 0.5 P_c$ ,  $C = \frac{P_c}{P_c - P} = 2$  while  $C_1 = 1.822$ . Calculations are the same as in the preceding example.

### § 163. Effect of Eccentric Compressive Force and Initial Curvature of Bar

A. In case of eccentric application the axial compressive force leads to eccentric compression, which, as shown earlier (Chapter 21) results in axial compression and bending (§ 162). By using the results obtained in § 162 we can take into account the effect of initial eccentricity  $e$  of the axial compressive force  $P$  (Fig. 404 (a)).

According to formula (28.17) the maximum deflection in this case is

$$f = f_0 C$$

where  $f_0$  is the deflection due to bending caused by moment  $M_0 = Pe$  and is equal to (Chapter 15)

$$f_0 = \frac{M_0 l^2}{8EJ} = \frac{P e l^2}{8EJ}$$

and coefficient  $C$  that accounts for the effect of axial forces on deflection (28.18) is:

$$C = \frac{1}{1 - \frac{P}{P_c}} = \frac{P_c}{P_c - P}$$

Consequently

$$f = \frac{P e l^2}{8EJ} \frac{1}{1 - \frac{P}{P_c}} \quad (28.29)$$

and the maximum compressive stress according to formula (28.12) is:

$$\sigma_{\max} = \frac{P}{S} + \frac{Pe}{W} + \frac{Pf}{W}$$

Substituting the value of  $f$ , (28.29), we obtain

$$\delta_{\max} = \frac{P}{S} + \frac{Pe}{W} + \frac{P}{W} \frac{P e l^2}{8EJ} \frac{1}{1 - \frac{P}{P_c}} = \frac{P}{S} + \frac{Pe}{W} \left( 1 + \frac{P l^2}{8EJ} \frac{1}{1 - \frac{P}{P_c}} \right) \quad (28.30)$$

After opening the brackets, we find that

$$\sigma_{\max} = \frac{P}{S} + \frac{M_0}{W} C_1, \quad \text{where } C_1 = \frac{P_c + 0.235P}{P_c - P} \quad (28.31)$$

**B.** If there is an initial curvature in the bar compressed by forces  $P$  (Fig. 404 (b)), the eccentricity of the point of application of force  $P$  is assumed to be known: in the middle of the span it is equal to  $f_0$  and the total deflection is (28.17):

$$f = f_0 C, \quad \text{or } f = f_0 \frac{1}{1 - \frac{P}{P_c}}$$

As in the earlier case of eccentric application of compressive forces, deflections rise sharply only when force  $P$  approaches the critical value,  $P_c$ . In both cases (A and B) the Euler critical force should be considered dangerous. Therefore, irrespective of eccentricity and initial curvature, the stability of a bar against buckling should be checked as in axial compression. The strength check is different,

because in these cases bending should be considered in addition to compression (see § 122).

Hence, when highly flexible bars ( $\sigma_{\max} \leq \sigma_p$ ) are subjected to axial compression, they lose stability upon the compressive force attaining the critical value determined by Euler's formula. Euler's critical force  $P = P_c$  should be taken as the breaking load. Neither the eccentric application of compressive force nor the presence of initial curvature have any influence upon the breaking load in these bars.

The above conclusion does not hold well for bars of small and medium flexibility. At critical stresses exceeding the limit of proportionality the above-mentioned factors considerably reduce  $\sigma_c$ . This has been observed experimentally and confirmed by theoretical attempts at calculating critical deformation. Experiments reveal that eccentricity of application of force considerably affects the stability of bars of small and medium flexibility, it also affects the stability of long

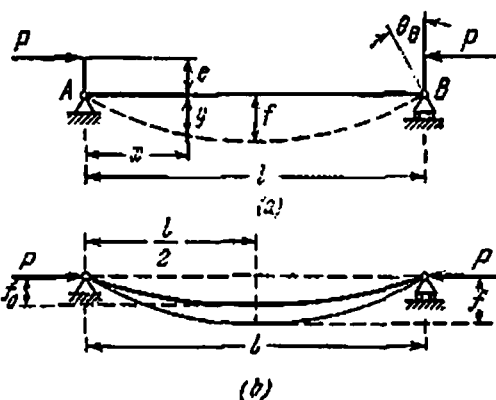


Fig. 404

bars, but to a much smaller degree. The additional factors, which have been discussed in this section, compel us to increase the stability factor for bars of small and medium flexibility and select a value which is slightly greater than the safety factor in the case of long bars. For proper evaluation of the influence of eccentricity and initial curvature on the strength and stability of compressed bars, we must get an idea about the numerical values of  $e$  and  $y_0$ .

In accurately manufactured bars we may expect an initial deflection  $y_0$  which is the  $\frac{1}{1000}$  of the length; if the manufacturing accuracy is not high, the initial deflection may be twice as large.

If the centering is proper, eccentricity may be the  $\frac{1}{750}$  of the length. Further, we must take into account the tolerances of the cross-sectional dimensions; it may be assumed that they are equivalent to an eccentricity of  $\frac{h}{40}$  and an initial deflection of the same magnitude. Here  $h$  is the cross-sectional dimension in the plane of possible buckling. In composite sections we must provide for an additional eccentricity of about  $\frac{h}{160}$  on account of the possible difference between the areas of individual elements.



Thus, for a solid section we may assume the following minimum values of  $e$  and  $y_0$ :

$$e = \frac{l}{750} + \frac{h}{40} \quad \text{and} \quad y_0 = \frac{l}{10(\kappa)} + \frac{h}{40}$$

Besides eccentricity and initial curvature, there are a number of other factors which affect the stability of compressed bars much more than the strength of beams and elements under tension. These factors include work hardening, initial stresses due to manufacturing inaccuracy of various parts, local defects in castings and knots in timber. In steel structures the effect of all these additional factors is taken into account by an increased (by 10-20%) stability factor (see § 153).

In conclusion let us note that in this section we discussed only a few problems in which critical force was determined at the instant when the bar crosses over from the existing state of equilibrium to a new one. It was assumed that bending was the only source that caused instability. However, it is known that loss of stability may occur in other forms too, in particular as bending plus torsion and pure torsion \* (in case of axial compression of thin-walled bars).

Instability is characteristic not only of bars. The theory of stability deals with many complicated problems of stability of complete structures and their individual elements—arches, frames, shells, plates, etc. Of special interest are problems of stability of such structures and their elements when subjected to dynamic loading \*\* and also investigations on stability in the process of elasto-plastic deformation and visco-elastic deformation (see Chapter 32).

It is impossible to solve these problems if a static approach is adopted towards problems of stability as problems of equilibrium in one or the other form. In all these problems deformation should be studied in time, i.e. the stability of movement must be investigated. Many complicated problems of stability are solved at present precisely on the basis of these principles. The reader can get acquainted with them in the special literature.\*\*\*

---

\* See N. M. Belyaev, *Strength of Materials*, Nauka, 1965 (in Russian), § 213.

\*\* The problem of dynamic stability of prismatic bars subjected to variable loading was first solved in 1924. See N. M. Belyaev, *Selected Works on Engineering Structures*, Leningrad, 1924 (in Russian).

\*\*\* See, for instance, I. I. Goldenblat, *Modern Problems of Vibration and Stability of Engineering Structures*, Stroitzdat, 1948 (in Russian); V. V. Bolotin, *Dynamic Stability of Elastic Systems*, Gostekhizdat, 1956 (in Russian); A. S. Volmir, *Stability of Deformable Systems*, Nauka, 1967 (in Russian).

# PART IX

## Dynamic Action of Forces

CHAPTER 29

### Effect of Forces of Inertia. Stresses due to Vibrations

#### § 164. Introduction

Until now we were solving the fundamental problem of strength of materials: determining cross-sectional sizes and selecting proper material for elements of structures by assuming the loading to be static.

It was explained in § 2 that loading may be considered static if there is no mechanical movement of the parts when pressure is transferred from one part to the other or when both parts are acted upon by body forces. Under such loading each element of the structure remains in equilibrium under the action of external forces and stresses.

The constancy of movement is characterized by constant velocity of the parts under consideration and complete absence of acceleration of these parts. If acceleration is experienced by the body or the parts contacting with it, the loading is said to be dynamic. For instance, the earth pressure on a bulkhead is an example of static loading, because neither the bulkhead nor the earth mass move, their velocities are constant and equal to zero.

Similarly, the force exerted on the rope by a load which is lifted by it may be considered static provided the load is raised with a constant velocity. On the other hand, the force exerted will be dynamic if the load is raised with acceleration. The connecting rods of steam and internal combustion engines experience dynamic loading, because their individual elements have different velocities. Two other examples of constructions working under dynamic loading are the foundation of a machine with rotating parts mounted eccentrically w.r.t. the axis of rotation (the foundation in this case experiences centripetal acceleration) and the foundation and piston rod of a steam hammer (in the process of forging the hammer block comes to a stop in a very short period on account of very strong retardation).

Even these examples are enough to make it clear that in practice we come across various types of acceleration which bodies under

consideration or bodies contacting with them have to experience. The acceleration may be constant in direction as well as magnitude or only in direction; it may also be reversible.

Under variable and reversible stresses the bodies fail due to a gradually increasing crack, and the failure is said to occur due to fatigue. If there is a sharp change in the velocity of an element of structure w.r.t. the force being exerted on it by adjacent elements, i.e. if the element experiences shock loading, the material of the element may behave as if it were brittle, although it is ductile under static loading. Therefore, in conducting a strength check for elements of structures subjected to dynamic loading, it is important to study not only the effect of external loading on the magnitude of stresses in the element but also its effect on the nature of resistance of the element material.

The effect of acceleration of elements of structures on the stressed state of the material may be accounted for as follows. If a body moves with acceleration, it is being acted upon (experiencing) by forces (pressure) from other bodies. From the law of equal reactions the body under consideration acts upon the other bodies with forces equal in magnitude and oppositely directed, namely the forces of inertia. This logic is also applicable to each element of the body moving with acceleration; the elements act on the contacting elements with a force equal to the force of inertia.

Thus, when elements of structures move with acceleration, they experience additional stresses which are equivalent to static stresses caused by forces of inertia; each element of the structure gives rise to stresses in the adjacent elements, as if the latter were acted upon by forces equal to the corresponding forces of inertia.

Here we must differentiate between three situations. If the magnitude and location of the external forces acting on the element under consideration does not depend upon the deformation of the element, i.e. if the deformation does not change the nature of motion of the body, then its acceleration is determined from the methods of kinematics of solid bodies, and the dynamic action of external forces is reduced to the addition of a static load corresponding to the inertial forces. This method is applicable to a majority of situations of practical importance (except shock loading).

If the acceleration changes, in the process, this invariably gives rise to vibrations in the element under consideration. The vibrations in their turn may cause resonance that results in a sharp increase in deformation and stresses. These stresses may be very high and must be added to the stresses obtained by considering the inertial forces as an additional static load.

Finally, there may be cases (shock loading) when the acceleration and consequently the corresponding forces of inertia depend upon the deformability of the element under consideration. In such cases

the mechanical properties of the material must be taken into account while calculating the inertial forces. The method of strength check in each of the above cases will be explained through the following examples.

§ 165. Determining Stresses in Uniformly Accelerated Motion of Bodies

We shall begin the study of strength check under dynamic loading with the simplest case when points on the element of structure under consideration move with constant acceleration without causing vibrations. As an example we shall study the uniformly accelerated lifting of load  $Q$  suspended from a steel cable of cross-sectional area  $S$ . The specific weight of the cable material is  $\gamma$ , the load is lifted with a constant acceleration  $a$  cm/sec<sup>2</sup> (Fig. 405). We shall determine the stresses in an arbitrary section at a distance  $x$  from the lower end of the cable. Let us cut the cable at this section and study the equilibrium of the lower cutoff portion. This portion moves upwards with acceleration  $a$ , which means that besides the force balancing its weight it is acted upon from the upper portion by a force equal to its mass times acceleration  $a$ , i.e.  $\frac{Q + \gamma Sx}{g} a$ , where  $g$  is the acceleration of gravity.

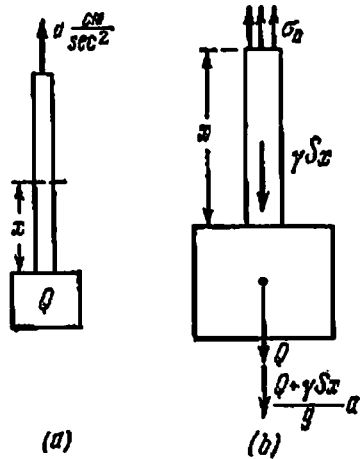


Fig. 405

From the law of equality of action and reaction the upper portion will experience a similar force acting downwards. Thus the dynamic stresses  $\sigma_D$  acting in the sectioned plane on the lower portion will balance not only the static load  $Q + \gamma Sx$  but also the additional force  $\frac{Q + \gamma Sx}{g} a$ . To determine these stresses we must study the equilibrium of the lower portion under the action of  $\sigma_D$ , static load  $Q + \gamma Sx$ , and the force of inertia  $\frac{Q + \gamma Sx}{g} a$  acting downwards (Fig. 405). We find that

$$\sigma_D = \frac{Q + \gamma Sx}{S} + \frac{Q + \gamma Sx}{gS} a = \frac{Q + \gamma Sx}{S} \left( 1 + \frac{a}{g} \right)$$

Ratio  $\frac{Q + \gamma Sx}{S}$  represents static stress  $\sigma_s$  in the section of cutting; therefore

$$\sigma_D = \sigma_s \left( 1 + \frac{a}{g} \right) \tag{29.1}$$

i.e. the dynamic stress is equal to the static stress multiplied by coefficient  $1 + \frac{a}{g}$ . This coefficient is called the dynamic coefficient and is denoted by  $K_D$ :

$$\sigma_D = K_D \sigma_s \quad (29.2)$$

This form of the formula for dynamic stresses shows why we paid special attention to calculating the stresses under static loading: in a large number of cases dynamic stresses may be expressed through static stresses by multiplying the latter with the appropriate dynamic coefficient.

The strength condition may be written

$$\sigma_{D \max} = \sigma_{s \max} \left( 1 + \frac{a}{g} \right) = K_D \sigma_{s \max} \leq [\sigma]$$

wherefrom

$$\sigma_{s \max} \leq \frac{[\sigma]}{1 + \frac{a}{g}} = \frac{[\sigma]}{K_D} \quad (29.3)$$

Thus in a number of cases dynamic analysis may be replaced by static by simply dividing the permissible stress with the dynamic coefficient  $K_D$ . This is done when it is difficult to obtain the dynamic coefficient theoretically and we have to be satisfied with the value of the dynamic coefficient determined experimentally. This method is employed, for example, in taking into account the dynamic nature of temporary loads acting on bridges.

### § 166. Stresses in a Rotating Ring (Flywheel Rim)

As a second example we shall determine the stresses in a uniform ring rotating at a high speed (Fig. 406(a)). The flywheel rim works under similar conditions, provided we neglect the effect of spokes.

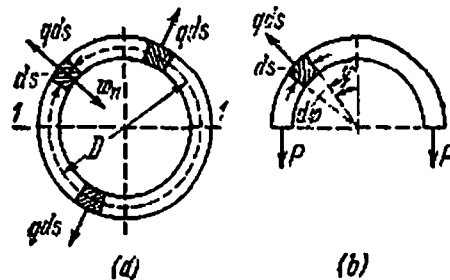


Fig. 406

Let  $S$  be the cross-sectional area of the ring,  $\gamma$  the specific weight of its material,  $n$  its number of revolutions per unit time,  $\omega$  its angular velocity of rotation and  $D$  the mean diameter of the ring.

Let us isolate an element of length  $ds$  from the ring. When the ring rotates, this element moves along a circular path with constant angular velocity  $\omega$ . Angular acceleration  $\varepsilon$  is zero. Therefore tangential acceleration of the element is  $\omega_t = \varepsilon D/2 = 0$ ; normal (centripetal) acceleration of the element is  $\omega_n = \omega^2 D/2$  and is directed toward the centre of the ring. In order to determine  $\sigma_D$ , the force of inertia must be applied to each and every element of the ring. This force is directed away from the centre and is equal to

$$\omega_n \frac{S\gamma}{g} ds = \frac{S\gamma \omega^2 D}{g \cdot 2} ds = q ds$$

where  $q$  is the intensity of the inertial force per unit length of the rim. Thus, the ring experiences stresses as if it were loaded by a radial force of intensity  $q$  per unit length (Fig. 406 (b)). Force  $P$  stretching the rim is (§ 19):

$$P = \frac{Dq}{2}$$

Stress  $\sigma_D$  is:

$$\sigma_D = \frac{P}{S} = \frac{Dq}{2S} = \frac{DS\gamma \omega^2 D}{2gS} = \frac{\gamma \omega^2 D^2}{4g} = \frac{\gamma v^2}{g}$$

where  $v = \omega D/2$  is the linear velocity of points on the surface of the ring. Thus, stresses in the rim depend only upon the specific weight of the rim material and the linear velocity of points on the rim surface. Let us solve the following problem to get an idea about the approximate value of these stresses:

$$n = 360 \text{ rpm}, \quad D = 4 \text{ m}, \quad \gamma = 7.5 \text{ gf/cm}^3$$

Angular velocity is:

$$\omega = \frac{2\pi n}{60} = \frac{2\pi \times 360}{60} = 12\pi \text{ sec}^{-1}$$

The stress is:

$$\sigma_D = \frac{\gamma \omega^2 D^2}{4g} = \frac{7.5 \times 144\pi^2 \times 16 \times 10^3}{4 \times 10^3 \times 981} = 435 \text{ kgf/cm}^2$$

## § 167. Stresses in Connecting Rods

Let us check the strength of connecting rod  $AB$  joining two wheel axles of a steam engine (Fig. 407); to the driving wheel  $O_1$  is transmitted a torque from the steam engine. The connecting rod is secured to the wheels at points  $A$  and  $B$  with the help of cylindrical hinges,  $AO_1$  and  $BO_1$  are both equal to  $r$ , diameter of the wheels is  $D$ , length of the connecting rod is  $l$  and the steam engine moves with a constant velocity  $v$ .

As the connecting rod is in movement, the first step in checking its strength is to establish whether the motion is with acceleration, i.e. solve a clear-cut problem of kinematics. The connecting rod is in relative motion w.r.t. the steam engine, and the engine imparts to it translational motion of velocity  $v$ .

As the translational motion is of constant velocity, the acceleration can appear only in the relative motion. Now in relative motion of the connecting rod two of its points  $A$  and  $B$  move identically, de-

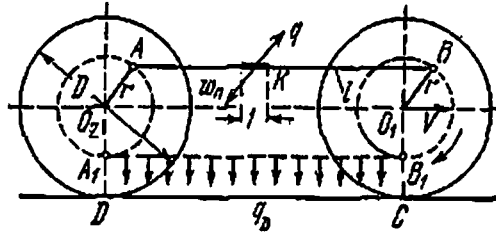


Fig. 407

scribing circles of radius  $r$  in a single plane. The relative motion of the connecting rod may therefore be considered plane-rectilinear and it may be safely concluded that all points of the connecting rod have the same velocity and acceleration as points  $A$  and  $B$ .

Point  $A$  moves with the second wheel describing a circle of radius  $r$ . If the steam engine is moving with uniform velocity, the angular velocity of rotation  $\omega$  of the wheels must also be constant. This means that angular acceleration must be zero and hence the tangential acceleration of point  $A$  must also be zero, i.e.  $\omega_t = 0$ . Point  $A$  experiences only centripetal acceleration directed from  $A$  towards  $O_2$  and equal to  $\omega^2 r$ . Any other point on the connecting rod, say, point  $K$ , experiences the same acceleration parallel to  $O_2 A$ .

To check the strength of the connecting rod, the load due to inertial forces must be added to its dead weight. The inertial force per unit length of the connecting rod is:

$$q = \frac{1 \times S \gamma}{g} \omega_n = \frac{S \gamma}{g} \omega^2 r$$

this force of inertia acts parallel to  $O_2 A$  but is directed opposite to the direction of acceleration.

In the position of the connecting rod shown in the diagram, bending caused by its dead weight is opposite to that caused by the forces of inertia. The connecting rod finds itself critically loaded in the lowermost position  $A_1 B_1$  when both the forces act in the same direction. The total load  $q_D$  per unit length of the connecting rod will in this case be

$$q_D = \gamma S + \frac{\gamma S}{g} \omega^2 r = \gamma S \left( 1 + \frac{\omega^2 r}{g} \right)$$

The connecting rod should be analyzed as a beam hinged at points  $A$  and  $B$  and loaded by a uniformly distributed force  $q_D$ . The maximum bending moment at the middle of span will be

$$M_{\max} = \frac{q_D l^2}{8} = \frac{\gamma S l^2}{8} \left( 1 + \frac{\omega^2 r}{g} \right)$$

The maximum stress in this section will be

$$\sigma_{D\max} = \frac{M_{\max}}{W} = \frac{S}{W} \frac{\gamma l^2}{8} \left( 1 + \frac{\omega^2 r}{g} \right)$$

**Example.** Analyze two following shapes of the connecting rod, (a) rectangular cross section and (b) I-section (Fig. 408), for the data given below:

$$\omega = 30 \text{ sec}^{-1}, \quad \gamma = 7.86 \text{ gf/cm}^3, \quad r = 50 \text{ cm}, \quad l = 150 \text{ cm}$$

In this example

$$\frac{\gamma l^2}{8} \left( 1 + \frac{\omega^2 r}{g} \right) = \frac{0.00786 \times 150^3}{8} \left( 1 + \frac{50 \times 30^2}{981} \right) = 1036 \text{ kgf/cm}$$

For the rectangular section

$$S = 10 \times 4.5 = 45 \text{ cm}^2, \quad W = \frac{4.5 \times 10^3}{6} = 75 \text{ cm}^3$$

$$\frac{S}{W} = \frac{45}{75} = 0.6 \text{ cm}^{-1}, \quad \sigma_{D\max} = 0.6 \times 1036 = 622 \text{ kgf/cm}^2$$

For the I-section:

$$S = 10 \times 4.5 - 2 \times 6 \times 1.5 = 27 \text{ cm}^2, \quad W = \frac{4.5 \times 10^3 - 2 \times 1.5 \times 6^3}{12 \times 5} = 64.2 \text{ cm}^3$$

$$\frac{S}{W} = \frac{27}{64.2} = 0.42 \text{ cm}^{-1}, \quad \sigma_{D\max} = 0.42 \times 1036 = 435 \text{ kgf/cm}^2$$

Hence, despite the decrease in the section modulus (almost by 15%) the maximum stresses in the second case are less by 1.5 times due to considerable decrease in the weight of the connecting rod.

Besides bending, the connecting rod is subjected to tension or compression due to force  $P$  with which wheel  $O_1$  acts on wheel  $O_2$ . In position  $A_1 B_1$  the connecting rod experiences compression. Neglecting the effect of deflection on the bending moment we may write the strength condition as follows:

$$\sigma_{\max} = \frac{P}{S} + \frac{\gamma S l^2}{8W} \left( 1 + \frac{\omega^2 r}{g} \right) \leq [\sigma]$$

In addition to the strength check the connected rod should also be checked for stability by considering it as simply supported in the



plane of bending caused by  $q_D$ , and as a bar fixed rigidly at one end in a perpendicular plane. While calculating flexibility the maximum value of the radius of gyration should be used in the first case and the minimum in the second.

We may similarly design connecting rod  $AB$  hinged at end  $A$  with the crank  $OA$  that is rotating about point  $O$  with angular velocity  $\omega$  (Fig. 409). If the crank rotates with constant angular velocity, point  $A$  of the connecting rod experiences only centripetal acceleration,

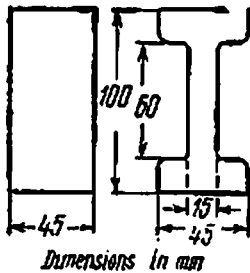


Fig. 408

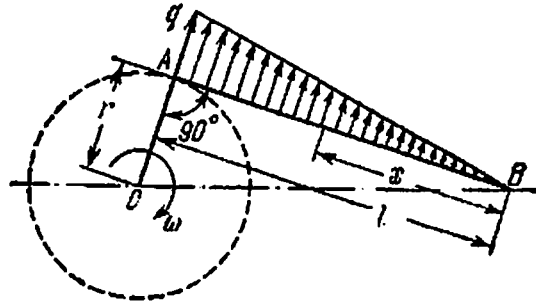


Fig. 409

whereas point  $B$  experiences only tangential acceleration. All other points of the connecting rod between points  $A$  and  $B$  experience both accelerations. Limiting ourselves to forces of inertia arising in the connecting rod due to centripetal acceleration only, let us study the position of the connecting rod when it is perpendicular to the crank and, consequently, when the centripetal acceleration of point  $A$  is perpendicular to the crank axis. Let us assume that the centripetal inertial force  $q$  is perpendicular to the crank at all points and changes linearly along the length of the connecting rod from  $q=q_0$  at point  $A$  to  $q=0$  at point  $B$ . The greater the length of the connecting rod as compared to the crank the higher is the accuracy of this assumption. The connecting rod may be considered as a simply supported beam hinged at points  $A$  and  $B$ . The bending moment is maximum at  $x = \frac{l}{\sqrt{3}}$  ( $x$  is measured from point  $B$ ) and is equal to (see § 59)

$$M_{\max} = \frac{q_0 l^2}{9\sqrt{3}}$$

Since  $q_0 = \frac{S\gamma \times l}{g} \omega^2 r$  and  $\sigma_{D\max} = \frac{M_{\max}}{W}$ , we get

$$\sigma_{D\max} = \frac{q_0 l^2}{9\sqrt{3}W} = \frac{S\gamma l^2 \omega^2 r}{9\sqrt{3}Wg}$$

### § 168. Rotating Disc of Uniform Thickness

The problem of determining stresses and deformation in shafts and discs rotating at high speeds is of considerable interest. Due to their high speeds of rotation, the steam turbine shafts and discs experience large centripetal forces. The stresses caused by these forces are distributed symmetrically about the axis of rotation of the disc.

Let us study a simple problem on analysis of discs of uniform thickness. The analysis of such discs lies at the base of several approximate methods employed in analyzing discs of an arbitrary shape. We shall use here some results obtained while deriving the formulas for the analysis of thick-walled cylinders (§ 144). Let us assume that stresses  $\sigma_r$  and  $\sigma_t$  remain constant over the width of the disc of unit thickness; we shall consider axial stress  $\sigma_z$  to be equal to zero.

Let us write the conditions of equilibrium of element  $AB$  isolated from the disc by two meridian sections and two concentric cylindrical surfaces (Fig. 410). In this case, besides the forces acting on element  $AB$ , we must also take into account inertial force

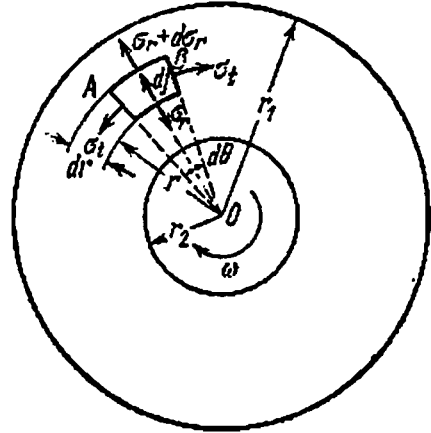


Fig. 410

$$dj = \omega^2 r \frac{\gamma r \times 1 \times dr d\theta}{g}$$

which acts from the centre of the disc towards its periphery. Equation (25.1) derived in § 144 may be replaced by the following relation:

$$\sigma_r - \sigma_t + r \frac{d\sigma_r}{dr} + \frac{\gamma \omega^2 r^2}{g} = 0 \quad (29.4)$$

Equation (25.4) of the same section (equation of joint deformation) remains valid in the present case also, i.e.

$$\frac{d\sigma_t}{dr} - \mu \frac{d\sigma_r}{dr} = \frac{1+\mu}{r} (\sigma_r - \sigma_t) \quad (29.5)$$

Substituting the value of  $(\sigma_r - \sigma_t)$  from equation (29.4) in equation (29.5), we get

$$\frac{d\sigma_t}{dr} = -\frac{d\sigma_r}{dr} - \frac{1+\mu}{g} \gamma \omega^2 r \quad (29.6)$$

Differentiating equation (29.4) with respect to  $r$  and substituting  $\frac{d\sigma_r}{dr}$  from equation (29.6), we get the following linear differential equation:

$$r \frac{d^2\sigma_r}{dr^2} + 3 \frac{d\sigma_r}{dr} + \frac{3+\mu}{g} \gamma \omega^2 r = 0$$

or

$$\frac{d}{dr} \left[ \frac{1}{r} \frac{d}{dr} (r^2 \sigma_r) \right] + \frac{3+\mu}{g} \gamma \omega^2 r = 0$$

Upon integration we obtain

$$\sigma_r = A + \frac{B}{r^2} - \frac{3+\mu}{8g} \gamma \omega^2 r^2 \quad (29.7)$$

It ensues from equations (29.4) and (29.7) that

$$\sigma_t = \sigma_r + r \frac{d\sigma_r}{dr} + \frac{\gamma \omega^2 r^2}{g} = A - \frac{B}{r^2} - \frac{1+3\mu}{8g} \gamma \omega^2 r^2 \quad (29.8)$$

In formulas (29.7) and (29.8),  $A$  and  $B$  are constants of integration, which must be determined from the conditions at the disc surface. In determining the constants we shall study the following two cases: (a) disc with a central hole, and (2) solid disc. Let us assume that ends of the disc are free of external forces.

For the disc with a central hole, stress  $\sigma_r$  must be zero at  $r=r_1$  as well as at  $r=r_2$  (Fig. 410). When the conditions at the disc surface are applied to formula (29.7) we get the following equations:

$$A + \frac{B}{r_2^2} - \frac{3+\mu}{8g} \gamma \omega^2 r_2^2 = 0$$

and

$$A + \frac{B}{r_1^2} - \frac{3+\mu}{8g} \gamma \omega^2 r_1^2 = 0$$

wherefrom

$$A = \frac{3+\mu}{8g} \gamma \omega^2 (r_1^2 + r_2^2), \quad B = -\frac{3+\mu}{8g} \gamma \omega^2 r_1^2 r_2^2$$

Substituting the values of  $A$  and  $B$  in formulas (29.7) and (29.8), we get

$$\sigma_r = \frac{3+\mu}{8g} \gamma \omega^2 \left( r_1^2 + r_2^2 - r^2 - \frac{r_1^2 r_2^2}{r^2} \right)$$

and

$$\sigma_t = \frac{\gamma \omega^2}{8g} \left[ (3+\mu) \left( r_1^2 + r_2^2 + \frac{r_1^2 r_2^2}{r^2} \right) - (1+3\mu) r^2 \right]$$

Assuming for brevity that

$$\frac{r_2}{r_1} = \alpha, \quad \frac{r}{r_1} = \rho, \quad \frac{3+\mu}{8g} \gamma \omega^2 r_1^2 = p, \quad \frac{1+3\mu}{3+\mu} = m$$

we may write the equations obtained above as follows:

$$\sigma_r = p \left[ 1 + \alpha^2 \left( 1 - \frac{1}{\rho^2} \right) - \rho^2 \right] \quad (29.9)$$

and

$$\sigma_t = p \left[ 1 + \alpha^2 \left( 1 + \frac{1}{\rho^2} \right) - m\rho^2 \right] \quad (29.10)$$

Let us point out that  $\sigma_r$  becomes zero at  $\rho=1$  and  $\rho=\alpha$ , i.e. at the internal and external peripheries of the disc. It is positive for values of  $\rho$  between 1 and  $\alpha$  and, as is not difficult to prove, becomes maximum at

$$\rho = \sqrt{\alpha} = \sqrt{\frac{r_2}{r_1}}$$

At this value

$$(\sigma_r)_{\max} = p(1-\alpha)^2 \quad (29.11)$$

Stress  $\sigma_t$  is also positive for all values of  $\rho$  and becomes maximum at the internal periphery of the disc, where  $\rho=\alpha$ :

$$(\sigma_t)_{\max} = p[2 + (1-m)\alpha^2] \quad (29.12)$$

From a comparison of equations (29.11) and (29.12) we can easily notice that  $(\sigma_t)_{\max}$  is always greater than  $(\sigma_r)_{\max}$ . Therefore irrespective of whether we check the strength of the disc by the theory of maximum shearing stresses or the distortion energy theory, the strength condition will be

$$(\sigma_t)_{\max} = \frac{3+\mu}{8g} \gamma \omega^2 r_1^2 [2 + (1-m)\alpha^2] \leq [\sigma] \quad (29.13)$$

Figure 411 shows curves depicting the change in values of  $\sigma_t^0 = \sigma_t/p$  along the disc radius for values of  $\alpha$  between 0 and 1 and for  $\mu=0.3$ . We note that the maximum values of  $\sigma_t$ , (29.12), (at the internal periphery of the disc) do not change much with the value of the hole's radius, i.e. with  $\alpha$  (curve *ab*). At  $\alpha \approx 0$ , i.e. when the radius of the central hole is very small, there is a sharp change in the value of  $\sigma_t$  at the hole edge due to stress concentration (curve *acd*). Under these conditions

$$(\sigma_t)_{\max} = 2p = \frac{3+\mu}{4g} \gamma \omega^2 r_1^2 \quad (29.14)$$

In a very thin circular ring, where  $r_1 \approx r_2$  and  $\alpha \approx 1$ ,

$$(\sigma_t)_{\max} = \frac{\gamma \omega^2 r_1^2}{g} \quad (29.15)$$

which is the same as obtained in § 166. In this case the maximum value of  $\sigma_t$ , (29.15), is only 20% greater than  $(\sigma_t)_{\max}$  for a disc with a very small hole (29.14).

It is evident from formulas (29.9) and (29.10) that stresses  $\sigma_r$  and  $\sigma_t$  increase sharply with the increase in the peripheral velocity  $v = \omega r_1$ . It should be noted that besides velocity  $v$  and mechanical properties of the material  $\mu$  and  $\gamma$  these stresses depend only upon dimension-

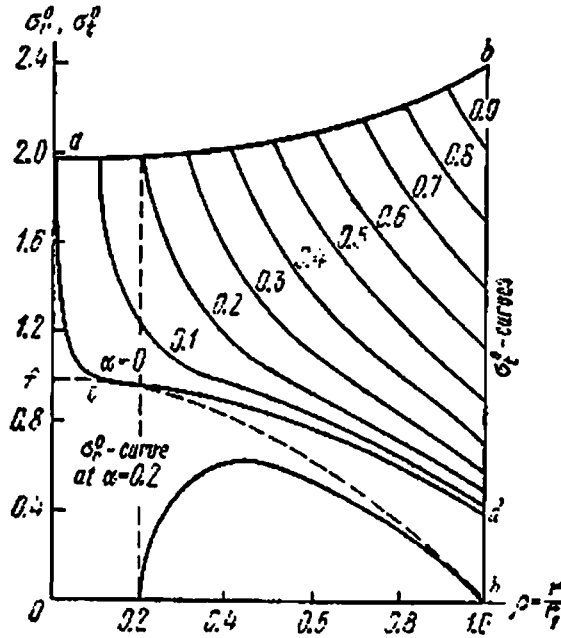


Fig. 411

less quantities  $\rho$  and  $\alpha$ . Hence  $\sigma_r$  and  $\sigma_t$  will be equal in two geometrically identical discs having same  $\rho$ 's. This property enables us to replace the actual testing of large discs by testing of small models in the laboratory.

In a solid disc,  $\sigma_r$  and  $\sigma_t$  are equal at the centre, where  $r=0$ . A comparison of formulas (29.7) and (29.8) indicates that this condition can be satisfied only if the constant of integration  $B$  is equal to zero. The other constant,  $A$ , can be found from the following condition: at  $r=r_1$ , i.e. at the external surface of the disc, stress  $\sigma_r$  must be zero. Therefore

$$A = \frac{3+\mu}{8g} \gamma \omega^2 r_1^2 = p$$

Substituting the above value of  $A$  and  $B=0$  in formulas (29.7) and (29.8), we obtain

$$\sigma_r = p(1 - \rho^2) \tag{29.16}$$

and

$$\sigma_t = \rho (1 - m\rho^2) \quad (29.17)$$

The corresponding curves showing variation of  $\sigma_r^0 = \frac{\sigma_r}{\rho}$  and  $\sigma_t^0 = \frac{\sigma_t}{\rho}$  along the disc radius are given in Fig. 411 (curves *fh* and *fd*). Both stresses are positive for all values of  $\rho$  and increase towards the centre. At  $\rho=0$

$$(\sigma_r)_{\max} = (\sigma_t)_{\max} = \rho = \frac{3+\mu}{8g} \gamma \omega^2 r_1^2 \quad (29.18)$$

Thus, in a disc with a very small central hole, stress  $\sigma_t$  at the edge of the hole is two times greater than at the centre of a solid disc on account of stress concentration (see formula (29.14)).

The above discussion was based on the assumption that the edges of the disc are free of external loading. This assumption generally does not correspond to reality. Usually the disc is mounted on the shaft in the hot state or by a hydraulic press with an interference fit, which ensures that deformation of the disc hole due to centripetal forces is always less than the deformation of the opposite sign incurred during mounting, i.e. the disc sits tightly over the shaft in normal working. The external periphery of the disc is usually fitted with a rim for mounting turbine blades; during rotation the rim gives rise to additional centripetal forces which are transmitted to the disc. Thus the internal and external peripheries of the disc are subjected to uniformly distributed tensile or compressive forces. The stresses caused by these forces may be computed by the formulas derived in the analysis of thick-walled cylinders (formulas (25.9), § 144). Upon adding the stresses obtained from formulas (25.9), (29.9) and (29.10) we can draw a complete diagram depicting distribution of stresses in a rotating disc.

### § 169. Disc of Uniform Strength

The formulas derived in the preceding section and the curves drawn in Fig. 411 show that there is considerable variation in the values of  $\sigma_r$  and  $\sigma_t$  along the radii of discs of uniform thickness. The most non-uniform distribution of stresses occurs in discs of uniform thickness with a central hole. The design of such discs is based on the maximum stress  $\sigma_t$  at the inner edge of the disc, which imposes restrictions on the limiting value of maximum velocity. For achieving high velocity of rotation the discs have to be made of variable thickness which decreases from the centre towards the periphery. The most economical shape of the disc is one in which the same stress acts on all points of the disc. Such discs are known as *discs of uniform strength*. While designing such discs it is assumed that the stresses remain

constant over the thickness of the disc; this generally gives a small error in the calculated stress value.

The basic formulas for designing discs of variable thickness can

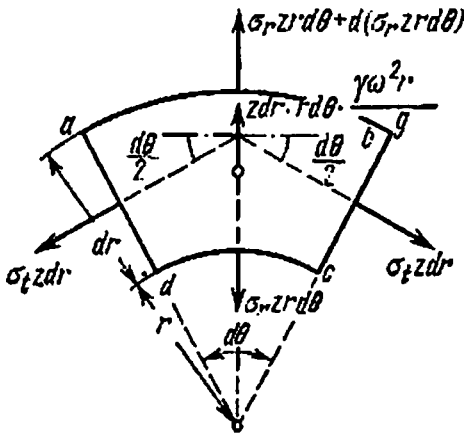


Fig. 412

be derived as before by considering the equilibrium of an element *abcd* (Figs. 410 and 412) of the disc. Let us denote by *z* the variable thickness, which is a certain function of the radius, *r*. Faces *ad* and *bc* of the element cut by meridian sections are acted upon by forces  $\sigma_t z dr$  making an angle  $d\theta$  with each other, face *dc* of the element is acted upon by a radial force  $\sigma_r z r d\theta$  directed towards the centre and face *ab* is acted upon by a radial force  $\sigma_r z r d\theta + d(\sigma_r z r d\theta)$  directed from the centre towards the outer

surface of the disc. To these forces we must add the force of inertia due to the mass of the element,

$$z dr r d\theta \frac{\gamma \omega^2 r}{g}$$

acting from the centre towards the periphery.

Projecting all the forces enumerated above on the radius, we get the following differential equation for the equilibrium of a disc of variable thickness:

$$d(\sigma_r z r d\theta) - \sigma_t z dr d\theta + z dr d\theta \frac{\gamma \omega^2 r^2}{g} = 0$$

or

$$\frac{d}{dr}(r z \sigma_r) - z \sigma_t + z \frac{\gamma \omega^2 r^2}{g} = 0$$

If  $z = \text{const}$ , the above equation transforms into equation (29.4) derived in the preceding section.

In a disc of uniform strength stresses  $\sigma_r$  and  $\sigma_t$  are constant at all points and are equal. Equating their value to the permissible stress  $[\sigma]$ , we can write the following equation of equilibrium:

$$\frac{d}{dr}(z r) - z + z \frac{\gamma \omega^2 r^2}{[\sigma] g} = 0$$

or

$$\frac{1}{z} \frac{dz}{dr} = - \frac{\gamma \omega^2 r}{[\sigma] g} = - 2nr$$

where

$$n = \frac{\gamma \omega^2}{2 [\sigma] g}$$

Upon integrating the above equation, we get

$$z = Ce^{-nr^2}$$

where  $C$  is a constant of integration. If the disc does not have a central hole then from the condition  $z=z_0$  at  $r=0$ , it ensues that  $C=z_0$ . The thickness of the disc at the centre ( $z_0$ ) is determined from conditions at its outer surface.

A solid disc of uniform strength can be used even at very high peripheral velocities. However, from the point of view of convenience of manufacturing, discs of variable thickness with central holes are generally used. These discs, which in shape are close to discs of uniform strength, provide the most advantageous distribution of stresses along the radius. The methods of analysis of such discs are discussed in special courses.

### § 170. Effect of Resonance on the Magnitude of Stresses

In the first two problems discussed in §§ 165 and 167, the acceleration was assumed to be fixed in direction w.r.t. the element on which it was acting; in the last example the acceleration was continuously changing its direction through  $360^\circ$  during one rotation of the wheel. In this case the stresses and deformations periodically changed their sign resulting in vibrations of the body.

A similar situation will arise if the beam is loaded with a machine which has a rotating load having eccentricity w.r.t. the axis of rotation (Fig. 413). The force of inertia of the rotating load will give rise to stresses and deformations in the beam which periodically change their sign. The beam will begin to vibrate with a period which is equal to the period of rotation of the load. These vibrations are known as *forced vibrations*. If the period of forced vibrations is the same as the period of natural vibrations of the beam, then resonance occurs and the amplitude of vibrations increases sharply with the passage of time. The amplitude of vibrations is in fact restricted by frictional forces and resistance of the atmospheric medium. However, despite these restrictions the amplitude may assume large values, which far exceed the deformations the beam would have experienced under the same acceleration of constant direction.

There was a case when due to resonance the angle of twist of a shaft increased six-fold as compared to the angle before resonance. This happened with the crankshaft of a motor of the airship *Graf Zeppelin* in its very first flight across the Atlantic ocean.



Thus, if resonance is not curbed at the very outset but is allowed to continue for some time, it results in a gradual growth of deformation and a corresponding increase in stresses ultimately leading to failure. Therefore, at the design stage it is essential to prevent resonance in structures which are subjected to variable acceleration of constant period.

Since the period of the exciting forces is generally given, the designer can control only the period of natural vibrations of the structure:

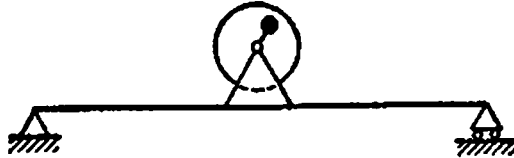


Fig. 413

the period of natural vibrations should be selected in such a way that it differs considerably from the period of the exciting forces.

Questions concerning the determining of period, frequency and amplitude of natural and forced vibrations are discussed in theoretical mechanics.\* Therefore, below (§ 171) we shall apply without proof the results of theoretical mechanics in determining stresses and checking the strength of elements of structures subjected to vibration.

### § 171. Determination of Stresses in Elements Subjected to Vibration

A. An elastic system disturbed from its stable state of equilibrium begins to vibrate. The vibrations occur near the position of elastic equilibrium in which the loaded system experiences static deformation  $\delta_s$  and a corresponding static stress  $p_s$  ( $\sigma_s$  or  $\tau_s$ , depending upon the nature of deformation). In a system subjected to vibration, to the static deformation is added dynamic deformation which depends upon the type of vibrations and their amplitude. This results in a change in the value of  $p_s$ . Hence, while checking the strength of a vibrating system it is essential to determine the dynamic deformation and the corresponding stresses in addition to the static deformation and stresses.

In a number of cases the nature of vibrations of the system can be completely defined by one quantity (one coordinate). Such systems are known as systems with a single degree of freedom; the examples of such systems are a light stretched or compressed spring with a weight suspended at its end performing longitudinal oscillations, a beam of

\* See, for instance, L. G. Loitsyanskii and A. I. Lurye, *A Course of Theoretical Mechanics* Gostekhizdat 1955 (in Russian) Part II.

small (as compared to  $Q$ ) dead weight (shown in Fig. 414) performing oscillations in a direction perpendicular to its own axis, etc.

In vibrating systems having one degree of freedom, the total deformation of an arbitrary section may be obtained by adding the static and dynamic deformations. Obviously, the strength check should

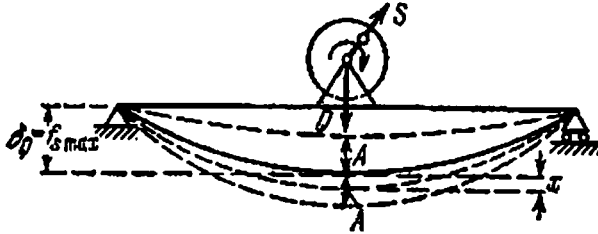


Fig. 414

be carried out for the section where the total deformation is maximum. In the simplest cases the total deformation is obtained by adding the maximum static deflection  $\delta_{s \max}$  and the maximum amplitude  $A$  of the vibrations:

$$\delta_D = \delta_{s \max} + A = \delta_{s \max} \left( 1 + \frac{A}{\delta_{s \max}} \right) = K_D \delta_{s \max} \quad (29.19)$$

As long as the system deforms within the elastic limits, the stresses are directly proportional to strain. Therefore

$$\rho_D = \rho_s \left( 1 + \frac{A}{\delta_{s \max}} \right) = K_D \rho_s \quad (29.20)$$

where

$$K_D = 1 + \frac{A}{\delta_{s \max}} \quad (29.21)$$

is the dynamic coefficient under vibration. The strength condition in this case is as follows:

$$\rho_D = K_D \rho_s \leq [\rho] \quad (29.22)$$

Thus, as in the previously discussed problem, in which forces of inertia of constant direction were considered, the determination of dynamic stresses and strength check under vibration can be replaced by the determination of static stresses and dynamic coefficient  $K_D$ . Since  $K_D$  depends upon  $A$ , we must know how to determine the maximum amplitude of vibrations under different situations.

It is well known that the differential equation of an oscillating load  $Q$  performing natural vibrations, may be written in the form of an equilibrium equation which takes into account the forces of inertia in addition to the external force (load  $Q$ ) and the force of elastic

resistance of the system:

$$\frac{Q}{g} x'' + P - Q = \frac{Q}{g} x'' + P_1 = \frac{Q}{g} x'' + cx = 0 \quad (29.23)$$

Here  $x$  is the coordinate which completely determines the location of load  $Q$  during vibration (see, for example, Fig. 414),  $P$  is the total elastic resistance of the system to vibrations,  $P - Q = P_1$  is the restoring force (an additional elastic force which appears in the system due to the displacement by  $dx$  of the point of application of force  $Q$  on account of vibration) which in the first elastic limit may be considered proportional to coordinate  $x$  ( $P_1 = cx$ ), and  $c$  is a proportionality constant which is equal to the force required to cause unit static deformation of the system in the direction of force  $Q$ . If the static deformation due to load  $Q$  is  $\delta_Q$ , then  $c = \frac{Q}{\delta_Q}$ .

After solving equation (29.23) we get the following formulas for calculating frequency  $\omega_0$  and period of the natural vibrations  $t_0$ :

$$\omega_0 = \sqrt{\frac{gc}{Q}} = \sqrt{\frac{g}{\delta_Q}}, \quad t_0 = \frac{2\pi}{\omega_0} = 2\pi \sqrt{\frac{\delta_Q}{g}}$$

Hence, natural vibrations of a weightless body are equivalent to simple harmonic motion with a frequency (period) equal to the frequency (period) of oscillation of a simple pendulum which is equal in length to the static deformation of the system due to load  $Q$ . For instance, if the load stretches a prismatic bar,

$$\omega_0 = \sqrt{\frac{g}{\Delta l}} = \sqrt{\frac{gES}{Ql}}$$

In the case of a simply supported beam loaded by a force  $Q$  acting at the middle of its span,

$$\omega_0 = \sqrt{\frac{g}{f_{\max}}} = \sqrt{\frac{48EJg}{Ql^3}}$$

**B.** If in addition to force  $Q$  and force of elastic resistance  $P$  the system is acted upon by an exciting force  $F$  and force of resistance of the atmospheric medium,  $R$ , then the differential equation of vibration may be written in the form of an equilibrium equation similar to equation (29.23):

$$\begin{aligned} \frac{Q}{g} x'' + P - Q - F + R &= \frac{Q}{g} x'' + P_1 - F + R \\ &= \frac{Q}{g} x'' + cx - F + R = 0 \end{aligned} \quad (29.24)$$

In a sufficiently large number of cases the resistance of the atmospheric medium,  $R$ , may be considered directly proportional to the

velocity of the vibrating body:  $R=rx'$ . If the exciting force varies according to the sine law

$$F = H \sin \omega t$$

where  $H=F_{\max}$  and  $\omega$  is the frequency of the exciting force, then equation (29.24) may be written as follows:

$$\frac{Q}{g} x'' + rx' + cx = H \sin \omega t$$

or

$$x'' + 2nx' + \omega_0^2 x = \frac{gH}{Q} \sin \omega t \quad (29.25)$$

Here  $n = \frac{rg}{2Q}$  is the *damping coefficient* and  $\omega_0$  is the frequency of natural vibrations which occur in the system even when the exciting force,  $F$ , and the force of resistance,  $R$ , are absent.

After solving equation (29.25) we get the following expression for amplitude  $A$  of the forced vibrations in the presence of damping:

$$\begin{aligned} A &= \frac{H}{\frac{Q}{g} \sqrt{(\omega_0^2 - \omega^2)^2 + 4n^2 \omega^2}} \\ &= \frac{gH}{Q\omega_0^2} \frac{1}{\sqrt{\left[1 - \left(\frac{\omega}{\omega_0}\right)^2\right]^2 + 4\left(\frac{n}{\omega_0}\right)^2 \left(\frac{\omega}{\omega_0}\right)^2}} \\ &= \frac{\delta_H}{\sqrt{\left[1 - \left(\frac{\omega}{\omega_0}\right)^2\right]^2 + 4\left(\frac{n}{\omega_0}\right)^2 \left(\frac{\omega}{\omega_0}\right)^2}} \end{aligned} \quad (29.26)$$

Here

$$\frac{gH}{Q\omega_0^2} = \frac{gH}{Q} \frac{\delta_Q}{g} = \frac{H}{Q} \delta_Q = \delta_H$$

is the static deformation of the system due to maximum exciting force  $F$  ( $F_{\max} = H$ ). The ratio of amplitude  $A$  of the forced vibrations to deformation  $\delta_H$  is called the *amplification factor* of vibrations and denoted by  $\beta$ :

$$\beta = \frac{A}{\delta_H} = \frac{1}{\sqrt{\left[1 - \left(\frac{\omega}{\omega_0}\right)^2\right]^2 + 4\left(\frac{n}{\omega_0}\right)^2 \left(\frac{\omega}{\omega_0}\right)^2}} \quad (29.27)$$

Therefore formula (29.21) for dynamic coefficient  $K_D$  may now be written as

$$K_D = 1 + \frac{A}{\delta_{s \max}} = 1 + \frac{\delta_H}{\delta_Q} \beta \quad (29.28)$$

The amplitude of natural vibrations has not been accounted for in the above expression, because it can have appreciable effect only at the beginning of vibrations; in presence of a resisting medium it sharply decreases with the passage of time.

Figure 415 contains curves depicting the variation of *amplification factor*  $\beta$  as a function of  $\frac{\omega}{\omega_0}$  for various values of the damping coefficient  $n$  (ratio  $\frac{\mu}{m_0}$ ). If the frequency of the exciting force is close to the frequency of natural vibrations, i.e. if  $\frac{\omega}{\omega_0} \approx 1$ , and if the damping coefficient is not large, then the denominators in formulas (29.26) and (29.27) for determining  $A$  and  $\beta$  will be very small and the am-

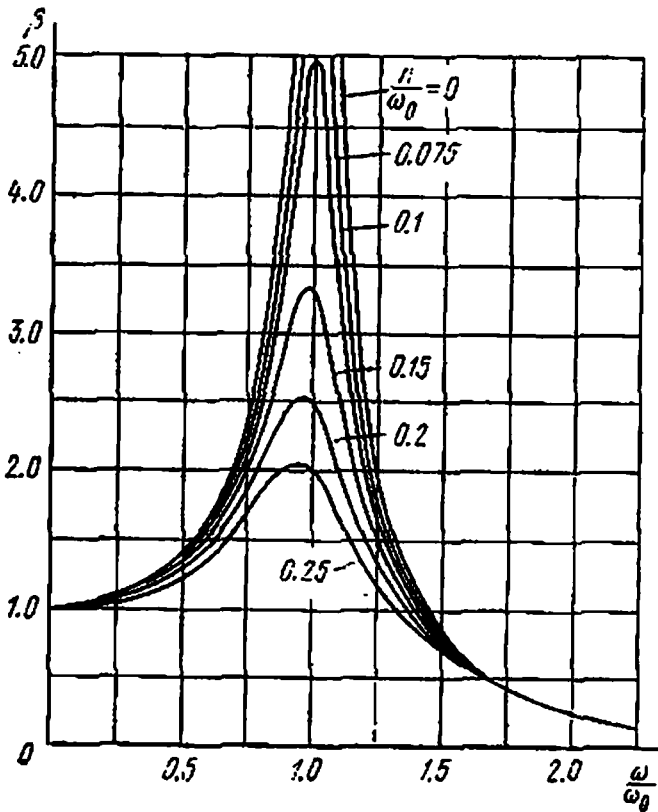


Fig. 415

plitude and amplification factor will be very large (Fig. 415). Under such circumstances even a small exciting force will result in high stresses (on account of resonance).

With the increase in damping resonance becomes less effective. It should, however, be noted that damping can considerably decrease the amplitude of forced vibrations only under near resonance con-

ditions ( $0.75 \leq \frac{\omega}{\omega_0} \leq 1.25$ ); the effect of damping is imperceptible if the ratio  $\frac{\omega}{\omega_0}$  is outside this range.

It is evident from formulas (29.26), (29.27) and (29.28) and Fig. 415 that if frequency  $\omega$  of the exciting force  $F$  is very low, then the amplitude of vibrations tends to  $\delta_H$ , the amplification factor tends to unity and the maximum stress can be calculated as the static stress due to load  $Q$  and maximum value of exciting force  $F$  ( $F_{\max} = H$ ). If the frequency of the exciting force is very high, then the amplitude of vibrations and the amplification factor tend to zero and force  $Q$  may be considered as a fixed load. The maximum stress in the system is in this case equal to the static stress due to load  $Q$ .

This is a factor of great practical importance; it is employed in the design of various types of dampers, seismographs, vibrographs and other instruments. In machine design the shock absorbers protecting the foundation from vibrations are selected in such a way that the frequency of natural vibrations of the machine mounted on the absorbers is considerably less than the frequency of the exciting force.

## § 172. The Effect of Mass of the Elastic System on Vibrations

A. If the vibrating system carrying load  $Q$  has a sufficiently distributed mass (meaning thereby that the number of the degrees of freedom is large), then the simplified calculations discussed in the preceding section will give a considerable error. In such cases the differential equations of motion should be written with the mass of the system being taken into account. Instead of solving such problems from equilibrium conditions, on the basis of which equations (29.23) and (29.24) were obtained, it is more convenient to solve them using the law of conservation of energy.

Assuming that the energy imparted to a system in disturbing it from its stable state of equilibrium is equal to the sum of kinetic and potential energies of the load and elastic system and is constant for natural vibrations, we get the following equation:

$$U + T = \text{const} \quad (29.29)$$

This equation shows that vibration is accompanied by continuous transformation of one type of energy into another without any loss. When the elastic system occupies one of the extreme positions, where the velocity of vibrations is zero and consequently the kinetic energy is zero ( $T=0$ ), the potential energy of the load and system is maximum,  $U=U_{\max}$ . On the other hand, when the system is in equilibrium,  $U=0$  and  $T=T_{\max}$ .

It should be noted that the principle applied in deriving equation (29.29) is applicable only to systems with a single degree of freedom, because the law of conservation of energy does not take into account the heat transfer, which occurs in systems with a big number of degrees of freedom. Hence, the problem of vibration of systems with more than one degree of freedom is reduced to the fundamental problem discussed in § 171, and we can approximately determine only one (principal) frequency of the natural vibrations.

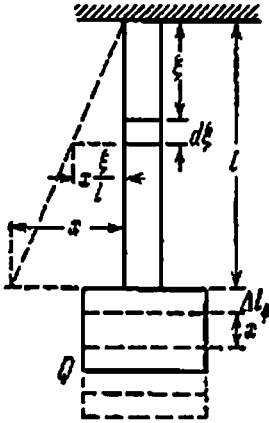


Fig. 416

Let us discuss a few examples on application of equation (29.29). B. As the first example we shall study the vibrations of load  $Q$  suspended from an end of a prismatic bar of length  $l$ , cross-sectional area  $A$  and specific weight  $\gamma$  (Fig. 416). If the suspended load is disturbed from the state of equilibrium and left to itself, it starts performing longitudinal vibrations about the position of equilibrium. Let us write down expressions for  $U$  and  $T$  for the vibrating load-bar system.

Potential energy of the system changes by  $U = U_t - U_0$  w.r.t. the potential energy in equilibrium; here  $U_0$  is the potential energy of the system at the initial moment (in equilibrium) and  $U_t$  is the potential energy at instant  $t$ .

Let us denote the potential energy of load  $Q$  at the initial moment by  $U_Q$ ; potential energy of the bar at the same moment is equal to  $\frac{Q\Delta l_s}{2}$ , where  $\Delta l_s$  is the static deformation of the bar due to load  $Q$ . Hence

$$U_0 = U_Q + \frac{Q\Delta l_s}{2}$$

At instant  $t$  when the load has lowered by a distance  $x$  and the bar has received additional deformation  $x$ , the potential energy of the load decreases by  $Qx$ , whereas the force of elastic resistance and static deformation of the bar increase by  $\frac{\Delta l_s + x}{\Delta l_s}$  times. Consequently,

$$\begin{aligned} U_t &= U_Q - Qx + \frac{1}{2} Q \frac{\Delta l_s + x}{\Delta l_s} \Delta l_s \frac{\Delta l_s + x}{\Delta l_s} \\ &= U_Q - Qx + \frac{Q\Delta l_s}{2} + Qx + \frac{Qx^2}{2\Delta l_s} = U_0 + \frac{Qx^2}{2\Delta l_s} \end{aligned}$$

and

$$U = U_t - U_s = \frac{Qx^2}{2\Delta l_t} \quad (29.30)$$

Kinematic energy of the system is the sum of the kinetic energy  $T_1$  of the load and  $T_2$  of the bar. Kinetic energy of the load is  $T_1 = \frac{Q}{2g}(x')^2$ . While calculating the kinetic energy of the bar, we must bear in mind that at instant  $t$  the load and consequently the lower face of the bar are moving with velocity  $x'$ , whereas the velocity of the upper face of the bar is zero. The velocities of intermediate sections will be within these two extremal values.

Let us assume that displacement of bar sections w.r.t. the fixed end follows the same law as in static tension, i.e. it is directly proportional to the distance of the section from the fixed end. Thus (Fig. 416), if the lower face gets displaced by  $x$ , then the section at a distance  $\xi$  from the fixed end must get displaced by  $x \frac{\xi}{l}$ , and the velocity of this section will be  $x' \frac{\xi}{l}$ . The kinetic energy of an element of length  $d\xi$  cut at a distance  $\xi$  from the fixed end will be  $dT_2 = \frac{\gamma A d\xi}{2g} x'^2 \left(\frac{\xi}{l}\right)^2$ .

Kinetic energy of the whole bar will be the sum of quantities  $dT_2$  over the bar's length:

$$T_2 = \int_0^l \frac{\gamma A d\xi}{2g} x'^2 \left(\frac{\xi}{l}\right)^2 = \frac{x'^2 \gamma A l}{2g \cdot 3}$$

Thus, the kinetic energy of the bar is equal to the kinetic energy of a concentrated load of mass  $\frac{\gamma A l}{3g}$ , i.e. it is equal to the kinetic energy of a load whose mass is  $1/3$  of the bar and which moves with the same velocity as the bar. The total kinetic energy of the load-bar system is:

$$T = T_1 + T_2 = \frac{x'^2}{2g} \left( Q + \frac{\gamma A l}{3} \right)$$

Substituting  $T$  and  $U$  (29.30) in equation (29.29) and differentiating the last with respect to  $t$ , we get

$$\frac{1}{g} \left( Q + \frac{\gamma A l}{3} \right) x'' + \frac{EA}{l} x = \frac{1}{g} \left( Q + \frac{\gamma A l}{3} \right) x'' + \frac{Q}{\Delta l_Q} x = 0$$

or

$$x'' + \frac{g}{\Delta l_Q} \frac{Q}{Q + \frac{\gamma A l}{3}} x = x'' + \frac{g}{\Delta l_t} x = 0$$



Here  $\Delta l$ , is the static deformation due to load  $Q + \frac{\gamma A l}{3}$ . The differential equation obtained above by taking into consideration the mass of the vibrating bar differs from equation (29.23) only in the factor before  $x$  and both equations become identical once the mass of the bar is ignored. Therefore, the correction due to mass of bar, which must be introduced in the calculations of the preceding section,

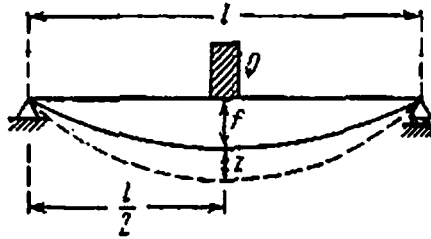


Fig. 417

consists in determining static deformations, required for calculating the frequency of natural vibrations, not for load  $Q$  but for a load  $Q$  plus one-third of the weight of the bar. Thus, the weight of the vibrating bar reduces the frequency of natural vibrations and increases their period. The quantity  $\frac{\gamma A l}{3g}$  is called the *reduced mass of the bar*.

C. As the second example we shall study a simply supported beam, loaded by force  $Q$  at the middle of its span (Fig. 417).

Let us denote the maximum static deflection of the beam due to load  $Q$  by  $f = \frac{Ql^3}{48EJ}$ , and the variable deflection of the middle section due to vibrations by  $z$ . Let us assume that the additional deflection of the beam due to vibrations varies along its length in the same manner as due to the static load  $Q$ ; the variation occurs according to the following equation (see § 85):

$$y = \frac{Ql^3}{48EJ} \frac{3l^2x - 4x^3}{l^3} = \frac{f}{l^3} (3l^2x - 4x^3) \quad (29.31)$$

Thus, if with respect to the position of static equilibrium  $z$  is the additional displacement of the middle section due to vibrations, then the displacement of the section at a distance  $x$  from the left support will be

$$y = \frac{z}{l^3} (3l^2x - 4x^3)$$

The velocity of vibration of the centre of gravity of this section will be

$$\frac{z'}{l^3} (3l^2x - 4x^3)$$

The kinetic energy of an element of length  $dx$  of the beam will be

$$dT_2 = \frac{\gamma A dx}{2g} z'^2 \left( \frac{3l^2 x - 4x^3}{l^3} \right)^2$$

and the kinetic energy of the whole beam will be

$$T_2 = 2 \frac{\gamma A}{2g} z'^2 \frac{1}{l^3} \int_0^{l/2} (3l^2 x - 4x^3)^2 dx = \frac{17}{35} \frac{\gamma A l}{2g} z'^2 \quad (29.32)$$

Kinetic energy of load  $Q$  is:

$$T_1 = \frac{Q}{2g} z'^2$$

Since potential energy of bending is calculated by the formula

$U = \int \frac{M^2 dx}{2EJ}$ , and  $M = EJ \frac{d^2 y}{dx^2}$ , we get

$$U = \int \frac{EJ}{2} \left( \frac{d^2 y}{dx^2} \right)^2 dx$$

As the middle section gets displaced by  $z$  from the position of static equilibrium,  $\frac{d^2 y}{dx^2} = -\frac{24}{l^3} zx$ . Therefore

$$U = \int \frac{EJ}{2} \left( \frac{d^2 y}{dx^2} \right)^2 dx = 2 \frac{EJ}{2} \int_0^{l/2} \left( \frac{24zx}{l^3} \right)^2 dx = \frac{24EJ}{l^3} z^2$$

Substituting the values of  $U$  and  $T = T_1 + T_2$  in equation (29.29) and differentiating it with respect to  $t$ , we get

$$z'' + \frac{48EJ}{l^3} \left( \frac{g}{Q + \frac{17}{35} \gamma A l} \right) z = z'' + \frac{g}{l} z = 0$$

It is evident from the above expression that the beam should be considered weightless and  $\frac{17}{35} = 0.486$  of its weight should be added to  $Q$  to account for its mass while determining the frequency and period of natural vibrations; the quantity  $\frac{17}{35} \frac{\gamma A l}{g}$  is called the reduced mass of the beam.

Let us point out that if the deflected beam be approximately considered as corresponding to the sine curve  $y = f \sin \frac{\pi x}{l}$ , then the reduced mass will be not  $\frac{17}{35} \frac{\gamma A l}{g}$  but  $\frac{1}{2} \frac{\gamma A l}{g}$ , which is sufficiently close to the actual value.

The reduced mass thus determined has been obtained on the assumption that the mass of the beam is small as compared to  $Q$ , because we have neglected the effect of mass of the beam on its deflection. Equation (29.31) of the deflected beam axis corresponds to a situation when it is loaded by a single concentrated force acting at the middle of its span.

D. Let us now consider the other extreme case, when the mass of the beam is very large in comparison with  $Q$  or when the vibrating beam is loaded by a continuous uniformly distributed force of intensity  $q$  (which includes the weight of the beam). The equation of the deflected beam is as follows (see § 86):

$$y = -\frac{q}{24EJ}(l^3x - 2lx^3 + x^4) = -\frac{16f}{5l^4}(l^3x - 2lx^3 + x^4)$$

where  $f$  is the deflection at the middle of the span.

The kinetic energy of an element of length  $dx$  at a distance  $x$  from the left support may be expressed through velocity  $z'$  of the middle section by the following formula:

$$dT = \frac{qdx}{2g} z'^2 \left(\frac{16}{5l^4}\right)^2 (l^3x - 2lx^3 + x^4)^2$$

Total kinetic energy of the beam is:

$$T = \frac{q}{2g} z'^2 \left(\frac{16}{5l^4}\right)^2 \int_0^l (l^3x - 2lx^3 + x^4)^2 dx = \frac{ql}{2g} z'^2 \frac{3968}{7875}$$

Potential energy of the beam is:

$$U = \frac{EJ}{2} \int_0^l \left(\frac{d^2y}{dx^2}\right)^2 dx = \frac{EJ}{2} \int_0^l \left[\frac{192}{5} \frac{z}{l^4} (x^2 - lx)\right]^2 dx = \frac{3072}{125} \frac{EJz^2}{l^3}$$

Substituting these expressions for  $U$  and  $T$  in equation (29.29) and differentiating it with respect to  $t$ , we get:

$$z'' + \frac{48EJg}{\left(\frac{31}{63}ql\right)l^3} z = 0$$

The reduced mass of the beam in this case is:

$$\frac{31}{63} \frac{ql}{g} = 0.492 \frac{ql}{g}$$

Thus, the equation of the deflected beam axis does not have much effect on the period of natural vibrations, as long as the general nature of deflection does not change.

If a simply supported beam deflects along a curve that has no points of discontinuity, then the curve may be assumed to be a sine curve of half wave length  $y=f \sin \frac{\pi x}{l}$ , and the reduced mass of the beam may be considered equal to  $\frac{0.5ql}{g}$ .

Thus, while determining the first frequency of natural vibrations of a system of distributed mass, the system may be assumed to be weightless and its reduced mass added to the mass of the concentrated

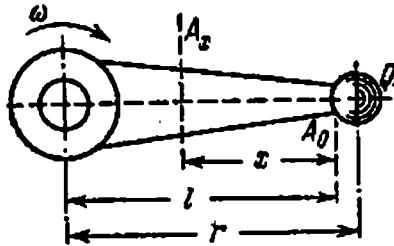


Fig. 418

force acting on the system; the "reduction" method holds well even in such cases of loading when  $Q=0$ .

**Example.** A non-uniform bar of length  $l$  carrying load  $Q$  at one end (Fig. 418) rotates with angular velocity  $\omega$  about an axis to which its other end is fixed. The distance between the centre of gravity of load  $Q$  and the axis of rotation is  $r$ . Find a relation between the cross-sectional area  $A_x$  and distance  $x$  of the section from the free end if stresses in all the sections are equal to  $[\sigma]$ . Specific weight of the material is  $\gamma$ .

Each point of the bar with abscissa  $x$  experiences centripetal acceleration  $\omega^2(l-x)$ . Therefore, to determine the stresses all elements of the bar must be loaded by forces of inertia acting away from the centre and equal to the mass of element multiplied by  $\omega^2(l-x)$ . An element of length  $dx$  cut by two adjacent sections with abscissas  $x$  and  $x+dx$  and cross-sectional areas  $A_x$  and  $A_x+dA_x$ , is acted upon by the force of inertia  $\frac{A_x \gamma dx}{g}(l-x)\omega^2$ , where  $g$  is the acceleration of gravity.

The size of the sections should change in such a way that this force of inertia give rise to stress  $[\sigma]$  on the area  $dA_x$  (see analysis of uniform strength bars under tension and compression, § 25). We obtain the following differential equation for  $A_x$ :

$$[\sigma] dA_x = \frac{A_x \gamma dx}{g} (l-x) \omega^2$$

After separating the variables and integrating, we get

$$\frac{dA_x}{A_x} = \frac{\gamma \omega^2}{g[\sigma]} (l-x) dx, \quad \text{or} \quad \ln A_x = \frac{\gamma \omega^2}{g[\sigma]} \left( lx - \frac{x^2}{2} \right) + C$$

Constant  $C$  can be determined from the boundary condition at  $x=0$ :  $A_x=A_0$  (cross-sectional area of the end faces of the bar). This area depends upon the force of inertia of load  $Q$ , which stretches the end face element:

$$A_0 = \frac{Qr\omega^2}{g[\sigma]}$$

Substituting in  $A_0=C$  in the expression for  $A_x$ , we get

$$\ln A_x = \frac{\gamma\omega^2 x}{2g[\sigma]}(2l-x) + \ln A_0, \quad \text{or} \quad A_x = A_0 \exp \left[ \frac{\gamma\omega^2}{2g[\sigma]}(2l-x)x \right]$$

## CHAPTER 30

### Stresses Under Impact Loading

#### § 173. Fundamental Concepts

Impact takes place when the velocity of the element under consideration or of elements adjoining it changes in a very short period of time.

In piling, a heavy load falls on the upper face of the pile from a certain height and drives it into the soil; the drop weight comes to a stop instantaneously, causing impact. A similar phenomenon takes place during forging; both the forged part and the hammer head experience impact as the latter comes to a sudden stop when it hits the part to be forged. During impact high pressures are created between the colliding bodies. The velocity of the falling body changes over a short period and in particular cases falls to zero as it comes to a stop. This means that the hammer head is subjected to a large acceleration from the forging in a direction opposite to that of its movement, i.e. the hammer head experiences reaction  $P_D$  which is equal to the product of its mass and the acceleration.

Denoting this acceleration by  $a$ , we can write reaction  $P_D = \frac{Q}{g}a$ , where  $Q$  is the weight of the falling body. In accordance with the law of equality of action and reaction a force of the same magnitude acts on the forging in the opposite direction (Fig. 419). These forces give rise to stresses in both bodies. Thus, the forging experiences stresses as if it were being acted upon by the force of inertia of the hammer head; these stresses may be calculated by considering (§ 164) the force of inertia  $P_D$  as a static load acting on the structure. The chief difficulty is how to compute this force. We do not know the duration of impact, i.e. the time during which the velocity falls to zero. Therefore, acceleration  $a$  and consequently force  $P_D$  remain unknown. Hence, although computation of stresses under impact loading is a

particular part of the general problem of taking into account forces of inertia (§ 164), a different method based on the law of conservation of energy has to be employed to calculate  $P_D$ , stresses and deformation.

During impact there is a sudden transformation of one type of energy into another: kinetic energy of the moving body is transformed into potential energy of deformation. By expressing this energy as a function of force  $P_D$  (stress or deformation (§ 98)), we can determine these quantities.

Engineering problems are generally solved by the theory of elastic impact, which makes use of the following main assumptions:

(1) The kinetic energy of the striking body completely changes into potential energy of deformation of the body which is hit; we ignore the energy that is spent on deforming the striking body and the base on which the hit body is placed.

(2) The distribution of stresses and strains over the volume of the hit body remains the same as under static loading; here we ignore the change in distribution of stresses and strains at the point of collision and also the stresses and strains arising from high-frequency vibrations which appear in the whole volume of the body due to impact.

The first assumption usually leads to a higher safety factor being specified, as the hit body is assumed to be in worse conditions than it really is; the second assumption does not add to the safety factor for the more stressed parts of the hit body.

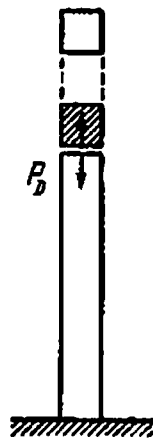


Fig. 419

### § 174. General Method of Determining Stresses Under Impact Loading

A. Imagine that a rigid body  $A$  of weight  $Q$  whose deformation may be neglected falls from a certain height  $H$  and hits another body  $B$  which rests on an elastic system  $C$  (Fig. 420). As a particular case we may consider a load falling on the face of a prismatic bar, the other end of which is rigidly fixed (longitudinal impact) or a load falling on a simply supported beam (bending impact).

Elastic system  $C$  undergoes deformation during a very short period of time. Let us denote by  $\delta_D$  the displacement of body  $B$  (whose own deformation may be neglected) in the direction of impact. In the particular cases enumerated above displacement  $\delta_D$  represents axial

elongation  $\Delta l_D$  in the case of longitudinal impact and deflection  $f_D$  of the section of impact in bending impact. As a result of the impact, system  $C$  experiences stresses  $p_D$  ( $\sigma_D$  or  $\tau_D$ , depending upon the type of deformation).

Assuming that kinetic energy  $T$  of the falling body is completely transformed into potential energy of deformation,  $U_D$ , of the system, we may write

$$T = U_D \quad (30.1)$$

By the time of completion of deformation the falling body covers a distance  $H + \delta_D$ ; therefore its kinetic energy can be expressed in terms of the work  $W_D$  done by it:

$$T = W_D = Q(H + \delta_D) \quad (30.2)$$

Let us now calculate  $U_D$ . If the deformation is static, potential energy  $U_s$  is numerically equal to half the product of the acting force and corresponding deformation (§ 98):

$$U_s = \frac{1}{2} Q\delta_s \quad (30.3)$$

Static deformation  $\delta_s$  of the section of impact may be calculated by Hooke's law and in general is written as

$$\delta_s = \frac{Q}{c}, \quad \text{or} \quad Q = c\delta_s$$

Here (see § 171)  $c$  is a proportionality factor (sometimes also known as rigidity of the system); it depends upon the properties of material, shape and size of the body, type of deformation and location of the section under impact. Thus, in simple tension or compression  $\delta_s = \Delta l_s = \frac{Ql}{EA}$  and  $c = \frac{EA}{l}$ ; in bending of a simply supported beam loaded at the middle of its span by a concentrated force  $Q$ , static deformation  $\delta_s = f_s \text{ max} = \frac{Ql^3}{48EJ}$  and  $c = \frac{48EJ}{l^3}$ ; etc.

Thus, formula (30.3) may be rewritten as follows:

$$U_s = \frac{1}{2} Q\delta_s = \frac{c}{2} \delta_s^2$$

This formula is based on two assumptions: (a) Hooke's law must be applicable, and (b) force  $Q$ , stress  $p_s$  and corresponding deformation  $\delta_s$  must increase gradually from zero to a finite value.

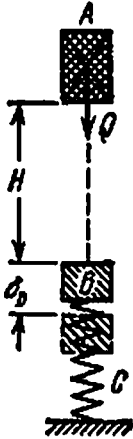


Fig. 420

Experiments on determination of the modulus of elasticity in bars subjected to vibrations within the elastic limits show that Hooke's law remains valid and the modulus of elasticity remains unaffected by the dynamic nature of loading. Of the nature of increase of stresses it must be said that although the increase is fast it is not instantaneous even in the case of impact loading:  $\delta_D$  increases gradually during a very short period of time from zero to a finite value, and the increase in stresses  $p_D$  runs parallel with the increase in deformation.

Reaction of system  $C$  to the falling weight  $Q$  (let us call it  $P_D$ ) appears as a result of the development of deformation  $\delta_D$ . It increases with  $\delta_D$  from zero to a finite maximum value and, if stress  $p_D$  does not exceed the limit of proportionality, is related to it by Hooke's law:

$$\delta_D = \frac{P_D}{c}$$

where  $c$  is the same proportionality constant, which retains the same meaning under impact loading also.

Thus, both conditions necessary for the validity of formula (30.3) are satisfied by impact loading too. Consequently, it may be considered that the formula for  $U_D$  under impact loading must be the same as obtained by loading system  $C$  with a static force of inertia  $P_D$ , i.e.

$$U_D = \frac{1}{2} P_D \delta_D = \frac{c}{2} \delta_D^2 = \frac{Q}{2\delta_s} \delta_D^2 \quad (30.4)$$

(here, as before, we consider  $c=Q/\delta_s$ ). Substituting the values of  $T$  and  $U_D$  in equation (30.1), we get

$$Q(H + \delta_D) = \frac{Q}{2\delta_s} \delta_D^2 \quad (30.5)$$

or

$$\delta_D^2 - 2\delta_s \delta_D - 2H\delta_s = 0 \quad (30.6)$$

wherefrom

$$\delta_D = \delta_s \pm \sqrt{\delta_s^2 + 2H\delta_s}$$

or, keeping the positive sign before the square root to determine the maximum deformation in the direction of impact, we obtain

$$\delta_D = \delta_s \left( 1 + \sqrt{1 + \frac{2H}{\delta_s}} \right) = K_D \delta_s \quad (30.7)$$

Since according to Hooke's law stresses are proportional to deformation,

$$p_D = p_s \left( 1 + \sqrt{1 + \frac{2H}{\delta_s}} \right) = K_D p_s \quad (30.8)$$



and

$$P_D = Q \left( 1 + \sqrt{1 + \frac{2H}{\delta_s}} \right) = K_D Q \quad (30.9)$$

It is evident from these formulas that impact strain, stress and force depend upon static deformation, i.e. upon the rigidity and longitudinal dimensions of the body under impact. This statement will be proved below with the help of individual examples. Constant

$$K_D = 1 + \sqrt{1 + \frac{2H}{\delta_s}} \quad (30.10)$$

in this case represents the dynamic coefficient. Substituting  $H$  in formula (30.10) by  $\frac{v^2}{2g}$ , where  $v$  is the velocity of the body under impact at the beginning of impact, we get

$$K_D = 1 + \sqrt{1 + \frac{v^2}{g\delta_s}} \quad (30.11)$$

Besides, since

$$\frac{2H}{\delta_s} = \frac{QH}{\frac{1}{2} Q\delta_s} = \frac{T_0}{U_s}$$

where  $T_0 = QH$  is the energy of the body under impact at the beginning of impact, the expression for the dynamic coefficient may also be written as follows:

$$K_D = 1 + \sqrt{1 + \frac{T_0}{U_s}} \quad (30.12)$$

**B.** If in formulas (30.7) and (30.8) we put  $H=0$ , i.e. if we apply force  $Q$  instantaneously, then  $\delta_D = 2\delta_s$  and  $p_D = 2p_s$ ; if force  $Q$  is applied suddenly, then the deformation and stress are two times the deformation and stress due to a statically applied load of the same magnitude.

On the other hand, if height  $H$  (or velocity  $v$ ) from which the load falls is large as compared to  $\delta_s$ , then 1 may be neglected as compared to  $\frac{2H}{\delta_s}$  in the radicand in formulas (30.7) to (30.11). The expressions for  $\delta_D$  and  $p_D$  may be written as follows:

$$\delta_D = \delta_s \left( 1 + \sqrt{\frac{2H}{\delta_s}} \right), \quad p_D = p_s \left( 1 + \sqrt{\frac{2H}{\delta_s}} \right) \quad (30.13)$$

If ratio  $\frac{2H}{\delta_s}$  is very large, then the first term in the parentheses may also be neglected and the expressions are written as follows:

$$\delta_D = \delta_s \sqrt{\frac{2H}{\delta_s}}, \quad p_D = p_s \sqrt{\frac{2H}{\delta_s}} \quad (30.14)$$

The dynamic coefficient in this case is:

$$K_D = \sqrt{\frac{2H}{\delta_s}} = \sqrt{\frac{T_s}{U_s}} \quad (30.15)$$

It should be noted that unity in the radicand be ignored if  $\frac{2H}{\delta_s} \geq 10$  (the error of the approximate formula will not exceed 5%), but unity in the radicand can be neglected only for very high values of the ratio  $\frac{2H}{\delta_s}$ . For example, in order to ensure that the error of approximate formulas (30.14) and (30.15) does not exceed 10%, the ratio  $\frac{2H}{\delta_s}$  must be greater than 110.

Formulas  $\delta_D = K_D \delta_s$  and  $p_D = K_D p_s$  in which  $K_D$  is expressed in terms of  $\frac{T_s}{U_s}$ , (30.12), may also be used for solving the problem on collision between bodies moving with a certain velocity, for determining the stresses in the cylinder of an internal combustion engine due to a sharp increase in gas pressure on account of ignition of fuel, etc. On this basis these formulas may be considered as general formulas for impact analysis.

Generalizing what has been said above, we can suggest the following method of determining stresses under impact. Applying the law of conservation of energy, we must (1) calculate kinetic energy  $T$  of the body under impact; (2) calculate potential energy  $U_D$  of the bodies experiencing impact, when they are loaded by the inertial forces (the potential energy may be expressed through stress ( $\sigma_D, \tau_D$ ) in a particular section, through deformation (elongation, deflection) or through the force of inertia  $P_D$  of the body under impact; and (3) equate  $U_D$  and  $T$  and from this equation determine either the dynamic stress directly, or first determine deformation and then applying Hooke's law find stress or force  $P_D$  and finally calculate the corresponding dynamic stress and deformation.

The method outlined above is based on the assumption that the kinetic energy of the body under impact is fully transformed into potential energy of deformation of the elastic system. This assumption is not very accurate. Kinetic energy of the falling body is partially transformed into heat and partially into the energy spent on inelastic deformation of the foundation on which the elastic system rests.

In addition, if impact occurs at a high velocity, then the deformation of the body suffering this impact does not get enough time to spread over the whole body, and local stresses of considerable magnitude, which sometimes exceed the yield stress of the material, appear in the region of impact. For example, if a steel beam is hit by a lead hammer, then a large portion of the kinetic energy is transformed into the energy of local deformation. A similar phenomenon

may occur even at low velocity of impact if the body suffering impact is very rigid or heavy.

All the situations discussed above pertain to a high value of  $\frac{2H}{\delta_s}$ . It may be stated that the method of analysis described above is applicable until  $\frac{2H}{\delta_s}$  does not exceed a certain value. Accurate investigations confirm that the error does not exceed 10% if  $\frac{2H}{\delta_s} \leq 100$ .

Now, since this ratio can be expressed in terms of  $\frac{T_0}{U_s}$  (see earlier discussion) it may be stated that the above method is applicable until the energy of impact does not become more than 100 times the potential energy of deformation due to static loading of the elastic system suffering impact by a force equal to the weight of the impacting body. Consideration of the mass of the body under impact (see § 178) helps in somewhat increasing the limits of applicability of this method in such cases when the impacting body has a big mass.

A more accurate theory of impact is given in the theory of elasticity.

### § 175. Concrete Cases of Determining Stresses and Conducting Strength Checks Under Impact

A. The formulas derived in § 174 show that qualitative changes may occur due to a quantitative change in the period of the force acting on a body.

Let us study some simple cases of deformation under impact loading. In this study we shall determine the dynamic coefficient with the help of formulas (30.10) and (30.12) and the approximate formula (30.15).

We shall determine  $\delta_D$ ,  $p_D$  and  $P_D$  by the following relations:

$$\delta_D = K_D \delta_s, \quad p_D = K_D p_s, \quad P_D = K_D Q$$

In the case of an axial tensile or compressive impact (Fig. 421),

$$\delta_s = \Delta l_s = \frac{Ql}{EA}, \quad p_s = \sigma_s = \frac{Q}{A}, \quad U_s = \frac{Q^2 l}{2EA} = \frac{\sigma_s^2 Al}{2E} = \frac{\Delta l_s^2 EA}{2l}$$

Dynamic coefficient  $K_D$  may be calculated from one of the following expressions:

$$\begin{aligned} K_D &= 1 + \sqrt{1 + \frac{2H}{\delta_s}} = 1 + \sqrt{1 + \frac{2T_0 EA}{Q^2 l}} \\ &= 1 + \sqrt{1 + \frac{2T_0 E}{\sigma_s^2 Al}} = 1 + \sqrt{1 + \frac{2T_0 l}{\Delta l_s^2 EA}} \end{aligned} \quad (30.16)$$

Having calculated  $K_D$  we can easily determine  $\sigma_D$  and  $P_D$  and  $\Delta l_D$ .

The approximate formula for determining stresses in this case is as follows:

$$K_D = \frac{1}{\sigma_s} \sqrt{\frac{2T_0 E}{AI}}, \quad \sigma_D = \sigma_s K_D = \sqrt{\frac{2T_0 E}{AI}} \quad (30.17)$$

It should be noted that under static as well as dynamic loading the stresses in the compressed bar depend upon the compressive force and the cross-sectional area of the bar.

If load  $Q$  is applied statically to the bar, then the force transmitted to the bar is equal to  $Q$  and does not depend upon its material and size. In the case of impact loading  $P_D$ , which gives rise to stresses in the bar, depends upon the acceleration with which the body suffering impact resists the impacting body, i.e.  $P_D$  depends upon the time during which the velocity of the impacting body changes. This period depends upon the axial dynamic deformation  $\Delta l_D$  and upon the pliability of the bar material. The greater the pliability, i.e. the smaller the modulus of elasticity  $E$  and the greater the bar length  $l$ , the longer is the duration of impact and the smaller are acceleration and force  $P_D$ .

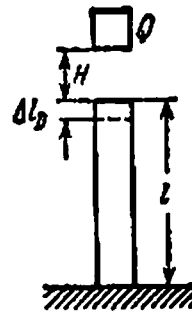


Fig. 421

Thus, if stress distribution is uniform in all the sections of the bar, dynamic stresses decrease with the increase in cross-sectional area and pliability (i.e. increase in length and decrease in modulus of elasticity  $E$ ). Only due to this reason springs placed between impacting bodies are able to damp the impact. The formulas derived earlier express the same idea. For example, formula (30.17) with certain approximation expresses the idea that in longitudinal impact the stresses depend not upon the cross-sectional area, but upon the volume of the bar.

Having determined the dynamic stress from formulas (30.8) and (30.16) or (30.17), we can now write the strength condition as follows:

$$\sigma_D \leq [\sigma_D] \quad (30.18)$$

where  $[\sigma_D]$  is the permissible normal stress under impact, which for a ductile material is equal to  $[\sigma_D] = \frac{\sigma_y}{k_D}$ . The safety factor  $k_D$  may be considered equal to the primary safety factor  $k_0$  under static loading (i.e., 1.5-1.6; § 16), because the dynamic nature of loading has

already been accounted for in formulas (30.16) and (30.17). However, keeping in mind the not too accurate theoretical basis of their derivations, a slightly higher value, up to 2, of the safety factor is employed. In addition, a better material is generally used in such cases (more uniform material having better plastic properties).

B. In bending, static deformation  $\delta_s$ , which represents static deflection  $f_s$  of the beam in the section of impact, depends upon the type of loading and constraints.

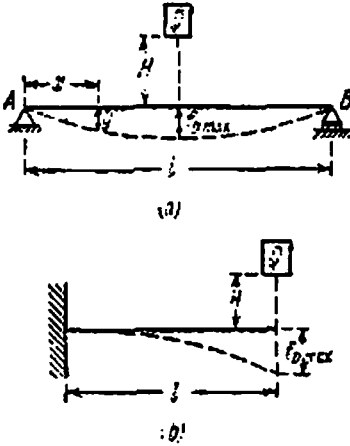


Fig. 422

Thus, in a simply supported beam of span  $l$  experiencing impact at its middle from a weight  $Q$ , falling from height  $H$  (Fig. 422 (a)), we get:

$$\delta_s = f_{s \max} = \frac{Ql^3}{48EJ}$$

$$p_s = \sigma_{s \max} = \frac{Ql}{4W}$$

and

$$U_s = \frac{Qf_{s \max}}{2} = \frac{Q^2 l^3}{96EJ}$$

In a cantilever experiencing impact at its free end from a falling weight  $Q$  (Fig. 422 (b))

$$\delta_s = f_{s \max} = \frac{Ql^3}{3EJ}, \quad p_s = \sigma_{s \max} = \frac{Ql}{W}$$

and

$$U_s = \frac{Qf_{s \max}}{2} = \frac{Q^2 l^3}{6EJ}$$

Substituting the values of  $\delta_s = f_{s \max}$  and  $U_s$  in the expression for  $K_D$ , we first determine  $K_D$  and then through it the dynamic stresses and deformation. For example,  $\sigma_{D \max}$  for a simply supported beam can be calculated by the following formula:

$$\sigma_{D \max} = K_D \sigma_{s \max} = \frac{Ql}{4W} \left( 1 + \sqrt{1 + \frac{96T_0 EJ}{Q^2 l^3}} \right) \quad (30.19)$$

Strength condition (30.18) may, in this case, be written as

$$\sigma_{D \max} = \frac{Ql}{4W} \left( 1 + \sqrt{1 + \frac{96T_0 EJ}{Q^2 l^3}} \right) \leq [\sigma_D] = \frac{\sigma_y}{k_D} \quad (30.20)$$

In case of impact on a simply supported beam (Fig. 422 (a)) the approximate formulas for calculating  $\sigma_{D \max}$  and  $f_{D \max}$  are as follows:

$$\begin{aligned} f_{D \max} &= K_D f_{s \max} = f_{s \max} \sqrt{\frac{T_0}{U_s}} \\ &= \frac{Q l^3}{48 E J} \sqrt{\frac{96 T_0 l J}{Q^2 l^3}} = \sqrt{\frac{T_0 l^3}{24 E J}} \end{aligned} \quad (30.21)$$

and

$$\sigma_{D \max} = K_D \sigma_{s \max} = \frac{Q l}{4 W} \sqrt{\frac{96 T_0 E J}{Q^2 l^3}} = \sqrt{\frac{6 T_0 E J}{W^2 l}} \quad (30.22)$$

Identical expressions for  $f_{D \max}$  and  $\sigma_{D \max}$  can be obtained in case of impact on a cantilever (Fig. 422 (b)). Keeping in mind that

$$J = i^2 A, \quad W = \frac{J}{z_{\max}}$$

and

$$\frac{J}{W^2} = \left( \frac{z_{\max}}{i} \right)^2 \frac{1}{A}$$

we can modify formula (30.22) as follows:

$$\sigma_{D \max} = \frac{z_{\max}}{i} \sqrt{\frac{6 T_0 E}{A l}} \quad (30.23)$$

From the approximate formula (30.23) it is obvious that the dynamic stresses in bending depend upon the modulus of elasticity of the beam material, volume of the beam, shape of cross section (ratio  $\frac{z_{\max}}{i}$ ) and the type of loading and constraints (in this particular example, the radicand contains  $6T_0$ ; in beams loaded and constrained in a different manner the numerical constant before  $T_0$  will be different). Thus, in a rectangular beam of height  $h$  and width  $b$ , the dynamic stress will be the same irrespective of whether the beam is placed on the thin or flat face and its magnitude is (according to the approximate formula):

$$\sigma_{D \max} = \sqrt{\frac{18 T_0 E}{A l}}$$

because in both cases

$$\frac{z_{\max}}{i} = \frac{\frac{h}{2}}{\sqrt{\frac{bh^3}{12bh}}} = \frac{\frac{b}{2}}{\sqrt{\frac{hb^3}{12bh}}} = \sqrt{3}$$

It should be recalled that under a similar static load the maximum stress in a beam placed on its flat face is  $\frac{h}{b}$  times more than the stress

in a beam placed on its narrow face. Obviously, the above statement is true only if the impact occurs within the elastic limits.

The resistance of beams to impact loading also depends upon their section modulus and rigidity. The greater the pliability (deformability) of a beam, the greater is the kinetic energy of impact which it can absorb at the same permissible stress. Maximum deflection occurs in a beam in which the maximum stress is the same in all sections, i.e. in beams of uniform strength. Such beams are capable of withstanding greater deflection than uniform beams having the same permissible stress; this means that uniform strength beams can absorb greater amount of impact energy. Precisely for this reason, springs are made in the shape of uniform strength beams.

C. Let us now study the problem of determining stresses under a twisting impact. If a rotating shaft is suddenly stopped by applying brakes at one of its ends and the other end is acted upon by force  $T_0$  of the flywheel which twists the shaft, then stresses in such a shaft can be determined by the method explained above. The shaft is twisted by two force couples (the force of inertia of the flywheel and the frictional force of the brakes) each of moment  $M$ .

In this example

$$\delta_s = \varphi_s = \frac{M}{GJ_p}, \quad \rho_s = \tau_{s \max} = \frac{M}{W_p}$$

and

$$U_s = \frac{M^2 l}{2GJ_p} = \frac{\tau_{s \max}^2 W_p^2 l}{2GJ_p} = \frac{\varphi_s^2 GJ_p}{2l}$$

Therefore

$$\delta_D = \varphi_D = K_D \varphi_s = \varphi_s \sqrt{\frac{T_0}{U_s}} = \sqrt{\frac{2T_0 l}{GJ_p}} \quad (30.24)$$

and

$$\rho_D = \tau_{D \max} = K_D \tau_{s \max} = \tau_{s \max} \sqrt{\frac{T_0}{U_s}} = \sqrt{\frac{2T_0 GJ_p}{lW_p^2}} = 2 \sqrt{\frac{T_0 G}{Al}} \quad (30.25)$$

because

$$J_p = \frac{\pi r^4}{2}, \quad W_p = \frac{\pi r^3}{2}, \quad \frac{J_p}{W_p^2} = \frac{2}{\pi r^2} = \frac{2}{A}$$

Keeping in mind that kinetic energy  $T_0$  of the flywheel is:

$$T_0 = \frac{J_0}{2} \omega^2$$

where  $J_0$  is the moment of inertia of the flywheel, and  $\omega$  its angular velocity, we may write

$$\tau_{D \max} = \omega \sqrt{\frac{2J_0 G}{Al}} \quad (30.26)$$

It should be noted that even under twisting impact the maximum dynamic stresses depend upon the modulus of elasticity and volume of the shaft.

### § 176. Impact Stresses in a Non-uniform Bar

It was explained in § 175 that the volume of the bar should be increased to reduce the stresses due to longitudinal impact. However, this is true only when the cross-sectional area of the bar does not change along its length—the stresses are equal in all sections. The situation will be entirely different if various portions of the bar have different areas of cross section (Fig. 423).

We know (formulas (30.16) or (30.17)) that dynamic stress in longitudinal impact depends upon the cross-sectional area of the bar as well as its pliability (deformability). The maximum stresses in a necked bar (Fig. 423 (a)) must, for example, be determined for the minimum cross-sectional area (at the neck) taking into consideration the compressibility of the bar, which depends upon the deformation of the whole bar and not only the neck portion.

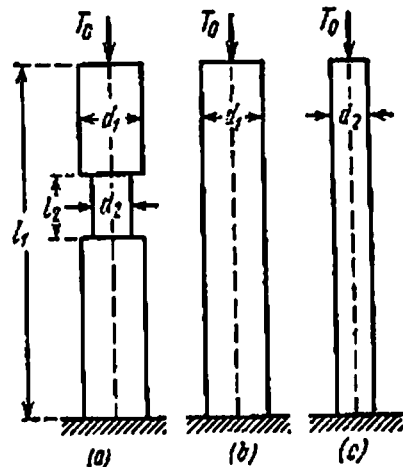


Fig. 423

Stresses in this case may be brought down in two ways. Firstly, by increasing the cross-sectional area of the neck portion (if this is permissible from design considerations) by using a bar of diameter  $d_1$  (Fig. 423 (b)); in doing so we increase the cross-sectional area and to a smaller extent decrease the compressibility of the bar. There is a slight increase in the force of inertia, but the cross-sectional area of the neck portion increases by a higher degree, thus resulting in an overall reduction in stress.

However, this (first) method cannot generally be applied because the design of structures demands that the neck be retained. In such cases the strength of the bar is increased by reducing its cross-sectional area in the thick portion, thus increasing its pliability. If we reduce the diameter of the whole bar to  $d_2$  (Fig. 423 (c)), we automatically increase its compressibility and consequently decrease the dynamic force  $P_D$  as well as the dynamic stress. Thus, a reduction in the magnitude of stresses may be achieved by two methods, both of which make the stresses uniform: by increasing the volume with the addition of material at the neck or by decreasing the volume with reduction in cross-sectional area of the thick portion.



These conclusions can be easily checked analytically. Let us determine the maximum dynamic stress in each of the three bars shown in Fig. 423 (a), (b), and (c), caused in each case by a longitudinal impact of energy  $T_0 = QH$ . For the bar shown in Fig. 423 (a) let  $A_1$  be the cross-sectional area of the thick portion and  $A_2$  the cross-sectional area of the neck; let  $\frac{A_2}{A_1} = q$  and  $\frac{l_2}{l_1} = p$ . We shall calculate the stresses by approximate formulas (30.14) and (30.17). According to formula (30.14) the maximum dynamic stress in the bar shown in Fig. 423 (a) is:

$$\rho_D = \sigma_a = \sigma_s \sqrt{\frac{2H}{\Delta l_s}} = \sigma_s \sqrt{\frac{2H}{\Delta l_s}} = \frac{Q}{A_2} \sqrt{\frac{2H}{\Delta l_s}} = \sqrt{\frac{2T_0 Q}{A_2^2 \Delta l_s}}$$

Since

$$\Delta l_s = \frac{Q l_2}{E A_2} + \frac{Q (l_1 - l_2)}{E A_1} = \frac{Q l_1}{E A_2} [p + q(1 - p)]$$

we find that

$$\sigma_a = \sqrt{\frac{2T_0 Q}{A_2^2 \frac{Q l_1}{E A_2} [p + q(1 - p)]}} = \sqrt{\frac{2T_0 E}{A_1 l_1 q [p + q(1 - p)]}} \quad (30.27)$$

Stresses in the uniform bars shown in Fig. 423 (b) and (c) may be calculated from formula (30.17):

$$\sigma_b = \sqrt{\frac{2T_0 E}{A_1 l_1}}, \quad \sigma_c = \sqrt{\frac{2T_0 E}{A_2 l_1}} = \sqrt{\frac{2T_0 E}{A_1 q l_1}} \quad (30.28)$$

Since  $[p + q(1 - p)] < q < 1$ , we find that  $\sigma_a > \sigma_c > \sigma_b$ . For instance, if  $\frac{d_2}{d_1} = 0.8$  and  $\frac{l_2}{l_1} = 0.1$ , then  $q = 0.64$  and  $p = 0.1$ ; after computing we get  $\sigma_a = 1.52\sigma_b$  and  $\sigma_c = 0.82\sigma_a = 1.25\sigma_b$ . Thus a neck which reduces the diameter by 20% over one-tenth of the total length of the bar results in a 50% increase in stresses; if the bar is made of a uniform section corresponding to the minimum diameter, the stresses reduce by 20%.

Although these calculations have been done on the basis of approximate formulas, the relation established between  $\sigma_a$ ,  $\sigma_b$ , and  $\sigma_c$  is quite close to the relation which we would have obtained by using the accurate formula (30.8) for a not very low value of impact energy  $T_0$ .

### § 177. Practical Conclusions from the Derived Results

The results of the preceding computations are of great practical importance. First of all they show that the nature of resistance of bars considerably differ from their resistance to static deformation.

Under static compression, thickness of a portion of the bar does not affect the stresses in sections of the remaining portion; under impact it increases these stresses. Reduction of cross-sectional area over a small length results in a sharp increase in stresses throughout the bar.

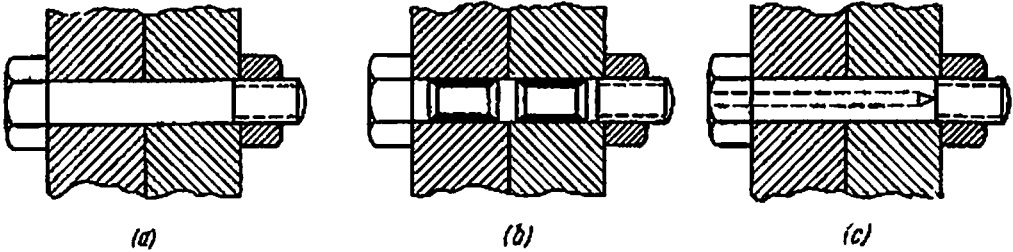


Fig. 424

The endeavour should be to reduce the stresses by increasing the pliability of the bar by increasing its length, adding a shock-absorber, using another material of lower modulus of elasticity and using a uniform cross-sectional area along the bar length. Generally, the most effective way is to reduce the bar to a uniform diameter equal to the minimum.

Therefore, while designing bars working under impact loading, it is essential to have a uniform section all along the bar length;

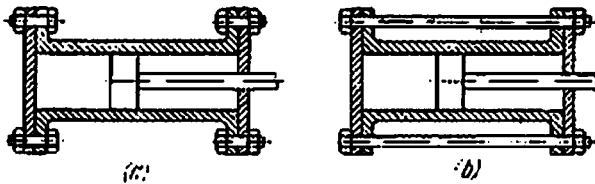


Fig. 425

greater thickness of some portions is permissible over a small length, but necking is highly undesirable even over a very small length. If a sufficiently strong bar cannot be designed under such conditions, then it is essential either to increase the length of the bar or to increase its cross-sectional area uniformly.

As an example let us study a bolt transmitting tensile impact from one part of the structure to another. The design shown in Fig. 424 (a) has poor impact resistance, because the threaded length of the bolt having smaller diameter acts as a neck. The greater part of the impact energy is absorbed by the threaded portion of the bolt. The chances of failure are high.

In a properly designed bolt the impact energy should be absorbed more or less uniformly by the whole bolt; this can be achieved by making the bolt diameter uniform over the whole (or almost the whole)

length and equal to the minimum diameter of the thread. For this we may either machine the bolt shank (Fig. 424 (b)) or drill a hole in it (Fig. 424 (c)).

As an example of increasing impact resistance of bolts by increasing their length we may study the design shown in Fig. 425 (a) and (b). The cylinder cover of a boring tool is sometimes subjected to strong impact from the boring tool. Small bolts securing the cover to the cylinder according to Fig. 425 (a) fail easily. Failure can be prevented by increasing their length as shown in Fig. 425 (b).

### § 178. The Effect of Mass of the Elastic System on Impact

Let us study how the mass of the body subjected to impact affects the impact stresses. As an example we shall consider impact in bending (Fig. 422). Weight  $Q$  drops on beam  $AB$  and at the moment of impact has a velocity  $v_w = \sqrt{2gH}$ , at the same instant the beam has a velocity  $v_b = 0$  (it is stationary). On account of impact all elements of the beam will acquire a certain velocity (different for each element) in a short time while the weight will correspondingly slow down. At the point of impact the weight and the beam material in immediate vicinity have identical velocities equal to  $v_m$ . Medium velocity  $v_m$  may be found from Carnot's theorem:

$$v_m = \frac{M_w v_w}{M_w + \alpha M_0} = \frac{Q}{Q + \alpha Q_0} v_w \quad (30.29)$$

Here  $Q$  and  $M_w$  are the weight and mass of the striking body,  $Q_0$  and  $M_0$  are the weight and mass of the body subjected to impact (beam), and  $\alpha$  is the mass reduction coefficient (less than unity) which has to be introduced to account for the fact that not all parts of the body suffering impact move after impact with the same velocity,  $v_m$  (see, for example, Fig. 422). For tension and compression  $\alpha = \frac{1}{3}$ ; if the beam is subjected to bending as shown in Fig. 422 (a), then  $\alpha = 17/35 \approx \frac{1}{2}$ ; etc.\* It is evident from (30.29) that  $v_m < v_w = \sqrt{2gH}$ ; the greater mass  $M_0$  of the body suffering impact the less is  $v_m$  as compared to  $v_w$ . Kinetic energy that remains in the beam-weight system after

---

\* Detailed derivation of the expression for coefficient  $\alpha$  for the beam shown in Fig. 422(a) is given in § 231 of N. M. Belyaev, *Strength of Materials*, Nauka, Editions 7-14 (in Russian).

impact is:

$$\begin{aligned}
 T_1 &= \frac{M_w v_m^2}{2} + \frac{\alpha M_0 v_m^2}{2} = \frac{1}{2} (M_w + \alpha M_0) \frac{M_w^2 v_m^2}{(M_w + \alpha M_0)^2} \\
 &= \frac{M_w v_w^2}{2} \frac{1}{1 + \alpha \frac{Q_0}{Q}} = \frac{T_0}{1 + \beta}
 \end{aligned}
 \tag{30.30}$$

i.e.  $1 + \beta$  times less than the kinetic energy of the weight if the latter strikes a weightless beam. Hence, if the mass of the body suffering impact is taken into consideration, the dynamic coefficient should be calculated not by formulas (30.10), (30.11) and (30.12), but by the formula

$$\begin{aligned}
 K_D &= 1 + \sqrt{1 + \frac{T_0}{U_s(1 + \beta)}} = 1 + \sqrt{1 + \frac{2H}{\delta_s(1 + \beta)}} \\
 &= 1 + \sqrt{1 + \frac{v_w^2}{g\delta_s(1 + \beta)}}
 \end{aligned}
 \tag{30.31}$$

i.e. if the mass of the body suffering impact is taken into account, the design stresses due to impact are reduced.

As an example of analysis of a complicated structure under impact, let us study the impact load  $Q$  at the middle of a beam which

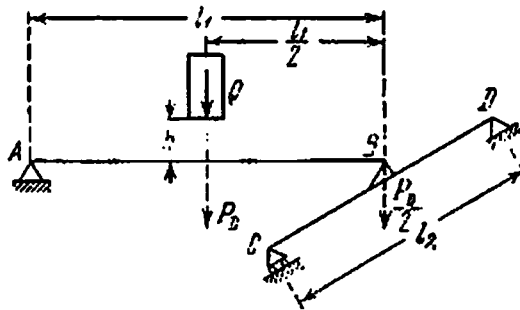


Fig. 426

is constrained by a fixed hinged support at end  $A$  and another hinged support at point  $B$  mounted at the middle of the second beam (Fig. 426). The first beam has span  $l_1$ , moment of inertia  $J_1$  and modulus of elasticity  $E$ , and the respective quantities for the second beam are  $l_2$ ,  $J_2$ , and  $E$ . The maximum dynamic stresses occur in the outer fibres of the middle sections of the beams (first as well as second). Our aim is to determine these stresses.

We shall solve this problem by multiplying the static stresses due to load  $Q$  in the first ( $AB$ ) and second ( $CD$ ) beams with the dynamic coefficient

$$K_D = 1 + \sqrt{1 + \frac{2H}{l_s}}$$

The static deflection of the first beam in the section of impact is determined by the deformation of the whole structure and is equal to  $f_0 = f_1 + \frac{1}{2}f_2$ , where  $f_1$  is the maximum static deflection of the first beam due to force  $Q$ , and  $f_2$  is the corresponding deflection of the second beam due to force  $\frac{Q}{2}$ . Since

$$f_1 = \frac{Ql_1^3}{48EJ_1} \quad \text{and} \quad f_2 = \frac{Ql_2^3}{96EJ_2}$$

we get

$$f_0 = \frac{Ql_1^3}{48EJ_1} + \frac{Ql_2^3}{192EJ_2} = \frac{Ql_1^3}{48EJ_1} \left[ 1 + \frac{J_1}{4J_2} \left( \frac{l_2}{l_1} \right)^3 \right]$$

and

$$K_D = 1 + \sqrt{1 + \frac{96LJ_1H}{Ql_1^3 \left[ 1 + \frac{J_1}{4J_2} \left( \frac{l_2}{l_1} \right)^3 \right]}}$$

The maximum stresses in the first and second beams are

$$\sigma_{D_1} = K_D \sigma_s = K_D \frac{Ql_1}{4W_1} \quad \text{and} \quad \sigma_{D_2} = K_D \sigma_s = K_D \frac{Ql_2}{8W_2}$$

As the potential energies due to impact accumulated by the first beam ( $U_{D_1}$ ), the second beam ( $U_{D_2}$ ) and both beams combined ( $U_D = U_{D_1} + U_{D_2} = T_0$ ) are proportional respectively to  $U_{s_1}$ ,  $U_{s_2}$ , and  $U_s$  (the square of the dynamic coefficient serves as the constant of proportionality), we get

$$\frac{U_{D_1}}{U_D} = \frac{U_{D_1}}{T_0} = \frac{U_{s_1}}{U_s} = \frac{\frac{1}{2} Ql_1}{\frac{1}{2} Ql_1 + \frac{1}{4} Ql_2} = \frac{f_1}{f_1 + \frac{1}{2} f_2} = \frac{f_{01}}{f_0} \quad (a)$$

and

$$\frac{U_{D_2}}{U_D} = \frac{U_{D_2}}{T_0} = \frac{U_{s_2}}{U_s} = \frac{\frac{1}{4} Ql_2}{\frac{1}{2} Ql_1 + \frac{1}{4} Ql_2} = \frac{\frac{1}{2} f_2}{f_1 + \frac{1}{2} f_2} = \frac{f_{02}}{f_0} \quad (b)$$

Deflection  $f_0$  represents the total *pliability* of the whole structure at the point of impact, deflections  $f_{01}$  and  $f_{02}$  represent fractions of the total pliability which depend upon the deformation of the first and second beams separately. It follows from formulas (a) and (b) that

$$U_{D_1} = T_0 \frac{f_{01}}{f_0} \quad \text{and} \quad U_{D_2} = T_0 \frac{f_{02}}{f_0}$$

Thus, distribution of impact energy between the beams is directly proportional to their pliability as a fraction of the total pliability

at the point of impact. If the dimensions of the beams are selected in such a way that  $f_{01} = f_{02}$ , then  $U_{D_1} = U_{D_2} = \frac{1}{2} T_0$ . Had there been a rigid support in place of the second beam, the total impact energy would have been absorbed by the first beam; the second beam helps in damping the impact on the first.

The same effect would have been observed if instead of rigid supports we had used very pliable supports made of rubber spacers or helical springs for constraining the beam ends.

### § 179. Impact Testing for Failure

It was pointed out earlier that dynamic action of force is distinguished not just by the fact that stresses (within elastic limits) under dynamic loading are different from stresses under static loading.

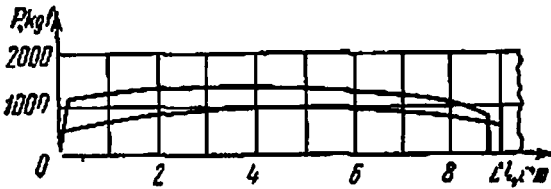


Fig. 427

The material itself reacts to dynamic loading in a different way than to a load which increases gradually. This is especially noticeable in impact loading.

Experiments on failure of specimens under impact loading show that the tension test diagram in this case is completely different from the tension test diagram under static loading. Figure 427 shows the tension test diagrams for mild steel under static and dynamic loads; the curve of impact loading is distinguished by a sharp increase in the yield stress and by a displacement of the maximum load towards the left. This shows that the velocity of impact also affects the mechanical properties of the material. There are cases when materials having excellent plastic properties under static loading behave as brittle materials under dynamic loading. Therefore, materials for elements subjected to dynamic loading are selected after conducting an *impact test*. In impact test specimens of the material are subjected to impact failure under tension, but more often under bending, and the energy required for breaking the specimens acts as a pointer to the properties of the material. Impact test under bending is most commonly employed.\*

\* For details see N. M. Belyaev, *Laboratory Experiments on Strength of Materials*, Gostekhizdat, 1951 (in Russian), § 89.

If  $T$  is the energy spent on breaking the specimen and  $A$  is the cross-sectional area of the specimen in the section of failure, then the impact strength of the specimen material is obtained by dividing  $T$  by  $A$ :

$$a_i = \frac{T}{A} \text{ kgf} \cdot \text{m/cm}^2$$

To reveal the properties of the specimen material during an impact test, the specimen is given a particular shape—a cut is made in the section of impact. Cuts of various shapes shown in Fig. 428 can be made; the one shown in Fig. 428 (b) is generally used at present.

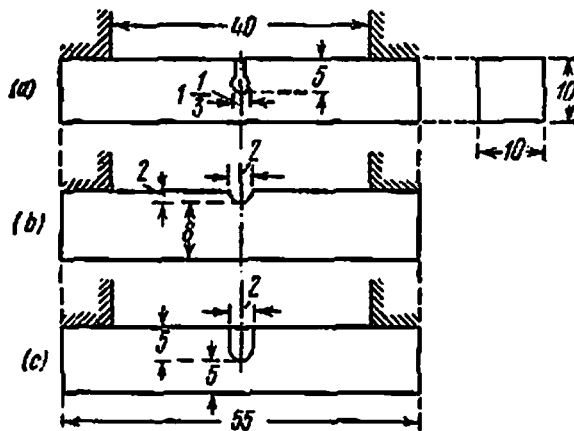


Fig. 428

The idea behind making the cut is to subject the specimen material to dynamic loading under the most unfavourable circumstances. The cut creates considerable weakening of the sections in the middle of the span, causing a sharp increase in bending stresses over a small length of the specimen.

We have already seen (§ 176) the strong effect which any local weakening of the section can have on the stresses. Almost all the energy of impact is absorbed by a small volume of material around the weakened section, causing a sharp increase in the dynamic stresses. In addition, the cut also gives rise to a local increase of stresses at its base, which are similar in nature to local stresses at the edges of holes (§ 15).

Figure 429 shows distribution of stresses in the section of a beam weakened by a cut. Curve *a* shows the diagram of stresses  $\sigma_x$  in a section without a cut; curve *b* shows the distribution of normal stresses in the section with a cut without taking into account the local stresses; finally, curve *c* shows the complete picture of variation of normal stresses  $\sigma_x$  under bending.

We see that just the decrease in the height of the section increases the stresses 2.25 times; if the local stresses are also taken into ac-

count, the coefficient of stress concentration comprises 5.22 w.r.t. the parent beam and 2.32 w.r.t. the beam of reduced height.

Generally, the local stresses result in the working of the material in three-dimensional stressed state; these conditions are not conducive to development of plastic deformation, and the material fails as if it were brittle.

Thus, in the example under consideration, in addition to normal stresses  $\sigma_1$  in sections perpendicular to the specimen axis there act tensile stresses  $\sigma_2$  in sections parallel to the axis. The distribution

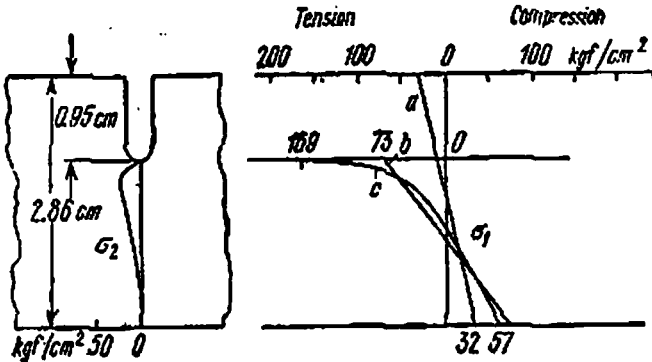


Fig. 429

curve for these stresses is also shown in Fig. 429. Besides, inside the specimen acts the third principal stress,  $\sigma_3$ , also tensile. Thus, the material near the base of the cut is subjected to three-dimensional tension, under which plastic deformation is very difficult. If the yield stress of the material under tension,  $\sigma_y$ , and stresses  $\sigma_2$  and  $\sigma_3$  are less than  $\sigma_1$ , for example  $0.2\sigma_1$ , the beginning of yielding in a three-dimensional stressed state is determined by the third theory of strength according to the following equation:

$$\sigma_1 - \sigma_3 = \sigma_y, \quad \text{or} \quad \sigma_1 - 0.2\sigma_1 = 0.8\sigma_1 = \sigma_y$$

Hence, the material at the base of the cut can undergo plastic deformation only for values of  $\sigma_1$  greater than  $\sigma_y$ , namely at  $\sigma_1$  equal to  $1.25\sigma_y$ . Due to such restrictions to plastic deformation the material may start behaving like a brittle material. This further aggravates the effect of impact loading.

Thus, the cut helps in a clear classification between materials which are more sensitive to adverse action of impact and those which are less sensitive. Here the various types of cuts show a varying degree of effect; for example, a sharp cut enhances the adverse effect of impact more than a round cut. Therefore, impact strength of various materials can be compared only if the specimens are alike.

The drawback of specimens shown in Fig. 428 is that the base of the cut falls in the stretched zone, where failure starts. Obviously, the strength of such a specimen depends upon the quality of the cut;



on the other hand, the cut makes it impossible to test specimens which must retain the contours of the actual part (this is sometimes of great importance).

The specimen (Fig. 430) prepared in the Strength Testing Laboratory of the Leningrad Institute of Railway Engineers is free of these drawbacks. When this specimen fails, the cut develops parallel to the direction of impact. Also, in this specimen almost all the energy of impact is concentrated in the weakened zone, but the failure is more close to the real one.

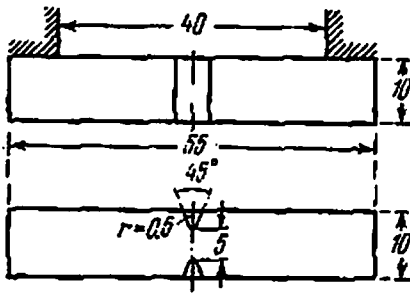


Fig. 430

There is a sharp difference between such broken specimens of ductile and brittle materials; considerable plastic deformation may be observed in the stretched zone for materials having low sensitivity to impact. However, failure of brittle materials occurs almost without an permanent deformation.

### § 180. Effect of Various Factors on the Results of Impact Testing

As a rule impact testing is carried out at room temperature on at least four identical specimens. This restriction on the minimum number of specimens to be tested is necessary to keep a check on random errors of manufacturing and testing, which may sometimes seriously affect the impact strength of the specimen.

As an example, Table 21 shows values of impact strength for a number of materials at room temperature; the tests were conducted on the type of specimen shown in Fig. 428 (b).

It can be easily noticed that impact strength is greatly affected by a number of factors, namely shape of the specimen, velocity of impact and most of all temperature of the specimen.

Impact strength of specimens of the same material falls as the temperature of testing is reduced. In some materials (mild steel) the fall is very sharp; in hardened and alloy steels (chrome-nickel) the fall is comparatively smooth. In Fig. 431 curves *a*, *b*, *c* show the variation of impact strength; the curves were obtained at the Strength Testing Laboratory of the Leningrad Institute of Railway Engineers (LIRE).

Before testing, the specimen is brought to the required temperature in a trough which can be heated by placing on an electric heater and cooled with the help of liquid air. Curves *a*, *b*, *c* shown in Fig. 431

Table 21

## Impact Strength for Some Materials

Type of steel and its chemical composition	Heat treatment			
	annealing		hardening and tempering	
	$\sigma_B$ ( $\text{kgf}/\text{mm}^2$ )	$a_1$ ( $\text{kgf} \cdot \text{m}/\text{cm}^2$ )	$\sigma_B$ ( $\text{kgf}/\text{mm}^2$ )	$a_1$ ( $\text{kgf} \cdot \text{m}/\text{cm}^2$ )
Carbon steels (carbon content)				
< 0.15	35-45	> 25	36-50	> 25
0.15-0.20	40-50	> 22	45-65	> 20
0.20-0.30	50-60	> 20	55-75	> 15
0.30-0.40	60-70	> 16	70-85	> 12
0.40-0.50	70-80	> 12	80-95	> 8
0.50-0.60	80-90	> 10	90-105	> 5
0.60-0.70	85-95	> 8	> 100	> 3
> 0.7	> 95	> 6	> 105	> 2
Alloy steels				
Nickel steel: C 0.20, Ni 3.0	50-58	25-20	70-80	24-18
Chrome-nickel steel: C 0.3, Ni 2.5-3.0, Cr 0.5-0.8	> 65	> 7	75-90	> 20
Chrome-nickel molybdenum steel: C 0.25-0.35, Ni 2.5-3.5, Cr 0.8-1.2, Mo 0.3-0.6	65-70	13	95-100	20-16

make it clear that a reduction in temperature may cause a sharp reduction in impact strength and thus cause brittle fracture of parts of structure. This phenomenon has been often observed in practice; cold brittleness of rails, rims and other elements used in railway transport has often been the cause of a number of problems.

A very important point in this context is that for quite a few materials (Fig. 431, curve *a*) the transition from plastic failure, having high impact strength, to brittle failure takes place in a small temperature interval. For instance, a material having good impact strength at room or nearly room temperature may experience brittle failure even with a small reduction in temperature. Therefore, results of the usual impact tests at room temperature cannot be considered sufficient for assessing the resistance of material to dynamic loading; it is necessary to obtain a more complete picture of impact strength as a function of temperature (Fig. 431, curves *a*, *b*, *c*).

The more to the left is the "critical" interval of fall-off of impact strength, the lower is the sensitivity of the material to temperature changes under dynamic loading and the greater is its reliability.

Variation of the shape of the specimen can, to some extent, be utilized to replace testing at various temperatures. Experiments show

that in wider specimens the "critical" temperature interval shifts towards the right, i.e. towards higher temperatures. Therefore, if the usual impact test at room temperature gives satisfactory results, then tests may be conducted on wider specimens to check whether the temperature of conducting the experiment is close to the critical

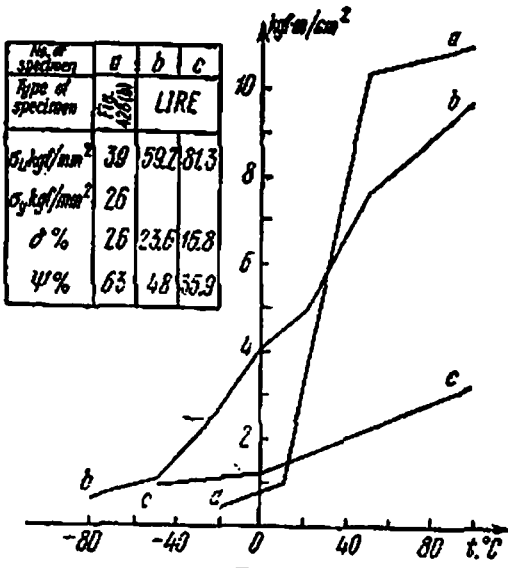


Fig. 431

interval. If brittle fracture occurs after this test, it means that the temperature of experiment is close to the critical interval.

Finally, it should be noted that ductile properties of a material may be seriously affected by residual stresses, which appear in the material after quenching, cold rolling, or rolling at low temperatures resulting in strain-hardening of the material. As a rule, these stresses cannot be assessed by simple tension test. Residual stresses generally occur in a three-dimensional stressed state of the material; this may

result in brittle fracture. Situations like this have been observed in manufacturing large I-beams having thin flanges. In the course of our experiments an I-beam No. 50 failed due to brittle fracture when it was dropped on earth on a frosty day. Tests under static loading and the chemical and metallurgical analysis revealed that the material of the beam was of good quality. Only under dynamic loading at different temperatures was cold brittleness observed in specimens cut near the flange edge—in the maximum hardened region. As for the effect of chemical composition of steel on brittleness, the impact strength decreases, as can be seen from Table 21, with an increase in carbon content, i.e. with an increase in ultimate strength and decrease in plastic properties of steel. Phosphorus has an extremely adverse effect on impact strength, especially at low temperatures. Therefore the percentage of phosphorus in steel should be restricted in every possible way if the steel is to be used in the manufacture of elements working under impact.

## CHAPTER 31

**Strength Check of Materials  
Under Variable Loading****§ 181. Basic Ideas Concerning the Effect of Variable  
Stresses on the Strength of Materials**

The resistance of materials to loads which systematically change in magnitude or magnitude and sign is considerably different from the resistance of the same materials to static and dynamic loads. Consequently, the problem of checking strength of materials under variable loads requires to be studied in a special chapter.

It is well known that machine parts subjected to cyclic loads sometimes fail suddenly, without any noticeable permanent deformation, at stresses which they reliably withstand under static loading. The attention of engineers was first directed to this problem by the observation that machine elements manufactured from materials showing under static tests excellent plastic properties—elongation, contraction and impact strength—failed without any noticeable plastic deformation, as if they were made of some brittle material.

When the engineers first started studying the causes of such failures (first half of the nineteenth century), they still did not have a clear idea about the structure of metals; it was assumed at that time that plastic metals have a "fibrous" structure, whereas brittle metals have a "crystalline" structure. As the failure of elements generally occurred not immediately but after a certain, considerably long, period of operation of the machine, it was assumed that under variable stresses the metal gets "fatigued" and changes its structure from fibrous to crystalline, becoming brittle in the process.

The surface of fracture itself seemed to support this hypothesis. As a rule, the surface had two distinct zones: a smooth, ground surface (the surface in which the crack developed gradually) and a coarse grained surface (surface of final failure of the section weakened by the crack). Figure 432 shows the surface of failure of a wagon axle; we can see the outer ring-shaped smooth surface and the inner coarse-grained surface, which is characteristic of brittleness.

However, at the beginning of the twentieth century, the study of the microstructure of metals under microscope proved that the hypothesis was not correct. It was observed that metals have a crystalline structure in the ductile state. Observations showed that when the element is subjected to variable stresses, no principal changes in the microstructure or in mechanical properties occur. The materials of the piston rods of steam engines and of the wagon axles retained their structure irrespective of how long they worked.

This precludes any talk of "recrystallization" from one form to another under the action of variable stresses.

The nature of failure under variable loading was discovered at the beginning of this century. Numerous experiments revealed that under the action of variable stresses, a crack appeared in the metal and gradually penetrated into its interior. Under variable deformation the edges of the crack approach each other at one instant and move away at another; this explains the ground, smooth surface in the zone of failure. As the fatigue crack develops, the cross section weakens more and more, and finally a chance impact is enough to cause complete failure, which occurs when the strength of the weakened cross section becomes insufficient.

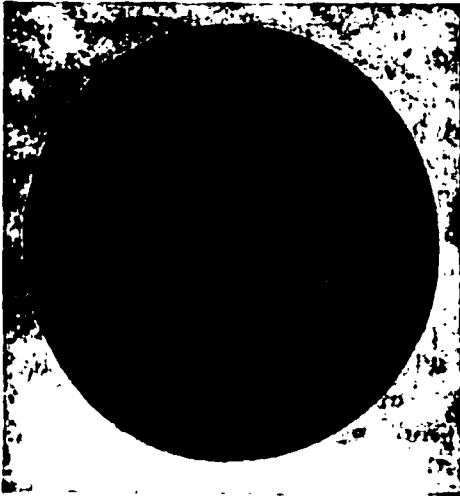


Fig. 432

The fatigue crack is a sharp cut on the surface of cross section, similar to the cut made on specimens used in impact testing. The base of the crack finds itself in a three-dimensional stressed state, which is conducive to brittle failure under impact (see § 179). This explains the presence of coarse-grained structure in the zone of failure, caused by brittle fracture.

The fatigue crack is a sharp cut on the surface of cross section, similar to the cut made on specimens used in impact testing. The base of the crack finds itself in a three-dimensional stressed state, which is conducive to brittle failure under impact (see § 179). This explains the presence of coarse-grained structure in the zone of failure, caused by brittle fracture.

Thus, brittle failure under variable loading is caused not because the material changes its microstructure and becomes brittle, but because of the appearance of a fatigue crack in the three-dimensional stressed state, which is conducive to brittle failure without any plastic deformation.

The failure under variable loading is of a localized nature and does not involve the material of the whole structure. Therefore, if a crack is seen to develop under variable loading, in many cases it is not necessary to change the whole structure: it suffices to replace the damaged part and remedy the factors which caused the crack.

The theory of failure discussed above is now accepted by engineers throughout the world. Consequently, the term "fatigue of material" has lost its physical meaning: while describing the process of failure under dynamic loading we must talk not about failure due to fatigue but about failure due to gradual growth of crack.

However, on account of its brevity and widespread use in technical literature, the term "fatigue of materials" is still in vogue, although it expresses a different meaning: from now on whenever we speak about "fatigue of material", it will mean failure due to gradual development of a crack.

Our aim now is to expose the factors which cause the crack, and

lay down such rules for design of machine elements and structures and strength check that guarantee safe working under variable loads.

This problem is very important, especially in machine building, where most often we have to deal with cyclic stresses. It can safely be assumed that approximately 90% of the total failures of machine parts occur due to development of the fatigue crack. These failures are very dangerous and often result in serious accidents, because it is not always possible to notice the developing hair-thin fatigue crack in time. Failures of wagon and engine axles are chiefly caused by these cracks and invariably result in derailment, accompanied by tragic consequences. Similar failures have been observed in aircrafts as well as in other branches of machine building.

## § 182. Cyclic Stresses

Stresses in the parts of machines and structures may change either due to change in the magnitude of load (for instance, stresses in the connecting rod and the cylinder wall of an internal combustion engine change due to change in pressure of gas mixture inside the cylinder) or due to change in position of the part under action of a constant load (for instance, if the constant weight of a wagon acts on the axle which is rigidly connected with the wheels, the bending stresses at any point of the axle's cross section vary as the point changes its location due to rotation of the axle).

The variation of stresses in parts of machines or structures may be unstable (for example, changes in stresses acting in a part of bridge due to moving trams, automobiles, pedestrians) or steady (for example, change in stresses acting in the connecting rod and cylinder wall of an internal combustion engine, rotating wagon axle, transmission shaft, etc.). From among the various types of steady variable stresses, cyclic stresses are the most important; besides, these stresses are the most widely investigated. A single repetition of stress (from minimum to maximum and back) is known as the *cycle of variation of stress*; if such a cycle is continuously repeated during functioning of a part, the stresses acting in the part are called *cyclic stresses*. Cyclic stresses act in wagon axles, shafts, connecting rods, turbine blades and many other parts of machines and structures.

Figure 433 depicts various types of cyclic stresses in "stress  $p$  ( $\sigma$  or  $\tau$ ) versus time  $t$ " coordinates: (1) constant sign cycle (Fig. 433(a)), in which stresses vary only in magnitude; (2) fluctuating (zero base) cycle (Fig. 433(d)), in which stresses vary between zero and a certain maximum value; (3) constant stress (Fig. 433(c)); (4) alternating cycle (Fig. 433(b)), in which stresses change in magnitude and in sign (all the cycles enumerated above are known as *asymmetrical cycles*); (5) *symmetrical cycle* (Fig. 433(e)), an alternating cycle in which the upper and lower limits of stress variation have the same abso-

lute values. The curves which describe the variation of stresses in time may considerably differ in appearance; variation of stresses in machine parts often follows the sinusoidal law.

The maximum absolute stress in the cycle is denoted by  $\rho_{\max}$  ( $\sigma_{\max}$ ,  $\tau_{\max}$ ), while the minimum is denoted by  $\rho_{\min}$  ( $\sigma_{\min}$ ,  $\tau_{\min}$ ). The ratio

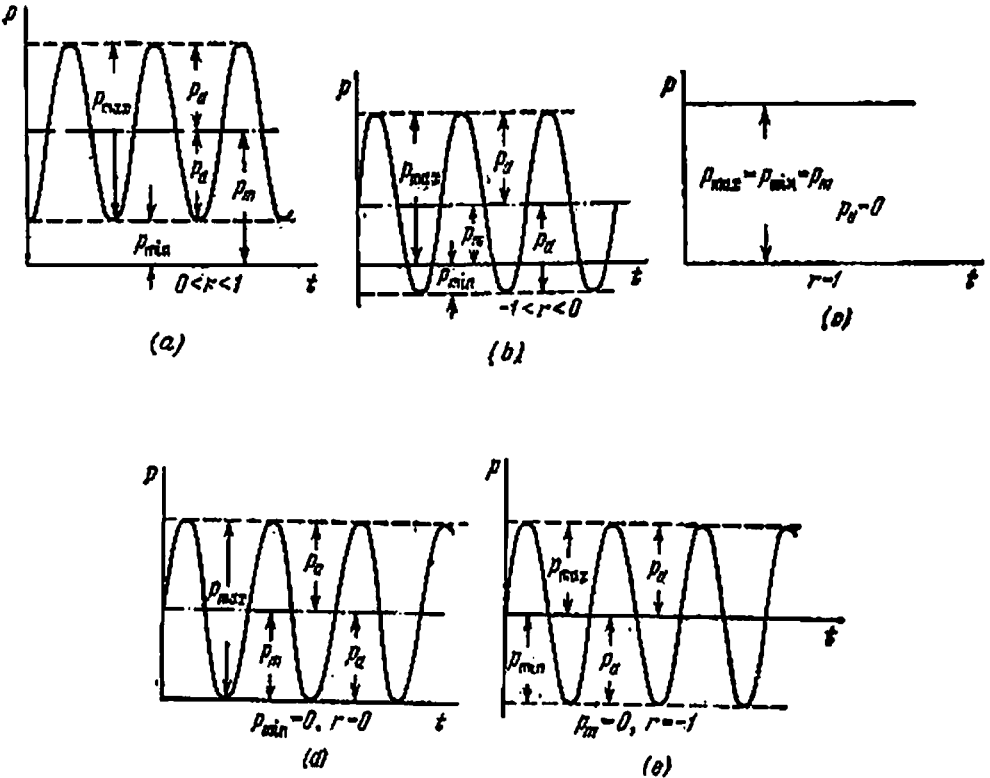


Fig. 433

of minimum stress to maximum with the signs taken into account is known as the *cycle characteristic*, or the *coefficient of asymmetry of cycle*,  $r = \rho_{\min} / \rho_{\max}$ . This coefficient varies between  $-1$  and  $+1$ ; in Fig. 433 the coefficient of asymmetry is given for all the cycles. The half of the sum of maximum and minimum stresses of a cycle (taking their signs into consideration) is known as the *constant component of cycle*, or *mean cycle stress*:

$$\rho_m = \frac{\rho_{\max} + \rho_{\min}}{2} = \frac{1+r}{2} \rho_{\max} \tag{31.1}$$

The half of the difference of maximum and minimum stresses (also taking their signs into consideration) is known as the *variable component of cycle*, or the *amplitude of stresses in the cycle*:

$$\rho_a = \frac{\rho_{\max} - \rho_{\min}}{2} = \frac{1-r}{2} \rho_{\max} \tag{31.2}$$

Thus, any cycle of stress variation may be obtained by superimposing a symmetrical stress cycle  $p'_{\max} = -p'_{\min} = p_a$  on a constant stress  $p''_{\max} = p_{\min} = p_m$ .

### § 183. Strength Condition Under Variable Stresses

Experiments show that gradually developing cracks appear only under variable stresses, oscillating systematically between extreme values.

It is also known that a large number of elements of machines and structures exhibit good resistance to variable loads over a long duration, provided the stresses remain within certain limits. Hence, just the fact that the stresses are variable is not enough to cause a crack—for the crack to appear it is essential that the maximum value of the variable stresses should exceed a particular value, which is known as *endurance strength*, or *endurance limit*. Endurance limit  $p_r$  represents the maximum value of a periodically changing stress which the material can withstand for a practically infinite period of time without fatigue cracks appearing in it.

The endurance limit for a variable stress cycle will be denoted by  $p_r$ ,  $\sigma_r$ , or  $\tau_r$  with a subscript representing the cycle characteristic:  $p_{-1}$  is the endurance limit of an asymmetrical cycle of characteristic  $r = -1$ ;  $p_{0.2}$  is the endurance limit of an asymmetrical cycle of characteristic  $r = 0.2$ ; etc.

Thus, the possibility of failure due to gradual development of a fatigue crack is subject to the following two conditions: (1) periodic oscillation of the variable stresses between two extreme values, and (2) the maximum value of the actual stresses in the element of structure exceeding the endurance limit of the material.

The strength condition in this case must express the fact that the maximum actual stress  $p_{\max}^D$  must be less than the endurance limit  $p_r$  and ensure a certain margin of safety:

$$p_{\max}^D \leq \frac{p_r}{k_r}$$

where  $k_r$  is the safety factor.

At present the endurance limit can be determined only experimentally. It depends mainly upon the (a) material (steel, iron, non-ferrous metals); (b) nature of deformation (bending, torsion, etc.); and (c) degree of asymmetry of the cycle, i.e. the interrelation between the extreme values of the variable stress.

A few additional factors affecting the endurance limit (corrosion, dimensions of elements) will be discussed separately (§§ 186 and 187).

As for the maximum dynamic stress  $p_{\max}^D$ , experiments show that contrary to failure under static loading the fatigue cracks in brittle as well as ductile prismatic bars appear not due to the maximum



design stress,  $\rho_{\max}$  (for example, in bending  $\sigma_{\max} = \frac{M}{W}$ ), but due to the local stresses (§ 15) which occur at places of deviation from the prismatic shape (cuts, scratches, holes, transition from a thin portion to a thick portion, etc.).

These local stresses  $\rho_l$  are considerably greater than the maximum stress and may be expressed by the following formula:

$$\rho_l = \alpha_c \rho_{\max}$$

here  $\alpha_c$  is the coefficient of stress concentration; its value depends upon the nature of deviation from the prismatic shape.

In the next sections we will explain how to determine the endurance limit and the coefficient of stress concentration.

#### § 184. Determination of Endurance Limit In a Symmetrical Cycle

Of maximum interest is the determination of the endurance limit in a symmetrical cycle ( $\rho_m = 0$ ), because this value is minimum. The endurance limit also varies depending upon the type of deformation—bending, axial deformation (tension and compression) and torsion.

Endurance limit in bending is determined on machines in which a round specimen is loaded through ball bearings or as a cantilever with a force acting at one end or as a simply supported beam acted upon by two symmetrical equal forces; the specimen rotates at 2000-3000 rpm. During each rotation the maximum stressed portion of the specimen material undergoes a symmetrical change of stress from maximum compressive to an equal maximum tensile, and vice versa. The number of cycles of the specimen is determined by its rpm, which can be registered by a special counting device.\* The contour of the specimen must be smooth, ruling out any possibility of occurrence of local stresses. The experiment for determining the endurance limit is carried out as follows. A batch of specimens consisting of 6-10 pieces is prepared from the material to be tested; the specimens are numbered 1, 2, 3, . . . .

The first specimen is placed in the machine and loaded in such a way that a particular value of maximum normal stress  $\sigma'$  is obtained; this value is generally taken 0.5-0.6 of the ultimate strength of the material. The machine is put into operation, and the specimen rotates experiencing variable stresses oscillating between  $+\sigma'$  and  $-\sigma'$  until ultimate failure. At this moment a special device switches off the motor, the machine stops and the counting device indicates the number of cycles,  $N_1$ , required to break the specimen at stress  $\sigma'$ .

\* For details see N. M. Belyaev, *Laboratory Experiments on Strength of Materials*, Gostekhizdat, 1958 (in Russian).

The second specimen is similarly tested at a stress  $\sigma''$ , less than  $\sigma'$ ; the third specimen is tested at stress  $\sigma''' < \sigma''$ , and so on. The number of cycles required to break the specimen increases respectively. Thus, if we go on reducing the test stress for each successive specimen, we reach a stage when the specimen does not fail even after withstanding a very large number of cycles. The stress corresponding to this stage is very close to the actual endurance limit.

Experiments show that if a steel specimen does not fail after  $10^7$  cycles, it can practically withstand an infinite number of cycles ( $10^9 \cdot 2 \times 10^8$ ). Therefore, while determining the endurance limit of a

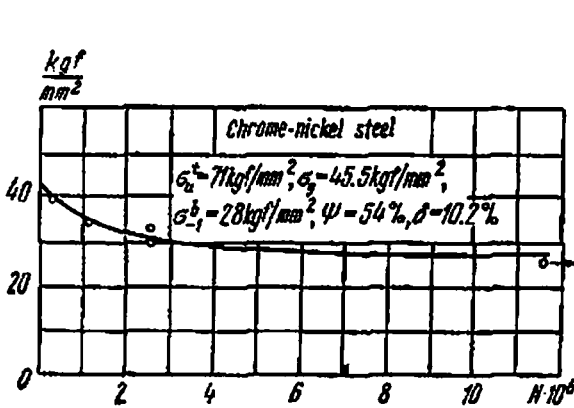


Fig. 434

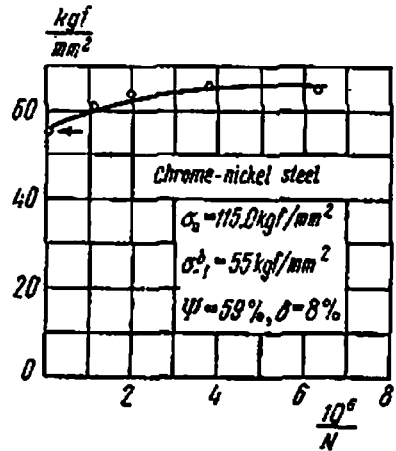


Fig. 435

material, the experiment is stopped if the specimen does not fail after  $10^7$  cycles. In a number of cases the tests are stopped after a smaller number of cycles, but never before completing  $5 \times 10^6$  cycles.

A similar dependence does not exist for non-ferrous metals, and to make sure that the specimen can really withstand a very large number of cycles at the given stress the experiment is stopped only after subjecting the specimen to  $2 \times 10^8$  and even  $5 \times 10^8$  cycles. Therefore, in the case of non-ferrous metals the endurance limit can be specified only for a particular number of cycles, say for  $10^7$  cycles, the material has one endurance limit and for  $3 \times 10^7$  cycles a different endurance limit.

The experimental results have to be processed graphically in order to determine the numerical value of endurance limit. Figures 434 and 435 show two such methods. In the first method stresses  $\sigma'$ ,  $\sigma''$ , ... are laid off the  $y$ -axis, and  $N_1$ ,  $N_2$ , ... are laid off the  $x$ -axis. The ordinate of the horizontal tangent (asymptote) to the curve gives the endurance limit  $\sigma_{e1}$ . In the second method, we lay off the quantity  $10^8/N$  along the  $x$ -axis. In this case the endurance limit is determined as the segment cut off on the  $y$ -axis by the extended curve,

because in this case the origin of coordinates corresponds to  $N = \infty$ . The second method is now more commonly used.

The endurance limit can be similarly determined under axial loading (tension and compression) and torsion; special testing machines (pulsators \*) are used for this purpose.

An enormous amount of experimental data is now available on determination of endurance limits of various materials. A greater part of the experimental studies pertain to steel, because steel is the most commonly used material in machine building. The results of these experiments show that for all grades of steel the endurance limit is related by a definite law to the ultimate tensile strength  $\sigma_u$ . For rolled and forged steels the bending endurance limit under a symmetrical cycle comprises  $(0.40-0.60)\sigma_u$ ; for cast steel the endurance limit varies between  $(0.40-0.46)\sigma_u$ .

Thus, with sufficient practical accuracy, we may write the following relation for all grades of steel:

$$\sigma_{-1}^b = 0.4\sigma_u = \beta_r\sigma_u$$

If the specimen is subjected to axial loading under a symmetrical cycle (variable tension and compression), then the corresponding endurance limit  $\sigma_{-1}^a$  is found to be less than the endurance limit under bending; the ratio between the two endurance limits may be taken equal to 0.7, i.e.

$$\sigma_{-1}^a = 0.7\sigma_{-1}^b$$

The reduction may be explained by the fact that in tension and compression all sections of the specimen experience equal stresses, and in bending maximum stresses occur only at the outer fibres (the remaining material remains underloaded and thus somewhat impedes the emergence of fatigue cracks); besides, there is always bound to be some eccentricity in the application of axial loads.

Finally, the torsional endurance limit under a symmetrical cycle comprises 0.55 of the bending endurance limit. Thus, under a symmetrical cycle we get the following values for steel:

$$\left. \begin{aligned} \sigma_{-1}^a &= 0.4\sigma_u \\ \sigma_{-1}^a &= 0.7\sigma_{-1}^b = 0.28\sigma_u \\ \sigma_{-1}^t &= 0.55\sigma_{-1}^b = 0.22\sigma_u \end{aligned} \right\} \quad (31.3)$$

These relations can be employed for obtaining formulas for the strength check.

In the case of nonferrous metals we get a more flexible relation between endurance limit and ultimate strength; the empirical for-

\* Ibid.

mula is

$$\sigma_{-1} = (0.24-0.50) \sigma_u$$

While using expression (31.3), it should be borne in mind that the endurance limit of a material depends upon a large number of factors (§ 187); the relations given in expression (31.3) were obtained on specimens of small diameter (7-10 mm) having a polished surface and no sharp changes of shape along the length.

### § 185. Endurance Limit in an Unsymmetrical Cycle

The equipment required for determining endurance strength under an unsymmetrical cycle is much more complicated than the equipment used for symmetrical cycles.

A special spring capable of stretching and compressing the specimen should be added to the simple testing machine discussed earlier, in which the specimen only rotates. Quite often we have to employ even more complicated machines, which are capable of exerting axial load on the specimen (tension, compression) under different extreme values of the variable stresses.

However, we now have at our disposal sufficient experimental data to obtain a graphical or analytical relation between the endurance limit and the cycle characteristic  $r$ , i.e.  $\frac{\rho_{\min}}{\rho_{\max}}$ .

Let us remind the reader about the notations used here:  $\rho_u$  represents the ultimate strength of the material,  $\rho_y$  the yield stress,  $\rho_r$  the endurance limit corresponding to a cycle of characteristic  $r$ ,  $\rho_{-1}$  the endurance limit in a symmetrical cycle,  $\rho_{\max}$  and  $\rho_{\min}$  the upper and lower extreme values of the cycle,  $\rho_m = \frac{\rho_{\max} + \rho_{\min}}{2}$  the mean stress in the cycle,  $\rho_a = \frac{\rho_{\max} - \rho_{\min}}{2}$  the amplitude of oscillations of the cycle,  $2\rho_a$  the double amplitude of the cycle, and  $r = \frac{\rho_{\min}}{\rho_{\max}}$  the characteristic of the cycle.

The values of  $\rho_{\max}$ ,  $\rho_{\min}$ ,  $\rho_a$  and  $\rho_m$  which correspond to working of the material at the endurance limit will be denoted by a subscript  $r$ :

$$\rho_{r \max}, \quad \rho_{r \min}, \quad \rho_{r m}, \quad \rho_{r a}$$

(the maximum absolute value of  $\rho_{r \max}$  or  $\rho_{r \min}$  must coincide with  $\rho_r$ ).

The results of experiments for determining endurance limit under different cycles are conveniently represented in the form of diagrams. The simplest among these diagrams is the diagram in the  $\rho_m$ - and  $\rho_a$ -coordinates (Hay's diagram) shown in Fig 436. On this diagram the values of  $\rho_m$  are laid off on the  $x$ -axis to a certain scale and the values of  $\rho_a$  are laid off on the  $y$ -axis in the same scale. Curve  $ABCD$  has been plotted on the basis of experiments for determining the endurance limit under different cycles of variable stresses. For deter-

mining with the help of this diagram the endurance limit  $p_r$  for a cycle having coefficient of asymmetry  $r$  we draw from the centre of coordinates  $O$  a straight line  $OS$  at an angle  $\beta$ , so that (see (31.1) and (31.3))

$$\tan \beta = \frac{p_a}{p_m} = \frac{1-r}{1+r} \tag{31.4}$$

and extend it until it intersects curve  $ABCD$  at point  $C$ ; from this point we then drop a normal  $CE$  on the abscissa. The sum of segments  $CE$  and  $EO$ , which are respectively equal to  $p_{aC}$  and  $p_{mC}$ , gives the endurance limit

$$p_{rC} = p_{max} = p_{aC} + p_{mC} \tag{31.5}$$

Thus, point  $A$  having ordinate  $OA = p_a = p_{-1}$  and abscissa  $p_m = 0$  represents the endurance limit under a symmetrical cycle:  $r = -1$ ,

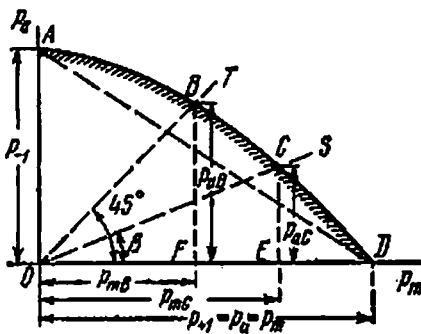


Fig. 436

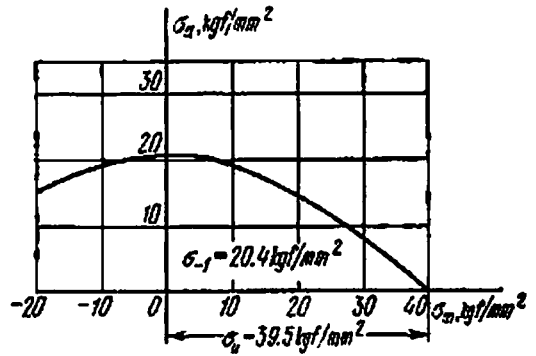


Fig. 437

$\beta = \pi/2$ , while point  $D$  having ordinate  $p_a = 0$  and abscissa  $OD = p_m = p_{+1} = p_u$  represents the endurance limit under static loading ( $r = +1$ ,  $\beta = 0$ ), which is equal to the ultimate strength of the material. If we draw a straight line  $OT$  at  $45^\circ$  inclination through the centre of coor-

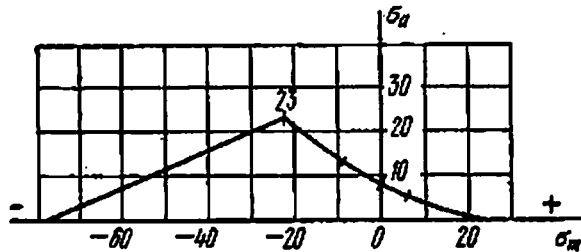


Fig. 438

ordinates, point  $B$ , where this line intersects curve  $ABCD$ , represents the endurance limit under fluctuating (zero base) load, because ordinate  $BF = p_{aB}$  of point  $B$  is equal to abscissa  $OF = p_{mB}$ , i.e. from (31.1) and (31.2)  $1+r = 1-r$ , and  $r = 0$ .

Figure 437 depicts Hay's diagram for common low-carbon steel, and Fig. 438 shows the same diagram for grey iron having the following properties:  $\sigma_{u,t} = 78 \text{ kgf/mm}^2$ ,  $\sigma_{u,c} = 22 \text{ kgf/mm}^2$ ,  $\sigma_{-1} = 7.3 \text{ kgf/mm}^2$ , and  $\sigma_{0,c} = 46 \text{ kgf/mm}^2$  ( $\sigma_{0,c}$  is the endurance limit under fluctuating cycle in compression). This diagram proves that under variable loading too cast iron has a much higher strength in compression to that in tension.

The endurance limit should be looked upon as a critical stress similar to ultimate strength under static loading, because a stress slightly greater than the endurance strength can cause failure within a practically feasible number of variations of the load. Therefore, curve  $ABCD$  in Fig. 436 represents a curve of critical (limiting) stresses for materials that do not have a yield zone. If the material is ductile and the critical stress for it under static loading is yield stress  $p_y$ , then it can be easily established from Fig. 439 that line  $AGH$  should be taken as the line of critical stresses. In the endurance limit

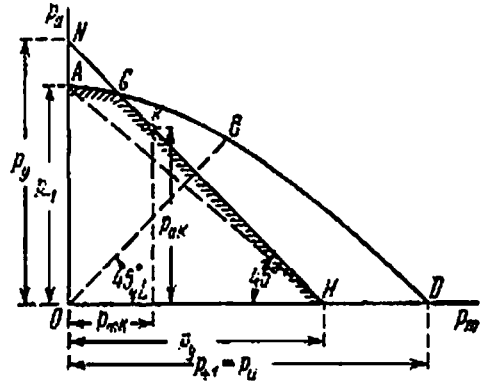


Fig. 439

diagram  $ABD$  (Figs. 436 and 439), if we cut segments  $OH$  and  $ON$  equal to yield stress  $p_y$  on the  $x$ - and  $y$ -axis, respectively, and join points  $N$  and  $H$  by a straight line  $NH$ , then the sum of the abscissa and ordinate of any point on this line is always equal to  $p_y$  (for instance, for point  $K$ ,  $OL + LK = p_{mK} + p_{aK} = OL + LH = p_y$ , as  $LK = LH$ ). Hence, straight line  $NH$  determines the critical limit of stresses under static loading, while curve  $ABD$  determines it under variable loading. In the region in which straight line  $NH$  lies above curve  $ABD$  (from the axis of ordinates to point  $G$ , the point of intersection of these lines) the critical limit of stresses is determined by curve  $AG$ . But where line  $NH$  lies below curve  $ABD$ , the critical limit of stresses is determined by the straight line  $NH$ . In Figs. 436 and 439 the critical stress lines are hatched.

On account of the fact that usually we determine experimentally  $p_y$ ,  $p_u$ , and  $p_{-1}$  while the endurance limits for other values of  $r$  are generally not determined, straight lines  $AD$  (Fig. 436) or  $AH$  (Fig. 439) have often to be accepted as the critical stress lines in the absence of experimental data. The critical stress curve is sometimes replaced by a straight line in order to simplify calculations; let us note that such an approximation adds to the existing safety factor.

A fairly large number of formulas were proposed for establishing the analytical relationship between endurance limit, ultimate strength

and the cycle's characteristic. Those deserving attention are:

$$\rho_r = \frac{2q_1}{1-r+(1+r)q_1} \rho_u \quad (31.6)$$

$$\rho_r = \frac{\sqrt{(1-r)^2 + 4(1+r)^2 q_1^2} - (1-r)}{(1+r)^2 q_1} \rho_u \quad (31.7)$$

and

$$\rho_{ra} = \rho_{-1} \left[ 1 - n_1 \frac{\rho_{rm}}{\rho_u} - n_2 \left( \frac{\rho_{rm}}{\rho_u} \right)^2 \right] \quad (31.8)$$

where  $q_1 = \rho_{-1}/\rho_u$ . Coefficients  $n_1$  and  $n_2$  in the last formula have different numerical values depending upon the material. For low-carbon steel  $n_1=0$  and  $n_2=1$ , and a parabolic relationship exists between  $\rho_{ra}$  and  $\rho_{rm}$ . On the other hand, for steels with high ultimate strength  $n_1=1$ ,  $n_2=0$ , and expression (31.8) is represented by a straight line.

As already mentioned, endurance limit  $\rho_r$  depends not only upon the material, nature of deformation and type of cycle, but also upon the shape of part and the condition of its surface, upon its dimensions, and so on. From among the factors listed the endurance limit  $\rho_r$  is affected most by the shape of part and the condition of its surface. As these factors are equally important in static loading also, they deserve a detailed discussion.

## § 186. Local Stresses

Uniform distribution of stresses over the section of the part under tension or compression and linear variation of normal stresses over the section of a beam subjected to bending or shearing stresses along the radius of section of a shaft subjected to torsion are valid only for uniform prismatic rods which are free of internal or external flaws and damages and only in sections that are sufficiently far away from the point of application of load. The distribution of stresses is violated at the point of application of load and also where the part has holes, recesses, transitions from one dimension and shape to another, internal and external flaws and damages, non-uniform structure of material, etc.

For instance, in a plate (Fig. 440(a)) stretched by forces  $P$  acting along its axis the normal stresses in section  $mn$  located sufficiently far from the point of application of force are distributed uniformly. In section  $m_1n_1$ , where there is a small circular hole in the plate, the distribution of stresses will be different. Near the edge of the hole the stress will be considerably (about three times if the hole is small) higher than in section  $mn$ . However, the high stresses act only on a small area of section  $m_1n_1$  near the hole; in the remaining area of the section the stresses are approximately the same as in section  $mn$ . These high stresses are known as local stresses  $\rho_l$  ( $\sigma_l$  or  $\tau_l$ ); the sources

of local stresses (holes, recesses, damages, etc.) are called *factors (sources) of stress concentration*. The ratio between the maximum local stress  $p_{l \max}$  to the *nominal stress*  $p_{\text{nom}}$ , i.e. to the stress at the same point in the absence of stress concentration source, is known as the *coefficient of stress concentration*,  $\alpha_c$ :

$$\alpha_c = \frac{p_{l \max}}{p_{\text{nom}}} \tag{31.9}$$

Even in a uni-axially loaded element the local stresses create a three-dimensional stressed state. In Fig. 440 it is shown that besides stresses in sections perpendicular to the bar axis additional normal stresses of smaller magnitude appear around the hole in a plane normal to the first ( $\sigma_2$ ).

The coefficient of stress concentration depends chiefly upon how fast the prismatic shape changes. If the transition from a large diameter to a smaller diameter takes place sharply, at right angles, the

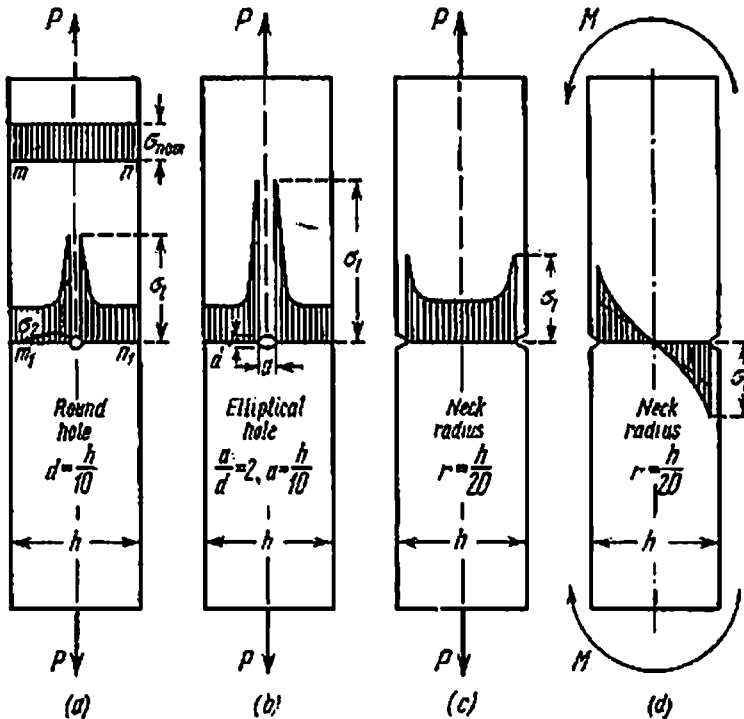


Fig. 440

maximum value of  $\alpha_c$  is obtained. If the transition is smoothed by making a fillet of certain radius, the value of  $\alpha_c$  becomes smaller and may even become equal to unity (Fig. 441 (a) and (b)).

Figure 440 depicts a few examples of stress concentration due to holes and recesses in parts subjected to tension or bending.



The following methods are employed for determining the coefficient of stress concentration. In a number of cases (for example, in tension and bending of bars with holes and necks) it is possible to determine the local stresses by the theory of elasticity. Another popular method is the experimental determination of local stresses in a planar stressed transparent model (made of glass, celluloid or bakelite) under polarized light; from the colour of various portions of the model we can find the difference between principal stresses at various points and then through some additional measurements and computations determine the principal stresses.

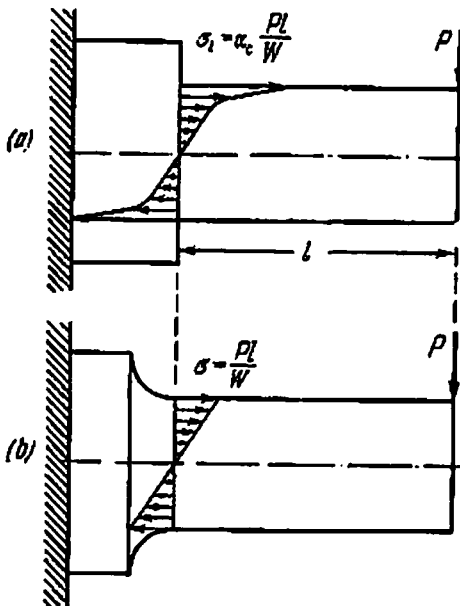


Fig. 441

The experimental methods include determining local stresses with the help of lacquer coatings or meshes\* (quadratic or circular of small diameter), which are applied to the surface of the specimen, and studying brittle (gypsum) models.

If we test the strength of a material (Fig. 441 (a) and (b)) on two specimens, one with local stresses and the other without, we

find that  $\sigma_u$  of the first specimen is less than  $\sigma_u$  of the second specimen (of course, using the same modulus of section of diameter  $d$ ); the ratio of these two values of ultimate strengths gives us the required coefficient of stress concentration,  $\alpha_c$ .

However, a more reliable method of obtaining  $\alpha_c$  is by determining the endurance limit of two specimens, one with local stresses and the other without. The first specimen gives a lower (on account of local stresses) endurance limit  $\sigma_r^*$  as compared to the second  $\sigma_r$ , the ratio  $\frac{\sigma_r^*}{\sigma_r}$  determines coefficient  $\alpha_c$ . It was noticed that the value of the stress concentration coefficient differs with the method employed, although the factor causing local stresses was the same in each case.

The first two methods—one based on the theory of elasticity and the other on optical study—give almost equal values of  $\alpha_c$ . This is obvious, because in both cases the results pertain to isotropic elastic materials. Also, the values of  $\alpha_c$  determined from endurance tests are found to be quite close to the values obtained by the first two

\* See, for example, G. A. Smirnov-Alyayev, *Strength of Materials Under Plastic Deformation*, Mashgiz, 1961 (in Russian).

methods for some materials (chrome-nickel, high strength carbon steel) and considerably less for other materials (mild steel). It was found that the coefficient of stress concentration depends not only upon the shape of the specimen, but also upon its material. The greater the ductility of material, the lower is its coefficient of stress concentration. The reasons for this have already been explained in § 16; the plasticity of a material creates a sort of buffer, which to a certain extent mitigates the effect of local stresses.

Thus, we have two coefficients of stress concentration: first, the theoretical one,  $\alpha_{c,t}$ , takes into account only the shape of the specimen and is mainly determined by any of the first two methods; the second, the actual one,  $\alpha_{c,a}$  is determined by the test on endurance and takes into account not only the shape but also the material of the specimen.

As this consideration affects only the amount by which the local stresses exceed the general, i.e. the quantities  $(\alpha_{c,t}-1)$  and  $(\alpha_{c,a}-1)$ , the sensitivity of a material to local stresses may be determined by the ratio of the two, known as the *sensitivity factor* of the material:

$$q = \frac{\alpha_{c,a} - 1}{\alpha_{c,t} - 1} \quad (31.10)$$

This factor depends upon the material; it may be equal to unity in high grade, heat-treated alloyed steels and may be as low as 0.5 in case of mild steels. It is found that iron is the least sensitive to local stresses; in the case of iron  $q$  is close to zero and the actual stress concentration factor,  $\alpha_{c,a}$ , is almost equal to unity. This can be explained by the fact that the ultimate strength of iron is strongly affected by microscopic graphite inclusions, which are actually nothing but sharp cracks in the base metal. The effect of these cracks, which are a regular feature of iron, is so strong that it almost completely makes iron immune to the effect of other stress concentration factors.

The sensitivity factor, however, depends not only upon the material but also upon the shape and size of the part, and  $q$  increases with the increase in dimensions of the body.

Sensitivity factor  $q$  for steel may be determined approximately (without accounting for the absolute dimensions of the body) with the help of the curves in Fig. 442, depending upon the ultimate strength of the material (between 40 and 130 kgf/mm<sup>2</sup>) and the theoretical stress concentration coefficient  $\alpha_{c,t}$  (Figs. 443 and 444). This diagram was obtained from experimental data on endurance testing of small (diameter of 7-10 mm) specimens of various grades of steel for different values of the theoretical stress concentration coefficient. It is evident from the diagram that the sensitivity factor increases with ultimate strength and theoretical stress concentration coefficient. The increase of  $\alpha_{c,t}$  beyond 1.8 ceases to have any effect on the sensitivity factor. For a highly alloyed steel having high ultimate strength

(130 kgf/mm<sup>2</sup>), coefficient  $q$  may be considered equal to unity, and  $\alpha_{c,t} = \alpha_{c,l}$ .

Much less data on the sensitivity factor for nonferrous metals are available. For cast Electron (an alloy of magnesium with aluminium,

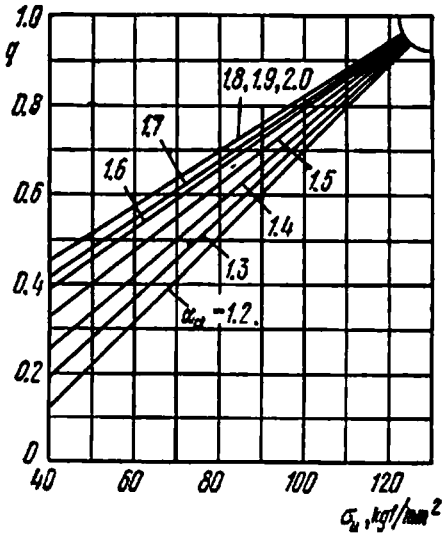


Fig. 442

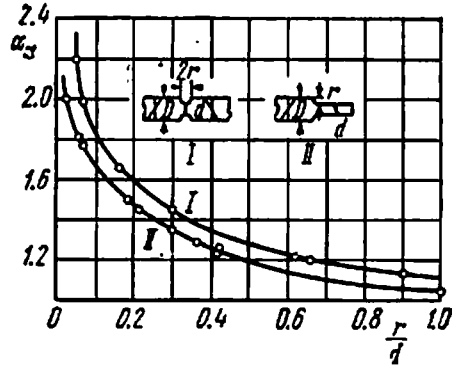


Fig. 443

zinc and manganese) this coefficient is 0.15; in rare cases it may go up to 0.25. The sensitivity factor is higher for rolled and stamped Electron and varies between 0.35 and 0.50. In case of aluminium alloys the values of this coefficient are still lower.

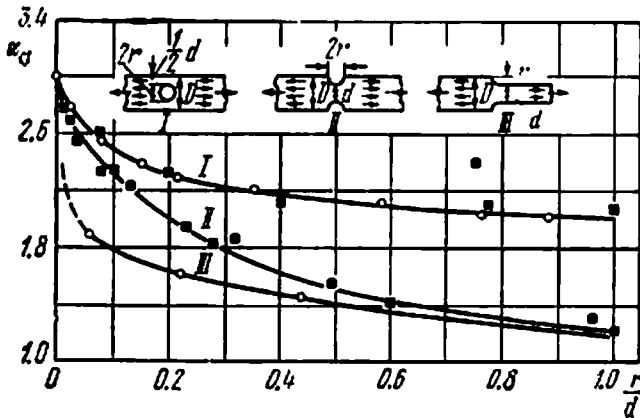


Fig. 444

The curves in Figs. 443 and 444 showing the variation of  $\alpha_{c,t}$  as a function of  $\frac{r}{d}$  may be used for determining the theoretical stress concentration coefficient in more common situations of stress con-

centration (holes, necks, fillets) depending upon the sharpness of change in shape of the part under tension or compression (Fig. 443) and pure bending (Fig. 444). The coefficients were determined for rectangular specimens by the optical method. In round specimens with necks and fillets the corresponding values of  $\alpha_{c,t}$  are found to be somewhat less. Some values of  $\alpha_{c,t}$  for round specimens are given in Table 22.

Table 22

## Coefficient of Stress Concentration

Type of deformation and source of stress concentration	$\alpha_c$
<b>I. Bending and tension</b>	
1. Semicircular neck on shaft, ratio of radius of neck to diameter of shaft	
0.1	2.0
0.5	1.6
1.0	1.2
2.0	1.1
2. Fillet, ratio of radius to height of section (diameter of shaft)	
0.0625	1.75
0.125	1.50
0.25	1.20
0.5	1.10
3. Transition at right angle	2.0
4. Sharp V-shape neck	3.0
5. Whitworth thread	2.0
6. Metric thread	2.5
7. Hole, the ratio of hole diameter to cross-sectional dimensions varies from 0.1 to 0.33	2.0
8. Scratches on surface due to cutting tool	1.2-1.4
<b>II. Torsion</b>	
1. Fillet, the ratio of fillet radius to the minimum shaft diameter	
0.02	1.8
0.10	1.2
0.20	1.1
2. Keyways	1.6-2.0

It should be emphasized that the curves in Figs. 443 and 444 and Table 22 help determine the theoretical, i.e. the maximum possible, values of the concentration coefficient. Knowing the theoretical stress concentration coefficient,  $\alpha_{c,t}$ , the actual stress concentration coefficient,  $\alpha_{c,a}$ , can be computed by the following formula:

$$\alpha_{c,a} = 1 + q(\alpha_{c,t} - 1) \quad (31.11)$$

which ensues from expression (31.10). However, if the sensitivity factor  $q$  is determined approximately from the curves in Fig. 442, then the actual stress concentration coefficient,  $\alpha_{c,a}$ , can also be determined only approximately. It is therefore desirable to determine  $\alpha_{c,a}$  directly by conducting endurance tests on specimens of required shape. The stress concentration coefficients,  $\alpha_{c,t}$  and  $\alpha_{c,a}$ , for a wide range of sources of stress concentration are given in handbooks, and the methods of their determination are a subject of study in special courses.\*

Quite a few simple approximate empirical formulas were proposed for determining the actual stress concentration coefficient of steel versus its ultimate strength. When the part does not have sharp angles, necks, or keyways and has a good finished (but not polished) surface,

$$\alpha_{c,a} = 1.2 + 0.2 \frac{\sigma_u - 40}{110} \quad (31.12)$$

and when the part has sharp angles, necks, or scratches,

$$\alpha_{c,a} = 1.5 + 1.5 \frac{\sigma_u - 40}{110} \quad (31.13)$$

These formulas are valid for steel with ultimate strength between 40 and 130 kgf/mm<sup>2</sup> and are sufficiently accurate for practical application;  $\sigma_u$  is expressed in kgf/mm<sup>2</sup>.

While talking of local stresses, it is necessary to emphasize the effect of surface damages on the endurance limit. Experiments show that the endurance limit of forged parts which do not undergo subsequent heat treatment is less than that of parts of the same materials in which the outer layer is machined and polished; in mild steels the difference may be 15-20%, and in high grade steels it may be as high as 50%.

A similar phenomenon is observed in springs made from high grade alloy steels if the spring wire is not machined after heat treatment (hardening and annealing). Such a surface can sometimes reduce the endurance limit two-fold. Even notches and scratches reduce the endurance limit by 10-20%.

A very important cause of considerable stress concentration is the interference fit between two parts, for example, the fit between disc or pulley hub and shaft or axle. Numerous experiments reveal that in interference fits the actual stress concentration coefficient may reach 1.8-2. It may be reduced by proper designing of the two parts (§ 191).

Poor surface finish can be the source of considerable stress concentration in machine parts made of high strength steels. For example,

---

\* See, for example, S. V. Serensen, I. M. Teitelbaum, and N. I. Prigorovskii, *Dynamic Strength in Mechanical Engineering*, Mashinostroenie, 1975 (in Russian).

for steels having ultimate strength between 50 and 140 kgf/mm<sup>2</sup> milling (denoted by  $\nabla$ ) without subsequent grinding and polishing creates a stress concentration equivalent to  $\alpha_r=1.25-2$  (here and farther on the lower value refers to steel having  $\sigma_u=50$  kgf/mm<sup>2</sup> while the greater value refers to steel having  $\sigma_u=140$  kgf/cm<sup>2</sup>). Rough grinding (denoted by  $\nabla\nabla$ ) reduces the stress concentration coefficient to 1.1-1.45; fine grinding and rough polishing (denoted by  $\nabla\nabla\nabla$ ) correspond to  $\alpha_r=1.05-1.15$ , and only after fine polishing (denoted by  $\nabla\nabla\nabla\nabla$ )  $\alpha_r=1$ . Nonferrous metals and alloys are somewhat less sensitive to the effect of surface finish on stress concentration.

The combined effect of local stresses and chemical reactions can result in a sharp reduction in the endurance limit of elements subjected to corrosion. Experiments reveal that the endurance limit registers a sharp reduction if the tests are conducted in water or some other fluid which can cause corrosion. However, this effect is less pronounced in case of stainless steel parts.

Finally, the microstructure of steel is another factor affecting the local stresses and consequently the endurance limit. The metal is a conglomerate of crystal grains of various sizes and arbitrary orientation; therefore the actual stress distribution is to some extent non-uniform even under simple tension. The degree of non-uniformity of stress distribution increases with the non-uniformity of grain size. Therefore, a fine grained homogeneous structure obtained by proper heat treatment helps to increase the endurance limit of the material.

In conclusion, it must be emphasized once again that the higher the strength of a steel the greater is its sensitivity to all types of cuts and surface damages and the higher is the quality of machining which it requires.

The expressions of endurance limit and coefficient of stress concentration derived in this section will be used in subsequent sections for laying down rules to be followed in selecting permissible stresses.

### § 187. Effect of Size of Part and Other Factors on Endurance Limit

The values of endurance limit in the preceding section were all obtained for small specimens of a diameter between 7 and 12 mm. In recent experiments endurance limits have been determined on larger specimens having diameter between 40 and 50 mm. There are fatigue testing machines which are capable of testing wagon axles of diameter 150 mm or even 300 mm.

The experiments reveal that, firstly, there is a large spread in data if a big specimen of this size is used for determining the endurance limit by the method given in Fig. 435. Secondly, the endurance limit, though not accurately known on account of the large spread,

is found to be less and sometimes much less than the endurance limit determined on small specimens. This decrease in endurance limit is more pronounced in alloyed steels; the effect of absolute dimensions on endurance limit is less in case of carbon steels.

The experimentally established fact that the endurance limit of parts is less than the endurance limit of small specimens tested in the laboratory is of utmost importance, particularly so, because this factor is not accounted for while determining the strength factor.

Unfortunately, the reduction has until now eluded a sound scientific explanation; obviously, it is due to a number of factors, which include the following:

(a) There is a greater possibility of the presence of internal sources of stress concentration in large specimens (inclusions, bubbles, etc.); the smaller specimens are more clear in this respect.

(b) In the process of manufacturing, the surfaces of specimens get work hardened, and work hardening is more pronounced in specimens of small size; it has been established experimentally that work hardening results in an increase in endurance limit.

(c) Finally, for the same value of maximum stress (in outer fibres), the decrease of stress as we move towards the interior of the body is more intense in case of small specimens than in large specimens, and their crystal grains work under less severe conditions.

All these ideas are, however, only assumptions. Experiments on determination of actual stress concentration coefficient with specimens of various sizes show that increasing the specimen size is to a certain extent equivalent to increasing the sensitivity factor of its material. These facts are of practical importance, because they show that sources of stress concentration causing local stresses are actually more dangerous than laboratory experiments on small specimens make them to be.

Hence, while checking the strength of a material, the effect of absolute dimensions on endurance limit must always be taken into account. Such a consideration can be avoided only if we determine the endurance limit on specimens of natural size. This, however, is not always possible. Moreover, sufficient experimental data is now available on comparative fatigue tests conducted on small (diameter 7-10 mm) and large specimens of the same material. Making use of this data and assessing the reduction in endurance limit due to increase of absolute size by the *scale factor*,  $\alpha_s$ , which represents the ratio of endurance limit  $p_r$  of a small specimen to  $p_r^e$  of a larger specimen or the element itself, we can approximately calculate the endurance limit of the element if the endurance limit of the smaller specimen is known. Since  $\alpha_s = p_r / p_r^e$ ,

$$p_r^e = \frac{p_r}{\alpha_s} \quad (31.14)$$

The scale factor  $\alpha_s$  can be determined as a function of absolute dimensions of the specimen or element by the curves shown in Fig. 445. The reduction of the endurance limit of the element is expressed through the endurance limit of a 10-mm diam. specimen obtained by fatigue testing. The value of  $\alpha_s$  depends not only upon the absolute dimensions of the element, but also upon its material and the sources of stress concentration. In Fig. 445 curve 1 is used for deter-

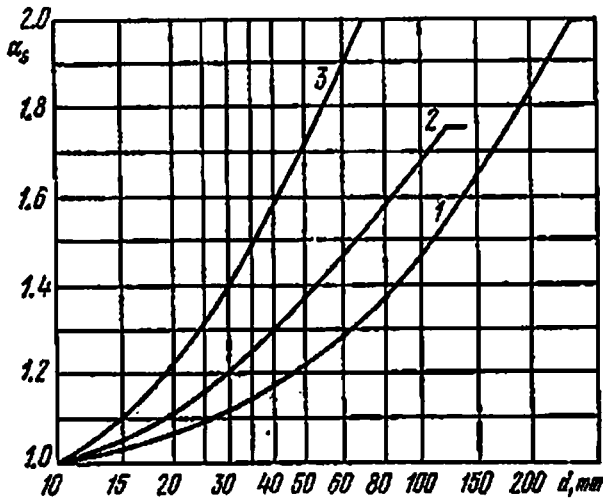


Fig. 445

mining the scale factor for carbon steel elements in absence of stress concentration, curve 2 is used for carbon steel elements with mild stress concentration ( $\alpha_{c,\sigma} < 2$ ) and alloy steel elements with no stress concentration, curve 3 is used for alloy steel elements with stress concentration. The curves in Fig. 445 can be used for smooth specimens only in bending and torsion, but can be used for specimens with stress concentration in all states of stress.

The production processes employed in manufacturing of parts (heat treatment and chemical heat treatment, metal cutting, rolling, drop forging, press fits, welding of joints, etc.) also create factors that influence the strength of materials to variable loading.

Some of these processes can lead to a reduction of the endurance strength; on the other hand, there are methods of surface treatment which improve the endurance strength of material. These methods are: (a) work hardening of the surface layer of finished part by burnishing with rolls or by shot peening; (b) chemical heat treatment of the surface: nitriding, case-hardening, cyaniding; (c) hardening of the surface layer by high frequency current (induction hardening) or by gas flame. The strengthening effect of these processes lies in the fact that residual compressive stresses are set up in the surface layer: when the latter add up with the alternating stresses due to external



load, we get asymmetrical stress cycles with a compressive mean stress  $p_m$ , which is less dangerous for the part.

The effect of production process and surface treatment may be taken into account (1) while determining the endurance limit on small laboratory specimens which are subjected to identical treatment before they are used for fatigue tests, (2) by correspondingly changing the stress concentration coefficient or by introducing a special coefficient for production process,  $K_p$ , which may have a value greater than unity (when the resistance of the part to variable loading decreases) as well as less than unity.

In a number of cases the conditions in which the part functions also considerably affect the endurance limit of the material. The most important are the effect of corrosion and temperature, as well as breaks, underloading and overloading of the part during its working.

If the part works in conditions that are conducive to corrosion (for example, if the part is under water), its resistance to variable loading decreases and the fatigue curve plotted in  $p-N$  coordinates does not have a portion which asymptotically approaches the horizontal. In such a case the part can have only a limited endurance strength corresponding to a definite number of cycles. The harmful influence of corrosion may be reduced by work hardening, nitriding, oxidation, chromium plating and some other methods of surface treatment. At the design stage the effect of corrosion may be taken into account by a corresponding increase in the coefficient of stress concentration.

The change in endurance limit of material must also be taken into consideration when the part functions in conditions with high or low temperatures. The endurance limit of metals (steel, cast iron, nonferrous metals) slightly improves at low temperatures, and this is true for smooth specimens as well as specimens having stress concentration. The same metals suffer a drop in endurance limit, at first gradually and then faster as the temperature is increased. If the part functions temporarily in conditions with low or high temperatures, this can be taken into account by introducing a special coefficient.

Parts of machines and structures are quite often subjected to short-term underloading and overloading. Breaks in operation, underloading and overloading for a relatively short period of time generally have a positive effect on the endurance limit of part material, i.e. they increase the endurance limit; overloading (stretching over a long period of time) reduces the endurance strength. Safe overloading value for a certain period of time or safe duration of overloading for a given load are found by plotting special curves known as *damage susceptibility curves*, but we shall not elaborate on this here. We also note the positive influence of the so-called "training": the part is made to work during a certain number of cycles under stresses that are just a little below the endurance strength.

While designing a part the effect of its operating conditions may be taken into account by a special coefficient  $K_{u,c}$ , which as coefficient  $K_p$  may be greater or less than unity.

The effect of the frequency of a variable stress cycle on the endurance limit is usually considered when the endurance limit is being determined. The existing fatigue testing machines give, as a rule, about 3000 stress cycles per minute. Experimental studies show that variation of the number of cycles between 500 and 10 000 does not have any appreciable effect on endurance strength. Therefore, while designing parts subjected to variable loading the special dynamic stress coefficient  $K_D$  should be used only when the cycle frequency is less than 500 or greater than 10 000 and also when the variable load is simultaneously an impact load.

### § 188. Practical Examples of Failure Under Variable Loading. Causes of Emergence and Development of Fatigue Cracks

Having established all aspects of failure under variable loading, let us study a few practical cases of such failures.

Figures 446 and 447 show the broken axle of a wagon (bending accompanied by torsion), in which failure occurred due to sharp change

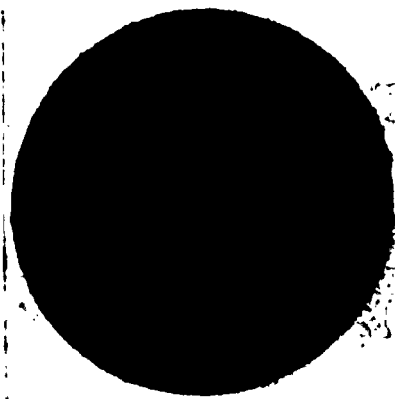


Fig. 446

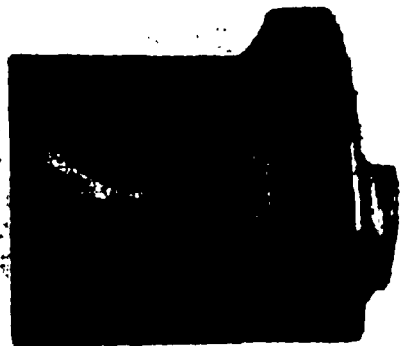


Fig. 447

from a thick portion to a thin portion; instead of a smooth fillet the transition was sharp, with rough notches on the surface left by the cutting tool. The fatigue crack appeared at the outer surface and developed along a ring shaped path. The material of the axle was satisfactory; this is borne out by the extremely small area of momentary rupture.

Figure 448 shows the fracture of a non-rotating axle which bends in the vertical plane. The material is shaft steel with an approximate

ultimate strength of  $50 \text{ kgf/mm}^2$ . The crack appeared and developed due to sharp transition (at right angles) from a square shape to a circular shape.

Figure 449 shows the longitudinal section of the other end of the same shaft, which has yet not ruptured; fatigue cracks developing



Fig. 448



Fig. 449

from the outer fibres towards the interior are clearly visible in the region of sharp transition.

The zone of fatigue cracks and the zone of ultimate failure are both clearly visible in Fig. 448. Pay attention to the series of curved strips and lines on the surface of the fatigue cracks. These are the

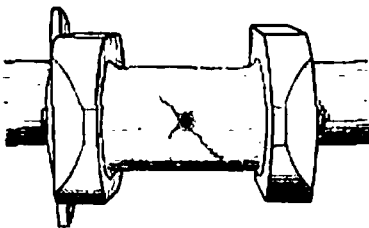


Fig. 450



Fig. 451

traces of gradual development of the cracks; the failure occurs approximately along the normal to these lines. Hence, by studying these lines, we can always point out the origin of the crack; as a rule, this is the point where the source of stress concentration is most effective,

resulting in the fatigue crack. The development of the crack can be explained by the fact that high local stresses appear at its base, thus helping the crack propagate towards the interior of the material.

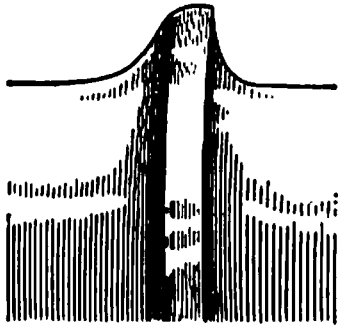


Fig. 452

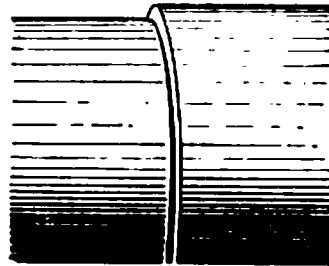


Fig. 453

It is interesting to note that fatigue cracks did not appear in the axles, the fracture of one of which is shown in Fig. 448, which were made from steel of lower strength ( $\sigma_u \approx 40 \text{ kgf/mm}^2$ ) although the same shape was retained. This can be explained by the fact that the steels have different sensitivity to local stresses.

Figure 450 shows the fatigue crack appearing in the oil hole of a crankshaft working under variable (in opposite directions) torsion. The cracks make an angle of  $45^\circ$  with the shaft axis and are perpendicular to the principal stresses.

Figure 451 shows the beginning of a fatigue crack on a car axle at the location of a very small (0.5-mm high) but very sharp recess. We find that the fatigue crack starts developing simultaneously at a number of points, which may not necessarily be all in the same plane. Later all these cracks merge into a single crack.

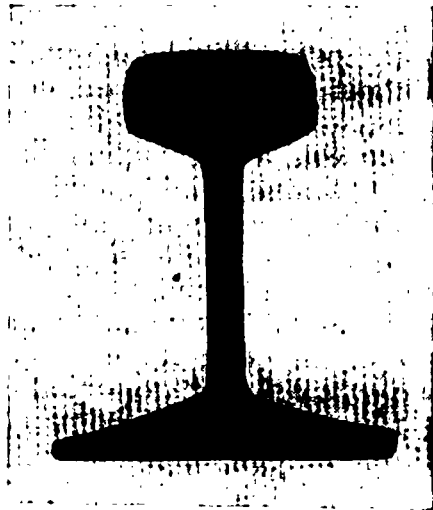


Fig. 454

Figures 452 and 453 show two steam engine axles out of which the one with smooth transitions worked satisfactorily for 40 years, whereas the other with sharp change served only for one year. The material of the second axle was better than that of the first.

Finally, Fig. 454 shows a fatigue crack which began due to internal sources of stress concentration. A bubble or a hollow inclusion in the rail head became the centre of local stresses. This resulted in gradual

development of the fatigue crack, weakening the section and leading to ultimate failure. In the section of failure the fracture looks like a silver spot.

The above examples are enough to show the salient features of fatigue failures.

Experience shows that the principal factor causing fatigue failure is not the poor quality of material (usually it was found to satisfy the required standard), but improper machining, which gives rise to considerable local stresses. Only rarely does it happen that poor quality of the material gives rise to a fatigue crack, which would not have occurred had the material been of standard quality. We can cite an example when failure occurred due to a point-size sharp mark on the axle's surface.

Before concluding this section it is necessary to explain the physical process by which the fatigue crack appears and develops.

Displacement of crystal grains, as in static tensile loading, begins under the action of high local stresses which are caused by one or the other source of stress concentration and are usually much greater than the yield stress. The only difference is that in tension the plastic deformation and displacement of crystal grains are caused by the same stress. Therefore, they affect the whole volume of the specimen and develop in a particular direction; under variable loading these deformations are concentrated in a small volume subjected to local stresses and reverse their direction at definite intervals. They, therefore, do not have any appreciable effect on the strength of the specimen as a whole, but the small portion experiencing local stresses gradually passes through all stages of plastic deformation which the material of a simple tensile test specimen has to bear on the whole.

At each cyclic change of loading, the permanently deformed portion of material which falls in the zone of high local stresses gets displaced in one and then the reverse direction; each displacement occurs in a plane different from that of the preceding one, because these displacements are accompanied by cold hardening of the material. With the increase in cold hardening the rigidity of the permanently deformed portion tends to the rigidity of the surrounding elastic material, taking a greater fraction of the load upon itself. This leads to a growth of actual maximum stresses in the small volume under consideration although the mean stress (measured) in the remaining portion remains constant. This reduces the load on the elastic zone, resulting in less strain over the whole zone including the permanently deformed portion within the elastic zone.

Hence, under variable loading there is a gradual increase of actual maximum stresses in the overstressed portion and a corresponding gradual decrease in its deformation. A fatigue crack does not appear if the attenuation of deformation ceases before the actual stresses reach the breaking point; the element works under stresses less than

the endurance limit. On the other hand, if the stresses reach the breaking point, a crack appears. The process is repeated at the bottom of the crack and results in gradual development of the crack; the element works under stresses which exceed the endurance limit.

In general the physical process of failure under variable loading does not differ much from failure under simple tensile loading. This conclusion is supported by the latest experimental studies of failure in both cases with the help of X rays.\*

### § 189. Selection of Permissible Stresses

With the help of diagrams shown in Figs. 436 and 439 we can determine the critical stress for any type of cycle. Let us now study the order in which the permissible stresses are established. For the sake of simplicity of analysis we shall consider  $AD$  (Fig. 436) the critical stress line for brittle materials and  $AH$  (Fig. 439) for ductile materials. In order to obtain the permissible stress the abscissa and ordinate of every point on both lines will be reduced in accordance with the accepted values of the safety factors; the latter will have different values for the constant and variable components of the stress cycle.

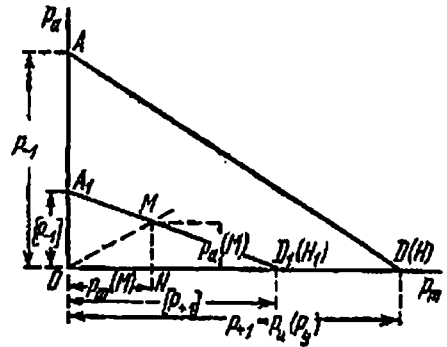


Fig. 455

Mean stress  $p_m$  may be looked upon as a certain constant static stress. It is known that under static loading the critical stress for brittle materials is the ultimate strength, whereas for ductile materials it is the yield stress. Factors like the manufacturing process and operating conditions, dimensions of the part and its surface finish, etc., have much less an effect upon the ultimate strength and yield stress as compared to the endurance limit. The effect of these factors can be taken into account by slightly changing the main safety factor,  $k_0$ , which usually accounts for errors in determining the properties of material, magnitude and location of applied load, errors of design, and other factors. No special provision need be made for stress concentration in case of ductile materials that have a suf-

\* See, for example, I. A. Oding and V. S. Ivanova, *Mechanism of Fatigue Failure of Metals*, Mashgiz, 1962 (in Russian); G. V. Uzhik (Editor), *Fatigue and Endurance of Metals*, IL, 1963 (in Russian); S. V. Serensen (Editor), *Problems of Mechanical Fatigue*, Mashinnstroenie, 1964 (in Russian); P. G. Forrest, *Fatigue of Metals*, Pergamon Press, Oxford, 1962.

ficiently large yield zone. Hence, for ductile materials the permissible stress under static loading may be found as (Fig. 455)

$$[\rho_{+1}] = \frac{\rho_y}{k_{01}} \quad (31.15)$$

whereas for brittle materials (Fig. 455)

$$[\rho_{+1}] = \frac{\rho_u}{k_{02}\alpha_{c,a}} \quad (31.16)$$

where  $\alpha_{c,a}$  is the actual stress concentration coefficient,  $k_{01}$  is the main safety factor for yield stress, and  $k_{02}$  is the main safety factor for ultimate strength.

Under a symmetrical cycle of loading the critical stress is the endurance limit, which as a rule is less than the yield stress of material. For a symmetrical cycle the permissible stress  $[\rho_{-1}]$  is found by dividing the endurance limit  $\rho_{-1}$  by the strength coefficient,  $k_r$ , which besides the main safety factor  $k_0$  includes the coefficient of actual stress concentration  $\alpha_{c,a}$ , the scale coefficient  $\alpha_s$  and, if necessary, coefficients  $K_p$  and  $K_{o,c}$  (coefficients of production process and operating conditions). If the variation of loads is not smooth but is accompanied by sharp impacts, then we must also use a *dynamic coefficient*  $K_d$ , which lies between one and two. Hence for brittle as well as ductile materials,

$$[\rho_{-1}] = \frac{\rho_{-1}}{k_r} = \frac{\rho_{-1}}{k_0\alpha_{c,a}\alpha_s} \quad (31.17)$$

or

$$[\rho_{-1}] = \frac{\rho_{-1}}{k_0\alpha_{c,a}\alpha_s K_p K_{o,c} K_d} \quad (31.18)$$

The stress diagram plotted in  $\rho_a$ - $\rho_m$  coordinates (Fig. 455) shows the critical stress line  $AD$  ( $AH$ ) and safe (permissible) line  $A_1D_1$ ; the last has been plotted for values  $[\rho_{+1}] = OD_1$  and  $[\rho_{-1}] = OA_1$  determined from formulas (31.15) and (31.17). For finding the permissible stress  $[\rho_r]$  for an arbitrary variable cycle having the coefficient of asymmetry equal to  $r$ , we must draw through the origin of coordinates  $O$  a straight line  $OM$  making an angle  $\beta$  ( $\tan \beta = \frac{1-r}{1+r}$ ) with the abscissa until it intersects line  $A_1D_1$  ( $A_1H_1$ ). The sum of the abscissa  $\rho_m(M)$  and ordinate  $\rho_a(M)$  of point  $M$  represents the permissible stress  $[\rho_r]$ :

$$[\rho_r] = \rho_{\max}(M) = \rho_m(M) + \rho_a(M) \quad (31.19)$$

It follows from similar triangles  $OA_1D_1$  and  $NMD_1$  that

$$\frac{OD_1}{ND_1} = \frac{OA_1}{NM}$$

or

$$\frac{[\rho_{+1}]}{[\rho_{+1}] - \rho_m(M)} = \frac{[\rho_{-1}]}{\rho_a(M)}$$

wherefrom

$$\rho_a(M)[\rho_{+1}] + \rho_m(M)[\rho_{-1}] = [\rho_{+1}][\rho_{-1}] \quad (31.20)$$

Since

$$\rho_a(M) = \frac{1-r}{2} \rho_{\max}(M) = \frac{1-r}{2} [\rho_r]$$

and

$$\rho_m(M) = \frac{1+r}{2} \rho_{\max}(M) = \frac{1+r}{2} [\rho_r]$$

it ensues from (31.20) that

$$[\rho_r] = \frac{2[\rho_{+1}][\rho_{-1}]}{(1+r)[\rho_{-1}] + (1-r)[\rho_{+1}]} \quad (31.21)$$

The strength condition may be written as

$$\rho_{\max} \leq [\rho_r] \quad (31.22)$$

This general method of determining permissible stresses may be elaborated as follows:

Given (a) type of deformation, (b) ratio of  $\rho_{\max}$  to  $\rho_{\min}$ , (c) shape of the part; (d) mechanical properties of the material ( $\sigma_u$ ). Find the permissible stress  $[\rho_r]$ .

Solution:

(1) Calculate

$$\rho_m = \frac{\rho_{\max} + \rho_{\min}}{2} \quad \text{and} \quad \rho_a = \frac{\rho_{\max} - \rho_{\min}}{2}$$

(2) Find

$$r = \frac{\rho_{\min}}{\rho_{\max}}$$

(3) Determine the endurance limit under a symmetrical cycle for the given type of deformation:

$$\rho_{-1} = \beta_r \sigma_u$$

(4) From the curves in Figs. 443 and 444 determine  $\alpha_{c,a}$ , depending upon the configuration of the part.

(5) Find  $q$  from the curve in Fig. 442.

(6) Calculate the actual coefficient of stress concentration

$$\alpha_{c,a} = 1 + (\alpha_{c,t} - 1) q$$



The actual stress concentration coefficient may also be calculated from the following formulas (§ 186):

$$\alpha_{c.a} = 1.2 + 0.2 \frac{\sigma_u - 40}{110} \quad \text{or} \quad \alpha_{c.a} = 1.5 + 1.5 \frac{\sigma_u - 40}{110}$$

if the technology of machining the part is known.

(7) Determine scale factor  $\alpha_s$  from the curve in Fig. 445, depending upon the size of the part.

(8) Determine permissible stress in a symmetrical cycle:

$$[p_{-1}] = \frac{p_{-1}}{k_0 \alpha_{c.a} \alpha_s}$$

(9) Find the yield stress  $p_{\eta} = \beta_r \sigma_u$ .

(10) Determine the permissible stress under static loading

$$[p_{+1}] = \frac{p_{\eta}}{k_0}$$

(11) Determine the required permissible stress

$$[p_r] = \frac{2 [p_{+1}] [p_{-1}]}{(1-r) [p_{+1}] + (1+r) [p_{-1}]}$$

This method of determining permissible stresses is not very accurate on account of the modifications introduced in the diagrams and also due to an insufficiently accurate accounting for the stress concentration factors. If desired, more accurate breaking stress diagrams may be used in which the dotted lines shown in Figs. 436 and 439 are not drawn. The accurate method of analysis may give much higher values of permissible stress for cycles having characteristics approximately equal to zero if the endurance limit is close to the yield stress; in all other situations the results obtained from the approximate and accurate diagrams are not much different.

### § 190. Strength Check Under Variable Stresses and Compound Stressed State

The above methods for checking the strength of materials under variable stresses were discussed in connection with the simplest types of deformation: tension, compression, torsion and bending. The question that now arises is: How to apply these methods in case of compound stressed state?

From a practical point of view the most important situation is that of combined bending and torsion. As explained earlier in § 125, strength check has to be carried out for an element of the material in a bi-axial stressed state; four of its faces are acted upon by shearing

stresses  $\tau = \frac{M_t}{2W}$  and two by normal stresses  $\sigma = \frac{M_b}{W}$ , where  $W = \frac{\pi r^3}{4}$  is the section modulus of the round shaft.

For a strength check under static loading we employed the following two conditions: condition (A) when the theory of maximum shearing stresses was applied, and (B) when the theory of distortion energy was applied:

$$(A) \sqrt{\sigma^2 + 4\tau^2} \leq [\sigma] \quad \text{and} \quad (B) \sqrt{\sigma^2 + 3\tau^2} \leq [\sigma]$$

Both formulas may be written in a general form by dividing them by  $[\sigma]$ :

$$(A) \sqrt{\frac{\sigma^2}{[\sigma]^2} + \frac{\tau^2}{\left(\frac{[\sigma]}{2}\right)^2}} \leq 1 \quad \text{and} \quad (B) \sqrt{\frac{\sigma^2}{[\sigma]^2} + \frac{\tau^2}{\left(\frac{[\sigma]}{\sqrt{3}}\right)^2}} \leq 1$$

or in the general form

$$\sqrt{\frac{\sigma^2}{[\sigma]^2} + \frac{\tau^2}{[\tau]^2}} \leq 1$$

where  $[\tau] = \frac{[\sigma]}{2}$  when the theory of maximum shearing stresses is applied, and  $[\tau] = \frac{[\sigma]}{\sqrt{3}}$  when the distortion energy theory is applied.

Thus, the strength check by both theories may be represented by a common equation

$$\frac{\sigma^2}{[\sigma]^2} + \frac{\tau^2}{[\tau]^2} \leq 1 \quad (31.23)$$

Since the fatigue crack is caused by the same physical processes of deformation of the material which result in failure under static loading, equation (31.23) may also be employed for checking the strength of materials under variable loading. Stresses  $\sigma$  and  $\tau$  may be broken into the components  $\sigma_m$ ,  $\sigma_a$  and  $\tau_m$ ,  $\tau_a$ :

$$\sigma = \sigma_m + \sigma_a, \quad \tau = \tau_m + \tau_a.$$

Here  $[\sigma]$  and  $[\tau]$  represent the permissible stresses under bending and torsion,  $[\sigma]_b$  and  $[\tau]_t$ , respectively, obtained from the simplified  $[\rho_a]$ - $[\rho_m]$  diagram (Fig. 455) by taking into consideration the stress concentration coefficient of the particular type of deformation and the cycle characteristic,  $\frac{\sigma_{\min}}{\sigma_{\max}}$  or  $\frac{\tau_{\min}}{\tau_{\max}}$ .

### § 191. Practical Measures for Preventing Fatigue Failure

The results derived in the preceding sections enable us to find means, which ensure sufficient strength of machine parts and structures under variable stresses.

These measures may be divided into two categories. On one hand, we must be able to manufacture elements of machines and structures from materials which have the greatest resistance to variable stresses. We have seen that in this respect the requirements of the material lead to the following two points: first, it is desirable to use a metal which has a high ultimate strength and sufficient ductility, because this is compatible with high endurance limit; second, the metal must be free of all internal factors of stress concentration (this requirement can be fulfilled by a material of uniform fine-grained structure without any residual stresses (e.g. after quenching) or disruption of uniformity in the form of cracks, gas bubbles, non-metallic inclusions, etc.).

These requirements explain why important parts subjected to variable loading are so often manufactured from alloyed steels (chrome-nickel, chrome-vanadium) having high ultimate strength and fine-grained structure free of internal stresses, which is imparted by proper heat treatment (hardening with subsequent annealing).

However, such steels are sometimes found to have microscopic cracks (especially in chrome-nickel steels), which are known as *flakes*. These flakes, just like inclusions, may sharply reduce the endurance limit of steel in spite of its having high ultimate strength.

The second category of measures ensuring sufficient strength under variable loading consists in careful design of the outer profile and proper finishing of the external surface of the element. The chief aim of the designer and technologist should be to reduce as far as possible the coefficient of stress concentration caused by sharp changes of the profile and defective machining. Reduction of local stresses can be achieved chiefly through smooth transitions of profiles, grooves, cuts and fillets. It is inadmissible to provide unsmoothed transitions, although the radius of the fillet curve may be very small. Whenever possible the radius should be large enough to affect noticeably the reduction in local stresses. The proper radii may be selected with the help of Figs. 443 and 444. It should be noted that sometimes just a small increase of the radius can rid the element from danger of failure.

We know of the failure of a large number of crankshafts of aircraft engines in the Royal Air Force. These failures occurred at the fillet near the mounting seat of the propeller; the failures stopped when the fillet radius was increased by just  $1/8$  in.  $\approx 3$  mm.

This can be explained as follows. At stresses close to the endurance

limit the curve depicting the relation between breaking stress and number of cycles is almost horizontal (Fig. 434). Therefore, if the actual stress even slightly exceeds the endurance limit, failure is inevitable, because a majority of the parts undergo cyclic changes which are large enough for the fatigue crack to appear.

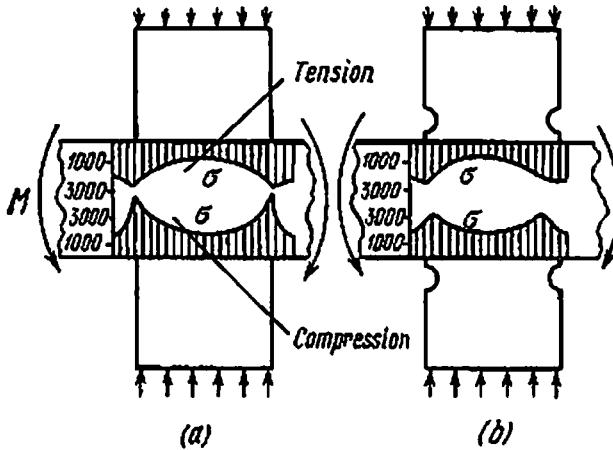


Fig. 456

On the other hand, the fatigue crack does not appear if we make the actual stress just a little less than the endurance limit by reducing the coefficient of stress concentration. The sharper the change of profile, the greater the difference between the rigidity of adjacent portions and the sharper the change of stress, the greater is the coefficient of stress concentration. Therefore the local stresses can be reduced not only by making the transitions smoother, but also by decreasing the difference between the rigidities of adjacent portions of the element in the sections where stress concentration is unavoidable. These considerations have recently led to the concept of *crippling cuts*. For example, when a gear or pulley is mounted on a shaft with interference fit, considerable local stresses appear in the shaft material (Fig. 456(a)).

The coefficient of stress concentration for normal stresses under bending in a section perpendicular to the shaft axis varies between 1.8 and 2. Figure 456(a) also shows the variation of normal stresses in the outer fibres of the shaft, on which the pulley is mounted with an interference fit. The stresses were determined by optical method.

It is evident from the diagram that there is a sharp local increase in stresses, especially in the compressed zone near the hub edge.

The local stresses decrease and become more uniformly distributed if a cut is made in the hub near the contacting surface to smooth down the sharp change in rigidity at the edge (Fig. 456(b)). The coefficient of stress concentration falls from 2 to 1.4; if, as shown in Fig. 457, the shaft diameter at the seat is increased in addition to

the cut already made, the coefficient of stress concentration may be reduced to 1.0-1.05. The local stresses may similarly be reduced by bossing the thicker part near the section of sharp transition (at right angles) (Fig. 458 (a) and (b)).

In all these examples the aim of changing the profile is to smooth the change of stress in the section of transition.

The resistance of materials to variable loading depends as much upon the surface finish as upon the smoothness of transitions in the

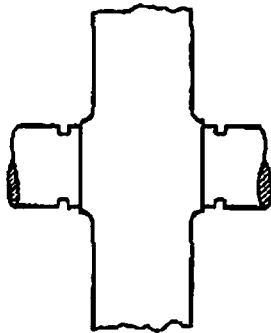


Fig. 457

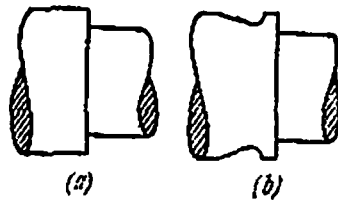


Fig. 458

profile. Any scratches or cuts left by the cutting tool can play an important role in subsequent failure of the part. We know of the failure of a large number of pistons of steam engine cylinders, when tapered hubs were fitted on the worn tapered ends of the plungers to increase

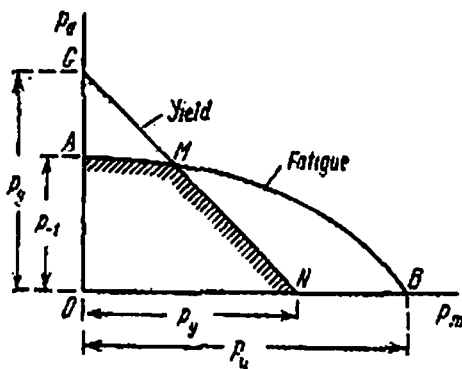


Fig. 459

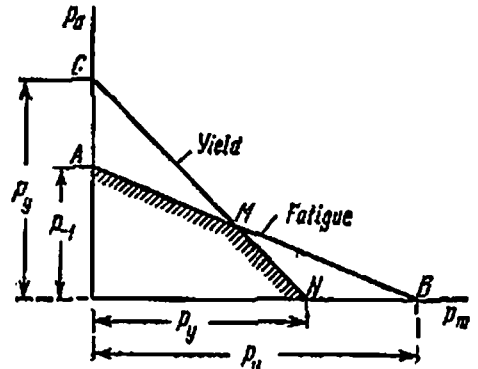


Fig. 460

their thickness. Before fitting the hub the worn out surface of the plunger was subjected to coarse turning without any subsequent finishing. The fatigue cracks appeared under the hub, beginning from the source of stress concentration in the form of a scratch left by the cutting tool. Therefore, fine finishing, nickel plating and varnishing, if the part works in a corroding medium, are not super-

fluous luxuries but absolute necessities for safe functioning of a majority of parts subjected to variable loading.

It should be noted that the questions of proper selection of material and rules regarding proper design of parts cannot be studied in isolation from one another. The better the material, the higher is its ultimate strength and the higher the quality of machining which it requires. If we use a costly alloyed steel and do not pay sufficient attention to the reduction of local stresses, we run the risk of bringing to nought the advantages that accrue from the use of high quality steel. The sensitivity factor of such a steel is much higher than that of mild steel. This was explained in § 186.

Figures 459 and 460 show the  $p_n$ - $p_m$  diagrams for mild and high grade alloyed steels. On these diagrams lines  $AMB$  correspond to failure due to development of a fatigue crack, and lines  $GN$  represent failure due to plastic deformation when the stresses exceed the yield stress.

Lines  $AMN$ , which are shaded on the diagrams, represent the curves of breaking stresses (in the wider sense of the word). It is obvious that the chances of failure due to development of fatigue crack are far greater in case of alloyed steel than in mild steel. The chances of reduction of local stresses due to plastic deformation are considerably less in the first case as compared to the second. This to a large extent explains the higher sensitivity of alloyed steels to stress concentration.

Summing up, we may conclude that the higher the grade of steel the higher is the quality of finishing which it requires so that all its properties may be fully exploited.

## CHAPTER 32

### Fundamentals of Creep Analysis

#### § 192. Effect of High Temperatures on Mechanical Properties of Metals

On account of the fast development of machine building, increasingly vital importance is being attached to strength analysis of machine parts working for long periods at high temperatures. Such parts include discs and blades of steam and gas turbines, pipes and other elements of steam generators, various parts of internal combustion engines, jet engines, chemical plants, etc.

The behaviour of the materials of such parts is affected by the absolute temperature as well as the duration for which the parts work at the high temperatures.

The properties of metals change considerably at high temperatures; therefore the known properties of strength and ductility at normal

(room) temperature cannot serve for the analysis of elements of the same metals working at high temperatures.

As the temperature increases, there is at first a gradual reduction of the modulus of elasticity and the limit of proportionality; beyond a particular temperature (for carbon steels after 300-350°C, for alloyed steels from 350-400°C, for nonferrous metals from 50-150°C) this reduction goes on getting steeper. Thus, for example, the modulus of elasticity of a commonly used steel is approximately 25-30% less at 600°C and 50% less at 800°C as compared to its value at room temperature. The reduction of the modulus of elasticity and limit of

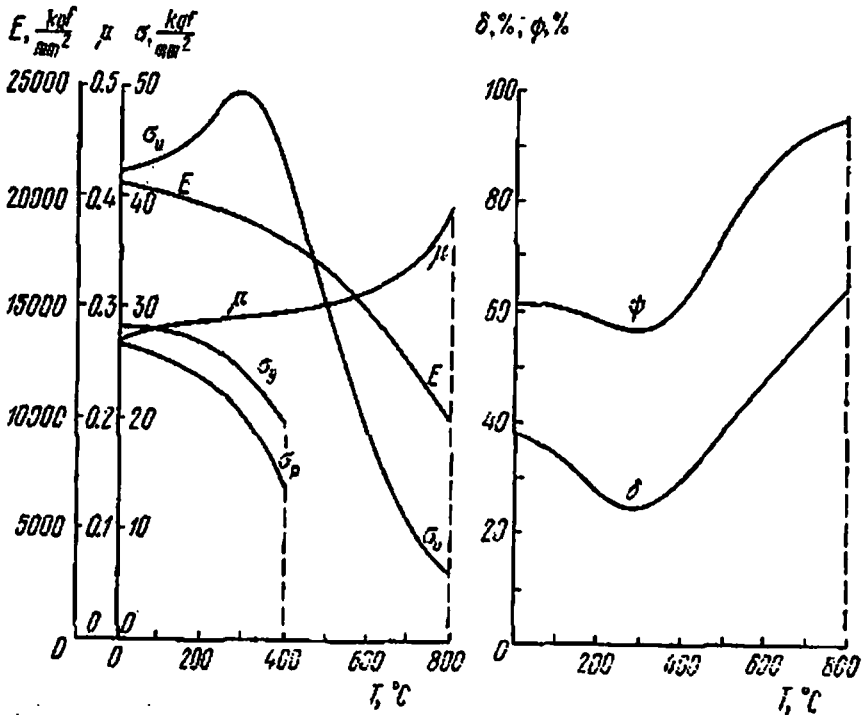


Fig. 461

proportionality is even more pronounced in case of nonferrous metals. The yield stress,  $\sigma_y$ , and ultimate strength,  $\sigma_u$ , of carbon steels increase at first with the increase in temperature and become maximum at a temperature of about 200-250°C, the maximum value is 10-20% greater than  $\sigma_u$  and  $\sigma_y$  at room temperature. If the temperature is further increased, the yield stress falls sharply: at 600°C the yield stress of steel is only 40% of its value at room temperature. In case of nonferrous metals and their alloys the increase of temperature is accompanied by a continuous decrease of yield stress. With increase in temperature the endurance limit varies in a manner which is more or less similar to the variation of ultimate strength.

The plastic properties (total relative elongation and reduction of cross-sectional area at the moment of failure) suffer a slight setback as the temperature is increased from 20 to 200-250°C; with a further increase in temperature the plastic properties, as a rule, again begin to improve. However, the plastic properties of austenitic chrome-nickel steels, bronze, brass and nickel are adversely affected by high temperatures. On the other hand, the plastic properties of aluminium and magnesium improve.

The curves in Fig. 461 show the variation of strength and plastic properties of mild steel (0.15% C) as the temperature is raised to 800°C.

### § 193. Creep and After-effect

The variation of strength and plastic properties with the increase in temperature is of vital importance in the design of elements of machines and structures. However, the most important factor affecting the behaviour of metals at high temperatures is *creep*.

Creep signifies a continuously (may be very slow) increasing deformation under constant forces (or stresses) and high temperature. In a number of metals (lead, brass, bronze, aluminium and a few other nonferrous metals and alloys) creep may occur even at room temperature.

The higher the temperature, the faster is the growth of deformation due to creep. Sometimes a gradual, continuously increasing deformation over a sufficiently long period of time at high temperatures may lead to failure of an element, even though the stresses induced in it are less than not only the ultimate strength but also the proportionality limit at room temperature.

For example, the diameter of a steam pipe working at high temperature and pressure increases continuously; finally it may fail due to rupture of its walls (this sometimes actually happens). The creep of discs and blades of steam turbines may result in overlapping of the gap between the blades and the turbine housing, leading to breakage of the blades.

Creep of metals is an irreversible (permanent) deformation, which may be studied as slow yielding. In a number of cases (especially in a compound stressed state) plastic deformation due to creep results not only in a change in stress but also their redistribution over the volume of the element. The change in stress is prominent when there is a restraint to total deformation of the body due to certain specific features of its working. In such cases, the elastic deformation experienced by the body during loading decreases with passage of time; this results in the beginning of plastic deformation, which subsequently continues to grow. It is accompanied by a reduction of stresses in the element. Such a reduction of stresses due to



gradual increase of plastic deformation at the cost of elastic is known as *after-effect*.

Due to after-effect a mild interference fit between two parts may loosen so much as to impede the normal functioning of the structure. For example, the loosening of the flange bolts of a gas pipe or the high pressure cylinder of a steam turbine may ultimately lead to leakage of gas or steam if the bolts are not tightened periodically; the loosening of fit between the turbine disc and the shaft may lead to clearance between the two resulting in the coming off of the disc.

As already stated, creep may occur in some nonferrous metals and their alloys even at room temperature. However, in steel, iron and a number of nonferrous metals and their alloys creep begins only when they are heated above a certain, unique for each metal, temperature (carbon steels and iron above 300-350°C, alloyed steels above 350-400°C, light alloys above 50-150°C, etc.). Creep is not observed in these metals if they are heated below the specified temperatures. Besides, even at temperatures equal to or higher than the specified, creep does not begin as long as the stresses remain less than a particular, specific for each metal, value. After-effect begins at approximately the same values of temperature and stress as creep.

Creep is especially prominent in metals. However, it occurs in a number of other materials also. For example, at room temperature creep can be observed in various plastics (celluloid, bakelite, polyvinyl chloride plastic, etc.), concrete and cement mortar. In reinforced concrete structures, creep, with the passage of time, leads to redistribution of stresses between concrete and reinforcement; the latter gets slightly overloaded whereas the stresses in concrete decrease. However, the creep of concrete and the ensuing redistribution of stresses have almost no effect on the load carrying capacity of the reinforced concrete structure. Creep at room temperature also occurs in timber under compression, and especially under bending.

Experimental study of the phenomenon of creep began quite recently (in 1910). These studies aroused widespread interest in the early twenties, when the first important results were published.

Creep testing presents a number of difficulties even in simple tension. These tests can be conducted only on a special apparatus capable of maintaining a constant load and temperature and measuring the specimen's deformation. The creep tests must be conducted with a high degree of accuracy if reliable results are desired, the duration of the tests should not differ much from the service life of the element, and this involves testing over tens of thousands of hours. All these factors make creep testing a complicated, time-consuming and costly affair. On account of all these difficulties the phenomenon of creep has until now not been studied experimentally sufficiently well even for simple tensile loading.

Testing for creep is still more complicated and cumbersome in com-

pound stressed state. The majority of these tests were conducted on thin-walled pipes subjected to a combination of internal pressure, torsion and tension. However, the number of such tests conducted until now is very small.

Scientists have not been successful in working out short tests on creep. The reason is that the stipulated duration of testing is a necessary and important condition for obtaining reliable results which may be used for creep analysis and design. The results of the accelerated tests can, as yet, serve only for an approximate qualitative estimate of the effect of high temperatures on the behaviour of metals.

### § 194. Creep and After-effect Curves

A. It was mentioned above that experimental study of creep, which forms the basis of design of elements of machines and structures working at high temperatures, is generally carried out on specimens subjected to simple tension. In creep testing the temperature and tensile force acting on the specimen must remain constant over the duration of the test.

The elongation of the specimen is measured at regular intervals of time; from the readings we plot a curve in the coordinate system relative elongation  $\epsilon$  versus time  $t$ , and the curve is known as the *creep curve of the material*. The shape of the curve depends upon the material, stress and temperature at which the test is conducted. A typical creep curve for metals is shown in Fig. 462 (curve OABCD).

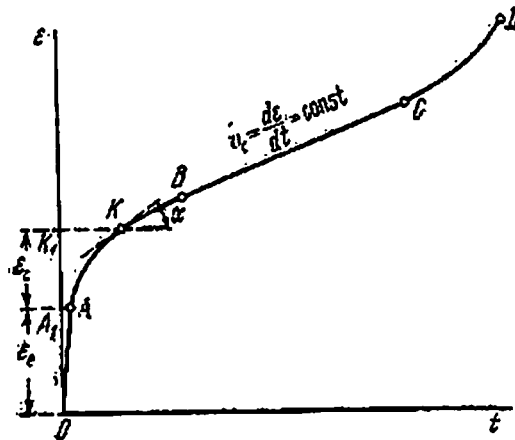


Fig. 462

When the specimen heated to a particular temperature  $T$  is loaded, its deformation increases fast in the beginning (depending upon the speed of loading) from zero to a certain value  $OA_1$  (it is assumed that loading of the specimen is stopped at a stage which corresponds to point  $A$  on the creep curve).

This is followed by gradual increase in deformation of the loaded specimen, and the material begins to creep. The growth of creep deformation is depicted by curve  $ABCD$ ; the ordinates of points on this curve (for example, the ordinate of point  $K$ ) represent the sum of elastic strain  $\varepsilon_e = \overline{OA}_1$  and creep strain  $\varepsilon_c = \overline{A_1K}_1$ :

$$\varepsilon = \varepsilon_e + \varepsilon_c$$

The rate of creep deformation at any point of the curve is determined by the slope which the tangent to the curve at the point makes with the abscissa, i.e.

$$v_c = \frac{de}{dt} = \tan \alpha$$

The whole process of creep may be divided into three successive stages. In the first stage, represented by segment  $AB$  on the creep curve, the deformation takes place with a non-uniform, continuously decreasing speed; this is the zone of *non-uniform*, or *unstable*, creep. Depending upon the material, stress and temperature, the duration of the first stage varies from a few hours to a few hundred and even (in exceptional cases) a few thousand hours.

The nature of creep in the first and second stages is affected mostly by the following two factors: (1) increase of strength of the material due to strain hardening, which occurs as a consequence of increase in residual (permanent) deformation, and (2) removal of strain hardening or decrease of strength due to high temperature. Creep can be studied as an interaction of these two factors, which are chiefly responsible in causing "pure" creep. This picture of creep may be complicated, especially during the subsequent stages, by various internal (for example, microstructure change and phase changes of the metal) and external (for example, corrosion) factors.

When the strengthening effect of strain hardening is balanced by the weakening effect of long exposure to high temperatures, the decrease of creep rate ceases and the second stage (segment  $BC$ ) begins, this is the stage of *uniform*, or *stable*, creep, in which creep occurs with a minimum uniform velocity.

This velocity remains constant until a neck begins to form on the specimen (point  $C$  on the creep curve). If the load on the specimen remains constant, then the local reduction of the cross-sectional area of the specimen in the third stage (segment  $CD$  on the creep curve) is accompanied by an increase of stresses, which in their turn result in a higher creep rate. This leads to ultimate failure of the specimen (point  $D$  on the creep curve).

The shape of the creep curve may change considerably if the temperature or stress is changed. Figure 463 shows creep curves at constant temperature,  $T$ , but different fixed values of stresses  $\sigma_i$  ( $\sigma_1 < \sigma_2 < \sigma_3 < \sigma_4 < \sigma_5$ ). The creep curves at fixed stress  $\sigma$  but different fixed

values of temperature  $T_i$  ( $T_1 < T_2 < T_3 < T_4 < T_5$ ) are identical to the above curves.

At low values of stress ( $\sigma = \sigma_1$ ) creep may be completely absent, i.e. for the loaded specimen the  $\epsilon-t$  diagram may be represented by a straight line passing through point  $A_1$  and parallel to the abscissa. At a somewhat higher value of stress ( $\sigma = \sigma_2$ ) there will be a short

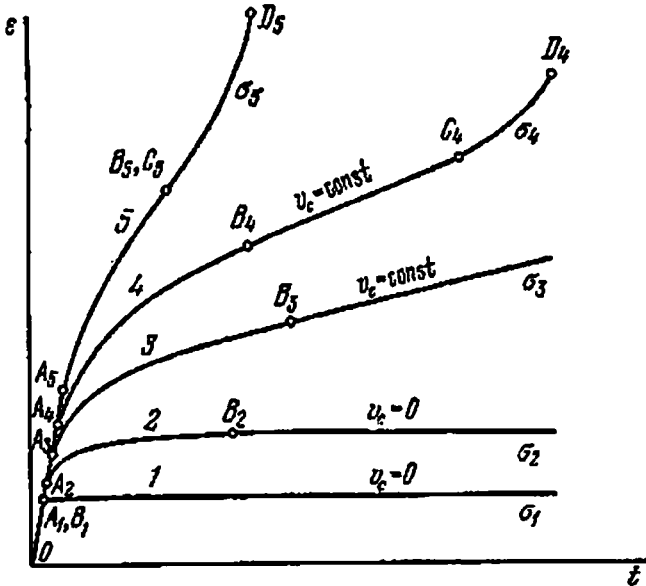


Fig. 463

period of unstable creep, which will stop when the rate of creep becomes zero. At a still higher value of stress ( $\sigma = \sigma_3$ ) the velocity of creep will not be zero but will be so small that failure due to creep will occur after a very long period, which far exceeds the service life of the element.

At stress  $\sigma = \sigma_4$  we get the creep curve shown in Fig. 462. If the stress or temperature is further increased, the creep curves also undergoes a further change: creep progresses at a faster rate, and the straight line portion of the curve—the zone of stable creep—goes on getting shorter till it reduces to a point (curve 5 in Fig. 463), i.e. the zone of unstable creep directly changes into the zone of failure. In this case the zone of stable creep is represented by an inflection point on curve  $ABCD$ , point  $B_s$ , which coincides with point  $C_s$ .

The nature of failure due to creep depends mainly upon the properties of the material at the given temperature. Carbon steels at temperatures less than  $550^\circ\text{C}$ , copper, lead and some other light alloys generally fail after large plastic deformation and neck formation. Special heat resistant steels having good creep strength fail after comparatively small deformation, the failure is brittle in nature and usually begins at the location of stress concentration.

B. As already stated, after-effect is the gradual reduction of stresses in a loaded element whose total deformation is constant and equal to the elastic deformation in the loaded state. The reduction of stresses takes place due to gradual decrease of elastic deformation and an equivalent increase in plastic deformation according to the following formula:

$$\varepsilon = \varepsilon_e + \varepsilon_c = \varepsilon_e^0 = \text{const} \quad (32.1)$$

The after-effect curve is shown in Fig. 464. The process of after-effect may be divided into two stages: in the first stage (segment *AB* on the after-effect curve) the stresses decrease very fast, and this is accompanied by a sharply decreasing after-effect rate; in the second stage (segment *BC* on the curve) the reduction of stresses is considerably slower and is accompanied by slowly decreasing after-effect rate.

Depending upon the material, initial stress and temperature, the duration of the first stage varies from several tens of hours to a few hundred hours. The physical process accompanying after-effect in the first and second stages has not yet been studied in sufficient details. There are still very few good experimental set-ups for studying after-effect, and this makes it difficult to compare the results of experiments on after-effect with those on creep. In majority of the machines which have been used until now for investigating after-effect it has been impossible to achieve pure after-effect.

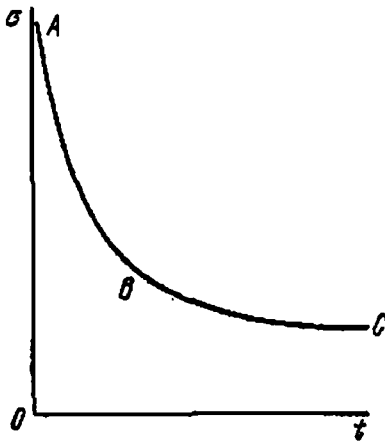


Fig. 464

It is generally assumed that growth of plastic deformation in after-effect is similar to its growth in creep and therefore the rate of after-

effect may be calculated from the creep velocity. If this assumption were true, there would be no need for studying after-effect separately. However, there is another view which holds that creep rate cannot be taken as the rate of after-effect, because these processes are basically different, the mechanism of origin and growth of plastic deformation in after-effect is somewhat different from that in creep.

In after-effect the reduction of stresses in the element is caused by the growth of plastic deformation at the cost of elastic deformation, and the length of the element remains constant. In creep the growth of plastic deformation is exclusively due to elongation of the element. The total deformation in creep is considerably greater than in after-effect; this is an important difference, because the magnitude of



the best results compatible with experimental data:

$$\left. \begin{aligned} (1) v_c &= k\sigma^n \\ (2) v_c &= a \sinh \frac{\sigma}{b} \end{aligned} \right\} \quad (32.3)$$

In these formulae  $k$ ,  $n$ ,  $a$ , and  $b$  are certain constants which depend upon the properties of the material and the testing temperature. The second relation is more compatible with experimental results than the first, but it considerably complicates computations. Besides, the data available on  $k$  and  $n$  of the first relation is much more than the data available on coefficients  $a$  and  $b$  of the second relation. Therefore, the first relation is more commonly used in creep analysis.

#### Coefficients in Formula (32.3)

No.	Type of steel	Chemical composition in %							
		C	Mn	Si	Mo	Cr	Ni	W	Nb
1	Carbon steel	0.15	0.50	0.23					
2	Carbon steel	0.43	0.68	0.20					
3	Molybdenum steel	0.13	0.49	0.25	0.52				
4	Chrome-molybdenum steel	0.11	0.45	0.42	0.50	2.08			
5	Chrome-molybdenum steel	0.48	0.49	0.62	0.52	1.20			
6	Chrome-nickel steel (18-8)	0.06	0.50	0.61		17.75	9.25		
7	Steel-69	0.52		0.82	0.57	13.51	15.2	2.01	
8	Steel Nb	0.19		0.72	0.69	1.71	0.87		0.77

Table 23 contains data on the values of coefficients  $k$  and  $n$  for some steels, tested for creep at various temperatures and stresses.

### § 195. Fundamentals of Creep Design

A. It is obvious that at high temperatures the most suitable operating conditions for a part are those which correspond to the first or second creep curve of Fig. 463 when creep deformation does not appear at all or disappears soon after the part is loaded. However, the corresponding stresses  $\sigma_1$ , equal to the creep limit and stresses  $\sigma_2$ , are usually so small in magnitude that if they were to be accepted as the upper stress limit, this would lead to an unjustified increase in the dimen-

Table 23

Heat treatment	Temperature (°C)	Stress range (kgf/cm <sup>2</sup> )	Values of coefficients in formula (32.3)	
			$n$	$k$ ((cm <sup>2</sup> /kgf) <sup><math>n</math></sup> hr <sup>-<math>n</math></sup> )
Annealing 844°C	427	1410-2110	6.35	$0.17 \times 10^{-20}$
	538	280-560	3.05	$0.12 \times 10^{-13}$
	593	110-250	3.10	$0.26 \times 10^{-12}$
	649	30-90	2.85	$0.16 \times 10^{-10}$
Annealing 844°C	427	1060-1690	6.0	$0.2 \times 10^{-21}$
	538	210-630	3.9	$0.14 \times 10^{-16}$
	649	30-180	1.7	$0.12 \times 10^{-8}$
Annealing 844°C	482	910-1410	5.40	$1.2 \times 10^{-23}$
	538	560-1060	4.60	$0.6 \times 10^{-19}$
	593	210-420	3.55	$0.23 \times 10^{-14}$
	649	60-120	3.10	$0.2 \times 10^{-12}$
Annealing 844°C	482	970-1410	8.35	$0.58 \times 10^{-20}$
	538	460-840	4.95	$0.14 \times 10^{-19}$
	593	280-560	6.90	$0.10 \times 10^{-23}$
	649	140-280	3.25	$0.17 \times 10^{-12}$
Annealing 844°C	427	1410-2110	6.35	$0.145 \times 10^{-26}$
	538	320-1060	3.55	$0.175 \times 10^{-16}$
	649	70-250	2.95	$0.365 \times 10^{-12}$
Hardening 1093°C	538	880-1340	4.4	$0.21 \times 10^{-19}$
	593	560-1060	4.3	$0.17 \times 10^{-19}$
	649	350-840	5.1	$0.14 \times 10^{-19}$
	816	110-280	4.7	$0.21 \times 10^{-16}$
Hardening 1175°C	600	800-2200	3.15	$0.65 \times 10^{-16}$
	650	400-1500	2.9	$0.29 \times 10^{-14}$
Normalization 850°C	500	1500-2500	4.3	$0.41 \times 10^{-20}$
	600	200-500	3.1	$0.59 \times 10^{-14}$



sions of machine parts. Therefore, a small creep deformation is generally permitted in machine parts (third curve in Fig. 463). However, it is necessary that the total strain  $\varepsilon_{\max}$  in the part equal to the sum of strain due to load,  $\varepsilon_l$ , and strain due to creep,  $\varepsilon_c$ , (Fig. 465) should not during the whole service life of the part,  $t_p$ , exceed a given permissible strain  $[\varepsilon]$  which depends upon the function of the part, its operating conditions etc. For instance, the permissible strain  $[\varepsilon]$  for the pipes of steam superheaters is 0.02, for steam pipes it is 0.003, while for steam-turbine cylinders its value is 0.001.

Hence, for uni-axial loading the design equation is:

$$\varepsilon_{\max} = \varepsilon_l + \varepsilon_c \leq [\varepsilon] \quad (32.4)$$

It follows from Fig. 465 that

$$\varepsilon_l + \varepsilon_c \approx \varepsilon_l + \varepsilon_{red} \quad (32.5)$$

where

$$\varepsilon_{red} = t_p \tan \alpha = t_p \nu_c = t_p k \sigma^n \quad (32.6)$$

is the uniform (stable) creep strain during the service life  $t_p$  of the part. Using formulas (32.5) and (32.6), equation (32.4) may be modified as follows:

$$\varepsilon_l + t_p k \sigma^n \leq [\varepsilon] \quad (32.7)$$

wherefrom

$$\sigma \leq \left\{ \frac{[\varepsilon] - \varepsilon_l}{k t_p} \right\}^{1/n} \quad (32.8)$$

Stress

$$\sigma = \left\{ \frac{[\varepsilon] - \varepsilon_l}{k t_p} \right\}^{1/n}$$

is sometimes called the *virtual creep limit for permissible total creep strain* and is denoted by  $\sigma_{ce}$ . Thus, the design equation for permissible creep strain may be written as

$$\sigma \leq \sigma_{ce} = \left\{ \frac{[\varepsilon] - \varepsilon_l}{k t_p} \right\}^{1/n} \quad (32.9)$$

If the elastic and unstable creep strains of the element are negligible as compared to the stable creep strain, then creep analysis may be based on the maximum permissible stable (minimum) creep rate. Obviously, the permissible creep rate should be determined from the condition that creep deformation increasing with this constant rate should not exceed, during the whole service life of the element, a certain permissible value of deformation which does not disrupt the normal functioning of the structure or machine. The corresponding maximum stress, which does not give rise to a creep rate greater than the permissible at the particular temperature, may be considered as the limiting stress. Often this stress is referred

to as the *creep limit of the material from consideration of the minimum permissible or uniform rate of deformation* ( $\sigma_{cv}$ ). Evidently  $\sigma_{cv}$  is a function of temperature and the minimum permissible creep rate.

Table 24

## Creep Velocity

Part	$[v_c]$ per hour
1 Turbine discs with tight fit	$10^{-9}$
2 Bolts, flanges and cylinders of steam turbines	$10^{-8}$
3 Steam pipes, welded joints of boiler pipes	$10^{-7}$
4 Pipes of steam superheaters	$10^{-6}$ - $10^{-5}$

As an example, Table 24 gives the approximate permissible values of the minimum relative creep rate,  $[v_c]$ , for a few parts of steam boilers and turbines.

In creep analysis based on minimum creep rate, the fundamental equation of uni-axial stressed state of the material may be written as follows:

$$v_c = k\sigma^n \leq [v_c] \approx \frac{[\epsilon]}{t_p} \quad (32.10)$$

since

$$\epsilon = v_c t_p$$

From equation (32.10) we get:

$$[\sigma] = \sigma_{cv} = \left\{ \frac{[v_c]}{k} \right\}^{1/n} \quad (32.11)$$

The strength condition in terms of stresses may be written as follows:

$$\sigma \leq [\sigma] = \left\{ \frac{[v_c]}{k} \right\}^{1/n} \quad (32.12)$$

**B.** It is implicit that in creep analysis from considerations of permissible deformation and permissible creep rate it is not enough to ensure that the creep deformation does not exceed a permissible value at a particular temperature during the whole service life of the element. It is also essential to provide a certain safety factor against the occurrence of such a failure. Hence, points  $K_1, K_2$ , and  $K_3$  (Fig. 466) on creep curves 1, 2, and 3 corresponding to abscissas  $t_{p1}, t_{p2}$ , and  $t_{p3}$ , and ordinates  $[\epsilon]_1, [\epsilon]_2$ , and  $[\epsilon]_3$  must lie on the segments corresponding to the first and second stages of creep.

This must always be checked analytically and therefore requires special investigation. As already explained, creep analysis from considerations of permissible deformation and permissible creep rate may be replaced by an analysis based on permissible stresses, the creep limits  $\sigma_{re}$  or  $\sigma_{rv}$ . However, it is essential to check beforehand that  $\sigma_r$  ( $\sigma_{re}$  or  $\sigma_{rv}$ ) does not exceed a permissible value, which is a certain fraction of the ultimate strength at the given temperature.

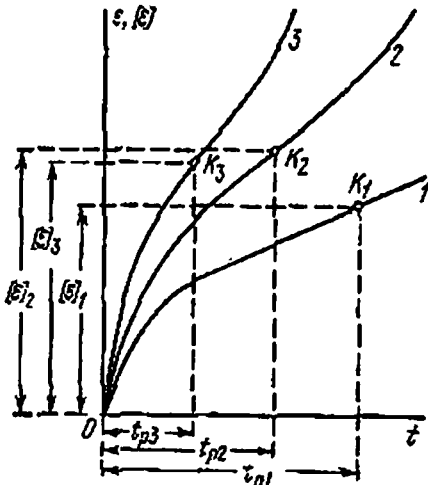


Fig. 466

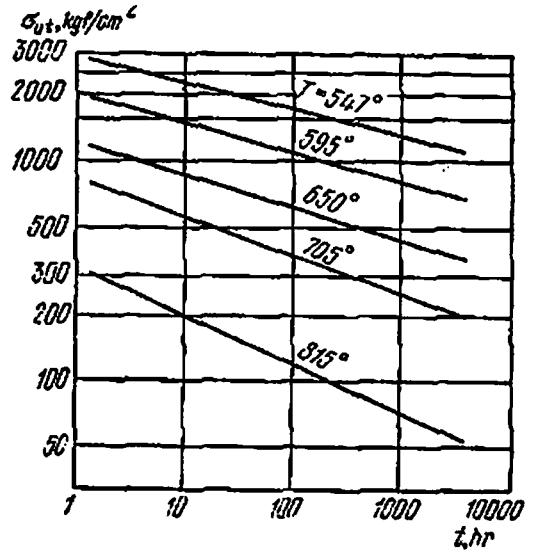


Fig. 467

It is known that at high temperatures the ultimate strength of materials is greatly dependent upon the duration of testing; a comparatively small increase in duration may cause considerable reduction in the ultimate strength. At a certain temperature (above 800°C for mild steels) the specimen may even fail under a load which induces stresses that are less than the limit of proportionality at room temperature, provided the specimen is subjected to this load for a sufficiently long time. Therefore, at present the strength of a material at high temperatures is characterized not by the ultimate strength, determined from short-term tests, but by the *long-term strength* ( $\sigma_{at}$ ). The long-term strength at a particular temperature characterizes the stress which will cause failure only after a specified period. The curves in Fig. 467 show the variation of long-term strength of chrome-molybdenum steel (0.1% C, 1.55% Si, 4.88% Cr, 0.51% Mo) as a function of time at various temperatures.

A few scientists are of the opinion that the non-uniformity of stress distribution at the locations of stress concentration is smoothed during creep and therefore stress concentration need not be taken into account in creep design. It is relevant to point out that machine parts working at high temperatures are, as a rule, manufactured from

special heat-resistant steels, which have poor tendency to creep; generally such parts fail after undergoing small deformation and the failure is brittle in nature. Consequently, in a majority of practical cases smoothening of the stresses does not occur and it is essential to account for stress concentration in creep design.

Therefore, while determining the long-term strength of heat resistant steels, the possibility of stress concentration should be taken into account, i.e. the experiments for determining  $\sigma_{ut}$  should be conducted on specimens of corresponding shape.

If the elements of machines are subjected to the simultaneous action of fatigue and creep, then the long-term strength should be determined from fatigue test at the appropriate temperature. Thus, the following important cases may be distinguished while calculating the strength of elements of machines and structures working under high temperatures.

If the temperature is not high enough to cause creep (§ 193), the critical state is determined by the yield stress or ultimate strength of the material at the given temperature, obtained by the usual tests. The strength condition is:

$$\sigma \leq [\sigma] = \frac{\sigma_a}{k} \quad (32.13)$$

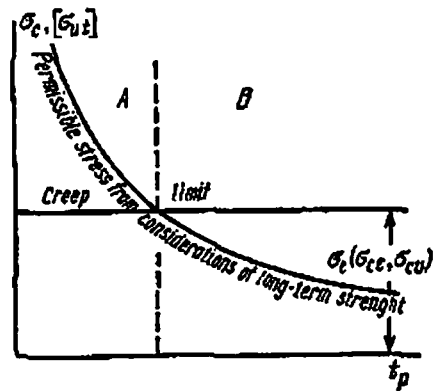


Fig. 468

If creep is possible at the given temperature (see § 193), then the first thing to do is to establish which of the permissible stresses is maximum for the total service life  $t_p$  of the element: the permissible stress from considerations of total creep deformation ( $\sigma_{ce}$ ) or minimum creep rate ( $\sigma_{cv}$ ), or the permissible stress from considerations of long-term strength  $[\sigma_{ut}] = \frac{\sigma_{ut}}{k_t}$ , where  $k_t$  is the long-term safety factor, which may be considered approximately equal to the usual safety factor  $k$  (Fig. 468).

If  $[\sigma] = \sigma_c (\sigma_{ce}, \sigma_{cv}) < [\sigma_{ut}]$ , zone A in Fig. 468, the creep design should be carried out according to formulas (32.4), (32.9), (32.10) or (32.12). If, on the other hand,  $[\sigma] = \sigma_c > [\sigma_{ut}]$ , zone B in Fig. 468, then creep design should be based on the formula

$$\sigma \leq [\sigma_{ut}] = \frac{\sigma_{ut}}{k_t} \quad (32.14)$$

If the elements experience after-effect, then care should be taken that the interference fit between them does not loosen beyond a per-

missible limit; reduced stress  $\sigma_t$  due to after-effect should not be less than a certain minimum value which ensures the required interference between the elements:

$$\sigma_t \geq \sigma_{\min}$$

From this condition we can specify periods after which the joints should be retightened to the required interference by special methods (for instance, by tightening the flange bolts of gas or steam pipes).

In conclusion it should be pointed out that this section dealt mainly with the methods of creep analysis in simple situations (uniaxial stressed state), which can be utilized for building up the analysis of more complex cases. The methods of creep analysis in compound stressed state are the subject of study in special monographs.\*

### § 196. Examples on Creep Design

**Example 1.** Determine the frequency of tightening flange bolts of a steam pipe to prevent leakage of steam, if the initial pull of  $P = 3000$  kgf on each bolt cannot be reduced by more than 40%. The temperature at which the bolts work is  $T = 425^\circ\text{C}$ . The cross-sectional area of each bolt is  $A = 3$  cm<sup>2</sup>; the bolts are made of mild steel having modulus of elasticity  $E_T = 1.77 \times 10^6$  kgf/cm<sup>2</sup> (at  $T = 425^\circ\text{C}$ ); the stable creep rate for the material may be determined from the formula  $v_c = k\sigma^n$ , and at

$$T = 425^\circ\text{C}, \quad k = 2.26 \times 10^{-26} \frac{\text{cm}^2 \cdot \text{hr}}{\text{kgf}^n} \quad \text{and} \quad n = 6$$

Solve the problem on the assumption that the flanges of the steam pipe are absolutely incompressible; the zone of unstable creep may be neglected.

**Solution.** If the flanges of the steam pipe are absolutely incompressible, then the total deformation of the bolt elongated during tightening by  $\Delta l_0$  must remain constant. During creep the elastic deformation of the bolt  $\Delta l_e$  will gradually change into plastic deformation  $\Delta l_p$ ; this will lead to the reduction of stresses in the bolt. The following condition must be satisfied

$$\Delta l_e + \Delta l_p = \Delta l_0 = \text{const}$$

or

$$\epsilon_t + \epsilon_p = \frac{\sigma}{E_T} + \epsilon_p = \epsilon_0 = \frac{\sigma_0}{E_T}$$

where  $\sigma_0$  is the initial tightening stress in the bolt,  $\sigma$  is the stress in the bolt at the instant of failure  $t$ , and  $E_T$  is the elasticity modulus

\* See, for example, I. M. Kachanov, *Theory of Creep*, Fizmatgiz, 1960 (in Russian); N. N. Malinin, *Applied Theory of Plasticity and Creep*, Mashinostroenie, 1975 (in Russian).

of the material at the given temperature  $T$ . Upon differentiating the above equation w.r.t.  $t$ , we obtain

$$\frac{1}{E_T} \frac{d\sigma}{dt} + \frac{d\varepsilon_p}{dt} = \frac{1}{E_T} \frac{d\sigma}{dt} + v_c = \frac{1}{E_T} \frac{d\sigma_0}{dt} = 0$$

Neglecting unstable creep and substituting  $k\sigma^n$  for  $v_c$ , we get the following differential equation:

$$\frac{d\sigma}{dt} + E_T k \sigma^n = 0$$

or

$$\frac{d\sigma}{\sigma^n} = -E_T k dt$$

Upon integrating this equation we obtain

$$\frac{1}{(n-1)\sigma^{n-1}} = E_T k t + C \quad (a)$$

where  $C$  is the constant of integration. Since  $\sigma = \sigma_0$  at  $t=0$ ,

$$C = \frac{1}{(n-1)\sigma_0^{n-1}}$$

Substituting this value of  $C$  in equation (a), we get the following formula correlating  $\sigma$  and  $t$ :

$$\sigma = \frac{\sigma_0}{[1 + (n-1) E_T k \sigma_0^{n-1} t]^{1/(n-1)}}$$

Substituting the numerical values given in this problem, we get

$$\sigma = \frac{\frac{3000}{3}}{\left[1 + (6-1) 1.77 \times 10^4 \times 2.26 \times 10^{-26} \left(\frac{3000}{3}\right)^{6-1} t\right]^{\frac{1}{6-1}}} = \frac{1000}{(1 + 2 \times 10^{-3} t)^{1/5}}$$

$$\text{or } t = \frac{1}{2} \left( 1000 - \frac{10^{18}}{\sigma^5} \right).$$

The values of  $t$  corresponding to different values of  $\sigma$  are given in Table 25, column A. If the stresses in the bolts are not to decrease by more than 40%, then the bolts must be tightened after every 5930 hours or approximately after 8.5 months.

This solution of the after-effect in bolts is approximate. Due to pliability of the steam pipe flanges the stresses in bolts will reduce at a much faster rate. However, if the pliability of the flanges is taken into account, the solution becomes quite complicated. Without considering this aspect in detail we give here the final results (see Table 25,

column B) obtained for the case when the elastic deformation of the flanges is  $\epsilon_{e,f} = 3 \times 10^{-3} P_t$ , and their creep rate is  $v_{c,f} = 5 \times 10^{-22} P_t^4$  (where  $P_t$  kgf is the pull on each bolt at instant  $t$ ).

Table 25

Values of  $t$

$\sigma$ (kgf/cm <sup>2</sup> )	$t$ (hours)		$\sigma$ (kgf/cm <sup>2</sup> )	$t$ (hours)	
	A	B		A	B
1000	0	0	600	5900	5000
900	347	335	500	15500	11900
800	1026	960	400	48300	31700
700	2475	2230			

Hence, if we follow the results of the more accurate solution, re-tightening should be carried out not at an interval of 5930 hours but at an interval of 5000 hours or about every 7 months. This period will be still less if we consider the zone of unstable creep during creep design.

**Example 2.** A round 24-mm diameter shaft working at  $T = 540^\circ\text{C}$ , is twisted by a constant torque  $M_t = 20$  kgf·m. The shaft is made of alloyed steel having shearing modulus  $G = 6 \times 10^6$  kgf/cm<sup>2</sup> (at  $T = 540^\circ\text{C}$ ). The stable creep rate may be calculated from the formula  $v_c = k\tau^n$ , at  $T = 540^\circ\text{C}$   $k = 2.5 \times 10^{-10}$  cm<sup>2n</sup>/(kgf<sup>n</sup>·hr) and  $n = 5$ .

Find the shearing stress distribution in the shaft's cross section and also its angle of twist after 1000 hours of working under load.

**Solution.** Let us assume that the hypothesis of plane sections under torsion remains in force during creep too (this hypothesis agrees sufficiently well with experimental data). Then two cross sections at a distance  $dx$  will remain planes and only turn w.r.t. each other by an angle  $d\varphi$ . Since the radii of the sections do not warp, we may use the usual (§ 47) formula for determining relative shear at a distance from the shaft centre:

$$\gamma_\rho = \rho \frac{d\varphi}{dx}$$

After loading the shearing strain begins to increase on account of creep of the shaft's material, the relative angle of twist  $\frac{d\varphi}{dx}$  also increases accordingly. The total shearing strain may be expressed as the sum of elastic strain  $\gamma_e$  and creep strain  $\gamma_c$ , i.e.  $\gamma = \gamma_e + \gamma_c$ . The rate of growth of the total shearing strain may be written as follows:

$$v = \frac{d\gamma}{dt} = \frac{d\gamma_e}{dt} + \frac{d\gamma_c}{dt} = v_e + v_c = \rho \frac{d^2\varphi}{dx dt}$$

For simplification, the relatively small rate of growth of the elastic deformation may be neglected in comparison with the large rate of growth of creep deformation. The exact solution, with  $v_e \neq 0$ , is much more difficult. Besides, neglecting the zone of unstable creep and assuming that  $v_c = k\tau^n$ , we get

$$v \approx v_c = k\tau^n = \rho \frac{d^2\varphi}{dx dt}$$

wherefrom

$$\tau = \left( \frac{1}{k} \frac{d^2\varphi}{dx dt} \right)^{\frac{1}{n}} \rho^{\frac{1}{n}} = \Phi \rho^{\frac{1}{n}} \quad (a)$$

where

$$\Phi = \left( \frac{1}{k} \frac{d^2\varphi}{dx dt} \right)^{\frac{1}{n}} \quad (b)$$

The condition representing the equality of the moments of external (torque) and internal forces about the shaft axis may be written as follows:

$$M = M_t = \int_A \tau \rho dA = \int_0^r 2\pi\rho\tau\rho d\rho = 2\pi\Phi \int_0^r \rho^{2+\frac{1}{n}} d\rho$$

where  $r$  is the shaft radius. By introducing the notation

$$2\pi \int_0^r \rho^{2+\frac{1}{n}} d\rho = \frac{2\pi n}{3n+1} r^{(3n+1)/n} = J_{pc}$$

we may write

$$\Phi = \frac{M_t}{J_{pc}} \quad (c)$$

and taking into account expression (a)

$$\tau = \frac{M_t}{J_{pc}} \rho^{\frac{1}{n}}$$

We see that the distribution of shearing stresses of creep over the cross section of the shaft is not linear.

Substituting in the expression for  $J_{pc}$  the values  $r=1.2$  cm and  $n=5$ , we obtain:

$$J_{pc} = \frac{2 \times 3.14 \times 5}{3 \times 5 + 1} \times 1.2^{\frac{3 \times 5 + 1}{5}} = 1.964 \times 1.2^{3.2} = 3.52 \text{ cm}^3$$

The shearing stresses at a distance  $\rho$  from the shaft are:

$$\tau = \frac{M_t}{J_{pc}} \rho^{\frac{1}{n}} = \frac{2000}{3.52} \rho^{\frac{1}{5}} = 568 \rho^{\frac{1}{5}}$$



Table 26

Values of  $\tau$ 

$\rho$ (mm)	$\tau_c$ (kgf/cm <sup>2</sup> )	$\tau_c$ (kgf/cm <sup>2</sup> )	$\rho$ (mm)	$\tau_c$ (kgf/cm <sup>2</sup> )	$\tau_c$ (kgf/cm <sup>2</sup> )
12	737	589	4	246	473
10	614	568	2	123	411
8	492	543	0	0	0
6	369	513			

Table 26 contains values of  $\tau$  corresponding to different values of  $\rho$ . The table also contains values of  $\tau$  from consideration of pure torsion of the shaft calculated by the formula

$$\tau = \frac{M_t \rho}{J_p} = \frac{2M_t \rho}{\pi r^4} = \frac{2 \times 2000}{3.14 \times 1.2^4} \rho = 614 \rho$$

Creep helps in equalizing the stresses over the shaft's cross section; the stresses at the surface register a small decrease, whereas the stresses near the axis increase considerably (Fig. 469).

Let us determine the angle of twist per unit length of the shaft. On the basis of (b) and (c) we may write

$$\frac{d^2 \varphi}{dx dt} = k \varphi^n = k \left( \frac{M_t}{J_p c} \right)^n$$

Integrating this expression w.r.t.  $t$ , we get:

$$\frac{d\varphi}{dx} = k \left( \frac{M_t}{J_p c} \right)^n t + C$$

Since  $\frac{d\varphi}{dx} = \left( \frac{d\varphi}{dx} \right)_0 = \frac{M_t}{GJ_p}$  at  $t=0$ , we see that  $C = \frac{M_t}{GJ_p}$  and

$$d\varphi = \left[ \frac{M_t}{GJ_p} + kt \left( \frac{M_t}{J_p c} \right)^n \right] dx$$

Integrating and putting  $x=1$  cm, we obtain

$$\varphi_1 = \frac{M_t}{GJ_p} + kt \left( \frac{M_t}{J_p c} \right)^n$$

Substituting the numerical values of this problem, we get

$$\begin{aligned} \varphi_1 &= \frac{2000 \times 2}{6 \times 10^5 \times 3.14 \times 1.2^4} + 2.5 \times 10^{-10} \left( \frac{2000}{3.52} \right)^6 1000 \\ &= 0.00102 + 0.01480 = 0.0158 \text{ rad/cm} \end{aligned}$$

It can be easily seen that on account of creep the angle of twist increased almost 16-fold as compared to the angle of twist under pure torsion (first term of the above result). Hence, the decrease of maximum shearing stress in the shaft does not mean that its working conditions improve due to creep.

**Example 3.** A 50-cm long simply supported beam 20 mm by 40 mm is acted upon at the middle of its span by a concentrated force  $P=$

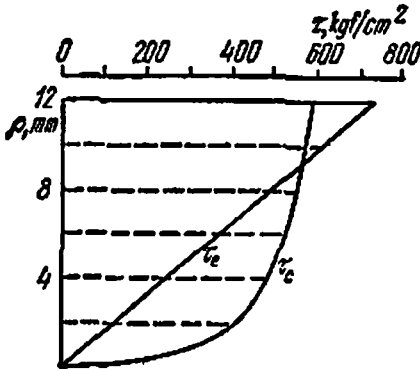


Fig. 469

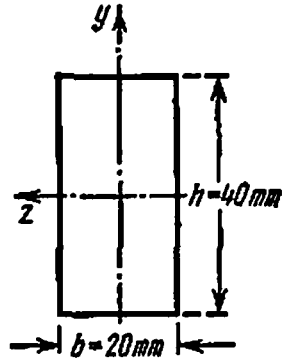


Fig. 470

$=400$  kgf (Fig. 470) works at  $T=500^\circ\text{C}$ . The beam is made of mild steel having modulus of elasticity  $E=1.6 \times 10^6$  kgf/cm<sup>2</sup> (at  $T=500^\circ\text{C}$ ). The stable creep rate is  $v_c=k\sigma^n$ , and at  $T=500^\circ\text{C}$

$$k = 1.5 \times 10^{-15} \left( \frac{\text{cm}^2}{\text{kgf}} \right)^n \text{ hr}^{-1} \quad \text{and} \quad n = 3$$

Neglecting the zone of unstable creep, find the distribution of normal stresses in the critical section and determine the maximum deflection of the beam after 10 000 hours of loading.

*Solution.* While solving this problem we shall neglect the effect of shearing stresses and assume that the hypothesis of plane sections under bending remains valid in creep too (this assumption agrees quite well with the experimental results). Assuming that the deformation of the beam's fibres follows the same law in the stretched and compressed zones, we may express the strain of a fibre at a distance  $y$  by the relation (§ 63)  $\epsilon = \frac{y}{\rho}$ , where  $\rho$  is the radius of curvature of the neutral surface of the beam.

In the loaded state the deformation of the beam fibres increases gradually on account of creep of the beam's material; the radius of curvature of the neutral surface also increases. The total relative deformation of an arbitrary fibre may be represented as the sum of elastic and creep strains, i.e.  $\epsilon = \epsilon_e + \epsilon_c$ . The rate of change of total

creep strain may be written as

$$v = \frac{de}{dt} = \frac{de_e}{dt} + \frac{de_c}{dt} = v_e + v_c = y \frac{d}{dt} \left( \frac{1}{\rho} \right)$$

For simplification we neglected, as in the preceding section, the rate of change of elastic strain. For an accurate solution of the problem (assuming  $v_e \neq 0$ ) consult special monographs (see footnote on page 620).

Neglecting, in addition, unstable creep and assuming  $v_c = k\sigma^n$ , we obtain

$$v \approx v_c = k\sigma^n = y \frac{d}{dt} \left( \frac{1}{\rho} \right)$$

wherefrom

$$\sigma = \left[ \frac{1}{k} \frac{d}{dt} \left( \frac{1}{\rho} \right) \right]^{1/n} y^{1/n} = \Phi y^{1/n} \quad (a)$$

where

$$\Phi = \left[ \frac{1}{k} \frac{d}{dt} \left( \frac{1}{\rho} \right) \right]^{1/n} \quad (b)$$

The condition expressing the equality of moments of the external and internal forces about the neutral axis may be written as follows:

$$M = \int_A \sigma y dA = 2\Phi \int_{A_{1/2}} y^{1+\frac{1}{n}} dA$$

Introducing the notation

$$2 \int_{A_{1/2}} y^{1+\frac{1}{n}} dA = J_{xc}$$

we get

$$\Phi = \frac{M}{J_{xc}}$$

and, if we recall (a),

$$\sigma = \frac{M}{J_{xc}} y^{\frac{1}{n}}$$

It should be noted that in creep the distribution of normal stresses over the height of the section is not linear.

If the beam has a rectangular section,

$$J_{xc} = 2 \int_{A_{1/2}} y^{1+\frac{1}{n}} dA = 2 \int_0^{\frac{h}{2}} y^{1+\frac{1}{n}} b dy = \frac{1}{\frac{n+1}{n}} \frac{n}{2n+1} bh \frac{2n+1}{n}$$

Substituting the numerical values of the problem in the expression for  $J_{zc}$ , we get

$$J_{zc} = \frac{3}{2^{\frac{3+1}{3}} (2 \times 3 + 1)} 2 \times 4^{\frac{2 \times 3 + 1}{3}} = \frac{3 \times 2 \times 4^{\frac{7}{3}}}{7 \times 2^{\frac{4}{3}}} = 8.64 \text{ cm}^{\frac{10}{3}}$$

The maximum bending moment is:

$$M_{\max} = \frac{Pl}{4} = \frac{400 \times 50}{4} = 5000 \text{ kgf} \cdot \text{cm}$$

The normal stresses in the rectangular beam may be calculated from the formula

$$\sigma = \frac{M}{J_{zc}} y^{\frac{1}{n}} = \frac{5000}{8.64} y^{\frac{1}{3}} = 579 y^{\frac{1}{3}}$$

The normal stresses computed from this formula for various values of  $y$  are given in Table 27. For comparison, the values of normal stresses under elastic deformation are given in the same table.

Table 27

$y$ (mm)	$\sigma$ (kgf/cm <sup>2</sup> )		$y$ (mm)	$\sigma$ (kgf/cm <sup>2</sup> )	
	Elastic deformation	Creep		Elastic deformation	Creep
20	938	729	4	188	426
16	750	677	2	94	339
12	563	615	0	0	0
8	375	537			

Due to creep the stresses over the beam's cross section level out. The stresses decrease in the fibres farthest from the neutral layer, whereas the stresses near the neutral layer increase (Fig. 471). The decrease in maximum stress is more pronounced in the rectangular beam as compared to the I-beam, because the latter is comparatively thinner near the neutral layer.

Let us determine the beam's deflection. Expressing the curvature of the beam by the approximate relation  $\frac{1}{\rho} = \frac{d^2y}{dx^2}$ , we may write  $\frac{d}{dt} \left( \frac{1}{\rho} \right) = \frac{d^3}{dx^2} \left( \frac{dy}{dt} \right)$ . Since from (b) and (c)

$$\frac{d}{dt} \left( \frac{1}{\rho} \right) = k D^n = k \frac{M^n}{J_{zc}^n}$$

we have

$$\frac{d^2}{dx^2} \left( \frac{dy}{dt} \right) = k \frac{M^n}{J_{zc}^n}$$

In the case of a simply supported beam (Fig. 472),  $M = (P/2)x$  and

$$\frac{d^2}{dx^2} \left( \frac{dy}{dt} \right) = k \frac{P^n x^n}{J_{zc}^n 2^n} = R x^n \tag{d}$$

where

$$R = \frac{k P^n}{2^n J_{zc}^n}$$

Integrating equation (d) w.r.t.  $x$ , we obtain

$$\frac{d}{dx} \left( \frac{dy}{dt} \right) = \frac{R}{n+1} x^{n+1} + C$$

or

$$\frac{dy}{dt} = \frac{R}{(n+1)(n+2)} x^{n+2} + Cx + D$$

where  $C$  and  $D$  are constants of integration. Since  $y=0$  for all values

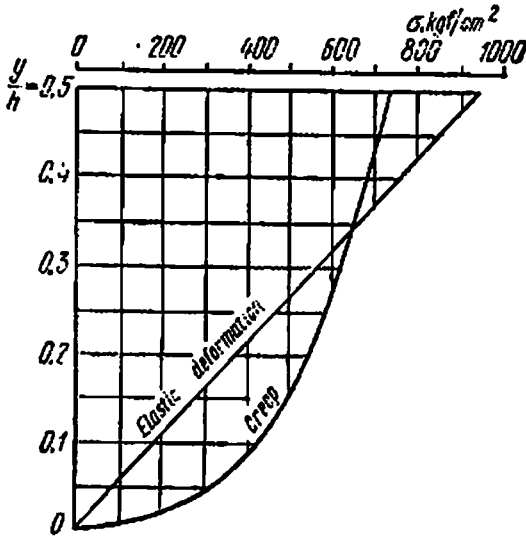


Fig. 471

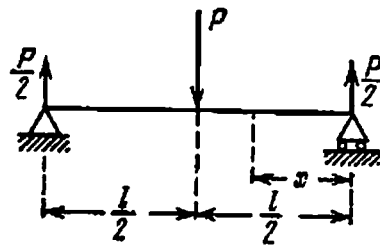


Fig. 472

of  $t$  when  $x=0$ , and  $\frac{dy}{dx} = 0$  when  $x = \frac{l}{2}$ , obviously  $\frac{dy}{dt} = 0$  at  $x=0$  and  $\frac{d}{dt} \left( \frac{dy}{dx} \right) = \frac{d}{dx} \left( \frac{dy}{dt} \right) = 0$  for  $x = \frac{l}{2}$ . Therefore

$$C = -\frac{R l^{n+1}}{(n+1) 2^{n+1}} \quad \text{and} \quad D = 0$$

The maximum deflection occurs in the section where  $x=l/2$ ; we get

$$\left(\frac{dy}{dt}\right)_{\max} = -\frac{Rl^{n+2}}{2^{n+2}(n+2)} = -\frac{kPn!n+2}{(n+2)2^{2(n+1)}J_z^n}$$

Integrating w.r.t.  $t$ , we obtain

$$y_{\max} = -\frac{kPn!n+2}{(n+2)2^{2(n+1)}J_z^n} t + H$$

where  $H$  is the constant of integration. Since at  $t=0$

$$y_{\max} = (y_{\max})_e = -\frac{Pl^n}{48EJ_z}$$

we have

$$H = (y_{\max})_e = -\frac{Pl^n}{48EJ_z}$$

The maximum deflection due to creep may therefore be written as

$$y_{\max} = -\frac{Pl^n}{48EJ_z} - \frac{kPn!n+2}{(n+2)2^{2(n+1)}J_z^n} t$$

$$J_z = \frac{bh^3}{12} = \frac{2 \times 4^3}{12} = 10.67 \text{ cm}^4$$

and

$$\begin{aligned} |y_{\max}| &= \frac{400 \times 50^3}{48 \times 1.6 \times 10^6 \times 10.67} + \frac{1.5 \times 10^{-16} \times 400^3 \times 50^{3+2}}{8.64^3 (3+2) \times 2^{2(3+1)}} 10\,000 \\ &= 0.0611 + 0.3634 = 0.425 \text{ cm} \end{aligned}$$

Under creep, the maximum load on the beam should be determined from consideration of permissible deformation. If, for instance, the maximum deflection of the rectangular beam should not exceed 1/500 of its length (0.1 cm) after 10 000 hours of operation, then the maximum permissible load may be calculated from the condition

$$\frac{Pl^n}{48EJ_z} + \frac{kPn!n+2}{(n+2)2^{2(n+1)}J_z^n} t \leq [f]$$

Substituting the numerical values, we get

$$\frac{50^3 P}{48 \times 10.67 \times 1.6 \times 10^6} + \frac{1.5 \times 10^{-16} \times 50^5}{5 \times 8.64^3 \times 2^8} 10\,000 P^3 \leq 0.1$$

or

$$P + 0.2326 P^3 \times 10^{-5} \leq 40.96$$

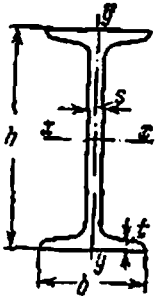
wherefrom

$$P \leq 40.8 \text{ kgf} \approx 40 \text{ kgf}$$

# Appendix

## Rolled Steel Profiles

(GOST 8239-72, 8240-72, 8509-72)



I-section

Profile No.	$h$	$b$	$s$	$t$	Area of section (cm <sup>2</sup> )	Mass of 1 m (kg)
	(mm)					
10	100	55	4.5	7.2	12.0	9.46
12	120	64	4.8	7.3	14.7	11.50
14	140	73	4.9	7.5	17.4	13.70
16	160	81	5.0	7.8	20.2	15.90
18	180	90	5.1	8.1	23.4	18.40
18a	180	100	5.1	8.3	25.4	19.90
20	200	100	5.2	8.4	26.8	21.00
20a	200	110	5.2	8.6	28.9	22.70
22	220	110	5.4	8.7	30.6	24.00
22a	220	120	5.4	8.9	32.8	25.80
24	240	115	5.6	9.5	34.8	27.30
24a	240	125	5.6	9.8	37.5	29.40
27	270	125	6.0	9.8	40.2	31.50
27a	270	135	6.0	10.2	43.2	33.90
30	300	135	6.5	10.2	46.5	36.50
30a	300	145	6.5	10.7	49.9	39.20
33	330	140	7.0	11.2	53.8	42.20
36	360	145	7.5	12.3	61.9	48.60
40	400	155	8.3	13.0	72.6	57.00
45	450	160	9.0	14.2	84.7	66.50
50	500	170	10.0	15.2	100.0	78.50
55	550	180	11.0	16.5	118.0	92.60
60	600	190	12.0	17.8	138.0	108.00

## Appendix

Table I

Tabulated values about axes						
<i>x-x</i>				<i>y-y</i>		
$J_x$ (cm <sup>4</sup> )	$W_x$ (cm <sup>3</sup> )	$t_x$ (cm)	$S_x$ (cm <sup>3</sup> )	$J_y$ (cm <sup>4</sup> )	$W_y$ (cm <sup>3</sup> )	$t_y$ (cm)
198	39.7	4.06	23.0	17.9	6.49	1.22 <sup>a</sup>
350	58.4	4.88	33.7	27.9	8.72	1.38
572	81.7	5.73	46.8	41.9	11.50	1.55
873	109.0	6.57	62.3	58.6	14.50	1.70
1290	143.0	7.42	81.4	82.6	18.40	1.88
1430	159.0	7.51	89.8	114.0	22.80	2.12
1840	184.0	8.28	104.0	115.0	23.10	2.07
2030	203.0	8.37	114.0	155.0	28.20	2.32
2550	232.0	9.13	131.0	157.0	28.60	2.27
2790	254.0	9.22	143.0	206.0	34.30	2.50
3460	289.0	9.97	163.0	198.0	34.50	2.37
3800	317.0	10.10	178.0	260.0	41.60	2.63
5010	371.0	11.20	210.0	260.0	41.50	2.54
5500	407.0	11.30	229.0	337.0	50.00	2.80
7080	472.0	12.30	268.0	337.0	49.90	2.69
7780	518.0	12.50	292.0	436.0	60.10	2.95
9840	597.0	13.50	339.0	419.0	59.90	2.79
13380	743.0	14.70	423.0	516.0	71.10	2.89
19062	953.0	16.20	545.0	667.0	86.10	3.03
27696	1231.0	18.10	708.0	808.0	101.00	3.09
39727	1589.0	19.90	919.0	1043.0	123.00	3.23
55962	2035.0	21.80	1181.0	1356.0	151.00	3.39
76806	2560.0	23.60	1491.0	1725.0	182.00	3.54





Channel Section with Sloping Flanges

Profile No.	$h$	$b$	$s$	$l$	Area of section (cm <sup>2</sup> )	Mass of 1 m (kg)
	(mm)					
5	50	32	4.4	7.0	6.16	4.84
6.5	65	36	4.4	7.2	7.51	5.90
8	80	40	4.5	7.4	8.98	7.05
10	100	46	4.5	7.6	10.90	8.59
12	120	52	4.8	7.8	13.30	10.40
14	140	58	4.9	8.1	15.60	12.30
14a	140	62	4.9	8.7	17.00	13.30
16	160	64	5.0	8.4	18.10	14.20
16a	160	68	5.0	9.0	19.50	15.30
18	180	70	5.1	8.7	20.70	16.30
18a	180	74	5.1	9.3	22.20	17.40
20	200	76	5.2	9.0	23.40	18.40
20a	200	80	5.2	9.7	25.20	19.80
22	220	82	5.4	9.5	26.70	21.00
22a	220	87	5.4	10.2	28.80	22.60
24	240	90	5.6	10.0	30.60	24.00
24a	240	95	5.6	10.7	32.90	25.80
27	270	95	6.0	10.5	35.20	27.70
30	300	100	6.5	11.0	40.50	31.80
33	330	105	7.0	11.7	46.50	36.50
36	360	110	7.5	12.6	53.40	41.90
40	400	115	8.0	13.5	61.50	48.30

Table 11

Tabulated values about axes							
<i>x-x</i>				<i>y-y</i>			<i>z<sub>0</sub></i> (cm)
$J_x$ (cm <sup>4</sup> )	$W_x$ (cm <sup>3</sup> )	$l_x$ (cm)	$S_x$ (cm <sup>3</sup> )	$J_y$ (cm <sup>4</sup> )	$W_y$ (cm <sup>3</sup> )	$l_y$ (cm)	
22.8	9.1	1.92	5.59	5.61	2.75	0.954	1.16
48.6	15.0	2.54	9.00	8.70	3.68	1.080	1.24
89.4	22.4	3.16	13.30	12.80	4.75	1.190	1.31
174.0	34.8	3.99	20.40	20.40	6.46	1.370	1.44
304.0	50.6	4.78	29.60	31.20	8.52	1.530	1.54
491.0	70.2	5.60	40.80	45.40	11.00	1.700	1.67
545.0	77.8	5.66	45.10	57.50	13.30	1.840	1.87
747.0	93.4	6.42	54.10	63.30	13.80	1.870	1.80
823.0	103.0	6.49	59.40	78.80	16.40	2.010	2.00
1090.0	121.0	7.24	69.80	86.00	17.00	2.040	1.94
1190.0	132.0	7.32	76.10	105.00	20.00	2.180	2.13
1520.0	152.0	8.07	87.80	113.00	20.50	2.200	2.07
1670.0	167.0	8.15	95.90	139.00	24.20	2.350	2.28
2110.0	192.0	8.89	110.00	151.00	25.10	2.370	2.21
2330.0	212.0	8.99	121.00	187.00	30.00	2.550	2.46
2900.0	242.0	9.73	139.00	208.00	31.60	2.600	2.42
3180.0	265.0	9.84	151.00	254.00	37.20	2.780	2.67
4160.0	308.0	10.90	178.00	262.00	37.30	2.730	2.47
5810.0	387.0	12.00	224.00	327.00	43.60	2.840	2.52
7980.0	484.0	13.10	281.00	410.00	51.80	2.970	2.59
10820.0	601.6	14.20	350.00	513.00	61.70	3.100	2.68
15220.0	761.0	15.70	444.00	642.00	73.40	3.230	2.75



Table III (Cont.)

Cylinder no.	$b$ (mm)	$d$ (mm)	Tabulated values about axes										Mass of 1 m (kg)
			Area of section (cm <sup>2</sup> )	$x-x$		$x_0-x_0$		$y_0-y_0$		$x_1-x_1$		$z_0$ (cm)	
			$J_x$ (cm <sup>4</sup> )	$i_x$ (cm)	$J_{x_0 \max}$ (cm <sup>4</sup> )	$i_{x_0 \max}$ (cm)	$J_{y_0 \min}$ (cm <sup>4</sup> )	$i_{y_0 \min}$ (cm)	$J_{y_0 \max}$ (cm <sup>4</sup> )	$i_{y_0 \max}$ (cm)	$J_{x_1}$ (cm <sup>4</sup> )		
4	40	3	2.35	3.55	1.23	5.63	1.55	1.47	0.79	6.35	1.09	1.85	
		4	3.08	4.58	1.22	7.26	1.53	1.90	0.78	8.53	1.13	2.42	
		5	3.79	5.53	1.20	8.75	1.54	2.30	0.79	10.73	1.17	2.97	
4.5	45	3	2.65	5.13	1.39	8.13	1.75	2.12	0.89	9.04	1.21	2.08	
		4	3.48	6.63	1.38	10.50	1.74	2.74	0.89	12.10	1.26	2.73	
		5	4.29	8.03	1.37	12.70	1.72	3.33	0.88	15.30	1.30	3.37	
5	50	3	2.96	7.11	1.55	11.30	1.95	2.95	1.00	12.40	1.33	2.32	
		4	3.89	9.21	1.54	14.60	1.94	3.80	0.99	16.60	1.38	3.05	
		5	4.80	11.20	1.53	17.80	1.92	4.63	0.98	20.90	1.42	3.77	
5.6	56	4	4.38	13.10	1.73	20.80	2.18	5.41	1.11	23.30	1.52	3.44	
		5	5.41	16.00	1.72	25.40	2.16	6.59	1.10	29.20	1.57	4.25	
6.3	63	4	4.96	18.90	1.95	29.90	2.45	7.81	1.25	33.10	1.69	3.90	
		5	6.13	23.10	1.94	36.60	2.44	9.52	1.25	41.50	1.74	4.81	
		6	7.28	27.10	1.93	42.90	2.43	11.20	1.24	50.00	1.78	5.72	
7	70	4.5	6.20	29.0	2.16	46.0	2.72	12.0	1.39	51.0	1.88	4.87	
		5	6.86	31.9	2.16	50.7	2.72	13.2	1.39	56.7	1.90	5.38	
		6	8.15	37.6	2.15	59.6	2.71	15.5	1.38	68.4	1.94	6.39	
		7	9.42	43.0	2.14	68.2	2.69	17.8	1.37	80.1	1.99	7.39	
		8	10.70	48.2	2.13	76.4	2.68	20.0	1.37	91.9	2.02	8.37	

Table III (Cont.)

Profile num	b	d	Area of section (cm <sup>2</sup> )	Tabulated values about axes										z <sub>0</sub> (cm)	Mass of t m (kg)
				x-x		x <sub>0</sub> -x <sub>0</sub>		y <sub>0</sub> -y <sub>0</sub>		x <sub>1</sub> -x <sub>1</sub>					
	(mm)			J <sub>x</sub> (cm <sup>4</sup> )	i <sub>x</sub> (cm)	J <sub>x</sub> max (cm <sup>4</sup> )	i <sub>x</sub> max (cm)	J <sub>x</sub> min (cm <sup>4</sup> )	i <sub>x</sub> min (cm)	J <sub>y</sub> min (cm <sup>4</sup> )	i <sub>y</sub> min (cm)	J <sub>x<sub>1</sub></sub> (cm <sup>4</sup> )			
7.5	75	5	7.39	39.5	2.31	62.6	2.91	16.4	1.49	69.6	1.49	69.6	2.02	5.80	
		6	8.78	46.6	2.30	73.9	2.90	19.3	1.48	83.9	1.48	83.9	2.06	6.89	
		7	10.10	53.3	2.29	84.6	2.89	22.1	1.48	98.3	1.48	98.3	2.10	7.96	
		8	11.50	59.8	2.28	94.9	2.87	24.8	1.47	113.0	1.47	113.0	2.15	9.02	
		9	12.80	66.1	2.27	105.0	2.86	27.5	1.46	127.0	1.46	127.0	2.18	10.10	
8	80	5.5	8.63	52.7	2.47	83.6	3.11	21.8	1.59	93.2	1.59	93.2	2.17	6.78	
		6	9.38	57.0	2.47	94.0	3.11	23.5	1.58	102.0	1.58	102.0	2.19	7.36	
		7	10.80	65.3	2.45	104.0	3.09	27.0	1.58	119.0	1.58	119.0	2.23	8.51	
		8	12.30	73.4	2.44	116.0	3.08	30.3	1.57	137.0	1.57	137.0	2.27	9.65	
9	90	6	10.60	82.1	2.78	130.0	3.50	34.0	1.79	145.0	1.79	145.0	2.43	8.33	
		7	12.30	94.3	2.77	150.0	3.49	38.9	1.78	169.0	1.78	169.0	2.47	9.64	
		8	13.90	106.0	2.76	168.0	3.48	43.8	1.77	194.0	1.77	194.0	2.51	10.90	
		9	15.60	118.0	2.75	186.0	3.46	48.6	1.77	219.0	1.77	219.0	2.55	12.20	
10	100	6.5	12.80	122.0	3.09	193.0	3.88	50.7	1.99	214.0	1.99	214.0	2.68	10.10	
		7	13.80	131.0	3.08	207.0	3.88	54.2	1.98	231.0	1.98	231.0	2.71	10.80	
		8	15.60	147.0	3.07	233.0	3.87	60.9	1.98	265.0	1.98	265.0	2.75	12.20	
		10	19.20	179.0	3.05	284.0	3.84	74.1	1.96	333.0	1.96	333.0	2.83	15.10	
		12	22.80	209.0	3.03	331.0	3.81	86.9	1.95	402.0	1.95	402.0	2.91	17.90	
		14	26.30	237.0	3.00	375.0	3.78	99.3	1.94	472.0	1.94	472.0	2.99	20.60	
	16	29.70	264.0	2.98	416.0	3.74	112.0	1.94	542.0	1.94	542.0	3.06	23.30		

Table III (Cont.)

Profile num	b	d	Area of section (cm <sup>2</sup> )	Tabulated values about axes										z <sub>0</sub> (cm)	Mass of J m (kg)
				x-x		x <sub>0</sub> -x <sub>0</sub>		y <sub>0</sub> -y <sub>0</sub>		x <sub>1</sub> -x <sub>1</sub>					
	(mm)			J x <sup>2</sup> (cm <sup>4</sup> )	l <sub>x</sub> (cm)	J x <sub>0</sub> max (cm <sup>4</sup> )	l <sub>x0</sub> max (cm)	J y <sub>0</sub> min (cm <sup>4</sup> )	l <sub>y0</sub> min (cm)	J x <sub>1</sub> (cm <sup>4</sup> )					
11	110	7	15.20	176.0	3.40	279.0	4.29	72.7	2.19	308.0		2.96	11.90		
		8	17.20	198.0	3.39	315.0	4.28	81.8	2.18	353.0		3.00	13.50		
12.5	125	8	19.7	294	3.87	467	4.87	122	2.49	516		3.36	15.5		
		9	22.0	327	3.86	520	4.86	135	2.48	582		3.40	17.3		
		10	24.3	360	3.85	571	4.84	149	2.47	649		3.45	19.1		
		12	28.9	422	3.82	670	4.82	174	2.46	782		3.53	22.7		
		14	33.4	482	3.80	764	4.78	200	2.45	916		3.61	26.2		
		16	37.8	539	3.78	853	4.76	224	2.44	1051		3.68	29.6		
14	140	9	24.7	466	4.34	739	5.47	192	2.79	818		3.78	19.4		
		10	27.3	512	4.33	814	5.46	211	2.78	911		3.82	21.5		
		12	32.5	602	4.31	957	5.43	248	2.76	1097		3.90	25.5		
16	160	10	31.4	774	4.96	1229	6.25	319	3.19	1356		4.30	24.7		
		11	34.4	844	4.95	1341	6.24	348	3.18	1494		4.35	27.0		
		12	37.4	913	4.94	1450	6.23	376	3.17	1633		4.39	29.4		
		14	43.3	1046	4.92	1662	6.20	431	3.16	1911		4.47	34.0		
		16	49.1	1175	4.89	1866	6.17	485	3.14	2191		4.55	38.5		
		18	54.8	1299	4.87	2061	6.13	537	3.13	2472		4.63	43.0		
		20	60.4	1419	4.85	2248	6.10	589	3.12	2756		4.70	47.4		



# Name Index

Belelyubskij, N. A. 283  
Beltrami, F. 145  
Belyaev, N. M. 5, 6, 7, 8, 26, 106, 148,  
188, 207, 290, 479, 499, 520,  
562, 565, 576  
Benardos, N. N. 158  
Bolotin, V. V. 520  
Bubnov, I. G. 353

Castigliano, A. 340  
Clapeyron, B. P. E. 335  
Clebsch, R. F. A. 304  
Coulomb, Ch. A. 140

Davidenkov, N. N. 148  
Druzhinin, S. I. 144

Engesser, F. 490  
Euler, L. 480

Fridman, Ya. B. 148  
Forrest, P. G. 597

Gadolin, A. V. 440, 446  
Galileo Galilei 18  
Goldenblat, I. I. 520  
Golovin, Kh. S. 440  
Guest, J. J. 140

Hencky, H. 145  
Huber, F. 145

Ivanova, V. S. 597

Kachanov, L. M. 136, 620  
Kachurin, V. K. 7  
Korman, Th. 490  
Kipnis, Ya. I. 8, 160  
Krylov, A. N. 305  
Kurkin, S. A. 163  
Kushelev, N. Yu. 8

Lamé, G. 138, 446  
Loitsyanskii, L. G. 538  
Lurye, A. I. 536

Malinin, N. N. 620  
Mariotte, Ed. 138  
Maxwell, J. C. 349  
Mises, R. 145  
Mohr, O. 349  
Müller-Breslau, H. F. B. 349

Navier, C. M. L. 138  
Navrotskii, D. I. 160  
Nikolaev, G. A. 163

Oding, I. A. 597  
Ovechkin, G. 163

Pavlov, A. P. 163  
Pirlet, 349  
Poncelet, J. V. 138  
Prigorovskii, N. I. 588  
Puzyrevskii, N. P. 305

Rankine, W. J. M. 138

Saint-Venant, B. 139, 189  
Serensen, S. V. 588, 597



Shtaerman, I. Ya. 96  
Sinitskii, A. K. 8  
Slavyanov, N. G. 158  
Smirnov-Alyayev, G. A. 584

Telelbaum, I. M. 588  
Timoshenko, S. P. 5, 188, 508  
Tresca, H. 140

Uzbek, G. V. 597

Vereslichagin, A. N. 349  
Vinokurov, V. A. 163  
Vlasov, V. Z. 188  
Vol'mir, A. S. 520

Yagn, Yu. I. 144  
Yasinskii, F. 490

Zhuravskii, D. I. 270

# Subject Index

- absolute displacement 129
- absolute elongation 33
- active force 312
- after-effect 608
- alternating cycle 573
- amorphous material 21
- amplification factor of vibrations 539
- amplitude of vibrations 535
- angle, twisting 169
- angle of shear 129
- anisotropic material 37, 56
- axes of inertia, principal 251
- axial compression 27
- axial force 29
- axial moment of inertia 233
- axial tension 27
- axis, neutral 227
  
- bar(s), compressibility of 559
  - curved 423
  - with large curvature 439
  - prismatic 27
  - rigidity of 34
  - with small curvature 439
- beam, cantilever 213
  - continuous 366
  - critical section of 200
  - deflection of 292
  - equation of deflected axis of 293
  - fictitious 314
  - riveted 289
  - simply supported 207
  - statically determinate 199
  - statically indeterminate 199, 356
  - of uniform rigidity 329
  - of uniform strength 324, 558
  - welded 290
- beam section, angle of rotation of 293
- beam supports, reaction of 197
  
- bending, pure 225
  - uni-planar 256
  - unsymmetric 379
- bending moment 203, 348
  - diagram of 204
- biaxial stress 102
- breaking away, failure by 101
- breaking load 457
- brittle failure, theory of 138
- brittle material 41, 52
- bulk modulus 123
- butt joint 159
  
  
- cable, flexible 92
- cantilever beam 213
- capacity, lifting 471
- Castigliano's theorem 340
- centre, flexural 387
- characteristic cycle 574
- circle, Mohr's 110
  - moment of inertia of 240
- Clapeyron's theorem 335
- coefficient, damping 539
  - dynamic 524
  - of dynamic response 60
  - of length 485
  - of operating conditions 475
  - of overloading 476
  - for production process 593
  - of reliability 475
  - of stress concentration 576
- comparison of displacements 361
- complementary shearing stresses 109
- complex figure, moment of inertia of 245
- component constant of cycle 574
- component variable of cycle 574
- composite stressed state 101
- compound loading 378

- compressibility of bars 559  
 compression, axial 27  
     eccentric 392  
 compressive stress 101  
 concentrated force 19  
 condition, of joint deformation 67, 80,  
     360  
     of strength 30  
 conditional stress 41  
 conical spring 186  
 connecting rod 525  
 conservation of energy 331  
 constancy of volume 50  
 constant sign cycle 573  
 constant stress cycle 573  
 constraint, redundant 357  
 contact stress 105  
 continuous beam 366  
 continuous load, intensity of 206  
 core of section 396  
 crack, fatigue 572  
 creep 607  
     stable 610  
     unstable 610  
 creep curve 609  
 creep limit 617  
 critical force 478  
 critical section 86  
 critical state, of material 63  
 critical stress 479  
 crushing of rivets 154  
 crystalline lattice 21  
 crystalline material 21  
 curved bar 423  
 cycle, alternating 573  
     characteristic 574  
     component constant of 574  
     constant sign 573  
     constant stress 573  
     fluctuating 573  
     mean stress of 574  
     of stress variation 573  
     zero base 573  
 cyclic stress 573  
 damage susceptibility curve 593  
 damping coefficient 539  
 dead weight 86  
 deflection of beam 292  
 deformation 21  
     elastic 21, 37  
     lateral 36  
     local 488  
     plastic 21, 47  
     total energy of 126  
 design load 476  
 design moment 406  
 diagram, of bending moment 204  
     of reduced moment 472  
     of shearing forces 204  
     stress-strain 47  
 differentiation, successive 313  
 displacement, absolute 129  
     generalized 333  
 distortion, potential energy of, theory  
     146  
 distributed force 19  
 distribution, uniform 29  
 double-shear rivet 153  
 ductile failure, theory of 140  
 ductile hinge 466  
 ductile material 41  
 dynamic coefficient 524  
 dynamic load 20  
 dynamic loading 521  
 dynamic response, coefficient of 60  
 dynamic stress 555  
  
 eccentric compression 392  
 eccentricity 392  
 eccentric tension 392  
 elastic deformation 21, 37  
     specific, work of 46  
 elasticity, limit of 23, 43  
     modulus of 34  
 elementary force 23  
 elongation, absolute 33  
     relative 33  
     relative residual 44  
 endurance limit 61, 62, 575  
 energy of deformation, total 126

- energy theory of strength 145  
 envelope 142  
 equal moments, method of 471  
 equation, of deflected axis 293  
     of method of initial parameters 305  
     of three moments 372  
 equatorial moment 233  
 Euler's formula 482  
 external force 19  
     method of 344
- factor of safety 24, 30  
     main 63, 64  
 factor of stress concentration 583  
 failure, by breaking away 101  
     due to shearing 101, 133  
     through rupture 132  
 fatigue 60, 572  
 fatigue crack 572, 594  
 fatigue limit 61  
 fictitious beam 314  
 fillet weld, joint with 162  
 fixed hinged support 197  
 fixed support 198  
     rigidly 198  
 flexibility 488  
 flexible cable 92  
 flexural centre 387  
 fluctuating cycle 573  
 force(s), active 312  
     axial 29  
     concentrated 19  
     critical 478  
     cumulative action of 335  
     distributed 19  
     external 19  
         method of 344  
     generalized 333  
     of interaction 19  
     normal 29  
     passive 312  
     of reaction 20  
     shearing 203  
     superposition of 83  
     volume 19
- forced vibrations 535  
 formula, Saint-Venant's 407  
 frame 351  
 free torsion 187
- generalized displacement 333  
 generalized force 333  
 generalized Hooke's law 335  
 graph-analytic method 313
- helical spring 181  
 hinge, ductile 466  
 hinged support, fixed 197  
     movable 197  
 Hooke's law 33  
     generalized 335  
 hydrostatic load 455
- impact load 20  
 impact test 565  
 initial parameters, method of 305  
 integration, successive 312  
 intensity of continuous load 206  
 interaction, force of 19  
 I-section 285  
 isotropic material 37
- joint, butt 159  
     lapped 151  
     riveted 159  
     welded 159  
     with side fillet weld 162  
 joint deformation, condition of 67, 80,  
     360
- lapped joint 151  
 lateral deformation 36  
 lattice, crystalline 21  
 law, Hooke's 33  
     generalized 335  
     of complementary shearing stresses 109  
     conservation of energy 331  
     constancy of volume 50  
     of cumulative action of forces 335

- lifting capacity 471
- limit, of elasticity 23, 43
  - endurance 61, 62, 575
  - of proportionality 41, 47
- limiting states, first group 474
  - second group 474
- limiting stress circle 139
- load, breaking 457
  - continuous, intensity of 206
  - design 476
  - dynamic 20
  - hydrostatic 455
  - impact 20
  - permanent 19
  - repeated variable 20
  - static 20
  - suddenly applied 20
  - temporary 19
  - ultimate 457
- load area 214
- load curve 214
- local deformation 488
- local stress 58, 61, 157, 576, 582, 583
- long-term strength 618
- loss of stability 483
  
- material, amorphous 21
  - anisotropic 35, 56
  - brittle 41, 52
  - critical state of 63
  - crystalline 21
  - ductile 41
  - isotropic 37
  - sensitivity factor of 585
  - strength of 18
- maximum rigidity, plane of 386
- maximum shearing stresses, theory of 140
- maximum tensile stresses, theory of 138
- Maxwell and Mohr theorem 347
- mean stress of cycle 574
- method, of comparison of displacements 361
  - of equal moments 471
  - of external force 344
  - graph-analytic 313
  - of initial parameters 305
  - of superposition of forces 223
  - Vereshchagin's 349
- modulus, bulk 123
  - of elasticity 34
  - reduced 490
  - tangential 490
  - section 236
- Mohr's circle 110
- Mohr's strength theory 141
- moment, bending 203
  - design 406
  - equatorial 233
  - of section, static 232
  - static, about neutral axis 267
- moment of inertia, axial 233
  - of circle 240
  - of complex figure 245
  - of parallelogram 240
  - polar 173, 250
  - principal 256
- multiple-shear rivet 154
  
- natural vibrations 535
- net area 31
- neutral axis 227
- neutral layer 227
  - radius of curvature of 231
  - of trapezoid 435
- normal force 29
- normal stress 100
  
- octahedral plane 120
- octahedral shearing stress 121
- operating conditions, coefficient of 476
- overloading, coefficient of 476
  
- parallelogram, moment of inertia of 240
- passive force 312
- permanent load 19

- permissible stress 24
- plane(s), of maximum rigidity 386
  - octahedral 120
  - principal 102
- plane of inertia, principal 255
- plastic deformation 21, 47
- pliability 555
  - of structure, total 564
- Poisson's ratio 37
- polar moment of inertia 173, 250
- potential energy of distortion, theory of 146
- principal axes of inertia 251
- principal moment of inertia 256
- principal plane 102
- principal plane of inertia 255
- principal radius of inertia 256
- principal stress(es) 102
  - trajectory of 282
  - shearing 120
- principle of superposition of forces 83
- prismatic bar 27
- production process, coefficient for 593
- product of inertia, of section 232, 247
- proportionality; limit of 41, 47
- pure bending 225
- pure shear 127
- pure torsion 187
  
- radius of curvature of neutral layer 231
- radius of inertia 256
  - principal 256
- reaction, of beam supports 197
  - force of 20
  - redundant 357
- reciprocity of displacements, theorem of 347
- reciprocity of works, theorem of 347
- reduced mass 544
- reduced modulus of elasticity 490
- reduced moment, diagram of 472
- reduced stress 147
- reduction of area, permanent relative 45
- redundant constraint 359
- redundant reaction 359
  
- redundant unknown 359
- relative elongation 33
- relative reduction of area, permanent 45
- relative residual elongation 44
- relative rigidity 36
- relative shear 129
- reliability, coefficient of 475
- repeated variable load 20
- reservoir, thin-walled 103
- residual elongation, relative 44
- resistance, to rupture 134
  - to shear 134
- resonance 535
- rigidity, of bar 34
  - maximum, plane of 386
  - relative 36
  - of system 550
  - torsional 177
- rigidly fixed support 198
- rirel(s), crushing of 154
  - double-shear 153
  - multiple-shear 154
- riveted beam 289
- riveted joint 159
- rod, connecting 525
  - thin-walled 194
- rupture, failure through 132
  - resistance to 134
  - theory of 138
- rupture strain, total true 51
  
- safety, factor of 24, 30
  - main factor of 63, 64
- Saint-Venant's formula 407
- scale factor 590
- section, of beam
  - critical 200
  - core of 396
  - critical 86
  - product of inertia of 232, 247
  - static moment of 232
- section modulus 174, 236
- sensitivity factor of material 585
- shear, angle of 129

- pure 127
- relative 129
- resistance to 134
- theory of 140
- shear centre 387
- shear centre line 387
- shearing, failure due to 101
  - modulus of elasticity for 131
- shearing force(s) 204
  - diagram of 204
- shearing stress(es) 100
  - complementary 109
  - maximum, theory of 140
  - octahedral 121
  - principal 120
- simply supported beam 207
- span 92
- specific work, of elastic deformation
  - 46
  - total 46
- spherical tensor 117
- spring, conical 186
  - helical 181
- stability check 477
- stable creep 610
- state(s), composite stressed 101
  - limiting 474
- statically determinate beam 199
- statically indeterminate beam 199, 356
- statically indeterminate problem 66
- statically indeterminate system 66
- static load 20
- static loading 60, 521
- static moment, about neutral axis 267
  - of section 232
- straight-line form, loss of stability of 483
- strength, condition of 30
  - energy theory of 145
  - long-term 618
  - of materials 18
  - tensile, ultimate 30
  - theory of 136
  - true ultimate 51
  - ultimate 23, 43
- strength endurance 575
  - in unsymmetric cycle 579
- strength theory, first 138
  - fourth 146
  - of Mohr 141
  - second 139
  - third 140
- stress, biaxial 102
  - compressive 101
  - conditional 41
  - contact 105
  - critical 479
  - of cycle, mean 574
- cyclic 573
- dynamic 555
- local 58, 61, 157, 576, 582, 583
- maximum shearing 140
- maximum tensile 138
- normal 100
- permissible 24
- principal 102
- reduced 147
- rupture, true 51
- shearing 100
  - octahedral 121
  - principal 120
  - tensile 100
  - triaxial 103
  - uniaxial 102
  - variable 575
- stress circle 111
  - limiting 139
- stress concentration, coefficient of 576
  - factor of 583
- stress deviator 124
- stress intensity 121
- stressed state, composite 101
- stress-strain diagram 47
- stress tensor 117
- stress variation, cycle of 573
- structure, total pliability of 564
- successive differentiation 313
- successive integration 312
- suddenly applied load 20
- superposition of forces, method of 223
  - principle of 83
- support, fixed 198
  - hinged, fixed 197

- movable 197
  - rigidly fixed 198
  - system, rigidity of 550
  - statically indeterminate 66
- 
- tangential modulus of elasticity 490
  - temporary load 19
  - tensile strength, ultimate 30
  - tensile stresses 100
    - maximum, theory of 138
  - tension, axial 27
    - eccentric 392
  - test, impact 565
  - theorem, Castigliano's 340
    - Clapeyron's 335
    - of Maxwell and Mohr 347
    - of reciprocity of displacements 347
    - of reciprocity of works 347
  - theory, of brittle failure 138
    - of ductile failure 140
    - of maximum tensile stresses 138
    - of maximum shearing stresses 140
    - of potential energy of distortion 146
    - of rupture 138
    - of shear 140
    - of strength 136
  - thin-walled reservoir 103
  - thin-walled rod 194
  - thin-walled vessel 454
  - three moments, equation of 372
  - torque 165
  - torsion, free 187
    - pure 187
  - torsional rigidity 177
  - total pliability of structure 564
  - total specific work 46
  - trajectory of principal stresses 282
  - trapezoid, neutral layer of 435
  - triaxial stress 103
  - true rupture strain, total 51
  - true rupture stress 51
  - true ultimate strength 51
  - T-section 243
  - twisting angle 169
- 
- ultimate load 457
  - ultimate strength 23, 43
    - true 51
  - ultimate tensile strength 30
  - uniaxial stress 102
  - uniform distribution 29
  - uni-planar bending 256
  - unit force, bending moment due to 348
  - unstable creep 610
  - unsymmetric bending 379
  - unsymmetric cycle, strength endurance in 579
- 
- variable load, repeated 20
  - variable stress 575
  - Vereshchagin's method 349
  - vessel, thin-walled 454
  - vibrations, amplification factor of 539
    - amplitude of 535
    - forced 535
    - natural 535
  - volume force 19
- 
- warping 488
  - weight, dead 86
  - welded beam 290
  - welded joint 159
  - work, of elastic deformation 46
    - specific 46
  - work hardening 590
- 
- zero base cycle 573
  - Zhuravskii's formula 284